Self -compacting concrete at fire temperatures

Persson, Bertil

2003

LUND INSTITUTE OF TECHNOLOGY
LUND UNIVERSITY

Division of Building Materials

SELF-COMPACTING CONCRETE AT FIRE TEMPERATURES

Bertil Persson

TVBM-3110 Lund 2003

ISRN LUTVDG/TVBM--03/3110--SE(1-200)
ISSN 0348-7911 TVBM
ISBN 91-631-3301-6
Revised September 2003
Lund Institute of Technology
Division of Building Materials
Box 118
SE-221 00 Lund, Sweden

Telephone: 46-46-2227415
Telefax: 46-46-2224427
www.byggnadsmaterial.lth.se

PREFACE

Concrete that does not require any energy for compacting in order to cover the reinforcement or fill out the mould has attracted a great deal of interest. Swedish experience now exists from 19 full-scale bridges and other full-scale projects with Self-Compacting Concrete, SCC. The technique has also been introduced for dwelling houses, tunnels and office buildings. A railway tunnel has been constructed with SCC and a double highway tunnel was recently made with SCC. SCC has also been introduced for the production of piles. Regarding concrete under severe circumstances for construction of bridges, dams, tunnels and so forth, the requirements of durability call for a higher level of documentation than for concrete that is used for dwelling houses or office buildings. The primary durability properties are chloride ingress, fire resistance, internal frost resistance, salt frost scaling and sulphate resistance for concrete in severe situations. All these properties except for the fire resistance were recently studied at our department. Salt frost scaling, internal frost resistance and sulphate resistance did not differ much from the corresponding properties of normal compacting concrete. The chloride ingress in a laboratory investigation showed larger chloride migration coefficient in SCC than in normal concrete, NC. An investigation of concrete with somewhat lower water-cement ratio, w/c, cast in the field showed smaller chloride migration coefficient in SCC than in NC. It is known from the Great Belt railway tunnel and also from the Channel railway tunnel that large-scale spalling of High-Performance Concrete, HPC, may occur during catastrophic fire, especially in concrete at low w/c. Such spalling is avoided by including polypropylene fibres in the concrete. However, a code of practice is lacking for how to use polypropylene fibre in order to avoid spalling in case of fire. In this project the objectives were to investigate mechanical performance under compressive loading at fire temperature conditions of SCC that contains different amount of polypropylene fibre, different types of cement and air content, preconditioned either in the air or in water. The objective was also to compare the result of performance under compressive loading at high temperature conditions with the corresponding properties of NC. The w/c of the concrete was either 0.40, 0.55 or 0.70. Finally the objectives were to give recommendations on how to produce a SCC that can withstand fire spalling. The following persons in the coordination group of the project are gratefully acknowledged:

- Christer Dieden (head of the group)
- Göran Fagerlund
- Ulf Jönsson
- Jens Oredsson

The following persons in the reference group of the project are also gratefully acknowledged for their participation:

- Patrik Groth
- Tomas Hermodsson
- Katarina Kieksi
- Robert Ronnebrant

Financial support from the following organisations and companies is also gratefully acknowledged:

- Brandforsk
- Skanska Prefab AB, SPAB
- The Development Fund of the Swedish Construction Industry, SBUF
- SP, Swedish Testing and Research Institute

Finally, thanks are due to the following persons for finalizing the report and carrying out the laboratory experiments:

- Britt Andersson
- Stefan Backe
- Peter Friberg
- Göran Klevbo
- Ingemar Larsson
- Thord Lundgren
- Martin Hansson
- Bengt Nilsson
- Sten Rodenstam
- Lennart Thorsson

Lars Boström was in charge of the full-scale tests.

Lund, 13 March 2003

Bertil Persson

CONTENTS **PAGE**

SYMBOLS

a,b constants for particle distribution
c cement content
c,e,g constants for current and residual properties of concrete at and after elevated temperatures
c/p cement-powder ratio
d sieve size ($0.1 < d < 10$ mm)
f filler content
f_c compressive cylinder strength (MPa)
$f_{ct,T}$ split tensile strength at elevated temperature (MPa)
$f_{ct,20}$ tensile strength at 20 °C (MPa)
$f_{ct,T20}$ split tensile strength at 20 °C after cooling from the elevated temperature (MPa)
f_{c28f} 28-day strength with filler (MPa)
f_{c28ppf} 28-day strength (fibre, MPa)
f_{c280} 28-day strength (no fibre, MPa)
h relative weight after evaporated or hydrated water losses
m resistance to water penetration after heating ($s/m^2 \cdot 10^6$)
n FTF (Hz)
o slope of the water suction between 0 and 4 min. versus square root of time
p material passing
p powder content (=cement + filler)
ppf polypropylene fibre amount (kg/m^3)
q slope of the water suction between 1000 and 4000 min. versus square root of time
r constant in order fully to describe suction between 1000 and 4000 min. (kg/m^2)
r residual and current relative properties of concrete at and after elevated temperatures
s particle passing through
t thickness of specimen (m
t time (h)
t concrete age ($2 < t < 28$ days)
w/b water-binder ratio
w/c water-cement ratio
w/p water-powder ratio
w/Pc the water-Portland cement ratio
A concrete A with Anläggningscement (Degerhamn) and air-entrainment
B concrete B with Byggcement and natural air content
B sealed curing
C_{to} torsional creep (rad/mm)
D air curing (drying)
D diameter of the specimen (in.)
E_{dyn} dynamic elastic modulus (obtained by FRF, GPa)
E_{stat} modulus of elasticity (at loading in the stress/strain tests, GPa)
FRF fundamental resonance frequency (Hz)
G Glass filler
G weight (kg)
HPC High Performance Concrete,
K limestone powder
K ratio of gyration (=d/4 for cylinder)
L length (in.)
NC normal compacting concrete
O optimisation
P testing
Pc/p the Portland cement –powder ratio
P_{cap} denotes the capillary porosity
S square beam
T manufacture of 20 cylinders
T temperature (°C)
T temperature at heating
R reference

RH relative humidity
SCC Self-Compacting Concrete
T_{sat} temperature of saturation (°C).
U executed testing
V/A half the hydraulic radius, volume to area
W weight of the specimen (lb.)
W weight after fire spalling
W_{dry} dry weight after heating 1 week at 105 °C and cooling in exsiccator at 20 °C
W_{wet} wet weight before heating
W_A weight after fire spalling of water-cured concrete A with type I cement
W_T weight in exsiccator at 20 °C after heating to 105 °C, 200 °C, 400 °C or 600 °C.
W_U weight under water at 20 °C after heating to 105 °C, 200 °C, 400 °C or 600 °C.
W_V weight after water ingress in vacuum at 20 °C after heating to 105 °C, 200 °C, 400 °C or 600 °C.
0 amount of polypropylene fibres (kg /m³)
40 w/c (%)
$\delta f_c/\delta t$ strength increase rate (MPa/day)

SUMMARY

1. General

This report describes experimental studies of the mechanical performance of Self-Compacting Concrete, SCC, under compressive loading at fire temperatures. The SCC contains different amounts of polypropylene fibre, different types of cement and air content, preconditioned either in the air or in water. The result of the studies was compared with the corresponding properties of normal concrete, with the same w/c and air content. Half a year's or one year's age applied at the time of testing. The strength development of the concrete was followed in parallel. Seven SCCs with w/c = 0.40, 0.55 or 0.70 and one normal concrete, NC, with w/c = 0.40 were studied for compressive strength in a fire temperature oven. The temperatures were 200 °C, 400 °C and 800 °C. Both testing at elevated temperature and after cooling took place. Elastic modulus, ultimate strain at maximum strength, dynamic modulus and relative humidity, RH, were studied in parallel. Supplementary tests of were performed, after cooling from 600 °C, of strength, elastic modulus, ultimate strain at maximum strength. Supplementary tests were also performed on capillary suction, porosity and resistance to water penetration at water suction. The results of the laboratory tests were compared with results of full-scale tests on twelve SCCs with w/c = 0.40, 0.55 or 0.70 and 4 NCs with w/c = 0.40, 0.55 or 0.70 on fire spalling carried out in a high-temperature oven. The same concrete was studied in the laboratory and in full-scale tests. The concrete was air-cured at an ambient RH = 60%, or water-cured from demoulding until testing. The effects of increased amount of polypropylene fibres, age, different types of cement and air content, capillary suction, porosity, moisture content, hydration losses, preconditioning either in the air or in water, were studied.

2. Mix proportions obtained at LTH

One fundamental point was the way to produce concrete with polypropylene fibre. Therefore the principles of the mix proportions are given even though it may seem too detailed. These results are based on concrete mix proportions defined by the grading curves of the fresh SCC. More fine materials were required in SCC than in NC in order to incorporate 4 kg/m³ of fibres in the mixed proportions. With 2 kg/m³ more traditional mix proportions of SCC were used.

3. Mechanical properties obtained at LTH

Glass or limestone filler additives increased strength substantially at normal temperature even though the cement content was somewhat lower in SCC than in NC. Probably a more efficient packing of the particles was the reason for the enlarged strength. Strength was increased by 0.07 MPa per kg/m³ increasing amount of filler added. Additives of polypropylene fibres decreased strength by 2.3% per kg/m³ increasing amount of fibre added. Water-cured cylinders of SCC, 100 mm in diameter, without polypropylene fibres, exhibited spalling at 480 °C/h heating rate. At 240 °C/h heating rate cylinders of SCC, 100 mm in diameter, without polypropylene fibres, exhibited no spalling. Once spalling was avoided, SCC and NC behaved similarly at high temperature except at 800 °C at which temperature SCC with limestone powder did not show any residual strength at all after cooling down to 20 °C, Figure 1. Figure 2 shows the properties of SCC with limestone powder. Comparison with HPC shows greater strength between 100 °C and 200 °C of SCC than that of HPC, Figure 3. Greater loss of the elastic modulus was obtained than seen before, Figure 4.

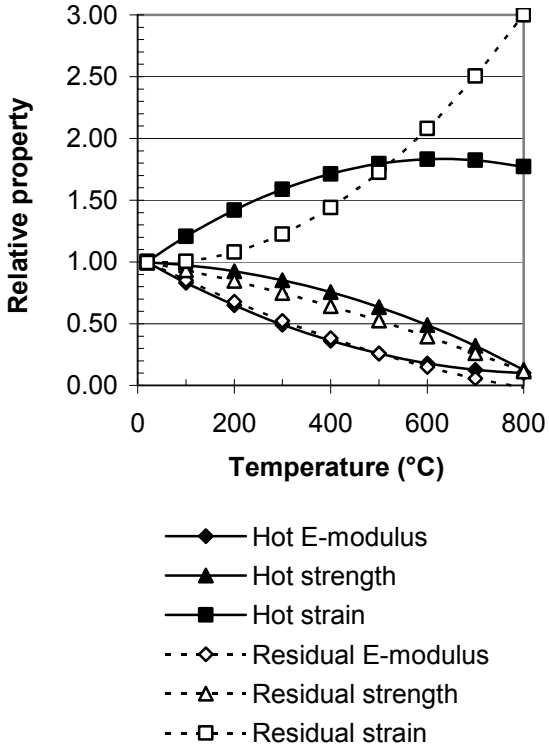

Figure 1 – Relative properties of concrete at/after elevated temperature except for residual property with limestone powder at 800 °C.

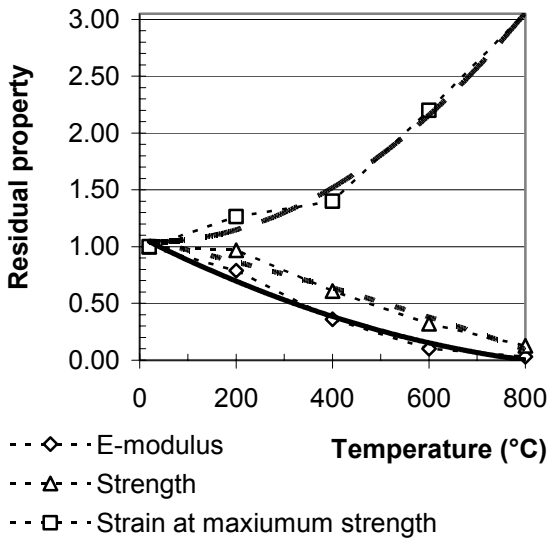

Figure 2 - Relative residual properties of SCC with limestone powder versus temperature.

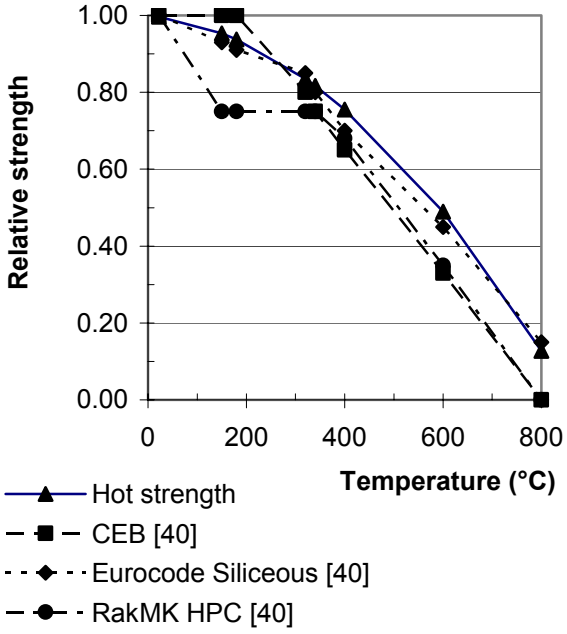

Figure 3 - Hot strength (64 specimens), CEB, Eurocode Siliceous and RakMP HPC code [40].

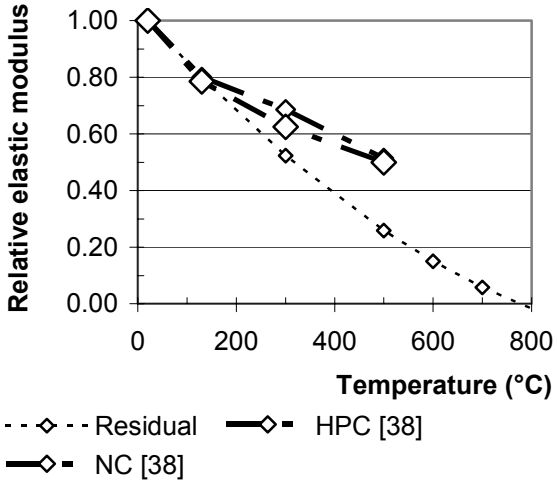

Figure 4 – E-modulus compared with [38].

4. Effect of properties of concrete on fire spalling tested at SP [94]

4.1 Moisture and isothermal behaviour

About 3% moisture in normal concrete is critical for the fire spalling to take place [79]. Even though the concrete was dried out to about 75%RH, very moisture content was observed. Moisture content as follows was measured:

- Previous research with HPC [40]: 2.2%
- Air-cured specimen: 3.6%
- Water-cured specimen: 5.9%

In comparison about 3.1% moisture content is sufficient to cause fire spalling at the stress level used in the experiments, about 15 MPa. The moisture content of SCC was compared with the isotherm of normal concrete. SCC showed larger moisture content than NC when RH was held constant, especially SCC with glass filler.

4.2 Effect of cement content, age and curing

It was observed that the cement-powder ratio, c/p, of the concrete had a substantial effect on the fire spalling – the lower the c/p, the larger the fire spalling. At water-cement ratio, w/c = 0.40, fire spalling was avoided with c/p $\geq$ 0.80 but became unacceptably large in concrete with c/p = 0.60. One way to avoid fire spalling seems to be to increase c/p. At half a year's age the same fire spalling was observed for a concrete with 4 kg/m³ fibres as for a one-year-old concrete with 2 kg/m³ of fibres. With water curing only half the resistance of water penetration of SCC was acceptable compared with the resistance of water penetration for air-cured concrete, probably due to a better hydration conditions with water curing.

4.3 Capillarity, water suction and fibres

At constant porosity both air and water-cured SCC showed greater resistance to water penetration than normal concrete, NC, did, which may be an explanation for the increased sensitivity of SCC to fire spalling compared with NC observed on tests performed at SP [94]. The largest increase of relative porosity with increasing temperature was observed for NC; the lowest increase of relative porosity was observed for SCC with low w/c without fibres. For SCC with fibres the increase of porosity was less than for NC, probably since larger water pressure than available in a 20-mm-concrete was required for the increase of porosity with fibres to take place. The smallest relative resistance to water penetration was consequently observed for NC. The observations of differences between porosity and resistance to water penetration of SCC and NC show that another structure

may be formed in SCC than in NC even though the isotherm performed similarly at normal temperature. At higher temperature the porosity increased more rapidly and the resistance to water penetration dropped more in NC than in SCC. For SCC with fibres increase of the relative resistance to water penetration was observed. For concrete with 2 kg/m³ polypropylene fibres larger resistance to water penetration at suction was observed at 105 °C than for the same concrete without fibres and than for concrete with 4 kg/m³ polypropylene fibres. For concrete with 4 kg/m³ polypropylene fibres larger resistance to water penetration at suction was observed at 200 °C than for the same concrete without fibres and for concrete with 2 kg/m³ polypropylene fibres. The reason for the increasing resistance to water penetration was probably an expansion and melting of the polypropylene fibres at 105-200 °C. These phenomena remained after the specimen has cooled to 20 °C and therefore decreased the water suction. As mentioned above, a much larger structure is required than 20 mm in thickness for the water pressure to form and to transport the melting, liquid polypropylene fibres out of the pores. During fire heating water transport will be prohibited inward in concrete with fibres. In this case the water pressure in concrete with fibres will increase more slowly than in concrete with no fibres as the water, instead of moving inward leaves the surface. This may explain the mechanism of polypropylene fibres in concrete at fire:

- Possible increase of polypropylene fibre volume and melting at 105-200 °C.
- Water movement inward concrete with fibre is diminished at 105-200 °C due to an increase in the resistance to water penetration.
- Water instead moves to the surface of concrete with fibres and fire spalling is avoided.

5. Polypropylene fibres to prevent spalling of 200-mm square reinforced columns

5.1 Calculation on cement and fibre content

Estimation was done for the amount of fibres versus w/c and c/p. According to a parameter study, the most important factor to prohibit fire spalling was a high cement-powder ratio, c/p. Figure 5 shows the amount of 32 µm fibres, ppf_{normal}, at constant moisture content and stress level in order to limit the fire spalling of SCC to that of normal concrete without fibres (kg/m³):

$$ppf_{normal}=(28\cdot(c/p)^2-26\cdot(c/p)-2.4)\cdot\ln(w/c)+45\cdot(c/p)^2-68\cdot(c/p)+23>0 \quad (1)$$

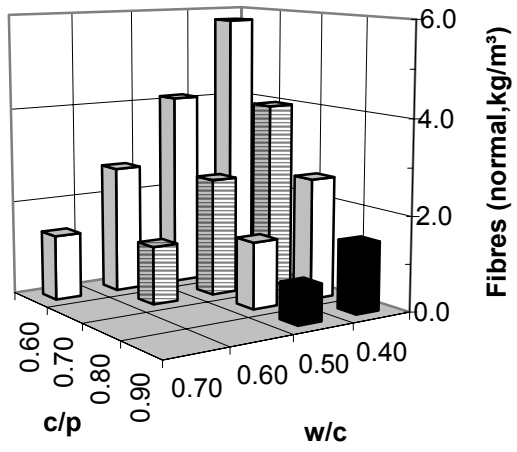

Figure 5 - Amount of fibres at constant moisture content and stress level in order to limit the fire spalling of SCC to that of normal concrete without fibres versus the cement-powder ratio, c/p, and the water-cement ratio, w/c.

Figure 6 shows the fibre requirement in order to limit the fire spalling at 15% at half a year's age. The following equation for the amount of polypropylene fibre in order to limit the fire spalling at 15% at half a year's age was obtained (32 µm fibres, kg/m³):

$$ppf_{85\%}=(-35\cdot(c/p)^2+34.9\cdot(c/p)-16.7)\cdot\ln(w/c)-25\cdot(c/p)+11.7>0 \quad (2)$$

c/p denotes the cement-powder ratio {0.50 < c/p < 1}
p denotes cement and powder (glass or limestone filler)
$ppf_{85\%}$ denotes the content of 32 µm polypropylene fibres to limit the fire spalling to 15% at half a years's age (32 µm fibres, kg/m³)

5.2 Calculation based on the fibre and Portland cement content

Another synthesis was required for the amount of fibres in concrete versus the water-Portland cement ratio, w/Pc and the Portland cement-powder ratio, Pc/p. Figure 7 shows the amount of 32 µm fibre at constant moisture content and stress level required for the same fire spalling of SCC like for normal:

$$ppf_{normal}=(13\cdot(Pc/p)-12.3)\cdot\ln(w/Pc)-2.69\cdot(Pc/p)^2+2.65\cdot(Pc/p)-0.2>0 \quad (3)$$

ppf_{normal} 32 µm fibres to obtain the same weight after fire of SCC like for normal
w/Pc denotes the water-Portland cement ratio
Pc/p denotes Portland cement-powder ratio

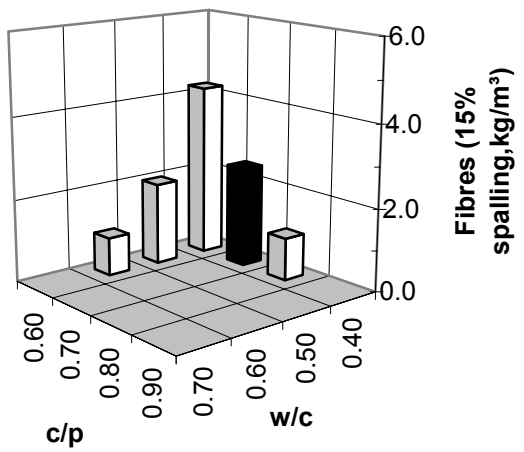

Figure 6 - Fibres based on 85% remaining weight after fire compared with the original one.

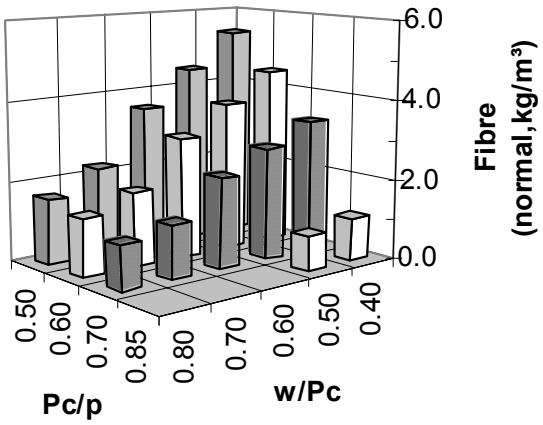

Figure 7 - Fibre amount at constant moisture content and stress level required for the same fire spalling of SCC like for normal concrete

Figure 8 shows the amount of fibres, ppf, to limit the fire spalling to 15% of that before fire at half a year's age (32 µm fibres, kg/m³):

$$ppf_{85\%}=(-43\cdot(Pc/p)^2+72\cdot(Pc/p)-31)\cdot\ln(w/Pc) - 14\cdot(Pc/p)^2+18.7\cdot(Pc/p)-6.2 \quad (4)$$

$ppf_{85\%}$ denotes 32 µm fibres to obtain 85% weight after fire of SCC of the original (kg/m³).

w/Pc denotes the water-Portland cement ratio
Pc/p denotes Portland cement-powder ratio

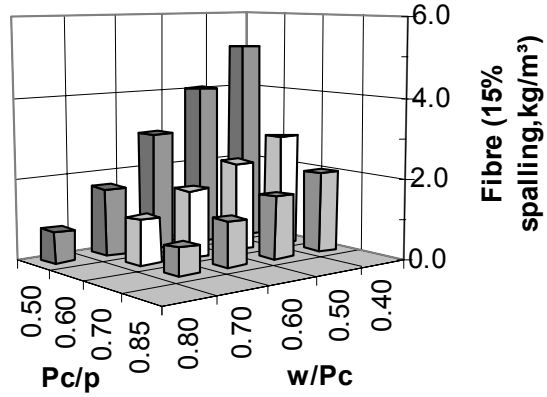

Figure 8 - Required amount of fibres in order to limit the amount of fire spalling to 15% of the original weight.

SAMMANFATTNING OCH SLUTSATSER

1. Allmänt

Denna rapport beskriver experimentella studier av mekaniska egenskaper hos självkompakterande betong, SKB, under tryckspänning vid brandtemperaturer. SKB innehåller olika mängder polypropylenfibrer, olika cement och lufthalt, förlagrad endera i luft eller i vatten. Resultaten av studierna jämförs med motsvarande egenskaper hos normal betong, NB, med samma vattencementtal, vct, och lufthalt. Ett halvt år eller ett års ålder används vid försöken. Hållfasthetsutvecklingen studerades parallellt hos betongen. Sju SKB med vct = 0.40, 0.55 eller 0.70 och en NB med vct = 0.40 studerades i fråga om hållfasthet vid temperaturförsök i ugn. Temperaturer var 200 °C, 400 °C och 800 °C. Försök utfördes såväl i varmt tillstånd som efter avsvalning. Elasticitetsmodul, brottstukning vid maximal hållfasthet, dynamisk elasticitetsmodul och relativ fuktighet, RF, studerades parallellt. Kompletterande försök utfördes efter avsvalning från 600 °C av hållfasthet, elasticitetsmodul, brottstukning vid maximal hållfasthet. Kompletterande försök utfördes även i fråga om motståndstal mot vatteninträngning, kapillaritet och porositet. Laboratorieresultaten jämfördes med fullskaleförsök på tolv SKB med vct = 0.40, 0.55 eller 0.70 och 4 NB med vct = 0.40, 0.55 eller 0.70 beträffande brandspjälkning utförda i en högtemperaturugn. Exakt samma betong studerades i laboratoriet som vid fullskaleförsöket. Betongen härdades endera i luft vid ca RF = 60% eller i vatten från tillverkning fram till fullskaleförsöken. Effekterna av ökad mängd polypropylenfibrer, ålder, olika typer av cement och lufthalt, kapillaritet, porositet, fukthalt, hydratationsförluster och härdningssätt, studerades.

2. Betongrecept framtagna vid LTH

En fundamental förutsättning var att självkompakterande betong, SKB, med polypropylenfibrer kunde produceras. Därför ges principer för betongproportionering även om detta kan verka att gå alltför djupt in i detalj. Resultaten bygger på betongrecept utförda med en ideal partikelfördelning i den färska betongen. Mer finmaterial erfordrades i ett recept för SKB än i recept för normal betong, NB, i syfte att receptet även skulle kunna innehålla 4 kg/m³ fibrer. För 2 kg/m³ fibrer kan ett mer traditionellt recept för SKB användas. Det kan dock inte rekommenderas att använda 4 kg/m³ fibrer i SKB eftersom arbetbarheten i en sådan betong minskar snabbt med tiden.

3. Mekaniska egenskaper erhållna vid LTH

Mineraliska tillsatser av glas- eller kalkstensfiller ökade hållfastheten avsevärt vid normal temperatur även om cementhalten minskades något hos SKB jämfört med NB. Förmodligen var en mer effektiv packning av partiklarna i den färska betongen orsaken till den ökande hållfastheten. Hållfastheten ökade med 0.07 MPa per kg/m³ ökad mängd filler. Tillsatser av polypropylenfibrer minskade hållfastheten med 2.3% per kg/m³ ökande mängd fibrer. Vattenhärdade cylindrar med 100 mm i diameter utan polypropylenfibrer, uppvisade brandspjälkning vid 480 °C/h i uppvärmningshastighet. Med 240 °C/h i uppvärmningshastighet av SKB med 100 mm i diameter, utan polypropylenfibrer, erhölls ingen spjälkning alls. När väl spjälkning kunde undvikas uppvisade SKB och NB liknande egenskaper vid höga temperaturer utom efter en upphettning till 800 °C då SKB med kalkstensfiller förlorade all hållfasthet efter avsvalning till 20 °C, figur 1. Figur 2 visar egenskaper hos SKB med kalkstensfiller. En jämförelse med högpresterande betong, HPB, visar högre hållfasthet hos SKB mellan 100 °C och 200 °C än hos HPB, figur 3. Elasticitetsmodulen minskade mer vid hög temperatur än vad som tidigare erfarits, figur 4.

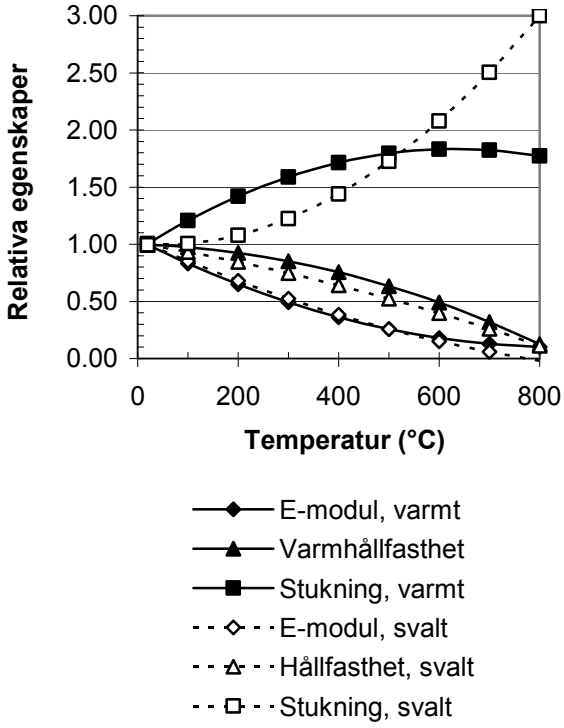

Figur 1 – Relativa egenskaper hos betong vid/efter förhöjd temperatur utom hos betong med kalkstensfiller efter uppvärmning till 800 °C.

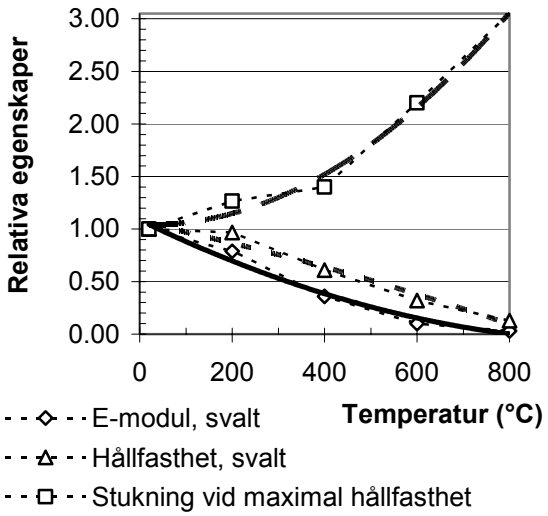

Figur 2 – Relativa kvarstående egenskaper hos SKB med kalkstensfiller versus temperatur.

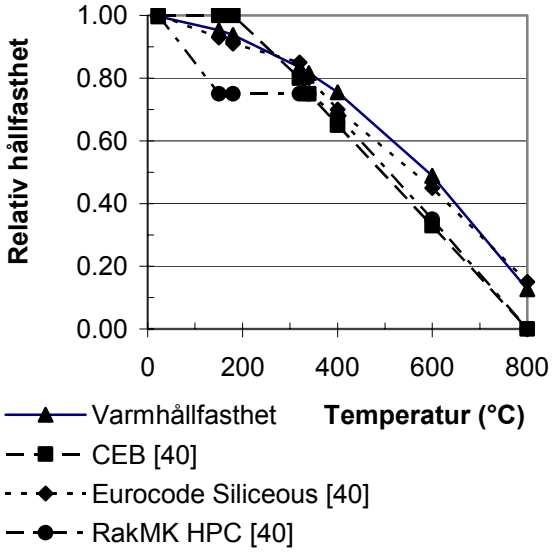

Figur 3 - Varmhållfasthet (64 specimens), CEB, Eurocode Siliceous and RakMP HPC code [40].

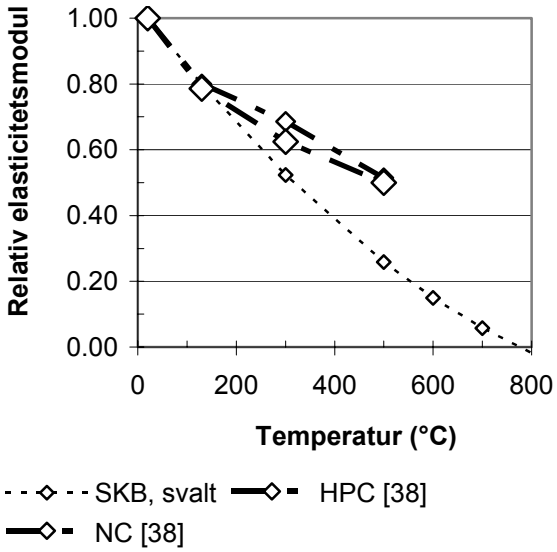

Figur 4 – E-modul jämfört med [38].

4. Spjälkning vid brandtemperaturer studerad vid SP [94]

Fukthalt och isoterm:

Omkring 3% fukthalt i normal betong är en kritisk fukthalt för att brandspjälkning skall kunna äga rum [79]. Även om betongen torkades till ca RF = 75% observerades höga fukthalter. I medeltal uppmättes följande fukthalter:

- Tidigare försök med HPB [40]: 2.2%
- Lufthärdade provkroppar: 3.6%
- Vattenlagrade provkroppar: 5.9%

Ca 3.1% fukthalt tillräckligt för att orsaka brandspjälkning vid spänningen vid experimenten, ca 15 MPa. Fukthalten i SKB jämfördes med isotermen för normal betong. SKB innehöll mer vatten än normal betong, speciellt SKB med glasfiller.

Effekt of cementhalt, ålder och härdning:

Det observerades att cementpulvertalet, cpt, hos betongen hade en avsevärd effekt på brandspjälkningen – ju lägre cpt desto större brandspjälkning. Vid vattencementtal, vct = 0.40, undveks brandspjälkning under förutsättning att cpt $\geq$ 0.80 men blev oacceptabelt stor vid cpt = 0.60. Ett sätt att undvika brandspjälkning förefaller vara att öka cpt. Vid ett halvt års ålder erhölls samma brandspjälkning för en betong med 4 kg/m³ fibrer som för en ett år gammal betong med 2 kg/m³ fibrer. Vid vattenlagring kunde motståndstalet för vatteninträngning hos SKB vara dubbelt så stort som för en luftlagrad betong till följd av en bättre hydratation av betongytan vid vattenlagring.

Kapillaritet, vattenuppsugning och fibrer:

Vid en konstant porositet visade såväl luftlagrad som vattenlagrad SKB större motståndstal mot vatteninträngning än NB, vilket kan vara en förklaring till känsligheten hos SKB för brandspjälkning studerad vid SP [94] jämfört med NB. Den största relativa ökningen av porositeten med ökande temperatur observerades hos NB; den lägsta ökningen i relativ porositet observerades för SKB med lågt vct utan fiberinnehåll. För SKB med fiber ökade porositeten mindre än för NB troligen beroende av att ett vattentryck större än det som erhölls i de 20 mm tunna proverna erfordras för att ge en ökad porositet. Det minsta relativa motståndstalet mot vatteninträngning erhölls på samma sätt för NB. De observerade skillnaderna i relativ porositet och i det relativa motståndstalet mot vatteninträngning mellan SKB och NB visar att en annan struktur troligen uppstår i SKB än i NB eftersom isotermen beter sig olikartat vid normal temperatur hos de bägge betongtyperna. Vid förhöjd temperatur ökar relativa porositeten

snabbare och minskar relativa motståndstalet mot vatteninträngning mer hos NB än hos SKB. För SKB med fibrer observerades ett ökande relativt motståndstal mot vatteninträngning. För betong med 2 kg/m³ polypropylenfibrer var det relativa motståndstalet mot vatteninträngning vid 105 °C större än hos samma betong utan fibrer och även större än hos betong med 4 kg/m³ polypropylenfibrer. För betong med 4 kg/m³ polypropylenfibrer var motståndstalet mot vatteninträngning vid 200 °C större än för samma betong utan fibrer. Orsaken till det ökade motståndstalet mot vatteninträngning vid 105-200 °C är troligen att fibrerna smälter och expanderar mer än betongen. Dessa iakttagelser kvarstod även efter avsvalning till 20 °C och minskade därför vatteninträngningen. Som nämnts ovan kan en större provkroppstjocklek än 20 mm krävas för att ett tillräckligt stort vattentryck skall uppstå i betongen under uppvärmning i syfte att ge en ökad porositet tillsammans med de smältande fibrerna. I samband med uppvärmning under brand förhindras transport av vatten inåt i betong med fibrer. I detta fall kommer vattentrycket i betong med fibrer att öka långsammare än i betong utan fibrer eftersom vattnet rör sig mot betongytan. Detta är en förklaring till mekanismen för polypropylenfibrer i betong vid brand:

- Ökande volym hos polypropylenfibrer och smältning vid 105-200 °C.
- Vattenrörelser förhindras inåt betongen vid 105-200 °C till följd av ett ökande motståndstalet mot vatteninträngning.
- Vattnet rör sig i stället utåt mot betongytan varvid spjälkning undviks.

5. Polypropylenfibrer för att undvika brandspjälkning

5.1 Beräkning byggd på cement- och fiberhalt

En syntes för att beräkna mängden polypropylenfibrer för att undvika brandspjälkning togs fram baserad på cementpulvertalet, cpt, och vattencementtalet, vct, figur 5. Figur 5 visar mängden 32 µm fibrer, ppf_{normal}, för att vid konstant fuktkvot och påkänningsnivå begränsa mängden spjälkning till samma nivå som för normal betong (kg/m³):

$$ppf_{normal}=(28\cdot(c/p)^2-26\cdot(c/p)-2.4)\cdot\ln(w/c)+45\cdot(c/p)^2-68\cdot(c/p)+23>0 \quad (1)$$

Figur 6 visar kravet på fibrer vid en största brandspjälkning om 15% vid ett halvt års ålder.

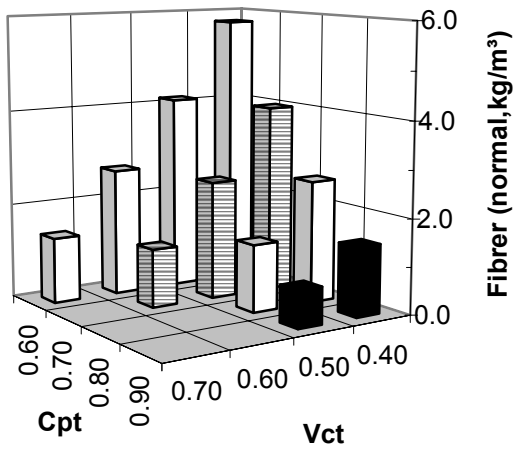

Figur 5 - Mängden 32 µm fibrer, ppf_{normal}, för att vid konstant fuktkvot och påkänningsnivå begränsa mängden spjälkning till densamma som för normal betong (kg/m³).

Fyra kg/m³ polypropylenfibrer kan emellertid inte rekommenderar från gjutbarhetssynpunkt. Följande ekvations erhölls för mängden polypropylenfibrer i syfte att begränsa brandspjälkningen till ca 15% vid ett halvt års ålder (32 µm, kg/m³):

$$ppf_{85\%}=(-35\cdot(c/p)^2+34.9\cdot(c/p)-16.7)\cdot\ln(w/c)-25\cdot(c/p)+11.7>0 \quad (2)$$

c/p betecknar cementpulvertalet, cpt {0.50 < c/p < 1}

p betecknar cement and pulverinnehåll (glas- eller kalkstensfiller)

$ppf_{85\%}$ betecknar 32 µm polypropylenfibrer vid 15% brandspjälkning (ett halvt års ålder, kg/m³)

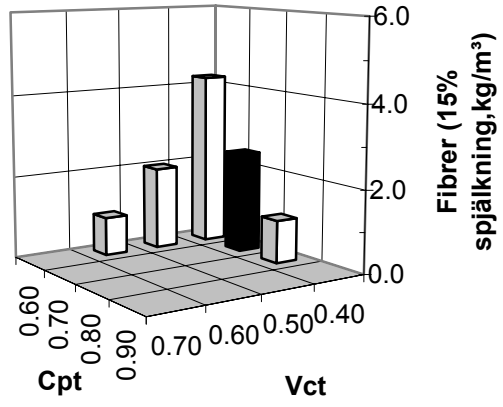

Figur 6 - Mängd 32 µm fibrer vid ca 15% brandspjälkning vid ett halvt års ålder fibrer (kg/m³). Cpt = cementpulvertalet, vct = vattencementtalet.

5.2 Beräkning baserad på fiber- och Portlandcementhalt

Ytterligare en syntes krävdes för att ta fram mängden fibrer i betong baserad på vattenportlandcementtalet, vPct, och Portlandcementpulvertalet, Pcpt. Figur 7 visar mängden 32 µm fibrer för att vid konstant fuktkvot och påkänningsnivå erhålla samma spjälkning som för normal betong:

$$ppf_{normal} = (13\cdot(Pc/p)-12.3)\cdot\ln(w/Pc) - 2.69\cdot(Pc/p)^2 + 2.65\cdot(Pc/p) - 0.2 > 0 \quad (3)$$

ppf_{normal} 32 µm fibrer för att erhålla samma spjälkning som för normal betong (kg/m³)
w/Pc betecknar vatten Portladcementtalet
Pc/p betecknar Portland cementpulvertalet

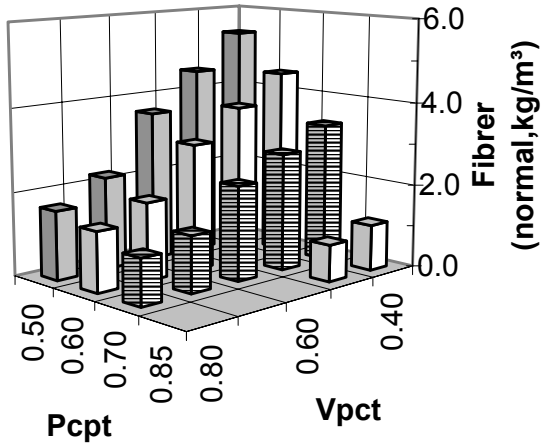

Figur 7 - Mängden 32 µm fibrer för att vid konstant fuktkvot och påkänningsnivå erhålla samma spjälkning som för normal betong.

Figur 8 visar mängd 32 µm fibrer för att erhålla 15% brandspjälkning vid ett halvt års ålder. Följande mängd fibrer, ppf, erhölls för att begränsa brandspjälkningen till 15% vid ett halvt års ålder (32 µm fibrer, kg/m³):

$$ppf_{85\%} = (-35\cdot(Pc/p)^2 + 34.9\cdot(Pc/p) - 16.7)\cdot\ln(w/Pc) - 25\cdot(Pc/p) + 11.7 > 0 \quad (4)$$

p betecknar innehåll av cement-, glas- och kalkstensfiller
ppf betecknar innehåll av 32 µm polypropylenfibrer för att begränsa brandspjälkningen till 15% vid ett halvt års ålder (kg/m³)
w/Pc betecknar vattenportlandcementtalet
Pc/p Portlandcementpulvertalet {0.50 < c/p < 1}

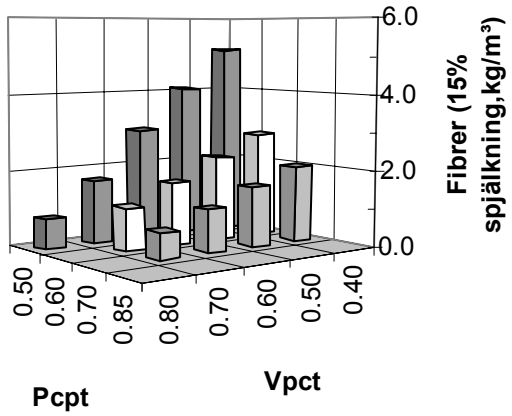

Figur 8 - Mängd 32 µm fibrer vid 15% brand spjälkning vid ett halvt års ålder.

1. INTRODUCTION, LIMITATIONS AND OBJECTIVE.

1.1 Introduction

Concrete that does not require any energy for compacting in order to cover the reinforcement or fill out the mould has attracted a great deal of interest in recent years. Swedish experience now exists from 19 full-scale bridges and other full-scale projects with SCC [1]. The technique has also been introduced for dwelling houses and office buildings [2]. A railway tunnel has been constructed with SCC [3], Appendix 1.1, and a double highway tunnel was recently made with SCC [4-6], a part of the highway E6. It consists of a 150-m long rock tunnel with twin-lane tubes. For the first time in Sweden, the water sealing system in a tunnel will be built as water drained concrete inner vault, cast directly on the concreted (shotcrete) rock surface. The water sealing consists of a 2-mm thick plastic membrane protected against the shotcrete by a geotextile cloth. The theoretical thickness of the concrete inner vault is 400 mm. The bottom part of this tunnel (barriers) was made of frost resistant SCC and drained by casting towards drained remaining concrete formwork [4-6]. Recently SCC has been introduced for the production of poles, piles and pillars [7-10], Appendix 1.2. Bridges, dams, tunnels and so forth require higher durability than concrete that is used for dwelling houses or office buildings. The primary durability properties are chloride ingress, fire resistance, internal frost resistance, salt frost scaling and sulphate resistance for concrete in severe situations. All these properties except for the fire resistance were recently studied at our department. Salt frost scaling, internal frost resistance and sulphate resistance did not differ much from the corresponding properties of normal compacting concrete. The chloride ingress was larger in SCC than in NC. It is known from the Great Belt railway tunnel and also from the Channel railway tunnel that large-scale spalling of the concrete may occur during catastrophic fire, especially in concrete at low water to cement ratio, w/c. Scaling is avoided by polypropylene fibre in concrete [11-13].

1.2 Limitations

The testing of the compressive strength at high temperature took place at about half a year's age only. Eight concrete were studied, one normal concrete, NC, with w/c = 0.40 and seven SCCs, with w/c = 0.40, 0.55 and 0.70. Tests of compressive spalling took place with 12 SCCs and 4 NCs, with w/c = 0.40, 0.55 or 0.70. The concrete was cured in air or water until testing. Strength specimens were 100 mm in diameter and 200 mm long. The fire spalling test specimens were 200 x 200 mm and 2 m long pre-stressed by cast-in tendon wires, 12 mm in diameter. The following parameters were studied, Table 1.1 [14]:

- w/c = 0.40, 0.55 or 0.70
- Polypropylene fibres, 32 μm, 0, 2 or 4 kg/m³
- Curing type, air or water
- Temperature, 20 °C, 200 °C, 400 °C, 800 °C
- High-temperature test or residual
- Different air content (1 or 6% vol.).

Table 1.1 – Parameters in the study

Testing status: hot or residual properties					
Temperature: 200 °C, 400 °C, 600 °C, 800 °C					
Concrete	w/c (%)	Cement–air - curing	Age (years)	Filler type	Fibre content (kg/m³)
40AG0	40	A	½	G	0
40AK0	40	A	½	K	0
40AK2	40	A	½	K	2
40AK4	40	A	½	K	4
40AR0	40	A	½	R	0
40BR0	40	A	½	R	0
40BK0	40	A	½	K	0
55BK0	55	B	1	K	0
55BK2	55	B	1	K	2
55BK4	55	B	½	K	4
55BR0	55	B	1	R	0
70BG0	70	B	½	G	0
70BK0	70	B	½	K	0
70BK2	70	B	½	K	2
70BK4	70	B	½	K	4
70BR0	70	B	½	R	0

A = water-cured concrete A with type I Anläggningscement and 5% air-entrainment; B = air-cured concrete B with type II Byggcement and natural air; G = glass filler; K = limestone filler; R = normal concrete without filler or fibres; 0 = 0 kg/m³ polypropylene fibres; 40 = w/c (%).

1.3 Objectives

The objectives were to investigate mechanical functioning of SCC under loading at high temperature conditions. The SCC contains increased amounts of polypropylene fibre, different types of cement and air content, preconditioned either in the air or in water. The objective was also to compare the result with the corresponding properties of NC. The objective was to recommend how to produce SCC able to withstand fire spalling.

2. PREVIOUS RESEARCH

2.1 Effect of stress and heating state on compressive strength

Influence of fire was studied [15]. The following conclusions were found:

- Compressive strength of the specimens during heating increased with the stress
- Strength in the hot state was greater than after cooling

Figure 2.1 shows results of high temperature tests on concrete with different types of aggregate [16].

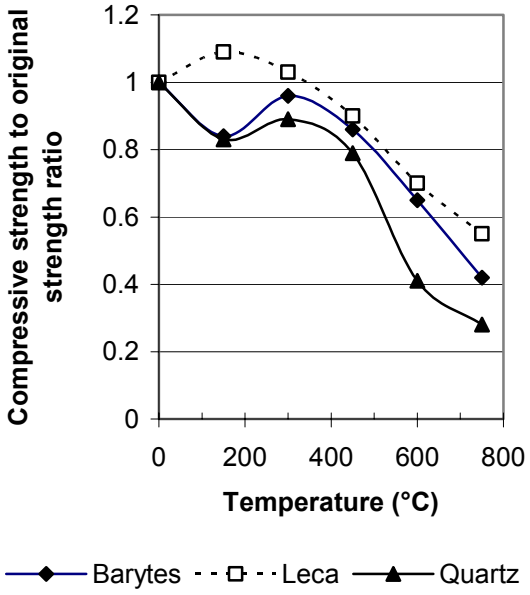

Figure 2.1 - Compressive strength to original strength ratio [16].

An aggregate of the quartz type seemed more unfavourable than the others tested [16-17]. In other tests the effect of compressive stress under heating on strength of concrete was tested [15,18]. The highest strength was obtained in the heated state provided that the specimen was loaded during the period of heating, at 25 or 40 % of the ultimate strength. The second highest strength was obtained on unloaded specimens that were tested at elevated temperature, the lowest on concrete that was heated to the stipulated temperature and then cured at 21 °C in an ambient relative humidity, RH = 65% before testing, Figure 2.2. The concrete contained aggregate of the quartz type. Figure 2.2 clearly demonstrates that strength increased with stress during loading and further that the strength at the heated state was larger than after cooling [15,18].

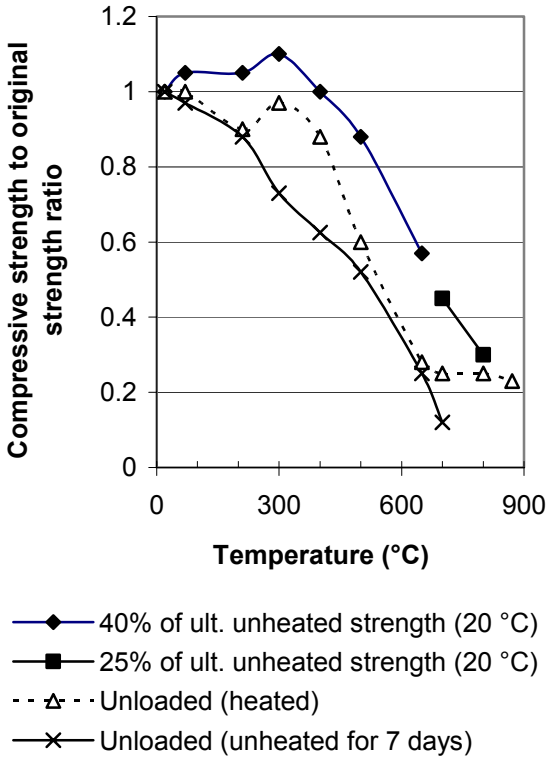

Figure 2.2 - Compressive strength to original strength ratio [15,18].

2.2 Effect of changes in cement paste

Figure 2.3 shows the effect of age and temperature on the strength of cement paste after heating at different age at start of testing [19,20]. In young cement paste an initial hydration during the heating increased the strength. Between 200 °C and 500 °C hydrated water leaves the cement paste. This results in large shrinkage [18]. Owing to the heating the cement paste is weakened and strength decreases somewhat. At the critical temperature, 500-600 °C, the calcium hydrates are decomposed into calcium oxide causing a substantial strength loss in the cement paste, Figure 2.3. The same applies to concrete [19,20].

2.3 Effect of thermal movements between aggregate and cement paste on compressive strength

Figure 2.4 shows the thermal dilatation of the following ingredients of concrete [19]:

1. Granite
2. Concrete with granite aggregate
3. Limestone
4. Sandstone
5. Cement paste under heating
6. Cement paste under cooling

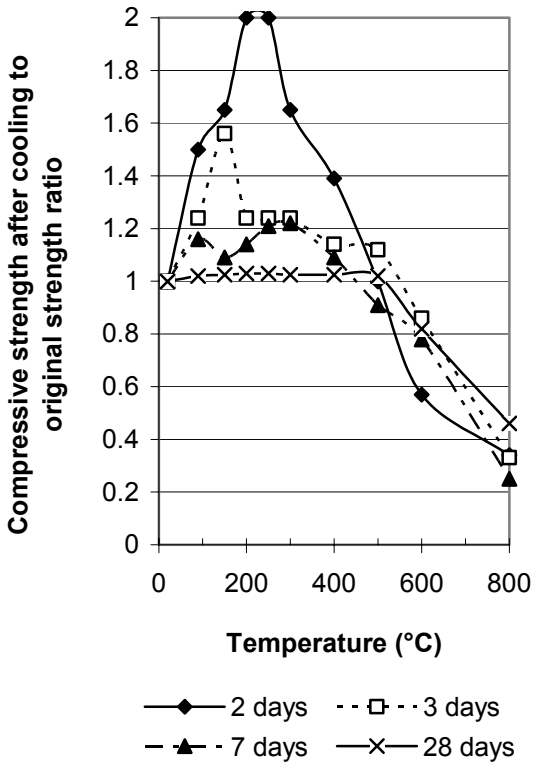

Figure 2.3 - Strength after cooling to original strength ratio [19,20]. The age of cement paste.

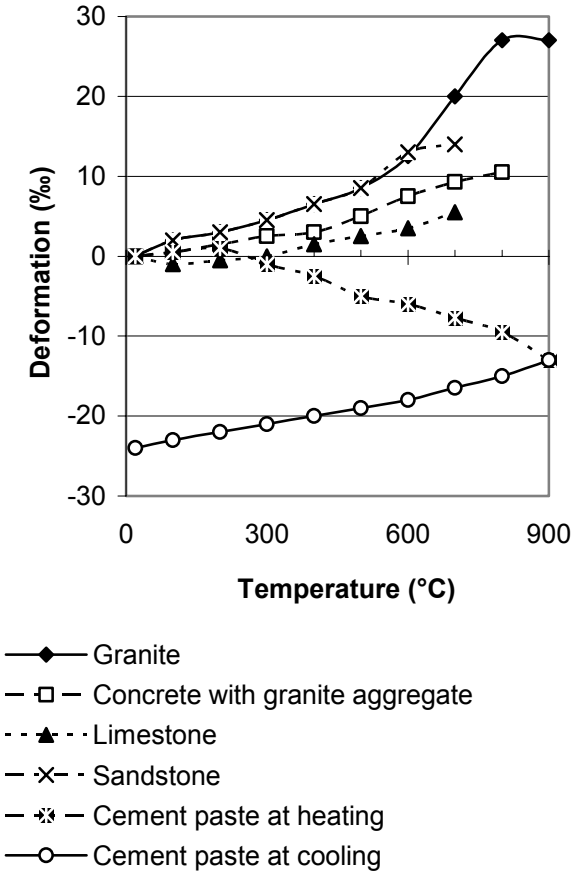

Figure 2.4 - Thermal dilatation of aggregate, cement paste and concrete [19].

It is quite clear that the aggregate expand during heating while the cement paste shrinks, mainly due to loss of water [18]. The movement of the concrete during heating almost follows the deformation of the aggregate. Therefore large deformations are imposed on the cement paste in concrete subjected to high temperature. The size of the compressive stress during heating of the concrete strongly affects the deformations, Figure 2.5. At high stress more than 50% of the ultimate, which is rare, no expansion takes place of the concrete during heating [16]. At no stress some expansion remains after heating but at low stress, 16.5 % of the ultimate strength, still a substantial shrinkage takes place after heating to 600 °C, figure 2.5.

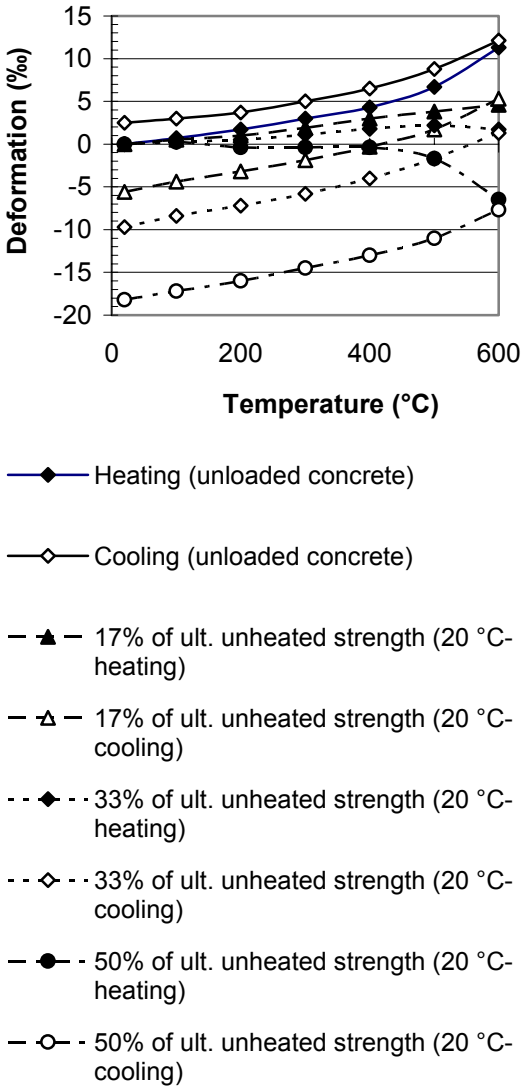

Figure 2.5 – Effect on deformations of stress during heating [16]. Black (full) mark = heating.

2.4 Tensile strength after heating

Two types of test applied either rapid or slow type of oven heating combined with two types of specimen, 50 or 94 mm in diameter [18], Figures 2.6-7. During the rapid type of oven heating large difference in temperature between surface and centre of concrete specimen may be avoided with insulation. The slow heating did not exceed 120 °C/h. In case of slow heating the difference in temperature between surface and centre of concrete specimen became small. Figure 2.8 shows the tensile strength at elevated temperature obtained with slow (Ø94 mm) or rapid heating (Ø50 mm) [21]. The tensile strength was not affected by the rate of heating or w/c. Table 2.1 provides the mix proportions of studied concrete [18]. The concrete was water-cured 4 days after casting and then in the air at RH = 60% for 1 month (w/c = 0.55 and w/c = 0.75) or for 2 months at RH = 60% (w/c = 0.50 or w/c = 0.68).

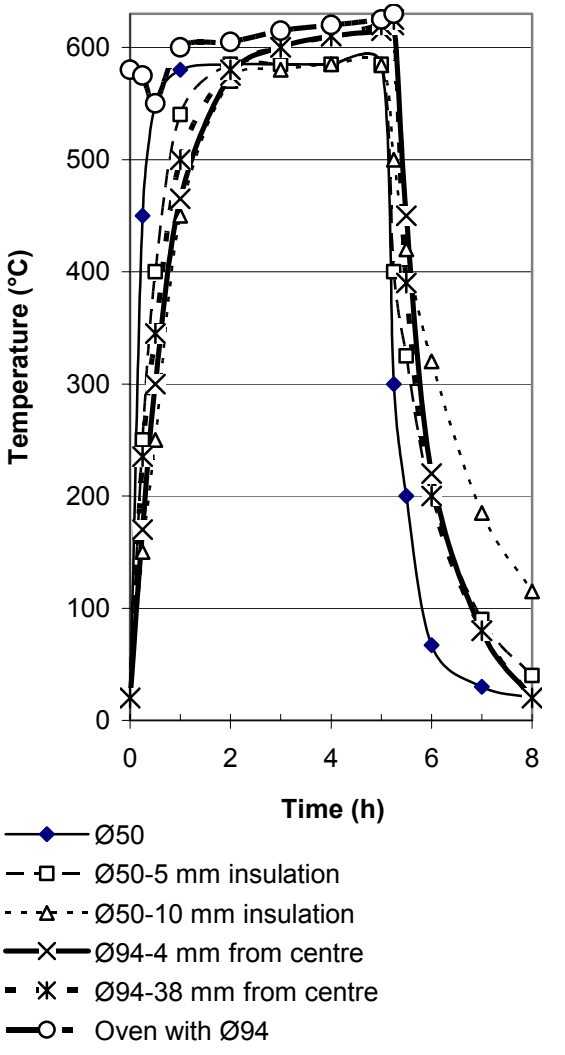

Figure 2.6 – Temperature rapid heating. Centre distance [18].

Table 2.1 - Mix proportions of studied concrete.

Concrete	Curing in RH = 60%	Cement/ sand/ aggregate	f_{cc} (28d, MPa)	f_{ct} (28days, MPa)
w/c=0.50	2 months	1:1.8:2.7		5.4
w/c=0.55	1 month	1:2:2.7	41	3.9
w/c=0.68	2 months	1:3.2:4.8		4.3
w/c=0.75	1 month	1:3.2:3.9	21	2.5

From Figure 2.8 the following equation was obtained by regression (dotted line):

$$f_{ct,T}/f_{ct,20}=-0.000001\cdot T^2-0.0003\cdot T+0.95 \qquad (2.1)$$

$f_{ct,T}$ denotes split tensile strength at elevated temperature (=1 at 20 °C)
$f_{ct,20}$ denotes tensile strength at 20 °C
T denotes temperature (20 < T < 800 °C)

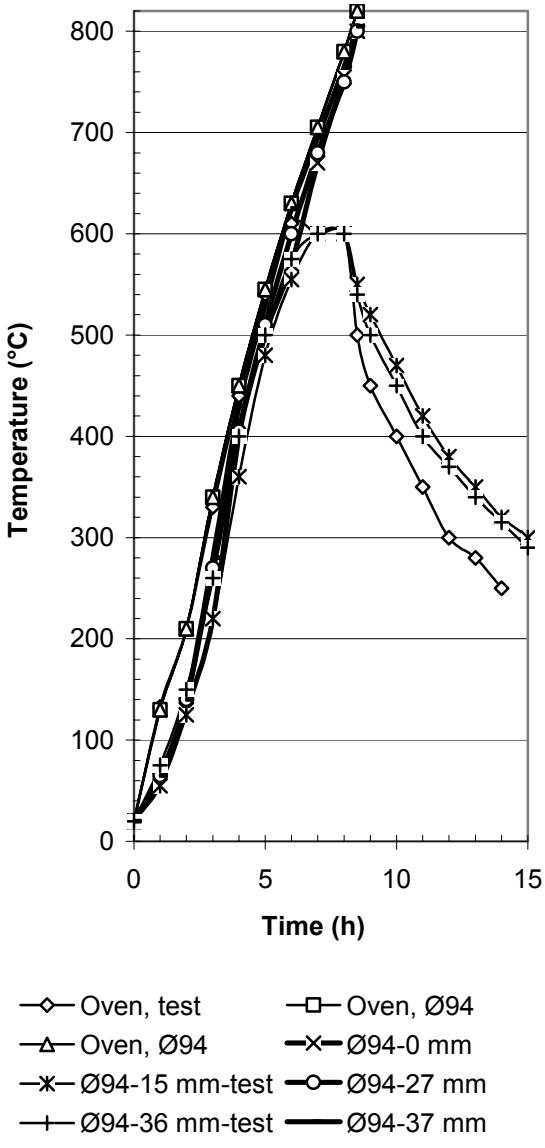

Figure 2.7 – Temperature at slowly heating. Centre distance [18].

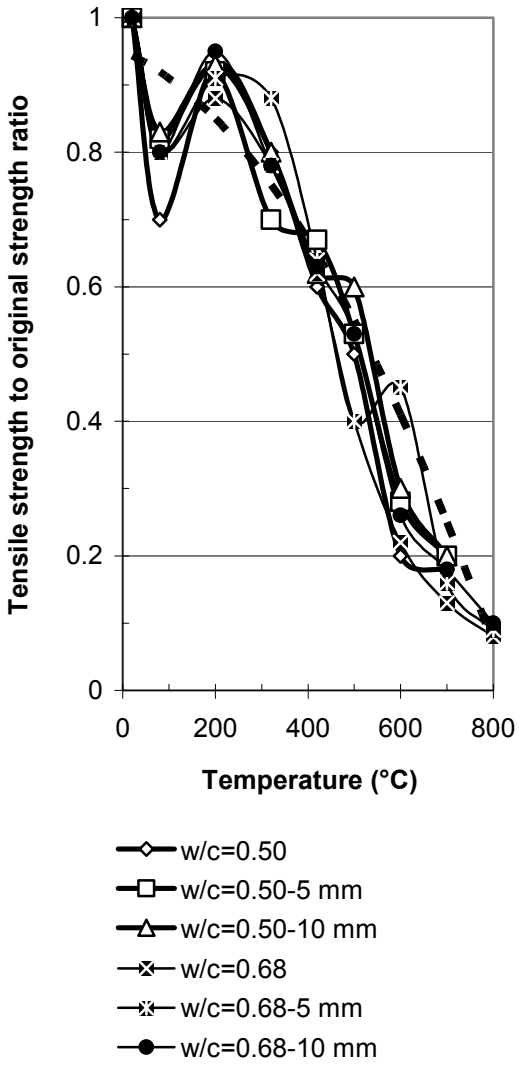

Figure 2.8 – Split tensile strength at elevated temperature obtained with slow (Ø94 mm) or rapid heating (Ø50 mm) [21]. Dotted line = equation (2.1).

In Figure 2.9 the effect of heating rate and temperature at testing on split tensile strength is shown [18]. Again it is shown that the rate of heating did not affect the split tensile strength. However, the temperature at testing had a substantial effect on the tensile strength at low temperature probably since the internal relative humidity, RH, of the concrete increases with the temperature [22-23]. The full dotted line in Figure 2.9 indicates equation (2.1) and an equation for split tensile strength at 20 °C after cooling from the elevated temperature (thin dotted line in Figure 2.9, equation (2.2)):

$$f_{ct,T20}/f_{ct,20}=-0.0000008\cdot T^2- 0.0006\cdot T+ 1.06 \quad (2.2)$$

$f_{ct,T20}$ denotes split tensile strength at 20 °C after cooling from the elevated temperature
$f_{ct,20}$ denotes tensile strength at 20 °C
T denotes temperature (20 < T < 800 °C)

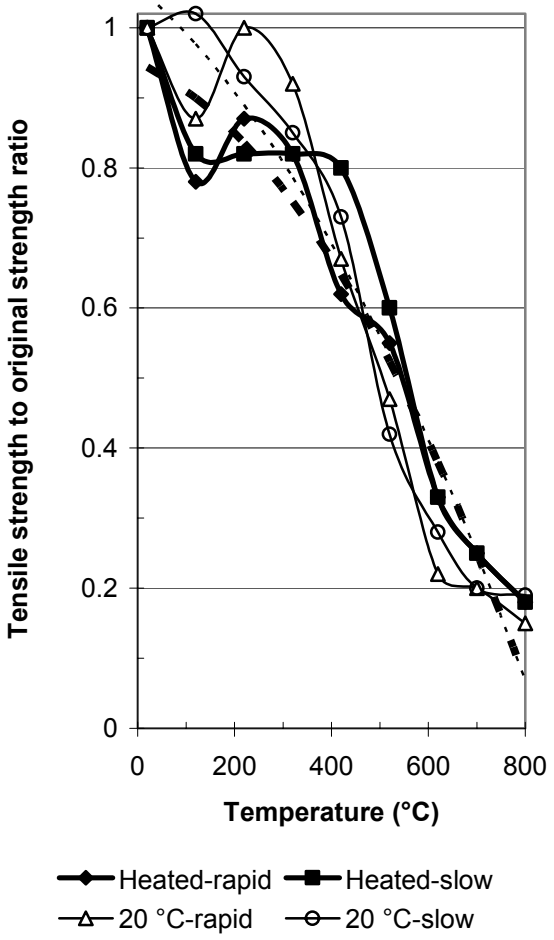

Figure 2.9 - The effect of heating rate and temperature at testing on split tensile strength is shown [18]. The full dotted line indicates equation (2.1) and thin dotted line equation (2.2).

Figure 2.10 shows the effect of w/c and testing temperature on the split tensile strength of the concrete [18]. At w/c = 0.55 the effect of the testing temperature was greater than at w/c = 0.75 probably since moisture of concrete with w/c = 0.75 evaporates more easily during heating than in concrete with w/c = 0.55. Figure 2.11 shows the development of tensile and compressive strength of concrete at elevated temperature [16].

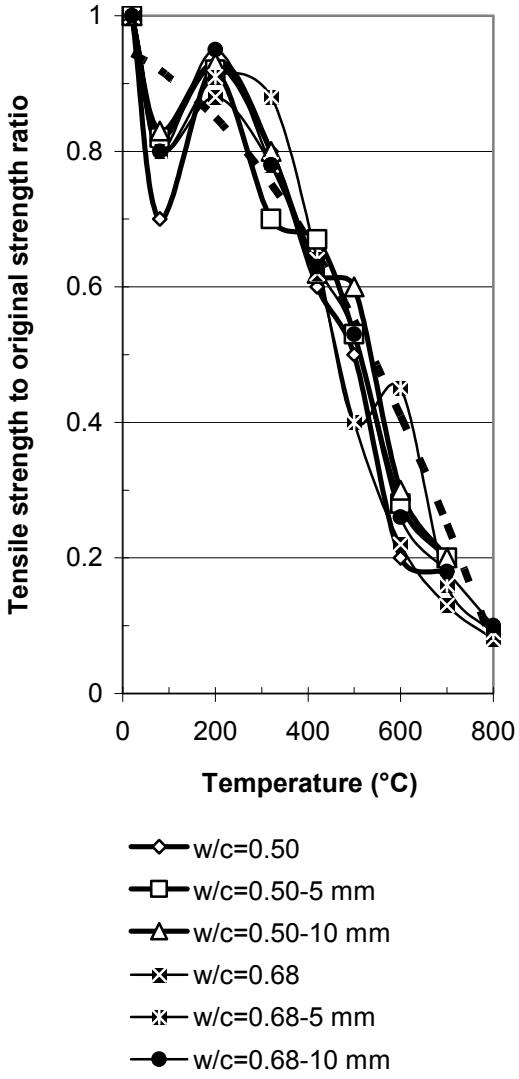

Figure 2.10 - Effect of w/c and temperature on the split tensile strength [18]. Full dotted line indicates equation; and thin dotted line (2.2).

2.5 Creep at varying temperatures and temperature gradients

The mechanical behaviour of concrete under torsional loading at transient, high-temperature conditions was studied in order to avoid the influence of thermal expansion during the tests [24]. By studying the twist angle versus time at different temperatures it was possible to determine the effect of temperature on the creep behaviour [24]. Table 2.2 provides the mix proportion of the studied concrete [24]. The strength scatter was fairly large.

Table 2.2 - Mix proportion of the concrete studied [24].

Concrete	Cement/ sand < 8 mm /crushed quartzite 8-12 mm	f_{cc} (28days, MPa)	f_{ct} (28days, MPa)
w/c=0.55	1:2.7:2	32-54	2.7-4.6

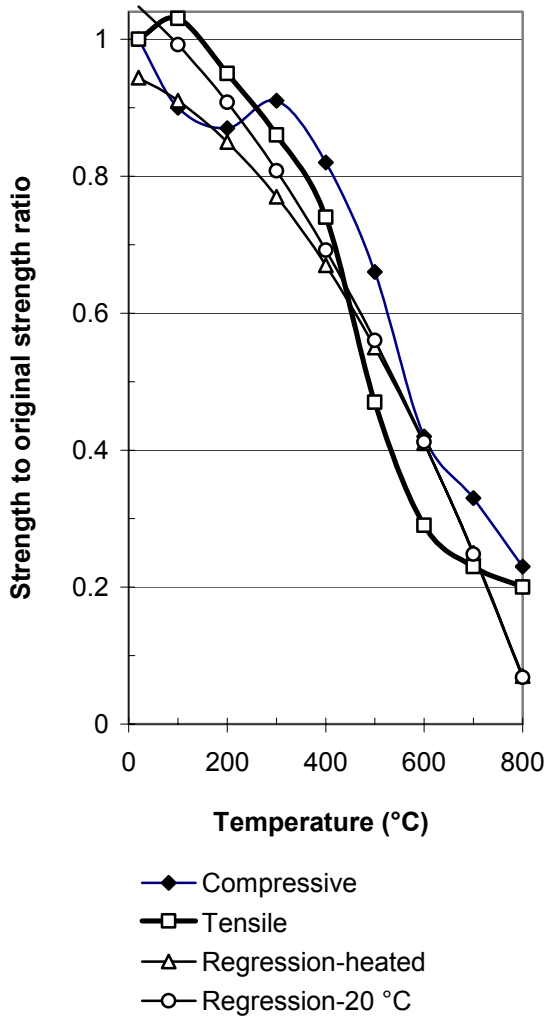

Figure 2.11 - Tensile and compressive strength of concrete versus temperature [16].

The size of the specimen was either circular Ø 150 mm or 150 x 150 mm. The length of the specimen was 1500 mm and the size at the supports was 200 mm square. At the middle of the specimen 800 mm in length was diminished to either 150 mm square or circular testing area. The stress to strength level at loading was 30% of the ultimate torque capacity. The rate of heating was 120 °C/h. Figure 2.12 shows development of the temperature in the Ø150 mm specimen together with the temperature development at other heating rates like 420 °C/h and with standard ISO 834 fire according to the following equation:

$$T = 345 \cdot \log(480 \cdot t + 1) + 20 \qquad (2.3)$$

t denotes time (h)
T denotes fire temperature (°C)

Figure 2.13-15 show the temperature profiles in the Ø150 mm cylinder at heating rates varying between 120 °C/h and 480 °C/h.

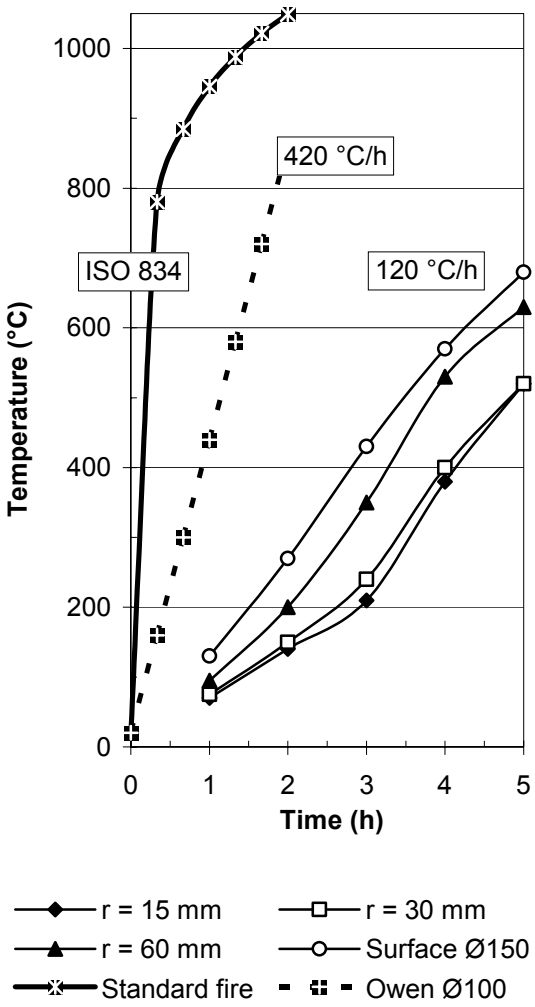

Figure 2.12 - Temperature in Ø150 mm specimen and at other heating rates like 420 °C/h or standard ISO 834 fire, equation (2.3). r = distance from centre of specimen.

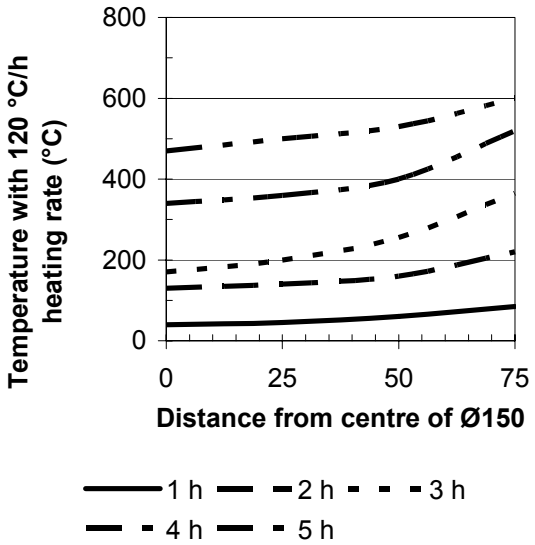

Figure 2.13 - Temperature in the Ø150 mm cylinder at 120 °C/h heating rate.

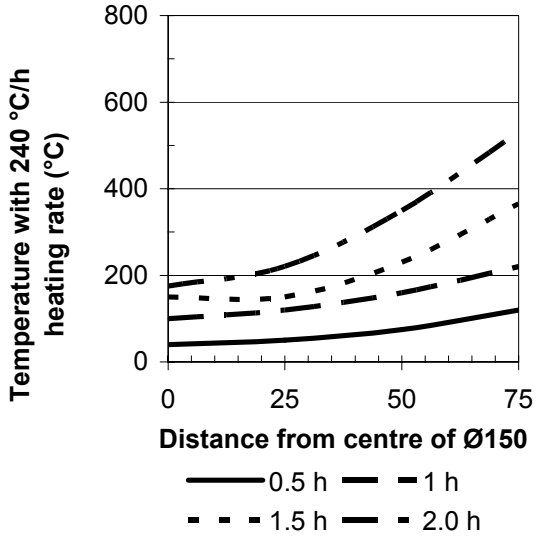

Figure 2.14 - Temperature in the Ø150 mm cylinder at 240 °C/h heating rate.

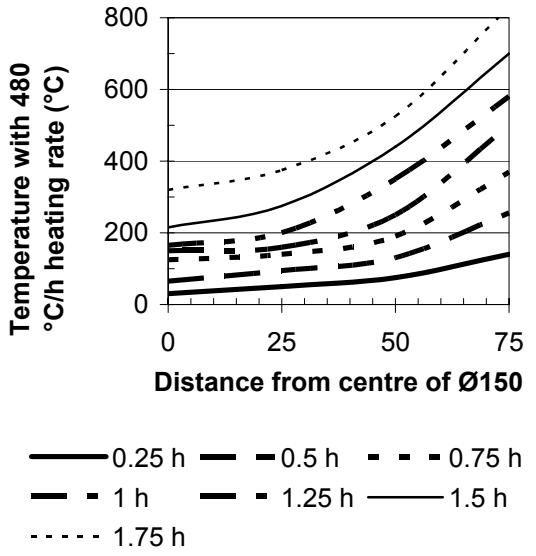

Figure 2.15 - Temperature in the Ø150 mm cylinder at 480 °C/h heating rate.

Figure 2.16-18 show temperature difference from the centre of the specimen. Internal and external mirrors at two points observed the creep of the concrete at different temperature [24]. Those performed the measurement of twist during fire tests. The total measurement length was 470 mm. The torsional creep at different temperature is shown in Figure 2.19:

$$C_{to}=(0.0013\cdot T-0.040)\cdot \ln(t)+ 0.0000056\cdot T^2+0.0023\cdot T+0.06 \quad (2.4)$$

C_{to} denotes torsional creep (rad/mm)
t denotes elapsed time ($0 < t < 4h$)
T denotes temperature ($20 < T < 400$ °C)

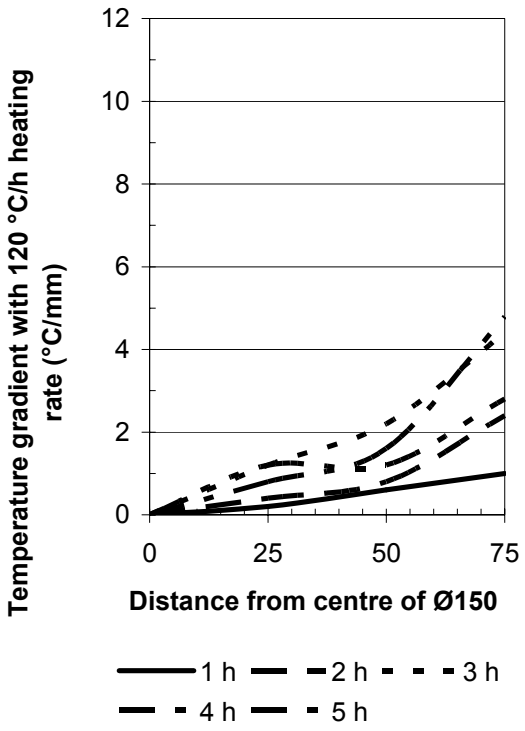

Figure 2.16 - Temperature gradient in Ø150 cylinder at 120 °C/h heating rate.

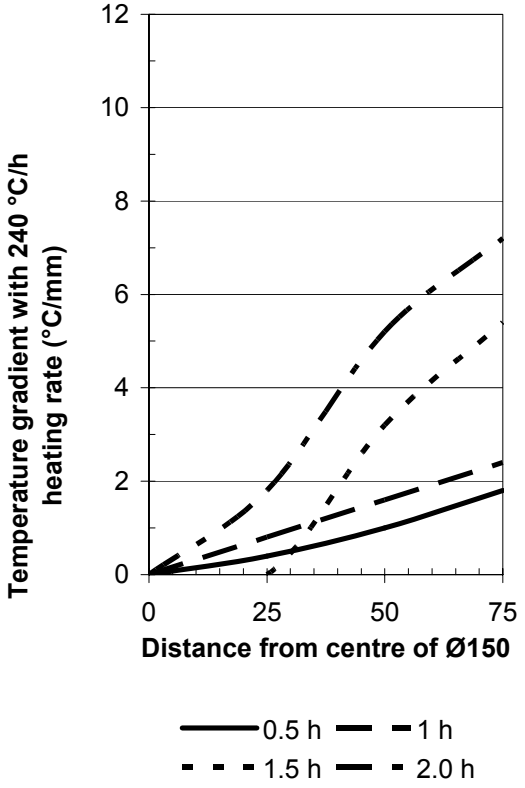

Figure 2.17 - Temperature gradient in Ø150 cylinder at 240 °C/h heating rate.

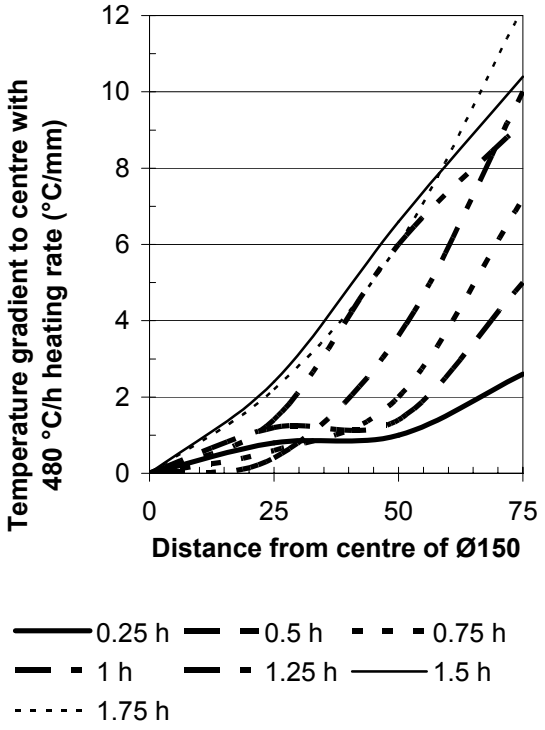

Figure 2.18 - Temperature gradient in Ø150 cylinder at 480 °C/h heating rate.

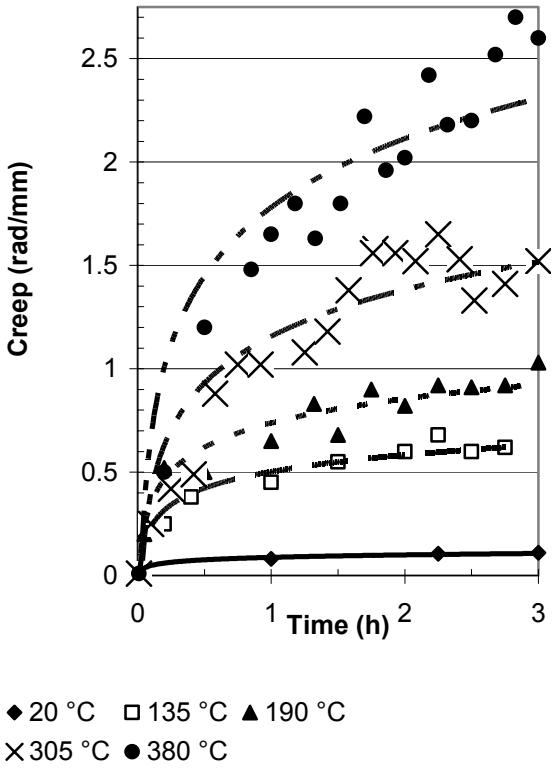

Figure 2.19 - The torsional creep at different temperature versus time [24].

Torsional strength decreases more rapid with temperature than tensile and compressive strength, Figures 2.11, 2.20 [24]. Compressive creep is therefore overestimated by equation (2.4).

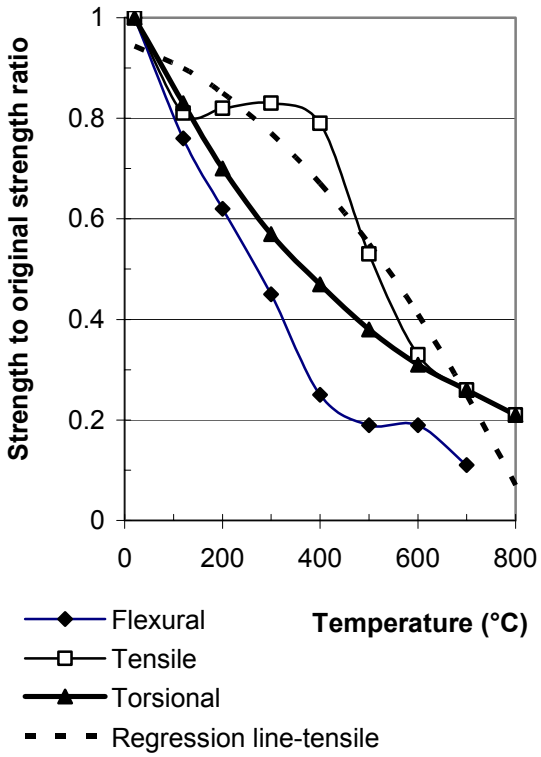

Figure 2.20 – Strength to original strength ratio [24]. Regression line with equation (2.1).

2.6 Steam pressure during heating

When concrete is heated the evaporable water expands more than the structure itself. This expansion leads to an increase of the relative humidity, RH, by about 0.35%/°C at w/c = 0.40, 20 °C [22-23]. RH saturation may take place in the pores and capillary transport take place instead of diffusion. Since the heat at fire comes from the surface the water will be transported inwards where the pores are not yet saturated. The pressure of the water in the pores will rapidly rise in turn causing a risk of surface spalling. The risk of spalling thus is linked closely to the tensile strength. Eventually, when the temperature of the concrete and the water reaches 275 °C explosive fracture takes place of the critical concrete zone. Figure 2.21-23 shows the steam pressure theory [24]. At about 275 °C 30 mm from surface explosion occurs.

2.7 High Performance Concrete, HPC

2.7.1 Swedish recommendations

Studies of the fire resistance on HPC were performed in a Swedish project of HPC [11]. First of all the strength of steel was studied versus the temperature, Figure 2.24. Prestressing steel was slightly more sensitive to high temperature than that normal steel was. However, at 450 °C only about half the strength of the steel remains, i.e. the cover layer is of great importance for reinforced structures with reinforcement bars, rebars.

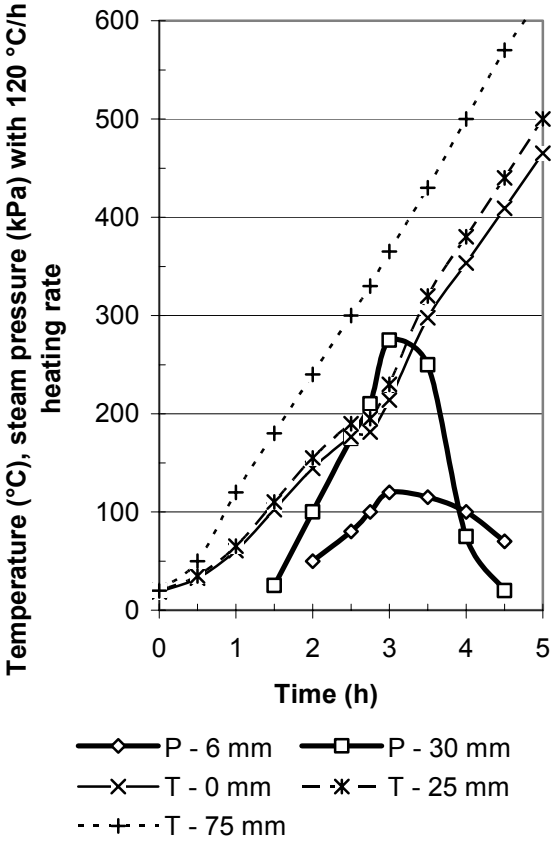

Figure 2.21 – Steam pressure with 120 °C/h heating rate. P=pressure, T=temp.

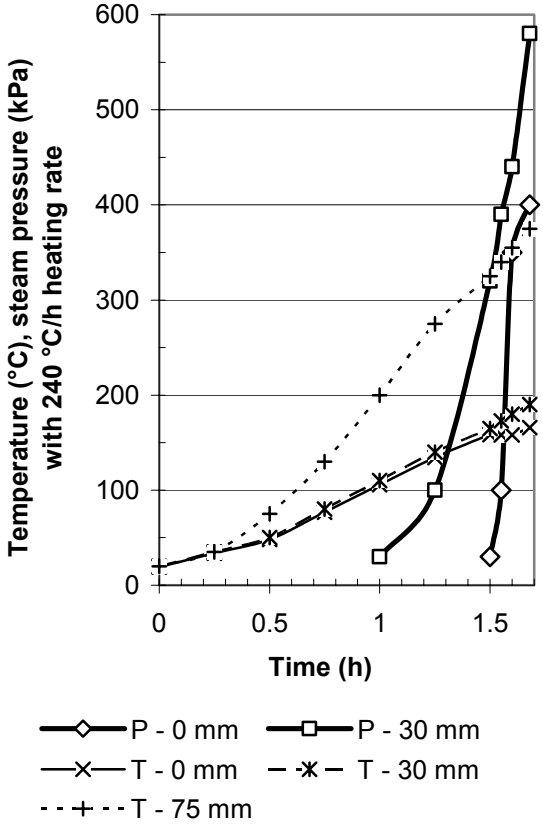

Figure 2.22 – Steam pressure with 240 °C/h heating rate. P=pressure, T=temp.

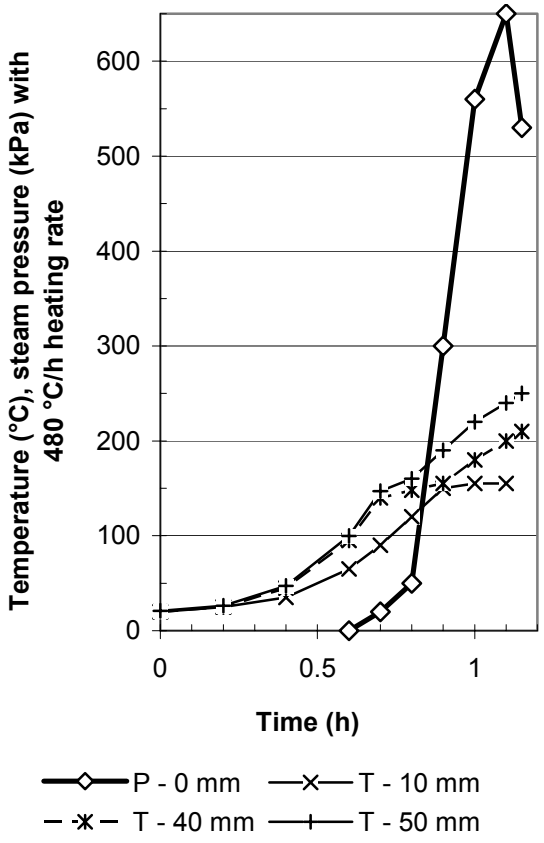

Figure 2.23 – Steam pressure with 480 °C/h heating rate. P=pressure, T=temp.

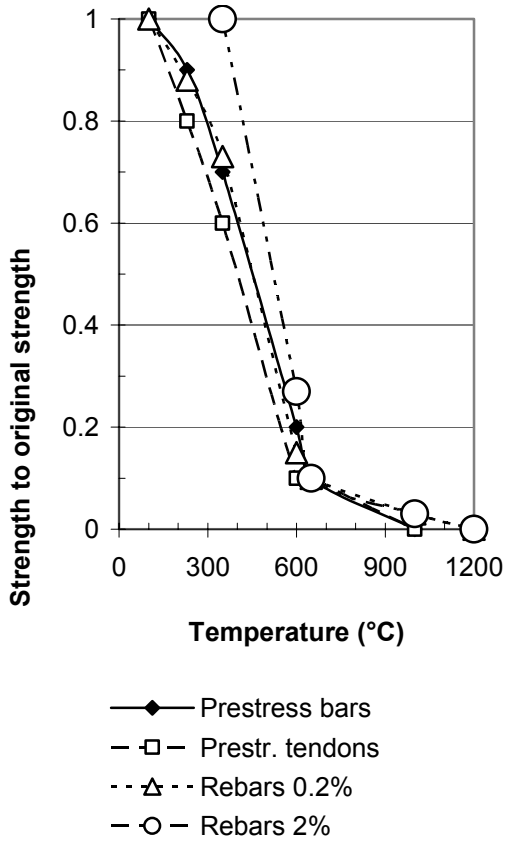

Figure 2.24. Steel strength vs temperature [11].

Other studies showed the corresponding decrease of the elastic modulus of the steel like the strength decrease versus temperature, Figure 2.25. Regarding spalling the following requirement were stated for concrete with 150-mm cube strength varying between 80 and 120 MPa:

- Water-binder ratio, w/b > 0.24
- Silica fume < 7% calculated on the basis of the cement content.
- ISO 834 fire exposure, Figure 2.12, equation (2.3)
- Concrete relative humidity, RH < 75%
- Stress to strength ratio < 0.45 at fire exposure

Still, even though the requirement were fulfilled the mix proportions of HPC required to be completed by the following amount of fibres of polypropylen [11] in order to avoid the risk of spalling of the concrete surface during fire [11]:

- 2 kg/m³ fibres at 0.28 < w/b $\leq$ 0.32
- 4 kg/m³ fibres at w/b $\leq$ 0.28

Therefore fibres of polypropylene were included in this project.

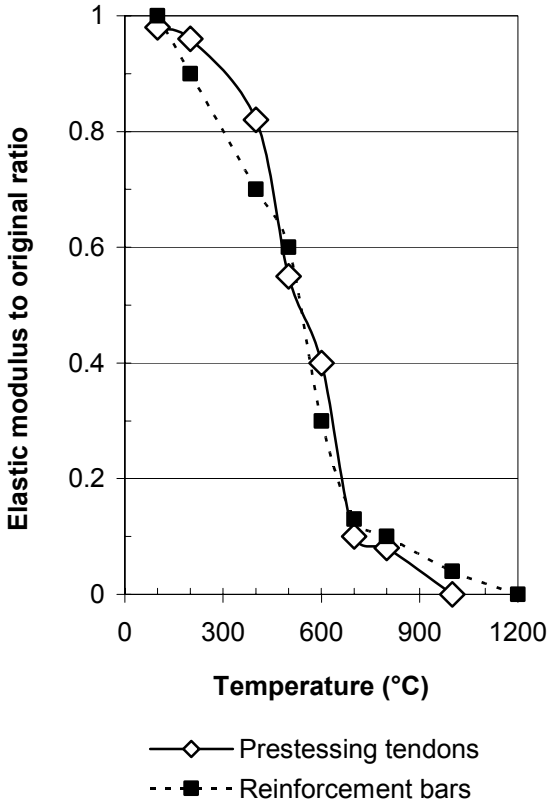

Figure 2.25 Decrease of elastic modulus versus temperature [11].

2.7.2 Swedish research on fire spalling

Spalling of concrete in the Swedish experiments was studied on concrete columns with mix proportions given in Appendix 2.1 [11,25]. The column studies were carried out on prestressed constructions. The type of column studied, 200 x 200 x 2000 mm, was symmetrically pre-stressed. It was the objective of the column studies to observed the risk of fire spalling at the standard ISO 834 fire, equation (2.3). The square columns were prestressed by alternatively 12 or 16 pieces of 12.5 mm strands. The strands were symmetrically placed in the column. The initial force of the strands varied between 90 and 135 kN before prestressing of the HPC. The force was hydraulically transferred to the HPC after a curing period varying between 2 and 4 days. Thus the stress in the HPC columns became more or less symmetrically distributed. After pouring, the HPC was heated in the mould. The cubes that were used to obtain the strength were placed in a hot box. The temperature in the box was adjusted to obtain the same heat development as the column. The columns were placed in a climate with a relative humidity of about 45%. All columns were studied at 20 °C after initial curing at about 48 °C. The cubes that were used to obtain the strength development of the square columns were placed in an insulated box on top of the column but inside the mould. The box was not insulated towards the column. The cubes thus obtained the same heat development as the column did. Different target values for the strength of the HPC before prestressing were used dependent on the force applied by the strands. Initially the HPC was cured in the steel mould. Plastic foil and 60 mm of heat insulation covered the top of the HPC. About 12 h before prestressing the columns were cooled to 20 °C. After prestressing the columns were cured at the same temperature as before (20 °C) but uncovered. After 1 h of creep measurement the columns were placed in an ambient climate of ≈ 45% relative humidity at 20 °C temperature [25]. The autogenous shrinkage and the drying shrinkage were measured for all the HPCs studied. The cylinder had a length of 300 mm and a diameter of 55.5 mm. The cylinders were cast on site and then transported to the laboratory where the HPC was demoulded. One cylinder of each batch of HPC was insulated by 2 mm butyl-rubber cloth; one cylinder was cured unprepared. Cast-in items were placed 25 mm from the ends of the 300-mm cylinder. After demoulding, stainless ground screws were placed in the cast-in items. The cylinders were placed in a 20 °C air-conditioned room with an ambient relative humidity of 55%. The first measurement took place after the HPC reached the same temperature as the ambient climate room. Measurements at three sides of the cylinders started at about 20 hours' age [25]. The measurement device (Proceq) was calibrated to an INVAR rod, cp. laboratory experiments. The measurements were carried out for 3 years. The weight of the cylinder was obtained parallel to the measurement of length to control losses of moisture from the specimen. cast-in items of steel were placed in the top of the column. The distance from the side of the column to the cast-in item was 100 mm. The horizontal distance between the cast-in items parallel to the column was 250 mm. After demoulding, the column consoles were fixed to the cast-in items. The measurement was carried out by LVDTs in the same way as described above. The LVDTs were calibrated before each measurement took place. A computer automatically collected the strain data. After 1 h the LVDT-measurements were replaced by mechanical measurements in stainless ground screws, that were placed in the cast-in items In the case of square column, cast-in plastic pipes were placed at the top of the column reaching the centre of the square section in order to measure the internal relative humidity. The pipe was tightened with a rubber plug between the measurements. During the measurement of internal relative humidity a dew-point meter (calibrated according to ASTM E 104-85, [26]) was placed in the pipe for at least 16 h. The instrument was covered with a hood to avoid temperature changes.

2.7.3 Research conditions for Swedish tests

The stress/strength level was documented by tests of creep and shrinkage before the fire spalling tests were carried out. Even though the creep and shrinkage tests do not give any fire spalling the results of the creep and shrinkage tests influences the stress/strength level substantially. Stress was supposed to have a substantial effect on fire spalling. Therefore the creep and shrinkage results are given as a method to measure and calculated the loss of prestressing. Figure 2.26 shows the results of internal relative humidity in the square columns. Columns with a higher grade of pre-stressing seem to dry out somewhat faster. Figure 2.27 shows the shrinkage of cylinders. The observed total strain at the middle upper edge of the square columns is shown in Figures 2.28-2.32. It was necessary to measure the strain in order to obtain the stresses in the concrete at the fire exposure. Figure 2.33 shows the moisture losses versus time. After about 50 days' age the concrete started to increase in weight due to carbonation. Figure 2.34 shows the shrinkage versus moisture losses of all columns.

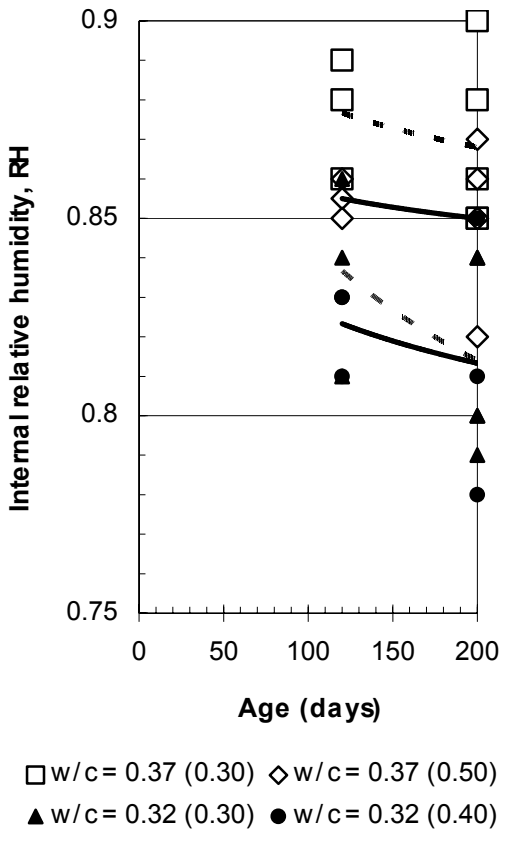

Figure 2.26 – Internal relative humidity, RH, in columns. ( ) = stress/strength level [25].

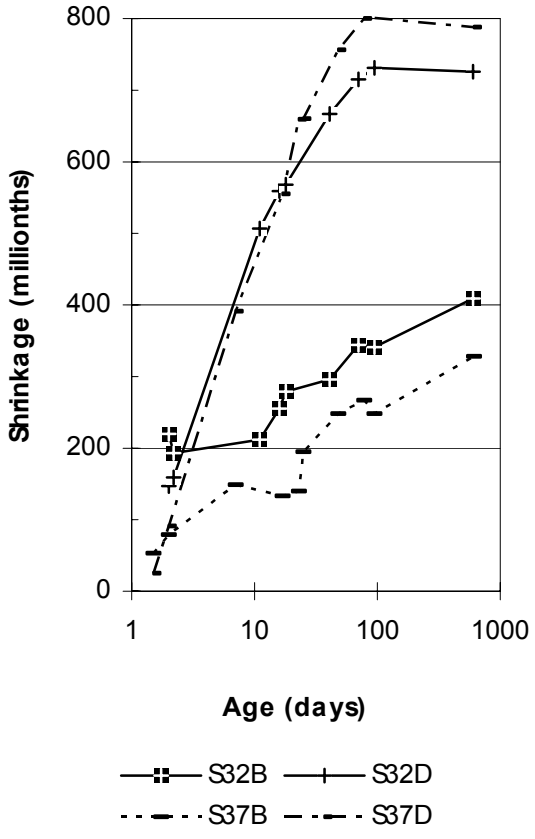

Figure 2.27 - Shrinkage cylinders versus age. B = sealed curing, D = air curing (drying), 37= water-cement ratio, w/c (per cent) [25].

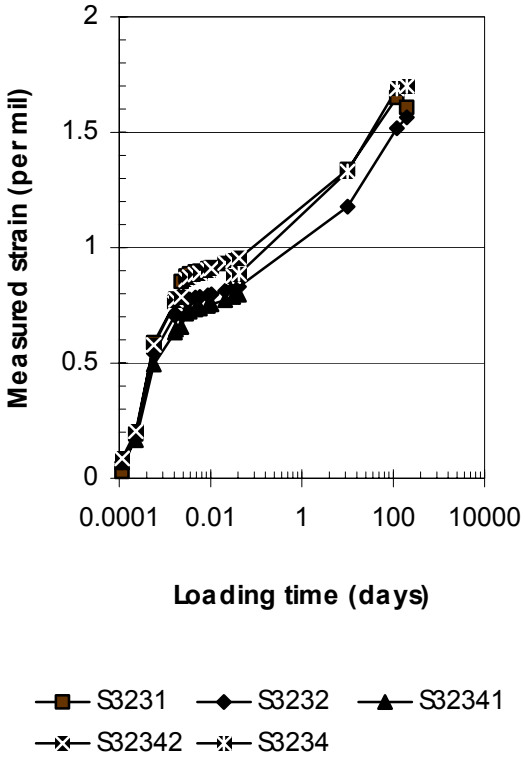

Figure 2.28 - Measured total strain of columns S323 versus loading time. S= square column; 32...=w/c (%); ..3.. = 10xprestress level,..1-4.= amount of plastic fibre; ..2= batch no [25].

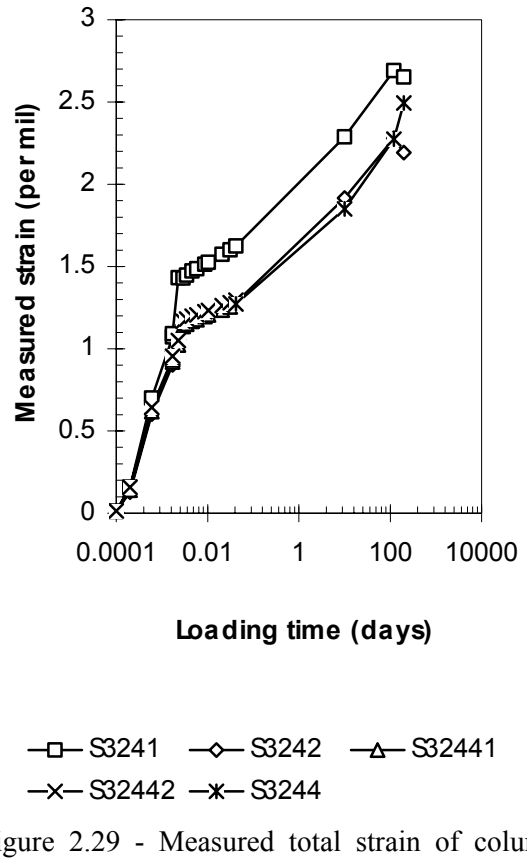

Figure 2.29 - Measured total strain of columns S324 versus loading time. S= square column; 32...=w/c (%); ..4.. = 10xprestress level,..1-4.= amount of plastic fibre; ...1= batch no [25].

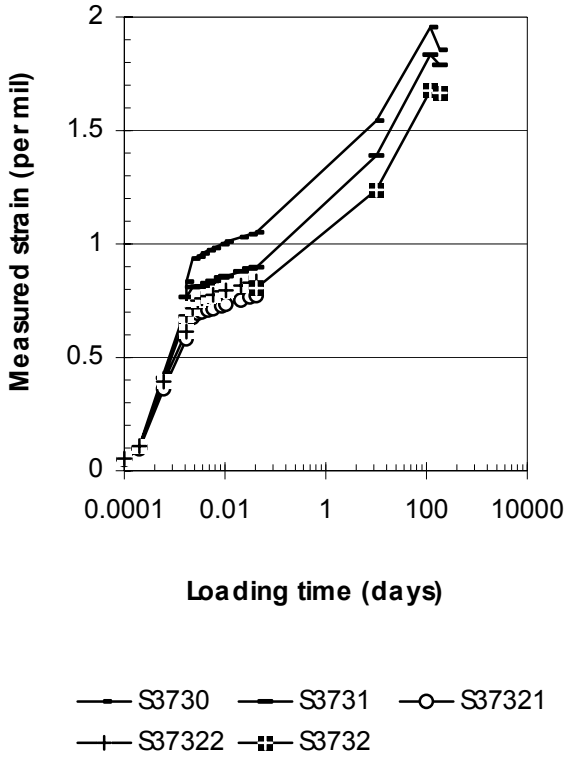

Figure 2.30 - Measured total strain column S373 at the middle top versus loading time. S= square column; 37...=w/c (%); ..3.. = 10xprestress level,..0-2..= amount of plastic fibre; ...2= batch no [25].

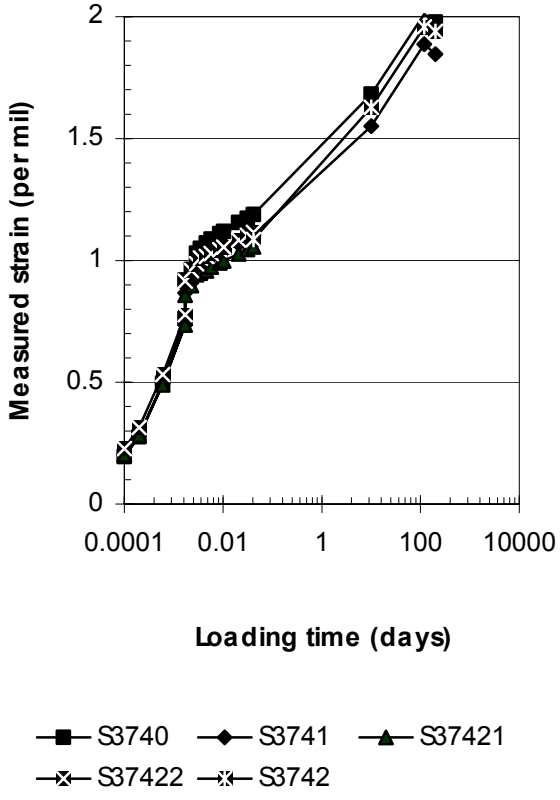

Figure 2.31 - Measured total strain of columns S374 versus loading time. S= square column; 37...=w/c (%); 4 = 10xprestress level,..0-2.= amount of plastic fibre; ...2= batch no [25].

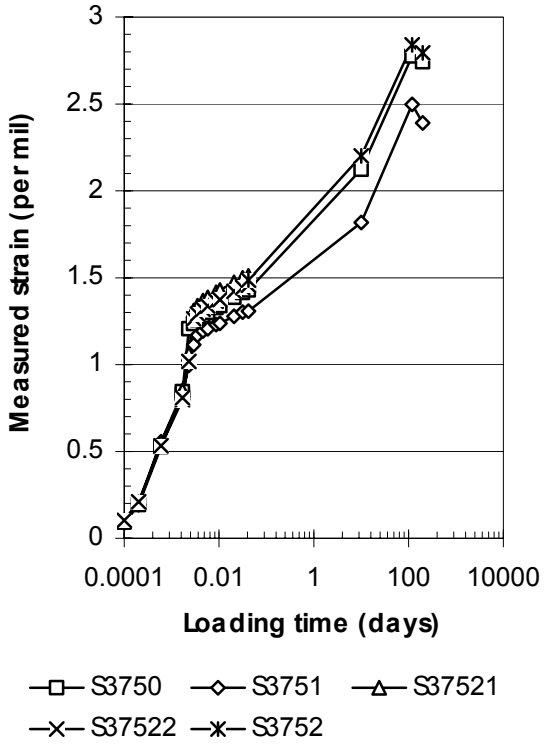

Figure 2.32 - Total strain of column S375 at the middle top versus loading time. S= square column; 37...=w/c (%); ..5.. = 10xprestress level, ..0-2...= amount of plastic fibre; ...2= batch no [25].

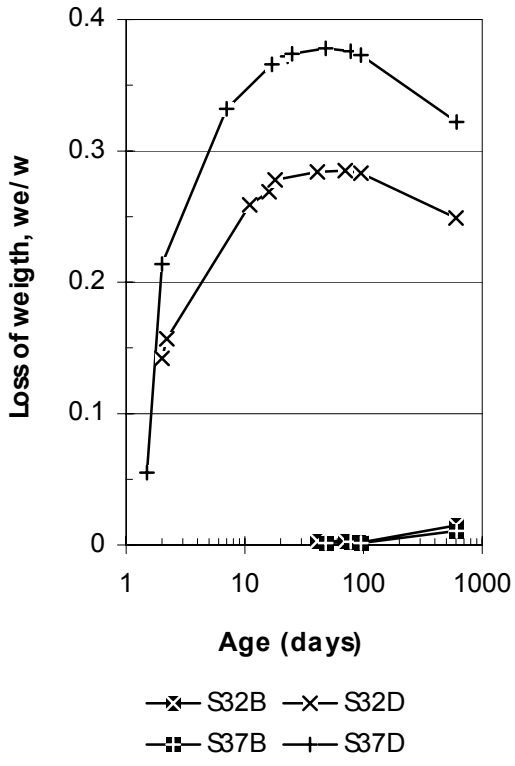

Figure 2.33 – Relative moisture losses versus time, we/w. w = mixing water, we = evaporated water. B= sealed curing, D= air curing, 32...=w/c (%).

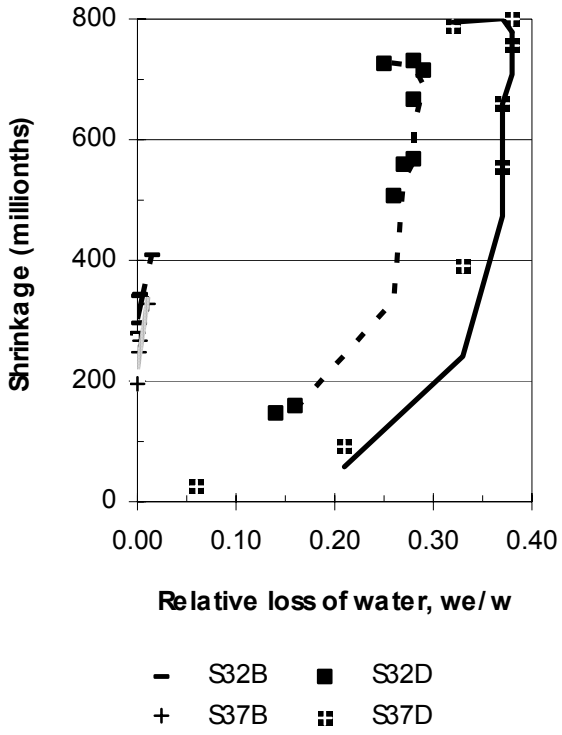

Figure 2.34 - Shrinkage versus moisture losses, we/w. B= sealed curing, D= air curing, S= square column, 32= water-cement ratio, w/c (%).

The square column was cooled to 20 °C before the prestressing of the HPC was performed. In an extensive investigation of the influence of the moisture profile on the measured shrinkage it was pointed out that the way of measurement was of great importance for obtaining a correct strain [27]. If the measurement points were placed at the surface, the measured shrinkage became larger than the average shrinkage of the column, due to the shrinkage of the surface. The maximum measured fault could be estimated as the difference between drying shrinkage and the autogenous shrinkage. Due to different admixture of plastic fibre in the columns the mixing was continued during the addition of plastic fibre, which may have influenced the compressive strength, perhaps ± 5 MPa. Some differences certainly existed between the ambient climate in the laboratory, where the shrinkage was measured, and the industry where the columns were cured, maybe ± 10% RH. The strain was mainly measured at 20 °C or recalculated to 20 °C accordant a thermal coefficient of dilatation of 0.01 per mil/°C. Some columns were identical as regards the structural properties, in which case only the average results are presented. Appendices 2.2-3 show the structural properties of the square columns S32 and S37. The estimations of the creep were carried out according to [25]. The elastic effect was added. The creep compliance was adjusted taking into account half the hydraulic radius of the specimen. Half the hydraulic radius of the square column was 0.05 m. Generally the ISO 834 fire tests of the columns S32 and S37 showed large spalling of concrete without fibres at w/c = 0.32 (w/b = 0.30) and no spalling at all of concrete with w/c = 0.37 (w/b = 0.35). Concrete with w/c = 0.32 and 4 kg/m³ did not obtain any spalling at all. Concrete with w/c = 0.32 and 2 kg/m³ did however obtain some spalling. The prestressing level did not seem to affect the spalling at all.

2.7.4 Performance of columns in fire

Extensive tests were carried out at the British Building Research Establishment (BRE)'s Cardington Laboratory [28-34]. The size of the 30 unreinforced columns tested in the laboratory was 200 x 200 x 1500 mm. ISO 834 834 standard procedure was used with a maximum temperature of 905 °C. The cylinder strength of the concrete fulfilled C85 (85 MPa). During the tests the columns were loaded, either at 40 % or 60 % of the ultimate load. Only 4 of the 30 columns survived the maximum temperature, three with polypropylene fibres, Figures 2.35 and 2.36. The results of the laboratory tests were utilised in a fire compartment, 225 m² and 2.25 m in height [28,30]. Timber cribs created the fire load of 40 kg/m² (720 MJ/m²). The predicted fire design scenario was based on Eurocode for actions [28,31]. Internal columns of 400 x 400 mm and external 250 x 400 mm were studied. All columns were grade C85 (28-day strength of 103 MPa, 4.2% moisture content) and 2.7 kg/m³ polypropylene fibres were added to the mix proportions of the concrete, which is more than 2.0 kg/m³ as specified in the Eurocode [28,31]. The thickness of the concrete floor was 250 mm. The total design load at the fire limit state was 9.25 kN/m² [28]. The design load is based on a 40% reduction in the partition and imposed load as stated in [32], [28]. During the test a main cable burnt through resulting in loss of all data from this point on. All columns behaved well during the fire and no spalling was observed. However, extensive spalling of the concrete floor occurred [28]. Material falling from the ceiling during spalling had an affect of suppressing the fire [28,33]. For this reason the maximum temperature in the compartment was lower than predicted by the Eurocode [28,34]. Since the loading level was unrealistically high in combination with unreinforced concrete 33% of ultimate loading was applied instead on concrete columns (the same dimension as stated above was studied). The following conclusions were drawn on the tests with reinforced concrete of different grades, with or without polypropylene fibres [28]:

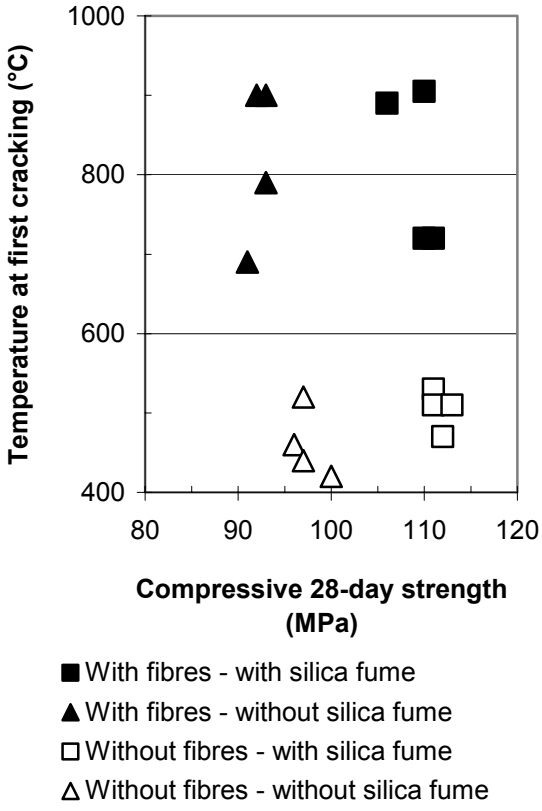

Figure 2.35 – Temperature at first cracking of unreinforced columns [28].

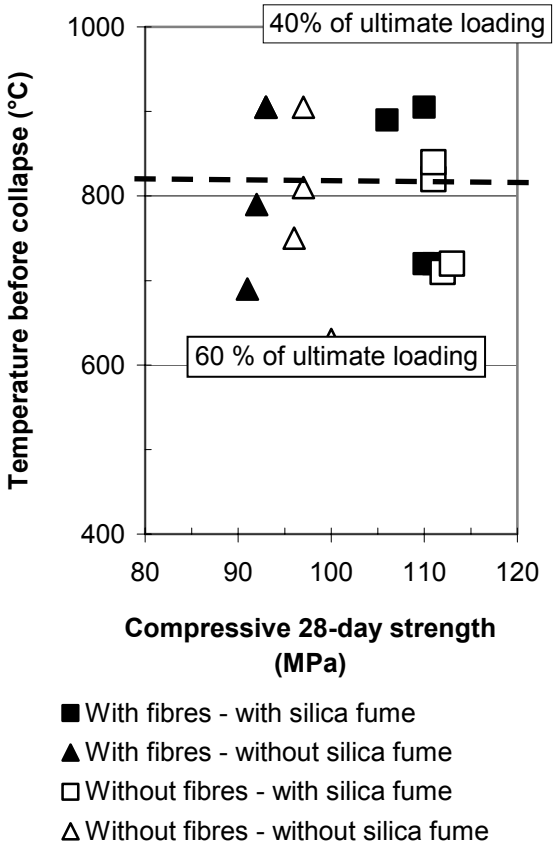

Figure 2.36 – Temperature before collapse of unreinforced columns [28].

1. For C45 no spalling took place
2. For C85 severe spalling took place in case of no polypropylene fibres
3. Spalling also occurred of C105 grade concrete without fibres

The largest benefit observed from the use of polypropylene fibres was for the C85 concrete. The strength increased from 55% of the ambient temperature strength in case of no fibres to 70% of the ambient temperature strength in the case with fibres. The research also gave the following main conclusions [28-29]:

1. When it is required to prevent spalling in high grade concrete, then polypropylene fibres should be included
2. The residual strength was not improved by use of polypropylene fibres
3. The compressive strength was decreased by use of polypropylene fibres in the concrete
4. The density was decreased by use of polypropylene fibres in the concrete
5. Silica fume did not affect the properties of concrete in fire

2.7.5 Effect of high temperature on the permeability

The effect of high temperature on the permeability was studied for three types of HPC, Appendix 2.4 [35-37]. The heating rate was slow: 60 °C/h, e.i. about 10 h from 20 to 600 °C. The size of the specimens was also fairly small, cylinders 150-160 mm in diameter and 300-320 mm long [35]. The following conclusions were drawn [35]:

1. Two kg/m³ of polypropylene fibres did not change the mechanical properties.
2. Explosive spalling occurred in light weight concrete probably due to high temperature gradient.
3. Under the same thermal treatment at 200 °C the increase of permeability is greater in HPC with polypropylene fibres due to the fibres melting.
4. Under the same thermal treatment at 600 °C the increase of permeability is equal in HPC with and without polypropylene fibres due to the fibres melting.
5. Under the same thermal treatment at 200 °C and 600 °C the permeability of light weight HPC is lower than that of normal weight HPC which also may explain the spalling.

2.7.6 Thermal stresses and water vapour pressure of HPC

Thermal stresses and water vapour pressure of HPC at high temperature was studied [38-39]. The specimen size was diameter 150 mm and length 320 mm. It was stored at relative humidity, RH = 95% and temperature = 22 °C 2 months before testing. The heating rate was slow, 60 °C/h. The mix proportions of the concrete are given in Appendix 2.5. Figure 2.37 shows that the residual (after cooling) relative tensile strength is slightly larger in HPC than in NC at higher temperature [38]. The same applies for the elastic modulus of HPC in comparison to NC, Figure 2.38 [38]. Table 2.3 gives the thermal expansion coefficient at elevated temperature [38].

Table 2.3 - Thermal expansion coefficient $\cdot 10^{-5}$ [38], Appendix 2.5.

Temp. (°C)	HPC	NC
20-50	$1.4 \cdot 10^{-5}$	1.1
50-90	1.5	1.2
90-200	1.6	1.3
200-275	1.7	1.5

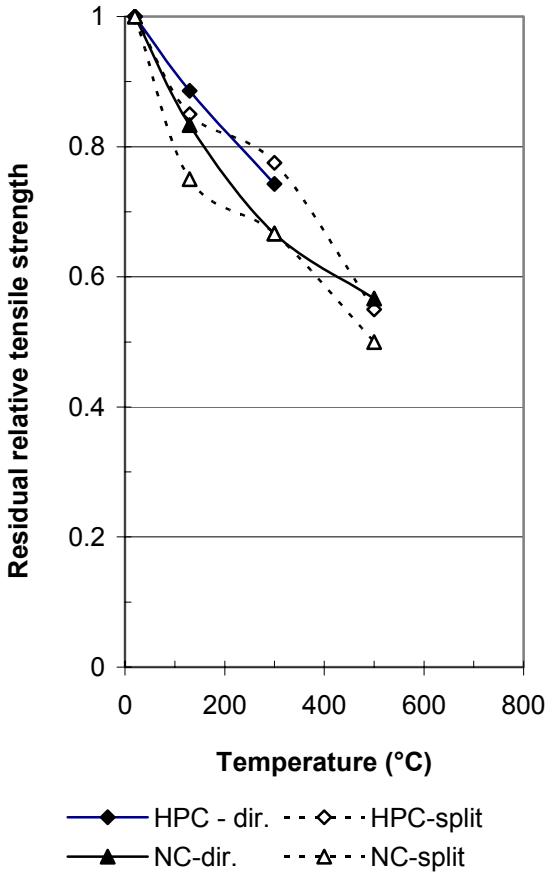

Figure 2.37 - The residual (after cooling) relative tensile strength is slightly larger in HPC than in NC at higher temperature [38], Appendix 2.5.

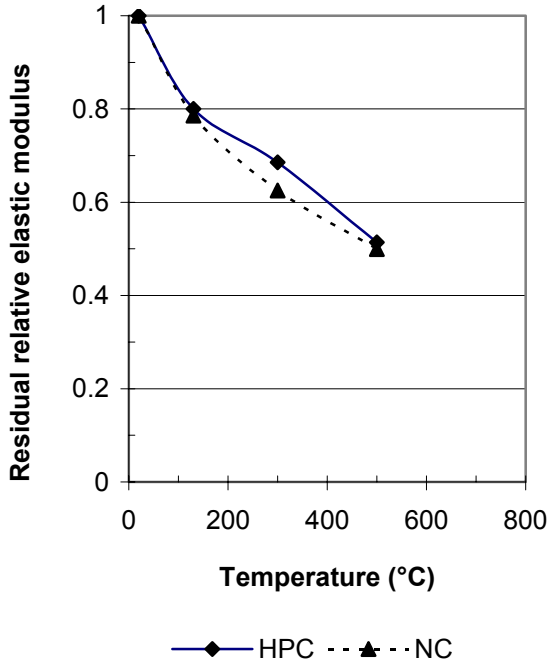

Figure 2.38 - The residual (after cooling) elastic modulus is slightly larger in HPC than in NC at higher temperature [38], Appendix 2.5.

In Figures 2.16-18 above it has been shown than temperature gradients of more than 5 °C/mm are required to obtain spalling in 150 mm cylinders [24]. The temperature gradient obtained by 60 °C/h heating rate was obviously too small to create spalling of 160 mm cylinders, Figure 2.41 [38]. Figure 2.41 shows the temperature gradient obtained by 60 °C/h heating rate of 160 mm cylinders [38], Appendix 2.5. Figure 2.39 shows the residual relative porosity at elevated temperature being 4% for both HPC and NC at 20 °C [38]. The porosity increase is larger for NC than for HPC in the critical temperature span between 200 and 300 °C. Since water in fluid state cannot exist above 275 °C it is of great importance that the water may be transported through the outer part of the concrete or be incorporated in an increased porosity. This is evidently possible in NC but not in HPC causing spalling in HPC. In order to establish the amount of spalling it is important to know the weight loss of concrete at elevated temperature. The losses come from evaporated and non-evaporable water and ignition losses from the aggregate, for example after fire spalling tests. Figure 2.40 shows the residual relative weight of HPC and NC after heating [38]. The weight loss was somewhat larger of NC than of HPC probably due to larger water content in NC than in HPC. Another important parameter to take into account during spalling is the temperature gradient within the concrete.

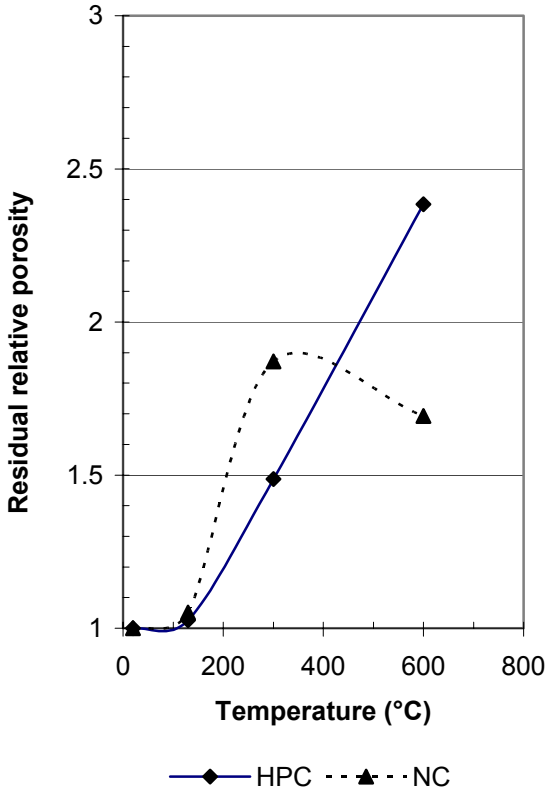

Figure 2.39 - Residual relative porosity at high temperature being 4% for HPC and NC at 20 °C [38], Appendix 2.5.

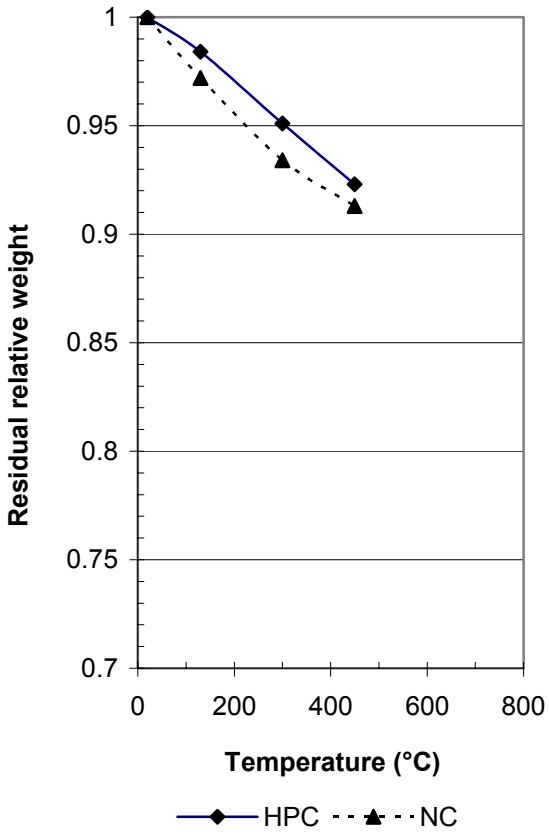

Figure 2.40 - Residual relative weight of HPC and NC after heating [38], Appendix 2.5.

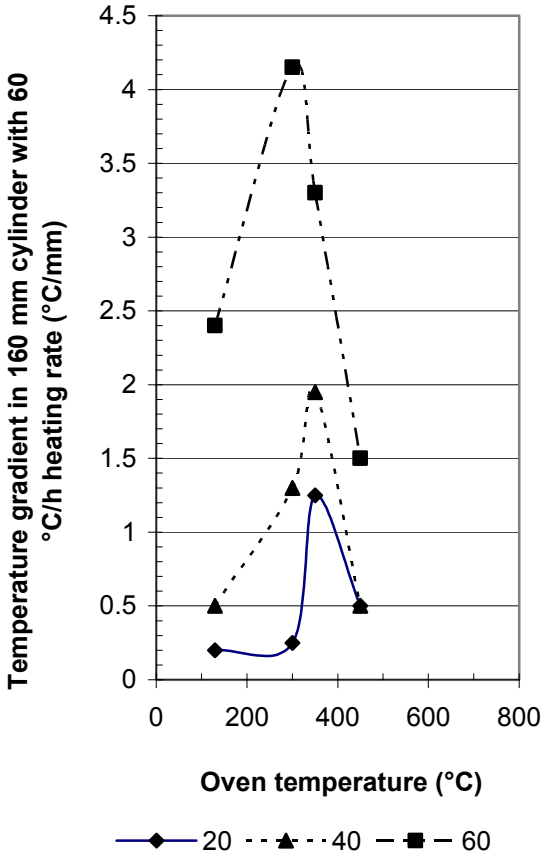

Figure 2.41 - Temperature gradient obtained by 60 °C/h heating rate of 160-mm cylinders [38], Appendix 2.5.

The maximum gradient was 4.2 °C/mm at about 275 °C oven temperature. At higher temperature fluid water may no longer exists but in this case the water may be transported towards the surface since the heating rate was fairly low. At higher heating rate no time is available for this transport, the gradient will be too large and spalling take place starting from the surface. In order to calculate the maximum pressure in a 160-mm cylinder at 60 °C/h heating rate some permeability values had to be used, Table 2.4 [38].

Table 2.4 - Permeability values [38].

Concrete	HPC	NC
w/b	0.56	0.53
w/c	0.56	0.61
w/p	0.56	0.44
Permeability (10^{-12} x(m/s))	3	15
Age (days)	30	30
RH (%)	95	95
Thermal conductivity (J/ms°C)	1.6	1.6
Heating rate (°/h)	60	60

Figure 2.42 shows the calculated maximum pressure in 160- mm cylinder at 60 °C/h heating rate [38], Appendix 2.5.

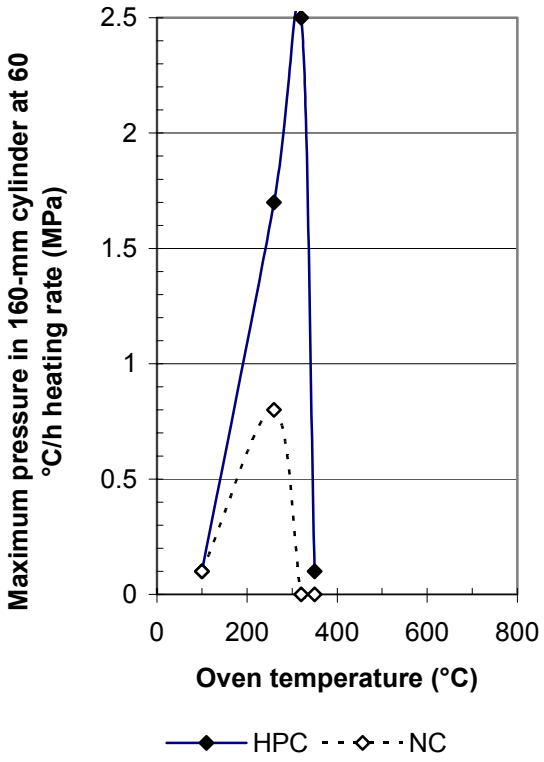

Figure 2.42 - Calculated maximum pressure in 160-mm cylinder at 60 °C/h heating rate [38], Appendix 2.5.

Again it is shown that the critical temperature where water formed due to the temperature increase and accompanying RH-increase no longer may exists is 275 °C, Figure 2.42. The pressure shown in Figure 2.42 is larger than those shown in Figures 2.21-23 which is explained by the type of concrete, HPC in Figure 2.42 and NC in Figures 2.21-23.

2.7.7 Rapid heating

In Figure 2.22-23 water pressure, heat and spalling of NC is registered [24]. Similar experiments but on HPC and with smaller specimens, cylinders 100 mm in diameter and 200 mm long, or blocks 100 x 200 x 200 mm subjected to fire from one side only, were performed [40-44]. The heating rate was set at 300 °C/h, i.e. slightly lower than that use in Figure 2.22-23. In Figure 2.22-23 extensive spalling occurred of 150-mm diameter NC cylinders at either 240 or 480 °C/h heating rate in the oven [24]. The temperature gradient then exceeded 5 °C/mm, Figure 2.16-17. The tests of HPC show the efficiency of using polypropylene fibres for mitigation of explosive spalling [40-44]. Materials and properties of the concrete in study are shown in Appendix 2.6 [40]. Spalling of the 100-mm diameter specimen took place after about 2.5 h at a oven temperature of 500 °C at a specimen centre temperature of about 275 °C [40]. This findings confirms results by [24], i.e. at 275 °C when fluid water no longer may exist a sudden explosion takes place when the water is transformed into vapour (initially the specimen contained water vapour but when the temperature increases also RH increase in the specimen and fluid water formed moving toward the specimen centre). In Figure 2.43 the temperature gradient of the 100-mm cylinder specimen of mix proportion 1, Appendix 2.6, versus time, the temperature rate and the calculated value gradient-rate ratio, g/r, are shown are shown [40]. Around g/r = 360 min/m or g/r = 6 h/m explosive spalling occurred [40]. What happened after spalling as concerns temperature development is of low interest and even difficult to measure. In Figure 2.44 the temperature gradient of a 100-mm slab specimen versus time, the temperature rate and the calculated gradient-rate ratio, g/r, are shown [40], mix proportion 1, Appendix 2.6. In this case the double g/r-value was acceptable due to twice the hydraulic radius of the specimen as compared to the 100-mm cylinder specimen. Figure 2.45 shows the pore pressure of a 100-mm slab for mix proportions 1-4, Appendix 2.6 [40]. Amount of polypropylene fibres is indicated.

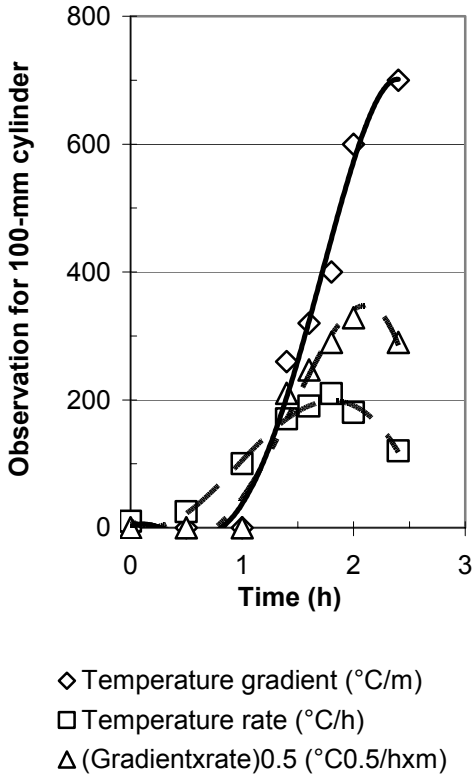

Figure 2.43 - Temperature gradient of 100-mm cylinder specimen versus time, the temperature rate and the calculated gradient-rate ratio, g/r, [40]. Mix proportion 1, Appendix 2.6.

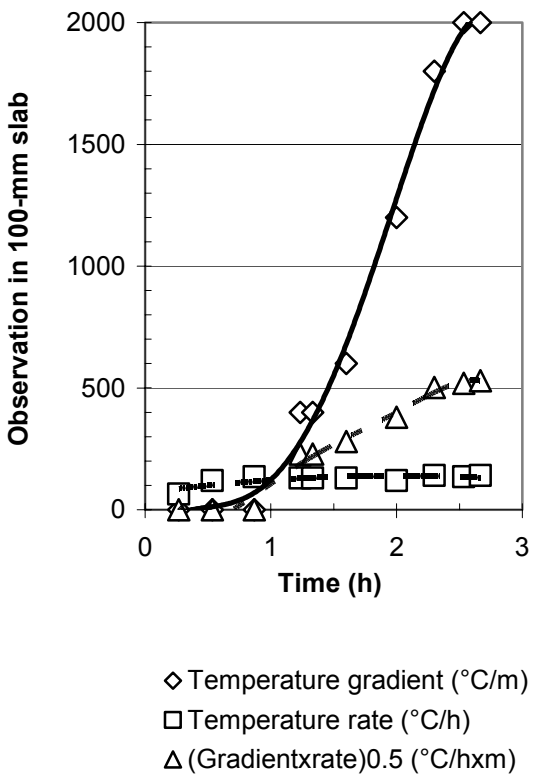

Figure 2.44 - Temperature gradient of 100-mm slab specimen versus time, the temperature rate and the calculated gradient-rate ratio, g/r, [40]. Mix proportion 1, Appendix 2.6.

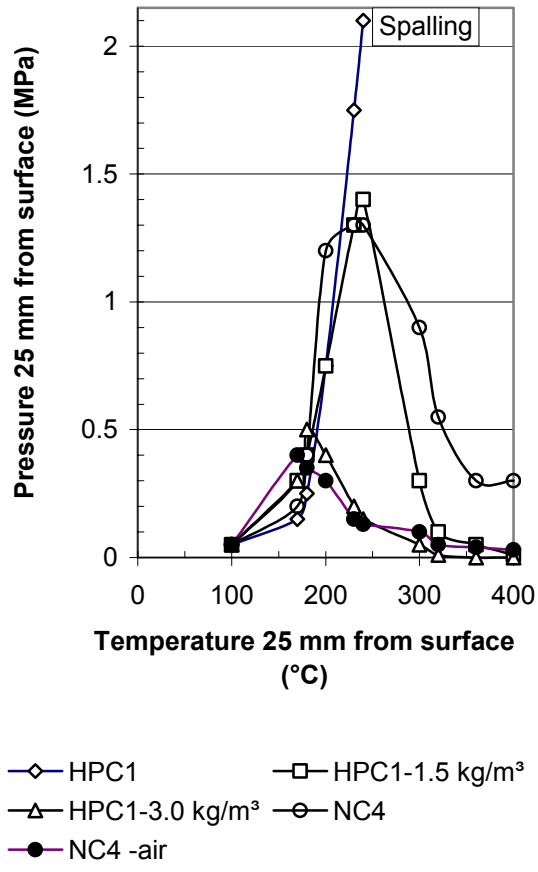

Figure 2.45 - Pore pressure of 100-mm slab for mix proportions 1-4, Appendix 2.6. Amount of polypropylene fibres is given [40].

Three kg/m³ of fibres had a very beneficial effect on the fire spalling resistance at w/b = 0.20. One-point-five kg/m³ of fibres was not sufficient to control the pressure but still spalling was avoided.

2.7.8 Relative strength

Figure 2.46 shows the development of relative stressed strength versus temperature of concrete given in Appendix 2.6 [40]. The stress was 40% of the 23 °C-strength and withhold throughout the testing. Figure 2.47 in turn shows the development of relative unstressed strength versus temperature of concrete given in Appendix 2.6 [40]. Both the stressed and the unstressed strength properties were tested at elevated temperature. Figure 2.48 shows the residual relative unstressed strength versus temperature, Appendix 2.6 [40]. The residual relative strength was normally lower than the stress and the unstressed strength on at elevated temperature, about 300 °C and higher except for w/b = 0.20 [40].

2.7.9 Comparison with European codes

Figure 2.49 shows a comparison of the relative stressed strength according to various European codes [40]. The lowest relative strength was obtained for HPC followed by the CEB code.

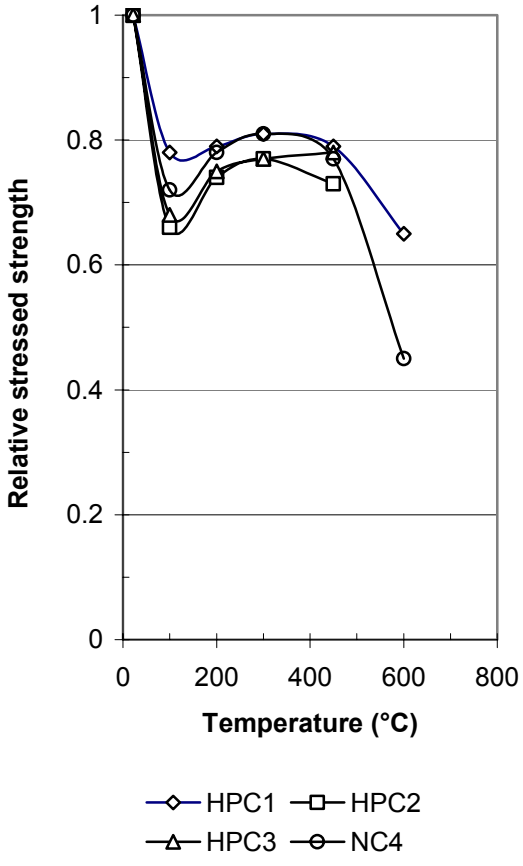

Figure 2.46 – Relative stressed strength versus temperature, Appendix 2.6 [40].

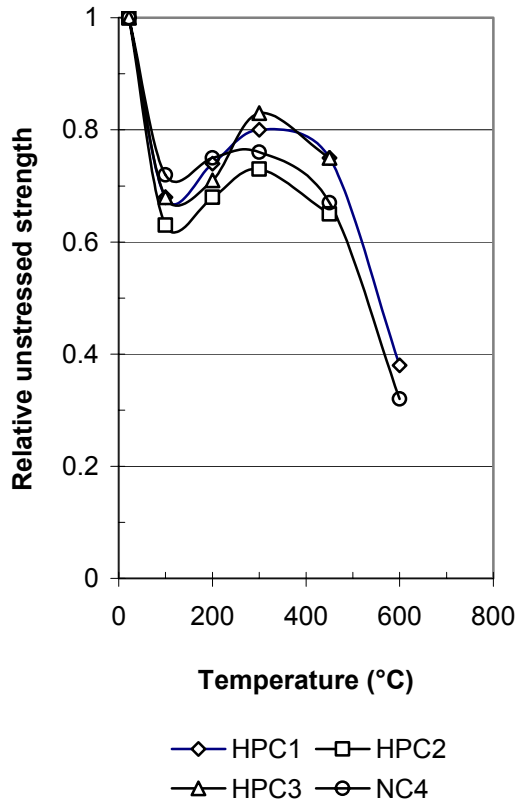

Figure 2.47 - Relative unstressed strength versus temperature, Appendix 2.6 [40].

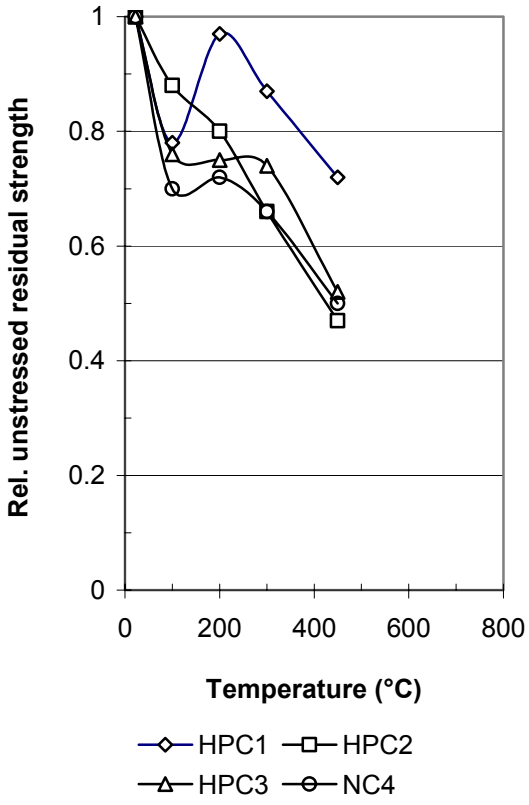

Figure 2.48 – Residual relative unstressed strength versus temperature, Appendix 2.6 [40].

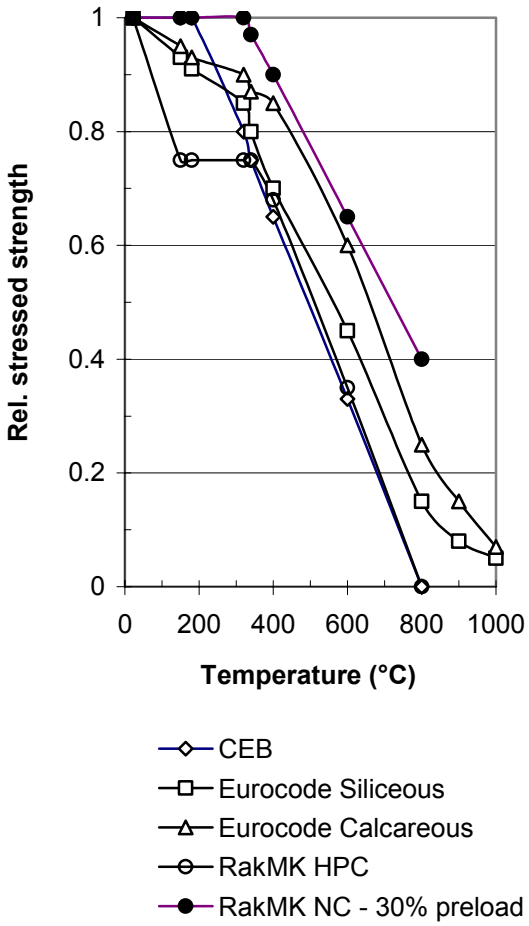

Figure 2.49 - Comparison of the relative stressed strength according to European codes [40].

The highest relative stressed strength was obtained by the Eurocode for calcareous material and by the Finnish code RakMK for normal concrete, 30% preloading of the ultimate strength [40]. Figure 2.50 shows the corresponding unstressed relative strength according to the Finnish code [40].

2.8 SCC with steel fibres

In order to incorporate steel fibres in SCC is was necessary to diminish the amount of large aggregate in the mix proportions [45-47]. Table 2.5 and Figure 2.51 give example of mix proportions and grading of SCC with steel fibres.

Table 2.5 - Mix proportions of SCC with steel fibres (kg/m³)

Cement	400
Fly ash	100
Steel fibrers	79
Water	190
w/b = w/p	0.38
w/c	0.43
Slump flow (mm)	620
28-day strength (MPa)	70

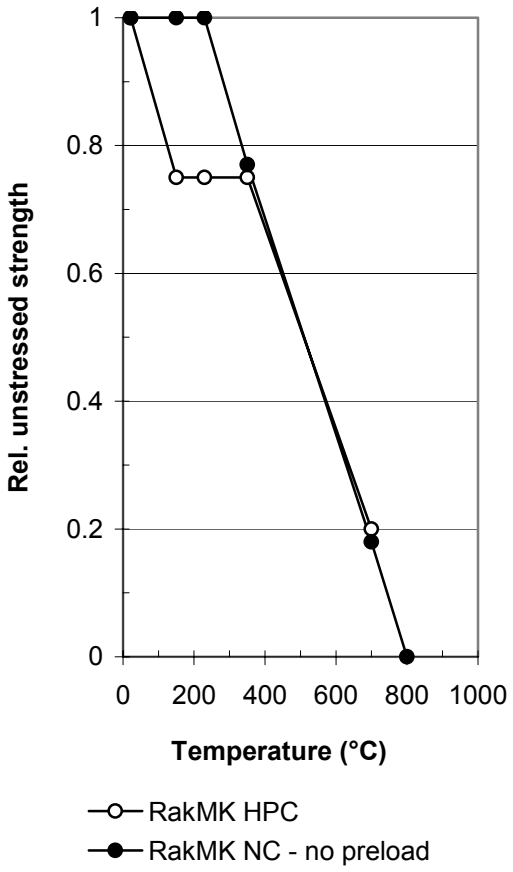

Figure 2.50 - Unstressed relative strength according to the Finnish code [40].

The following ideal grading was obtained for SCC with steel fibers:

$$p = 0.50 \cdot (d)^{0.26} \qquad (2.4)$$

p denotes material passing
d denotes sieve size (0.1<d<10 mm)

2.9 German code for SCC

A proposal for a German SCC code was presented but still not accepted [48]:

- Content of filler and cement in SCC to vary between 450 and 650 kg/m³
- Slump flow ≥ 700 mm
- Slump flow with J-ring ≥ 650 mm
- Difference between slump flow with and without J-ring ≤ 50 mm
- SCC to fulfil other NC requirements

A J-ring consists of 12 rebars 12 mm in diameter place in a 300-mm diameter cylindrical circle. The J-ring is placed around the slump flow cone before testing. Generally the German code is very simple and concentrated on the risk of separation of SCC, i.e. to keep the amount of filler + cement at an acceptable level. The risk of separation is also taken into account by the difference of the two slump flow measurements, with and without J-ring, Figure 2.52, also a test method well suited for the practise. SCC is also to fulfil all other requirement for NC, separation as well as bleeding, also in the hardened state. The reason for the pending acceptance of the German code is lacking data on creep, shrinkage and durability of SCC, especially with limestone filler [49]. Mix proportions of SCC were also studied in some Master Thesis at LTH and other works as a fundamental approach for the mix proportions in this study [50-78].

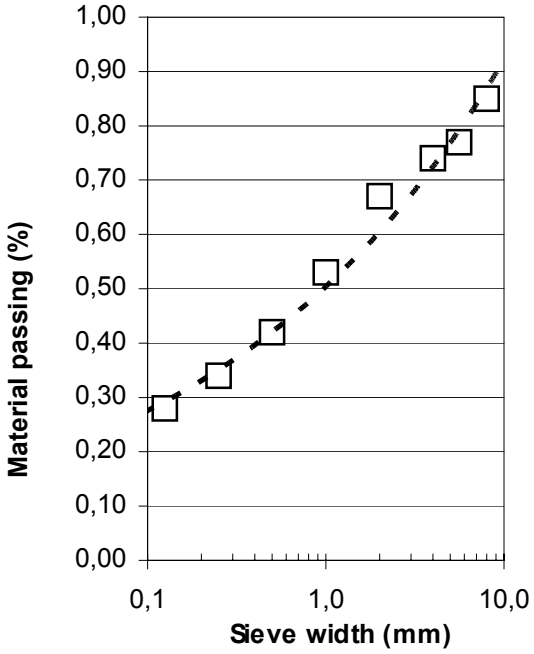

Figure 2.51 - Grading of SCC with steel fibres.

Figure 2.52 - Slump flow measurements, with and without J-ring.

2.10 Explosive fire spalling of normal concrete

2.10.1 Conditions for fire spalling

Khoury [79] states the following types of spalling for normal concrete:

- Aggregate spalling
- Explosive spalling
- Surface spalling
- Corner spalling

The first three types occur between the first 20 and 30 minutes of fire and are influenced by the heating rate mainly. The fourth type of spalling (corners) takes place after 30 to 60 minutes after fire and is influenced by the maximum temperature. All types of spalling are violent except for the fourth ones. Khoury [79] also states that the fire spalling is influenced by the following material parameters:

- Permeability
- Saturation level
- Aggregate size
- Aggregate type

The shape and size are geometric factors that significantly influences on the risk of fire spalling [79]. Few environmental factors are critical for the fire spalling to occur, Table 2.6 and Figure 2.53:

- The heating rate
- The heating profile
- The load level

The heating rate is supposed to be more than between 120 and 180 °C/h and the pore saturation level to be more than between 2 and 3% for the fire spalling to occur, Figure 2.53. The applied stress in a way work hand in hand with the concrete quality, i.e. for HPC the stress will automatically be larger than in NC. For a 100-MPa HPC a normal applied stress may be 30 MPa but in NC of 30 MPa only around 10 MPa. The critical moisture level then is around 2.5% for HPC to give fire spalling and around 3.5% for NC. HPC also has low permeability, which is another factor to take into account when estimating the risk of fire spalling even though the tensile strength is substantially larger in HPC than in NC. The low permeability in HPC affects the pore pressure rise parallell with the temperautre rise also due the much more horizontal isotherm in HPC than in NC. A small change of moisture when the water in the pores moves inwards during fire influences RH more in HPC than in NC. This is due to a finer pore system in HPC than in NC.

Table 2.6 – Factors effecting fire spalling [79].

Spalling	Time (h)	Kind	Sound	Effect	Root
Aggregate	0.11-0.5	Split-ting	Pop-ping	Super-ficial	A,D, S,H,W
Corner	0.5-1.5	Non-violent	None	Can be serious	A,F, R,T
Explosive	0.11-0.5	Violent	Load bang	Serious	A,F_s, G,H, L,O, P,Q, R,S, W,Z
Surface	0.11-0.5	Violent	Cracking	Can be serious	F_t,H, P,W

A aggregate thermal expansion
D aggregate thermal diffusivity
F_s Shear strength of concrete
F_t Tensile strength of concrete
G age of concrete
H heating rate
L loading restraint
O heating profile
P Permeability
Q Section shape
R Reinforcement
S Aggregate size
T Maximum temperature
W Moisture content
Z Section size

Figure 2.53 gives an equation for the risk of fire spalling [79]:

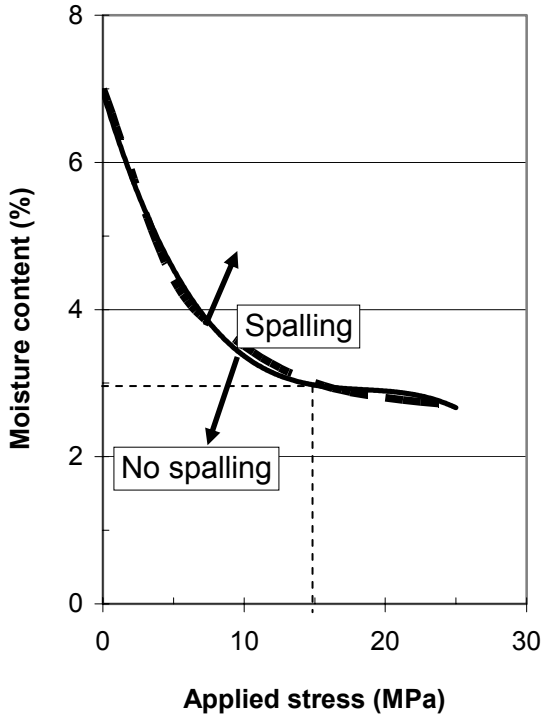

Figure 2.53 – Risk of fire spalling in concrete versus stress and moisture content [79].

$$u = -0.000617 \cdot \sigma^3 + 0.0341 \cdot \sigma^2 - 0.638 \cdot \sigma + 7 \quad (2.5)$$

u denotes moisture content (%)
σ denotes stress ($0 < \sigma < 25$ MPa)

In this project the stresses applied were around 15 MPa which gives a risk for spalling at u > 3.0%.

Khoury defines three types of mechanisms in order to explain fire spalling [79]:

- Pore pressure spalling depending on moisture content, heating rate and the permeability of the concrete
- Thermal stress spalling that occurs in ceramics
- Combined pore pressure and thermal stress spalling

Khoury also indicate different ways of avoiding fire spalling [79]:

- Protective layer of thermal barrier, vermiculite, intumescent paints or even a low grade concrete
- Polypropylene fibres that melt at 160 °C

According to Khoury 18 µm fibres act more effectively than larger ones. A recent development also allows for low melt polypropylene fibres, 130 °C [79]. The mechanism of the fibres is not yet understood. It seems that either continues canals in the concrete form when the fibres melt or the micro-cracking occur in the concrete when the fibres are heated (larger thermal expansion coefficient than tat of concrete). However, in ultra HPC or in reactive powder concrete fire spalling may not be prevented even though adding large quantities of polypropylene fibres, especially with silica fume [79]. Finally, Khoury sum up values of compressive strength of HPC versus temperature [79], Figure 2.54.

2.10.2 Tests on Self Compacting concrete, SCC

A exploratory study on plain SCC was carried out based on concrete cylinder 150 mm in diameter and 300 mm long with a strength of about 65 MPa [80]. Mix proportions and so forth are given in Table 2.7. The cylinders were subjected to a ISO 834 fire. The largest damaged was observed for the SCC with fly ash – the lowest for the SCC with limestone powder and for the NC. The spalling correlated with the moisture content [80]. SCC 1 exhibited the largest fire spalling. This concrete also contained the largest partition of type III cement, i.e. slag cement. It is known from research on frost resistance that concrete with slag cement has low tensile strength causing large frost scaling. The same conditions may apply for the fire spalling tests when large amounts of type III slag cement are included in the mix proportions.

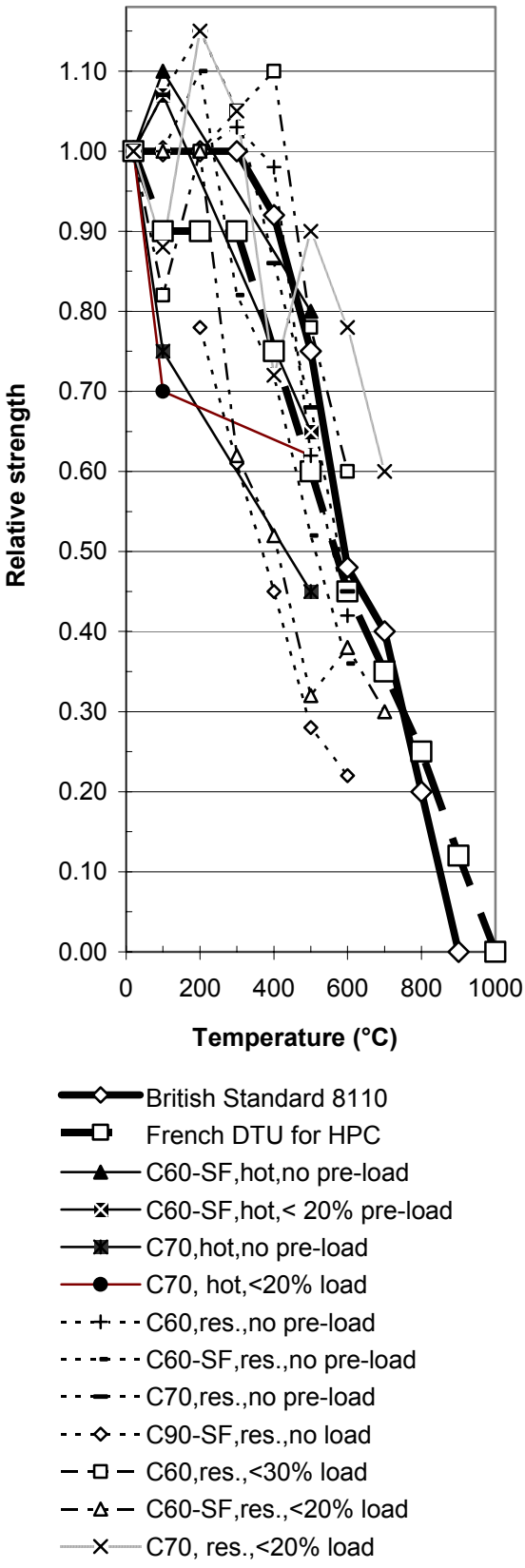

Figure 2.54 - Values of compressive strength of HPC versus temperature [79].

Table 2.7 - Mix proportions, spalling and so forth of study on SCC (kg/m³) [80].

Concrete	NC	SCC1	SCC2	SCC3
CEMI R A			260	240
CEMI R E	100	185	80	
CEMIII B	300	185		110
CEMIII C				
Fly ash		185		
Limestone filler			250	250
Sand 0-4 mm	830	660	790	770
Pea gravel 4-16 mm		900		
Crushed 4-16 mm	975			
Gravel 4-16 mm			860	
Limestone 4-14 mm				840
Plasticiser		2.3	2.4	2.4
Cement	400	370	340	350
Cement + fly ash	400	555	340	350
Powder	400	555	590	600
Water	156	177	119	133
c/p	1	0.67	0.57	0.58
(c+fly ash)/p	1	1	0.57	0.58
w/c	0.39	0.48	0.35	0.38
w/p	0.39	0.32	0.20	0.22
E-modulus (GPa)	37	34	40	37
Moisture, unsealed (%)	2.7	3.4	3.3	3.9
Spalling, unsealed (%)	6.0	6.9	7.2	6.5
Moisture, sealed (%)	3.9	4.7	4.0	4.6
Spalling, sealed (%)	7.1	9.6	7.2	7.4
Damage, sealed (%)	5	14	0	3
Moisture, saturated (%)	4.2	5.7	4.6	4.9

CEMI = Portland cement; CEMIII = slag cement.

3. MATERIALS AND METHODS

3.1 Material

Cement type I Degerhamn and type II Byggcement Skövde were used, Appendix 3.1. Crushed aggregate 8-11 and 11-16 mm and natural sand 0-8 mm, based on gneiss and filler of glass (brand SGÅ) or limestone (brand Limus 40) were used. Grading of the aggregates, filler and cements are given in Appendix 3.2. Superplasticiser of melamine formaldehyde or polycarboxyl ether were used. Air-entrainment agent was fir oil-based. Polypropylene fibres 32 μm in diameter were used (brand Bagrat LMF).

3.2 Optimisation of SCC

Optimisation took place during the first half of 2001 mainly based on the following requirement to be fulfilled for the concrete:

- Slump flow > 650 mm
- Slump flow to 500 mm < 10 s
- L-box ratio < 0.8, i.e. height in L-box at front to height at shaft
- Separation cylinder ratio < 0.9
- Air-content 5% for concrete with Degerhamn Std cement

Mix proportions of NC were obtained from the production of concrete at Skanska Prefab, SPAB, in Bollebygd. When the optimisations were finished, field tests were carried out. The field test in the first half of 2001 failed since it was not possible to adjust the amount of superplasticiser during the mixing procedure. Thus the decision was taken to re-optimise all the SCC [81-82].

3.3 Fabrication of concrete specimen

The specimen size for fire test were either cylinders 100 mm in diameter and 200 mm long. Beside also cubes were cast and tested, either 100-mm or 150-mm. All columns were produced at the factory at SPAB. A 1000-l compulsive mixer was used. At LTH the concrete was mixed in a 40-l compulsive mixer. The same material was used in SPAB like in Lund. At fabrication of specimen in Lund the following mixing procedure was used:

- Mixing with water and air-entrainment, ½ min
- Mixing with superplasticiser for 2 min.
- Test of slump flow
- Adjustment of superplasticiser
- Mixing with superplasticiser for 2 min.

In the first half of 2001 the following mixing procedure was used during fabrication of specimen at SPAB (concrete 55BK0, 55BK2 and 55BR0):

- Mixing with water and air-entrainment, ½ min
- Mixing with superplasticiser for 2 min.

In second half of 2001 at SPAB:

- Mixing with water and air-entrainment, ½ min
- Mixing with superplasticiser for 2 min.
- Test of slump flow
- Adjustment of superplasticiser
- Mixing with superplasticiser for 2 min.

Concrete with Byggcement intended for house building was cured at ambient RH = 60%, at least half a year before testing. Concrete with Degerhamn cement intended for outdoor constructions was cured in water half a year before testing. The water curing was supposed to simulate the conditions for a tunnel wall subjected to water pressure from one side and air from the other. The cubes for compressive strength testing were cured likewise. Details of the oven are shown in Appendices 3.3-6. The specimen for the oven tests were used in the following way:

20 °C 2 pieces for strength and RH
200 °C 2+2 pieces for strength at elevated temperature and after cooling
400 °C 2+2 pieces for strength at elevated temperature and after cooling
800 °C 2+2 pieces for strength at elevated temperature and after cooling

3.4 Mechanical behaviour of concrete

The following equipment was used at LTH:

- Testing machine with high-temperature oven completed with cooling equipment
- Stainless steel supports 100 mm in diameter, SIS 2368 M3 253A (brand: Avesta Sheffield) at tests with 20 °C, 200 °C, 400 °C and 800 °C oven temperature
- Protective net on the specimen, Appendix 3
- Testing with 0.5 N/(s·mm²) loading rate
- Vaisala HMP 44 probes for RH
- Grindosonic frequency indicator
- Two LVDTs for deformation measurements
- Thermocouples cast in the specimen and placed in the oven
- Scale
- Humidity generator (for calibration of the RH probe, before and after measurements)

The testing equipment was calibrated before the testing took place, both the compressive testing machine and the LVDTs. In all about 140 cylinders were tested. The following were obtained:

- Weight and fundamental frequency at 20 °C before testing
- RH before strength testing
- Temperature inside and at the surface of the specimen
- Deformation of specimen at the outside of the oven after deduction of deformations of equipment
- Compressive stress during testing
- Residual properties were obtained at 20 °C and RH = about 40% after 7 days of cooling

4. RESULTS

4.1 Time schedule

The cylinders were cast during 2001-2002 and tested in the autumn of 2002, Appendix 4.1. Cylinder were older than concrete cast in Bollebygd: 160 days' age at fire spalling test except for concrete 55BK0, 55BK2 and 55BR0 (320 days' age).

4.2 Optimisation and strength

Concrete optimised and cast at LTH and Bollebygd are given in Appendices 4.2-4.6 [81-84]. Figures 4.1-4.6 and Appendices 4.7-4.8 show the concrete strength. Figure 4.7 shows similar 28-day strength of concrete cast at LTH and at SPAB. Notations: A = Degerhamn cement (6% air), B = Byggcement (1% air), G = Glass filler, K = Limestone powder, R = reference, SGÅ = Svensk Glasåtervinning; NKK = Nordkalk; 0 = 0 kg polypropylenfibre/m³, 40 = w/c (%).

4.3 Pre-testing in oven at LTH

The LTH oven was pre-tested at 20 °C, 200 °C, 400 °C and 800 °C, with steel, Figures 4.8-11 and with concrete, Figures 4.12-15. The tests with steel were performed in order to obtain its elastic modulus, which was set at 184 GPa for loading. The temperature development in the oven was much slower than the standard fire, equation (2.3), Figures 2.12 and 4.16 but the objective was to avoid fire spalling. The LVDT deformation gauges and the load cells in use were calibrated. From the pre-tests it was concluded that the elastic modulus and the strength declined with the temperature but that the ultimate strain increased up to 400 °C, Figures 4.17-18.

4.4 Stress/strain tests in oven

A summary of the number of Appendices and Tables in which the result of strain/stress tests are shown is given in Table 4.1.

Table 4.1 - Summary of Appendices and Tables with result of strain/stress tests.

Concrete	Appendices	Figures
40AG0	4.9-4.15	4.19-4.22
40AK0	4.16-4.21	4.23-4.26
40AK2	4.22-4.27	4.27-4.30
40AK4	4.28-4.33	4.31-4.34
40BR0	4.34-4.40	4.35-4.38
55BK0	4.41-4.46	4.39-4.42
70BG0	4.47-4.53	4.43-4.46
70BK0	4.54-4.59	4.47-4.50

Notations: A = Degerhamn cement with 6% air – entrainment, B = Byggcement with natural air content (about 1%), G = Glass filler, K = Limestone powder, R = Reference, 0 = 0 kg polypropylenfibre/m³, 40 = w/c (%).

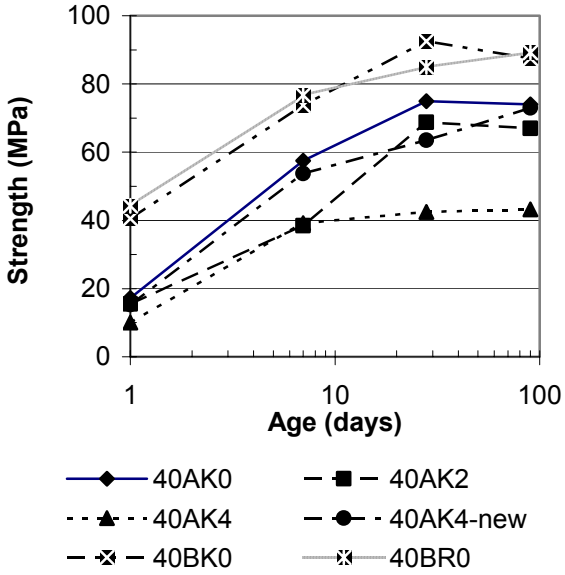

Figure 4.1 –Strength with w/c = 0.40 (LTH).

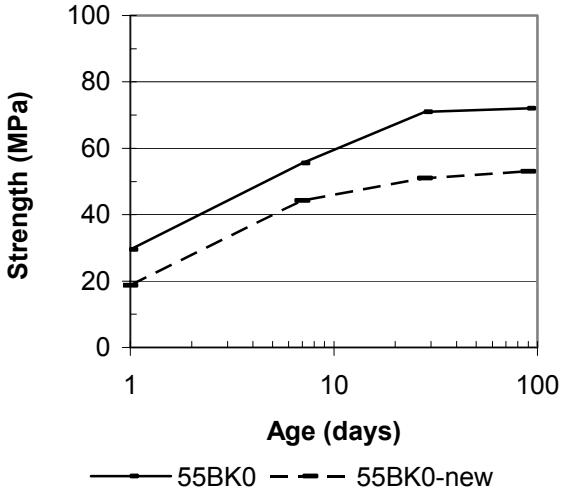

Figure 4.2 – Strength with w/c = 0.55 cast at LTH.

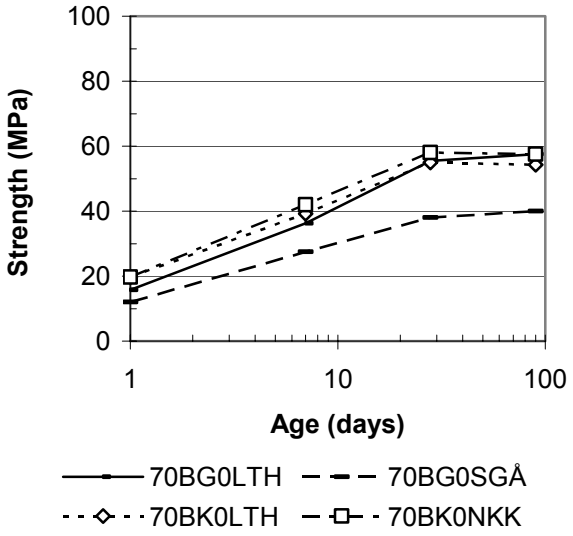

Figure 4.3 – Concrete strength at LTH (w/c=0.70).

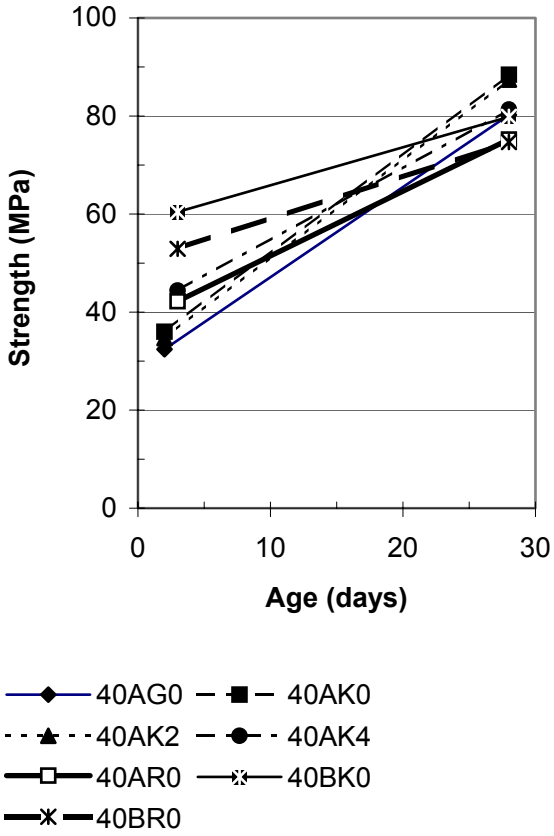

Figure 4.4 – Strength of concrete with w/c = 0.40 cast at SPAB, Bollebygd.

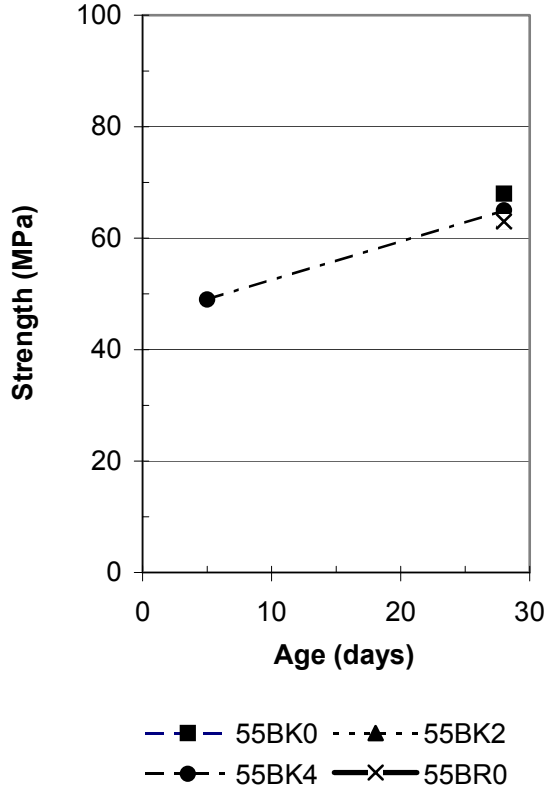

Figure 4.5 – Strength of concrete with w/c = 0.55 cast at SPAB, Bollebygd.

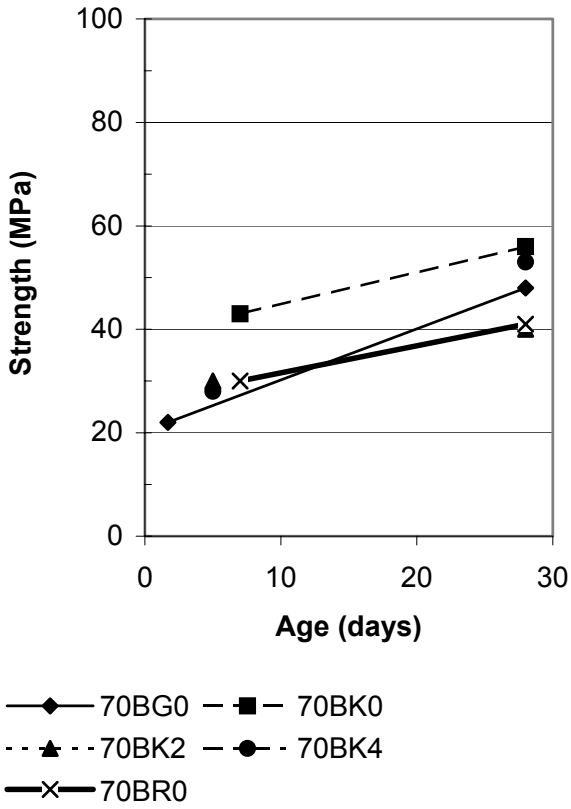

Figure 4.6 – Strength of concrete with w/c = 0.55 cast at SPAB, Bollebygd.

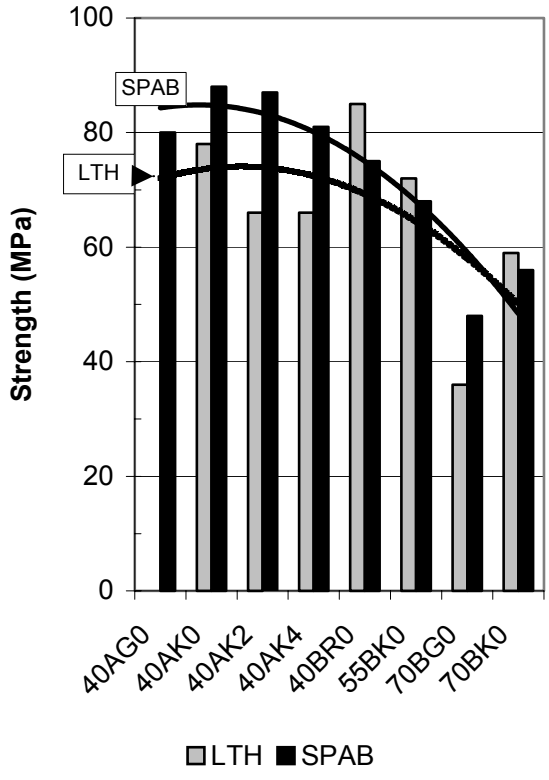

Figure 4.7 – Comparison of 28-day strength for concrete cast at LTH and at SPAB. Upper regression line = average strength of concrete cast at SPAB; lower regression line = average strength of concrete cast at LTH.

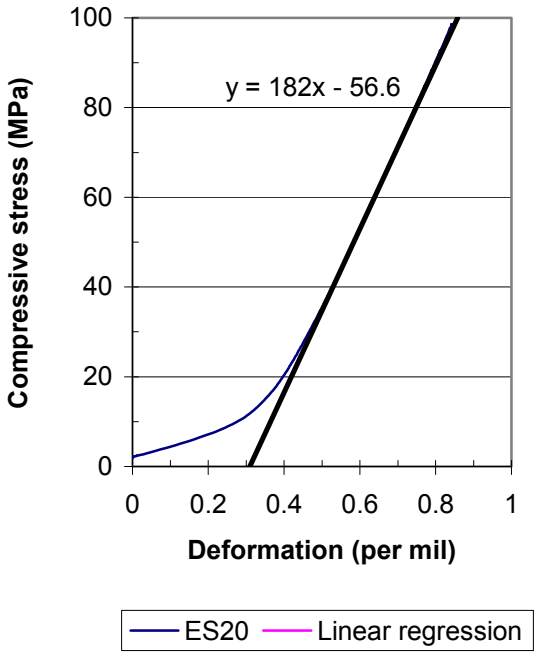

Figure 4.8 – Deformation and stress of steel at 20 °C. …...x = evaluated E-modulus (GPa).

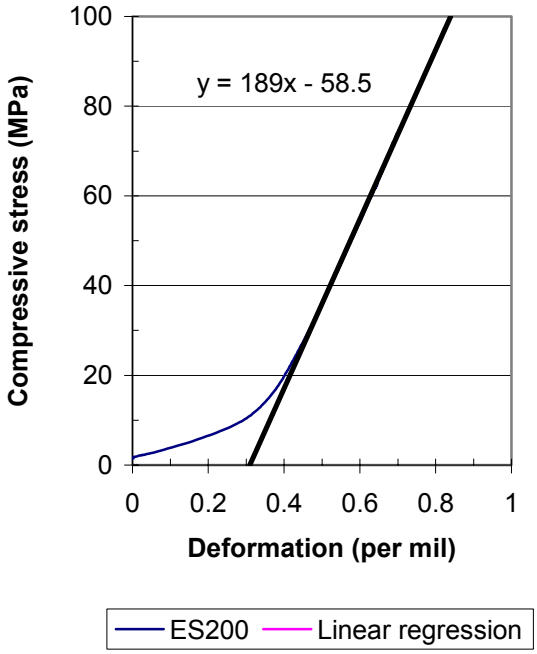

Figure 4.9 – Deformation and stress of steel at 200 °C. …...x = evaluated E-modulus (GPa).

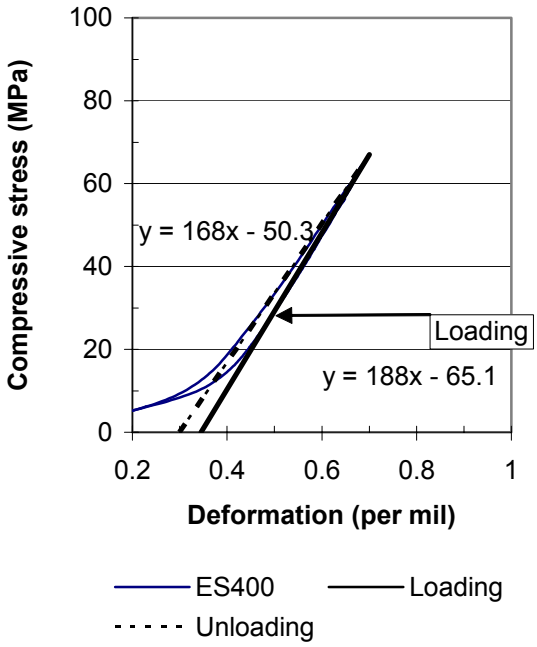

Figure 4.10 – Deformation and stress of steel at 400 °C. …...x = evaluated E-modulus (GPa).

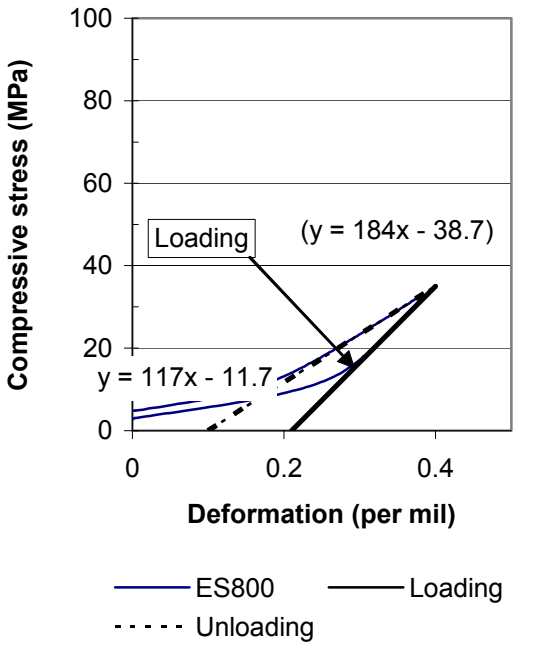

Figure 4.11 – Deformation and stress of steel at 800 °C. …...x = evaluated E-modulus (GPa).

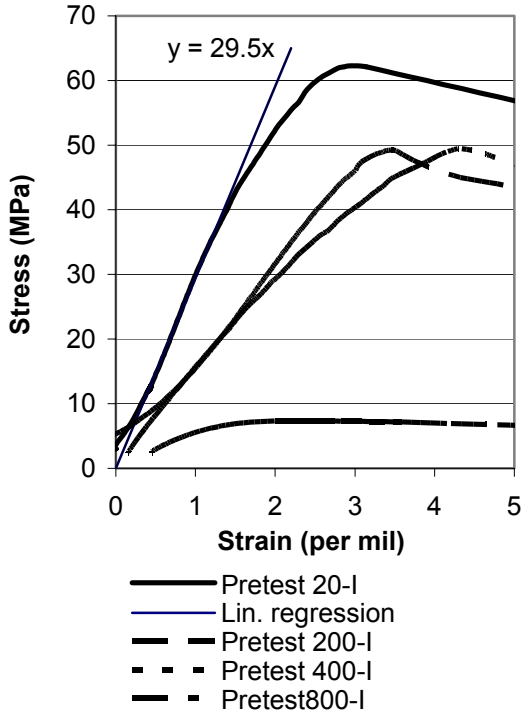

Figure 4.12 – Deformation and stress of concrete at 20 °C, 200 °C, 400 °C and 800 °C. …...x = evaluated E-modulus (GPa).

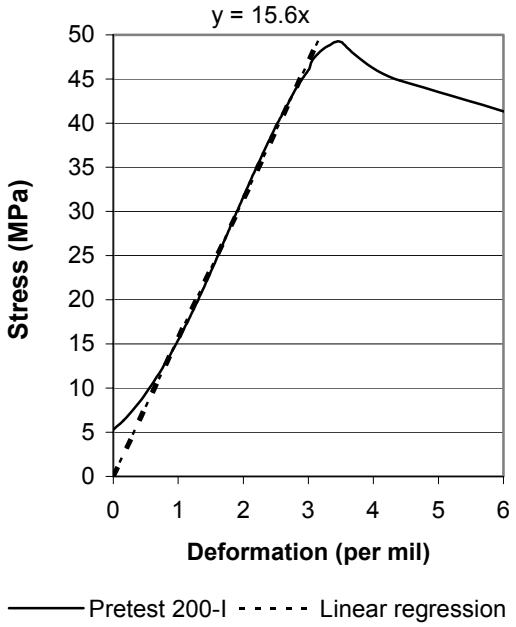

Figure 4.13 – Deformation and stress of concrete at 200 °C. …...x = evaluated E-modulus (GPa).

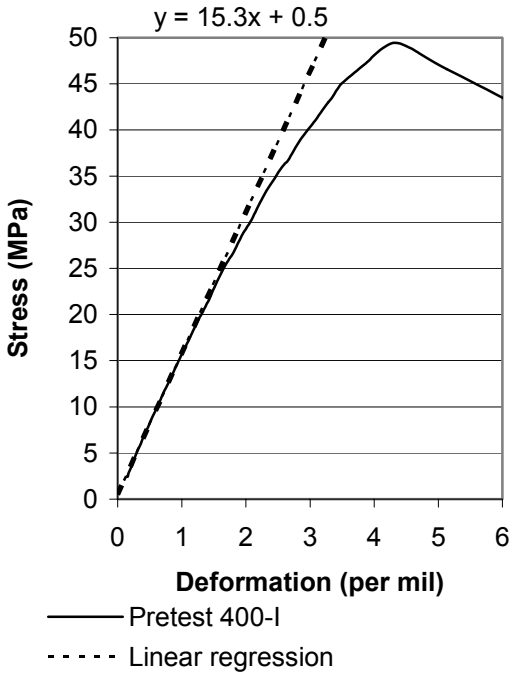

Figure 4.14 – Deformation and stress of concrete at 400 °C. …...x = evaluated E-modulus (GPa).

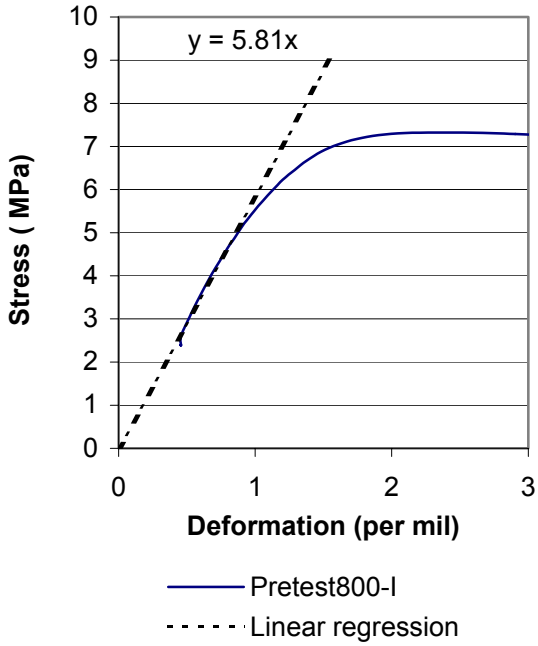

Figure 4.15 – Deformation and stress of concrete at 800 °C. …...x = evaluated E-modulus (GPa).

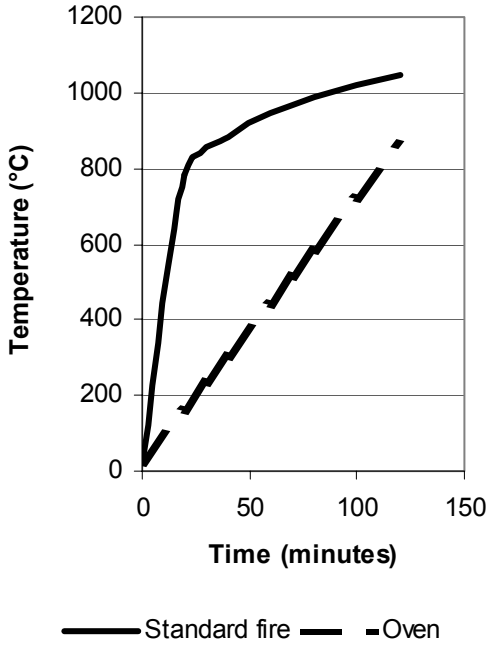

Figure 4.16 – Temperature with standard fire and in LTH oven.

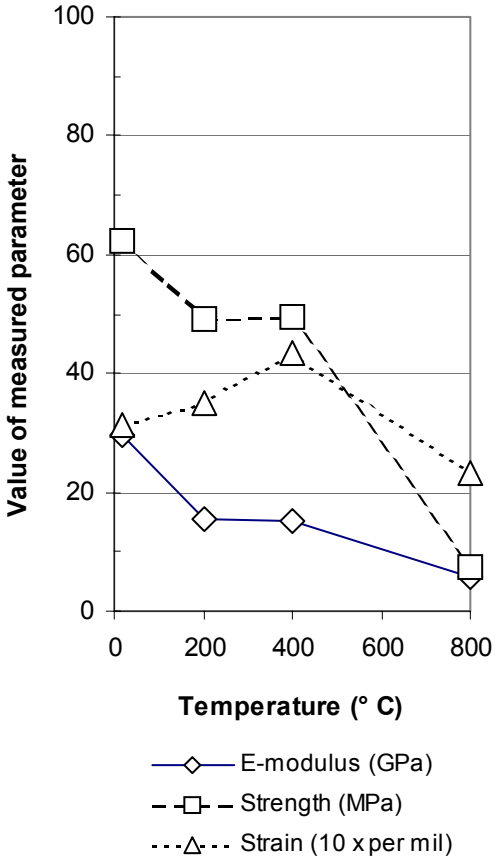

Figure 4.17 – Elastic modulus and the strength declined with the temperature but that the ultimate strain increased somewhat up to 400 °C.

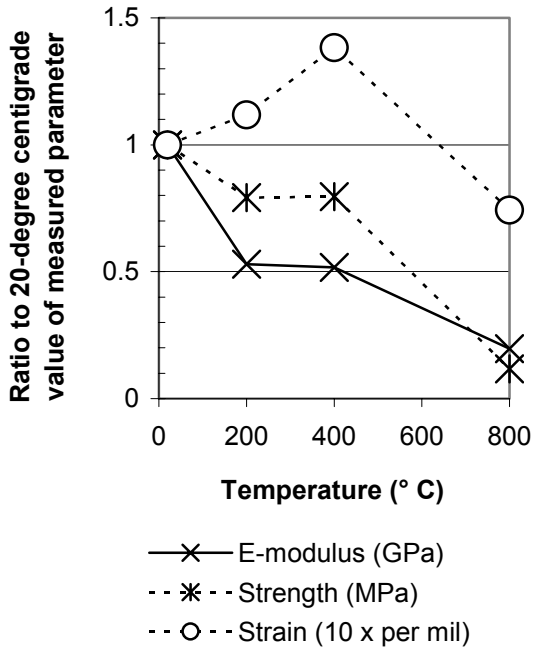

Figure 4.18 –Relative elastic modulus and relative strength declined with the temperature but the relative ultimate strain increased up to 400 °C.

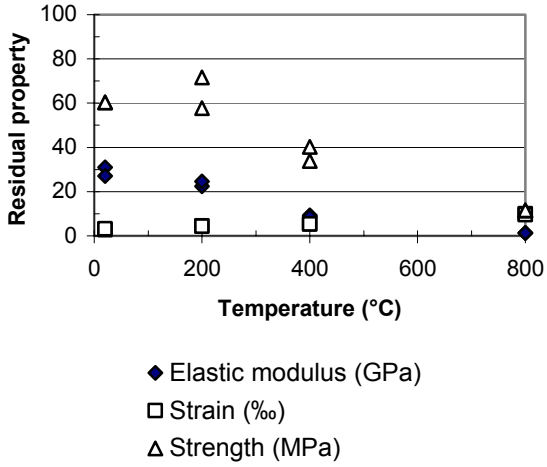

Figure 4.19 – Residual property of concrete 40AG0 versus temperature.

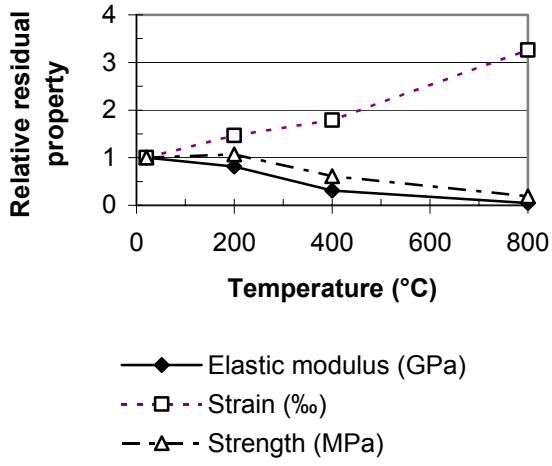

Figure 4.20 – Relative residual property of concrete 40AG0 versus temperature.

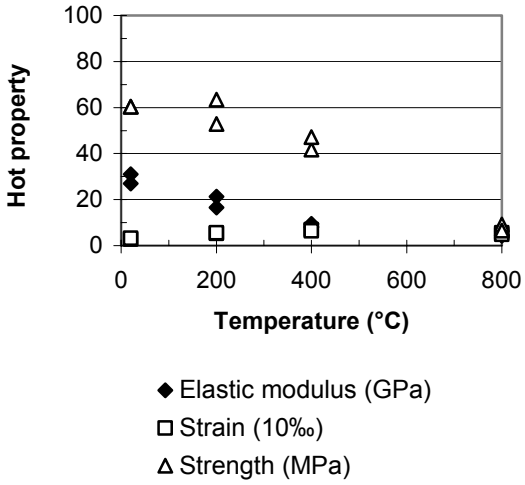

Figure 4.21 – Hot property of concrete 40AG0 versus temperature.

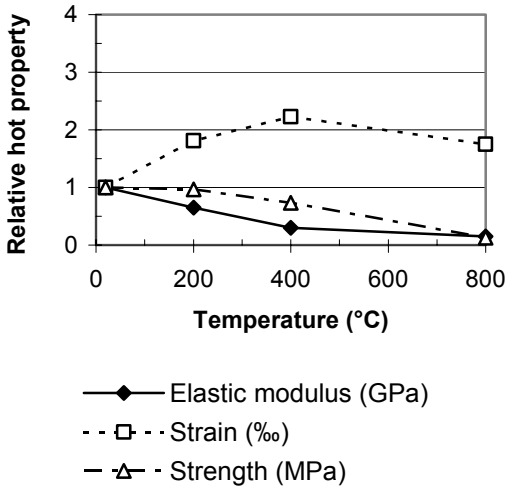

Figure 4.22 – Relative hot property of concrete 40AG0 versus temperature.

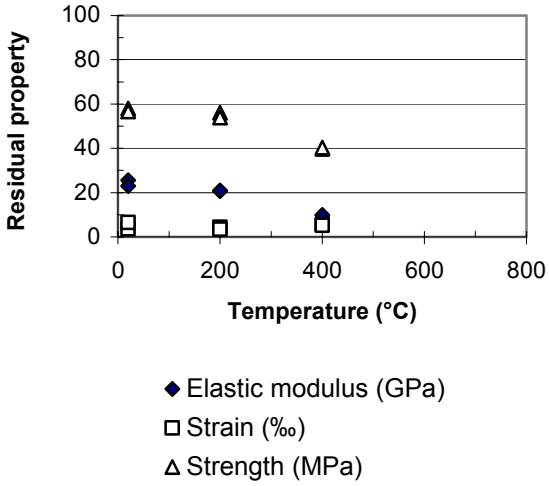

Figure 4.23 – Residual property of concrete 40AK0 versus temperature.

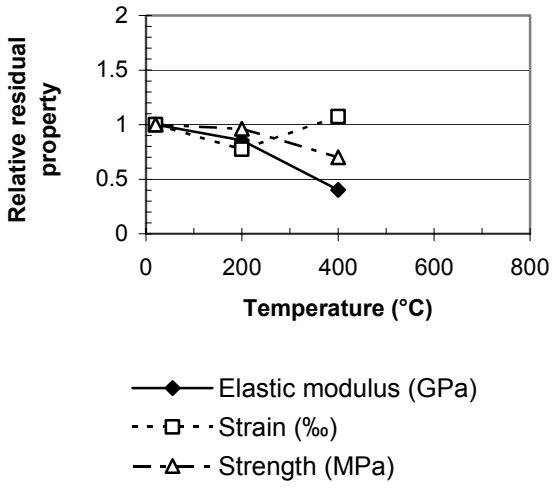

Figure 4.24 – Relative residual property of concrete 40AK0 versus temperature.

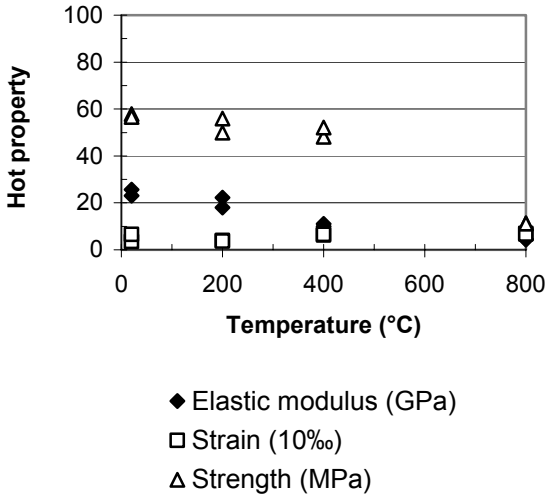

Figure 4.25 – Hot property of concrete 40AK0 versus temperature.

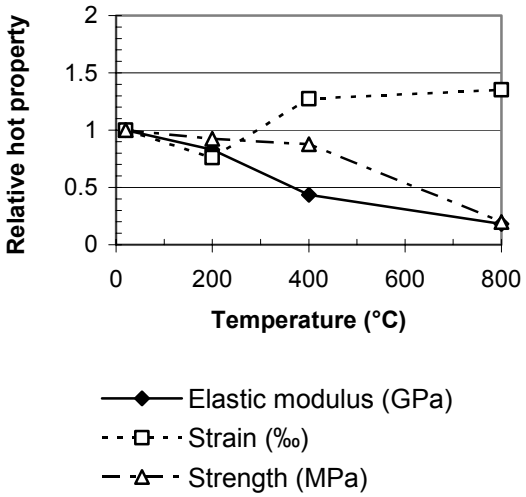

Figure 4.26 – Relative hot property of concrete 40AK0 versus temperature.

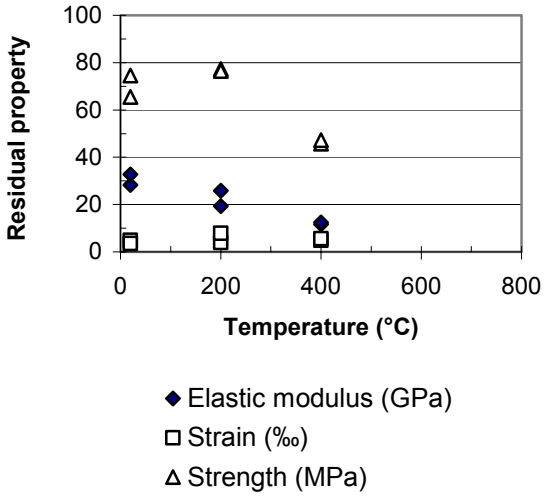

Figure 4.27 – Residual property of concrete 40AK2 versus temperature.

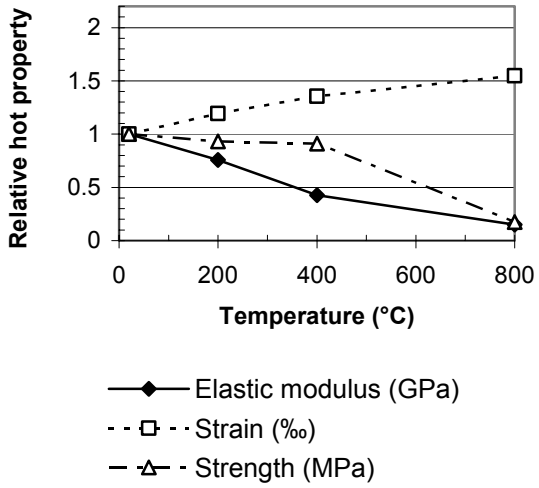

Figure 4.30 – Relative hot property of concrete 40AK2 versus temperature.

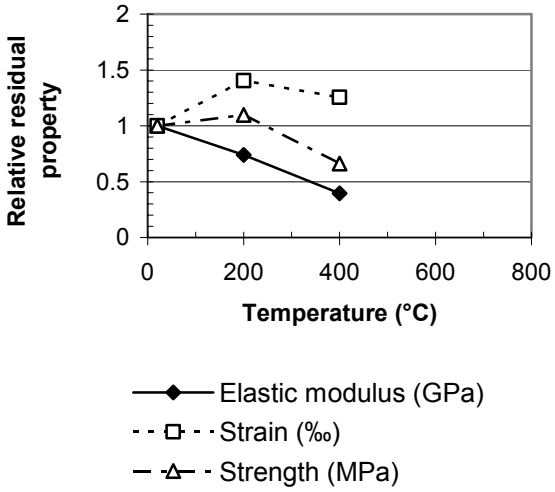

Figure 4.28 – Relative residual property of concrete 40AK2 versus temperature.

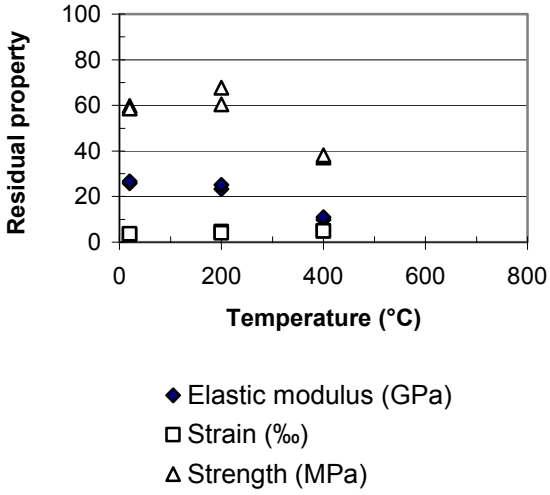

Figure 4.31 – Residual property of concrete 40AK4 versus temperature.

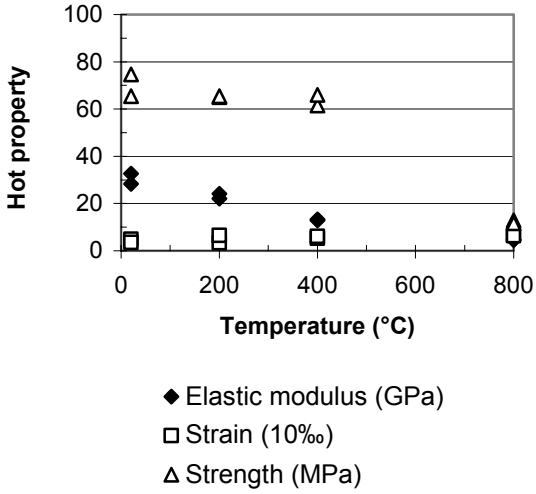

Figure 4.29 – Hot property of concrete 40AK2 versus temperature.

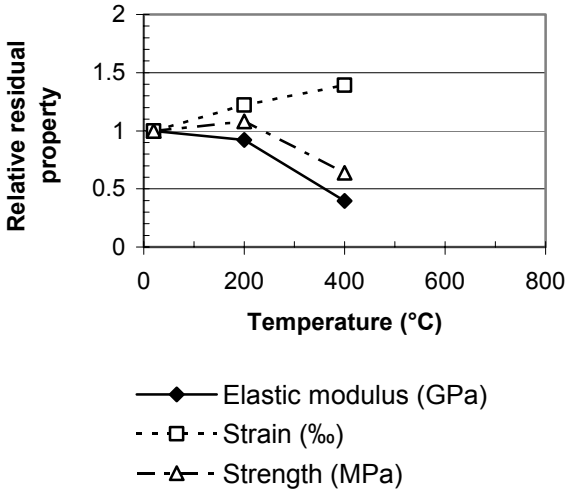

Figure 4.32 – Relative residual property of concrete 40AK4 versus temperature.

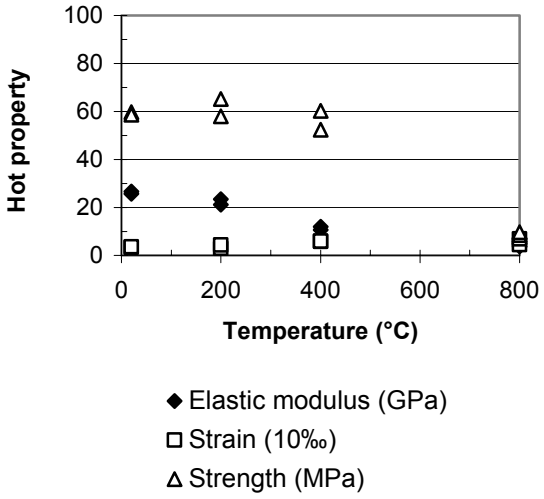

Figure 4.33 – Hot property of concrete 40AK4 versus temperature.

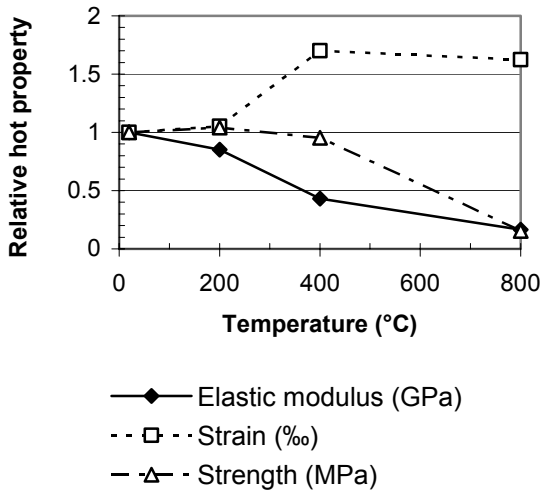

Figure 4.34 – Relative hot property of concrete 40AK4 versus temperature.

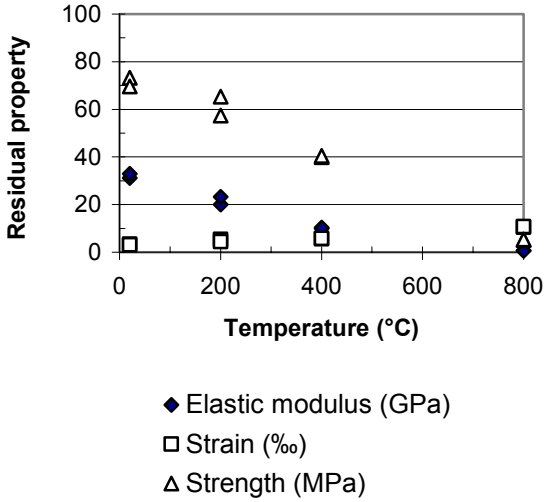

Figure 4.35 – Residual property of concrete 40BR0 versus temperature.

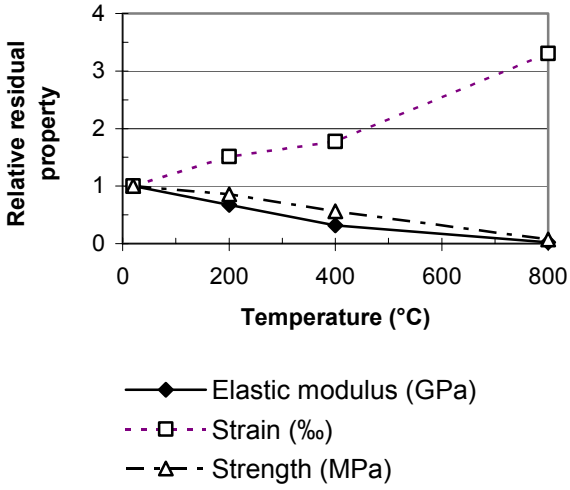

Figure 4.36 – Relative residual property of concrete 40BR0 versus temperature.

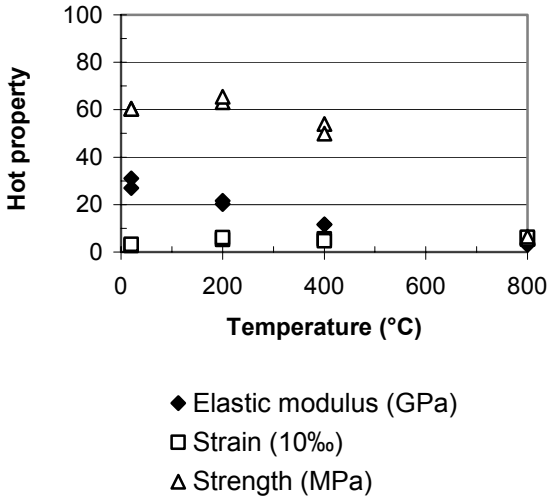

Figure 4.37 – Hot property of concrete 40BR0 versus temperature.

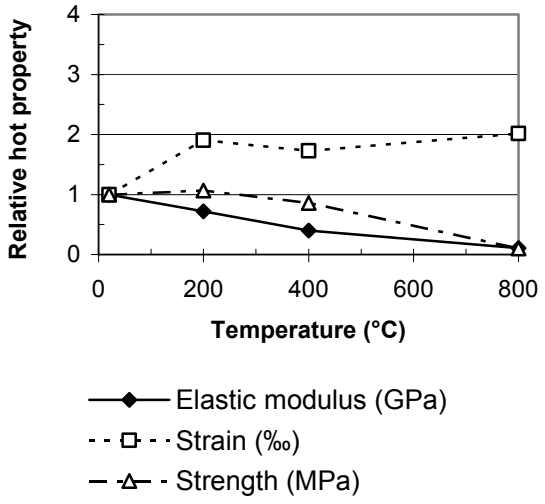

Figure 4.38 – Relative hot property of concrete 40BR0 versus temperature.

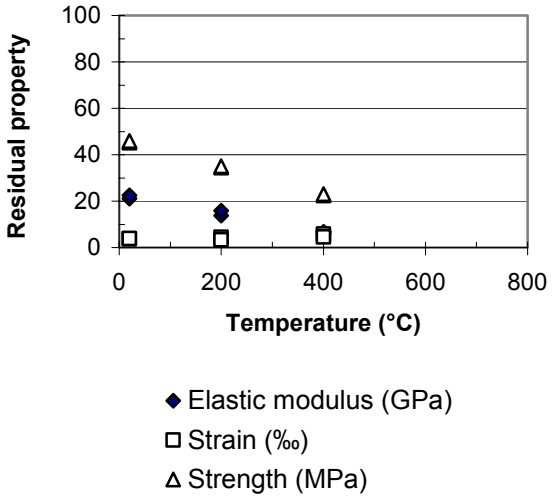

Figure 4.39 – Residual property of concrete 55BK0 versus temperature.

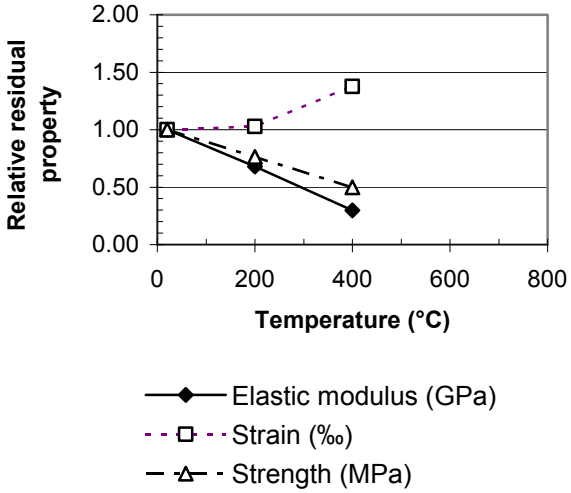

Figure 4.40 – Relative residual property of concrete 55BK0 versus temperature.

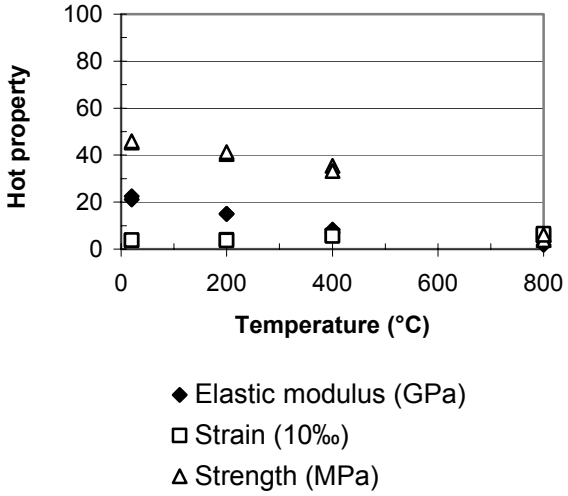

Figure 4.41 – Hot property of concrete 55BK0 versus temperature.

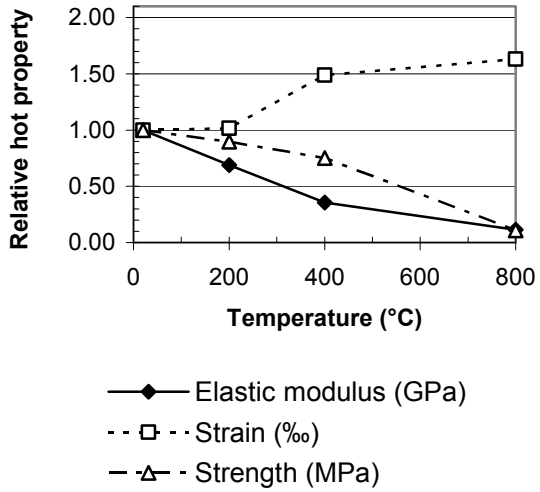

Figure 4.42 – Relative hot property of concrete 55BK0 versus temperature.

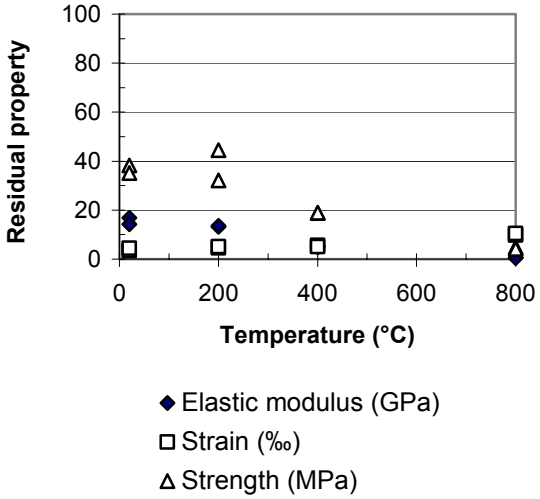

Figure 4.43 – Residual property of concrete 70BG0 versus temperature.

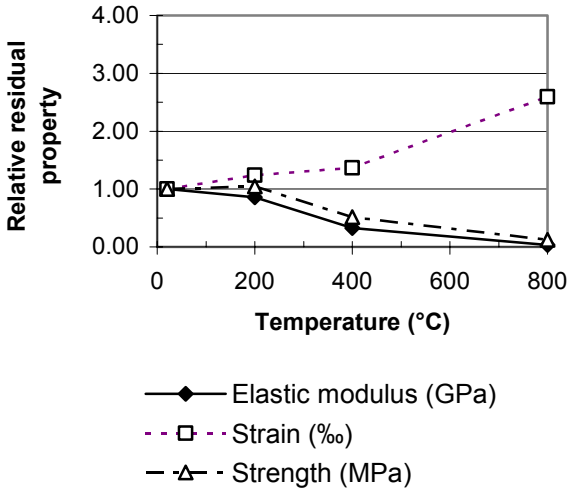

Figure 4.44 – Relative residual property of concrete 70BG0 versus temperature.

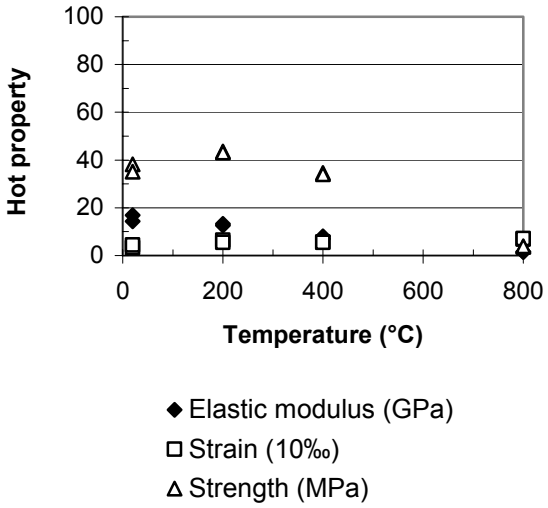

Figure 4.45 – Hot property of concrete 70BG0 versus temperature.

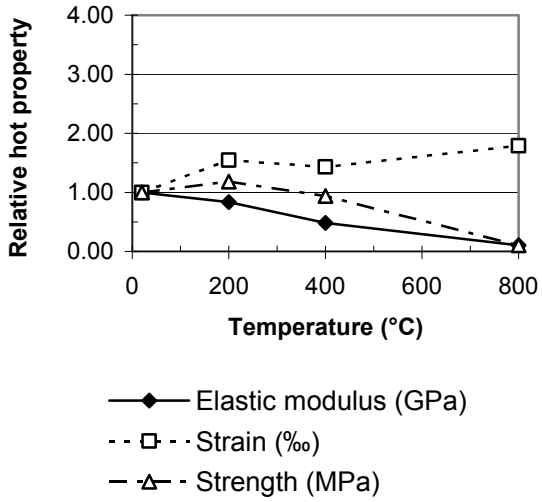

Figure 4.46 – Relative hot property of concrete 70BG0 versus temperature.

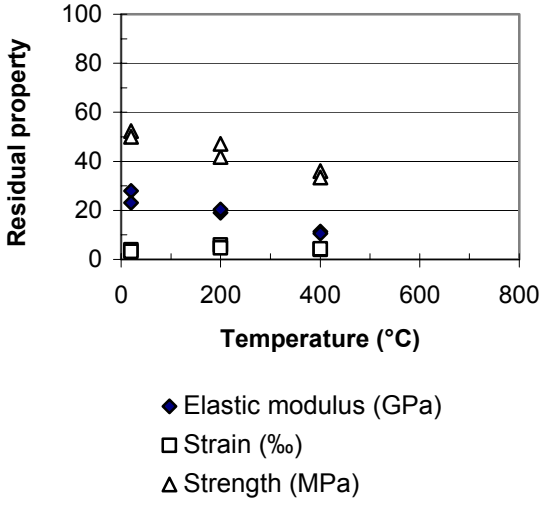

Figure 4.47 – Residual property of concrete 70BK0 versus temperature.

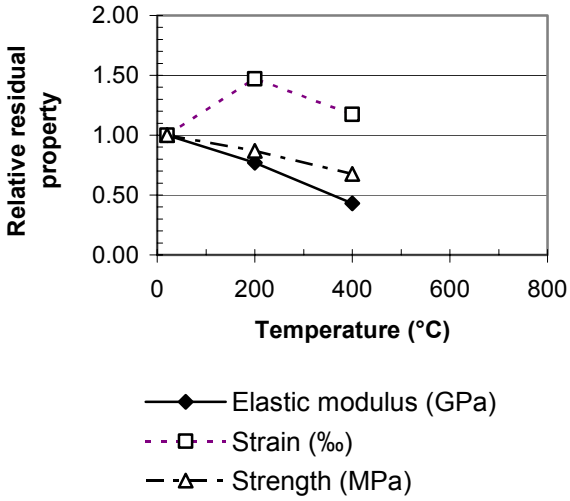

Figure 4.48 – Relative residual property of concrete 70BK0 versus temperature.

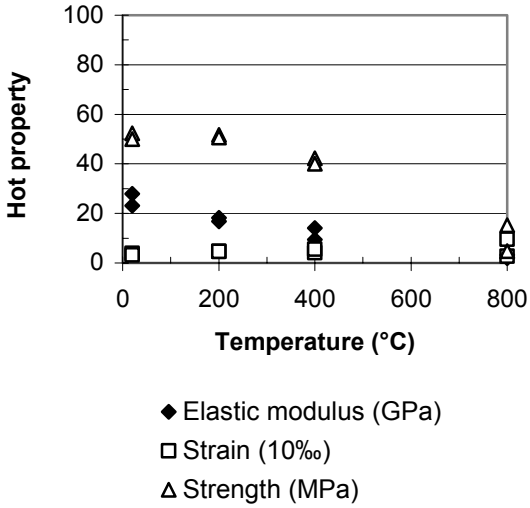

Figure 4.49 – Hot property of concrete 70BK0 versus temperature.

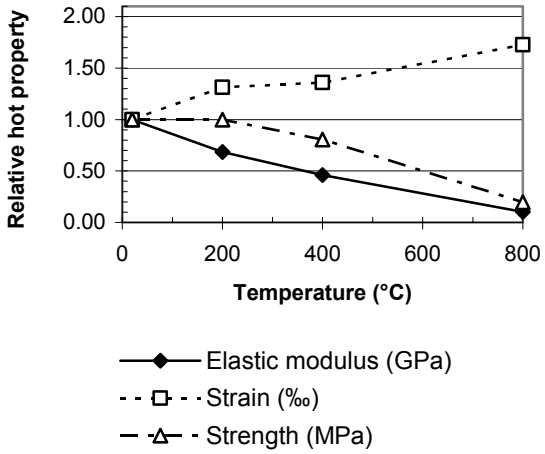

Figure 4.50 – Relative hot property of concrete 70BK0 versus temperature.

5. ANALYSIS

5.1 Optimisation

5.1.1 Optimisation at LTH

Since a great deal of the project was spent on the optimisation of the concrete it was important to analyse the reason for this. The optimisations at LTH were performed under the principles of a linear logarithmic distribution of the particles in the fresh concrete [85-88]. The mix proportions obtained at LTH more or less fulfilled the requirement of workability. The main problem was adding as much as 4 kg/m³ plastic fibres to the mix proportions, which works in the opposite direction to SCC, giving a very stiff mix. Therefore Japanese experience was taken into account by diminishing the maximum size of the aggregate from 16 mm to 11 mm [45-47]. Four kg/m³ of plastic fibres is comparable to 79 kg/m³ steel fibres accounting for the volume that the fibres occupy. The mix proportions with 4 kg/m³ obtained at LTH were later on used during the full-scale production of columns at SPAB [85-88].

5.1.2 Re-optimisation at LTH

In principle, the main problem that initialised the re-optimisation at LTH was that it initially was not possible to adjust the amount of superplasticiser at SPAB in order to achieve a good workability of the SCC. Very small faults of the amount of moisture in the gravel and aggregate or small changes of the particles distribution of the different materials may caused changes of the workability of SCC. Therefore it was suggested to perform control trial mixing of the different concretes before the full-scale production at SPAB. Since this was not possible at SPAB the first half of 2001 the SCC was cast directly without adjusting the amount of superplasticiser. In the first half of 2001 it was not possible the restart the mixer at SPAB once it was stopped after mixing.

The re-optimisation at LTH of the mixes was performed with the principle of gap-grading which increases the workability of the concrete but also the risk of blocking and segregation [89]. During the re-optimisation of the mix proportions the crushed aggregate between 8 and 11 mm was abandoned. The mix proportions obtained by Nordkalk and Svensk Glasåtervinning, SGÅ, at the re-optimisation at LTH more or less fulfilled the requirement of workability. The main problem was the risk of segregation according to the test with the segregation cylinder of following mixes:

- 70AK0
- 70BK0

Another problem during the re-optimisation performed by Nordkalk and SGÅ, at LTH, was the risk of blocking according to the test with the L-box [82,84], of the following mix proportions:

- 40AK4
- 55BK4
- 70BG0
- 70BK4

As mentioned above the mix proportions with 4 kg/m³ plastic fibre performed well at SPAB once the amount of superplasticiser was adjusted afterwards. However, the mix proportion 70 BG0 did not performed well during the fabrication of cylinders at LTH. The mixing had to be repeated twice before acceptable. The main reason was segregation of this mix proportions due to low content of cement + filler (only about 400 kg/m³ which was much less that 450 kg/m³ [48]).

5.1.3 Differences of mixes

Analyses were performed on the differences of particle grading in fresh concrete of the different mixes. In [85] the following particle grading of fresh NC was foreseen, Figure 5.1, Appendix 5.1:

$$s = a \cdot d^b \quad \{0.125 < d < 0.7 \cdot d_{max}\} \qquad (5.1)$$

s denotes particle passing through
a 38%
b constant according to Table 5.1
d particle diameter (0.1 < d < 10 mm)
K cube strength of concrete (MPa)

Table 5.1 - Constant b in equation (5.1)

K	25	60	90	120	150
b	0.32	0.24	0.20	0.18	0.16

Particle grading obtained at LTH is shown in Figure 5.2, Appendix 5.2 [82]. NC followed more or less the grading foreseen in Figure 5.1, i.e. much less fines than in SCC. In Table 5.2 the particles distributions obtained at LTH are given following equation (5.1). For NC and sieves varying between 0.063 mm and 16 mm a = 37% and b varying between b = 0.24 (corresponds to K60) and b = 0.35 (K30) were obtained. For sieves varying between 0.063 mm and 16 mm and SCC without fibres a = 47% was obtained with b varying between b = 0.24 (K60) and b = 0.27 (slightly more inclined, correspond to K30).

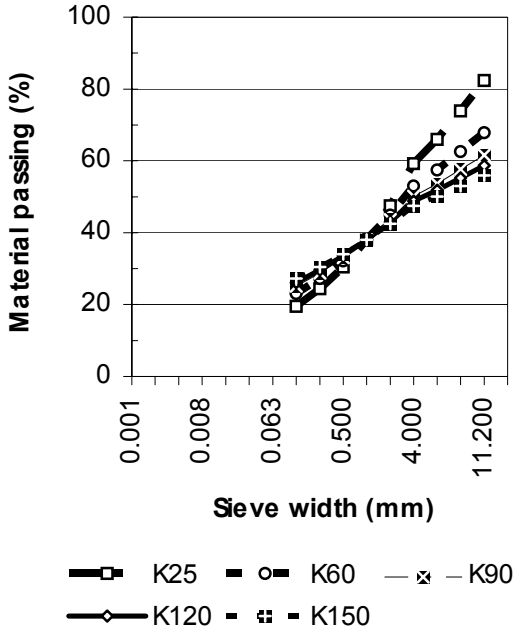

Figure 5.1 – Ideal particle grading of fresh NC.

Table 5.2 - Particle grading obtained at LTH for sieves varying between 0.063 mm and 16 mm.

Concrete	a	b
40AG0	49	0.24
40AK0	48	0.25
40AK4	55	0.24
40BK0	48	0.25
40BR0	37	0.24
55BK0	47	0.27
55BK4	54	0.25
55BR0	38	0.31
70BG0	47	0.26
70BK0	46	0.27
70BK4	56	0.27
70BR0	36	0.35

For sieves varying between 0.063 mm and 16 mm and SCC with 2 kg/m³ polypropylene fibres a = 48% was obtained with b varying between b = 0.23 (corresponds to K60) and b = 0.26 (slightly more inclined, correspond to K30).

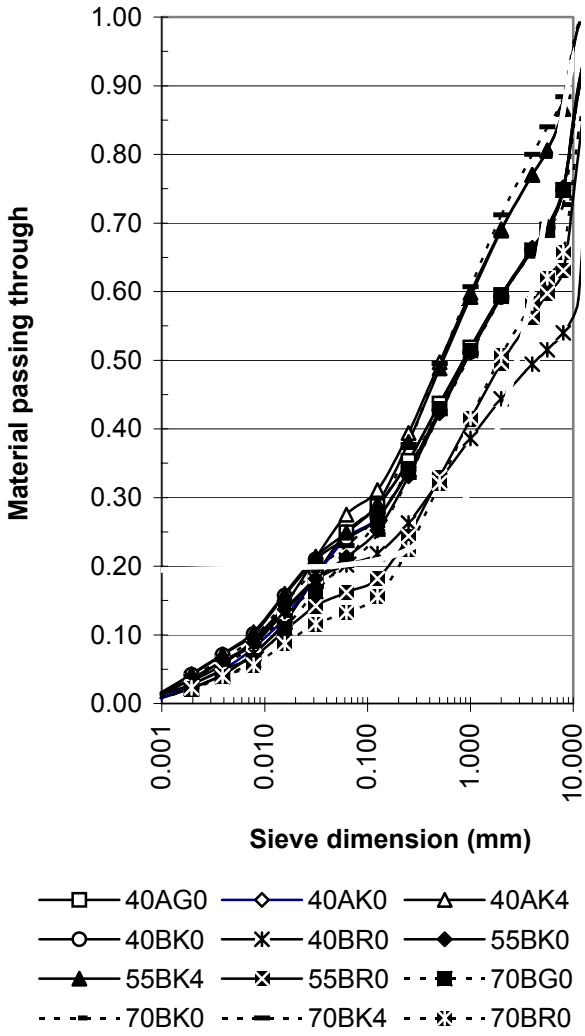

Figure 5.2 – Particle grading obtained at LTH.

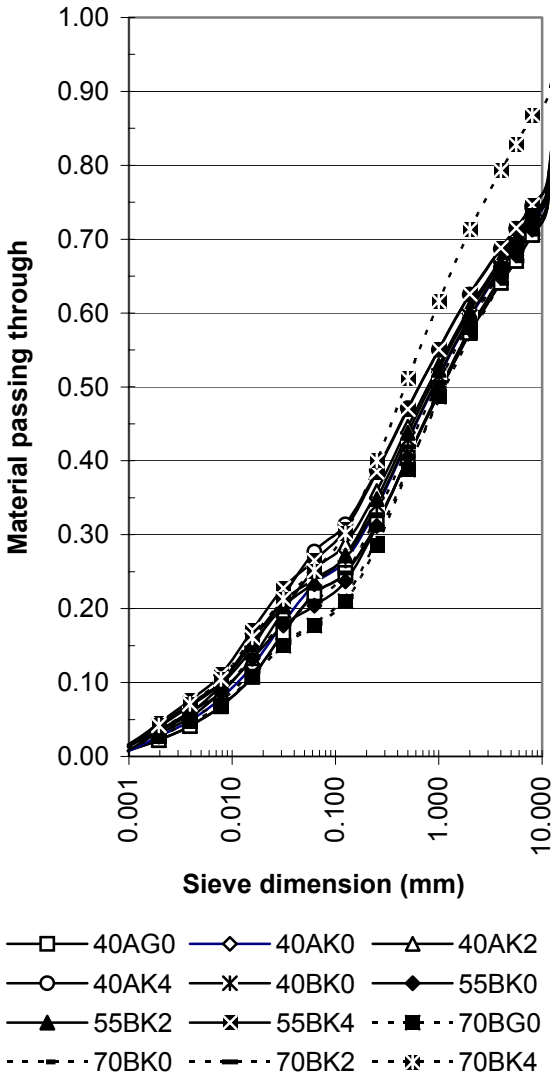

Figure 5.3 – Particle grading by SGÅ and Nordkalk [84].

The conclusion was that much more fines were required in SCC than in NC, about 10% more particles less than 1 mm, i.e. about 220 kg/m³ more fines < 1 mm in SCC than in NC. For SCC corresponding to K60 the inclination of the distribution of the particles in the fresh concrete was more or less the same like in NC, b = 0.24, but for K30 less inclination of the grading curve was observed in SCC than in NC, i.e. the grading of the particles of NC was steeper for K30 made of NC than in a K30 made of SCC [82]. For SCC with 4% plastic fibres a = 55% and b varying between b = 0.24 (K60) and b = 0.27 (K30) was obtained. Japanese experience indicated a = 50% and b = 0.26, i.e. less fines and steeper grading [45-47]. Figure 5.3, Table 5.3 and Appendix 5.3 shows grading of particles of fresh concrete optimised by SGÅ and Nordkalk [84].

Table 5.3 - Particle grading obtained by Nordkalk for sieves between 0.063 mm and 16 mm [84].

Concrete	a	b
40AG0	45	0.25
40AK0	47	0.24
40AK2	49	0.23
40AK4	51	0.21
40BK0	47	0.24
55BK0	45	0.26
55BK2	48	0.24
55BK4	51	0.22
70BG0	43	0.29
70BK0	43	0.28
70BK2	46	0.26
70BK4	51	0.22

Good workability of SCC without fibre as optimised by SGÅ and Nordkalk was obtained with a ≈ 46% and b ≈ 0.24-0.26. Bad workability of SCC without fibre as optimised by SGÅ and Nordkalk was obtained with a ≈ 43% and b ≈ 0.28-0.28 (segregation; too little cement + filler and too steep grading; 70BG0 and 70 BK0). Bad workability of SCC with 4% fibre as optimised by Nordkalk was obtained with a = 51% and b = 0.22 (blocking; too little cement + filler and too flat grading). Japanese experience indicated that a = 50% and b = 0.26 was needed in order to obtain good workability of SCC [45], i.e. much less steep grading than foreseen by Nordkalk [84].

5.1.4 Conclusions on particle grading

The following consideration should be taken when constructing a grading curve for fresh SCC without fibre as described by equation (5.1):

$$s = a \cdot d^b \quad \{0.125 < d < 0.7 \cdot d_{max}\} \qquad (5.1)$$

s denotes particle passing through

d particle diameter (mm)

- a = 47%
- b = 0.27 (K30)
- b = 0.24 (K60)

With 2 kg/m³ polypropylene fibres the following constants in equation (5.1):

- a = 48%
- b = 0.26 (K30)
- b = 0.23 (K60)

With 4 kg/m³ fibres the following constants in equation (5.1):

- a = 55%
- b = 0.27 (K30)
- b = 0.24 (K60)

Little cement + filler in SCC gave a risk of segregation. i.e. low a-value in equation (5.1); too flat grading gave a risk of blocking for concrete with 4% fibres, i.e. too low b-value in equation (5.1).

5.2 Strength

5.2.1 Effect of fibres

Figure 5.4 shows the effect of fibres on strength based on this limited investigation. The filler, aggregate and the cement content was change simultaneously when the fibres were added. Thus it is a combined effect shown in Figure 5.4. The following equation was evaluated:

$$f_{c28ppf} = f_{c280} \cdot (1 - 0.023 \cdot ppf) \qquad (5.2)$$

ppf denotes amount of 32 µm polypropylene fibre ($0 < ppf < 4$ kg/m³)

f_{c28ppf} denotes 28-day strength (fibre, MPa)

f_{c280} denotes 28-day strength (no fibre, $30 < f_{c280} < 60$ MPa)

5.2.1 Effect of filler

Figure 5.5 shows the effect of filler but also some effect of change of cement content based on this limited investigation. Adding filler was beneficial for strength. For concrete 40BK the amount of coarse aggregate was diminished from 1004 to 602 kg/m³, which explains the negative effect of filler observed. The effect of filler was evaluated:

$$f_{c28f} = f_{c280} + f \cdot 0.07 \qquad (5.3)$$

f denotes limestone/glass filler ($0 < f < 250$ kg/m³)

f_{c28f} denotes 28-day strength with filler (MPa)

f_{c280} denotes 28-day strength (no filler, $30 < f_{c280} <$ 60 MPa MPa)

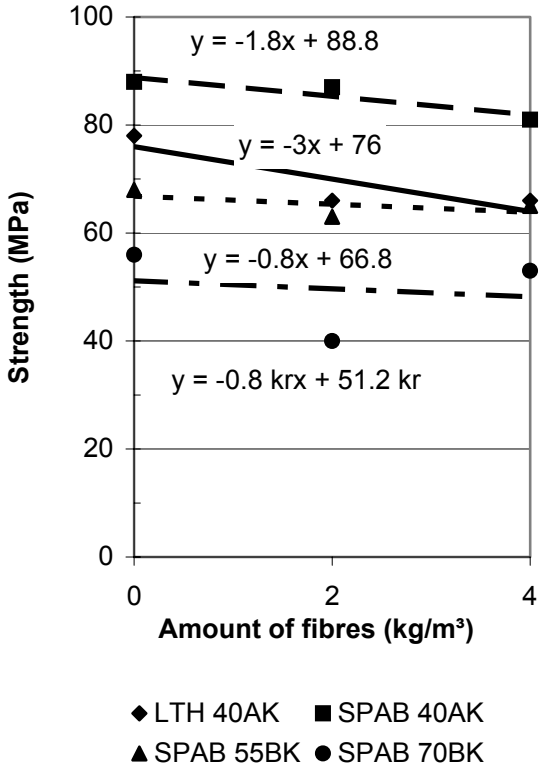

Figure 5.4 - Effect of fibres on strength.

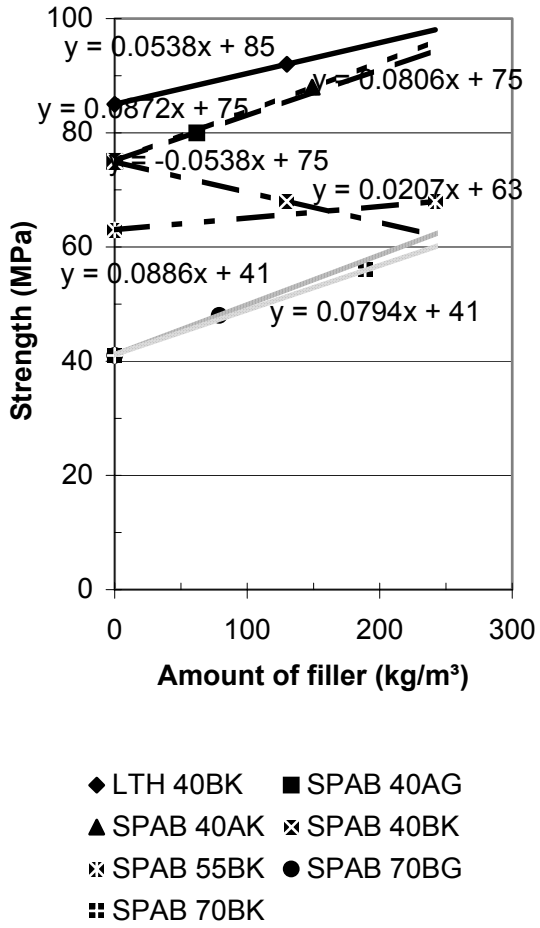

Figure 5.5 - Effect of filler on strength.

The strength development before 28-day age was more dependent on the cement type than the content of filler in the concrete. At w/c = 0.40 one-day strength was twice as large with Byggcement compared with Degerhamn Cement. A logarithmic development of strength was evaluated. For Byggcement the following strength increase rate, $\delta f_c/\delta t$, was obtained (MPa/day):

$$\delta f_c/\delta t = 9/t \qquad (5.4)$$

and for Degerhamn cement:

$$\delta f_c/\delta t = 18/t \qquad (5.5)$$

t denotes concrete age ($2 < t < 28$ days)

5.3 Unstressed properties

5.3.1 Residual properties at 20 °C

Figures 5.6-8 and Appendix 5.4 show the residual properties of the concrete at 20 °C (residual elastic modulus, residual strength and residual strain at maximum strength). After heating to 800 °C the concrete with limestone powder did not exhibit any residual strength after cooling to 20 °C. Figure 5.9-11 show the relative residual properties of the concrete at 20 °C (residual elastic modulus, residual strength and residual strain at maximum strength). Figure 5.12 shows the on average residual properties of the concrete except for concrete with limestone powder at 800 °C.

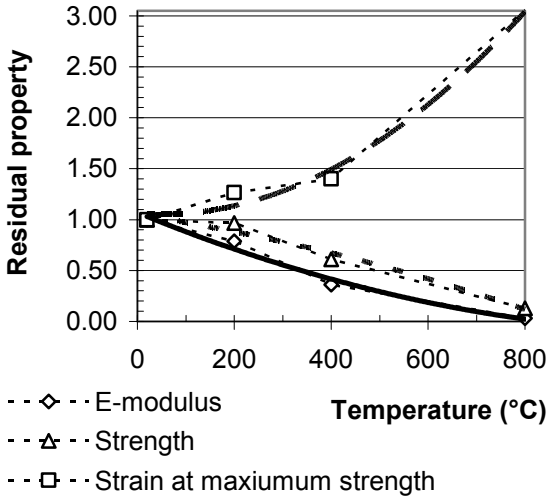

Figure 5.12 - Residual properties after cooling to 20 °C and RH = about 40% 1 week from elevated temperature except with limestone powder at 800 °C (= 0; one point = 16 measurements average).

5.3.2 Hot properties

Figures 5.13-19 and Appendix 5.5 show the corresponding hot properties of the concrete at elevated temperatures. In this case strength still was observed at 800 °C even for concrete with limestone powder.

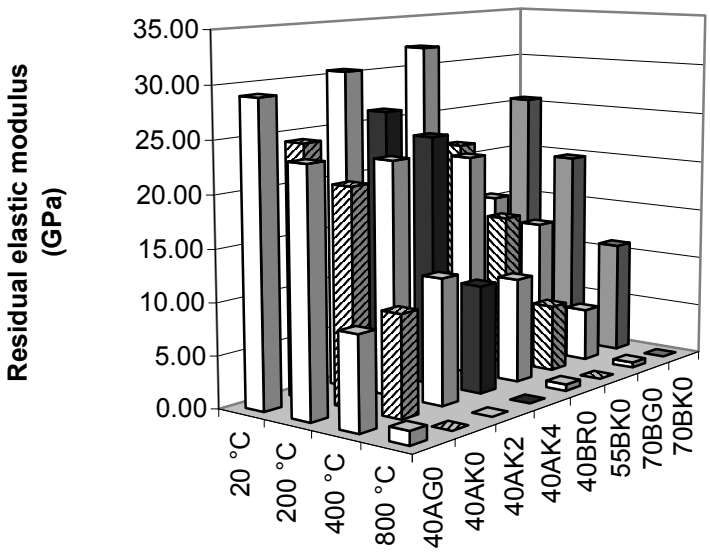

Figure 5.6 – Residual elastic modulus at 20 °C.

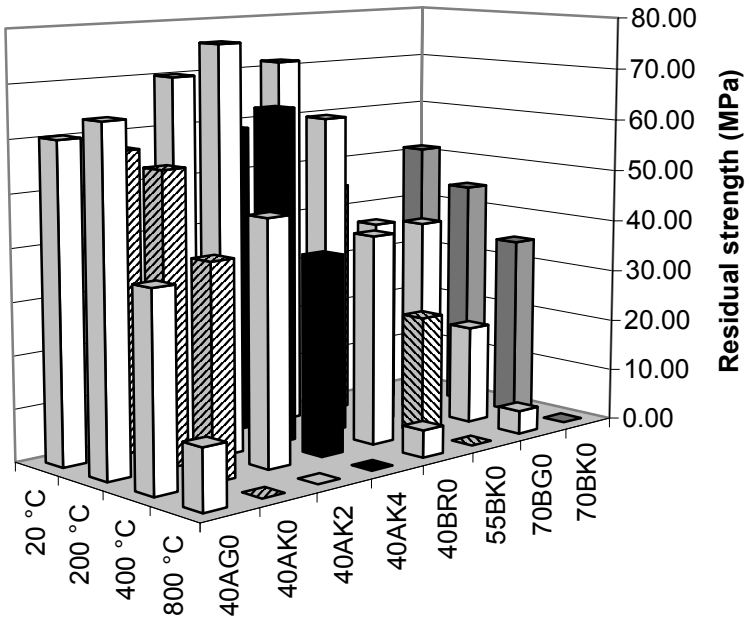

Figure 5.7 – Residual strength at 20 °C.

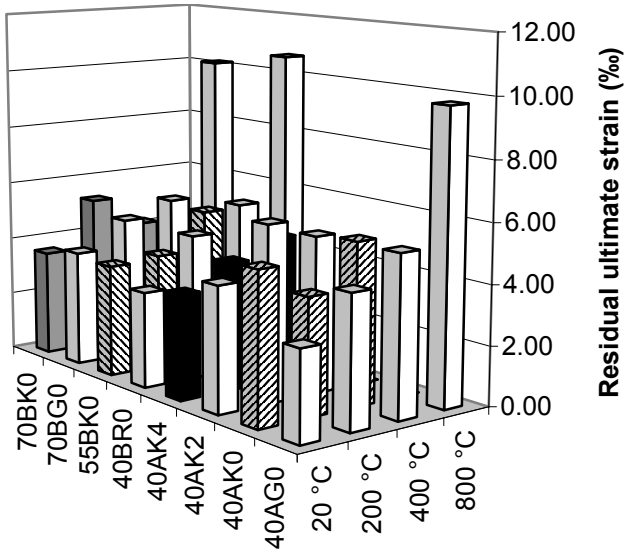

Figure 5.8 – Residual strain at maximum strength at 20 °C.

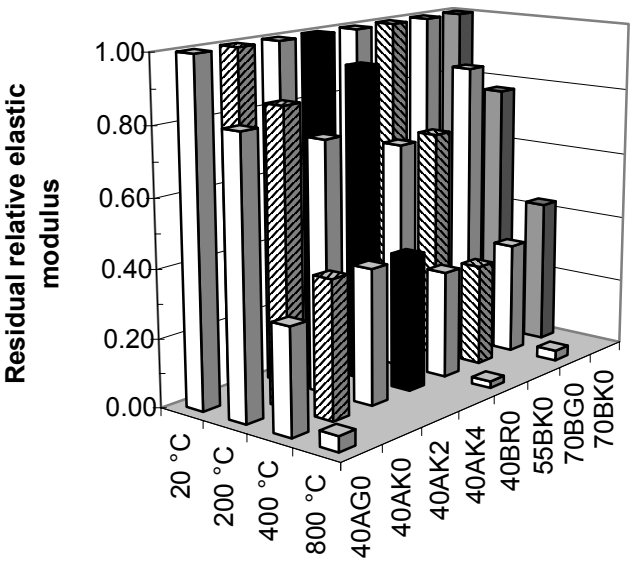

Figure 5.9 – Residual relative elastic modulus at 20 °C (= 0 at 800 °C for concrete with limestone powder).

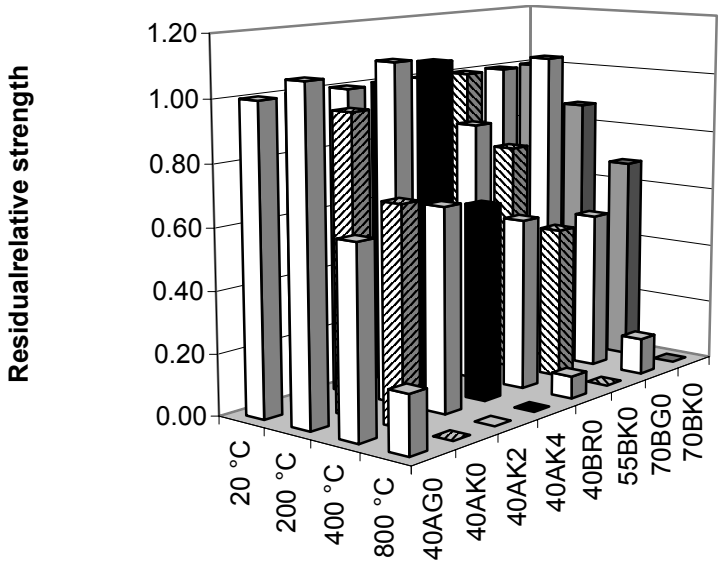

Figure 5.10 – Residual relative strength at 20 °C (= 0 at 800 °C for concrete with limestone powder).

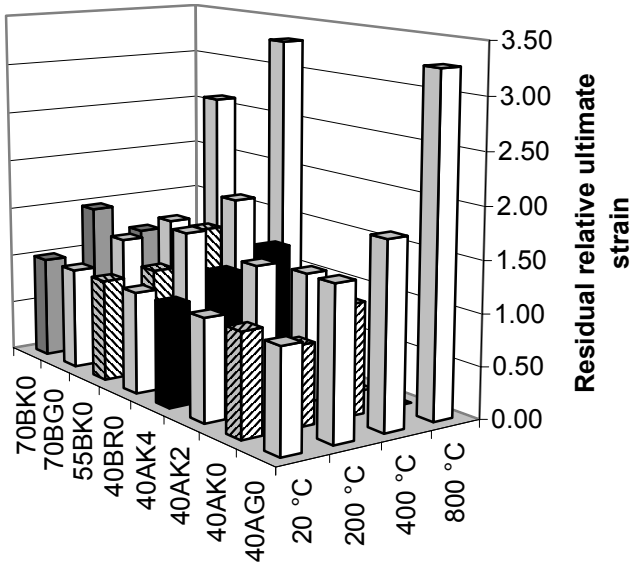

Figure 5.11 – Residual relative strain at maximum strength at 20 °C (= 0 at 800 °C for concrete with limestone powder).

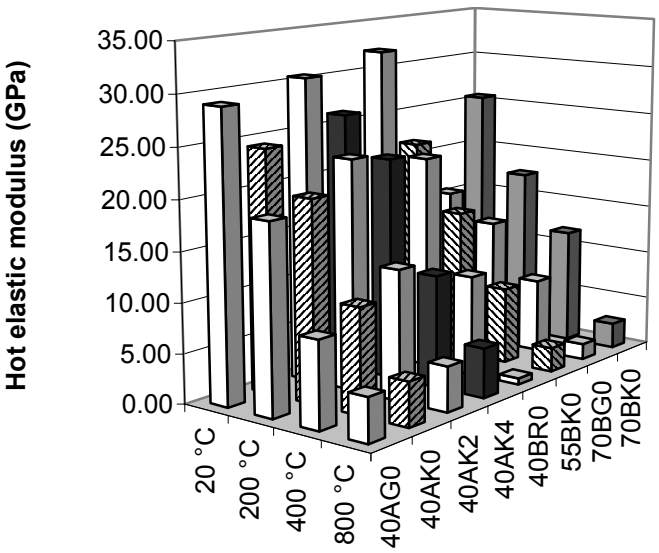

Figure 5.13 – Hot elastic modulus at 20 °C.

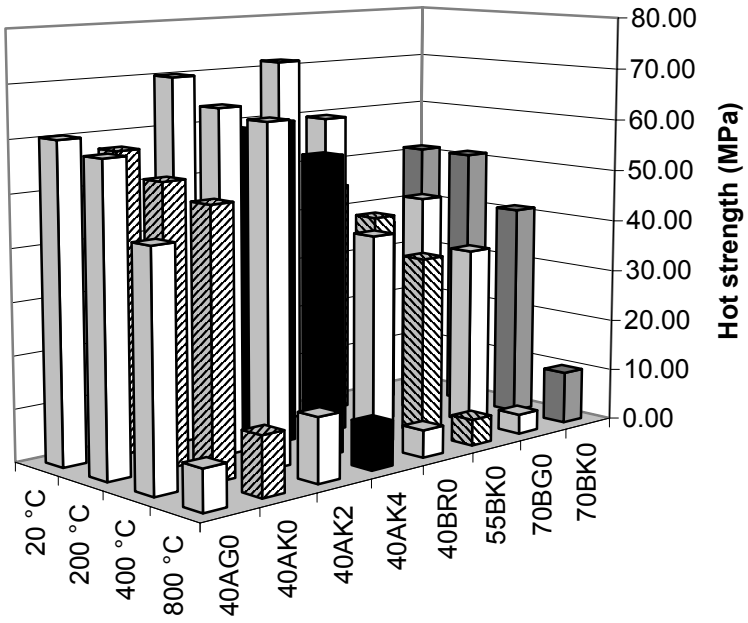

Figure 5.14 – Hot strength at 20 °C.

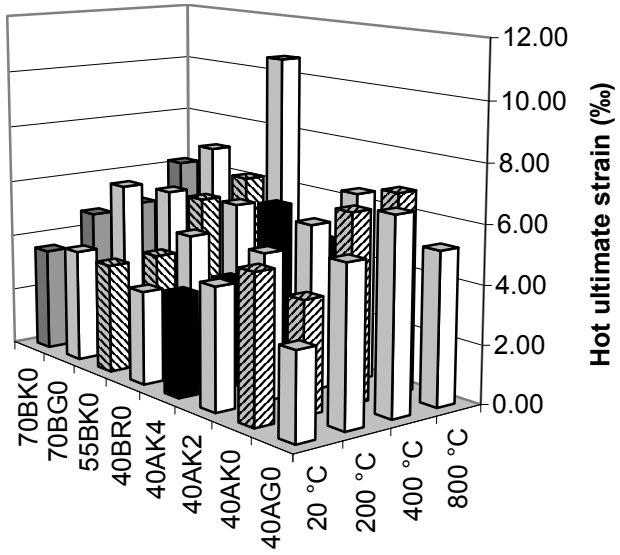

Figure 5.15 – Hot strain at maximum strength at 20 °C.

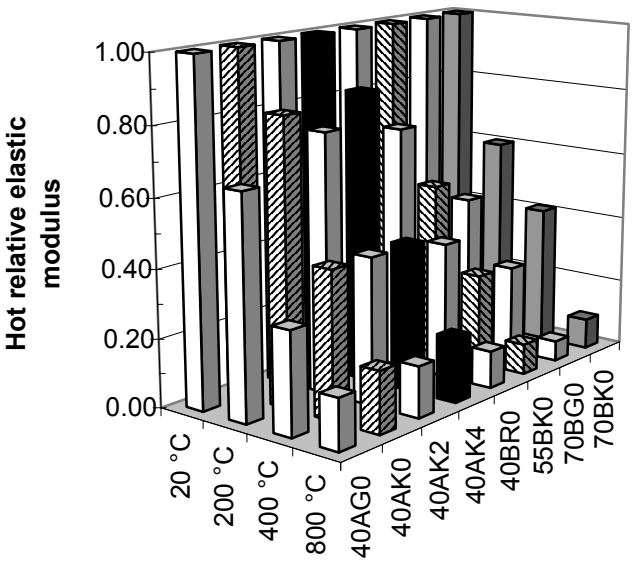

Figure 5.16 – Hot relative elastic modulus at 20 °C.

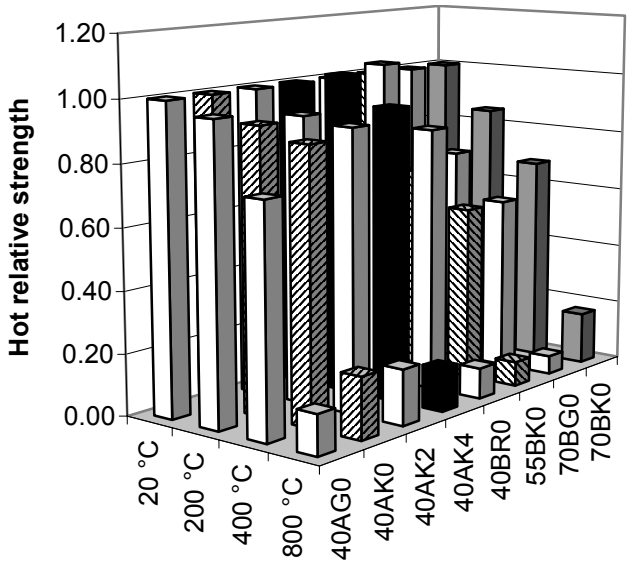

Figure 5.17 – Hot relative strength at 20 °C.

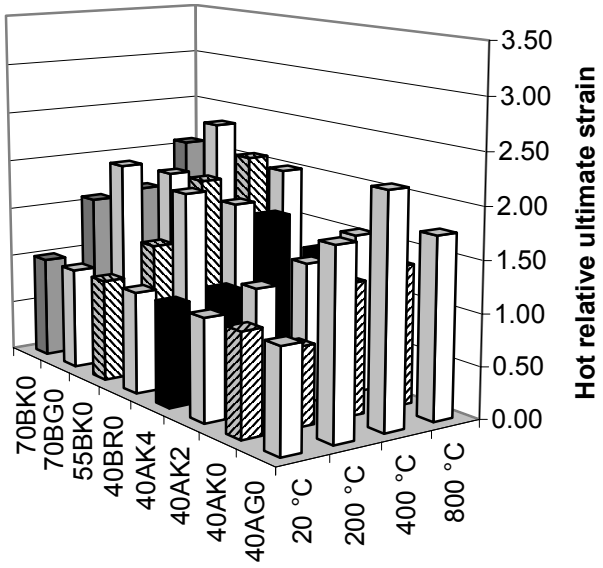

Figure 5.18 – Hot relative strain at maximum strength at 20 °C.

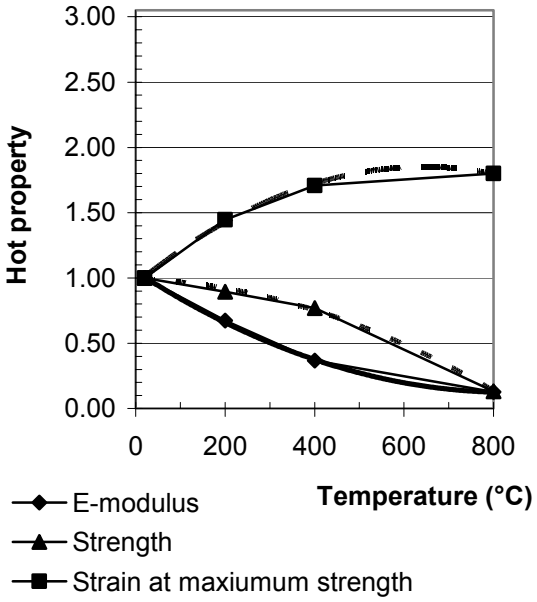

Figure 5.19 - Summary on average of hot properties (each point represents average on 16 measurements).

5.3.3 Formulas

The following formula was obtained for the relative properties after or at elevated temperature, Figure 5.12 and 5.19.

$$r = c \cdot T^2 + e \cdot T + g \qquad (5.6)$$

c,e,g constants for hot and residual properties of concrete at and after elevated temperatures given in Table 5.4.

r denotes residual and hot relative properties of concrete at and after elevated temperatures.

T denotes temperature ($20 < T < 800$ °C).

Table 5.4 – Constants in equation (5.2).

Property	Constant	Hot	Residual
E-modulus	c	0.0000013	0.00000080
	e	- 0.00221	-0.00196
	g	1.04	1.04
Strength	c	-0.0000012	-0.0000005
	e	- 0.000131	- 0.000729
	g	0.99	1.01
Strain	c	-0.0000022	0.0000035
	ec	0.00279	- 0.000301
	g	0.95	1

Elastic modulus of concrete behaved similar during high temperature and after cooling. However, strength and strain differed somewhat due to the testing temperature, Figure 5.20. Generally, residual strength was lower after cooling than at high temperature due to movements between the cement paste and the aggregate, Figure 2.4.

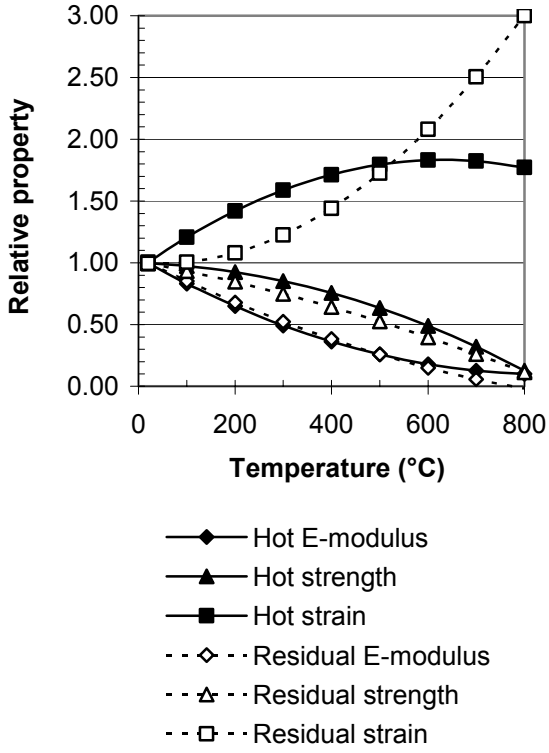

Figure 5.20 – Relative properties at/after elevated temperature with equation (5.6) except for residual property with limestone powder at 800 °C.

5.3.4 Comparison with others

First of all a comparison was done with a concrete with cylinder strength, f_c = 27.5 MPa, Figure 5.21 [90,91]. Figure 5.21 shows the hot and residual strength according to equation (5.6) and [90,91]. The hot strength coincide well between the experiments and [88,91] except for the temperature between 200 °C and 500 °C where the experiments showed about 15% larger strength than [90,91]. The residual strength from the experiments and [90,91] coincided well. Figure 5.22 shows the experimental hot strength at high temperature according to equation (5.6) and the corresponding strength according to Figure 2.1 [16]. The strength with light weight aggregate Leca is also shown (higher strength than with quartzite aggregate). The reference strength was somewhat lower at 150 °C than obtained in the experiments, Figure 5.22 [16]. According to Figure 5.23 the experiments showed slightly larger hot strength, about 7%, than [16] did. The results of the residual strength coincided well between the experiments and [16]. Figure 5.24 show that the experimental results coincided well with the Eurocode Siliceous material which aggregate was used in this case [40]. Compared with the CEB code and the Finnish code RakMP HPC, the experiments of SCC showed larger relative strength above 300 °C, Figure 2.49, Figure 5.24, Table 5.5 [40].

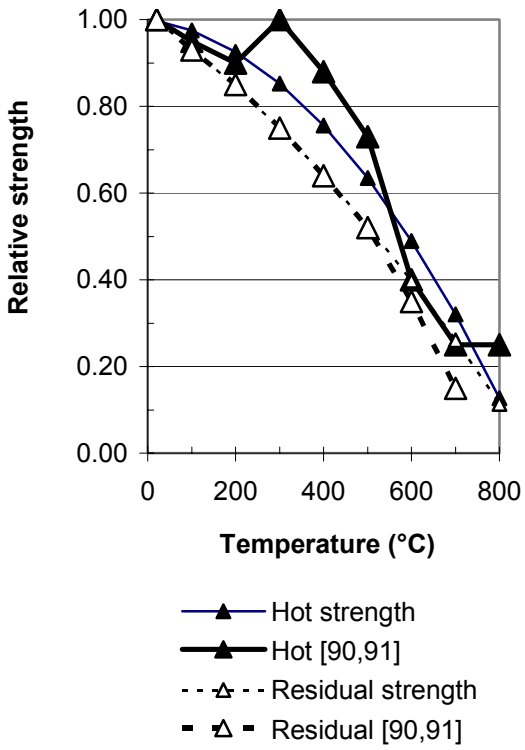

Figure 5.21 - Hot and residual strength according to equation (5.6) and [90,91].

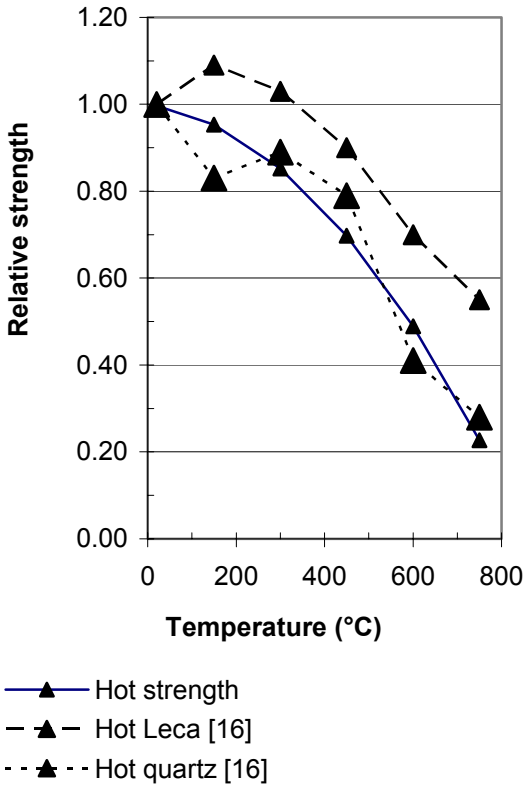

Figure 5.22 - Hot strength according to equation (5.6) and corresponding strength, Figure 2.1 [16].

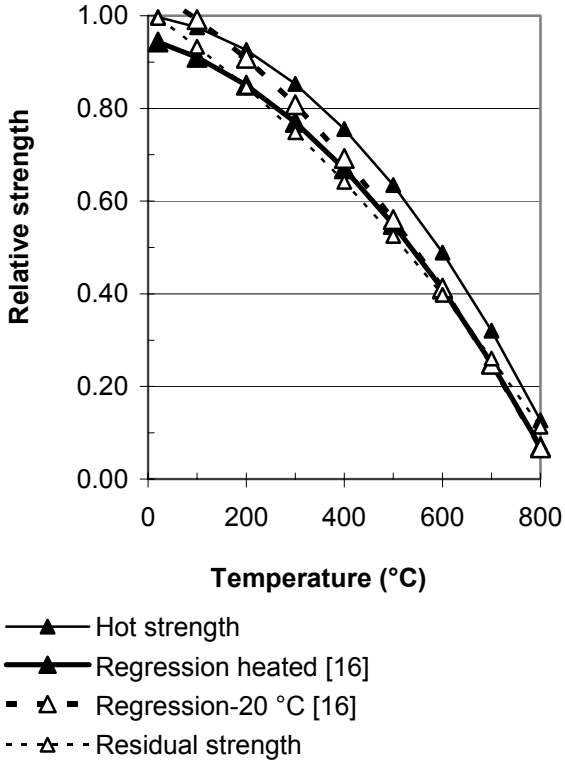

Figure 5.23 - Hot and residual strength according to experiments and figure 2.11 [16].

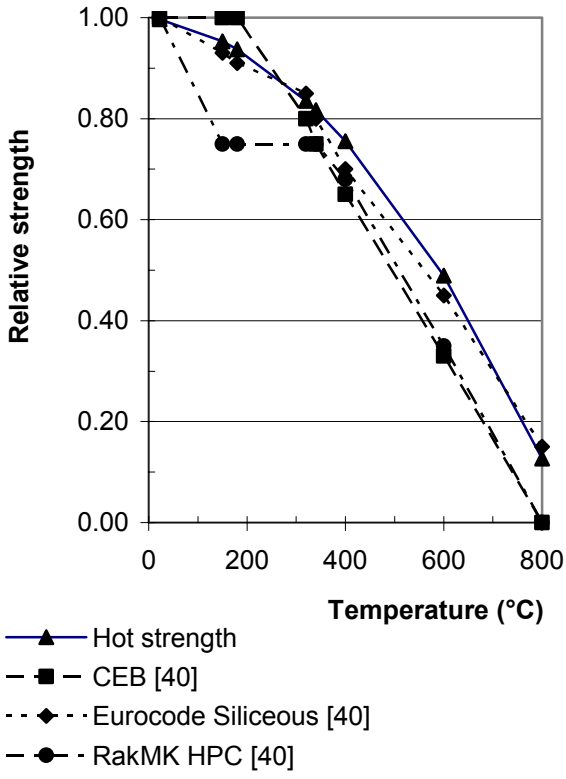

Figure 5.24 - Hot strength (64 specimens), CEB, Eurocode Siliceous and RakMP HPC code [40].

At 180 °C CEB showed about 5% larger relative strength than the experimental results on 16 specimens indicated but the RakMP HPC code, on the other hand about 20% lower relative strength [40]. The present study showed half the elastic modulus at 500 °C compared with [40], Figure 5.25.

Table 5.5 – Comparison of hot strength (in all 64 specimens), CEB and RakMP HPC code [40].

Temperature (°C)	CEB	RakMK HPC
20	0.00	0.00
150	-0.05	0.20
180	-0.06	0.19
320	0.04	0.09
340	0.07	0.07
400	0.11	0.08
600	0.16	0.14
800	0.13	0.13
Average	0.05	0.11

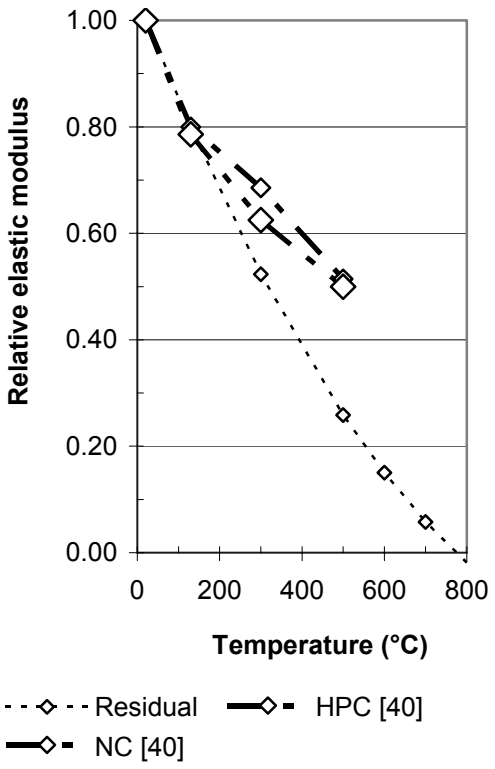

Figure 5.25 – E-modulus compared with [38].

5.4 Elastic modulus

5.4.1 Dynamic elastic modulus

Before each stress/strain tests, the dynamic elastic modulus, E_{dyn}, was established by measurements of the fundamental resonance frequency, FRF, in the 100 mm cylinders, 200 mm in length. A non-destructive testing method of the elastic modulus was of great interest for the purpose of studying damage in the concrete that was related to possible interior detriment due to, for example, heating. E_{dyn}, of SCC was detected by the FRF. A vibration was applied to the centre of the SCC specimen and FRF obtained at one end of the specimen. The evaluation of E_{dyn} was dependent on the weight, the shape of the specimen, RH and on Poisson's ratio. Xu studied E_{dyn} on prisms of cement mortar stored at different ambient RH and supposed to be equal to the internal RH [92]. A large dependence of RH on E_{dyn} was found to exist [25,92]. Between RH = 0.40 and RH = 0.95 E_{dyn} rose from 30 to around 36 GPa, i.e. ≈ 20%. It was the objective of the studies of E_{dyn} to compare the results with the static modulus of elasticity (at loading in the stress/strain tests), E_{stat}, of the SCC specimens. It was also the aim of the studies to correlate the influence of moisture on the measured E_{dyn}.

5.4.2 Evaluation of dynamic elastic modulus

Right before the stress/strain tests of the very same specimen was tested related to E_{dyn}. Supplementary tests were also performed. During test conditions according to Section 3 applied. The following testing procedure was used:

- Weight and shape were measured.
- FRF was detected by a pickup applied to the centre at one side of the concrete specimen.
- The driver (vibrator) was placed at one side of one end of the specimen.
- RH measured on fragment (parallel specimen)
- Calibration of RH devices according to [26].
- E_{dyn} was taken within ½ h of the stress/strain.
- Poisson's ratio, υ, was assumed to be υ=1/6.

The evaluation of E_{dyn} was carried out according to ASTM C 215-85 [93]:

$$E_{dyn} = 0.00416 \cdot (L^3 \cdot T/d^4) \cdot W \cdot n^2 \qquad (5.7)$$

D denotes the diameter of the specimen (in.)
n denotes FRF (Hz)
K ratio of gyration (=d/4 for cylinder)
L denotes the length (in.)
T = 1.09 for υ=1/6 and K/L=0.125 [=100/(4·200]
W denotes the weight of the specimen (lb.)

A simplification was done of equation (5.7, GPa):

$$E_{dyn} = 2.14 \cdot 10^{-6} \, G \cdot n^2 \qquad (5.8)$$

G denotes the weight (kg)

5.4.3 Comparison between E_{dyn} and E_{stat}

Table 5.6 gives Figures and Appendices with an experimental comparison between E_{dyn}, E_{stat} and strength. Table 5.7 gives a summary of the constants h and j in the following equation (GPa):

$$E = (h \cdot (f_c) + j) \cdot f_c \qquad (5.9)$$

f_c denotes cylinder strength (MPa)
h,j denotes constants given in Table 5.6
E denotes elastic modulus (GPa)

Table 5.6 - Figures and Appendices with comparison between E_{dyn}, E_{stat} and compressive strength.

Temperature (°C)	Appendix	Figure
20-20	5.6, 5.13	5.26
200–20	5.7, 5.14	5.27
200-200	5.8, 5.15	6.28
400-20	5.9, 5.16	5.29
400-400	5.10, 5.17	5.30
800-20	5.11, 5.18	5.31
800-800	5.12, 5.19	5.32

400-20 = heated to 400 °C, tested at 20 °C.

Table 5.7 - Constants h and j in equation (5.9).

Temp. (°C)	E_{dyn}, h	E_{dyn}, j	E_{stat}, h	E_{stat}, j
20-20	-0.00412	0.821	-0.00079	0.500
200–20			-0.00240	0.503
200-200			0.00021	0.334
400-20			-0.0014	0.319
400-400			-0.00075	0.252
800-20	0.0014	0.201	-0.00107	0.127
800-800			-0.031	0.74

400-20 = heated to 400 °C, tested at 20 °C.

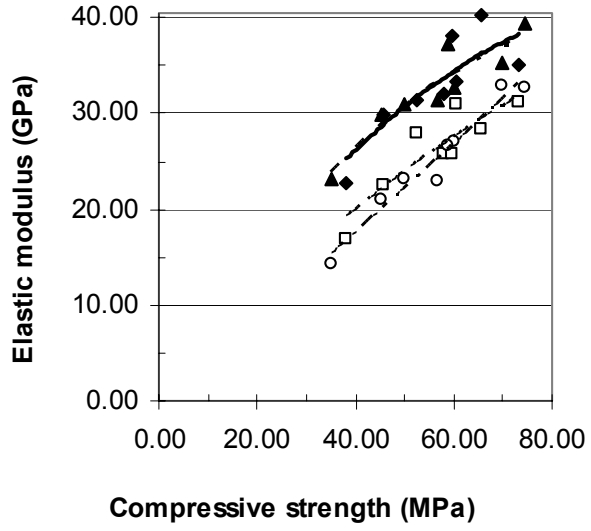

Figure 5.26 - E_{dyn} and E_{stat} versus compressive strength at 20 °C.

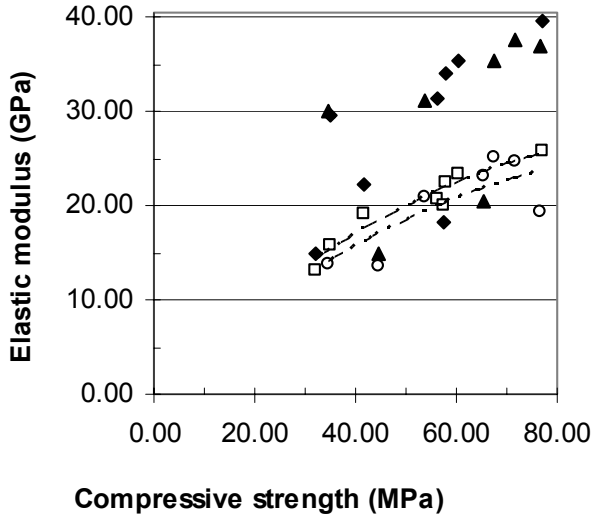

Figure 5.27 - E_{dyn} and E_{stat} versus compressive strength at 20 °C after heating to 200 °C.

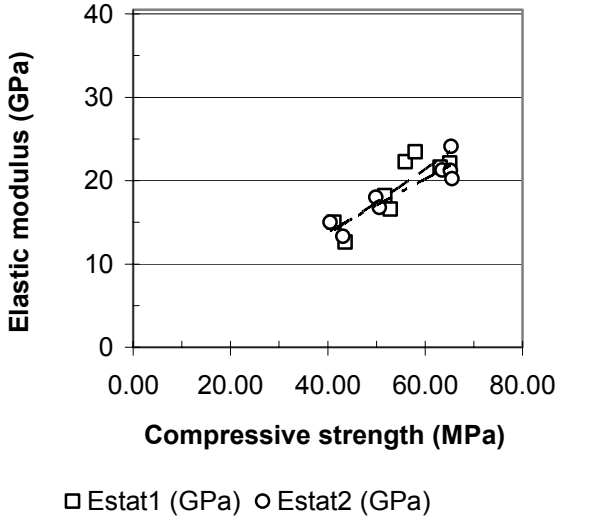

Figure 5.28 - E_{dyn} and E_{stat} versus compressive strength after heating to 200 °C.

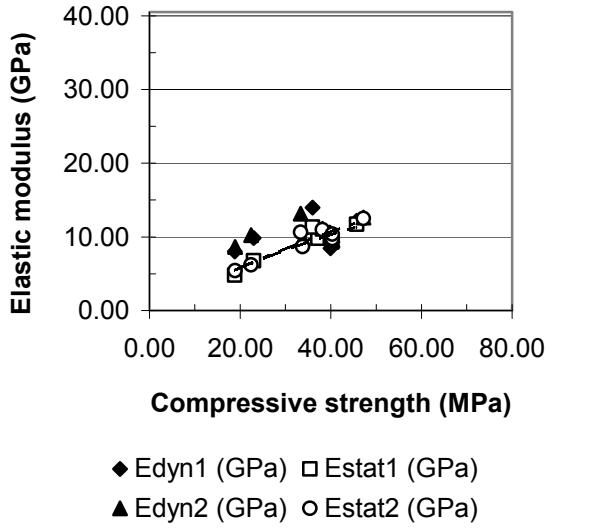

Figure 5.29 - E_{dyn} and E_{stat} versus compressive strength at 20 °C after heating to 400 °C.

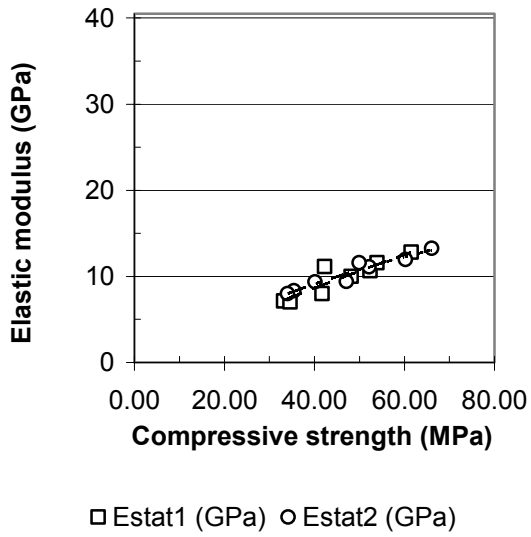

Figure 5.30 - E_{dyn} and E_{stat} versus compressive strength after heating to 400 °C.

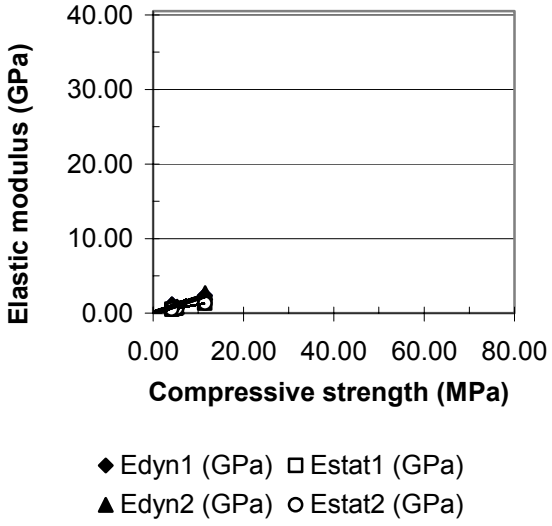

Figure 5.31 - E_{dyn} and E_{stat} versus compressive strength at 20 °C after heating to 800 °C.

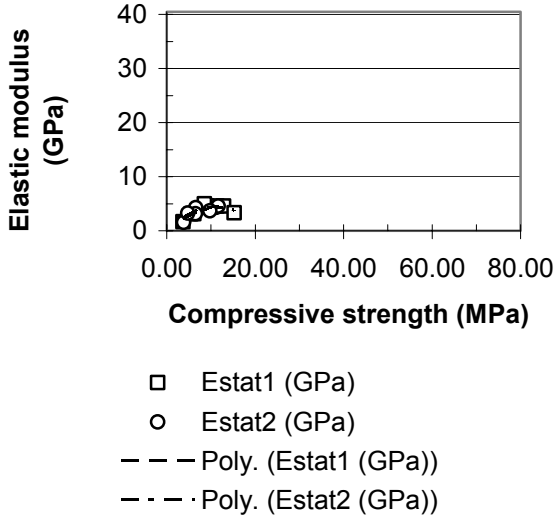

Figure 5.32 - E_{dyn} and E_{stat} versus compressive strength after heating to 800 °C.

5.4.4 Elastic moduli, E_{dyn} and E_{stat}

Based on the experimental results given in Tables 5.6-5.7 the following formulas were obtained on the elastic modulus, E, Figure 5.33-5.35 (GPa):

$$E_{dyn} = ((0.0000071 \cdot T - 0.00426) \cdot (f_c) + (-0.00079 \cdot T + 0.837)) \cdot (f_c) \quad (5.10)$$

$$E_{stat,hot} = ((-0.0000000916 \cdot (T)^2 + 0.0000374 \cdot T - 0.00211) \cdot (f_c) + (0.00000232 \cdot (T)^2 - 0.00161 \cdot T + 0.540)) \cdot f_c \quad (5.11)$$

$$E_{stat,residual} = (-0.00152 \cdot (f_c) + (-0.000263 \cdot T + 0.507)) \cdot (f_c) \quad (5.12)$$

f_c denotes cylinder strength ($5 < f_c < 60$ MPa)

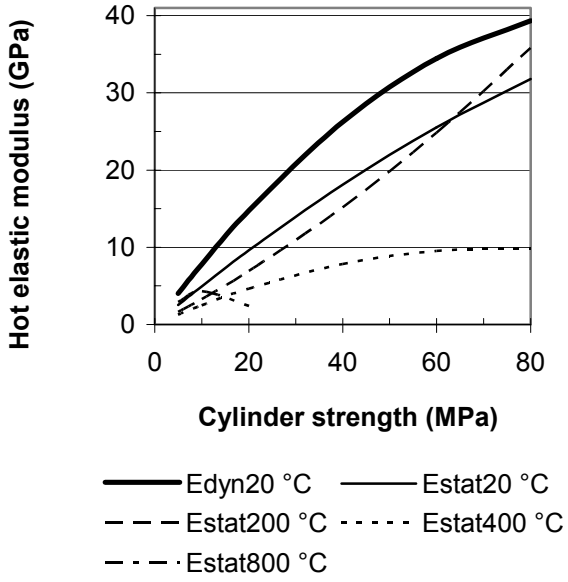

Figure 5.33 – Hot elastic modulus at different temperatures versus cylinder strength.

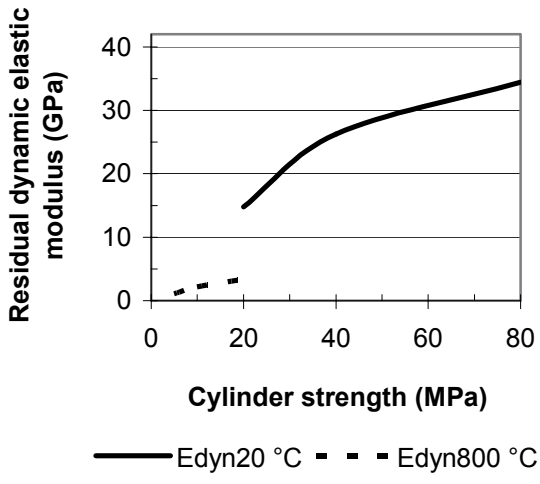

Figure 5.34 – Dynamic modulus at 20 °C and dynamic elastic modulus at 20 °C after heating to 800 °C versus cylinder strength.

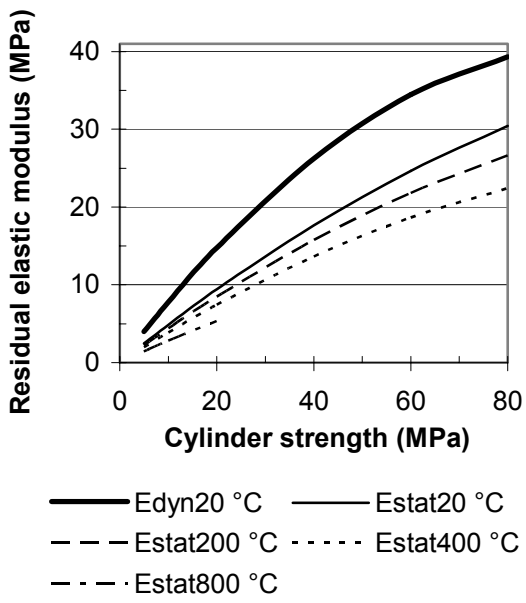

Figure 5.35 – Dynamic and static elastic modulus at 20 °C after heating versus cylinder strength.

5.5 Moisture losses at heating

In Figure 5.36 and Appendix 5.20 the moisture losses of different concretes are compared to [40,94]. The reference concrete, BR0, and concrete with high w/c normally give the smallest weight losses at 400 °C since these concrete contains a larger amount of aggregate. However, at 800 °C all weight was lost of limestone filler concrete AK and BK since the specimen showed no strength after cooling, Figure 5.36. At 800 °C about 94% of the initial weight remains of the reference concrete 40BR0 and of the glass filler concrete 70BG0 due to large aggregate content.

5.6 Comparison of RH in columns and cylinders

Figure 5.37 and Appendix 5.21 show RH at 20 °C before heating, both of columns, 200 x 200 mm and 2 m long, cast of the same concrete like in the experiments with cylinders and of cylinders [94]. A comparison showed that RH of water-cured columns was somewhat smaller than that of cylinders which is a size effect and explained by the effect of self-desiccation. In larger specimen (columns 200 x 200 mm) the effect of self-desiccation is more pronounced than in a cylinder 100 mm in diameter. On the other hand air-cured cylinders showed lower RH than the columns, even after ½ a years, Figure 5.37

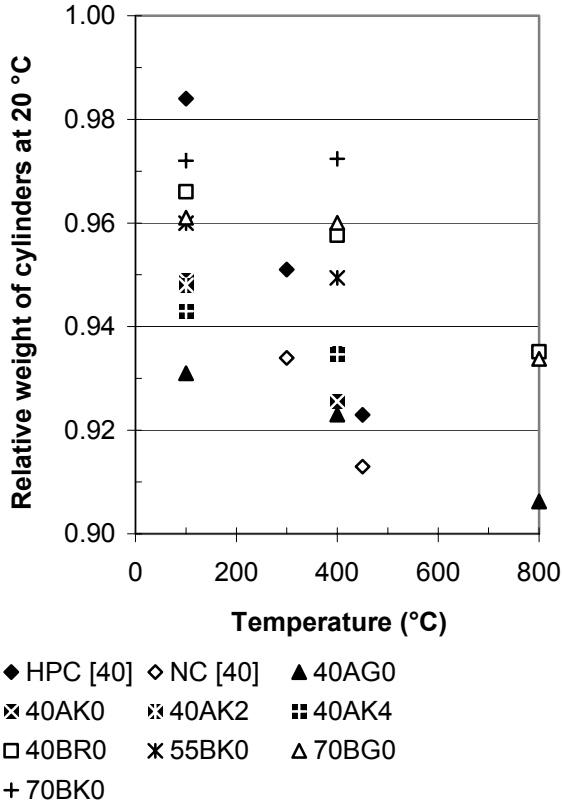

Figure 5.36 - Moisture losses [40,94].

5.7 Spalling of cylinders at slow heating

Even at slow heating rate, 240 °C/h., a small, water-cured specimen, cylinders 100 mm in diameter, showed explosive spalling. The following conditions were observed at the time of spalling:

External temperature:	350 °C
Internal temperature:	185 °C
Heating rate	240 °C/h

It was great interest to compare the conditions at explosive spalling of the cylinder with previous studies, Figure 2.43, also cylinders 100 mm in diameter [40]. The following values were calculated for the present cylinders:

Temperature gradient:	3300 °C/m
Temperature rate: 4 °C/min.=	360 °C/h
Gradient-rate ratio:	825 min/m

However, the values of the present exploding cylinder and the previous studies did not coincide probably since different concrete were used. Anyhow the heating rate exceeded 120-180 °C/h in the present experiments with probably was the critical parameter in this case [79].

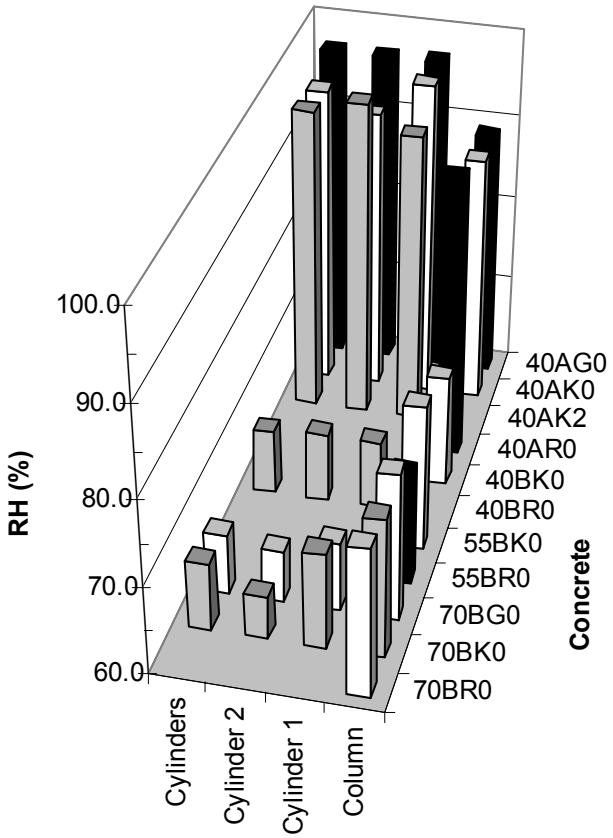

Figure 5.37 - RH at 20 °C before heating, of columns, 200 x 200 mm [95] and of cylinders, 100 mm in diameter.

6. TEST SIGNIFICANCES AND SOURCES OF ERROR

6.1 Sources of error

The following sources of error may be identified:

- Weighing faults at fabrication of concrete
- Moisture differences of aggregate
- Curing faults
- Variance in loading rate at testing
- Equipment faults at testing
- Exchange of specimens
- Age of specimens
- Temperature measurements and changes

6.2 Test significance

The moisture of the aggregate was taken daily before mixing in order to avoid any difference of water added to the mix proportions. The weight of the materials in the mix proportions was double checked and sometime checked three times before the mixing took place (in the field test the weight was measured automatically by computer). The concrete was possible to mix within a w/c-fault of ± 0.002, i.e. a fault of about ± 2 MPa. The variation of RH during curing was measured continuously and measured to be ± 3% RH. In the field tests the ambient RH was used which probably gave a larger in RH than in the laboratory. Figures 6.1-3, Table 6.1 and Appendix 6 show the test significance of repeated laboratory tests at LTH, in all three tests. The test results of the strength and of elastic modulus at high temperature in the oven at LTH showed good test significance while the test significance of the strain tests was lower (however, less than 10% variance).

Table 6.1 – Test significance of repeated laboratory tests at LTH, in all three tests.

Test/Concrete			
Elastic modulus (GPa)	Std	Average	Varians (%)
40BR0-200-200	0.87	20.46	4.27
70BG0-200-200	0.45	12.74	3.51
70BK0-200-200	2.51	19.19	13.05
Strain (per mil)	Std	Average	Varians (%)
40BR0-200-200	0.52	5.41	9.59
70BG0-200-200	0.51	6.25	8.12
70BK0-200-200	0.25	4.86	5.05
Strength (MPa)	Std	Average	Varians (%)
40BR0-200-200	1.61	65.21	2.48
70BG0-200-200	0.20	43.33	0.46
70BK0-200-200	1.11	51.88	2.13

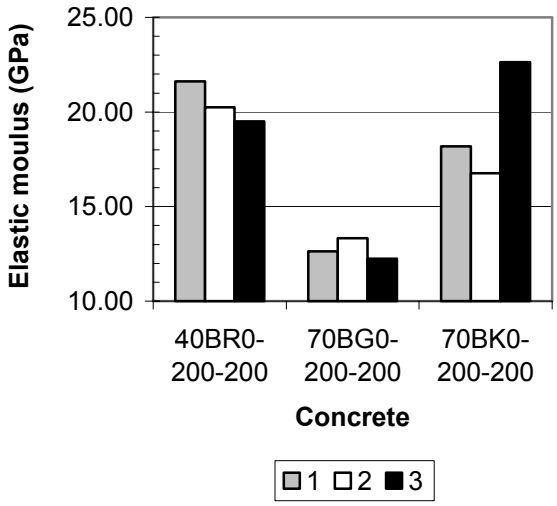

Figure 6.1 – Test significance of elastic modulus.

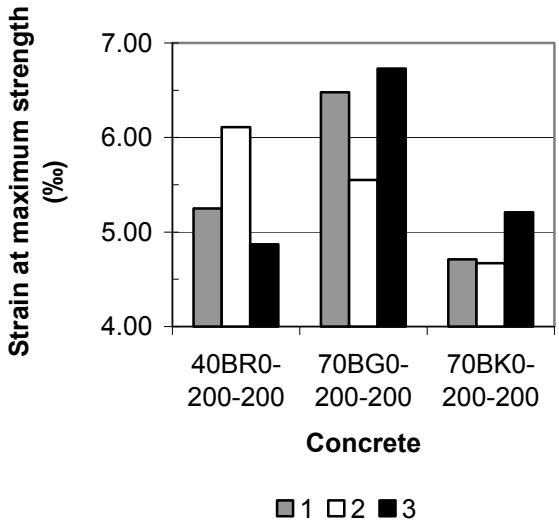

Figure 6.2 – Test significance of strain (‰).

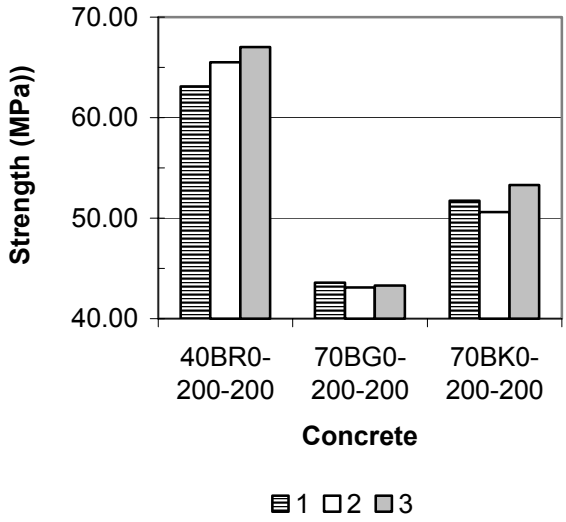

Figure 6.3 – Test significance of strength (MPa).

7. SUPPLEMENTARY TESTS

7.1 General

Concrete with lime stone powder showed no strength after cooling from 800 °C. Therefore it was of great interest to measure the properties after heating to 600 °C using precisely the same method like on tests at other temperatures. The objective of the Supplementary tests was to obtain residual elastic modulus, residual strength and residual strain at ultimate strength. It was also of great interest to measure the porosity and the resistance to water penetration of the concrete since it affected the strength, elastic modulus and also the risk of fire spalling. The objectives of the Supplementary tests were also to obtain the capillary porosity and the resistance to water penetration of the concrete. The size of the specimen was circular disc 100 mm in diameter and 20 mm in thickness. The test were performed with specimen treated with either at 105 °C, 200 °C, 400 °C or 600 °C. After the heating the concrete was cooled in an exsiccator with drying compound, blue gel, about 10% RH. The following tests were performed:

- Residual elastic modulus after 600 °C.
- Residual strength after 600 °C.
- Residual strain at maximum strength after heating to 600 °C.
- Capillary porosity.
- Resistance to water penetration at suction.

7.2 Residual elastic modulus strength at 600 °C

The same procedure as described in Chapter 3 above applied. The concrete was slowly heated at 600 °C (the precise temperature of the concrete varied between 595 and 625 °C dependent on the location in the oven). After heating the specimen were cooling for 1 week in the laboratory air at about RH = 30%. The stress/strain properties were then obtained. Appendix 7.1-8 show the results of the tests after heating to 600 °C. Figure 7.1-22 give a Supplementary view of the residual properties after heating to 600 °C. For concrete without limestone powder the equations given in Chapter 5 still apply. For limestone powder concrete new formulas for residual properties were estimated, Figure 7.23, Table 7.1:

$$r = c \cdot T^2 + e \cdot T + g \qquad (7.1)$$

c,e,g constants for residual properties at and after elevated temperatures given in Table 7.1.
r denotes residual relative properties of concrete at and after elevated temperatures.
T denotes temperature (°C).

Table 7.1 – Constants in equation (7.1).

Residual property	Constant	Without limestone powder	Limestone powder
E-modulus	c	0.0000013	0.000000994
	e	- 0.00221	-0.00215
	g	1.04	1.09
Strength	c	-0.000000349	-0.000000349
	e	- 0.000131	- 0.00094
	g	0.99	1.07
Strain	c	-0.0000022	0.00000333
	e	0.00279	- 0.000142
	g	0.95	1.04

The residual elastic modulus and the residual strength were lower of concrete with limestone powder than without the mineral additive. However, the strain at ultimate strength was somewhat larger, Figure 7.17-22.

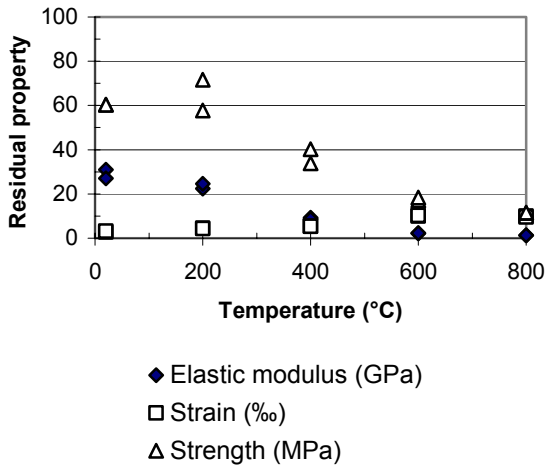

Figure 7.1 – Residual properties of concrete 40 AG0 after cooling 1 week at 20 °C and RH = 30%.

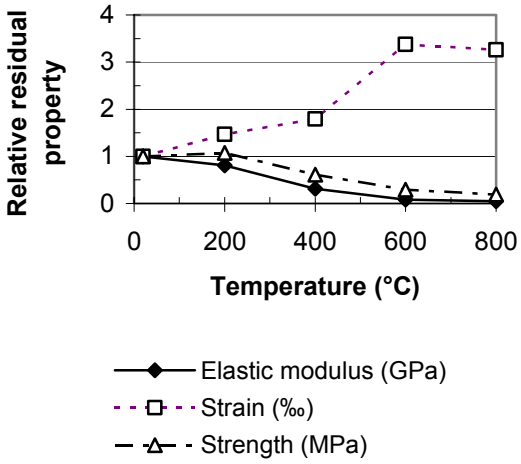

Figure 7.2 – Relative residual properties of concrete 40 AG0 after cooling 1 week at 20 °C and RH = 30%.

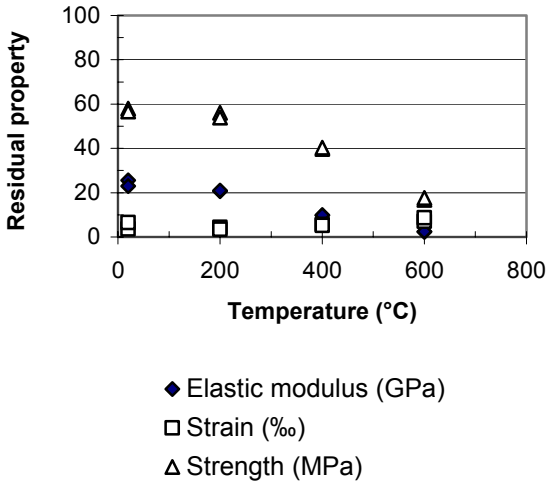

Figure 7.3 – Residual properties of concrete 40 AK0 after cooling 1 week at 20 °C and RH = 30%.

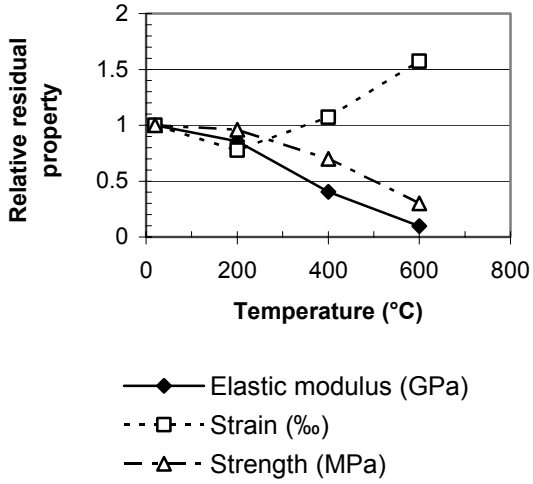

Figure 7.4 – Relative residual properties of concrete 40 AK0 after cooling 1 week at 20 °C and RH = 30%.

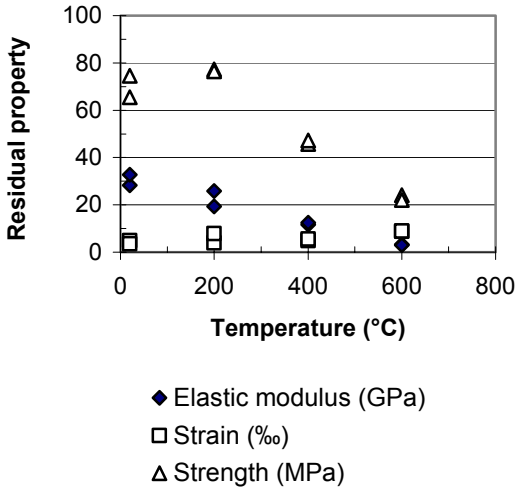

Figure 7.5 – Residual properties of concrete 40 AK2 after cooling 1 week at 20 °C and RH = 30%.

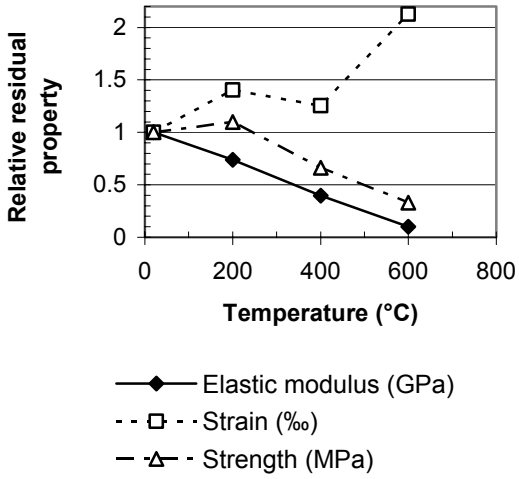

Figure 7.6 – Relative residual properties of concrete 40 AK2 after cooling 1 week at 20 °C and RH = 30%.

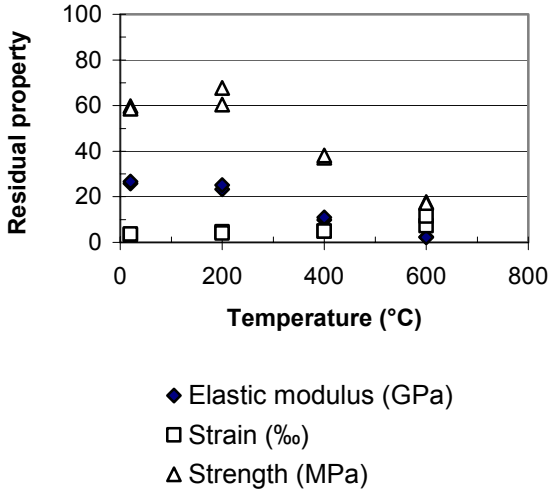

Figure 7.7 – Residual properties of concrete 40 AK4 after cooling 1 week at 20 °C and RH = 30%.

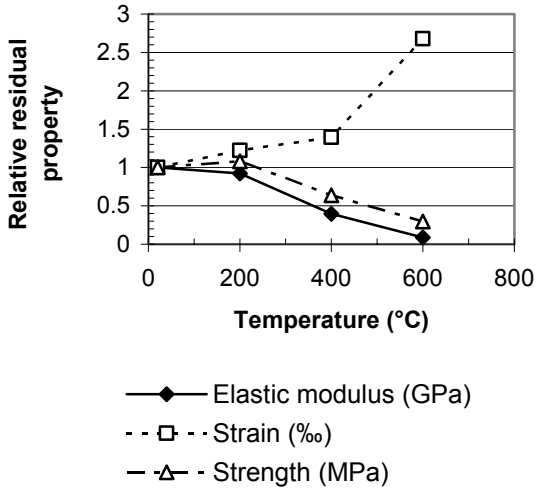

Figure 7.8 – Relative residual properties of concrete 40 AK4 after cooling 1 week at 20 °C and RH = 30%.

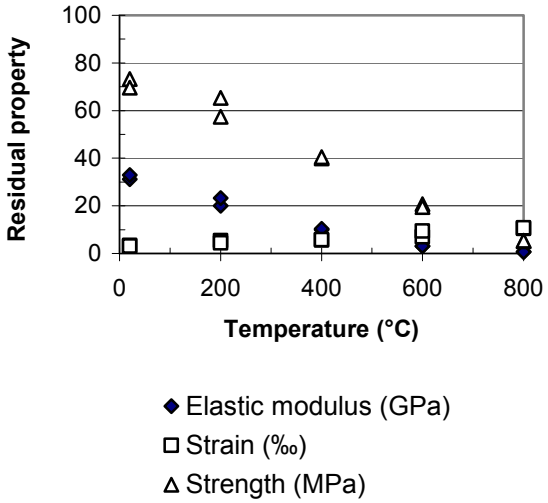

Figure 7.9 – Residual properties of concrete 40 BR0 after cooling 1 week at 20 °C and RH = 30%.

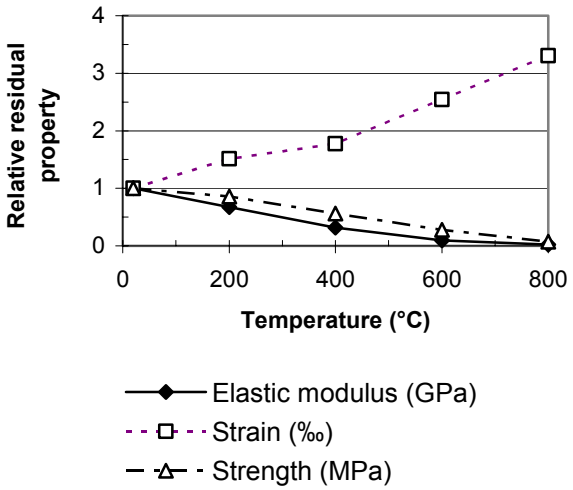

Figure 7.10 – Relative residual properties of concrete 40 BR0 after cooling 1 week at 20 °C and RH = 30%.

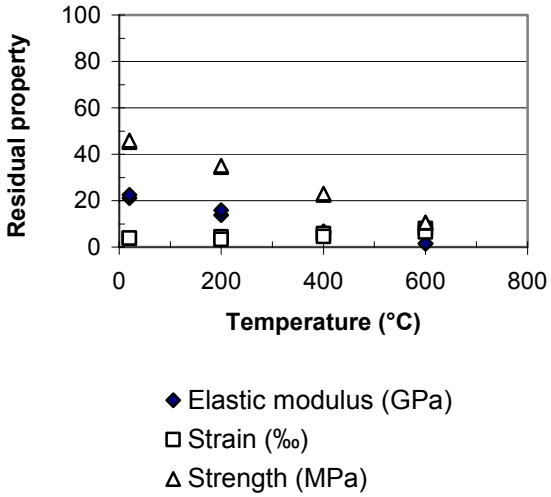

Figure 7.11 – Residual properties of concrete 55 BK0 after cooling 1 week at 20 °C and RH = 30%.

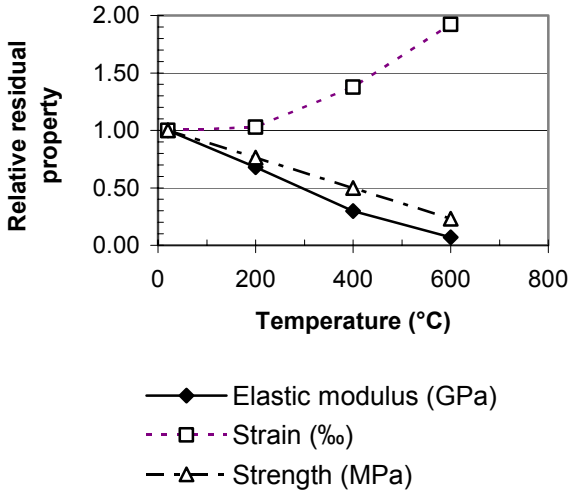

Figure 7.12 – Relative residual properties of concrete 55 BK0 after cooling 1 week at 20 °C and RH = 30%.

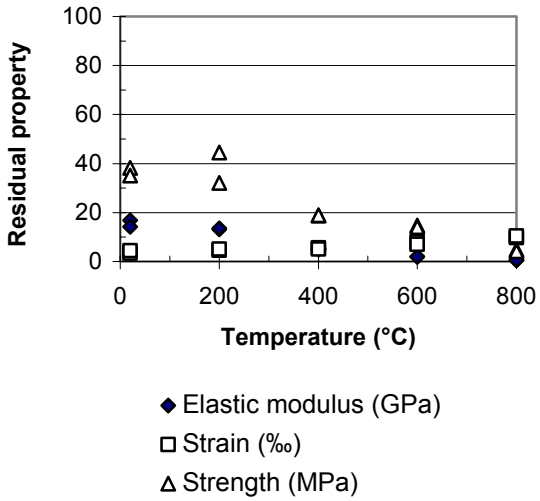

Figure 7.13 – Residual properties of concrete 70 BG0 after cooling 1 week at 20 °C and RH = 30%.

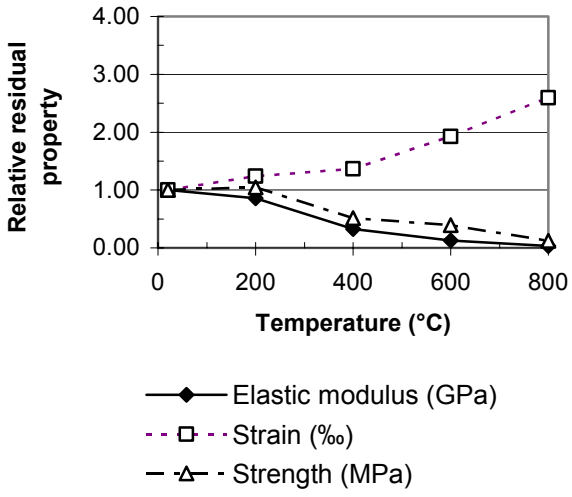

Figure 7.14 – Relative residual properties of concrete 70 BG0 after cooling 1 week at 20 °C and RH = 30%.

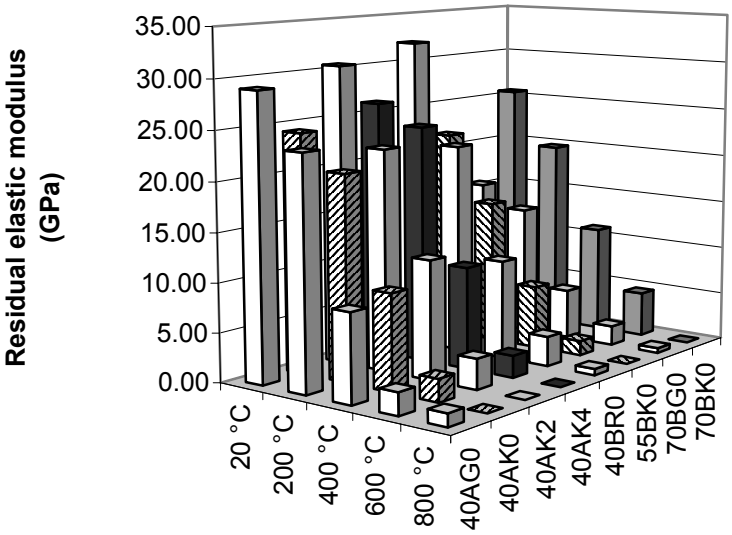

Figure 7.17 – Residual elastic modulus at 20 °C.

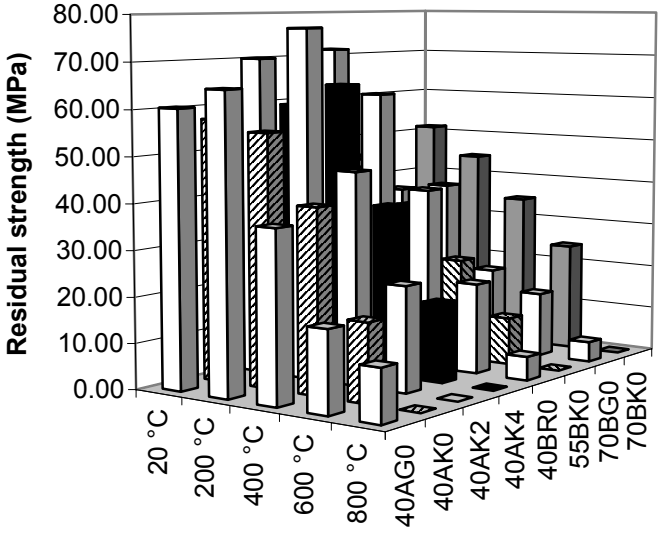

Figure 7.18 – Residual strength at 20 °C.

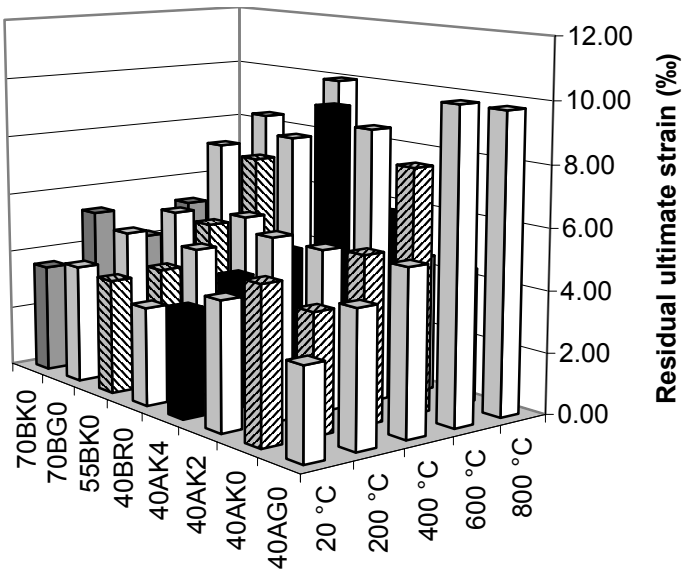

Figure 7.19 – Residual strain at maximum strength at 20 °C.

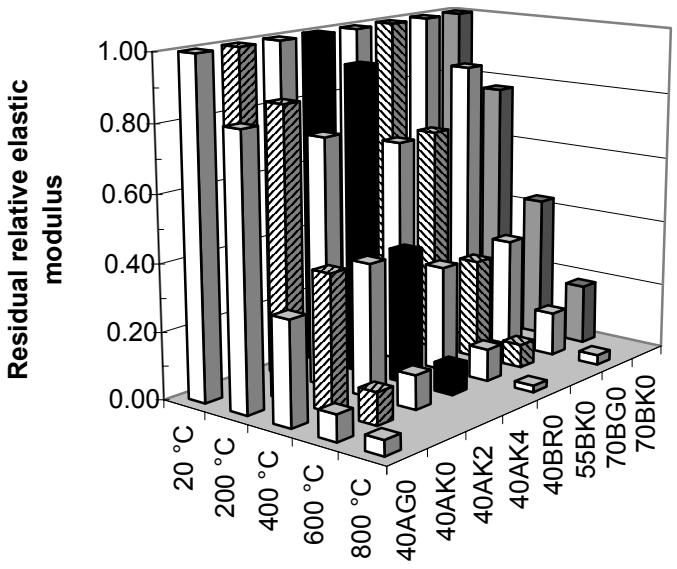

Figure 7.20 – Residual relative elastic modulus at 20 °C (= 0 at 800 °C for concrete with limestone powder).

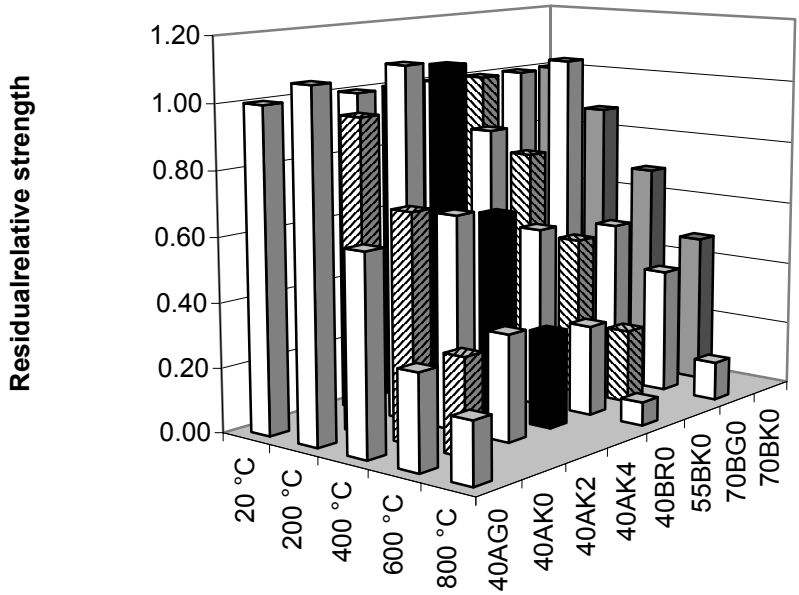

Figure 7.21 – Residual relative strength at 20 °C (= 0 at 800 °C for concrete with limestone powder).

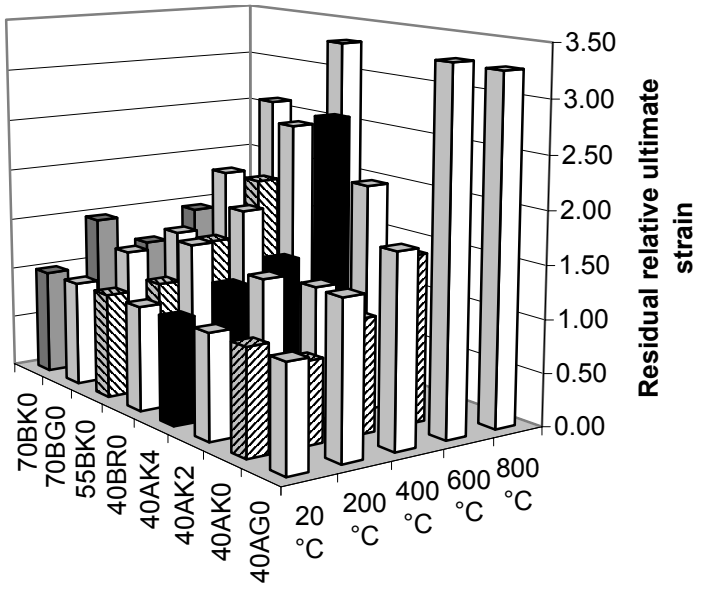

Figure 7.22 – Residual relative strain at maximum strength at 20 °C.

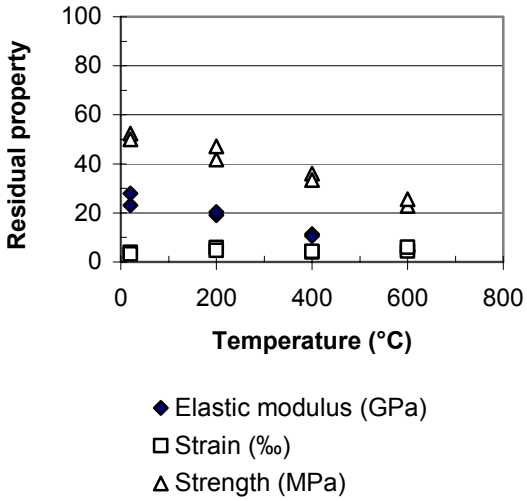

Figure 7.15 – Residual properties of concrete 70 BK0 after cooling 1 week at 20 °C and RH = 30%.

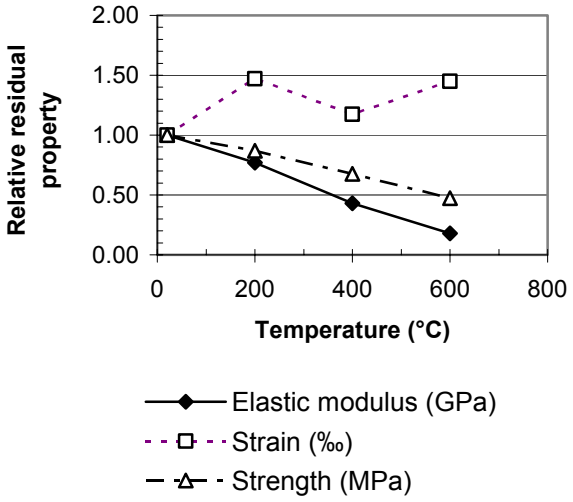

Figure 7.16 – Relative residual properties of concrete 70 BK0 after cooling 1 week at 20 °C and RH = 30%.

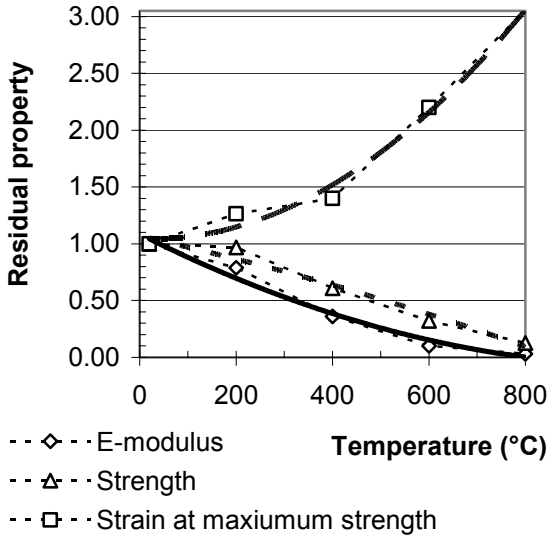

Figure 7.23 - Relative residual properties of SCC with limestone powder versus temperature.

The reason for the different behaviour of concrete with and without limestone powder is probably the variation of the aggregate content. In concrete with limestone powder a great deal of the aggregate is replaced by limestone powder which absorbs water from the air during cooling. The absorption of water leads to expansion of the limestone powder during the cooling phase, which is not the case for the aggregate. A comparison was also performed between the elastic modulus and the strength of the concrete, Figure 7.24. From Figure 7.24 the following equation for the elastic modulus at 20 ° after heating to 600 °C, was estimated, $E_{600\text{-}20}$:

$$E_{600\text{-}20} = (0.0025 \cdot (f_c) + 0.0994) \cdot f_c \qquad (7.2)$$

f_c denotes cylinder strength ($5 < f_c < 25$ MPa)

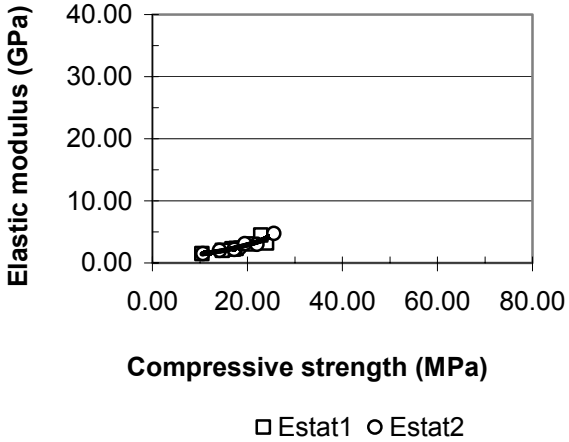

Figure 7.24 – Elastic modulus versus compressive strength at 20 °C after heating to 600 °C and cooling for 1 week in RH = 30%.

7.2 Porosity at water suction

The specimen size was 100 mm in diameter and 20 mm in thickness, three of each concrete. Porosity at water suction was measured. In the Supplementary test series the weight of the concrete was first taken at 20 °C. Then the concrete was heated to 105 °C for 1 week. After this heating the concrete was weighed again and further heated to either 105 °C, 200 °C, 400 °C or 600 °C. The concrete was then cooled to 20 °C in an exsiccator and weighed again. Then the concrete was vacuum treated for 24 h. Water was then immersed a vacuum tank and fully penetrating the concrete. The weight was then taken again at 20 °C, both in the air and under water by the wire method. Table 7.3 and Figures 7.25-26 give results of the capillary porosity of the concrete. The concrete capillary porosity was calculated according the following formula [95]:

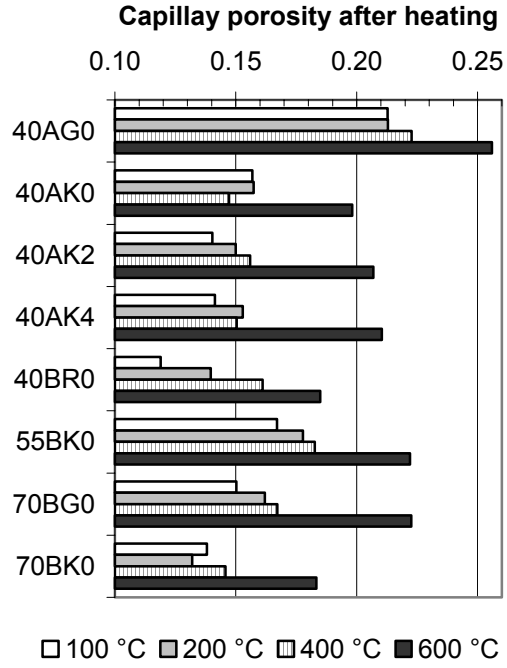

Figure 7.25 - Results of the capillary porosity at water suction of the concrete.

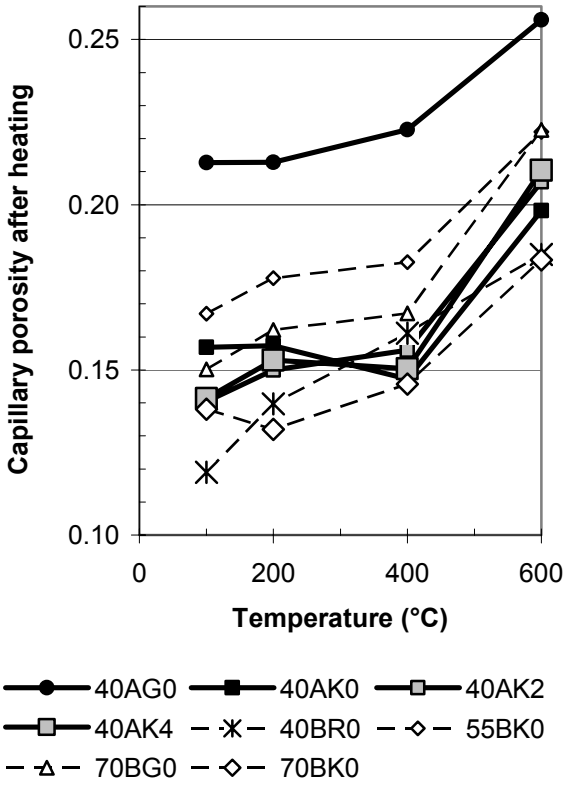

Figure 7.26 - Results of the capillary porosity at water suction of the concrete versus temperature.

$$P = (W_V - W_T)/(W_V - W_U) \quad (7.3)$$

W_T denotes the weight in exsiccator at 20 °C after heating to 105 °C, 200 °C, 400 °C or 600 °C.

W_U denotes the weight under water at 20 °C after heating to 105 °C, 200 °C, 400 °C or 600 °C.

W_V denotes the weight after water ingress in vacuum at 20 °C after heating to 105 °C, 200 °C, 400 °C or 600 °C.

Table 7.3 - Results of the capillary porosity at water suction of the concrete.

Concrete	105 °C	200 °C	400 °C	600 °C
40AG0	0.213	0.213	0.223	0.256
40AK0	0.157	0.157	0.147	0.198
40AK2	0.140	0.150	0.156	0.207
40AK4	0.141	0.153	0.150	0.210
40BR0	0.119	0.140	0.161	0.185
55BK0	0.167	0.178	0.183	0.222
70BG0	0.150	0.162	0.167	0.223
70BK0	0.138	0.132	0.146	0.183

The porosity was larger for the glass filler concrete 40BG0 than for the other concrete. An explanation for the increased porosity of glass filler concrete is the thermal expansion of glass that is larger than for concrete. Another possible explanation is an alkali-silica reaction between glass and the alkalis of the cement. A major increase of porosity was observed between 400 °C and 600 °C probably due to the quartzite transformation and releases hydrated water from the cement gel when the calcium hydrates recomposed into calcium oxide. The largest increase in porosity was observed for the reference concrete 40BR0: the smallest from concrete with limestone powder. Slightly larger increase of porosity at water suction was observed in concrete with polypropylene fibres than in concrete without fibres.

7.3 Resistance to water penetration at suction

The specimen size was 100 mm in diameter and 20 mm in thickness, three of each concrete. The concrete was treated at different temperatures either 105 °C, 200 °C, 400 °C or 800 °C. After cooling in a exsiccator at about RH = 10%, the weight was taken at 20 °C. The concrete was then subjected to suction by the flat side of the specimen. The water was penetrating the flat side of the specimen and the rim by about 1 mm in height. The weight was taken after 1, 2, 3, 4, 1050 and 4000 min. after start of the suction until it stabilised. The resistance to water penetration was calculated from the slopes of the abscissas of the water suction versus the square root of time, both between 0 and 4 min and between 1000 and 4000 min., Appendices 7.9-12, Table 7.4 and Figures 7.27-28 [95]:

$$m=(r/((o-q)\cdot t))^2 \quad (7.4)$$

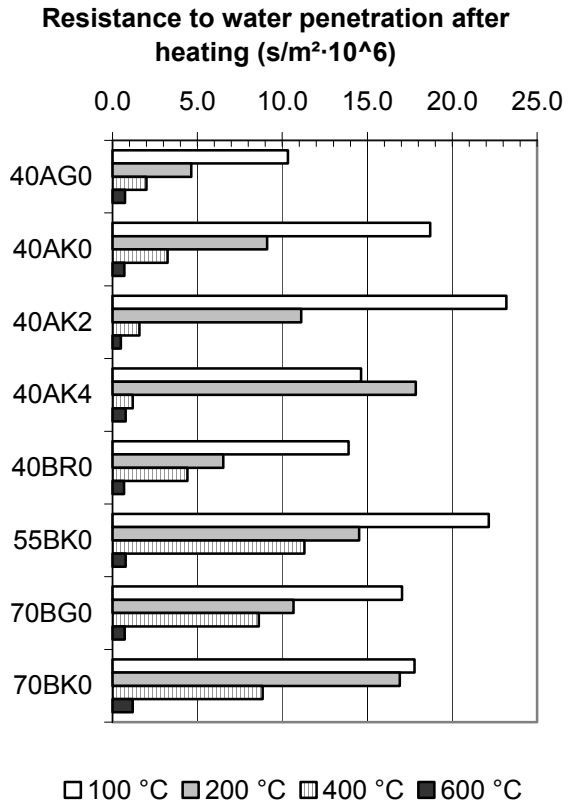

Figure 7.27 - Resistance to water penetration at suction after heating (s/m²·10^6).

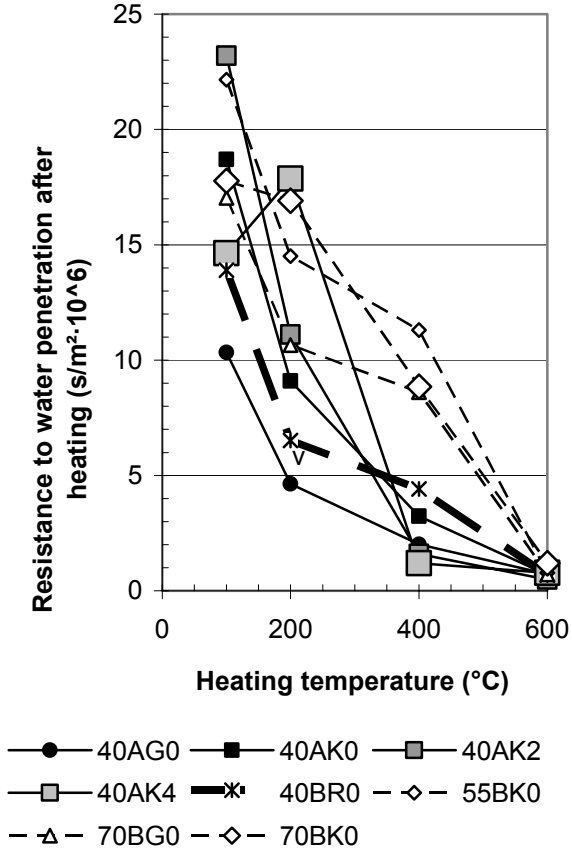

Figure 7.28 - Resistance to water penetration at suction after heating (s/m²·10^6) versus time.

m denotes the resistance to water penetration after heating (s/m²·10^6)
o slope of the water suction between 0 and 4 min. versus square root of time
q slope of the water suction between 1000 and 4000 min. versus square root of time
r constant in order fully to describe suction between 1000 and 4000 min. (kg/m²)
t thickness of specimen (m)

Table 7.4 - Resistance to water penetration after heating (s/m²·10^6).

Concrete	105 °C	200 °C	400 °C	600 °C
40AG0	10.3	4.64	2.01	0.727
40AK0	18.7	9.10	3.24	0.693
40AK2	23.2	11.1	1.59	0.486
40AK4	14.6	17.9	1.19	0.779
40BR0	13.9	6.52	4.40	0.676
55BK0	22.2	14.5	11.3	0.777
70BG0	17.0	10.7	8.62	0.713
70BK0	17.8	16.9	8.85	1.20

The lowest resistance to water penetration at suction was obtained for the glass filler concrete 40BG0 followed by the reference concrete 40BR0. These results coincide well with the observations of the porosity at water suction above. However, for concrete with 2 kg/m³ polypropylene fibres larger resistance to water penetration at suction was observed at 105 °C than for the same concrete without fibres and than for concrete with 4 kg/m³ polypropylene fibres. For concrete with 4 kg/m³ polypropylene fibres larger resistance to water penetration at suction was observed at 200 °C than for the same concrete without fibres and for concrete with 2 kg/m³ polypropylene fibres.
The reason for the increasing resistance to water penetration was probably an expansion and melting of the polypropylene fibres at 105-200 °C. These phenomena remained also after cooling the specimen at 20 °C and therefore decreased the water suction. During fire heating water transport thus may be prohibited inward concrete with fibres. In this case the water pressure in concrete with fibres may increase slower than in concrete with fibres as the water instead of moving inward will leave the surface of the concrete. This is probably explaining the mechanism of the polypropylene fibres in concrete at fire:

- Possible increase of the polypropylene fibre volume and melting at 105-200 °C.
- Water movement inward concrete with fibre is diminished at 105-200 °C due to an increase in the resistance to water penetration.
- Water instead moves the surface of concrete with fibres and thus fire spalling is avoided.

7.4 Capillary water suction and porosity

Normally a relationship exists between capillary suction (resistance to water penetration) and capillary porosity. Figure 7.29 shows that normal concrete had lower resistance to water penetration at capillary suction than SCC did when the capillary porosity is held constant. Especially with glass filler concrete with w/c=0.40 exhibited larger resistance to water penetration as compared to normal concrete at the same w/c=0.40. This is probably due to the glass filler content in SCC, which prohibit water movement, more than in normal concrete. It may also be due to a larger absorption of water in concrete with larger amount of filler that the absorption in concrete without filler, i.e. the isotherm of concrete might be affected. From Figure 7.29 the following formula was obtained, Figure 7.30:

$$m = d \cdot (P_{cap})^e \qquad (7.5)$$

d,e denotes constants given in Table 7.5

m denotes resistance to water penetration ($s/m^2 \cdot 10^6$)

P_{cap} denotes capillary porosity $\{0.14<P_{cap}<0.24\}$

Table 7.5 - Constants in equation (7.5)

	Normal concrete - air	SCC - air	SCC - water
d	0.0001	0.0001	0.000000064
e	-5.72	-6.23	-10.1

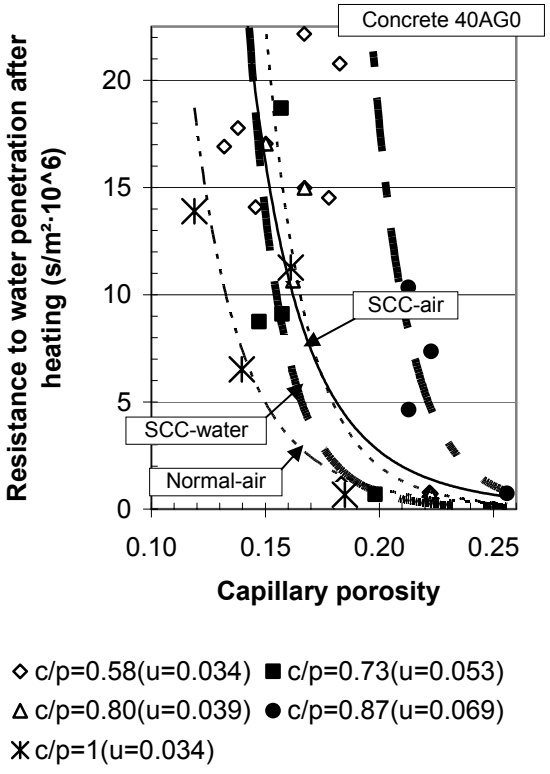

Figure 7.29 - Resistance to water penetration at capillary suction versus the capillary porosity. c = cement; p = powder (cement + filler); u = moisture content (weight wet/dry – 1).

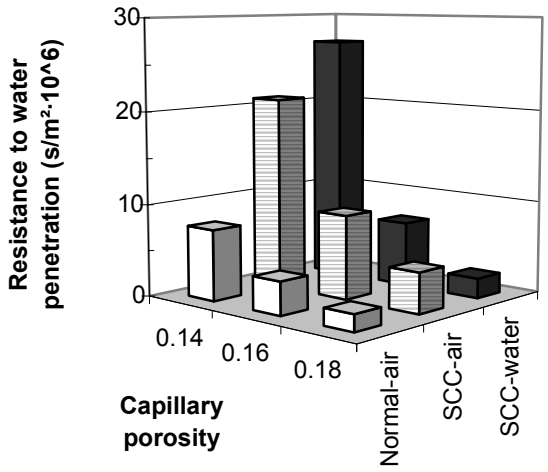

Figure 7.30 – Calculation of the resistance to water penetration with equation (7.5) for normal concrete and for SCC.

8. DISCUSSION

8.1 General

SCC is characterised by its large amount of fine material, cement and filler, in the purpose of achieving a high stability and for avoiding segregation during casting of the concrete. These requirements causes too a large tightness and low permeability of SCC. This in turn affects the conditions at the ingress of a fire for the concrete to transport water vapour present in the concrete out of the concrete. The water vapour is instead forced to be transported inward in the concrete where it is transformed into the liquid phase when the temperature is rapidly increasing during occasion of fire. Water has namely a larger coefficient of expansion than the concrete structure causing the pores of the concrete to be saturated by water rapidly as the temperature increases (the relative humidity, RH increases in concrete on the same time as the temperature increases). After few minutes of fire also the pressure in the water filled pores of the concrete increases. At a certain critical temperature water may no longer exist but is transforms into vapour, which may spall the concrete. After the time of explosion of the concrete liquid water may be seen flushing down the surface of the remaining part of a fire spalled vertical column, which indicates that liquid water is formed even though the column is well dried before the testing. At RH = 70%, initially in concrete with w/c = 0.40, a temperature rise of 100 °C is sufficient to cause saturation provided sealed conditions, Figure 8.1 [22,96]. Figure 8.1 shows the temperature of saturation for normal concrete (varying w/c and RH at start of fire) provided sealed conditions. Generally RH varies between 60% and 90% in the concrete at start of fire since the concrete normally obtains about 5% higher RH than the average RH of the ambient atmosphere. When polypropylene fibres are included the water transport inward the concrete probably is diminished between 100 °C and 200 °C. From Figure 8.1 the following equation was evaluated:

$$T_{sat} = 115 \cdot (1.07 - RH) \cdot \exp((2.52 - 0.95 \cdot RH) \cdot w/c) \quad (8.1)$$

w/c denotes water-cement ratio (0.35 w/c <0.75)
RH denotes RH before fire (0.30 < RH < 0.90)
T_{sat} denotes temperature of saturation (°C).

Explosion of concrete during heat spalling seems to take place at lower temperature than the critical one (275 °C). A temperature observed at the time of explosion is 185 °C with 350 °C at the surface of the concrete, Figure 8.2.

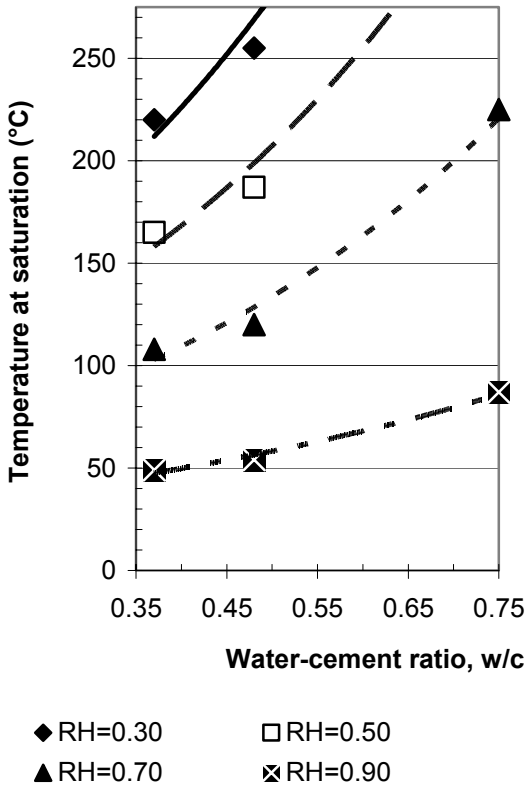

Figure 8.1 - Temperature at saturation of concrete with varying w/c and RH at start of fire provided sealed conditions [22,96].

Figure 8.2 – Performance of concrete 40AK0 after heating with 350 °C surface temperature and 185 °C concrete temperature at the time of explosion.

During fire spalling testing at SP not only part of the tested columns were damaged but also a security window glass that was placed in the wall of the large oven. The forces at fire spalling thus are enormous and may be a hazard for the fire rescue personnel at the start of a fire.

8.2 Effect of high temperature on mechanical properties of concrete tested at LTH

Normal concrete consists to its main part of aggregate, gravel and coarse aggregate. A minor part, about 25%, consists of hardened cement paste; approximately equal parts by weight of water and cement. The ratio of water and cement defines the water-cement ratio, w/c, of the concrete. When the concrete is heated the aggregate expands parallel to shrinkage of the cement paste. Water leaves the hardened cement paste parallel to the temperature increase causing large deformation as compared to the deformation of the aggregate. These interacting deformations ground the basis for shear stresses in the interfacial zone between aggregate and the hardened cement paste. In the hot state strength of SCC is not affected much up to a temperature of 400 °C, Figure 5.19. The hardened cement paste still has fairly plastic properties during the phase of heating at fire so the hardened cement paste may well deform itself with the aggregate up to 575 °C, anyhow, at which temperature the quartzite transformation takes place. The elastic modulus of concrete is much more affected by fire temperatures than the strength is (the deformation of the concrete is affected). The elastic modulus may be halved up to 400 °C when tested in the hot state, Figure 7.23. It is positively for SCC that no drop of strength seems to exist between 105 °C and 200 °C like occurs for High Performance Concrete, HPC, Figure 5.24. For HPC the strength was diminished about 20% between 105 °C and 200 °C, which is a disadvantage. After heating and when the concrete cools to normal temperature, large movements for a second time happens between the aggregate and the hardened, partly de-watered, cement paste. Both aggregate and the remaining part of the hardened cement paste shrinks, but the cement paste less since it absorbs water from the ambient air, especially after cooling. Especially SCC is affected after heating up to 800 °C and cooling for a week or more at 20 °C. SCC with limestone powder then loses its strength totally and is pulverised autonomy, Figure 7.23. The calculated residual properties are not affected much since no strength for concrete above 500 °C normally is taken into account. Damages may also occur after long since SCC loosens its strength after the fire.

8.3 Influence of mix proportions on fire spalling of concrete columns tested at SP [94]

In the laboratory at SP, Borås, hanging pre-stressed columns, 200 mm square and 2 m long, were tested during at least standard ISO 834 fire conditions (close to Hydro Carbon fire enhanced ISO 834 fire conditions for water-cured columns, equation (2.3), Figure 2.12). The age of the columns was either ½ or 1 year. The pre-stressing force (either 104 kN or 112 kN) was 30% of the current ultimate compressive 150-mm cube strength, i.e. about 40% of the ultimate strength of the columns, Appendix 4.6. Pre-stressing was carried out at about 2 days' age. About 14 columns were hanging at each fire test occasion. Data from the work has been used in order to correlate the weight of tested concrete to w/p, Figure 8.3 [94,97-100]. For water-cured concrete A with cement type I, the fire spalling results seems logical, Table 8.1. The following parameters was studied, Appendix 8:

- RH in the concrete before fire testing.
- Moisture in the concrete before fire testing.
- Weight of concrete before and after fire.
- Temperature of the column.
- Temperature in the fire room.
- Fire spalling of the surface (video cameras).

Table 8.1 – Age, mix proportions (kg/m³) and weight of columns after fire spalling [94,97-100].

Con-crete	Age (days)	Wa-ter	Ce-ment	Filler	w/p	We-ight	Air (%)
40AG0	170	172	430	62	0.35	0.82	5
40AK0	170	164	411	149	0.29	0.68	5.1
40AK2	170	173	433	181	0.28	0.88	2.5
40AK4	170	195	487	171	0.30	0.94	2.8
40AR0	170	206	518	0	0.40	0.93	4
40BR0	170	175	436	0	0.40	0.95	-
40BK0	170	179	518	130	0.28	0.76	-
55BK0	320	170	308	242	0.31	0.73	1.3
55BK2	320	189	344	241	0.32	0.85	1.1
55BK4	160	210	382	233	0.34	0.86	-
55BR0	320	192	348	0	0.55	0.86	1.5
70BG0	170	225	321	80	0.56	0.87	1.7
70BK0	170	188	268	189	0.41	0.82	2.6
70BK2	160	209	298	229	0.40	0.97	-
70BK4	160	214	306	331	0.34	0.86	-
70BR0	170	195	278	0	0.70	0.92	5

p = powder (cement + filler); w = water; A = Anläggningscement; B = Byggcement; K = limestone filler; R = normal concrete; 0 = 0 kg/m³ polypropylene fibres; 40 = w/c (%).

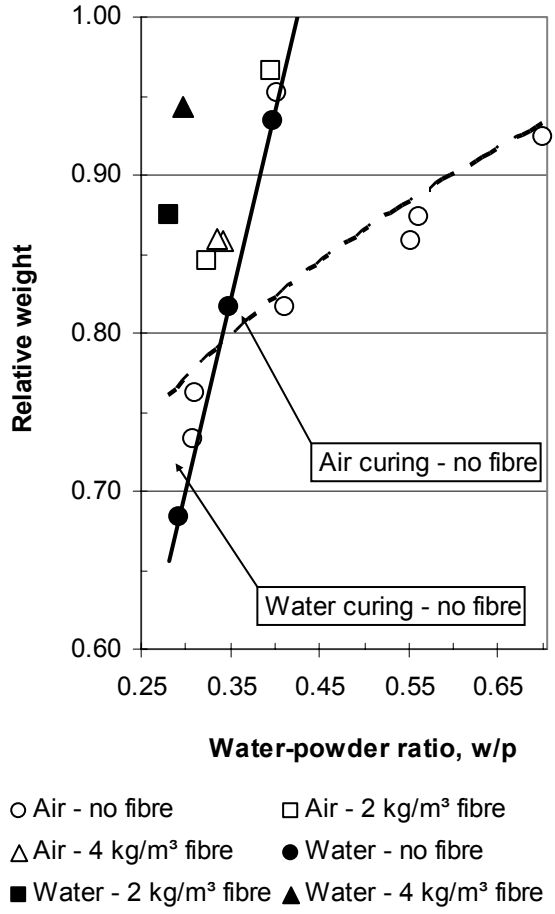

Figure 8.3 - Fire spalling versus w/p.

The concrete contained large amount of limestone powder which was due to the available aggregate. More than 200 kg/m³ of limestone powder was used in the following mix proportions:

- 55BK0
- 55BK2
- 55BK4
- 70BK2
- 70BK4

In a way the limestone powder content in the mentioned mix proportions shows that SCC cannot be produced with all kinds of aggregate except adding unreasonable amounts of limestone powder. Another aspect is that the early age water curing increased the tensile strength of the surface of the concrete, which may increase the resistance to fire spalling but also the resistance to fire spalling. The relative weight of the concrete A with type I cement subjected to water curing was reduced in the following way:

$$W_A = 2.39 \cdot (w/p) - 0.019 \qquad (8.2)$$

w/p denotes water-powder ratio ($0.25 < w/p < 0.40$)
W_A denotes weight after fire spalling concrete A

8.4 Parameters affecting fire spalling tests performed at SP [94]

8.4.1 Concrete A with Portland cement type I

From above significant effect of w/p was observed on the weight of concrete after fire spalling. Further parameter analyses were performed in order to explain some inconsistent observations above, Figures 8.4-5.

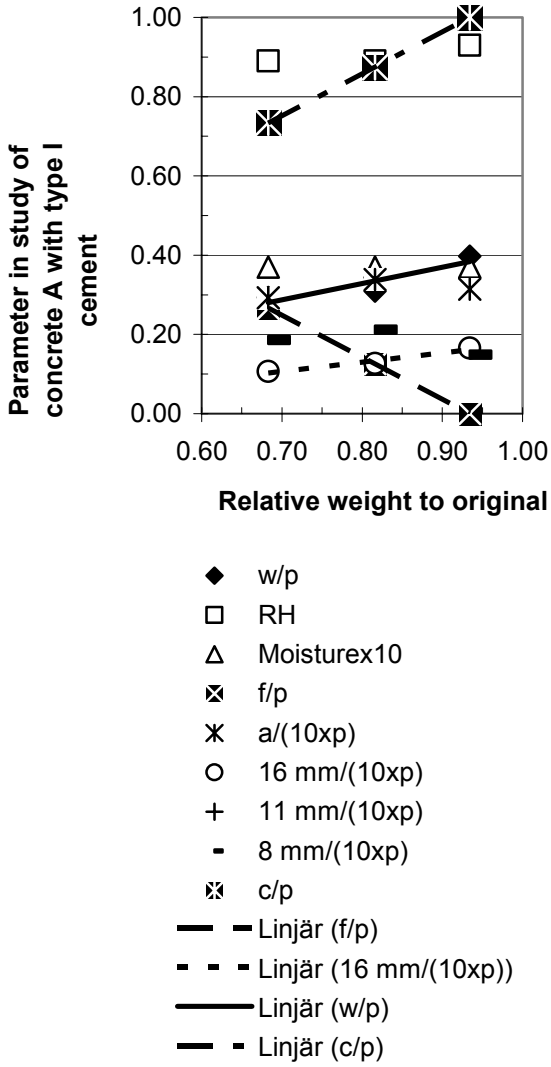

Figure 8.4 – Parameter analysis of spalling on concrete A with cement type I without fibres.

The following relationships were found for concrete A with cement type I without fibres:

$$n = k \cdot (1-W) + m \qquad (8.3)$$

c denotes cement content
k, m denotes constants given in Table 8.2
f denotes filler content
n denotes parameter in study
p denotes powder content (cement+filler)
W denotes weight after fire spalling

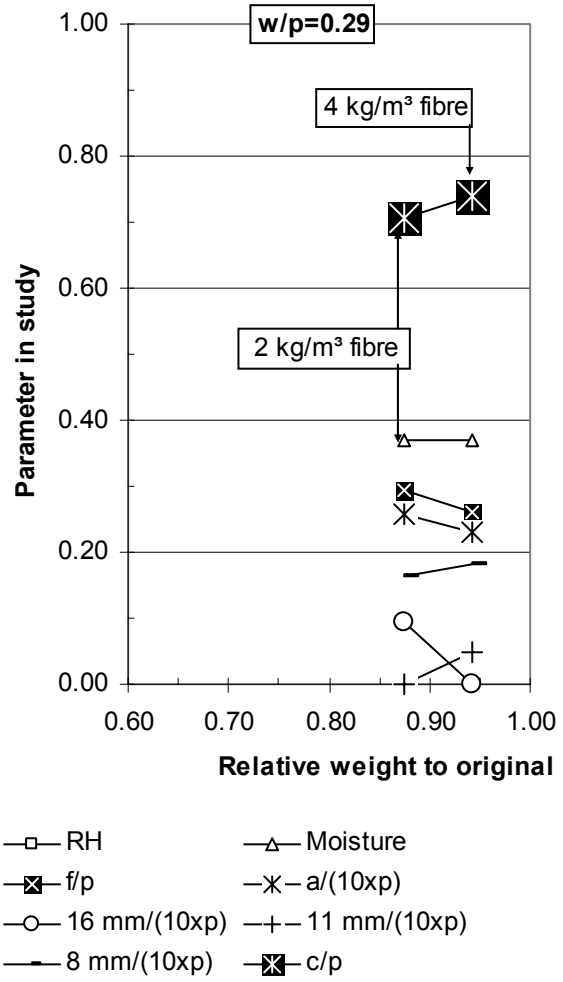

Figure 8.5 – Parameter analysis of spalling on concrete A with cement type I with fibres.

Table 8.2 – Parameters in equation (8.3).

Parameter, n	k	m
Aggregate 11-16 mm/(10·p)	-0.234	0.177
c/p	-1.060	1.070
f/p	1.060	-0.070
w/p	-0.411	0.411

Some of the parameters affected the fire spalling in parallel so that they are difficult to separate. The following result was obtained by the parameter analysis on fire spalling of concrete A with cement type I without fibres:

- Less aggregate 11-16 mm gave larger amount of spalling since k was negative.
- Lower c/p-ratio influenced on the spalling so that larger spalling was obtained.
- Subsequently larger f/p-ratio imposed larger spalling.
- Lower w/p-ratio gave larger spalling as found above.

For concrete A with 2% and 4% of fibres the fire spalling was decreased in a logical way by the increased of the amount of fibres, Figure 8.5.

8.4.2 Concrete B with filler cement type II

Figures 8.6 and 8.7 show a summary of factors influencing the weight of concrete B with filler cement type II. The following relationships were found on concrete B without fibres, Figure 8.6:

$$s = q \cdot (1-W) + r \qquad (8.4)$$

c denotes cement content
f denotes filler content
p denotes powder content (cement+filler)
q, r denotes constants given in Table 8.3
s denotes parameter in study
W denotes weight after fire spalling

Table 8.3 – Parameters in equation (8.4).

Parameter, s	q	r
Aggregate /(10xp)	-1.23	0.609
Aggregate 0-8 mm /(10xp)	-0.917	0.394
Aggregate 8-11 mm /(10xp)	-0.323	0.151
c/p	-1.59	0.943
f/p	1.87	0.110
Moisture	0.0286	0.747
w/p	-1.30	0.659

Again, some of the parameters affected the fire spalling in parallel so that they are difficult to separate. The following result was obtained by the parameter analysis on fire spalling of concrete B with cement type II without fibres (cement type II was recalculated into Portland cement):

- Less aggregate content gave larger spalling.
- Less aggregate 0-8 mm gave more spalling.
- Less aggregate 8-11 mm increased spalling.
- Content of aggregate 11-16 mm did not influence on the spalling.
- Lower c/p-ratio influenced on the spalling so that larger spalling was obtained.
- Larger f/p-ratio imposed larger spalling.
- Larger RH caused more spalling.
- Lower w/p-ratio gave larger spalling.

For concrete with B with 2% and 4% of fibres the increasing fire spalling was not logical, Figure 8.7. Possible reasons for the same amount of fire spalling of concrete 55BK2 and 55BK4 (even though the fibre content increased from 2 to 4 kg/m³) is shown in Table 8.4:

- Increase of testing age from 160 days (55KB4) to 320 days (55BK2).
- Decreased amount of aggregate.
- Increased amount of water.
- RH was 6% larger in 55BK4 than in 55BK2.

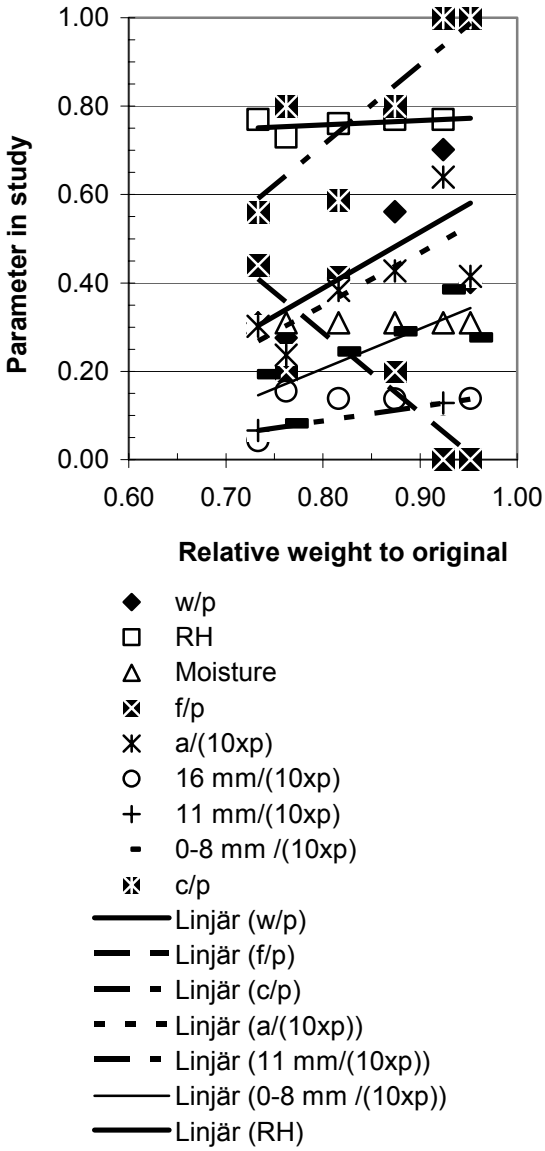

Figure 8.6 – Parameter analysis of spalling on concrete B with cement type II without fibres.

According to Anderberg [101] the age of concrete has a fundamental effect on the risk of spalling mainly due to the strength increase over time but also due to internal drying of the concrete. RH was not measured either in concrete 55BK4 or in 55BK2, which is unfortunate, since it is known that the moisture content and then also RH in the concrete affects the risk of fire spalling substantially. However, RH in concrete 55BK0 was know at 320 days' age, RH = 0.77, Appendix 8. Calculations with TorkaS [101] indicates that RH in concrete 55BK4 at 160 days' age was about 6% larger, i.e. RH = 83%, than in concrete 55BK2 at 320 days' age, i.e. RH = 77%. It is shown in the experiments that 4 kg/m³ of polypropylene fibres gave the same fire spalling at 160 days' testing age (55BK4) like 2 kg/m³ of polypropylene fibres did at 320 days' testing age (55BK2).

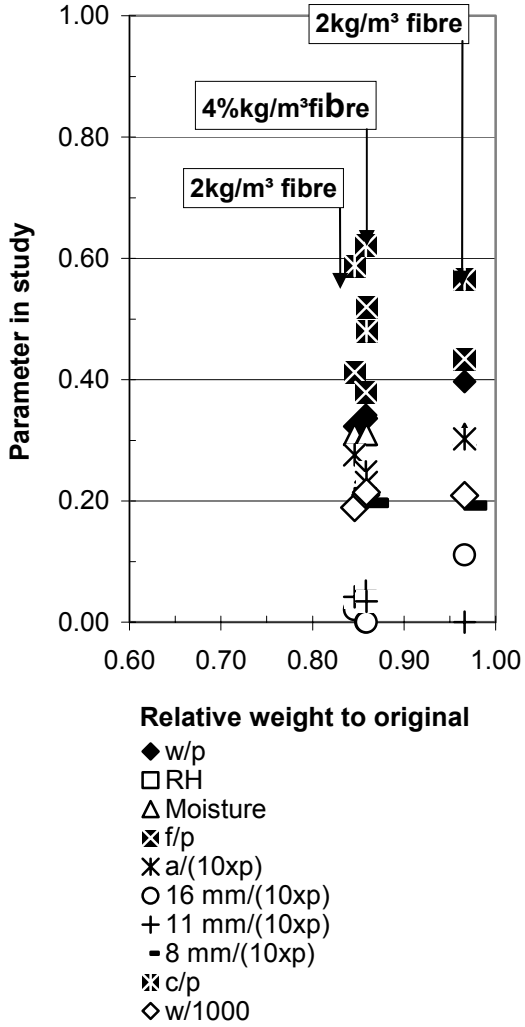

Figure 8.7 – Parameter analysis of spalling on concrete B with cement type I with fibres.

One-hundred-and-sixty days' age at testing of concrete was an quite unrealistic low age. Then 320 days' age is more appropriate and would indicate that 2 kg/m³ of polypropylene fibres is sufficient to reduce the fire spalling to 15%. For the comparable reference, normal concrete 55BR0 the age at testing was 320 days with a fire spalling of 14%. It is not reasonable to increase the requirements of fire spalling in SCC as compared to normal concrete. For concrete 70BK2 and 70BK4 the decrease of c/p and w/p probably was a reason for the increased spalling.

Table 8.4 - Mix proportions and other properties of concrete (kg/m³).

Con-crete	Age (d)	Spal-ling	w/p	f/p	c/p	w	a/(10xp)
55BK2	320	0.15	0.32	0.41	0.50	189	0.28
55BK4	160	0.14	0.34	0.38	0.62	210	0.25
70BK2	160	0.03	0.40	0.43	0.57	209	0.30
70BK4	160	0.14	0.34	0.52	0.48	214	0.23

d = days

8.4.3 Summary of parameter study on fire spalling tests performed at SP [94]

An increase of the following parameters was favourable in order to reduce fire spalling:

- age
- c/p
- w/p
- Aggregate /(10xp)
- Aggregate 0-8 mm /(10xp)
- Aggregate 8-11 mm /(10xp)
- Fibre content

Decrease of the following parameters reduced spalling:

- f/p
- Moisture content
- RH

8.5 Outcome of cement content on fire spalling

Additionally for SCC as compared to normal concrete is the large content of filler which is included in the powder content together with cement. The filler behaves in a way to fill gaps in the concrete pore structure causing higher compressive strength of the concrete. However, filler does not affect the tensile strength in parallel that is required to give a high fire spalling resistance of SCC. The tensile strength of concrete may be crucial in order to achieve high fire spalling resistance. If the amount of powder in concrete is exchanged too much by limestone filler, the concrete may not resist fire spalling like a pure Portland cement (type I) concrete does. The comparative conditions apply for other properties of concrete like chloride migration, when the amount of cement of the concrete is diminished and exchanged by limestone filler in parallel [103]. The exchange affect may be expressed by the cement-powder ratio, c/p, i.e. c/p = 1 for a concrete with Portland cement only (type I) like Anläggningscement in this project. For concrete with Byggcement (type II) c/p = 0.85 in fact apply but for practical reasons c/p = 1 is used in this project also for concrete with Byggcement (if c/p was changed then also w/c would change in parallel). For the tested concrete in this project, c/p as low as c/p = 0.48 was used (in fact c/p = 0.43 taking into account the limestone filler in Byggcement), i.e. less than half of the powder contained cement, which is little. The reason for the large amount of limestone filler was the requirement of workability in combination with an unsuitable aggregate, Figure 8.8, Appendix 8 [94]. SCC without any powder may be produced but is more expansive and unstable than SCC with large powder content [104]. Bleeding in small surface areas may also suddenly occur in SCC without filler, which may cause aesthetic affects on the surface, also after curing. However, full-scale production of SCC without limestone filler takes place in many factories so this method obviously is operable [104]. A summary of spalling of the tested concrete is given in Figure 8.8, Table 8.1 [94]. Figure 8.9 shows the influence of cement-powder ratio, c/p, on weight after fire spalling of concrete with Byggcement (air curing). No tendencies to fire spalling larger than 15% was observed for concrete with w/p > 0.50, Figure 8.9. Normal concrete with c/p = 1 exhibited up to 15% of weight fire spalling which is judged to be acceptable. It is not reasonable to have more conservative requirements for SCC than for normal concrete. Such enhanced requirements for SCC would have a reversing affect on SCC as compared to normal concrete and an obvious drawback for the new technique. However, at w/p $\leq$ 0.50, large fire spalling was observed for concrete with Byggcement (type II) combined with c/p $\leq$ 0.80. Figure 8.10 shows fires spalling of concrete with cement of type I (Anläggningscement, water curing - effect of the cement-powder ratio, c/p, on the weight after fire spalling). For concrete A cement of type I a slightly lower w/p < 0.37 was acceptable with a fire spalling not exceeding 15% (c/p = 0.90).

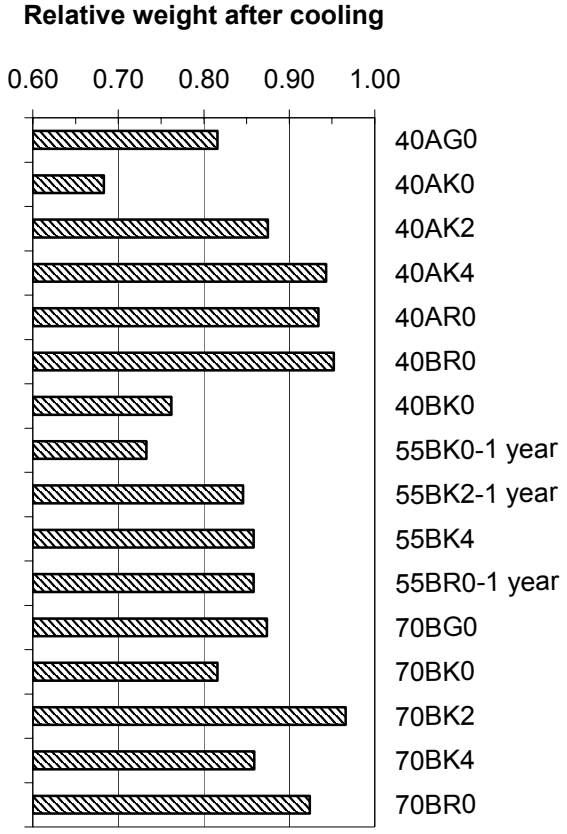

Figure 8.8 - Summary of spalling of concrete [94].

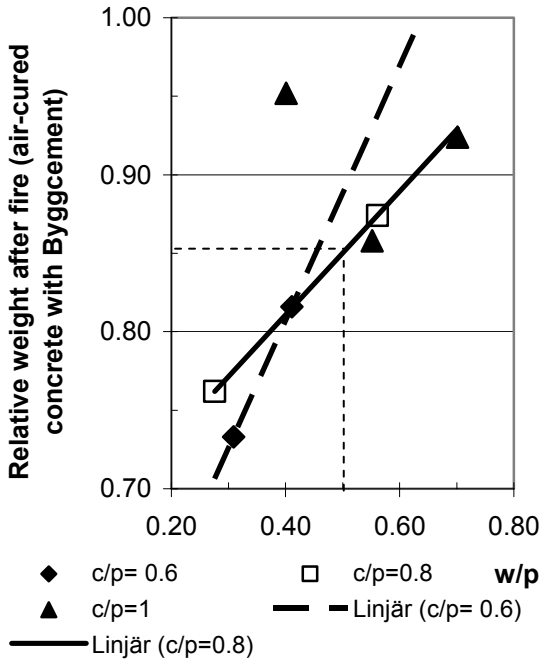

Figure 8.9 - Influence of cement-powder ratio, c/p, and water-powder ratio, w/p, on weight after fire spalling of concrete B (air curing).

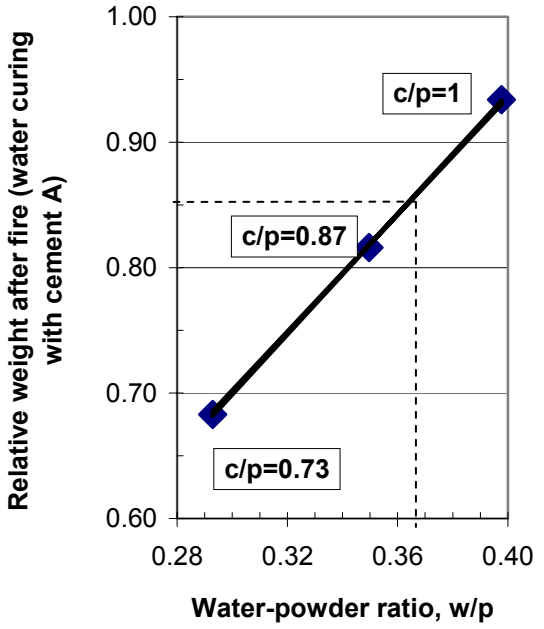

Figure 8.10 - Weight after fire spalling of concrete A with cement of type I (water curing, Anläggningscement, effect of c/p).

Obviously a relationship also exists between the parameters the cement-powder ratio, c/p and the water-powder ratio, w/p. Both these parameters increased in parallel when w/c was held constant. The question was how to express fire spalling in the best way, by w/c or w/p. w/c is the most well-known parameter of concrete affecting both strength and durability so this parameter was preferable to be further evaluated. From Figure 8.10 and equation (8.2) the following simplified equation was obtained for the relative weight of water-cured concrete after fire, W_w:

$$W_w = 2.4 \cdot w/p \qquad (8.5)$$

w/p denotes water-powder ratio ($0.25 < w/p < 0.40$)

8.6 Weight of curing, air entrainment and testing age on fire spalling

Effect of type of curing on the weight of concrete after fire spalling may be judged on the result of two concrete according to Figure 8.8, 40AR0 and concrete 40BR0, Table 8.5 [94]. Concrete 40AR0 (water-cured with Anläggningscement; w/c = w/p = 0.40; c/p = 1) obtained 93% of weight after fire spalling and concrete 40BR0 (air-cured with Byggcement; w/c = w/p = 0.40; c/p = 1) obtained 95% of weight [94]. The similar fire spalling of the concrete 40AR0 and 40 BR0 was astonishing. Even though the curing type varied from water to air more or less the same amount of spalling was observed. This may be due to a lower c/p for Byggcement, w/p = 0.85, than for Anläggningscement, w/p = 1. If the definition for w/p is altered w/c is also affected, in case an increase from w/c = 0.40 to w/c = 0.47 for concrete 40BR0 (calculation with pure Portland cement). In any case sufficient amount of water was available in the concrete for fire spalling to take place. A comparison with Figure 8.1 shows that an increase of temperature of 50 °C was necessary for concrete with w/c = 0.40 and RH = 90% initially to obtain saturation but about 105 °C increase of temperature for concrete with w/c = 0.40 and RH = 70%. Still much higher temperature changes takes place during fire, enough for the saturation of the pores to take place. Sufficient amount of water was available in the pore system even at RH = 70% in order to obtain saturation and fire spalling rapidly. Another reason for the low fire spalling of concrete A with water curing compared with concrete B with air curing may be the air content, 5% air content in concrete 40AR0 and natural air in concrete 40BR0 [94]. The effect of age on the amount of fire spalled concrete may be judge from Figure 8.8 and Table 8.6 [94]. Concrete 55BR0, that was 1 year at the time of testing lost 14% in weight at fire spalling compared with on average 7% for the comparable concrete at an age of half a year, 40AR0, 40BR0 and 70BR0. Neither in this case it seemed like age had a significant effect on fire spalling, rather a reversed effect. Normal air-cured concrete may obtain 14% of fire spalling even after 1 year of air-curing with RH = 73% in centre of the columns when it was tested, 55BR0. It also was interesting to compare

the fire spalling of the concrete 55BK2 (2 kg/m³ plastic fibre, 1 year old) with the same concrete 55BK4 (4 kg/m² fibre, ½ year). Both concrete obtained about 15% of fire spalling, i.e. in this case the ageing seems to halve the requirement of spalling to an acceptable level, Table 8.6. In general it seemed like the age, half a year or 1 year, did not affect the fire spalling at all, Table 8.6. These results are noticeable and in contrast to previous research. Probably the time of drying, half a year or 1 year still was too short in order to obtain significant difference to water curing. The question is also at what an age the concrete is required to be resistant to fire? Previous research shows that the same type of concrete construction sensible to fire spalling at half a year of age resisted the same type of fire at 5 years' age [105].

Table 8.5 –Properties of concrete 40AR0 and 40BR0 weight after fire [94, 97-100].

Concrete	40AR0	40BR0
Air content	4%	-
Cement-powder ratio, c/p	1	1
Curing (6 months)	Water	Air
Portland cement-powder ratio, c/p (real c/p))	1	0.85
RH	73%	93%
Water-cement ratio, w/c	0.40	0.40
Water-powder ratio	0.40	0.40
Water-Portland cement ratio, w/Pc	0.40	0.47
Weight after fire	93%	95%

Table 8.6– Effect of age on weight after fire [94].

Concrete	c/p	w/c	w/p	RH	Weight
40AR0	1.00	0.40	0.40	0.93	0.93
40BR0	1.00	0.40	0.40		0.95
55BK0-1 year	0.56	0.55	0.31	0.77	0.73
55BK2-1 year.	0.59	0.55	0.32		0.8585
55BK4	0.62	0.55	0.34		0.86
55BR0-1 year	1.00	0.55	0.55	0.73	0.86
70BR0	1.00	0.55	0.70	0.77	0.92

p = powder (cement + filler); w = water; A = Anläggningscement; B = Byggcement; K = limestone filler; R = normal; RH = rel. humidity; 0 = 0 kg/m³ polypropylene fibres; 40 = w/c (%).

8.7 Consequence of amount and type of fibre

For some combinations of cement-powder ratio, c/p < 0.80, and water-powder ratio, w/p ≤ 0.50, other measures were required to secure the fire spalling resistance at a maximum limit of 15% of the original weight before the fire. In the present investigation the fibre in use had a 32-µm diameter in contrast to another type of fibre of 18-µm which exhibited half the amount of spalling provided the same condition for the other parameters [79]. The amount of fibres given here is based on the 32-µm-diameter fibre at half a year of age and a maximum 15% of fire spalling. If the age of testing is increased from half a year to 1 year the required amount seem to be half, Table 8.6. The required amount of fibres will then be further diminished in order to secure SCC for fire spalling. However, first of all the amount of limestone powder is to be lowered in concrete before adding fibres. Figure 8.11 shows the weight after fire spalling of concrete B with Byggcement type I at varying amount of fibre and w/p. Amount of fibre is based on diameter 32 µm and half a year age. The effect of fibre was substantial in order to obtain a concrete resistant to fire spalling, Figure 8.11. In the same way the Figure 8.12 show the weight after fire spalling of concrete with Anläggningscement at varying amount of fibre and w/p. The amount of fibre is based on diameter 32 µm and half a year age and a 15% maximum level of fire spalling. At constant w/p ≈ 0.29 the effect of polypropylene fibres on the relative weight after fire exposure was observed on concrete A with Type I cement, Figure 8.12, Table 8.7.

Table 8.7. - Effect of polypropylene fibres on the relative weight of concrete A at w/p ≈ 0.29.

Fibre content (kg/m³)	Relative weight (%)
0	68
2	88
4	94

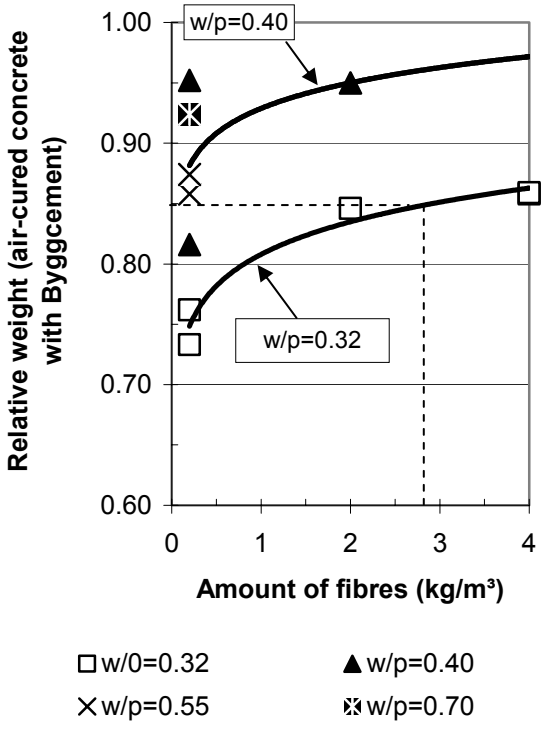

Figures 8.11 - Weight after fire spalling at half a year's age of concrete with Byggcement versus amount of 32 µm fibre and w/p.

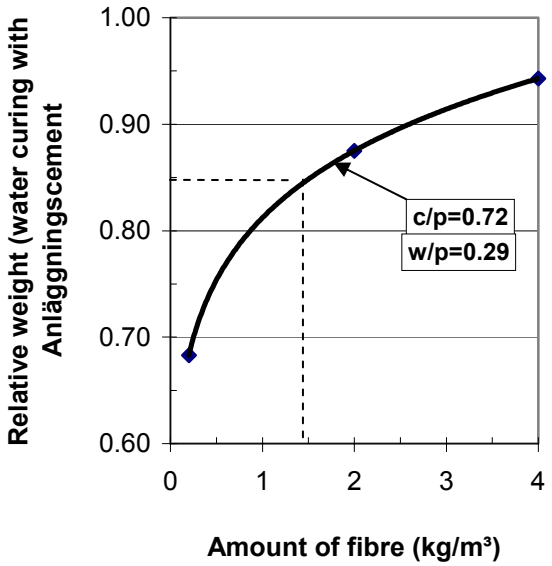

Figures 8.12 - Weight after fire of concrete A with type I cement at varying amount of fibre.

The effect of polypropylene fibres on the weight of the concrete A at w/p ≈ 0.29 after fire exposure was calculated in the following way, Figure 8.12:

$$W_{A,w/p\approx0.29} = 0.82\cdot(ppf)^{0.11} \quad \{0.2<f<4 \text{ kg/m}^3\} \quad (8.6)$$

ppf denotes fibre ($0.2 < f < 4$ kg/m³)
w/p denotes water-powder ratio ($0.25 < w/p < 0.40$)
$W_{A,w/p\approx0.29}$ denotes weight after fire of concrete A with Type I cement w/p≈0.29.

Together with equation (8.5) the Figure 8.13 was obtained in order to demonstrate the effect of fibre content and water-powder ratio, w/p on the relative weight of water-cured concrete after fire. The effect of the amount of polypropylene fibres, ppf, was not linear. The relative weight of concrete B with type II cement, W_B, was lower than that of concrete A, Figure 8.14:

$$W_B = (1.5\cdot(w/p)+0.32)\cdot(ppf)^{(-0.19\cdot(w/p)+0.11)} \quad (8.7)$$

ppf denotes plastic fibres $\{0.2 < ppf < 4$ kg/m³$\}$
w/p denotes the water-powder ratio
W_B denotes weight after fire spalling of concrete B $\{0.30< w/p< 0.40\}$

The equation (8.7) showed low significance particularly due to the different behaviour of the concrete with and without limestone powder. In order to avoid fire spalling of concrete B with type II cement (15% limestone powder), high filler content and therefore a low w/p, polypropylene fibres are required in the mix proportions. However, the effect of amount of polypropylene fibres was not logical as concerns the relative weight after fire exposure of concrete B with type II cement (15% limestone powder), Table 8.8. About 15% of fire spalling was observed even though 4 kg/m³ was added to the mix. At higher w/p the same difference was obtained, Table 8.9. Both w/p and the amount of fibres affected the weight after fire spalling. As shown above the cement-powder ratio, c/p, affected the weight after fire spalling much more than the water-powder ratio did, Figures 8.9-11. For one concrete with c/p = 1 almost no spalling took place at w/p = 0.40 but for low c/p = 0.5 large spalling took place when w/p was held constant at w/p = 0.40. Thus an equation of the fibre amount based on c/p and w/c was required.

Table 8.8– Relative weight after fire spalling [94].

Con-crete	Fibres (kg/m³)	Rel. weight	w/c	w/p	Age (years)
55BK0	0	0.73	0.55	0.31	½
55BK2	2	0.85	0.55	0.32	½
55BK4	4	0.86	0.55	0.34	1
70BK4	4	0.86	0.70	0.34	½

Table 8.9– Relative weight after fire spalling [94].

Con-crete	Fibre content	Rel. weight	w/c	w/p	Age (years)
40AR0	0	0.93	0.40	0.40	½
40BR0	0	0.95	0.40	0.40	½
70BK0	0	0.82	0.70	0.41	½
70BK2	4	0.97	0.70	0.40	½

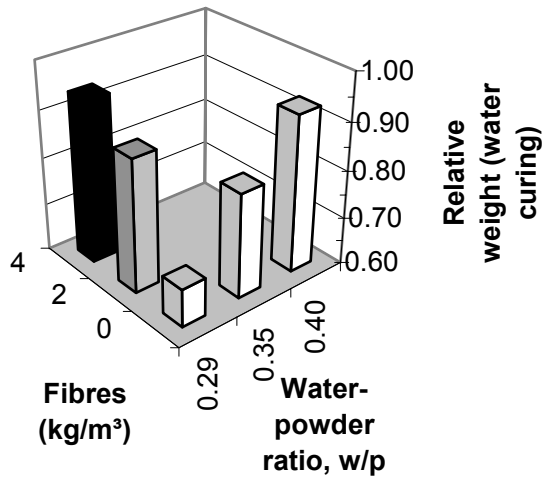

Figure 8.13 - Relative weight of water-cured concrete after fire spalling versus 32 µm fibre content and w/p.

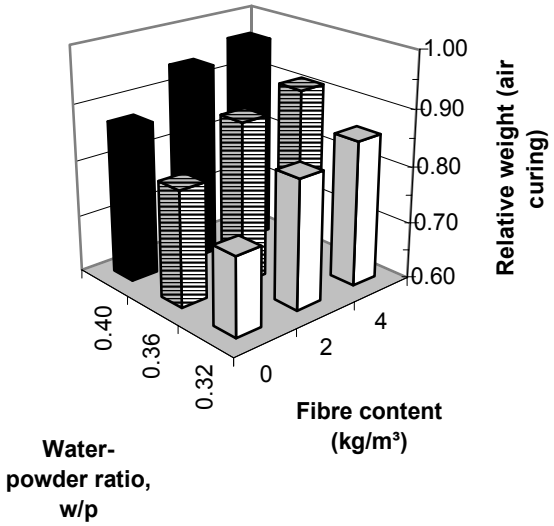

Figure 8.14 - Relative weight of concrete B with type II cement at different fibre content and w/p.

8.8 Effect of moisture and hydration losses

8.8.1 Moisture content

The moisture content of the concrete was not measured before the fire spalling test [94], but at the cylinder tests and also before the water suction and the porosity tests. (At full-scale tests it is necessary to cast dummies in order to obtain the moisture content.) In parallel also RH was measured in concrete, at half a years' age. Figure 8.15 shows the moisture content, u, in some concrete, either water-cured or in the air together with some previous result [40]. The moisture content, u, was calculated in the following way:

$$u=W_{wet}/W_{dry}-1 \qquad (8.8)$$

W_{dry} denotes the dry weight after heating 1 week at 105 °C and cooling in exsiccator at 20 °C
W_{wet} denotes the wet weight before heating

About 3% moisture in normal concrete is critical for the fire spalling to take place [79,101]. Even though the concrete was dried to about 75%RH high moisture content was observed. On average the following moisture content was found:

- Previous research [40]: 2.2%
- Air-cured specimen: 3.6%
- Water-cured specimen: 5.9%

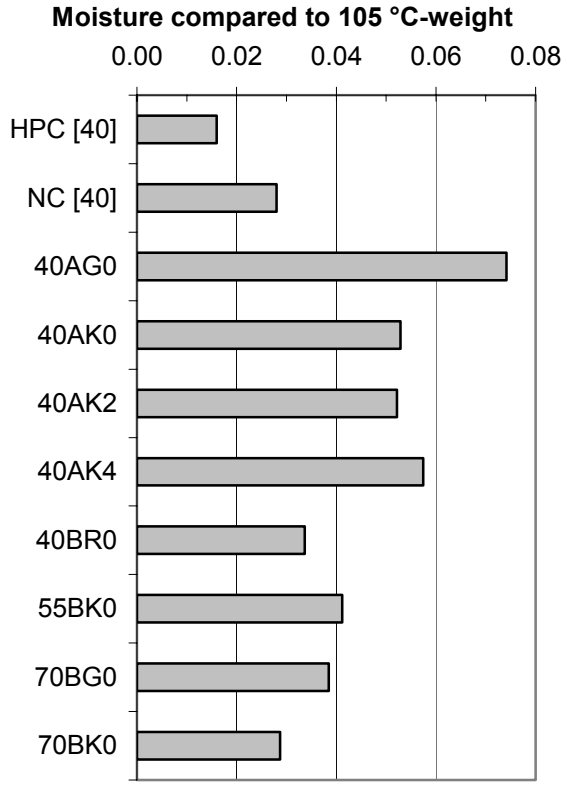

Figure 8.15 - Moisture content in concrete, either water- or air-cured with some previous result [40].

8.8.2 Isothermal behaviour

In Figure 8.16 the moisture content of the concrete was compared with the isotherm of normal concrete with either w/c = 0.40 or w/c = 0.70 [104]. Figure 8.16 shows that normal concrete 40BR0 performed as expected and followed the isotherm like concrete with w/c = 0.40 [106]. All other concrete with filler (SCC) showed isothermal properties above normal concrete. Especially concrete 40AG0 and 70BG0 contained more water than given by the isotherm. This in turn clearly shows that SCC contains more water than normal concrete when RH is held constant (especially concrete with glass filler). The observation shows that the reason for larger fire spalling of SCC may be a different isotherm. A structure with filler may absorbs more moisture than the gravel and aggregate does causing a larger moisture content shown by the isotherm (especially concrete with glass filler), Figure 8.16.

8.8.3 Hydration losses

It was important to calculate correct hydration losses at every temperature. If the hydration losses were incorrect part of the weight attributed to fire spalling may be hydration losses. From a practical point of view the following calculations were performed:

$$h= 1-W_{dry}/W_{wet} \qquad (8.9)$$

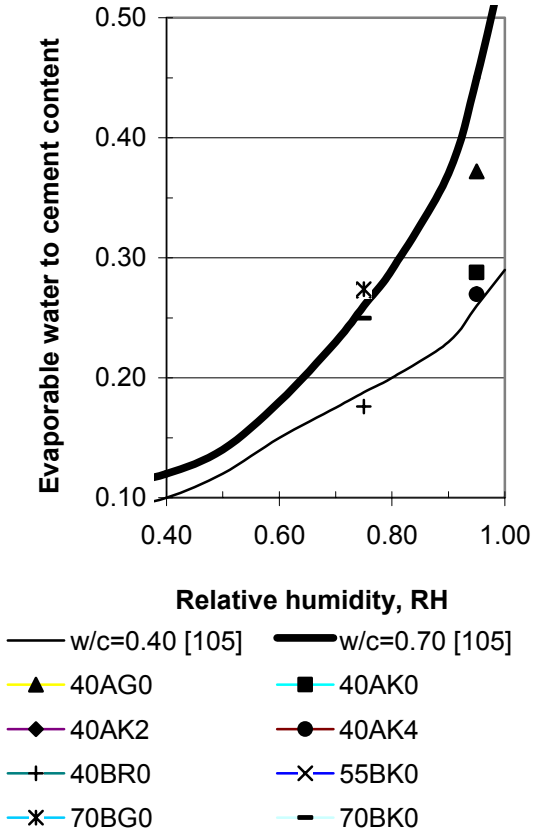

Figure 8.16 - Moisture content compared with the isotherm of normal concrete either with w/c= 0.40 or w/c= 0.70 [106]. A = Anläggningscement; B = Byggcement; G = glass; K = limestone; R = normal; 0 = 0 kg/m³ plastic fibres; 40 = w/c (%).

h denotes the relative weight after evaporated or hydrated water losses

W_{dry} denotes the dry weight after heating 1 week at 105 °C and cooling in exsiccator at 20 °C

W_{wet} denotes the wet weight before heating

The relative hydration losses thus are slightly larger than the relative moisture content. Figure 8.17 and Table 8.10 show the relative weight of the tested concrete after evaporated or hydrated water losses. The largest evaporated and hydration water losses were obtained for concrete with glass filler, 40AG0, which confirms the previous results of capillary porosity, Chapter 7.

Table 8.10 – Relative weight of the tested concrete after evaporated or hydrated water losses.

T (°C)	40AG0	40AK0	40AK2	40AK4	40BR0	55BK0	70BG0	70BK0
20	1.00	1.00	1.00	1.00	1.00	1.00	1.00	1.00
100	0.93	0.95	0.95	0.95	0.97	0.96	0.96	0.97
200	0.93	0.95	0.95	0.94	0.96	0.95	0.96	0.97
400	0.91	0.94	0.93	0.93	0.95	0.95	0.95	0.97
600	0.90	0.92	0.92	0.92	0.95	0.94	0.94	0.95
800	0.91	0.00	0.00	0.00	0.94	0.00	0.93	0.00

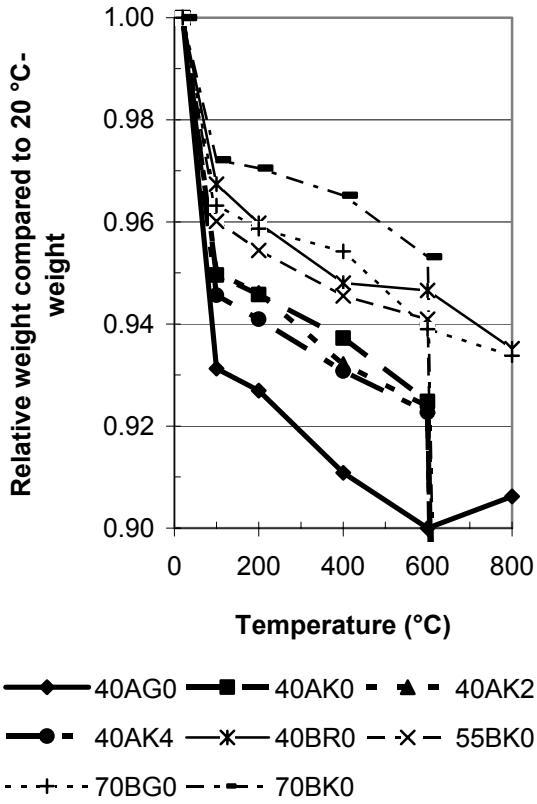

Figure 8.17 – Relative weight of concrete after evaporated or hydrated water losses.

8.9 Effect of porosity on fire spalling

Porosity and fire spalling were compared [94]. Figures 8.18-23 show the development of fire spalling versus capillary porosity at 20 °C after heating to different temperatures, 105 °C, 200 °C, 400 °C and 600 °C. The same observations apply after heating to 200 °C like after heating to 105 °C except for the porosity of SCC with fibres that became the same that for concrete without fibres when the other mix proportions of the concrete was held constant.
The following conclusions were drawn:

- Water-curing concrete showed less relative weight after fire spalling compared to air-cured concrete when the porosity was held constant (no fibres).
- Larger c/p-ratio gave larger weight after fire spalling when the porosity was held constant.
- Polypropylene fibres lowered the porosity after treating the concrete at 105 °C compared with the porosity without fibres.
- The relative weight after fire spalling became larger in SCC with fibres even though the porosity with fibres became smaller.
- Larger porosity of concrete with fibres than of concrete without fibres was observed after heating to 400 °C.

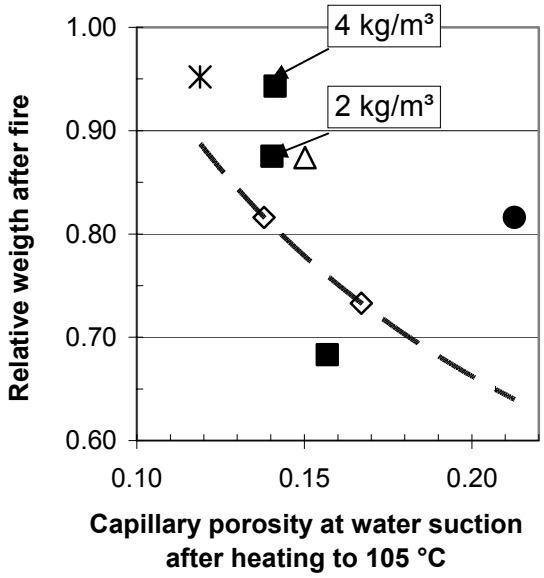

◇ c/p=0.58(u=0.034) ■ c/p=0.73(u=0.053)
△ c/p=0.80(u=0.039) ● c/p=0.87(u=0.069)
✳ c/p=1(u=0.034)

Figure 8.18 - Development of fire spalling versus capillary porosity at 20 °C after heating to 105 °C.

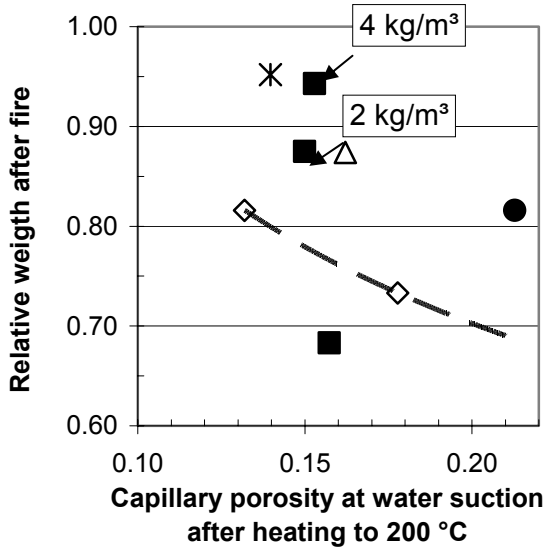

◇ c/p=0.58(u=0.034) ■ c/p=0.73(u=0.053)
△ c/p=0.80(u=0.039) ● c/p=0.87(u=0.069)
✳ c/p=1(u=0.034)

Figure 8.19 - Development of fire spalling versus capillary porosity at 20 °C after heating to 200 °C.

After heating to 400 °C and 600 °C the porosity increased more for concrete with polypropylene fibres than for concrete with the same mix proportions but without fibres. The pore volume for transport of water vapour increased more in concrete with fibres. The following equation was found for the relative weight after fire spalling of air-cured SCC with c/p=0.58, W_{fs}, Figure 8.24:

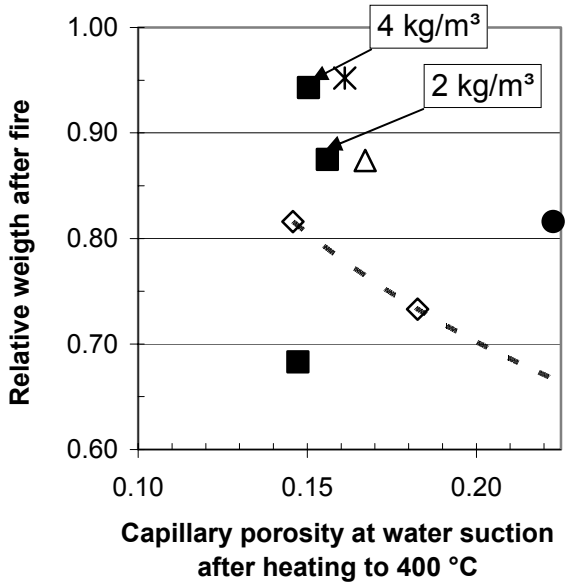

◇ c/p=0.58(u=0.034) ■ c/p=0.73(u=0.053)
△ c/p=0.80(u=0.039) ● c/p=0.87(u=0.069)
✳ c/p=1(u=0.034)

Figure 8.20 - Development of fire spalling versus capillary porosity at 20 °C after heating to 400 °C.

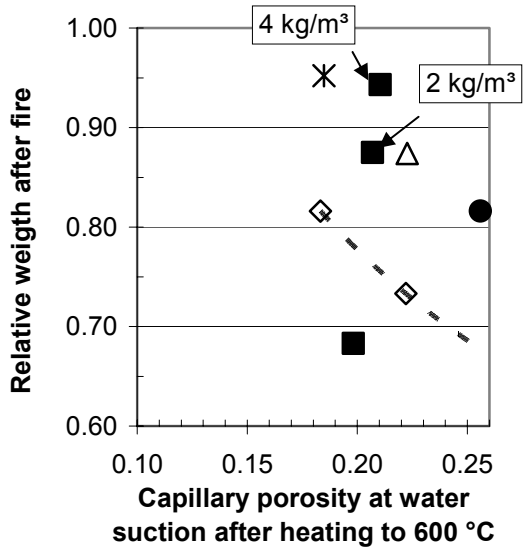

◇ c/p=0.58(u=0.034) ■ c/p=0.73(u=0.053)
△ c/p=0.80(u=0.039) ● c/p=0.87(u=0.069)
✳ c/p=1(u=0.034)

Figure 8.21 - Development of fire spalling versus capillary porosity at 20 °C after heating to 600 °C.

$$W_{fs} = (-1.02 \cdot 10^{-6} \cdot (T)^2 + 0.000734 \cdot T + 0.232) \cdot (P_{cap})^{(-2.22 \cdot 10^{-6} \cdot (T)^2 + 0.00144 \cdot T - 0.644)} \quad (8.10)$$

P_{cap} denotes capillary porosity at suction
T denotes temperature at heating (°C)
W_{fs} denotes relative weight after fire spalling of air-cured SCC with c/p=0.58

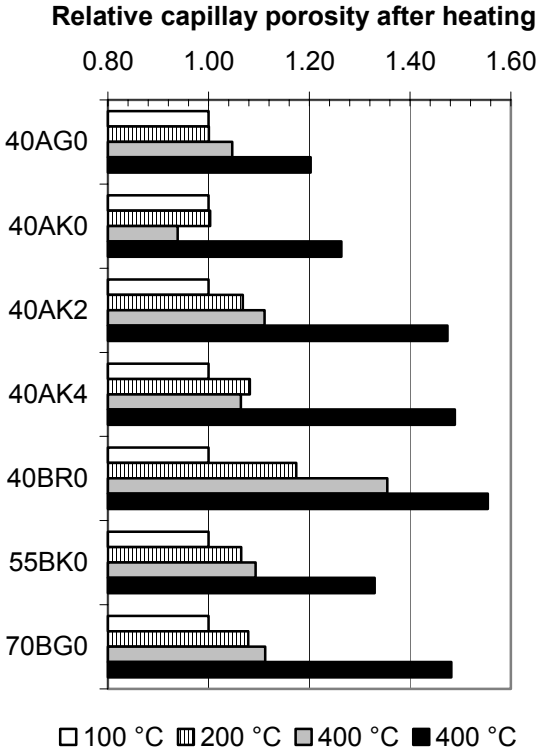

Figure 8.22 - Temperature and relative porosity. Notations: A = Anläggningscement; B = Byggcement; G = glass filler; K = limestone filler; R = normal concrete; 0 = 0 kg/m³ polypropylene fibres; 40 = water-cement ratio, w/c (%).

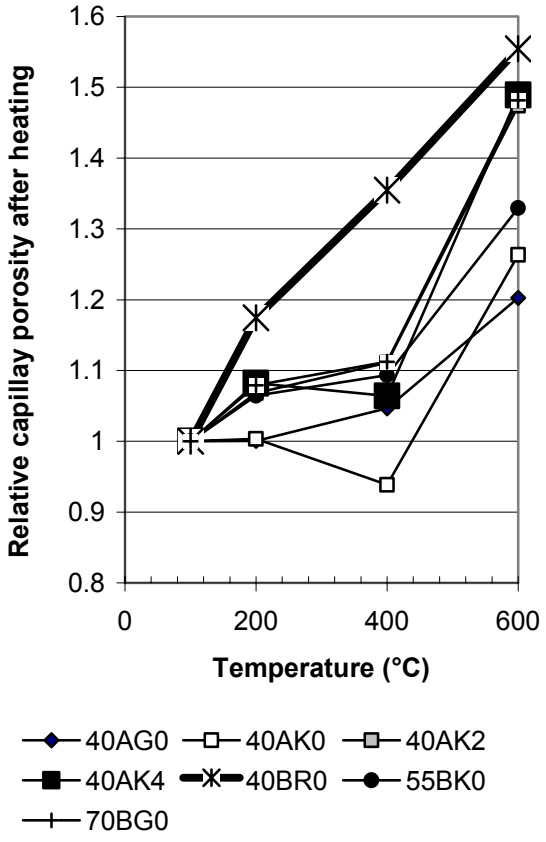

Figure 8.23 - Development of relative porosity versus temperature.

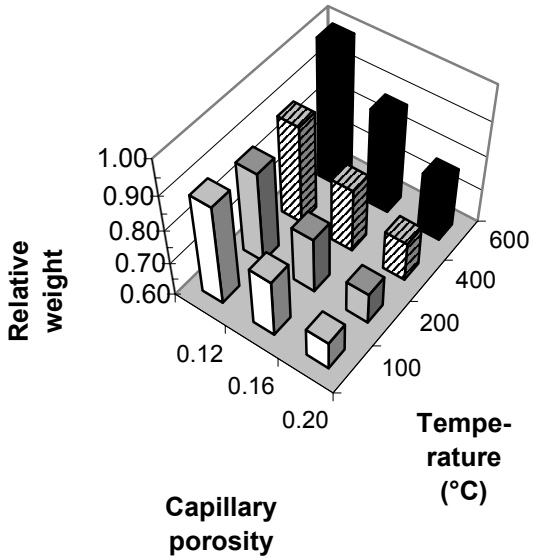

Figure 8.24 - Relative weight after fire spalling of air-cured SCC with c/p=0.58.

8.10 Influence of resistance to water penetration at water suction

8.10.1 General

The concrete was treated at different temperatures either 105 °C, 200 °C, 400 °C, 600 °C or 800 °C. The specimen size was 105 mm in diameter and 20 mm in thickness, three of each concrete. After cooling in a exsiccator at about RH = 10%, the weight was taken at 20 °C. The concrete was then subjected to suction from the flat side of the specimen. The water was penetrating the flat side of the specimen and the rim at about 1 mm in height. The weight was taken after 1, 2, 3, 4, 1000 and 4000 min. after start of the suction until it stabilised. The resistance to water penetration was calculated from the slopes of the abscissas of the water suction versus the square root of time, both between 0 and 4 min and between 1000 and 4000 min. In Chapter 7 it was found that the resistance to water penetration was much larger for SCC with filler than for normal concrete when the porosity was held constant. It was also seen in Chapter 7 that the resistance to water penetration increases with polypropylene fibres in the concrete, up to about 200 °C temperature. This may prohibit water from moving inward in the concrete at the start of a fire. The concrete will then resist fire better with fibres than without since the water in case of fibres present has to move out of the surface of the concrete. Since water movements in the concrete plays a key role to explain the fire spalling it was of great interest to correlate the resistance to water penetration to the weight of concrete after fire spalling.

8.10.2 Conditions after heating to 105 °C

The resistance to water penetration at water suction, m, is easily measure and a good tool to judge whether the concrete is sensitive to fire spalling or not. Figure 8.25 shows the results obtained after heating to 105 °C and measuring at 20 °C. The following observations were done:

- The resistance to water penetration at water suction, m, was about twice as large for air-cured concrete as for water-cured concrete at the same amount of fire spalling.
- For air-cured concrete maximum m = 17 s/m²·10^6 was found to give more than 85%-weight after fire spalling occurred.
- For water-cured concrete maximum m = 8.5 s/m²·10^6 was found to give more than 85%-weight after fire spalling occurred.
- Early water curing probably decreased the porosity of the surface of the concrete affecting the resistance to water penetration at water suction, c.p. Chapter 7.
- For 2 kg/m³ of polypropylene fibre increase of the resistance to water penetration at water suction was observed.
- For 4 kg/m³ of polypropylene fibre slight decrease of the resistance to water penetration at water suction was observed.

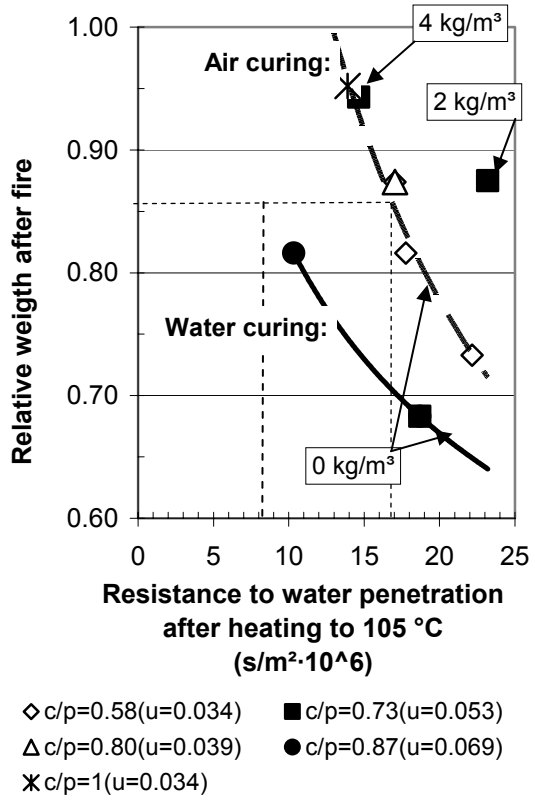

Figure 8.25 – Relative weight after fire spalling versus resistance to water penetration after heating to 105 °C and measuring at 20 °C. u = moisture content.

The following equation was evaluated in order to describe the fire spalling versus the resistance to water penetration at water suction:

$$W_i = h \cdot (m)^j \quad < 1 \qquad (8.11)$$

i = A denotes air curing; = W denotes water curing
h, j denotes constants given in Table 8.11.
m denotes the resistance to water penetration at water suction (s/m²·10^6)
W denotes the relative weight of concrete after fire spalling

Table 8.11 - Constants in equation (8.11).

Air curing, A			Water curing, W		
T (°C)	h	j	T (°C)	h	j
100	4.29	-0.570	100	1.65	-0.300
200	1.44	-0.220	200	1.22	-0.264
400	2.12	-0.438	400	1.01	-0.328
600	0.813	-0.164	600	2.65	3.70

It was probably the effect on hydration of the water curing that causes a lower resistance to water penetration at water suction in water-cured than in air-cured. However, for durability reasons it is preferred to cure the concrete well with water. For indoor use it seems an advantage to avoid too long water curing in order to limit the fire spalling of the concrete. It was also interesting to observe that the polypropylene fibres expands more than the concrete structure due to larger coefficient of thermal expansion and in a way tightened up the pores as regards water transports.

8.10.3 Conditions after heating to 200 °C

Figure 8.26 shows the performance of fire spalling versus the resistance to water penetration at water suction. Two-hundred °C is an interesting temperature since fire spalling occurs around this temperature. The polypropylene fibres are supposed to melt at about 170 °C but then become solid again as the temperature drops to 20 °C. The observations were as follows:

- The resistance to water penetration at water suction, m, was more than twice as large for air-cured concrete as for water-cured concrete at the same amount of fire spalling.
- For air-cured concrete maximum m = 10 s/m²·10^6 was found to give more than 85%-weight after fire spalling occurred.
- For water-cured concrete maximum m = 4.0 s/m²·10^6 was found to give more than 85%-weight after fire spalling occurred.
- Early water curing probably decreased the porosity of the surface of the concrete affecting the resistance to water penetration.

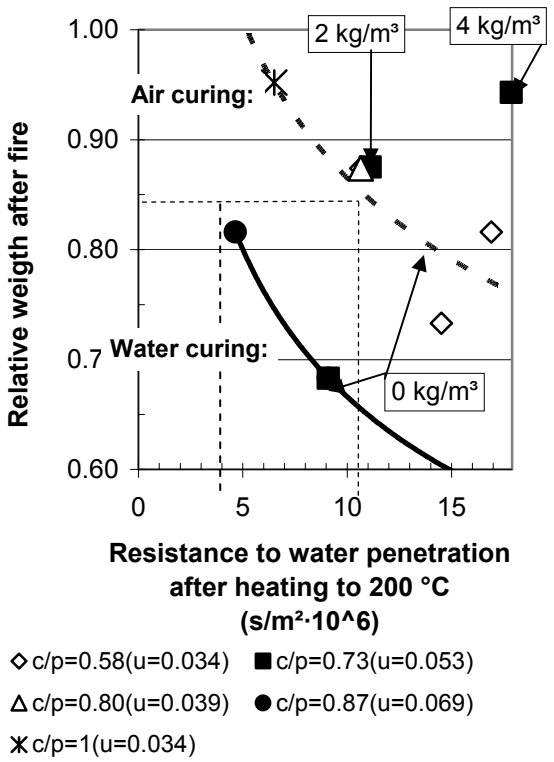

Figure 8.26 - Relative weight after fire spalling versus resistance to water penetration after heating to 200 °C and measuring at 20 °C. u = moisture content.

- For 2 kg/m³ of polypropylene fibre increase of the resistance to water penetration at water suction was observed.
- For 4 kg/m³ of polypropylene fibre a substantial increase of the resistance to water penetration at water suction was observed.
- Equation (8.10) describes the fire spalling.

8.10.4 Conditions after heating to 400 °C

Figure 8.27 shows the performance of fire spalling versus the resistance to water penetration at water suction. Four-hundred °C also is an interesting temperature since fire spalling certainly has occurred at lower temperature. The polypropylene fibres have melted and it is questioned if they evaporates or become solid again as the temperature drops to 20 °C. The observations were as follows:

- The resistance to water penetration at water suction, m, was more than four times as large for air-cured concrete as for water-cured concrete at the same amount of fire spalling.
- For air-cured concrete maximum m = 8.0 $s/m^2 \cdot 10^6$ was found to give more than 85%-weight after fire spalling occurred.
- For water-cured concrete maximum m = 2.0 $s/m^2 \cdot 10^6$ was found to give more than 85%-weight after fire spalling occurred.
- Early water curing probably decreased the porosity of the surface of the concrete affecting the resistance to water penetration at water suction, c.p. Chapter 7.
- For 2-4 kg/m³ of polypropylene fibre substantial decrease of the resistance to water penetration at water suction was observed.
- The decrease of resistance to water penetration shows that the fibres evaporate.

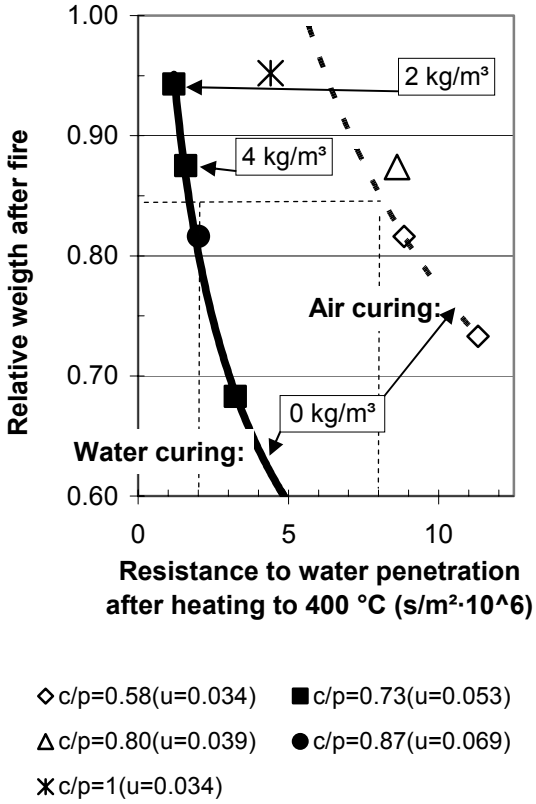

Figure 8.27 - Relative weight after fire spalling versus resistance to water penetration after heating to 400 °C and measuring at 20 °C. u = moisture content..

8.10.5 Conditions after heating to 600 °C

At 600 °C both the quartzite transformation and the release of carbon-dioxide from the limestone powder has taken place leaving large porosity in the concrete and thus decreasing the resistance to water penetration at water suction substantially. Figure 8.28 shows the fire spalling versus the resistance to water penetration at water suction after heating to 600 °C. The observations were as follows:

- The resistance to water penetration at water suction, m, was the same for air-cured concrete as for water-cured concrete at the same amount of fire spalling.

- For air-cured and for water-cured concrete maximum m = 0.7 s/m²·10^6 was found to give more than 85%-weight after fire spalling occurred.
- For 2-4 kg/m³ of polypropylene fibre the concrete did not show any difference in the resistance to water penetration at water suction compared with no fibres.

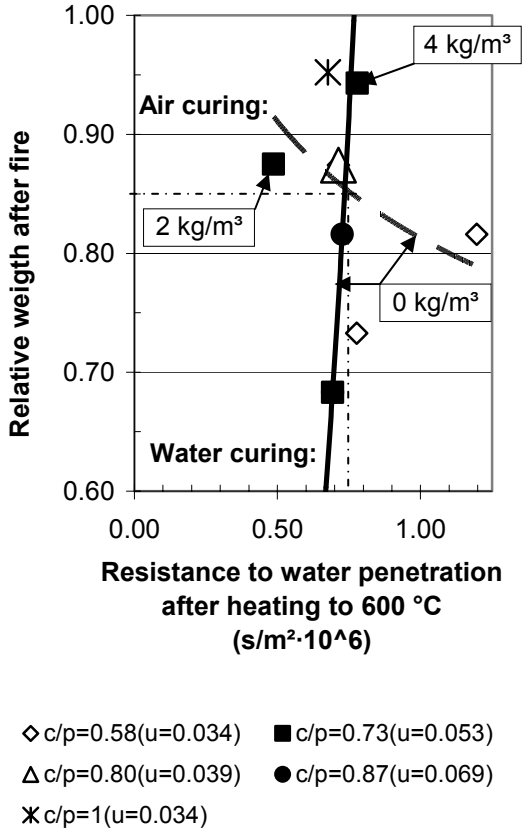

Figure 8.28 - Relative weight after fire spalling versus resistance to water penetration after heating to 600 °C and measuring at 20 °C. u = moisture content.

8.10.6 Summary of influence of resistance to water penetration at water suction

Figures 8.29-30 show a summary of the development of relative resistance to water penetration at water suction. The following equations were evaluated for the relative weight after fire, Figures 8.31-32:

$$W_A = 8.27 \cdot T^{(-0.36)} \cdot (m)^{(-0.000124 \cdot T - 0.27)} \quad (8.12)$$

$$W_B = 106 \cdot T^{(-0.731)} \cdot (m)^{(0.00053 \cdot T - 0.52)} \quad (8.13)$$

m denotes resistance to water penetration at water suction on fire spalling (s/m²·10^6)
B denotes air curing of concrete B
T denotes temperature (°C)
A denotes water curing of concrete A

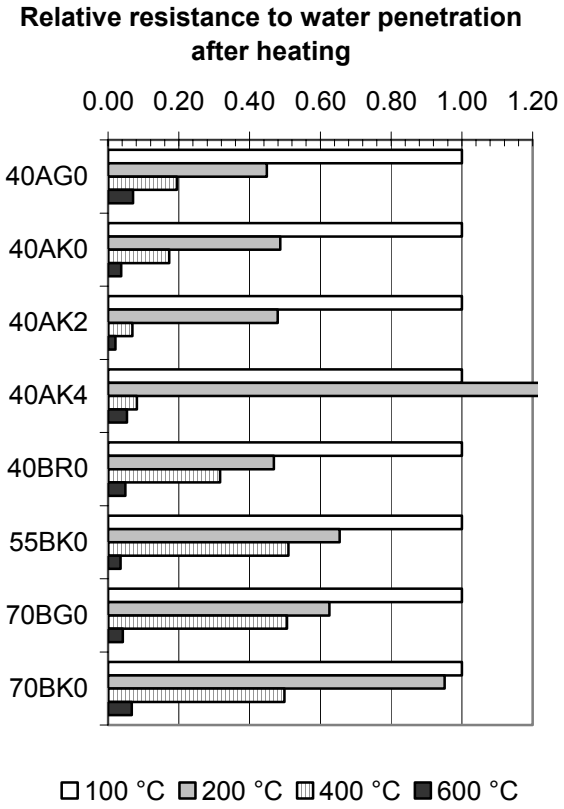

Figure 8.29 - Development of relative resistance to water penetration.

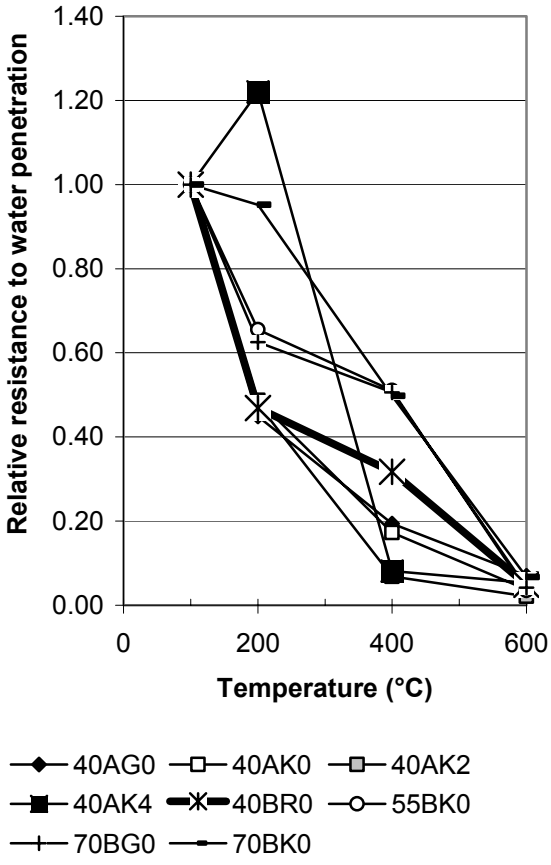

Figure 8.30 - Development of relative resistance to water penetration at water suction at different temperatures.

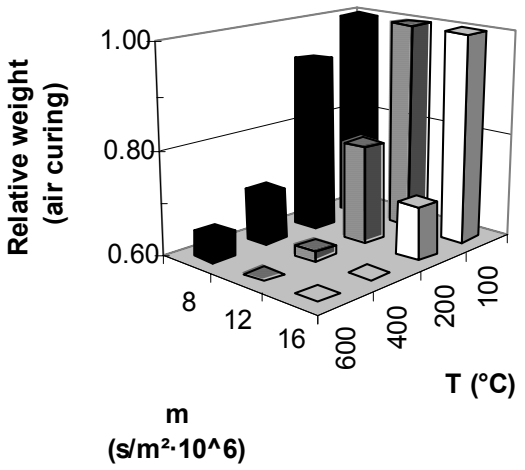

Figure 8.31 - Calculations with equation (8.13). m = resistance to water penetration (s/m²·10^6).

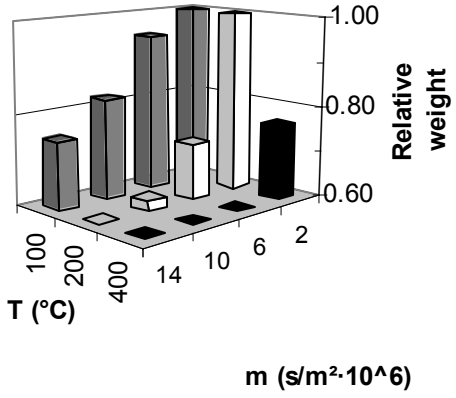

Figure 8.32 - Calculations with equation (8.12). m = resistance to water penetration (s/m²·10^6).

8.11 Amount of fibres to prevent fire spalling of 200-mm square reinforced columns

8.11.1 Calculation based on the cement content and the fibre content

A synthesis was required for the amount of fibres in combination with w/c and the cement-powder ratio, c/p. Figure 8.33 shows the weight after fire spalling independent of type of curing and cement type versus c/p, w/c and amount of fibres [94]. From Figure 8.33 the following equation was estimated for the relative weight of concrete without fibres after fire, W (no fibres):

$$W = (-5.29\cdot(c/p)^2 + 6.80\cdot(c/p) - 1.62)\cdot(w/c)+0.115\cdot\exp(2.11\cdot c/p) \quad (8.14)$$

Figure 8.34 and Table 8.12 show the resulting weight after fire of concrete without fibres as a result of equation (8.13). For concrete with 2 kg/m³ polypropylene fibres the results shown in Table 8.13 were obtained from equation (8.13) and Figure 8.33. Figure 8.35 shows the weight after fire of concrete with 2 kg/m³ fibres based on results in Figure 8.33 combined with equation (8.13) and Table 8.13. Figure 8.36 and Table 8.14 show the required amount of fibres in order to limit the amount of fire spalling of SCC to that of normal concrete without fibres, based on Figures 8.34-35. It is shown in Table 8.14 that the c/p-ratio substantially affected the fibre requirement. From Figures 8.34-36 and Table 8.14 the following equation for the amount of 32 µm fibres, ppf_{normal}, to limit the fire spalling of SCC to the same level of normal concrete without fibres was obtained (kg/m³):

$$ppf_{normal}=(28\cdot(c/p)^2-26\cdot(c/p)-2.4)\cdot\ln(w/c)+45\cdot(c/p)^2- 68\cdot(c/p)+23 > 0 \quad (8.15)$$

Table 8.12 - Weight after fire of concrete without fibres as a result of equation (8.13).

	c/p=					
w/c	0.50	0.60	0.70	0.80	0.90	1.00
0.40	0.51	0.63	0.72	0.80	0.85	0.90
0.50	0.56	0.69	0.78	0.84	0.88	0.89
0.60	0.60	0.74	0.83	0.88	0.90	0.88
0.70	0.65	0.80	0.89	0.93	0.92	0.87

Table 8.13 - Weight after fire of concrete with 2 kg/m³ fibres as a result of equation (8.13).

	c/p=					
w/c	0.50	0.60	0.70	0.80	0.90	1.00
0.40	0.62	0.74	0.83	0.91	0.96	1
0.50	0.68	0.81	0.90	0.96	1	1
0.60	0.73	0.87	0.94	1	1	1
0.70	0.79	0.94	1	1	1	1

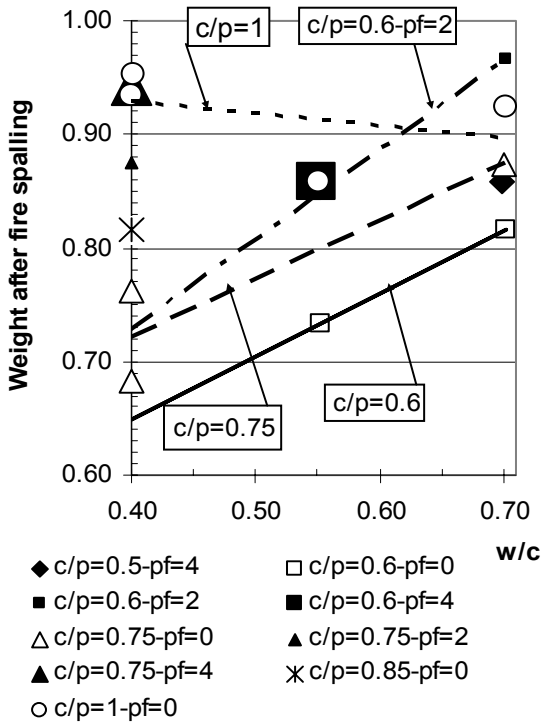

Figure 8.33 – Relative weight after fire spalling versus cement-powder ratio, c/p, w/c, and amount of fibres, ppf (kg/m³) [94].

Table 8.14 - Fibres to obtain the same weight of SCC after fire spalling like for normal concrete (kg/m³).

	c/p =				
w/c	0.60	0.70	0.80	0.90	1.00
0.40	5.8	4.0	2.6	1.5	
0.50	4.1	2.5	1.4	0.8	
0.60	2.7	1.2			
0.70	1.4				

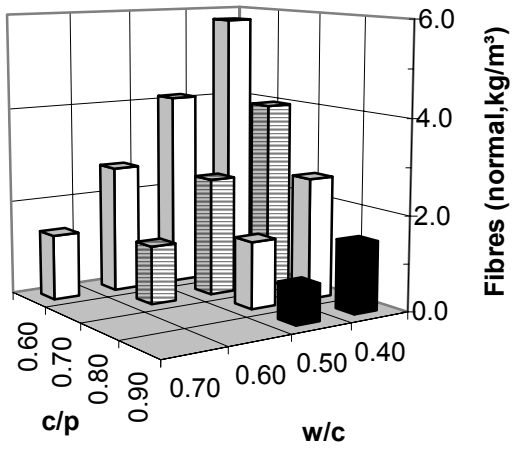

Figure 8.36 - Fibres in order to limit the fire spalling of SCC to the same level of normal concrete without fibres versus the cement-powder ratio, c/p, and the water-cement ratio, w/c.

The lowest observed weight of normal concrete after fire was 85% of the original weight. Therefore an alternative estimation of the amount of fibres was done in this case based on 85% remaining weight after fire compared with the original one, Table 8.15 and Figure 8.37. The following equation was obtained in order to simulate 85% remaining weight:

$$ppf_{85\%}=(-35\cdot(c/p)^2+34.9\cdot(c/p)-16.7)\cdot\ln(w/c)-25\cdot(c/p)+11.7 > 0 \quad (8.16)$$

c/p denotes the cement-powder ratio

$ppf_{85\%}$ denotes the amount of 32 μm fibres in order to obtain 85% weight of the original one after fire spalling (kg/m³)

w/c denotes the water-cement ratio

Table 8.15 - Fibres to obtain 85% remaining weight after fire spalling (kg/m³).

	c/p =				
w/c	0.60	0.70	0.80	0.90	1.00
0.40	4.2	2.4	1.0		
0.50	2.0				
0.60	0.9				
0.70					

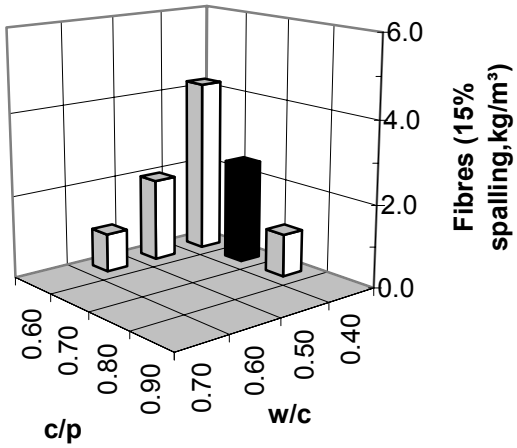

Figure 8.37 - Fibres based on 85% remaining weight after fire compared with the original one.

8.11.2 Calculation based on the Portland cement content and the fibre content

Another synthesis was done for the amount of fibres combined with the water-Portland cement ratio, w/Pc, and the Portland cement-powder ratio, Pc/p, Figure 8.38 [94]. From Figure 8.38 the following equation was estimated for the relative weight of concrete without fibres after fire:

$$W = (-0.336\cdot(Pc/p)^2 - 0.375\cdot(Pc/p) + 0.762)\cdot(w/Pc) + 0.182\cdot\exp(1.67\cdot Pc/p) - 0.02 \quad (8.17)$$

w/Pc denotes the water-Portland cement ratio
Pc/p denotes the Portland cement-powder ratio
W denotes the relative weight of concrete without fibres after fire

Figure 8.39 and Table 8.16 show the weight after fire of concrete without fibres based on equation (8.16). For concrete with 2 kg/m³ polypropylene fibres results shown in Table 8.17 and Figure 8.40 were obtained. Figure 8.38 gave the amount of 32 μm fibre required for the same fire spalling of SCC like for normal, Figure 8.41 and Table 8.18:

$$ppf_{normal} = (13\cdot(Pc/p) - 12.3)\cdot\ln(w/Pc) - 2.69\cdot(Pc/p)^2 + 2.65\cdot(Pc/p) - 0.2 > 0 \quad (8.18)$$

ppf_{normal} 32 μm fibres to obtain the same weight after fire of SCC for like normal (kg/m³)
w/Pc denotes the water-Portland cement ratio
Pc/p denotes Portland cement-powder ratio.

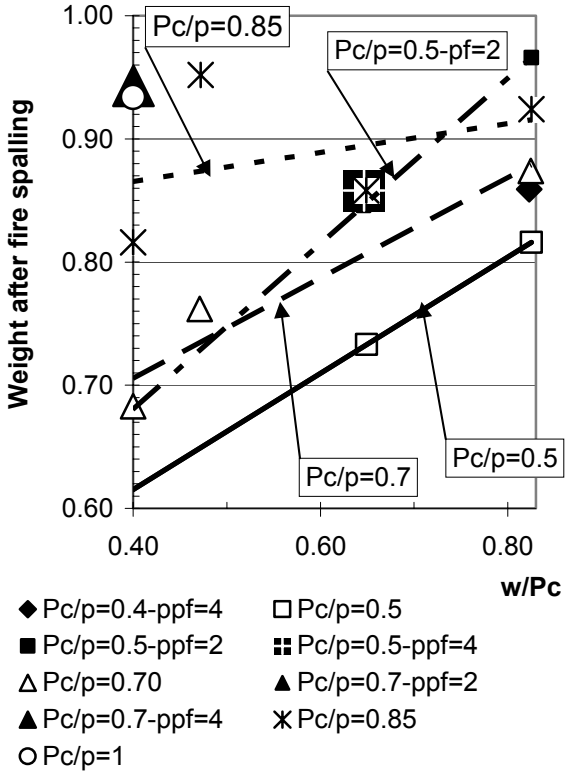

Figure 8.38 – Relative weight after fire spalling versus cement-powder ratio, Pc/p, w/Pc, and amount of fibres (kg/m³) [94].

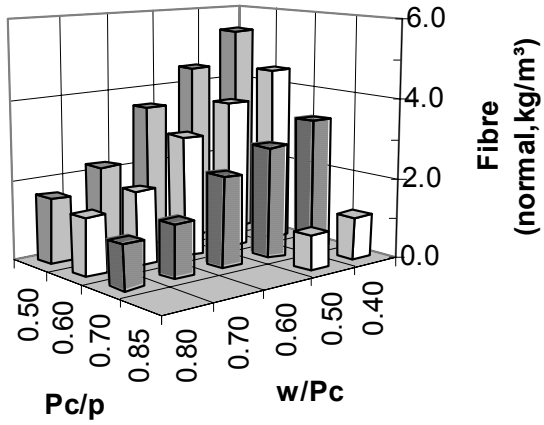

Figure 8.41 - Fibre amount required for the same fire spalling of SCC like for normal concrete.

Figure 8.42 and Table 8.19 show fibres to limit fire spalling at 15% of original weight (kg/m³):

$$ppf_{85\%} = (-43\cdot(Pc/p)^2 + 72\cdot(Pc/p) - 31)\cdot\ln(w/Pc) - 14\cdot(Pc/p)^2 + 18.7\cdot(Pc/p) - 6.2 \quad (8.19)$$

$ppf_{85\%}$ denotes the amount of 32 μm fibres to obtain 85% weight after fire of SCC of the original one (kg/m³).
w/Pc denotes the water-Portland cement ratio
Pc/p denotes Portland cement-powder ratio

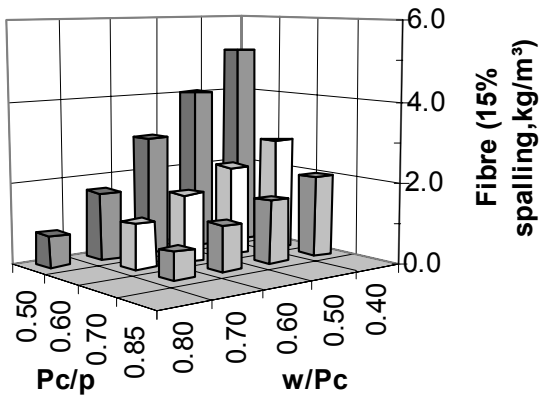

Figure 8.42 - Fibres in order to limit the amount of fire spalling to 15% of the original weight.

Table 8.16 - Weight after fire of concrete without fibres as a result of equation (8.15).

	Pc/p =				
w/Pc	0.50	0.60	0.70	0.85	1.00
0.40	0.61	0.66	0.72	0.83	0.98
0.50	0.66	0.70	0.75	0.85	0.99
0.60	0.71	0.74	0.79	0.87	0.99
0.70	0.76	0.79	0.82	0.89	1.00
0.80	0.81	0.83	0.85	0.91	1.00

Table 8.17 - Weight after fire of concrete with 2 kg/m³ fibres as a result of equation (8.16).

	Pc/p =				
w/Pc	0.50	0.60	0.70	0.85	1.00
0.40	0.70	0.75	0.81	0.92	1
0.50	0.77	0.81	0.85	0.95	1
0.60	0.83	0.86	0.90	0.99	1
0.70	0.89	0.91	0.95	1	1
0.80	0.95	0.97	0.99	1	1

Table 8.18 - Amount of fibres to limit the amount of fire spalling to that of normal concrete (kg/m³).

	Pc/p =				
w/Pc	0.50	0.60	0.70	0.85	1.00
0.40	5.4	4.5	3.3	1.1	
0.50	4.5	3.8	2.8	0.9	
0.60	3.6	3.0	2.3	0.7	
0.70	2.2	1.9	1.4		
0.80	1.7	1.4	1.1		

Table 8.19 - Amount of fibres to limit the fire spalling to 15% of the original weight (kg/m³).

	Pc/p =				
w/Pc	0.50	0.60	0.70	0.85	1.00
0.40	4.7	3.8	2.6		
0.50	3.6	2.9	1.9		
0.60	2.6	2.0	1.2		
0.70	1.4	1.0			
0.80					

8.11.3 Comparison between results with equations and experiments

It was important to compare the results with equations (8.14) and (8.17) and the experiments. Figure 8.43 and 8.44 show the calculated weight of the concrete versus the measured weight after fire spalling. Equation (8.17) showed the highest significance probably since it was based on the Portland cement content.

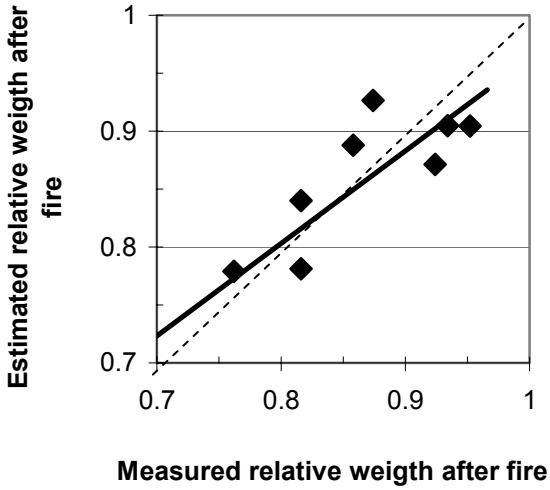

Figure 8.43 – With equation (8.14) calculated weight of the concrete versus the measured weight after fire spalling.

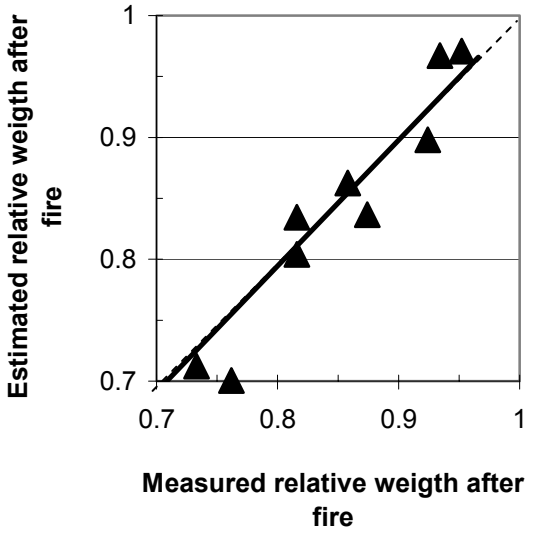

Figure 8.44 – With equation (8.17) calculated weight of the concrete versus the measured weight after fire spalling.

8.12 Evaluation of equations

8.12.1 General

It was important to evaluate the equations ion order to confirm the validity and the limits of application. Reference are given to main Chapters.

8.12.2 Previous research

Tensile strength after heating:

Table 8.20 shows an evaluation of equation (2.1):

$$f_{ct,T}/f_{ct,20}=-0.000001\cdot T^2-0.0003\cdot T+0.95 \qquad (2.1)$$

$f_{ct,T}$ denotes split tensile strength at elevated temperature (=1 at 20 °C)
$f_{ct,20}$ denotes tensile strength at 20 °C
T denotes temperature (20 < T < 800 °C)

Table 8.20 - An evaluation of equation (2.1):

Temperature (°C)	$f_{ct,T}/f_{ct,20}$	$f_{ct,T20}/f_{ct,20}$
100	0.91	0.99
200	0.85	0.91
300	0.77	0.81
400	0.67	0.69
500	0.55	0.56
600	0.41	0.41
700	0.25	0.25
800	0.07	0.07

Table 8.20 shows an evaluation of equation (2.2):

$$f_{ct,T20}/f_{ct,20}=-0.0000008\cdot T^2- 0.0006\cdot T+ 1.06 \qquad (2.2)$$

$f_{ct,T20}$ denotes split tensile strength at 20 °C after cooling from the elevated temperature
$f_{ct,20}$ denotes tensile strength at 20 °C
T denotes temperature (20 < T < 800 °C)

Creep at varying temperatures and temperature gradients:

Table 8.21 shows the temperature development with ISO 834 fire, equation (2.3):

$$T = 345\cdot\log(480\cdot t+1)+20 \qquad (2.3)$$

t denotes time (h)
T denotes fire temperature (°C)

The torsional creep is shown in Table 8.22:

$$C_{to}=(0.0013\cdot T-0.040)\cdot\ln(t)+ 0.0000056\cdot T^2 + 0.0023\cdot T + 0.06 \qquad (2.4)$$

C_{to} denotes torsional creep (rad/mm)
t denotes elapsed time (h)
T denotes temperature (20 < T < 400 °C)

Table 8.21 - The temperature development with ISO 834 fire, equation (2.3).

Time (h)	T (°C)
0.1	603
0.2	705
0.3	766
0.4	809
0.5	842
0.6	869
0.7	892
0.8	912
0.9	930
1	945

Table 8.22 - The torsional creep according to equation (2.4).

	Time (h)			
T (°C)	1	2	3	4
20	0.1	0.1	0.1	0.1
100	0.3	0.4	0.4	0.5
200	0.7	0.9	1.0	1.0
300	1.3	1.5	1.6	1.7
400	1.9	2.2	2.4	2.5

Explosive fire spalling of normal concrete:

Table 8.23 shows the critical moisture level at fire spalling of concrete, equation (2.5):

$$u = 0.000617\cdot\sigma^3 + 0.0341\cdot\sigma^2 - 0.638\cdot\sigma + 7 \qquad (2.5)$$

u denotes moisture content (%)
σ denotes stress (0 < σ < 25 MPa)

Table 8.23 - The critical moisture levels at fire spalling of concrete, equation (2.5).

Stress (MPa)	Moisture content (%)
1	6.4
2	5.9
3	5.4
4	5.0
5	4.6
10	3.4
15	3.0
20	2.9
25	2.7

8.12.3-4 Material and methods

No equations are available.

8.12.5 Analysis

Grading of particles in fresh concrete:

The particle grading of fresh NC was foreseen, Table 8.24 and equation (5.1). Table 8.25 shows the particle grading of the fresh SCC that was studied in the project, equation (5.1).

$$s = a\cdot d^b \ \{0.125 < d < 0.7\cdot d_{max}\} \qquad (5.1)$$

s denotes particle passing through

a 38%
b constant according to Table 5.1
d particle diameter (0.1 < d < 10 mm)
K cube strength of concrete (MPa)

Table 5.1 - Constant b in equation (5.1)

K	25	60	90	120	150
b	0.32	0.24	0.20	0.18	0.16

Table 8.24 - Grading of particle in fresh NC, equation (5.1). K = 150-mm cube strength.

d (mm)	K25	K60	K90	K120	K150
0.125	0.20	0.23	0.25	0.26	0.27
0.25	0.24	0.27	0.29	0.30	0.30
0.5	0.30	0.32	0.33	0.34	0.34
1	0.38	0.38	0.38	0.38	0.38
2	0.47	0.45	0.44	0.43	0.42
4	0.59	0.53	0.50	0.49	0.47
5.6	0.66	0.57	0.54	0.52	0.50
11.2	0.82	0.68	0.62	0.59	0.56

K = 150-mm cube strength.

Table 8.25 - Particle grading of fresh SCC that was studied in the project, equation (5.1).

d	SCC0-K30	SCC0-K60	SCC2-K30	SCC2-K60	SCC4-K30	SCC4-K60
0.13	0.27	0.29	0.28	0.30	0.31	0.33
0.25	0.32	0.34	0.33	0.35	0.38	0.39
0.50	0.39	0.40	0.40	0.41	0.46	0.47
1	0.47	0.47	0.48	0.48	0.55	0.55
2	0.57	0.56	0.57	0.56	0.66	0.65
4	0.68	0.66	0.69	0.66	0.80	0.77
5.6	0.75	0.71	0.75	0.71	0.88	0.83
11.2	0.90	0.84	0.90	0.84	1.00	0.98

K = cube strength. SCC2 = Self-Compacting Concrete (2 kg/m³ polypropylene fibres.

Effect of fibres and filler on strength:
Table 8.26 shows the effect of fibres on strength, equation (5.2):

$$f_{c28ppf} = f_{c280} \cdot (1 - 0.023 \cdot ppf) \qquad (5.2)$$

ppf denotes amount of polypropylene fibre (0 < pp f <4 kg/m³)
f_{c28ppf} denotes 28-day strength (fibre, MPa)
f_{c280} denotes 28-day strength (no fibre, 30 < f_{c280} < 80 MPa)

Table 8.27 shows the effect of fibres, eq. (5.3):

$$f_{c28f} = f_{c280} + f \cdot 0.07 \qquad (5.3)$$

f denotes filler (0 < f < 250 kg/m³)
f_{c28f} denotes 28-day strength with filler (MPa)
f_{c280} denotes 28-day strength (no filler, MPa)

Table 8.26 - Effect of fibres on strength, equation (5.2).

Strength (MPa)	Fibres (kg/m³)			
	1	2	3	4
30	29.3	28.6	27.9	27.2
40	39.1	38.2	37.2	36.3
40	39.1	38.2	37.2	36.3
60	58.6	57.2	55.9	54.5
70	68.4	66.8	65.2	63.6
80	78.2	76.3	74.5	72.6

Table 8.27 shows the effect of fibres, equation (5.3).

Strength	Filler (kg/m³)			
(MPa)	50	100	150	200
30	33.5	37	40.5	44
40	43.5	47	50.5	54
40	43.5	47	50.5	54
60	63.5	67	70.5	74
70	73.5	77	80.5	84
80	83.5	87	90.5	94

Elastic modulus, strength and strain at maximum strength:
The following formula was obtained for the relative hot properties at elevated temperature, Table 8.28, equation (5.6):

$$r = c \cdot T^2 + e \cdot T + g \qquad (5.6)$$

c,e,g constants for hot and residual properties of concrete at and after elevated temperatures given in Table 5.4.
r denotes residual and hot relative properties of concrete at and after elevated temperatures.
T denotes temperature (20 < T < 800 °C).

Table 5.4 – Constants in equation (5.2).

Property	Constant	Hot	Residual
E-modulus	a	0.0000013	0.0000008
	c	- 0.00221	-0.00196
	g	1.04	1.06
Strength	a	-0.0000012	-0.0000005
	c	- 0.000131	- 0.000729
	g	0.99	1.01
Strain	a	-0.0000022	0.0000035
	c	0.00279	- 0.000301
	g	0.95	1

Table 8.28 shows the relative hot properties at elevated temperature, equation (5.6). Table 2.29 shows the relative residual properties after treatment at elevated temperature, equation (5.6).

Table 8.28 - Relative hot properties at elevated temperature, equation (5.6).

Temperature	Hot properties		
(°C)	E-modulus	Strength	Strain
100	0.83	0.96	1.21
200	0.67	0.92	1.42
300	0.53	0.84	1.59
400	0.41	0.75	1.71
500	0.32	0.62	1.80
600	0.25	0.48	1.83
700	0.21	0.31	1.83
800	0.19	0.12	1.77

Table 8.29 - Relative residual properties after treatment at elevated temperature, equation (5.6).

Temperature	Residual properties		
(°C)	E-modulus	Strength	Strain
100	0.87	0.93	1.00
200	0.70	0.84	1.08
300	0.54	0.75	1.22
400	0.40	0.64	1.44
500	0.28	0.52	1.72
600	0.17	0.39	2.08
700	0.08	0.25	2.50
800	0.00	0.11	3.00

Table 8.30-32 give an experimental comparison between E_{dyn} , E_{stat} and strength, equation (5.9). Table 5.7 gives a summary of the constants h and j in the following equation (GPa):

$$E = (h \cdot f_c + j) \cdot f_c \qquad (5.9)$$

f_c denotes 100-mm cylinder strength (MPa)
h,j constants given in Table 5.7.

Table 5.7 - Constants h and j in equation (5.9).

Temp. (°C)	E_{dyn}, h	E_{dyn}, j	E_{stat}, h	E_{stat}, j
20-20	-0.00412	0.821	-0.00079	0.500
200–20			-0.00240	0.503
200-200			0.00021	0.334
400-20			-0.0014	0.319
400-400			-0.00075	0.252
800-20	0.0014	0.201	-0.00107	0.127
800-800			-0.031	0.74

400-20 = heated to 400 °C, tested at 20 °C.

Table 8.30 - Hot static elastic modulus based on equation (5.9).

Temperature	fc (MPa)				
(°C)	5	20	40	60	80
20	2.5	9.7	18.7	27.2	34.9
200	1.7	6.8	13.7	20.8	28.1
400	1.2	4.7	8.9	12.4	15.4
800	2.9	2.4			

Table 8.31 - Residual dynamic elastic modulus based on equation (5.9).

Temperature	fc (MPa)				
(°C)	5.0	20.0	40.0	60.0	80.0
20	4.0	14.8	26.2	34.4	39.3
200					
400					
800	1.04	4.58			

Table 8.32 - Residual static elastic modulus based on equation (5.9).

Temperature	fc (MPa)				
(°C)	5	20	40	60	80
20	2.5	9.7	18.7	27.2	34.9
200	2.5	9.1	16.3	21.5	24.9
400	1.6	5.8	10.5	14.1	16.6
800	0.6	2.1			

Based on the experimental results the following formulas were obtained also shown in Tables 8.33-8.35:

$$Edyn = ((0.0000071 \cdot T - 0.00426) \cdot (f_c) + (-0.00079 \cdot T + 0.837)) \cdot (f_c) \qquad (5.10)$$

$$Estat,hot = (-0.0000000916 \cdot (T)^2 + 0.0000374 \cdot T - 0.00211) \cdot (f_c)^2 + (0.00000232 \cdot (T)^2 - 0.00161 \cdot T + 0.54) \cdot f_c \qquad (5.11)$$

$$Estat, residual = -0.00152 \cdot (f_c)^2 + (-0.000263 \cdot T + 0.507) \cdot (f_c) \qquad (5.12)$$

Table 8.33 - Residual dynamic E-modulus based on equation (5.10), (MPa).

Temperature	fc (MPa)				
(°C)	5	20	40	60	80
20	4.0	14.8	26.3	34.4	39.3
100	3.7	13.7	24.6	32.7	37.9
200	3.3	12.4	22.6	30.5	36.1
300	2.9	11.1	20.6	28.3	34.4
400	2.6	9.9	18.6	26.1	32.6
500	2.2	8.6			
600	1.8	7.3			
700	1.4	6.0			
800	1.1	4.7			

Table 8.34 - Hot static E-modulus based on equation (5.11), (MPa).

Temperature	fc (MPa)				
(°C)	5	20	40	60	80
20	2.5	9.6	18.1	25.5	31.8
100	2.0	8.3	17.3	26.8	36.8
200	1.6	6.9	15.3	25.0	36.2
300	1.4	5.7	12.2	19.6	27.7
400	1.3	4.7	8.2	10.5	11.5
500	1.4	3.9			
600	1.7	3.4			
700	2.2	3.0			
800	2.9	2.8			

Table 8.35- Residual static E-modulus based on equation (5.12), (MPa).

Temperature	fc (MPa)				
(°C)	5	20	40	60	80
20	2.5	9.4	17.6	24.6	30.4
100	2.4	9.0	16.8	23.4	28.7
200	2.2	8.5	15.7	21.8	26.6
300	2.1	8.0	14.7	20.2	24.5
400	2.0	7.4	13.6	18.6	22.4
500	1.8	6.9			
600	1.7	6.4			
700	1.6	5.9			
800	1.4	5.3			

8.12.6 Test significance
No equations are available.

8.12.7 Supplementary tests
Residual properties:
Tables 8.37-38 shows estimations with equation (7.1):

$$r = c \cdot T^2 + e \cdot T + g \qquad (7.1)$$

c,e,g constants for residual properties at and after elevated temperatures given in Table 7.1.

r denotes residual relative properties of concrete at and after elevated temperatures.

T denotes temperature (°C).

Table 7.1 – Constants in equation (7.1).

Residual property	Con-stant	Without limestone powder	Limestone powder
E-modulus	c	0.0000013	0.000000994
	e	- 0.00221	-0.00215
	g	1.04	1.09
Strength	c	-0.000000349	-0.000000349
	e	- 0.000131	- 0.00094
	g	0.99	1.07
Strain	c	-0.0000022	0.00000333
	e	0.00279	- 0.000142
	g	0.95	1.04

Tables 8.36 - Estimations of relative properties for concrete with no limestone powder, equation (7.1).

Temperature (°C)	E-modulus	Strength	Strain
100	0.83	0.96	1.21
200	0.67	0.92	1.42
300	0.53	0.84	1.59
400	0.41	0.75	1.71
500	0.32	0.62	1.80
600	0.25	0.48	1.83
700	0.21	0.31	1.83
800	0.19	0.12	1.77

Table 8.37 - Estimations of relative properties for concrete with limestone powder, equation (7.1).

Temperature (°C)	E-modulus	Strength	Strain
100	0.88	0.88	1.06
200	0.70	0.87	1.14
300	0.53	0.76	1.30
400	0.39	0.64	1.52
500	0.26	0.51	1.80
600	0.16	0.38	2.15
700	0.07	0.24	2.57
800	0.01	0.09	3.06

Residual elastic modulus at 600 °C:
The elastic modulus was estimated for the E-modules at 20 ° after heating to 600 °C, $E_{600\text{-}20}$:

$$E_{600\text{-}20} = (0.0025 \cdot (f_c) + 0.0994) \cdot f_c \qquad (7.2)$$

f_c denotes cylinder strength ($5 < f_c < 25$ MPa)

Table 8.38 shows estimations with equation (7.2) of elastic modulus at 20 ° after heating to 600 °C.

Table 8.38 - Estimations with equation (7.2) of the elastic modulus at 20 ° after heating to 600 °C.

Cylinder strength (MPa)	Static E-modulus (GPa)
5	0.6
10	1.2
15	2.1
20	3.0
25	4.0

Resistance to water penetration:
Table 8.39 shows estimations with equation (7.5):

$$m = d \cdot (P_{cap})^e \qquad (7.5)$$

d,e denotes constants given in Table 7.5

m denotes resistance to water penetration ($s/m^2 \cdot 10^6$)

P_{cap} denotes capillary porosity $\{0.14 < P_{cap} < 0.24\}$

Table 8.39 - Estimations of resistance to water penetration with equation (7.5) (s/m²·10⁶).

Porosity	Normal - air	SCC - air	SCC - water
0.12	18.5		
0.14	7.7	20.9	
0.16	3.6	9.1	7.0
0.18	1.8	4.4	2.1
0.20	1.0	2.3	0.7
0.22	0.6	1.2	0.3
0.24	0.4	0.7	0.1

8.12.8 Discussion

Temperature of saturation:

Table 8.40 shows estimations with equation (8.1):

$$T_{sat} = 115 \cdot (1.07 - RH) \cdot \exp((2.52 - 0.95 \cdot RH) \cdot w/c)) \quad (8.1)$$

w/c denotes water-cement ratio ($0.35 < w/c < 0.75$)
RH denotes RH before fire ($0.30 < RH < 0.90$)
T_{sat} denotes temperature of saturation (°C).

Table 8.40 - Estimations of temperature of saturation with equation (8.1) (°C).

	RH before heating				
w/c	0.35	0.45	0.55	0.65	0.75
0.35	178	148	120	94	69
0.40	199	165	133	103	76
0.45	222	183	147	114	83
0.50	247	203	162	125	91
0.55		225	179	138	99
0.60		250	198	151	109
0.65			219	166	119
0.70			242	183	130
0.75			268	201	143

Relative weight after fire spalling:

Table 8.41 shows the relative weight of the concrete A with type I cement (water curing), equation (8.2):

$$W_A = 2.39 \cdot (w/p) - 0.019 \quad (8.2)$$

w/p denotes water-powder ratio ($0.25 < w/p < 0.40$)
W_A denotes weight after fire spalling concrete A

Table 8.41 - The relative weight of the concrete A with type I cement (water curing), equation (8.2).

w/p	Relative weight after fire
0.25	0.58
0.30	0.70
0.35	0.82
0.40	0.94

Parameter study:

Table 8.42 shows estimations with equation (8.3) of a parameter study of the weight after fire spalling of concrete A with type I cement without fibres:

$$n = k \cdot (1 - W) + m \quad (8.3)$$

c denotes cement content
k, m denotes constants given in Table 8.2
f denotes filler content
n denotes parameter in study
p denotes powder content (cement + filler)
W denotes weight after fire spalling

Table 8.2 – Parameters in equation (8.3).

Parameter, n	k	m
Aggregate 11-16 mm/(10·p)	-0.234	0.177
c/p	-1.060	1.070
f/p	1.060	-0.070
w/p	-0.411	0.411

Table 8.42 - Estimations with equation (8.3) of a parameter study of the weight after fire spalling of concrete A with type I cement without fibres

Relative weight	Aggr 11-16 mm/(10·p)	c/p	f/p	w/p
0.60	0.08	0.65	0.35	0.25
0.70	0.11	0.75	0.25	0.29
0.80	0.13	0.86	0.14	0.33
0.90	0.15	0.96	0.04	0.37

Tables 8.43 -44 show estimations with equation (8.4) of a parameter study of the weight after fire spalling of concrete B with filler cement type II without fibres:

$$s = q \cdot (1 - W) + r \quad (8.4)$$

c denotes cement content
f denotes filler content
p denotes powder content (cement + filler)
q, r denotes constants given in Table 8.3
s denotes parameter in study
W denotes weight after fire spalling

Table 8.3 – Parameters in equation (8.4).

Parameter, s	q	r
Aggregate /(10xp)	-1.23	0.609
Aggregate 0-8 mm /(10xp)	-0.917	0.394
Aggregate 8-11 mm /(10xp)	-0.323	0.151
c/p	-1.59	0.943
f/p	1.87	0.110
Moisture	0.0286	0.747
w/p	-1.30	0.659

Table 8.43 - Estimations with equation (8.4) of a parameter study of the weight after fire spalling of concrete B with filler cement type II without fibres.

Relative weight	Aggr/(10·p)	Aggr 0-8 mm/(10·p)	Aggr 8-11 mm/(10·p)
0.70	0.24	0.12	0.06
0.75	0.30	0.16	0.07
0.80	0.36	0.21	0.09
0.85	0.42	0.26	0.10
0.90	0.49	0.30	0.12
0.95	0.55	0.35	0.14

Table 8.44 - Estimations with equation (8.4) of a parameter study of the weight after fire spalling of concrete B with filler cement type II without fibres.

Relative weight	c/p	f/p	Moisture	w/p
0.70	0.47	0.67	0.76	0.27
0.75	0.55	0.58	0.75	0.33
0.80	0.63	0.48	0.75	0.40
0.85	0.70	0.39	0.75	0.46
0.90	0.78	0.30	0.75	0.53
0.95	0.86	0.20	0.75	0.59

Effect of polypropylene fibres:

Table 8.45 shows the effect of polypropylene fibres on the weight of the concrete A at w/p ≈ 0.29 after fire exposure calculated with equation (8.6):

$$W_{A,w/p\approx0.29} = 0.82\cdot(ppf)^{0.11} \quad \{0.2<f<4\ kg/m^3\} \quad (8.6)$$

ppf denotes fibre ($0.2 < f < 4$ kg/m³)
w/p denotes water-powder ratio ($0.25 < w/p < 0.40$)
$W_{A,w/p\approx0.29}$ denotes weight after fire of concrete A with Type I cement w/p≈0.29.

Table 8.45 - Effect of polypropylene fibres on the weight of the concrete A at w/p ≈ 0.29 after fire exposure calculated with equation (8.6).

Fibres (kg/m³)	Relative weight after fire
0.2	0.69
1	0.82
2	0.88
3	0.93
4	0.96

Table 8.46 shows in the same way the relative weight of concrete B with type II cement, W_B, versus fibre content and w/p based on equation (8.7):

$$W_B = (1.5\cdot(w/p)+0.32)\cdot(ppf)^{(-0.19\cdot(w/p)+0.11)} \quad (8.7)$$

ppf denotes plastic fibres $\{0.2 < ppf < 4\ kg/m^3\}$
w/p denotes the water-powder ratio
W_B denotes weight after fire spalling of concrete B $\{0.30< w/p< 0.40\}$

Table 8.46 - Relative weight of concrete B with type II cement, W_B, versus fibre content and w/p based on equation (8.7).

Fibres (kg/m³)	w/p		
	0.3	0.35	0.4
0.2	0.71	0.79	0.87
1	0.77	0.85	0.92
2	0.80	0.87	0.94
3	0.82	0.89	0.96
4	0.83	0.90	0.96

Effect of porosity on fire spalling:

Table 8.47 shows the effect of porosity and temperature on weight after fire spalling based on equation (8.10):

$$W_{fs} = (-1.02\cdot10^{-6}\cdot(T)^2+0.000734\cdot T+0.232)\cdot (P_{cap})^{(-2.22\cdot10\text{^-}6\cdot(T)\text{^}2+0.00144\cdot T-0.644)} \quad (8.10)$$

P_{cap} denotes capillary porosity at suction
T denotes temperature at heating (°C)
W_{fs} denotes relative weight after fire spalling of air-cured SCC with c/p=0.58.

Table 8.47 - Effect of porosity and temperature on weight after fire spalling based on equation (8.10).

Porosity	Temperature (°C)			
Pcap	100	200	400	600
0.14	0.82	0.81	0.83	0.95
0.16	0.77	0.76	0.79	0.88
0.18	0.72	0.72	0.75	0.82
0.2	0.68	0.69	0.72	0.78
0.22	0.65	0.66	0.69	0.73
0.24	0.62	0.64	0.66	0.70

Effect of resistance to water penetration on fire spalling:

Tables 8.48-49 shows the effect of resistance to water penetration and temperature on the relative weight after fire spalling based on equation (8.11):

$$W_i = h\cdot(m)^j \quad (8.11)$$

i = A denotes air curing; = W denotes water curing
h,j denotes constants given in Table 8.11.

m denotes the resistance to water penetration at water suction (s/m²·10^6)
W denotes the relative weight of concrete after fire spalling

Table 8.11 - Constants in equation (8.11).

Air curing, A			Water curing, W		
T (°C)	h	j	T (°C)	h	j
100	4.29	-0.570	100	1.65	-0.300
200	1.44	-0.220	200	1.22	-0.264
400	2.12	-0.438	400	1.01	-0.328
600	0.813	-0.164	600	2.65	3.70

Tables 8.48 - Effect of resistance to water penetration and temperature on relative weight of air-cured concrete after fire spalling based on equation (8.11).

m	Temperature (°C)			
(s/m²·10^6)	100	200	400	600
0.5				0.91
0.75				
1				0.81
5				0.62
10		0.87	0.77	
15	0.92	0.79	0.65	
20	0.78	0.74		
25				

Tables 8.49 - Effect of porosity and temperature on relative weight of water-cured concrete after fire spalling based on equation (8.11).

m	Temperature (°C)			
(s/m²·10^6)	100	200	400	600
0.5				0.21
0.75				0.85
1			1.00	0.81
5		0.94	0.59	
10	0.83	0.78		
15	0.73	0.70		
20	0.67	0.65		
25				

The following Tables 8.50-51 show estimation of the relative weight after fire with equations (8.12-13):

$$W_A = 8.27 \cdot T^{(-0.36)} \cdot (m)^{(-0.000124 \cdot T - 0.27)} \quad (8.12)$$

$$W_B = 106 \cdot T^{(-0.731)} \cdot (m)^{(0.00053 \cdot T - 0.52} \quad (8.13)$$

m denotes resistance to water penetration at water suction on fire spalling (s/m²·10^6)
B denotes air curing of concrete B
T denotes temperature (°C)
A denotes water curing of concrete A

Tables 8.50 - Estimation of the relative weight of water-cured concrete after fire with equations (8.12).

m	Temperature (°C)			
(s/m²•106)	100	200	400	600
0.5				
0.75				0.91
1			0.96	0.83
5		0.76	0.57	
10	0.82	0.62		
15	0.73	0.55		
20	0.68			
25				

Tables 8.51 - Estimation of the relative weight of air-cured concrete after fire with equations (8.13).

m	Temperature (°C)			
(s/m²·10^6)	100	200	400	600
0.5				
0.75				
1				0.99
5			0.81	0.71
10		0.85	0.65	0.62
15		0.72	0.58	
20	0.90	0.64		
25	0.81			

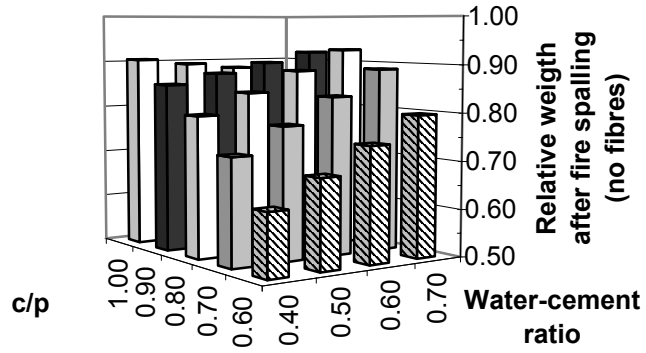

Figure 8.34 – Resulting weight after fire of concrete without fibres as a result of equation (8.13).

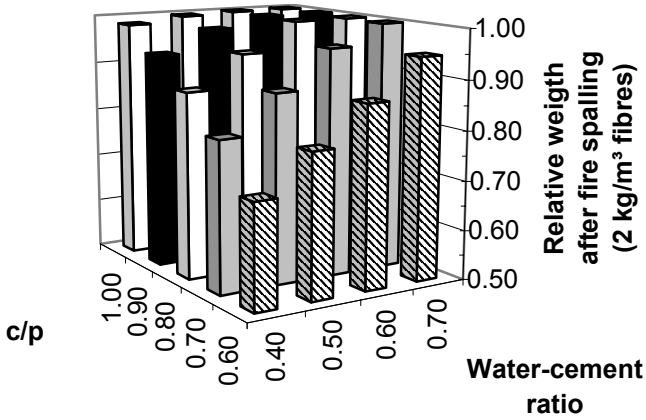

Figure 8.35 - Weight after fire of concrete with 2 kg/m³ fibres based on results in Figure 8.33 combined with equation (8.13) and Table 8.12.

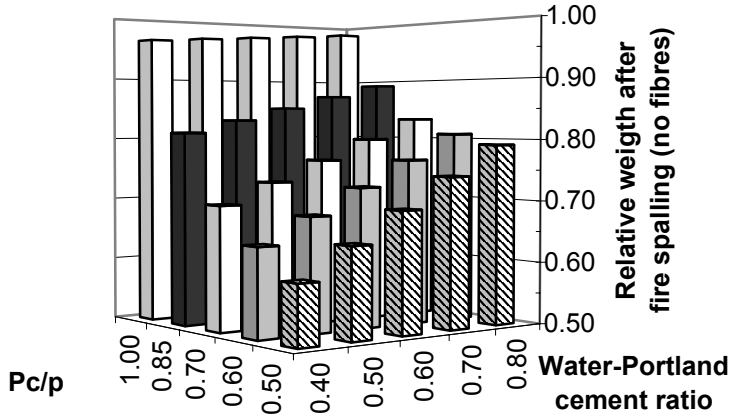

Figure 8.39 – Resulting weight after fire of concrete without fibres as a result of equation (8.15).

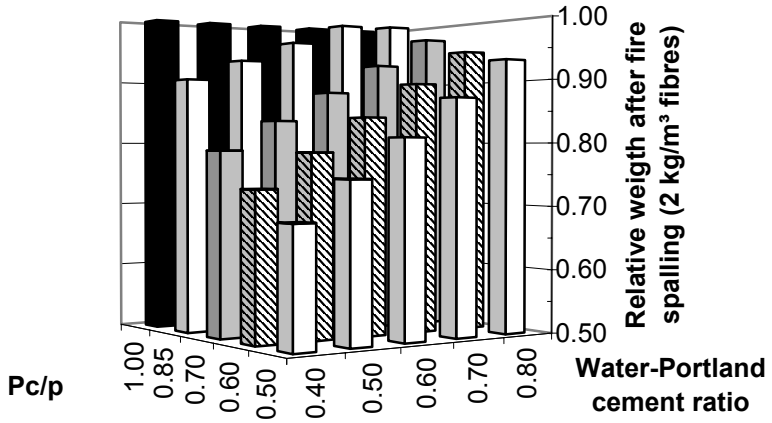

Figure 8.40 - Weight after fire of concrete with 2 kg/m³ fibres based on results in Figure 8.39 combined with equation (8.16) and Table 8.16.

9. CONCLUSIONS AND SYNTHESES

9.1 General

This report describes experimental studies of the mechanical performance of Self-Compacting Concrete, SCC, under compressive loading at fire temperatures. The SCC contains different amounts of polypropylene fibre, different types of cement and air content, preconditioned either in the air or in water. The result of the studies was compared with the corresponding properties of normal concrete, with the same w/c and air content. Half a year's or one year's age applied at the time of testing. The strength development of the concrete was followed in parallel. Seven SCCs with w/c = 0.40, 0.55 or 0.70 and one normal concrete, NC, with w/c = 0.40 were studied for compressive strength in a fire temperature oven. The temperatures were 200 °C, 400 °C and 800 °C. Both testing at elevated temperature and after cooling took place. Elastic modulus, ultimate strain at maximum strength, dynamic modulus and relative humidity, RH, were studied in parallel. Supplementary tests of were performed, after cooling from 600 °C, of strength, elastic modulus, ultimate strain at maximum strength. Supplementary tests were also performed on capillary suction, porosity and resistance to water penetration at water suction. The results of the laboratory tests were compared with results of full-scale tests on twelve SCCs with w/c = 0.40, 0.55 or 0.70 and 4 NCs with w/c = 0.40, 0.55 or 0.70 on fire spalling carried out in a high-temperature oven. The same concrete was studied in the laboratory and in full-scale tests. The concrete was air-cured at an ambient RH = 60%, or water-cured from demoulding until testing. The effects of increased amount of polypropylene fibres, age, different types of cement and air content, capillary suction, porosity, moisture content, hydration losses, preconditioning either in the air or in water, were studied.

9.2 Mix proportions obtained at LTH

One fundamental point was the way to produce concrete with polypropylene fibre. Therefore the principles of the mix proportions are given even though it may seem too detailed. These results are based on concrete mix proportions defined by the grading curves of the fresh SCC. More fine materials were required in SCC than in NC in order to incorporate 4 kg/m³ of fibres in the mixed proportions. With 2 kg/m³ more traditional mix proportions of SCC were used. However, with 4 kg/m³ of polypropylene fibres the workability decreased rapidly in the concrete.

9.3 Mechanical properties obtained at LTH

Glass or limestone filler additives increased strength substantially at normal temperature even though the cement content was somewhat lower in SCC than in NC. Probably a more efficient packing of the particles was the reason for the enlarged strength. Strength was increased by 0.07 MPa per kg/m³ increasing amount of filler added. Additives of polypropylene fibres decreased strength by 2.3% per kg/m³ increasing amount of fibre added. Water-cured cylinders of SCC, 100 mm in diameter, without polypropylene fibres, exhibited spalling at 480 °C/h heating rate. At 240 °C/h heating rate cylinders of SCC, 100 mm in diameter, without polypropylene fibres, exhibited no spalling. Once spalling was avoided, SCC and NC behaved similarly at high temperature except at 800 °C at which temperature SCC with limestone powder did not show any residual strength at all after cooling down to 20 °C, Figure 9.1. Figure 9.2 shows the properties of SCC with limestone powder. Comparison with HPC shows greater strength between 100 °C and 200 °C of SCC than that of HPC, Figure 9.3. Greater loss of the elastic modulus was obtained than seen before, Figure 9.4.

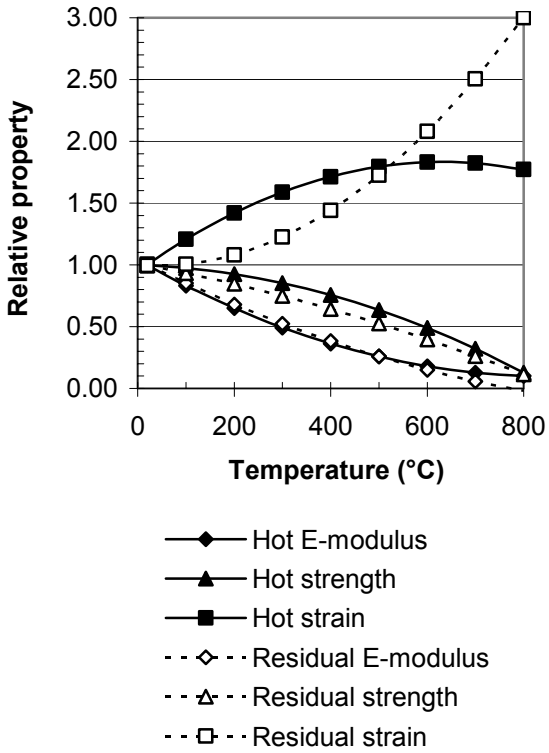

Figure 9.1 – Relative properties of concrete at/after elevated temperature except for residual property with limestone powder at 800 °C.

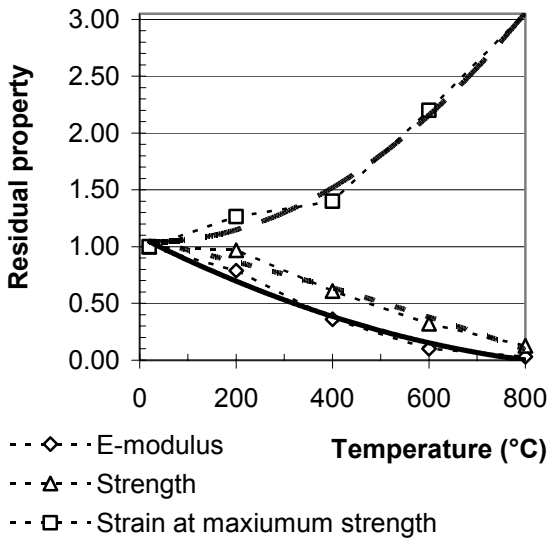

Figure 9.2 - Relative residual properties of SCC with limestone powder versus temperature.

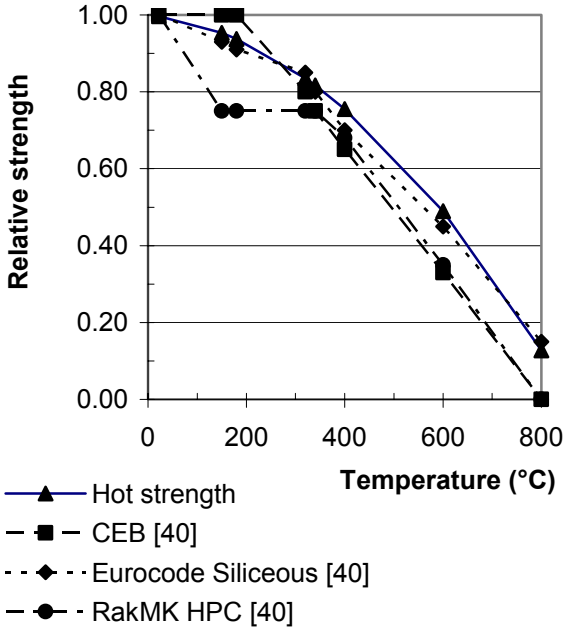

Figure 9.3 - Hot strength (64 specimens), CEB, Eurocode Siliceous and RakMP HPC code [40].

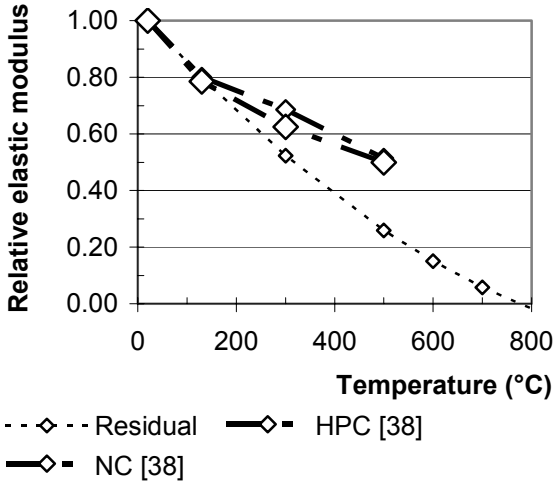

Figure 9.4 – E-modulus compared with [38].

9.4 Effect of properties on fire spalling of concrete tested at SP [94]

9.4.1 Moisture and isothermal behaviour

About 3% moisture in normal concrete is critical for the fire spalling to take place [79]. Even though the concrete was dried out to about 75%RH, high moisture content was observed. The following moisture content was found:

- Previous research with HPC [40]: 2.2%
- Air-cured specimen: 3.6%
- Water-cured specimen: 5.9%

In comparison about 3.1% moisture content is sufficient to cause fire spalling at the stress level used in the experiments, about 15 MPa. The moisture content of SCC was compared with the isotherm of normal concrete. SCC showed larger moisture content than NC when RH was held constant, especially in SCC with glass filler.

9.4.2 Effect of cement content, age and curing

It was observed that the cement-powder ratio, c/p, of the concrete had a substantial effect on the fire spalling – the lower the c/p, the larger the fire spalling. At water-cement ratio, w/c = 0.40, fire spalling was avoided with c/p $\geq$ 0.80 but became unacceptably large in concrete with c/p = 0.60. One way to avoid fire spalling seems to be to increase c/p. At half a year's age the same fire spalling was observed for a concrete with 4 kg/m³ fibres as for a one-year-old concrete with 2 kg/m³ of fibres. With water curing only half the resistance of water penetration of SCC was acceptable compared with the resistance of water penetration for air-cured concrete, probably due to a better hydration conditions with water curing.

9.4.3 Capillarity, water suction and fibres

At constant porosity both air and water-cured SCC showed greater resistance to water penetration than normal concrete, NC, did, which may be an explanation for the increased sensitivity of SCC to fire spalling compared with NC observed on tests performed at SP [94]. The largest increase of relative porosity with increasing temperature was observed for NC; the lowest increase of relative porosity was observed for SCC with low w/c without fibres. For SCC with fibres the increase of porosity was less than for NC, probably since larger water pressure than available in a 20-mm-concrete was required for the increase of porosity with fibres to take place. The smallest relative resistance to water penetration was consequently observed for NC. The observations of differences between porosity and resistance to water penetration of SCC and

NC show that another structure may be formed in SCC than in NC since the isotherm performed different at normal temperature. At higher temperature the porosity increased more rapidly and the resistance to water penetration decreased more in NC than in SCC. For SCC with fibres increase of the relative resistance to water penetration was observed. For concrete with 2 kg/m³ polypropylene fibres larger resistance to water penetration at suction was observed at 105 °C than for the same concrete without fibres and than for concrete with 4 kg/m³ polypropylene fibres. For concrete with 4 kg/m³ polypropylene fibres larger resistance to water penetration at suction was observed at 200 °C than for the same concrete without fibres and for concrete with 2 kg/m³ polypropylene fibres. The reason for the increasing resistance to water penetration was probably an expansion and melting of the polypropylene fibres at 105-200 °C. These phenomena remained after the specimen has cooled to 20 °C and therefore decreased the water suction. As mentioned above, a much larger structure is required than 20 mm in thickness for the water pressure to form and to transport the melting, liquid polypropylene fibres out of the pores. During fire heating water transport will be prohibited inward in concrete with fibres. In this case the water pressure in concrete with fibres will increase more slowly than in concrete with fibres as the water, instead of moving inward has to leave the surface of the concrete. This probably explains the mechanism of the polypropylene fibres in concrete affected by fire:

- Possible increase of polypropylene fibre volume and melting at 105-200 °C.
- Water movement inward concrete with fibre is diminished at 105-200 °C due to an increase in the resistance to water penetration.
- Water instead moves to the surface of concrete with fibres and spalling is avoided.

9.5 Polypropylene fibres to prevent spalling

9.5.1 Calculation on cement and fibre content

Estimation was done for the amount of fibres versus w/c and c/p. According to a parameter study, the most important factor to prohibit fire spalling was a high cement-powder ratio, c/p. Figure 9.5 shows the amount of 32 µm fibres, ppf_{normal}, at constant moisture content and stress level to limit the fire spalling of SCC to that of normal concrete without fibres (kg/m³):

$$ppf_{normal}=(28\cdot(c/p)^2-26\cdot(c/p)-2.4)\cdot\ln(w/c)+45\cdot(c/p)^2-68\cdot(c/p)+23>0 \quad (9.1)$$

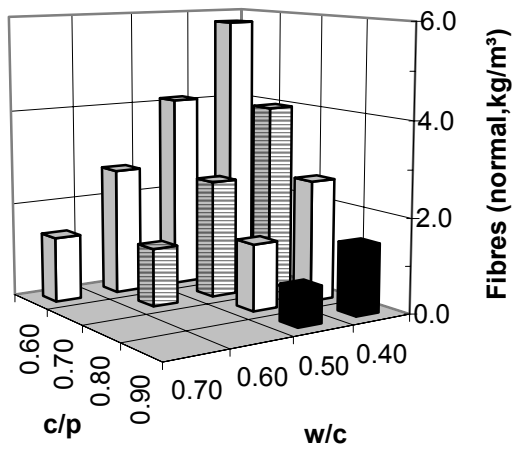

Figure 9.5 - Amount of fibres at constant moisture content and stress level in order to limit the fire spalling of SCC to that of normal concrete without fibres versus the cement-powder ratio, c/p, and the water-cement ratio, w/c.

Figure 9.6 shows the fibre requirement in order to limit the fire spalling at 15% at half a year's age. The following equation for the amount of polypropylene fibre in order to limit the fire spalling at 15% at half a year's age was obtained (32 µm fibres, kg/m³):

$$ppf_{85\%}=(-35\cdot(c/p)^2+34.9\cdot(c/p)-16.7)\cdot\ln(w/c)-25\cdot(c/p)+11.7>0 \quad (9.2)$$

c/p denotes the cement-powder ratio {0.50 < c/p < 1}

p denotes cement and powder (glass or limestone filler)

$ppf_{85\%}$ denotes the content of 32 µm polypropylene fibres to limit the fire spalling to 15% at half a years's age (32 µm fibres, kg/m³)

9.5.2 Calculation based on the fibre and Portland cement content

Another synthesis was required for the amount of fibres in concrete versus the water-Portland cement ratio, w/Pc and the Portland cement-powder ratio, Pc/p. Figure 9.7 shows the amount of 32 µm fibre at constant moisture content and stress level required for the same fire spalling of SCC like for normal:

$$ppf_{normal}=(13\cdot(Pc/p)-12.3)\cdot\ln(w/Pc)-2.69\cdot(Pc/p)^2+2.65\cdot(Pc/p)-0.2>0 \quad (9.3)$$

ppf_{normal} 32 µm fibres to obtain the same weight after fire of SCC like for normal

w/Pc denotes the water-Portland cement ratio
Pc/p denotes Portland cement-powder ratio

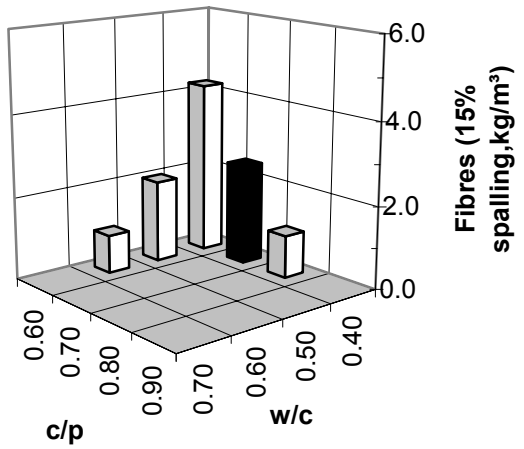

Figure 9.6 - Fibres based on 85% remaining weight after fire compared with the original one.

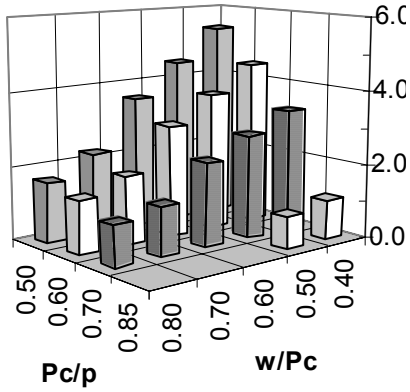

Figure 9.7 - Fibre amount at constant moisture content and stress level required for the same fire spalling of SCC like for normal concrete

Figure 9.8 shows the amount of fibres, ppf, to limit the fire spalling to 15% of that before fire at half a year's age (32 μm fibres, kg/m³):

$$ppf_{85\%}=(-43\cdot(Pc/p)^2+72\cdot(Pc/p)-31)\cdot\ln(w/Pc) - 14\cdot(Pc/p)^2+18.7\cdot(Pc/p)-6.2 \quad (9.4)$$

$ppf_{85\%}$ denotes the amount of 32 μm fibres to obtain 85% weight after fire of SCC of the original one (kg/m³).
w/Pc denotes the water-Portland cement ratio
Pc/p denotes Portland cement-powder ratio

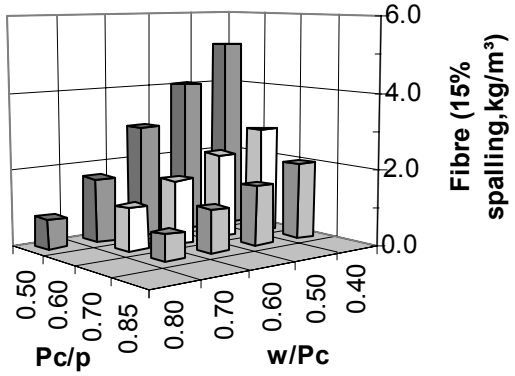

Figure 9.8 - Required amount of fibres in order to limit the amount of fire spalling to 15% of the original weight.

REFERENCES

1. Nilsson, M., Petersson, Ö., The First Bridge Made of SCC. "Första bron utförd i självkompakterande betong." Väg- och Vattenbyggaren 2/98 (1998) 28-31. (In Swedish.)
2. Söderlind, L., Full-scale Tests of SCC for Dwelling Houses. RILEM Symposium on SCC. Ed.: Skarendahl and Petersson (1999) 723-728.
3. Trägårdh, J., Very Good Frost Resistance of SCC – A case Study of the Stäket Tunnel. "Mycket god frostbeständighet i självkompakterande betong– en fallstudie från Stäkettunneln." Bygg & Teknik. 2001/07, 26-27.
4. Bergholtz, A., Lundgren, S., Concrete Inner Vault in the Grind Tunnel, "Motgjuten betonginkädnad i tunnel vid Grind", Swedish Road Administration and Scandiaconsult Sverige AB respectively, Rock Mechanics Meeting, Swedish Rock Engineering and National Group of International Society for Rock Mechanics, ISSN 0281-4714, 2000, 227-236.
5. Tunnel 99, Swedish Road Administration, 1999:138.
6. Tunnel 95, Swedish Road Administration, 1995:32.
7. Persson, B., Mix Proportions and Strength of SCC for Production of High Strength Poles, Piles and Pillars. Contribution to "1. Münchener Baustoffseminar Selbstverdichtender Beton" 9 oktober 2001. Ed.: Peter Schiessl. 2001, 31-39.
8. Persson, B., High Performance SCC. Proceedings of the 6th International Symposium on Utilization of High Strength/High Performance Concrete. University of Leipzig. Ed.: König, G., Dehn, F., Faust, T., Leipzig. 2002, 1273-1290.
9. Persson, B., SCC with High Performance. Proceedings of the 18th Symposium on Nordic Concrete Research. Nordic Research Projects, Elsinore, Ed.: Bager, D., Glavind, M., Publisher: The Norwegian Concrete Association. Oslo. 2002, 327-330.
10. Persson, B., SCC, with High Performance, HP, Proceedings of the Congress on Challenges of Concrete Construction, Dundee, Ed.: Dhir, R. K., Publisher: The University of Dundee, Dundee, 2002, 16 pp.
11. Anderberg, Y., Oredsson, J., Rise, G., High Performance Concrete Structures – Design Handbook. Svensk Byggtjänst, Stockholm, 2000, 49-58.
12. Persson, B., An International Workshop on High-Performance Concrete. "Internationellt arbetsmöte beträffande högpresterande betong." Betong 2/96. 1996. Stockholm, 27-29. (In Swedish.)
13. Diedrichs, U., Jumppanen, U.-M., Schneider, U., High Temperature Properties and Spalling Behaviour of High Strength Concrete. Weimar. Red.: F.H. Wittmann and P. Schwesinger. Freiburg and Unterengstringen. 1995, 129-143.
14. Oredsson, J., Application to the Development Fund of the Swedish Construction Industry, SBUF: "Fire Resistance of SCC", Skanska Perfab Ltd, 2000-04-14.
15. Malhotra, H.L., The Effect of Temperature on the Compressive Strength of Concrete, Magazine of Concrete Research, Vol. 28, 1956, 85.
16. Weigler, H., Fischer, R., Concrete at Temperatures between 100 °C and 750 °C. "Beton bei Temperaturen von 100 °C bis 750 °C." Beton 2, 1968.
17. Abrams, M.S., Compressive Strength of Concrete at Temperature to 1600 °F (871 °C), PCA, Ser. 1387-1, 1968.
18. Thelandersson, S., Effect of the Temperatures on Tensile Strength of Concrete, Bulletin 26, Div. Structural Mechanics and Concrete Construction, Reprint from nordisk Betong 1972:2, 1972, 28 pp.
19. Nekrassow, K., Fire Resistance concrete. "Hetzebeständiger Beton." Bauverlag, Wiesbaden – Berlin, 1961.
20. Nekrassow, K., Influence of Temperature on the Physical-Mechanical Properties of Concrete, "Einfluss hoher Temperaturen auf die physikalisch-mechanischen Eigenschaftens des Betons, Symposium Feuerwiderstandsfähigkeit von Spannbeton, Bauverlag GmbH, Wiesbaden-Berlin, 1966, 67-74.
21. Jönsson, G., Lassen, C., Experimental Investigation of the Temperature Dependence of the Tensile Strength for Concrete in Temperature Associated with Fires. "Experimentell undersökning för betong av draghållfasthetens temperaturberoende vid för brand aktuellt temperaturområde." Div. Structural Mechanics and Concrete Construction. 1968.
22. Nilsson, L.O., Temperature Effects in Relative Humidity Measurements on Concrete – Some Preliminary Studies. The Moisture Group. Report 1987:1. BFR. 1987, 84.
23. Persson, B., Compatibility between Floor Material and Concrete – Effect of Production Methods on Volatile Organic Compound, Moisture and Carbonation. "Kompa-

tibilitet mellan golvmaterial och betong – Effekt av produktionsmetoder på emissioner, fukt och karbonatisering." Report TVBM-7149 (assignment for Svenska Byggbranschens Utvecklingsfond, SBUF, PEAB AB, Bostik AB, EssBetong KB, Tarkett Sommer AB, Swerock AB, Svensk Glasåtervinning AB, ECOBETON A/S, Norge). Division of Building Materials. Lund Institute of Technology. Lund University. Lund. 2000, 133 pp. (In Swedish.)

24. Thelandersson, S., Mechanical Behaviour of Concrete under Torsional Loading at Transient, High-Temperature Conditions, Bulletin 46, Div. Structural Mechanics and Concrete Construction, 1974, 25-35.
25. Persson, B., Quasi-instantaneous and Long-term Deformations of High-Performance Concrete with Some Related Properties. Doctoral Thesis. Report TVBM-1016. Division of Building Materials. Lund Institute of Technology. Lund University, Lund, 1998, 500 pp.
26. ASTM E 104-85. Standard Practice for Maintaining Constant Relative Humidity by Means of Aqueous Solutions. ASTM. Philadelphia, (1985), 33-34, 637.
27. Alvaredo, A. M., Wittmann F. H. Shrinkage as Influenced by Strain Softening and Crack Formation. Proceedings of the Fifth International RILEM Symposium on Creep and Shrinkage in Barcelona. 1993. E & FN Spon. London, 1993, 103-114.
28. Lennon, T., Bailey, C., Clayton, N., The Performance of High Grade Concrete Columns in Fire, Symposium on Utilization of High Strength/High Performance Concrete. University of Leipzig. Ed.: König, G., Dehn, F., Faust, T., Leipzig. 2002, 341-353.
29. Clayton, N., Lennon, T., Effect of Polypropylene Fibres on Performance in Fire of High Grade Concrete, Building Research Establishment. publication 395. 2000.
30. DD ENV 1992-1-1. Design of Concrete Structures, British Standard Institution, London, 1992.
31. DD ENV 1991-1: 1996. Basis of Design and Actions in Structures, British Standard Institution, London, 1996.
32. PrEN 1991-1-2, Eurocode 1 – Actions on Structures: part 1.2: General Action – Action on Structures Exposed to Fire, European Committee for Standardisation, Brussels.
33. BS6399 Part 1:1996, Loading of Buildings Part 1, Code of Practise for Daeda and Imposed Loads, British Standard Institution, London, 1996.
34. Natural Fire Concept, Full Scale Tests, Implementation in the Eurocodes and Development of a userfriendly design tool, Techincal Report 5, Profil Arbed Recherches, 2000.
35. Noumowe, N. A., Debicki, G., Effect of Elevated Temperature from 200 to 600 °C on the Permeability of HPC, Symposium on Utilization of High Strength/High Performance Concrete. University of Leipzig. Ed.: König, G., Dehn, F., Faust, T., Leipzig. 2002,431-444.
36. Noumowe, N. A., Clastres, P., Debicki, G., Costaz, J.-L., Transient Heating Effect on High Strength Concrete, Nuclear Engineering and Design, No 166, Elsevier, 1966.
37. Noumowe, N. A., Clastres, P., Debicki, G., Bolvin, M., High Temperature Effect on HPC: Strength and Porosity, Third CANMET/ACI International Conference on Duarbility of Concrete, Nice, 1994, 157-172.
38. Noumowe, N. A., Clastres, P., Debicki, G., Costaz, J.-L., Thermal Stresses and Water Vapour Pressure of HPC at High Temperature, Symposium on Utilization of High Strength/High Performance Concrete, Ed.: de Larrard, F., Lacroix, R., Paris, 1996, 561-570.
39. Noumowé, A. N., Effet de Hautes Températures (20-600 °C) sur le Béton, Cas particulier du Béton à Hautes Performances, Thése de Doctorat de l'INSA, Lyon, 1995, 232 pp.
40. Phan, L., High-Strength Concrete at High Temperarture – An Overview, Symposium on Utilization of High Strength/High Performance Concrete, Ed.: de Larrard, F., Lacroix, R., Paris, 1996, 501-518.
41. Phan, L.T., Carino, N.J., Mechanical Properties od High Strength Concrete at Elevated Temperartures, NISTIR 6726, Gaithersburg, 2001.
42. Phan, L.T., Carino, N.J., Review of Mechanical Properties of HSC at elevated temperatures, Materials in Civil engineering, ACI, Vol. 10, 1998, 58-64.
43. Phan, L.T., Carino, N.J., Effects of Test Conditions and Mixture Proportions on Behaviour of High-Strength Concrete Exposed to High Temperatures, ACI Materials Journal, ACI, Vol. 99, 2002, 54-66.
44. Phan, L. T., Lawson, J. R., Davis, F. R., Effects of Elevated Temperature Exposure on Heating Characteristics, Spalling and Residual Properties of HPC, Materials and Structures, Vol. 34, 2001, 83-91.

45. Persson, B., Tunnel Through Water-distributing Sediments – Without Injection in Advance. “Tunnel genom vattenförande sediment – utan föregående injektering.” Bygg & Teknik 1/99. Stockholm. 1999, 28-29 (In Swedish.)
46. Persson, B., Japan Society for the Promotion of Science Fellowship for Research in Japan. Research Report 9803:12. Division of Building Materials. Lund Institute of Technology. Lund University. Lund. 2000, 3 pp.
47. Sakata, K., Personal communication. Okayama University, 1998.
48. DAfStb-Richtlinie ”Selbstverdichtender Beton”, Beuth Verlag, Berlin, 2001.
49. Harald Müller. Universität Karlsruhe. Personal information. 2002.
50. Andersson, R., Sjökvist, L.-G., SCC for the Element Industry – Technical Analyses. “Självkompakterande betong i prefabriceringsindustrin – en teknisk och ekonomisk analys.” Report TVBM-5039. Division of Building Materials. Lund Institute of Technology. Lund University. Lund. 1999, 48 pp. (In Swedish with English summary.)
51. Dieden, C., SCC for House Production – Composition, strength and Shrinkage. “Självkompakterande husbyggnadsbetong – sammansättning, hållfasthet och krympning.” Report TVBM-5040. Division of Building Materials. Lund Institute of Technology. Lund University. Lund. 1999, 50 pp. (In Swedish with English summary.)
52. Pujol, A. (Hugas), Mix Proportions and Properties of SCC. Report TVBM-5041. Division of Building Materials. Lund Institute of Technology. Lund University. Lund. 1999, 56 pp.
53. Charkas, M., and Fayli, W., SCC with Glass Filler – Studies on Aspects on Materials and Production. “Material- och produktionstekniska studier av självkompakterande betongmed glasfiller.” Report TVBM-5042. Division of Building Materials. Lund Institute of Technology. Lund University. Lund. 1999, 80 pp. (In Swedish with English summary.)
54. Boubitsas, D., Paulou, K., SCC for Marine Environment. “Självkompakterande betong för havsmiljö.” TVBM-5048. Lund Institute of Technology. Lund University. Lund. 2000, 55 pp. (In Swedish with English summary.)
55. Kakazoukis, N., Rheology of SCC – Results of Different Testing Methods. “Reologiska egenskaper hos självkompakterande betong– En undersökning av olika provningsmetoder. TVBM-5049. Lund Institute of Technology. Lund University. Lund. 2000, 35 pp. (In Swedish with English summary.)
56. Persson, B., Strength and Shrinkage of SCC. Proceedings of an International RILEM Workshop on Shrinkage in Concrete. Paris. 2000. Ed. by V Baroghel-Bouny and P-C Aïtcin. 2000, 81-99.
57. Persson, B., A Comparison between Deformations of SCC and Corresponding Properties of NC. Cement and Concrete Research. 31. 2001, 193-198.
58. Persson, B., SCC - Chloride Ingress and Frost Resistance. Nordic Mini Seminar. fib Commission 5.5. Gothenburg. 2001.
59. Persson, B., Chloride Migration Coefficient of SCC. Nordic Seminar on Durability of Exposed Concrete Containing Secondary Cementitious Materials. Hirtshals. Ed.: D. Bager. 2001, 20 pp.
60. Persson, B., The Bridge System between Honshu and Shikoku: Japanese Record Bridges. “Brosystemet mellan Honshu och Shikoku: Japanska rekordbroar.” Bygg & Teknik 2/99. Stockholm. 1999, 56-60 (In Swedish.)
61. Persson, B., Japanese Research on Strength and Elastic Modulus in Wall Made of SCC. “Japanska försök avseende hållfasthet och E-modul i väggar av vibreringsfri betong.” Betong 2/99. Stockholm. 1999, 16-17. (In Swedish.)
62. Persson, B., Production and Some Properties of SCC. ”Produktion av och vissa egenskaper hos Självkompakterande betong.” Bygg & Teknik 7/99. Stockholm. 1999, 26-28 (In Swedish.).
63. Persson, B., Modern Concrete and Filigree Form Work Conditions for a Record Construction in Malmö. “Modern betong och filigranform förutsättningarna för ett rekordbygge i Malmö.” Husbyggaren 6/99. 1999, 34-43 (In Swedish.)
64. Persson, B., Glass Filler Concrete without Superplasticiser in a Rapid-constructed Building in Malmö. “Flytmedelsfri betong med glasfillerinblandning i snabbyggt malmöhus” Husbyggaren 1/2000. 2000, 26-29 (In Swedish.)
65. Persson, B., SCC – A Quiet Revolution for the Building Industry. “Självkompakterande betong – en tyst revolution inom byggandet.” Husbyggaren 2/2000. 2000, 20-24 (In Swedish.)
66. Persson, B., The Cheapest Dwelling House in Sweden was Built in Concrete. ”Sveriges billigaste bostadshus byggdes i betong. Betong 2/2001, 14-15 (In Swedish).

67. Persson, B., SCC Offers a Short Fabrication Cycle and a Rational Production "Självkompakterande betong ger kort omloppstid och rationell produktion." Husbyggaren 6/2001, 10-13. (In Swedish.)
68. Persson, B., Assessment of Chloride Migration Coefficient, Salt Frost Resistance, Internal Frost Resistance and Sulphate Resistance of SCC. Report TVBM-3100 (assignment for SBUF and Skanska AB, Malmö). Division of Building Materials. Lund Institute of Technology. Lund University. Lund. 2001, 86 pp.
69. Persson, B., Strength of Concrete for Tunnel Elements. Working Report 0009:10 (assignment for Swerock AB, Helsingborg). Division of Building Materials. Lund Institute of Technology. Lund University. Lund. 2000, 13 pp. (In Swedish.)
70. Persson, B., Air Void Structure of Concretes KN, KO and RO within the Durability Project of SBUF (the Swedish Board of Building Research and the Development Foundation of the Swedish Contractors). "Luftporstruktur hos betongerna KN, KO och RO inom SBUF:s beständighetsprojekt". Report U00.15 (assignment for Skanska Asfalt och Betong AB, Malmö). Division of Building Materials. Lund Institute of Technology. Lund University. Lund. 2000, 23 pp. (In Swedish.)
71. Persson, B., Self-compacting Bridge Concrete with Mixed Filler. "Självkompakterande brobetong med blandfiller". Report U00.14 (assignment for Skanska Asfalt och Betong AB, Malmö). Division of Building Materials. Lund Institute of Technology. Lund University. Lund. 2000, 8 pp. (In Swedish.)
72. Persson, B., Japan Society for the Promotion of Science Fellowship for Research in Japan. Research Report 9803:12. Division of Building Materials. Lund Institute of Technology. Lund University. Lund. 2000, 3 pp.
73. Persson, B., Shrinkage and Strength of SCC with Different Kinds of Filler. Report U00.13 (assignment for Svensk Glasåtervinning AB, Hammar). Division of Building Materials. Lund Institute of Technology. Lund University. Lund. 2000, 22 pp.
74. Persson, B., Evaluation of Present and Remaining Research on SCC with Glass filler. "Utvärdering av föreliggande forskningsinsatser samt återstående forskningsbehov beträffande självkompakterande betongmed glasfillerinblandning." Report U00.10 (assignment for Svensk Glasåtervinning AB, Hammar). Division of Building Materials. Lund Institute of Technology. Lund University. Lund. 2000, 6 pp. (In Swedish.)
75. Persson, B., Chloride Penetration and Frost Resistance of Self-compactiong Concrete. "Frostbeständighet och kloridinträngning hos självkompakterande anläggningsbetong." Report U00.05 (assignment for Skanska Sverige AB). Division of Building Materials. Lund Institute of Technology. Lund University. Lund. 2000, 5 pp.
76. Persson, B., Self-Compacting Construction Concrete - Workability and Deformations. "Självkompakterande anläggningsbetong - gjutbarhet och deformationer ". Report U99.23 (assignment for Skanska Asfalt and Betong Ltd. Farsta). Division of Building Materials. Lund Institute of Technology. Lund University. Lund. 1999, 14 pp. (In Swedish.)
77. Persson, B., Workability of SCC with Viscocrete 3. "Gjutbarhet hos självkompakterande betong med Viscocrete 3. Report U99.11. (assignment for Sika Ltd. Järfälla). Division of Building Materials. Lund Institute of Technology. Lund University. Lund. 1999, 1 pp. (In Swedish.)
78. Persson, B., SCC. "Självkompakterande betong." Report U98.07 (assignment for Sydsten Ltd. Malmö). Division of Building Materials. Lund Institute of Technology. Lund University. Lund. 1998, 1 p. (In Swedish.)
79. Khoury, G. A., Passive Fire Protection in Tunnels. Imperial College. Concrete. 2002, 26 pp.
80. Blontrock, H., Taerwe, L., Exploratory Study on SCC. Proceedings of the 6th International Symposium on Utilization of High Strength/High Performance Concrete. University of Leipzig. Ed.: König, G., Dehn, F., Faust, T., Leipzig. 2002, 659-666.
81. Persson, B., Does plastic fibres prevent fire spalling even in SCC? "Förebygger plastfibrer brandspjälkning även hos Självkompakterande betong?" Husbyggaren 2/2002, 26-30 (In Swedish.)
82. Persson, B. Mechanical Performance of Self-Compacting Concrete under Compressive Loading at Transient, High Temperature Conditions - with Some Interrelated Properties. Report 0204:02. Division of Building Materials. Lund Institute of Technology. Lund University. Lund. 2002, 91 pp.
83. Persson, B. Self-Compacting Concrete at High Temperature Report 0212:02. Division of Building Materials. Lund Institute of

Technology. Lund University. Lund. 2002, 148 pp.
84. Rodenstam, S., Summary after re-optimisation. “Sammanställning av recept-optimering.” Nordkalk, Malmö, 2001, 31 pp. (In Swedish)
85. Persson, B., Ideal Distribution of Particles in High-Performance Concrete. “Ideal partikelfördelning i högpresterande betong.” Betong 95/3. 1995. Stockholm, 6-8, 39. (In Swedish with English summary.)
86. Dreux, D., Guide pratique du béton. Collection de l’Institute Technique du Bâtiment et des Travaux Public, Paris, 1970.
87. Persson, B., Experiences after visit at LCPC. Division of Building Materials. Lund Institute of Technology. Lund University. Lund. 1995.
88. Larrard, F., Personal communication, LCPC, Paris, 1995.
89. Neville, A.M., Brooks, J. J., Concrete Technology, Longman, Singapore, 1987 (updated 1999), 70.
90. Abrams, M.S., Compressive Strength of Concrete at Temperatures of 1600 °F (871 °C). Symposium on the Effect of Temperature on Concrete. ACI SP-25. Detroit. 1971.
91. Thelandersson, S., Concrete Structures at High Temperatures – a overview. “Betongkonstruktioner vid höga temperaturer - en översikt. VAST. Stockholm. 1974. Bulletin no 43. Div. Structural Mechanics and Concrete Construction, 1974.
92. Xu, A., Structure of Hardened Cement-fly Ash Systems and Their Related Properties. Report P-92:7. Division of Building Materials. Chalmers University of Technology. Gothenburg. 1992. Pp. IV: 15-19.
93. ASTM C 215-85 (1985). Standard Test Method for Fundamental Transverse, Longitudinal, and Torsional Frequencies of Concrete Specimens. ASTM. Philadelphia. 1985, 119-122.
94. Boström, L., The Performance of Some SCC when Exposed to Fire. Report 2002:23. Fire Technology. Swedish National Testing and Research Institute, 37 pp.
95. Persson, B., Hydration, Structure and Strength of High-Performance Concrete. “Högpresterande betongs hydratation, struktur och hållfasthet.” Report TVBM-1009. Division of Building Materials. Lund Institute of Technology. Lund University. Lund. 1992. 400 pp.
96. Bertil Persson. Flooring on Concrete – A Synthesis as Concerns Moisture, Chemical Volatile Compound and Adhesion. “Golvsystem på betong – fuktpåverkan, kemisk emission och vidhäftning.” Report TVBM-7165. Div. Building Materials. Lund Institute of Technology. Lund, 2003, 157 pp.
97. Boström, L., SCC with plastic fibres withstands fire. “Självkompakterande betong med plastfibrer klarar brand.” Brandposten no 26. SP. 2002, 15 (In Swedish).
98. Boström, L., SCC with plastic fibres withstands fire. “Självkompakterande betong med plastfibrer klarar brand.” Betong 3/2002, 32. (In Swedish).
99. Boström, L., SCC Exposed to Fire, “ Självkompakterande betong utsatt för brand.” Bygg & Teknik. 2002/06, 36-38 (In Swedish).
100. Persson, B., Resistance of Self-compacting Concrete with Limestone Powder. “Hållbarhet hos självkompakterande betong med kalkstensfiller.” Bygg & Teknik 07/2002, 35-38.
101. Anderberg, A., Personal communication. Fire Safe Design, Lund. 2002.
102. TorkaS 2.0. Calculation of RH in concrete. SBUF. 2002.
103. Persson, B., Chloride Migration Coefficient of Self-Compacting Concrete. RILEM Materials and Structures. 2001, 20 pp. (Accepted for publication).
104. Lillieblad, J., Personal communication. A-betong, Växjö. 2002.
105. Wickström, U., Personal communication. SP. Borås. 2002.
106. Nilsson, L. O., Hygroscopic Moisture in Concrete – Drying, Measurements & Related Material Properties. Report TVBM-1003. Div. Building Materials. Lund Institute of Technology. Lund, 1980.
107. Boström, L. Personal communication. SP. Borås. 2003.

APPENDICES

Appendices 1 –Constructions in SCC

Appendix 1.1 – Stäket tunnel in SCC at Bålsta

Appendix 1.2 – Part of pile in SCC of high -strength

Appendix 1.1 – Stäket tunnel in SCC at Bålsta

Appendix 1.2 – Part of pile in SCC of high -strength

Photo: Giovanni Terrasi.

Appendices 2 – Previous research

Appendix 2.1 – Mix proportions studied in the Swedish spalling project

Appendix 2.2 - Forces, stresses, compliance and shrinkage of columns S32.

Appendix 2.3 – Stresses and compliance (millionths/MPa), etcetera for columns S37.

Appendix 2.4 – Mix proportions and other properties of HPC in tests of permeability after high temperature (kg/m³)

Appendix 2.5 – Mix proportions and other properties of HPC in tests of thermal stresses and water vapour pressure (kg/m³)

Appendix 2.6 – Mix proportions and other properties of HPC in rapid heating tests (kg/m³)

Appendix 2.1 – Mix proportions studied in the Swedish spalling project.

Material/ mix	3230	3240	3730	3740	3750
Coarse aggregate 12-16 mm	425	425	425	380	380
Coarse aggregate 8-12 mm	425	425	425	380	380
Coarse aggregate 4-8 mm	325	325	325	190	190
Gravel 0-8 mm	775	775	775	790	790
Fibre	1-4	1-4	0-2	0-2	0-2
Cement, c, low-alkali (302 m^2/kg Blaine)	500	500	500	480	480
Silica fume, s (fineness 17.5 m^2/g)	35	35	35	33	33
Superplasticiser, melamine formaldehyde	10	10	10	4.8	4.8
w/c	0.32	0.32	0.37	0.35	0.35
w/b	0.30	0.30	0.35	0.33	0.33
s/c	0.07	0.07	0.07	0.07	0.07
Density	2500	2500	2500	2390	2390
Age at loading (h)	69	65	48	71	92
Strength at loading (150-mm cube, MPa)	57-69	62-72	42-46	49-55	56-62
Strength at 28 days' age (MPa)	62-88	100-105	77-88	81-89	85-88

Appendix 2.2 - Forces, stresses, compliance and shrinkage of columns S32.

Property/column	3231	3232	3234[1)]	3241	3242	3244[1)]
Force (kN) in strands at 100 s	1082	1108	1102	1512	1601	1596
10 d after prestressing	972	1010	974	1236	1353	1364
200 d after prestressing	908	919	886	1120	1266	1170
Stress (MPa) in HPC after 100 s	28	29	28	39	42	42
10 d after prestressing	25	26	25	32	35	36
200 d after prestressing	23	23.7	22.6	28.9	32.5	30.1
Compliance (millionths/MPa) after 100s	31.4	26.7	27.8	35.9	27.2	27.6
10 d after prestressing	54	45	53	71	54	53
200 d after prestressing	68.5	66	64.9	91.7	67.5	82.7
Elastic effect (millionths/MPa) at 10d	2.5	2.4	2.5	4	3.7	3.2
200 d after prestressing	1.9	2.3	2.2	2.2	1.6	3.6
Reduction of compliance (millionths/MPa) for shrinkage after 10 d	8.5 (22)	8.5 (22)	8.5 (22)	7 (16)	6 (14.5)	6 (14)
200 d after prestressing	17 (32)	17 (32)	17 (32)	13 (25)	12 (23)	13 (24)
Resulting creep compliance (millionths/MPa) at 10d	17 (4)	11 (-2)	19 (6)	32 (23)	25 (16)	22 (14)
200 d after prestressing	23 (8)	24 (9)	22 (7)	45 (33)	31 (20)	46 (35)
Estimated creep compliance 10 d after prestressing	12.7 (20.6)	9.2 (14.8)	8.8 (15.2)	23.2 (38.9)	20.2 (33.7)	18.9 (31.6)
200 d after prestressing (millionths/MPa)	21.0 (32.3)	16.5 (25.2)	15.2 (25.6)	31.7 (53.4)	28.8 (47.4)	27.4 (44.9)

1) average of 2 columns, d= loading time (days); s= seconds; (....)= drying shrinkage.

Appendix 2.3 – Stresses and compliance (millionths/MPa), etcetera for columns S37.

Property/column	3730	3731	3732[1)]	3740	3741	3742[1)]	3750	3751	3752[1)]
Force (kN) after 100 s	857	888	910	1111	1130	1136	1327	1347	1319
10 d after prestressing	713	750	769	907	950	924	1116	1188	1097
200 d after prestressing	639	655	684	813	856	826	968	1052	956
Stress (MPa) at 100 s	22	23	23	29	30	30	34	35	34
10 d after prestressing	18	19	20	24	25	24	29	31	28
200 d after prestressing	16	17	18	21	22	21	25	27	25
Compliance at 100s	43	35	31	36	33	32	36	33	37
10 d after prestressing	84	72	66	71	63	68	74	59	78
200 d of prestressing	113	106	95	94	84	91	110	88	114
Elastic effect at 10d	4.3	4.2	3.9	4.1	4	4.8	3.5	2.7	4.2
200 d after prestressing	2.6	2.5	2.4	3	3	3	3.3	3.3	2.6
Reduction for shrinkage after 10 d (mill./MPa)	8 (22)	8 (21)	7 (20)	6 (17)	6 (16)	6 (17)	5 (14)	5 (13)	5 (14)
200 d after prestressing	15 (47)	15 (47)	14 (46)	12 (38)	11 (36)	12 (38)	10 (32)	9 (30)	10 (32)
Resulting compliance (millionths/MPa, 10 d)	37 (23)	33 (20)	31 (18)	33 (22)	28 (18)	35 (24)	37 (28)	24 (16)	40 (31)
200 d after prestressing	58 (24)	59 (27)	52 (20)	51 (23)	43 (18)	50 (24)	67 (45)	49 (28)	70 (48)
Estimated creep compliance after 10 d	26.6 (46)	28.5 (49)	27.2 (47)	25.3 (44)	23.7 (41)	24.9 (43)	24.1 (42)	21.1 (37)	20.3 (35)
200 d after prestressing (millionths/MPa)	40.8 (68)	42.9 (72)	41.6 (69)	38.7 (65)	37.1 (62)	38.1 (65)	37.0 (63)	33.9 (57)	32.9 (55)

1) average of 2 columns; d= loading time (days); s= seconds; (....)= drying shrinkage.

Appendix 2.4 – Mix proportions and other properties of HPC in tests of permeability after high temperature (kg/m³)

Concrete	B2	B3	B4
Coarse aggregate 8-20 mm	815	815	
Medium aggregate 4-10 mm	318	318	
Sand 0-5 mm	782	782	782
Cem I 52.5	450	450	450
Silica fume	45	45	45
Water	150	150	150
Superplasticiser	12	12	12
Polypropylene fibres		2	
Light weigth aggregate			494
w/b	0.30	0.30	0.30
Density	2569	2571	1930
Compressive strength (MPa)	70	72	45
Splitting tensile strength (MPa)	4.8	4.9	3.0
Permeability ($x10^{-12}$ m² at 1.5 bars) – 20 °C	0.0015	0.0013	0.0033
- 200 °C	0.0055	0.0102	0.003
- 600 °C	3.6	2.89	0.174

Appendix 2.5 – Mix proportions and other properties of HPC in tests of thermal stresses and water vapour pressure (kg/m³)

Concrete	Normal (NC)	HPC
Gravel 13-24 mm	784	815
Fine gravel 5-13 mm	316	318
Lime stone sand 0-5 mm	772	782
Lime stone filler	0	57
Cement CPJ 55 PM	350	266
Silica fume	0	40
Plasticiser	12.2	0
Water reducer	0	9.1
Retarder	0	0.9
Water	195	161
w/b	0.56	0.53
w/c	0.56	0.61
w/p	0.56	0.44
Compressive strength (MPa)	38.1	61.1
Tensile splitting strength (MPa)	3.6	4
Tensile direct strength (MPa)	3	3.5

Appendix 2.6 – Mix proportions and other properties of HPC and NC in rapid heating tests (kg/m³)

Mix proportion	HPC1	HPC2	HPC3	NC4
Coarse aggregate	846	846	846	854
Fine aggregate	734	734	734	868
Cement	596	596	662	376
Silica fume	66	66	0	0
Superplasticiser	0.4	0.35	0.15	0
Water	133	199	194	213
Density	2376	2408	2436	2311
w/b	0.20	0.30	0.29	0.57
w/c	0.22	0.33	0.29	0.57
w/p	0.22	0.33	0.29	0.57
Aggregate content	0.66	0.66	0.65	0.75
Slump (mm)	240	230	35	76
Air content (%)	3.2	2.8	2	2.5
Moisture content (%)	5	6.1	6.3	7.3
Compressive strength (MPa), 28-d	75	66	53	41
58-d	87	80	59	42
400-d	98	81	72	47
Dynamic modulus (GPa), 58-d	34	37	37	34
400-d	47	44	44	37

Appendices 3 – Material and methods

Appendix 3.1 – Chemical composition and physical properties of cements (%)

Appendix 3.2 - The grading of the aggregates, filler and cements

Appendix 3.3 – Details of water -cooled oven

Appendix 3.4 – Details of water -cooled oven with specimen

Appendix 3.5 – Details of water -cooled oven with LVDTs before testing

Appendix 3.6 – Details of water -cooled oven with connected LVDTs after testing

Appendix 3.1 – Chemical composition and physical properties of cements (%).

Components	Byggcement, CEM II/A -L 42.5 R Skövde	Cement Degerhamn Std, CEM I 42.5 BV/SR/LA
CaO	63.4	65
SiO_2	19.4	21.6
Al_2O_3	3.5	3.5
Fe_2O_3	2.6	4.4
K_2O	1.4	0.58
Na_2O	0.30	0.05
MgO	2.9	0.78
SO_3	3.4	2.07
Ignition losses	7.0	0.47
CO_2	4.4	0.14
Clinker minerals: C_2S	12.6	21
C_3S	51	57
C_3A	7	1.7
C_4AF	6	13
Water demand	28.2%	25%
Initial setting time	151 min.	145 min.
Density	3065 kg/m^3	3214 kg/m^3
Specific surface	475 m^2/kg	305 m^2/kg

Appendix 3.2 - The grading of the aggregates, filler and cements

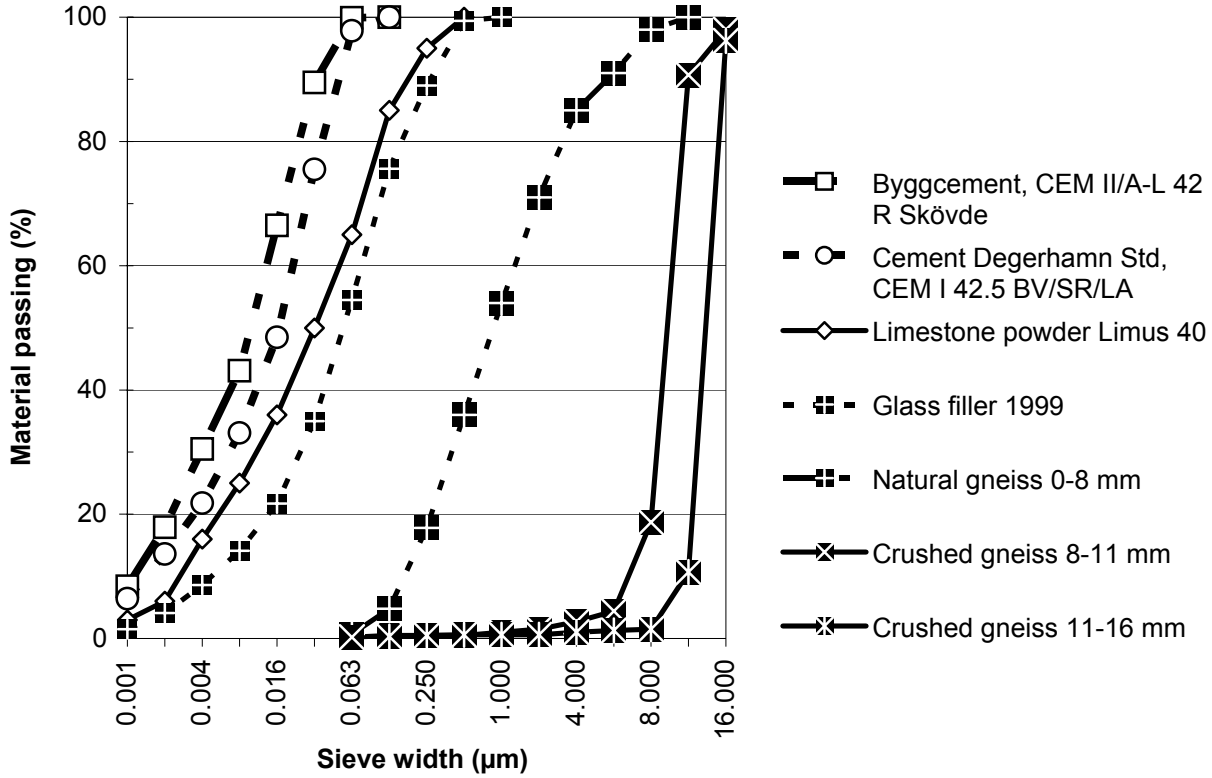

Appendix 3.3 – Details of water -cooled oven

Appendix 3.4 – Details of water -cooled oven with specimen

Appendix 3.5 – Details of water -cooled oven with LVDTs before testing

Appendix 3.6 – Details of water -cooled oven with connected LVDTs after testing

Appendices 4 – Results

Appendix 4.1 – Time schedule

Appendix 4.2 –Mix proportions and properties for concretes optimised by LTH (kg/m³ dry weight)

Appendix 4.3 –Mix proportions and properties for concretes optimised by NORDKALK and SGÅ (kg/m³ dry weight)

Appendix 4.4 –Difference between mix proportions and properties of concretes optimised by LTH and by Nordkalk and SGÅ (kg/m³ dry weight)

Appendix 4.5 –Difference between cost of concretes optimised by LTH and by Nordkalk and SGÅ (SEK/m³)

Appendix 4.6 – Mix proportions and properties of concrete cast in Bollebygd (kg/m³ dry weight)

Appendix 4.7 – Strength development of concrete cast at LTH (MPa)

Appendix 4.8 – Strength development of concrete cast at SPAB, Bollebygd (MPa)

Appendix 4.9 – Stress/strain results of concrete 40AG0 at 20 °C.

Appendix 4.10 – Stress/strain results of concrete 40AG0 at 200 °C – 20 °C.

Appendix 4.11 – Stress/strain results of concrete 40AG0 at 200 °C – 200 °C.

Appendix 4.12 – Stress/strain results of concrete 40AG0 at 400 °C – 20 °C.

Appendix 4.13 – Stress/strain results of concrete 40AG0 at 400 °C – 400 °C.

Appendix 4.14 – Stress/strain results of concrete 40AG0 at 800 °C – 20 °C.

Appendix 4.15 – Stress/strain results of concrete 40AG0 at 800 °C – 800 °C.

Appendix 4.16 – Stress/strain results of concrete 40AK0 at 20 °C.

Appendix 4.17 – Stress/strain results of concrete 40AK0 at 200 °C – 20 °C.

Appendix 4.18 – Stress/strain results of concrete 40AK0 at 200 °C – 200 °C.

Appendix 4.19 – Stress/strain results of concrete 40AK0 at 400 °C – 20 °C.

Appendix 4.20 – Stress/strain results of concrete 40AK0 at 400 °C – 400 °C.

Appendix 4.21 – Stress/strain results of concrete 40AK0 at 800 °C – 800 °C.

Appendix 4.22 – Stress/strain results of concrete 40AK2 at 20 °C.

Appendix 4.23 – Stress/strain results of concrete 40AK2 at 200 °C – 20 °C.

Appendix 4.24 – Stress/strain results of concrete 40AK2 at 200 °C – 200 °C.

Appendix 4.25 – Stress/strain results of concrete 40AK2 at 400 °C – 20 °C.

Appendix 4.26 – Stress/strain results of concrete 40AK2 at 400 °C – 400 °C.

Appendix 4.27 – Stress/strain results of concrete 40AK2 at 800 °C – 800 °C.

Appendix 4.28 – Stress/strain results of concrete 40AK4 at 20 °C.

Appendix 4.29 – Stress/strain results of concrete 40AK4 at 200 °C – 20 °C.

Appendix 4.30 – Stress/strain results of concrete 40AK4 at 200 °C – 200 °C.

Appendix 4.31 – Stress/strain results of concrete 40AK4 at 400 °C – 20 °C.

Appendix 4.32 – Stress/strain results of concrete 40AK4 at 400 °C – 400 °C.

Appendix 4.33 – Stress/strain results of concrete 40AK4 at 800 °C – 800 °C.

Appendix 4.34 – Stress/strain results of concrete 40BR0 at 20 °C.

Appendix 4.35 – Stress/strain results of concrete 40BR0 at 200 °C – 20 °C.

Appendix 4.36 – Stress/strain results of concrete 40BR0 at 200 °C – 200 °C.

Appendix 4.1 – Time schedule

2001	2	3	4	5	6	7	8	9	10	11	12	13	14	15	16	17	18	19	20	21	22	23	24	25	26	27	32	33	34	35	36	37	38	39	40	41	42	43	44	45	46	47	48	49
40AG0																																												
40AK0					O								T									P					O																	
40AK2						O									T									P				O																
40AK4							O									T									P				O															
40BR0								T									P													T														
55BK0																																												
70BG0		O							T									P							O					T													
70BK0	O							T										P							O					T													
2002	2	3	4	5	6	7	8	9	10	11	12	13	14	15	16	17	18	19	20	21	22	23	24	25	26	27	32	33	34	35	36	37	38	39	40	41	42	43	44	45	46	47	48	49
40AG0																																									P	P		
40AK0																																							P	P				
40AK2																																					P	P						
40AK4																																			P	P								
40BR0																																	P	P										
55BK0												T																			P	P												
70BG0																													P	P														
70BK0																											P	P																
Week	2	3	4	5	6	7	8	9	10	11	12	13	14	15	16	17	18	19	20	21	22	23	24	25	26	27	32	33	34	35	36	37	38	39	40	41	42	43	44	45	46	47	48	49

A = Degerhamn cement with 6% air -entrainment
B = Byggcement with natural air content (about 1%)
G = Glass filler
K = Limestone powder
O = Optimisation
P = Testing
T = Manufacture of 20 cylinders
R = Reference
U = Executed testing
0 = 0 kg polypropylenfibre/m³
40 = w/c (%)

Appendix 4.2 –Mix proportions and properties for concretes optimised at LTH (kg/m³ dry weight)

Date: 2001 -08 -30

Concrete	40AG 0	40AK 0	40AK 2	40AK 4	40BK 0	40BR 0	55BK 0	55BK 2	55BK 4	55BR 0	70BG 0	70BK 0	70BK 2	70BK 4	70BR 0
Crushed stone 12 -16	202	225	112	0	238	1045	236	118	0	455	229	238	119	0	371
Crushed stone 8 -11	407	363	341	318	384	0	365	342	318	362	373	377	300	223	366
Gravel 0 -8	972	996	1072	1147	1052	772	1058	1132	1205	1035	1001	1069	1163	1256	1134
Glass filler	163								0		322			0	0
Limestone powder	0	117	142	167	131	0	244	239	234	0	0	315	288	260	0
Byggcement	0	0	0	0	451	454	311	342	373	348	250	248	272	295	278
Degerhamn cement	436	433	447	460											
Air -entrainment agent	1.199	0.550	1.22	1.883											
Water	174	173	179	184	181	182	171	188	205	192	175	173	190	207	195
Superplasticiser (wet)	8.09	4.68	7.7	10.67	12.00	2.73	8.16	10.14	12.14	2.09	12.01	6.63	8.9	11,1	0,00
Plastic fibre			2	4.000				2	4.00				2	4	0
Superplast (%)	1.4	0.85	1.3	1.7	2	0.6	1.5	1.75	2		2.1	1.2	1.6	2	
Air content (%)		6	5.9	5.7											
Density	2364	2355	2323	2290	2450	2455	2400	2373	2347	2394	2362	2430	2372	2313	2345
Slump flow (mm)	740	740		600	695	160	665		600		695	740		600	
T_{500} (s)	10	6		10	8		8		8		13	5		7	

Notations: A = Degehamn cement (6% air), B = Byggcement (about 1 % air), G = Glass filler, K = Limestone powder, R = reference, 0 = 0 kg polypropylenfibre/m³ , 40 = w/c (%)

Appendix 4.3 –Mix proportions and properties for concretes optimised by Nordkalk (kg/m³ dry weight)

Date: 2001 -08 -30

Concrete	40AG 0	40AK 0	40AK 2	40AK 4	40BK 0	40BR 0	55BK 0	55BK 2	55BK 4	55BR 0	70BG 0	70BK 0	70BK 2	70BK 4	70BR 0
Crushed stone 12 -16	620	582	583	548	603	1045	615	572	533	455	559	631	590	254	371
Crushed stone 8 -11	0	0	0	0	0	0	0	0	0	362	0	0	0	0	366
Gravel 0 -8	1036	1018	1017	958	1054	772	1075	1000	931	1035	1183	1109	1027	1190	1134
Glass filler	62										80			0	0
Limestone powder	0	146	184	232	130	0	149	216	291	0	0	189	229	331	0
Byggcement	0	0	0	0	447	454	346	365	377	348	321	268	298	306	278
Degerhamn cement	427	402	441	454											
Air -entrainment agent	0.235	0.13	0.132	0.136											
Water	171	161	176	182	179	182	190	201	207	192	225	188	209	214	195
Superplasticiser (wet)	4.05	4.82	8.2	9.35	9.78	2.73	5.57	7.05	7.76	2.09	5.3	9.41	4.89	6.57	0
Plastic fibre			2	4				2	4				2	4	0
Superplast (%)	1	1.2	1.85	2.06	2.2	0.6	1.61	1.93	2.06		1.65	3.5	1.64	2.15	
Air content (%)		7	-	-											
Density	2314	2310	2405	2378	2423	2455	2385	2368	2356	2394	2374	2394	2357	2301	2345
Slump flow (mm)	700	705	710	650	685	160	685	710	655		695	705	705	620	
T_{500} (s)	7	5	8	8	6		6	5	6		2	3	3	6	

Notations: A = Degehamn cement (6% air), B = Byggcement (about 1 % air), G = Glass filler, K = Limestone powder, R = reference, 0 = 0 kg polypropylenfibre/m³ , 40 = w/c (%)

Appendix 4.4 –Difference between mix proportions and properties of concretes optimised by LTH and by Nordkalk (kg/m³ dry weight)

Date: 2001 -08 -30

Concrete	40AG 0	40AK 0	40AK 2	40AK 4	40BK 0	40BR 0	55BK 0	55BK 2	55BK 4	55BR 0	70BG 0	70BK 0	70BK 2	70BK 4	70BR 0
Crushed stone 12 -16	418	357		548	365		379		533		330	393		254	
Crushed stone 8 -11	-407	-363		-318	-384		-365		-318		-373	-377		-223	
Gravel 0 -8	64	22		-189	2		17		-274		182	40		-66	
Glass filler	-101	0		0	0		0		0		-242	0		0	
Limestone powder	0	29		65	-1		-95		57		0	-126		71	
Byggcement	0	0		0	-4		35		4		71	20		11	
Degerhamn cement	-9	-31		-6	0		0		0		0	0		0	
Air -entrainment agent	-0.96	-0.43		-1.75	0		0		0		0	0		0	
Water	-3	-12		-2	-2		19		2		50	15		7	
Superplasticiser (wet)	-4.04	0.14		-1.32	-2.22		-2.59		-4.38		-6.71	2.78		-4.53	
Plastic fibre	0	0		0	0		0		0		0	0		0	
Superplast (%)	-0.4	0.35		0.36	0.2		0.11		0.06		-0.45	2.3		0.15	
Air content (%)	-	1			0		0		0		0	0		0	
Density	-50	-45		88	-27		-15		9		12	-36		-12	
Slump flow (mm)	-40	-35		50	-10		20		55		0	-35		20	
T_{500} (s)	-3	-1		-2	-2		-2		-2		-11	-2		-1	

A = Degehamn cement (6% air), B = Byggcement, G = Glass filler, K = Limestone powder, R = reference, 0 = 0 kg polypropylenfibre/m³ , 40 = w/c (%)

Appendix 4.5 –Difference between cost of concretes optimised by LTH and by Nordkalk (SEK/m³)

Date: 2001 -08 -30

Concrete	40AG 0	40AK 0	40AK 2	40AK 4	40BK 0	40BR 0	55BK 0	55BK 2	55BK 4	55BR 0	70BG 0	70BK 0	70BK 2	70BK 4	70BR 0
Crushed stone 12 -16	62.70	53.55	0.00	82.20	54.75	0.00	56.85	0.00	79.95	0.00	49.50	58.95	0.00	38.10	0.00
Crushed stone 8 -11	-61.05	-54.45	0.00	-47.70	-57.60	0.00	-54.75	0.00	-47.70	0.00	-55.95	-56.55	0.00	-33.45	0.00
Gravel 0 -8	12.80	4.40	0.00	-37.80	0.40	0.00	3.40	0.00	-54.80	0.00	36.40	8.00	0.00	-13.20	0.00
Glass filler	-60.60	0.00	0.00	0.00	0.00	0.00	0.00	0.00	0.00	0.00	193.60	0.00	0.00	0.00	0.00
Limestone powder	0.00	8.70	0.00	19.50	-0.30	0.00	-28.50	0.00	17.10	0.00	0.00	-37.80	0.00	21.30	0.00
Byggcement	0.00	0.00	0.00	0.00	-2.40	0.00	21.00	0.00	2.40	0.00	42.60	12.00	0.00	6.60	0.00
Degerhamn cement	-7.20	-24.80	0.00	-4.80	0.00	0.00	0.00	0.00	0.00	0.00	0.00	0.00	0.00	0.00	0.00
Sum	-53.35	-12.60	0.00	11.40	-5.15	0.00	-2.00	0.00	-3.05	0.00	-121.05	-15.40	0.00	19.35	0.00

A = Degehamn cement (6% air), B = Byggcement, G = Glass filler, K = Limestone powder, R = reference, 0 = 0 kg polypropylenfibre/m³ , 40 = w/c (%).

Appendix 4.6 – Mix proportions and properties of concrete finally cast (kg/m³ dry weight)

Concrete	40AG0	40AK0	40AK2	40AK4	40AR0	40BK0	40BR0	55BK0	55BK2	55BK4	55BR0	70BG0	70BK0	70BK2	70BK4	70BR0
Crushed 12 -16	624	595	572	0	857	602	1004	234	119	0	452	551	631	583	0	356
Crushed 8 -11	0	0	0	326		0	0	362	244	316	360	0	0	0	220	351
Gravel 0 -8	1043	1040	998	1176	758	1052	742	1049	1140	1198	1029	1166	1109	1015	1241	1088
Glass filler	62									0		79			0	0
Limestone powder	0	149	181	171		130	0	242	241	233	0	0	189	226	256	0
Byggcement	0	0	0	0		447	436	308	344	382	346	316	268	294	312	267
Degerhamn cement	430	411	433	487	518											
Cementa 88L					0.161											
Microair				0.188												
Sikaair HPV	0.235															
Sikaair15B		0.13	0.132													
Water	172	164	173	195	206	179	175	170	189	210	191	222	188	207	219	195
Glenium (wet)				10.67						12.14					11.1	
Peramin F					10.4		2.73				2.09					0
Sikament 56	4.05	4.82	8.2			9.78		8.16	10.14			5.3	9.41	4.89		
Plastic fibre			2	4					2	4				2	4	0
Flytmedel (%)	1	1.2	1.85	1.7	2	2.2	0.6	1.5	1.75	2	0.57	1.65	3.5	1.64	2	
Density	2330	2360	2360	2370	2350	2420	2360	2380	2390	2350	2380	2340	2394	2330	2320	2250
Air content (%)	5.0	5.1	2.5	2.8	4.0	-	-	1.3	1.1	-	1.5	1.7	2.6	-	-	5.0
Slump (flow) (mm)	620	680	670	600	200	660	90	670	630	600	220	630	600	660	600	80
T_{500} (s)	6	5	8	10		6		8		8		2	3	3	7	
Prestress. (kN)	900	900	900	900	900	900	900	730	730	620	730	620	620	620	620	620
Approximate stress (20% stress losses; MPa)	18	18	18	18	18	18	18	15	15	12	15	12	12	12	12	12
Concrete	40AG0	40AK0	40AK2	40AK4	40AR0	40BK0	40BR0	55BK0	55BK2	55BK4	55BR0	70BG0	70BK0	70BK2	70BK4	70BR0

Notations: A = Degehamn cement (6% air), B = Byggcement (about 1 % air), G = Glass filler, K = Limestone powder, R = reference, 0 = 0 kg /m³ polypropylene fibre, 40 = w/c (%).

Appendix 4.7 – Strength development of concrete cast at LTH (MPa)

Concrete	40AK0	40AK2	40AK4	40AK4-new	40BK0	40BR0	55BK0	55BK0-new	70BG0LTH	70BG0SGÅ	70BK0LTH	70BK0NKK
Date	21.5.01	2.5.02	11.6.01	28.5.02	9.5.01	2.4.01	9.5.01	20.6.02	10.5.01	14.8.01	19.4.01	7.5.01
1 days	17.5	13.5	10	15.5	41	44	29	18	15.5	21	19.5	19
	17	17.5	10	15	40	44.5	30	19.5	16	21	20	20.5
1 days, av.	17.25	15.5	10	15.25	40.5	44.25	29.5	18.75	15.75	21	19.75	19.75
7 days	56	32.5	38.5	54.5	73	77	55	44.5	36	27	38	43
	59	44.5	40	53	74.5	76.5	56	44	36.5	28	40.5	41
7 days, av.	57.5	38.5	39.25	53.75	73.75	76.75	55.5	44.25	36.25	27.5	39.25	42
28 days	80.5	64	42	67.5	91	85	72.5	53.5	54	33	52.5	60
	75	68.75	42.5	63.5	92.5	85	71	51	55.5	38	55	58
28 days, av.	77.75	66.375	42.25	65.5	91.75	85	71.75	52.25	54.75	35.5	53.75	59
90 days	77	67	43	71	89.5	86	73		58	40	53	57
	71	67	43.5	75	85.5	92.5	71		57		55.5	58
90 days, av.	74	67	43.25	73	87.5	89.25	72	53	57.5	40	54.25	57.5

Notations: A = Degerhamn cement (6% air), B = Byggcement (1% air), G = Glass filler, K = Limestone powder, R = reference, SGÅ = Svensk Glasåtervinning; NKK = Nordkalk; 0 = 0 kg polypropylenfibre/m³, 40 = w/c (%).

Appendix 4.8 – Strength development of concrete cast for SP at SPAB, Bollebygd (MPa)

Concrete	Age	Prestressing strength (MPa)	Age (days)	Cube 1 (MPa)	Cube 1 (MPa)	Av. (MPa)	Density (kg/m³)
40AG0	2d	32.4	28	80.0	80.4	80.2	2380
40AK0	2d	36.0	28	88.4	88.4	88.4	2390
40AK2	2d	34.7	28	87.6	87.1	87.4	2420
40AK4	3d	44.4	28	84.4	78.2	81.3	2380
40AR0	3d	42.2	28	75.6	74.7	75.2	2400
40BK0	3d	60.4	28	80.9	78.7	79.8	2420
40BR0	3d	52.9	28	74.7	74.7	74.7	2460
55BK0	-	-	28	68.9	67.1	68.0	2360
55BK2	-	-	28	64.0	62.2	63.1	2370
55BK4	5d	48.9	28	65.8	64.9	65.4	2330
55BR0	-	-	28	63.6	62.7	63.2	2390
70BG0	40h	22.2	28	48.0	48.0	48.0	2320
70BK0	7d	42.7	28	55.6	55.6	55.6	2390
70BK2	5d	30.2	28	39.1	40.0	39.6	2340
70BK4	5d	37.8	28	53.3	52.9	53.1	2320
70BR0	7d	30.2	28	40.4	40.9	40.7	2270

Notations: A = Degehamn cement (6% air), B = Byggcement (about 1 % air), G = Glass filler, K = Limestone powder, R = reference, 0 = 0 kg polypropylenfibre/m³ , 40 = w/c (%)

Appendix 4.9 – Stress/strain results of concrete 40AG0 at 20 °C.

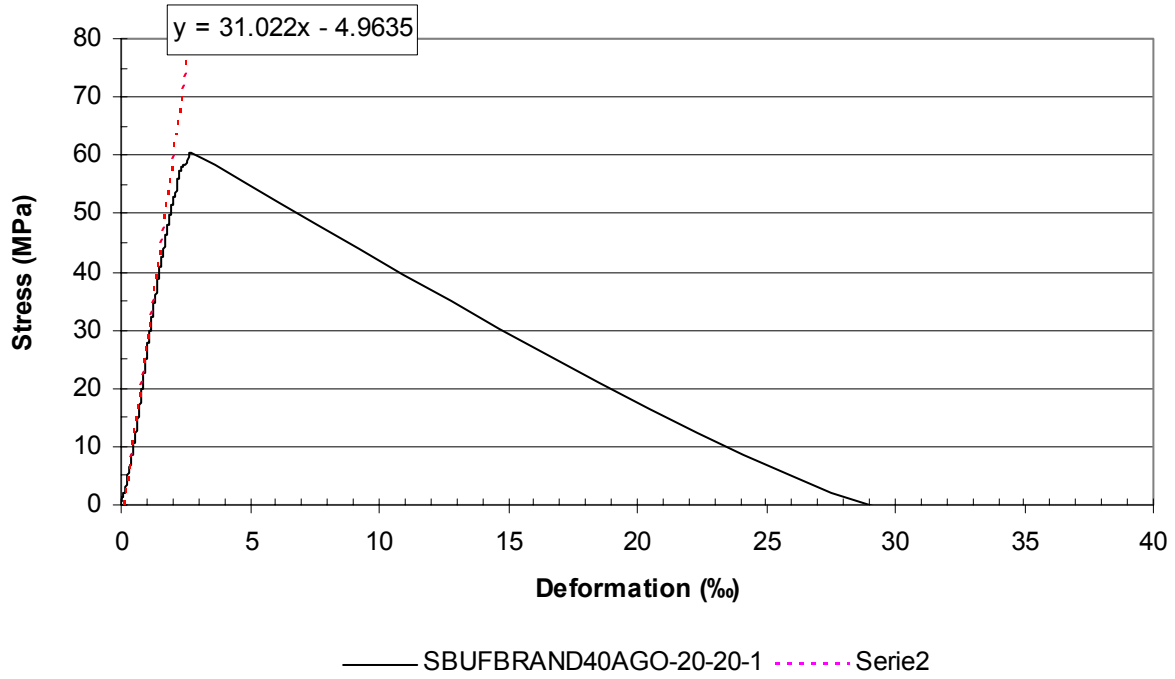

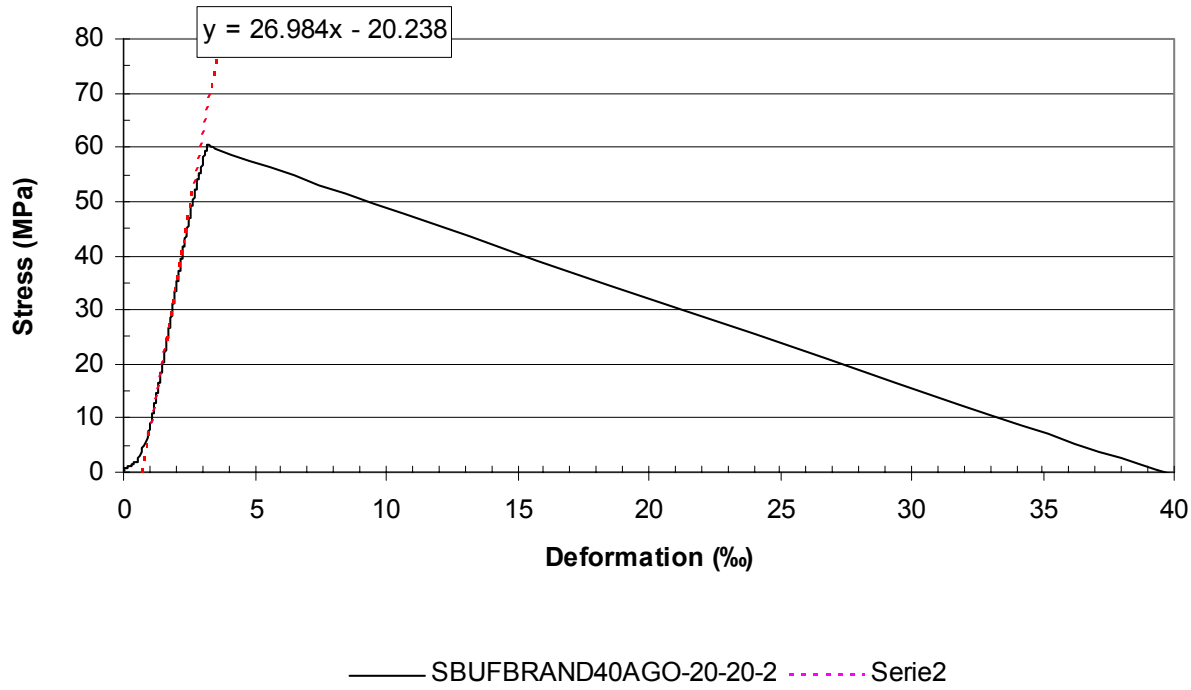

Appendix 4.10 – Stress/strain results of concrete 40AG0 at 200 °C – 20 °C.

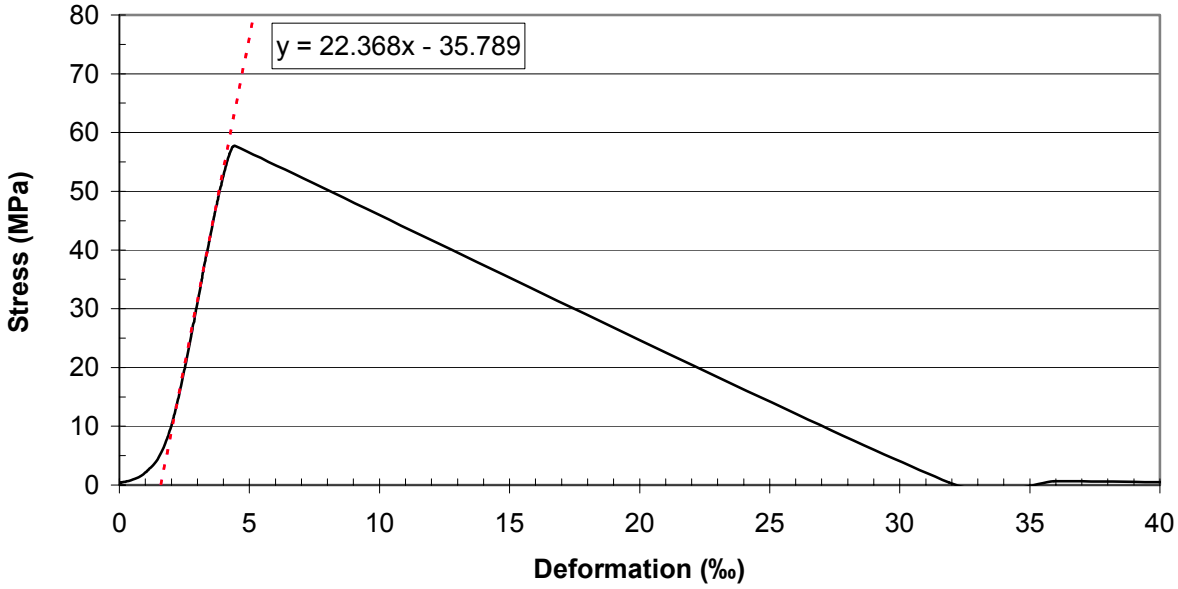

SBUFBRAND40AGO-200-20-1 Serie2

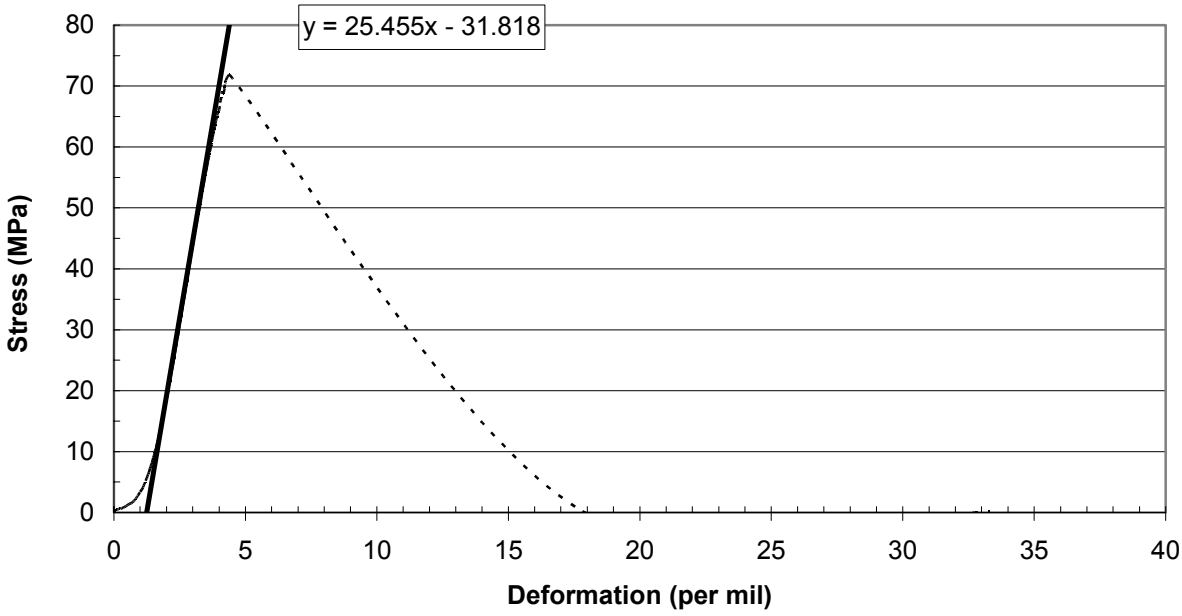

SBUFBRAND40AG0-200-20-2

Appendix 4.11 – Stress/strain results of concrete 40AG0 at 200 °C – 200 °C.

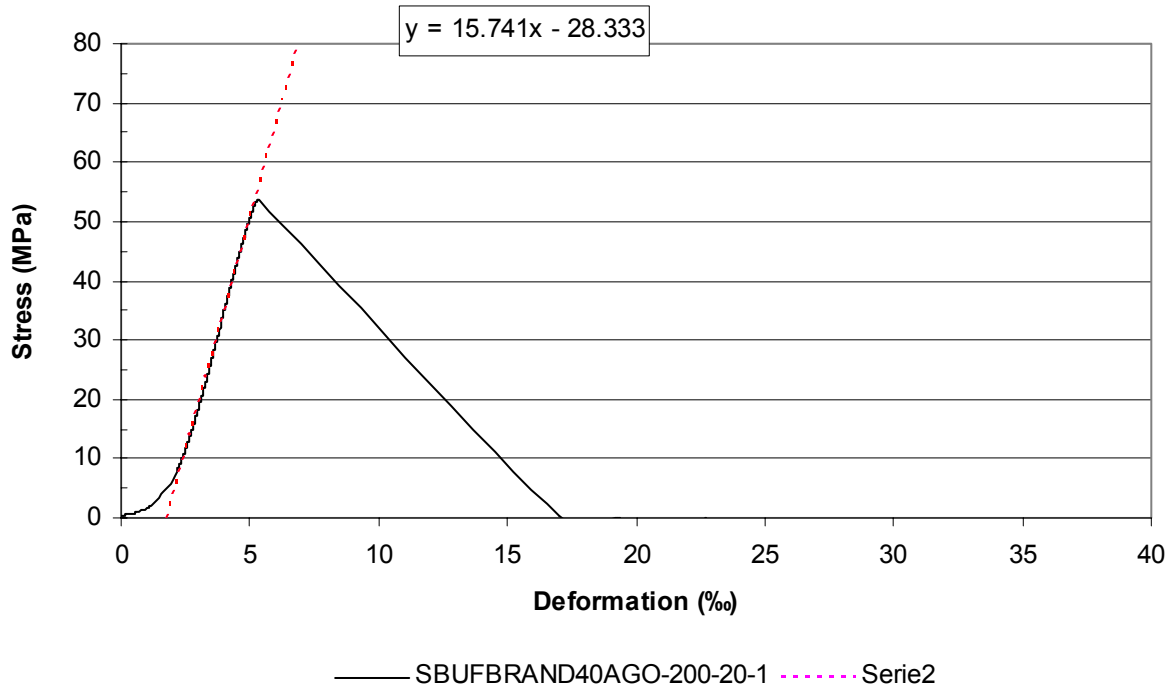

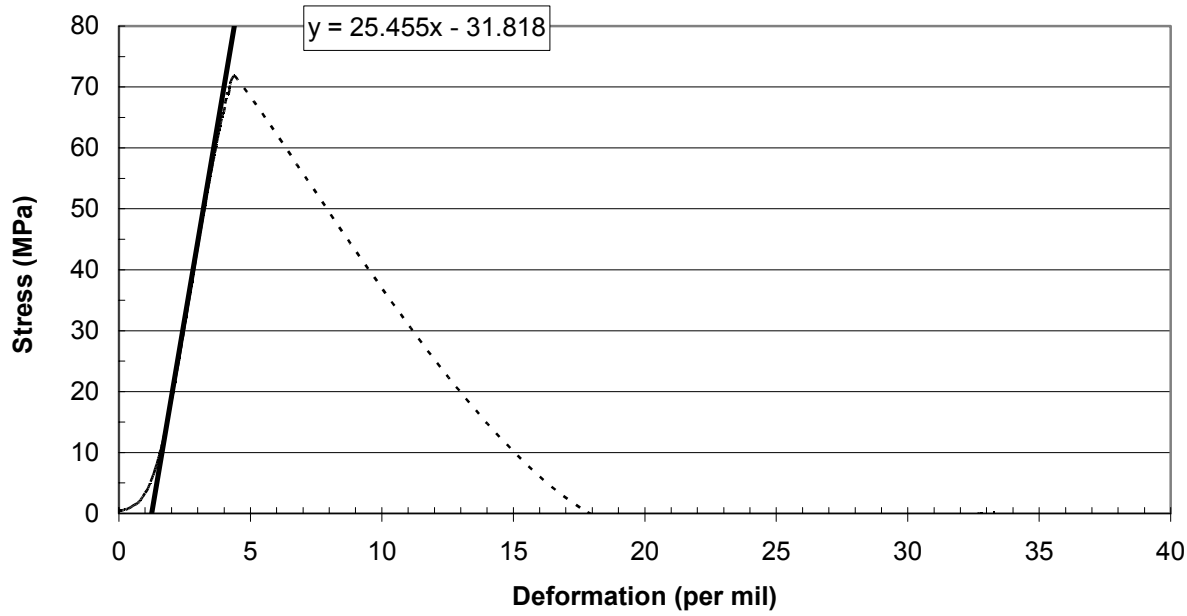

SBUFBRAND40AG0-200-20-2

Appendix 4.12 – Stress/strain results of concrete 40AG0 at 400 °C – 20 °C.

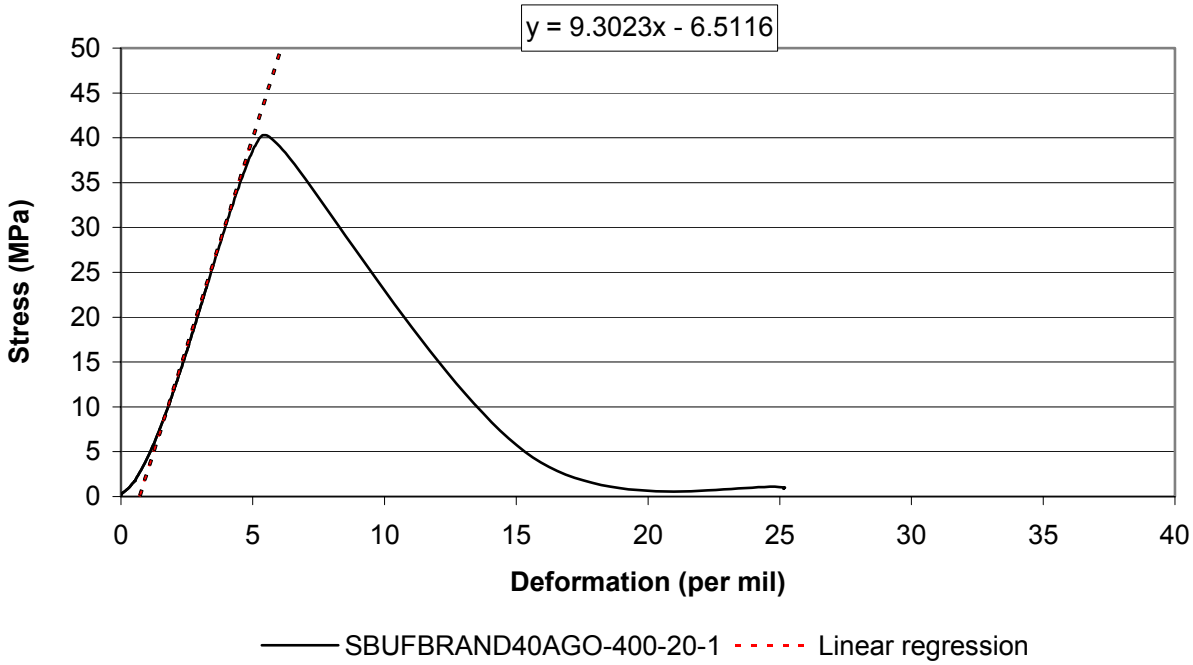

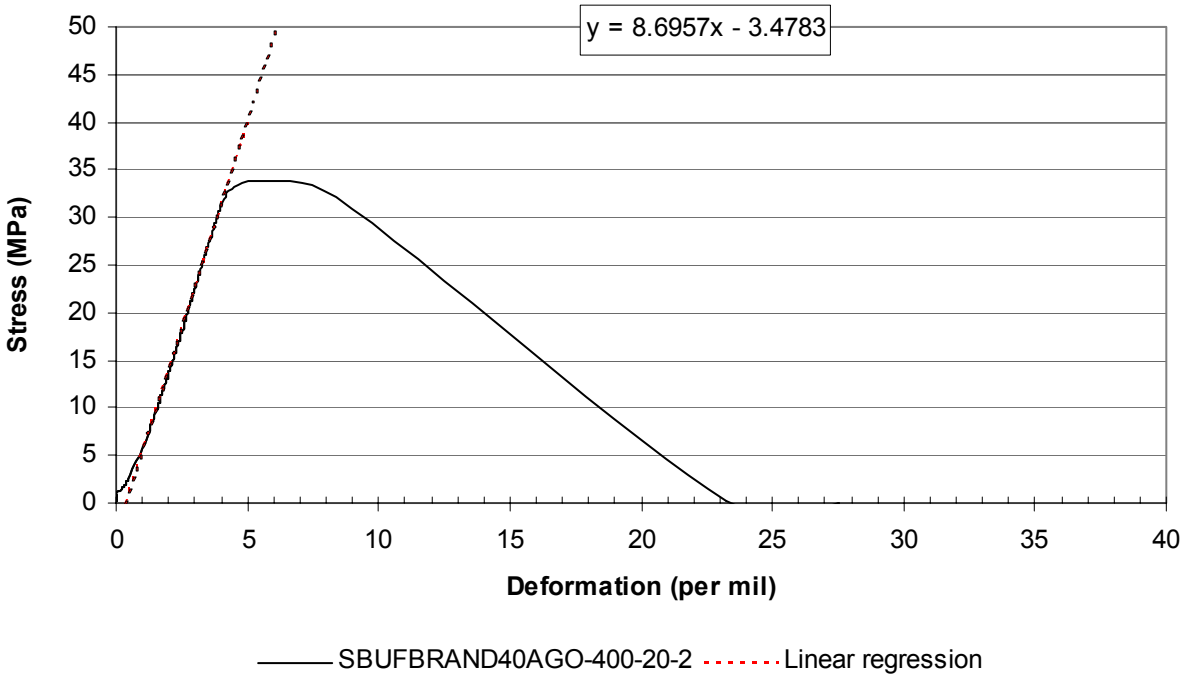

Appendix 4.13 – Stress/strain results of concrete 40AG0 at 400 °C – 400 °C.

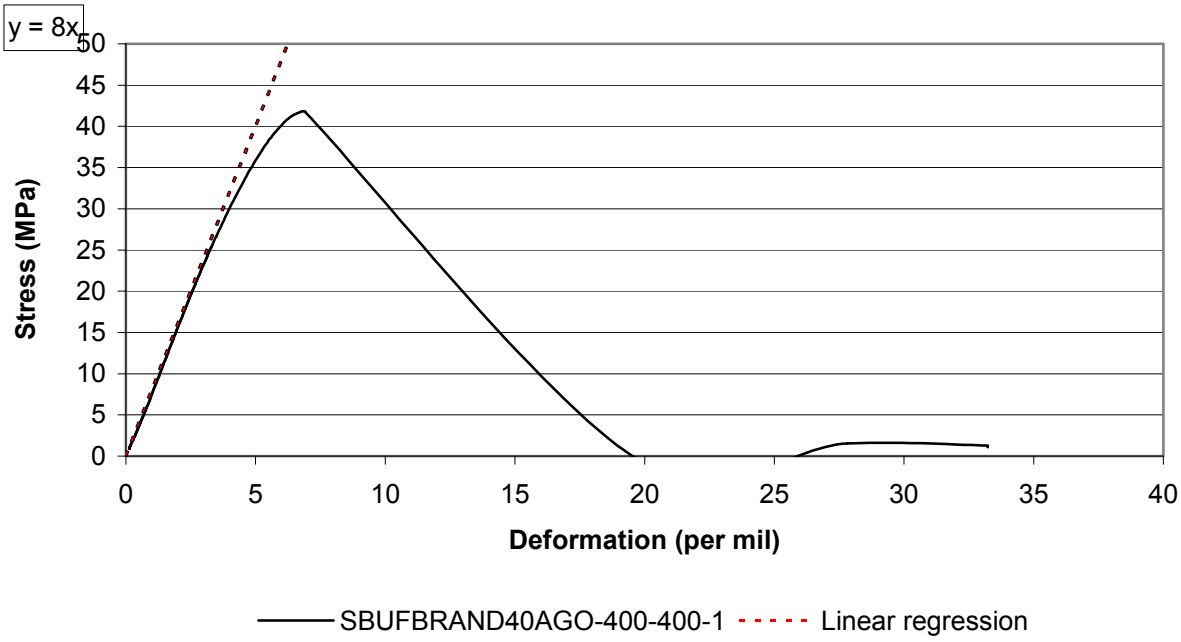

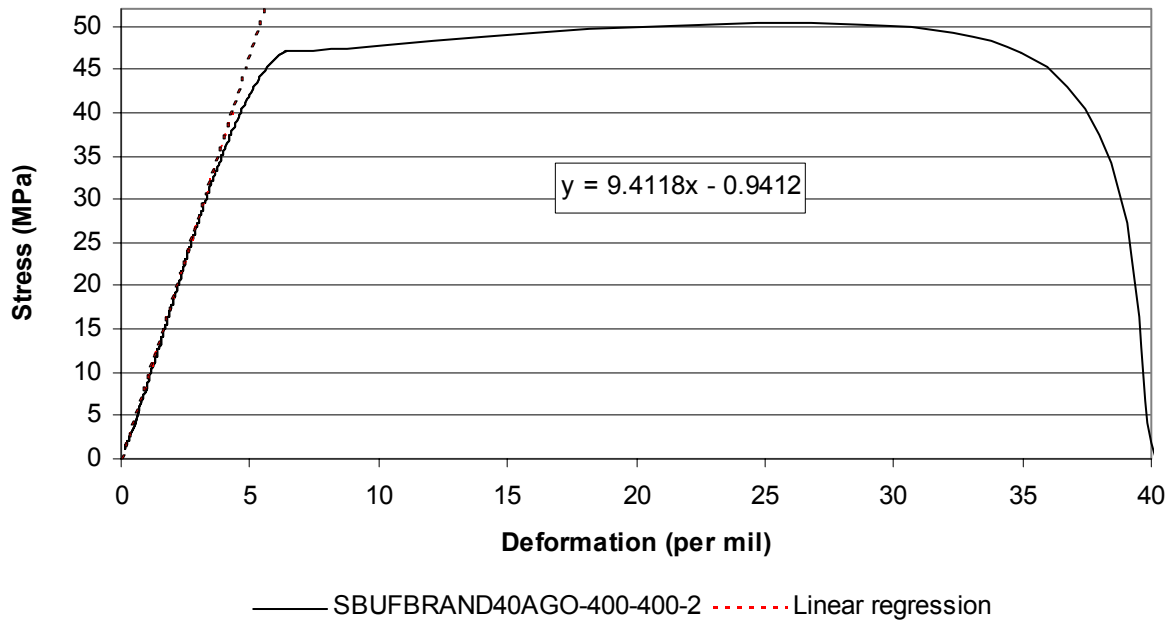

Appendix 4.14 – Stress/strain results of concrete 40AG0 at 800 °C – 20 °C.

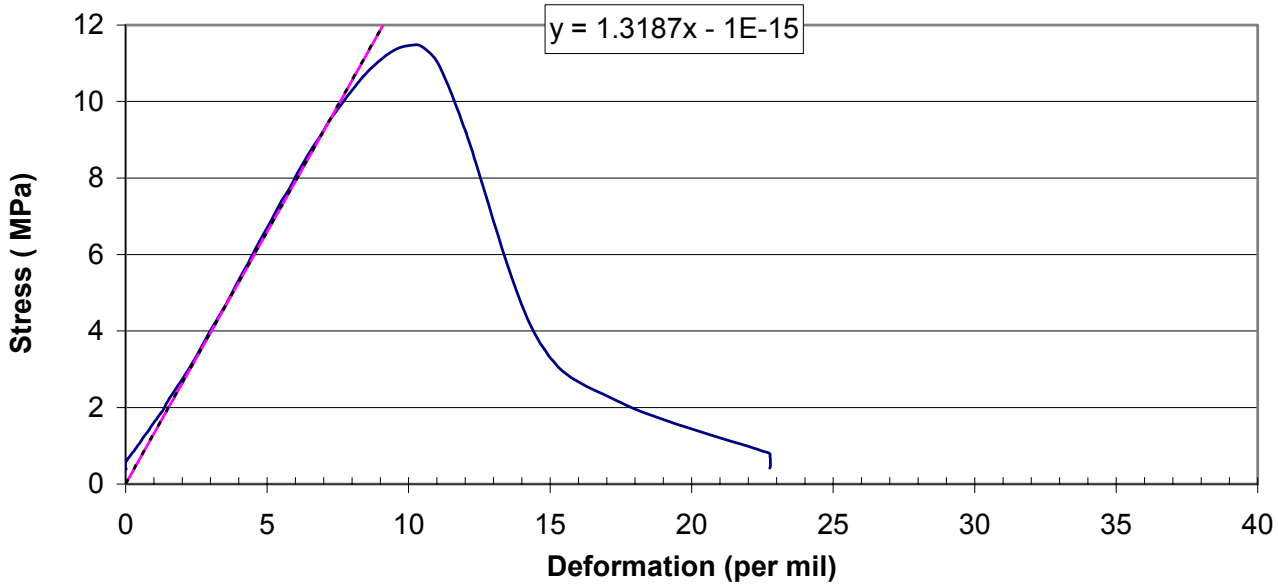

SBUFBRAND800-20-1

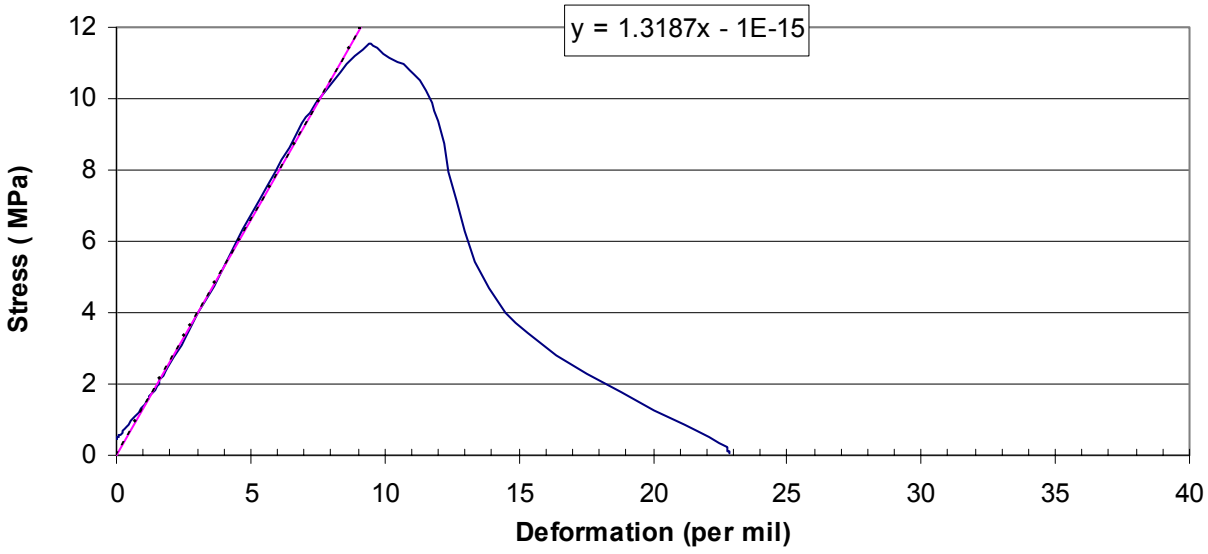

SBUFBRAND40AG0-800-20-2

Appendix 4.15 – Stress/strain results of concrete 40AG0 at 800 °C – 800 °C.

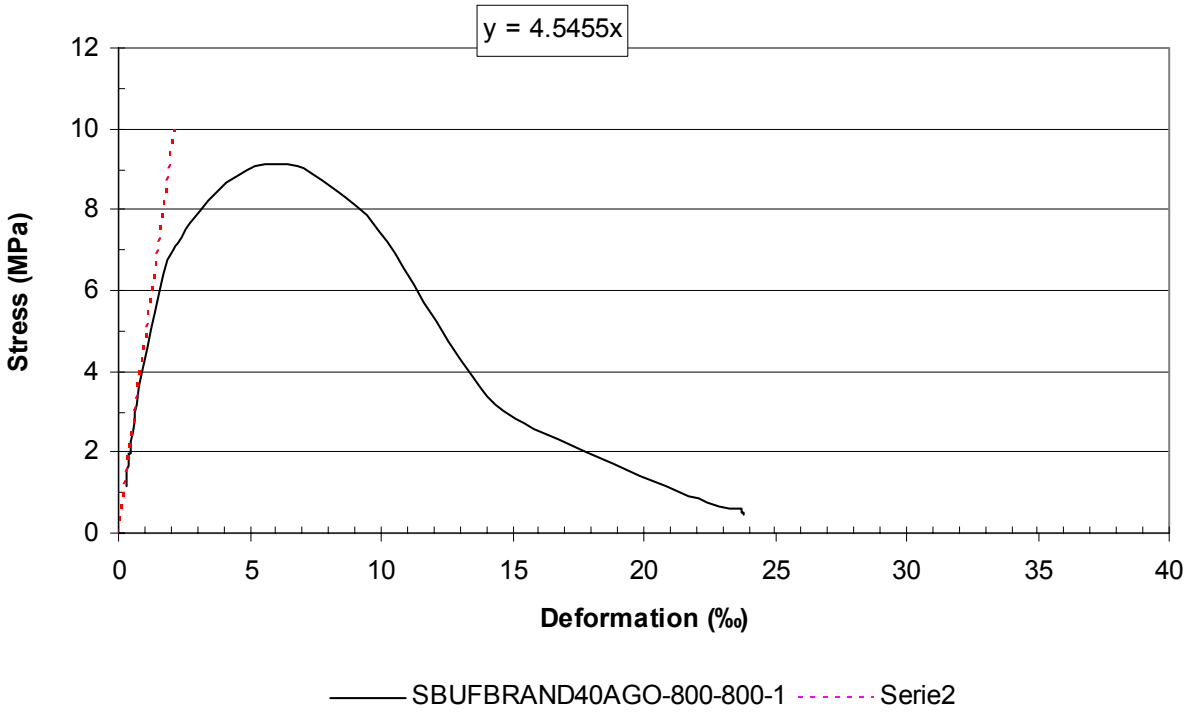

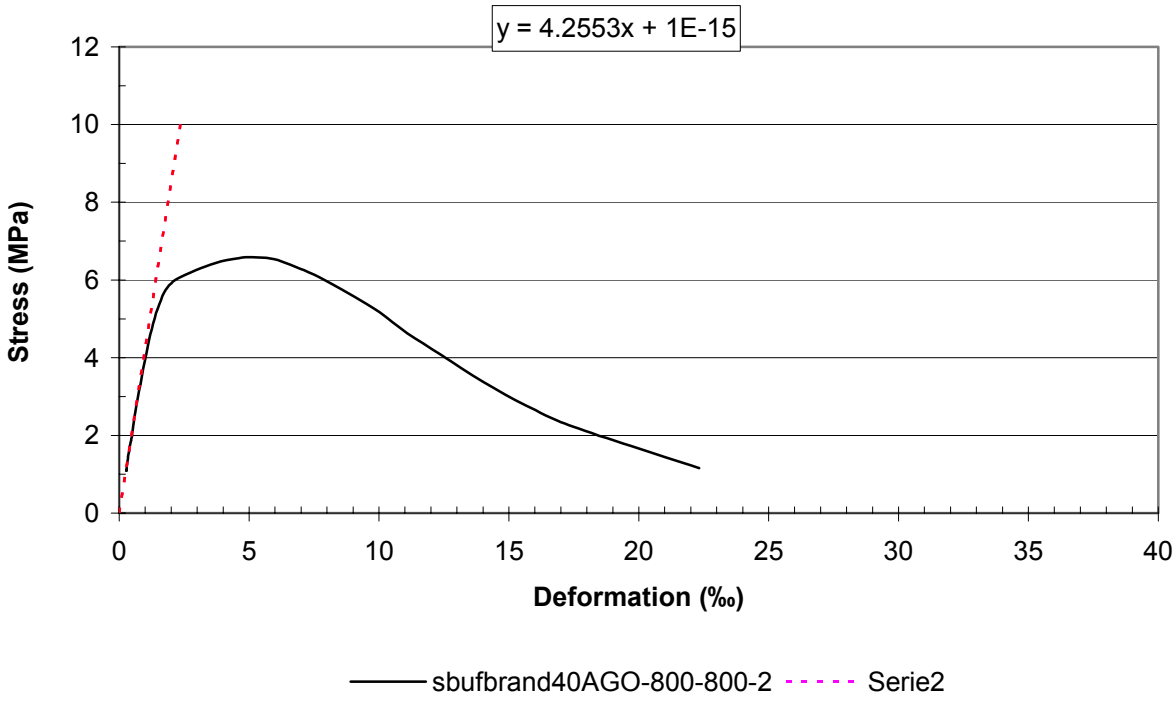

Appendix 4.16 – Stress/strain results of concrete 40AK0 at 20 °C.

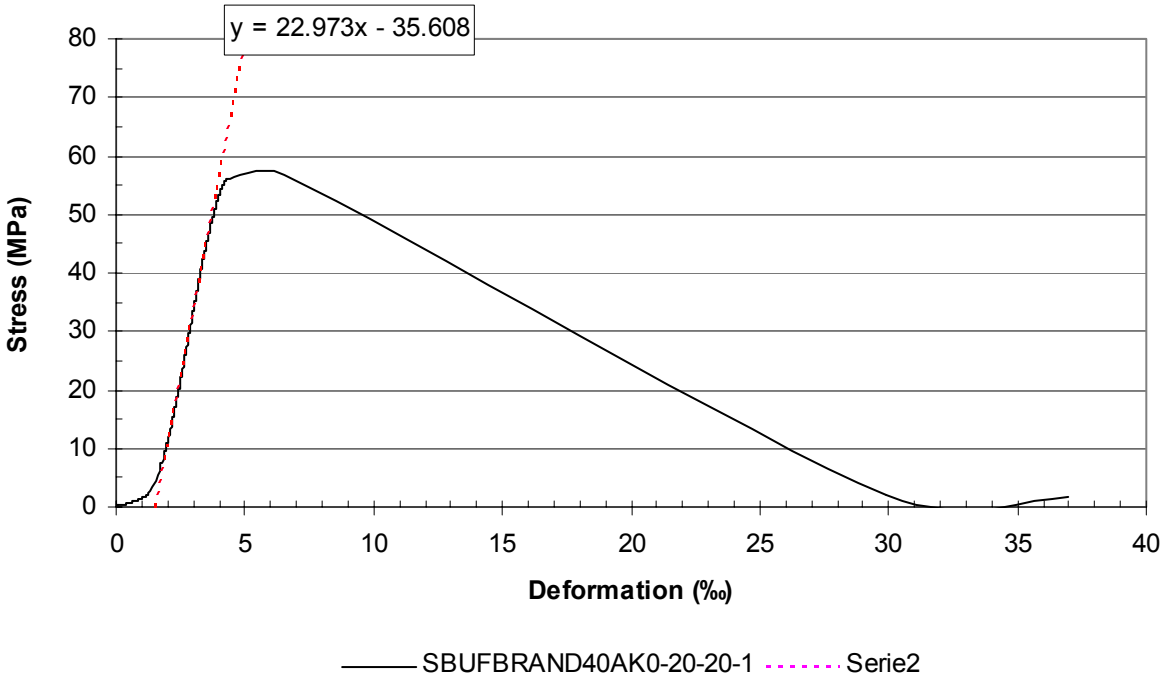

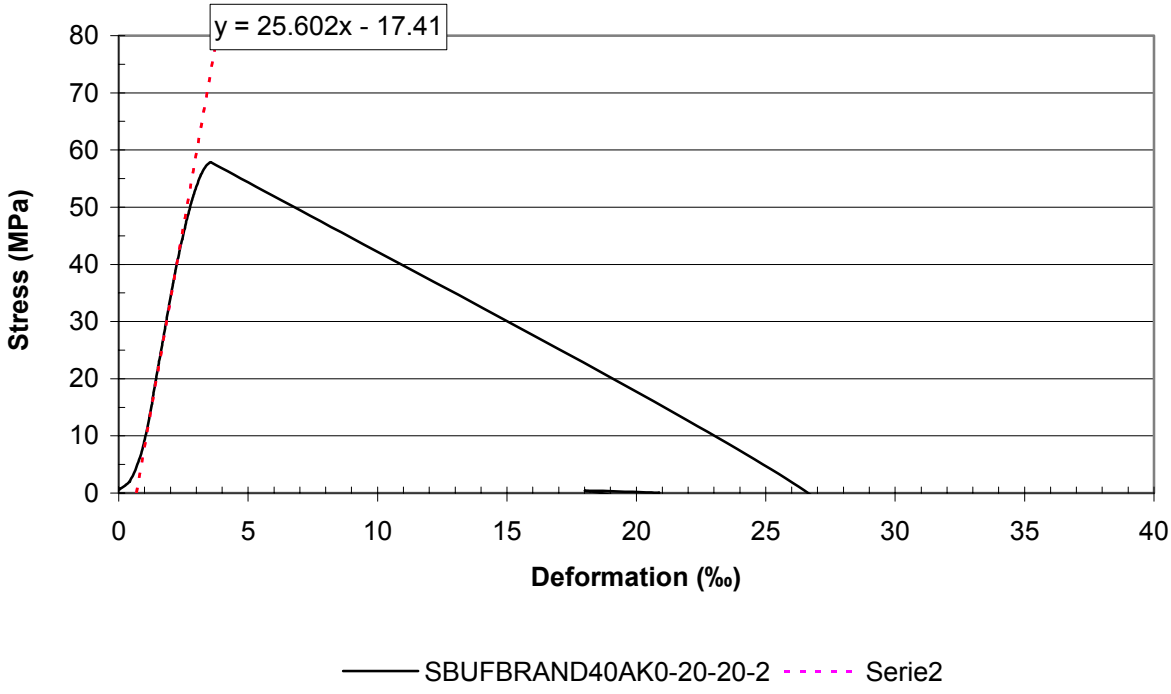

Appendix 4.17 – Stress/strain results of concrete 40AK0 at 200 °C – 20 °C.

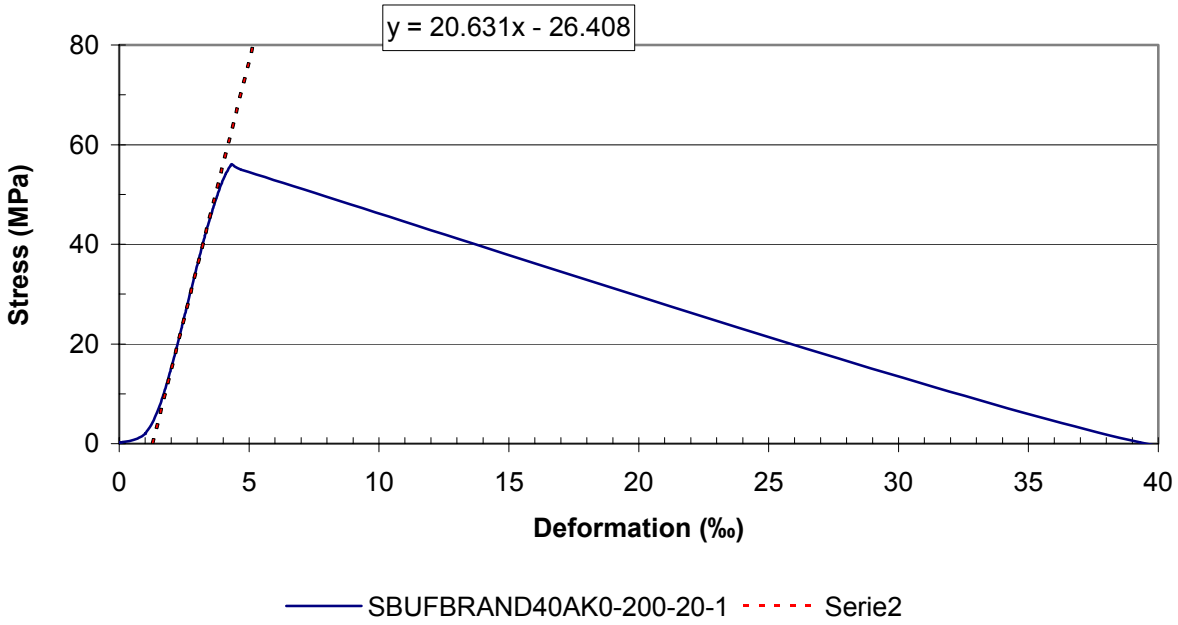

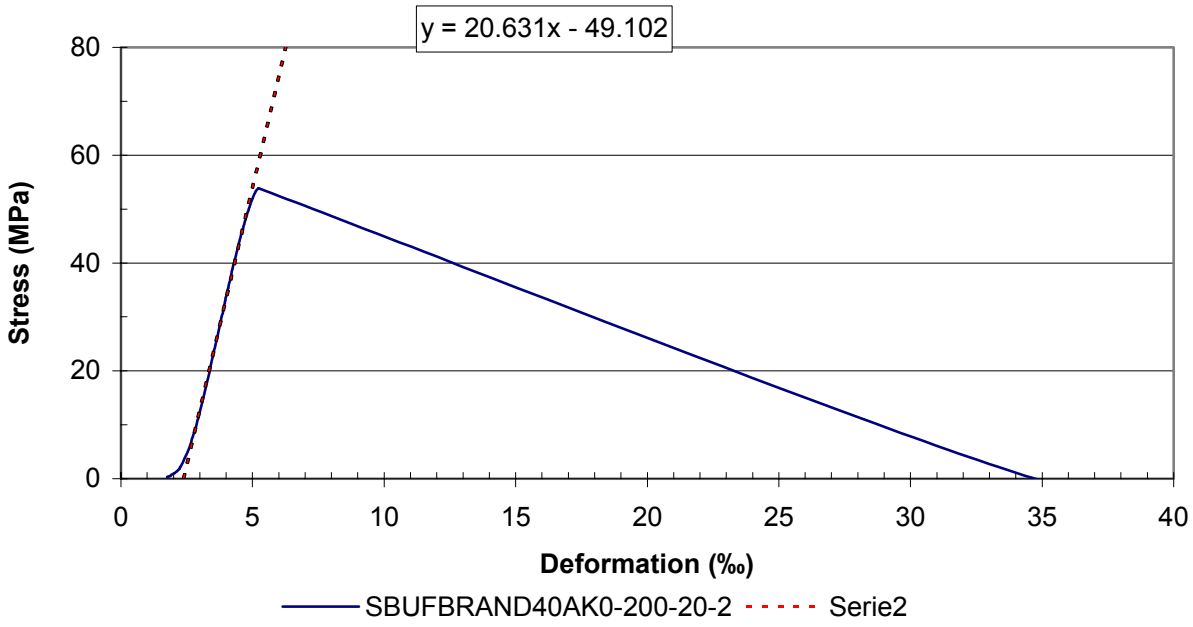

Appendix 4.18 – Stress/strain results of concrete 40AK0 at 200 °C – 200 °C.

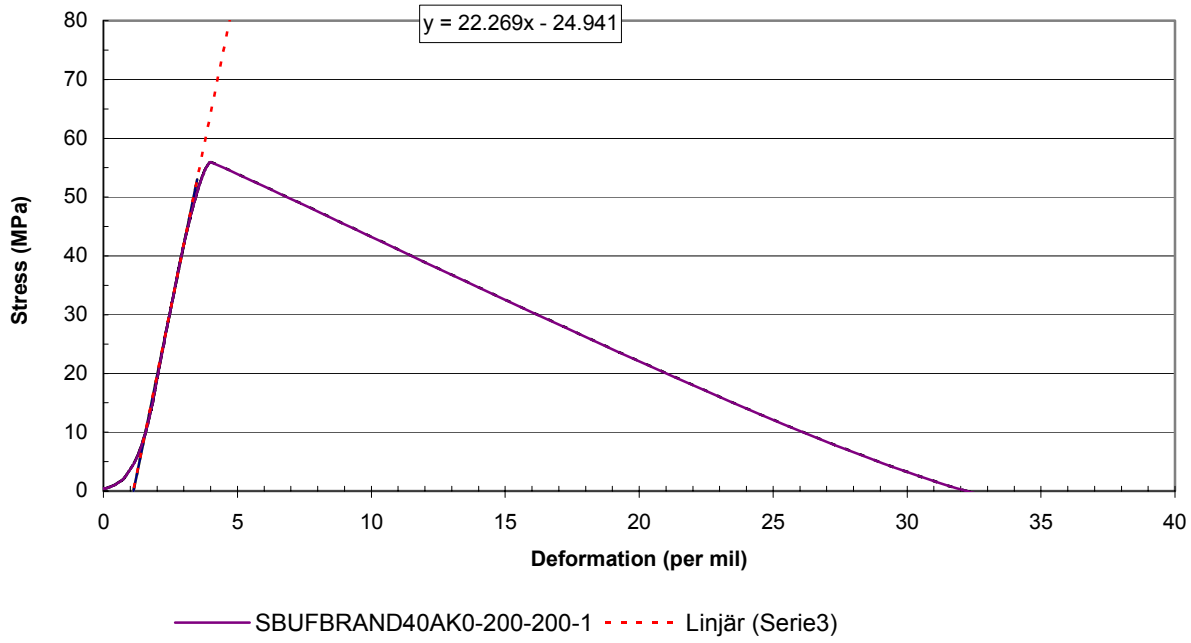

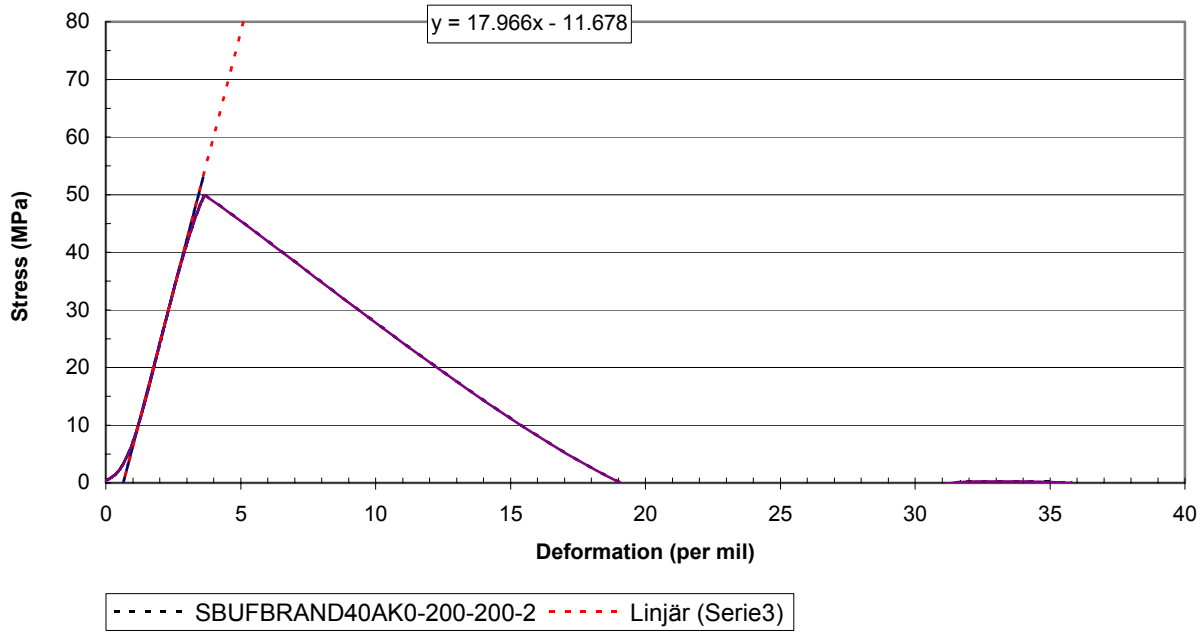

Appendix 4.19 – Stress/strain results of concrete 40AK0 at 400 °C – 20 °C.

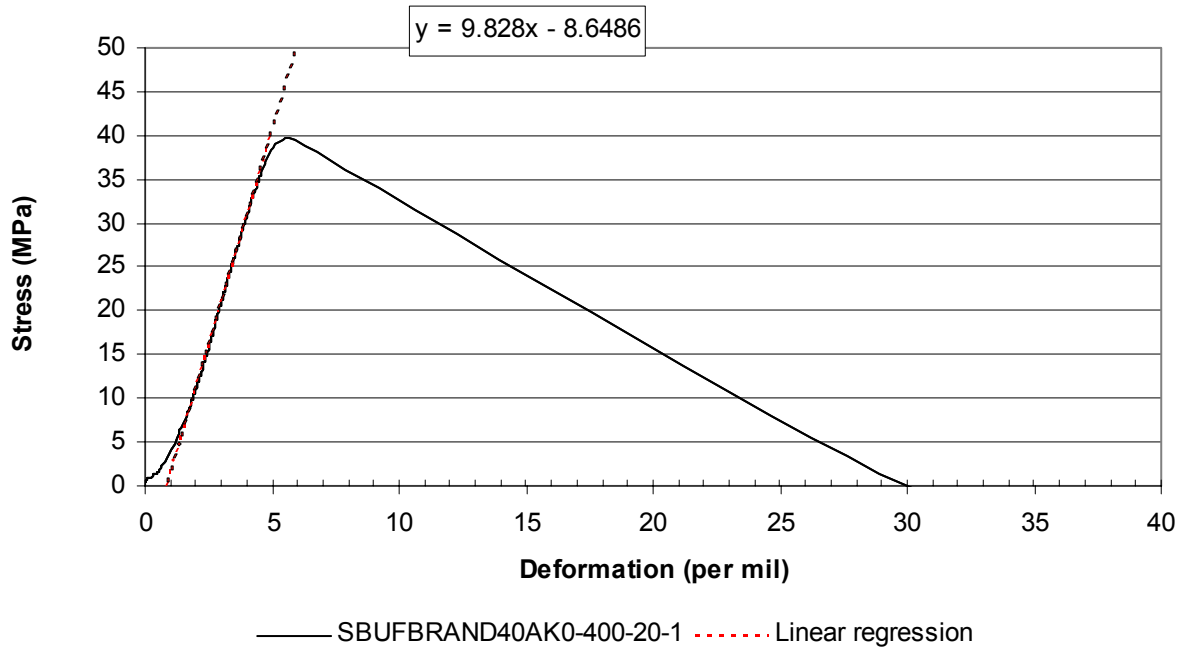

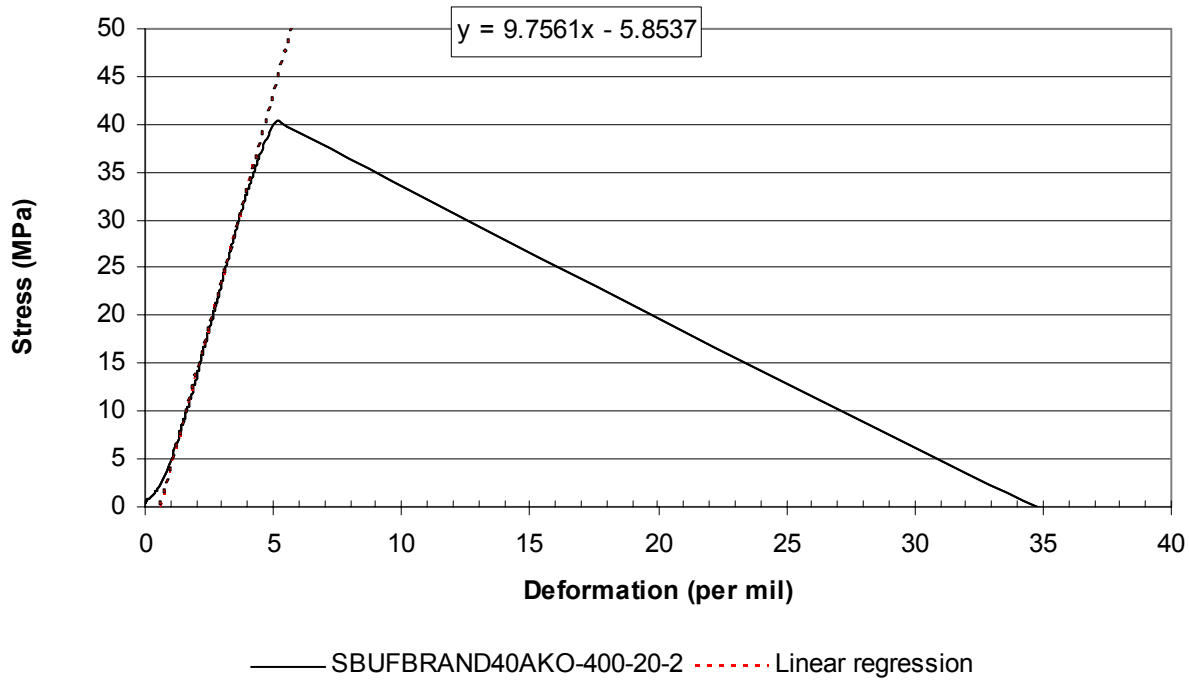

Appendix 4.20 – Stress/strain results of concrete 40AK0 at 400 °C – 400 °C.

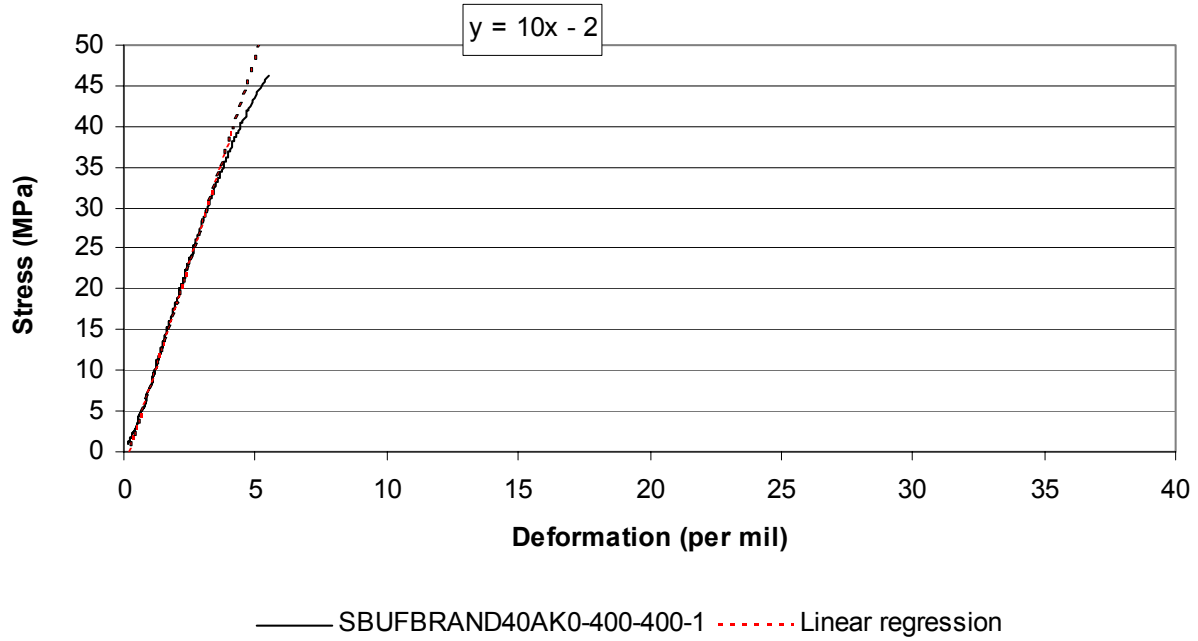

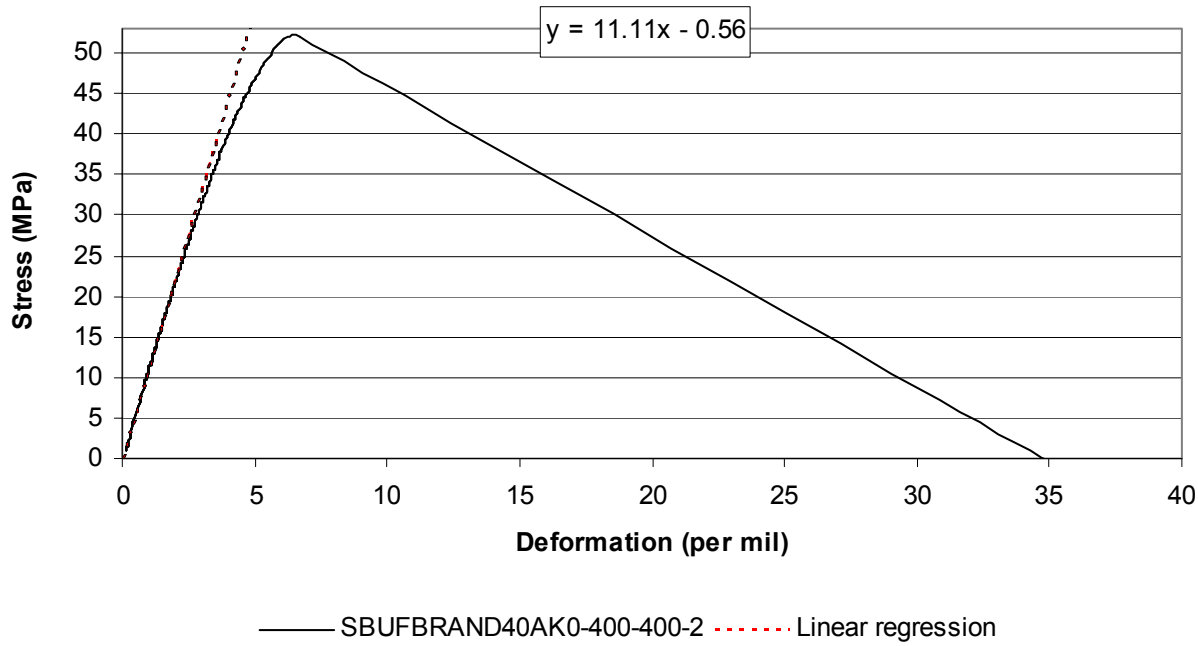

Appendix 4.21 – Stress/strain results of concrete 40AK0 at 800 °C – 800 °C.

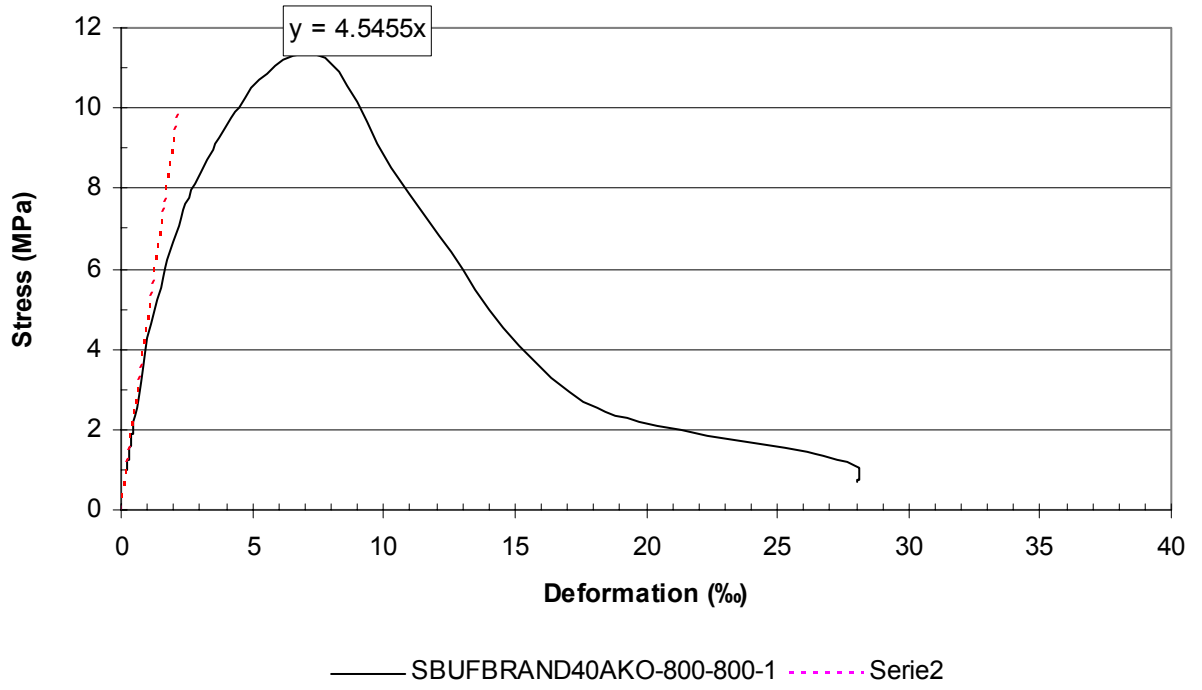

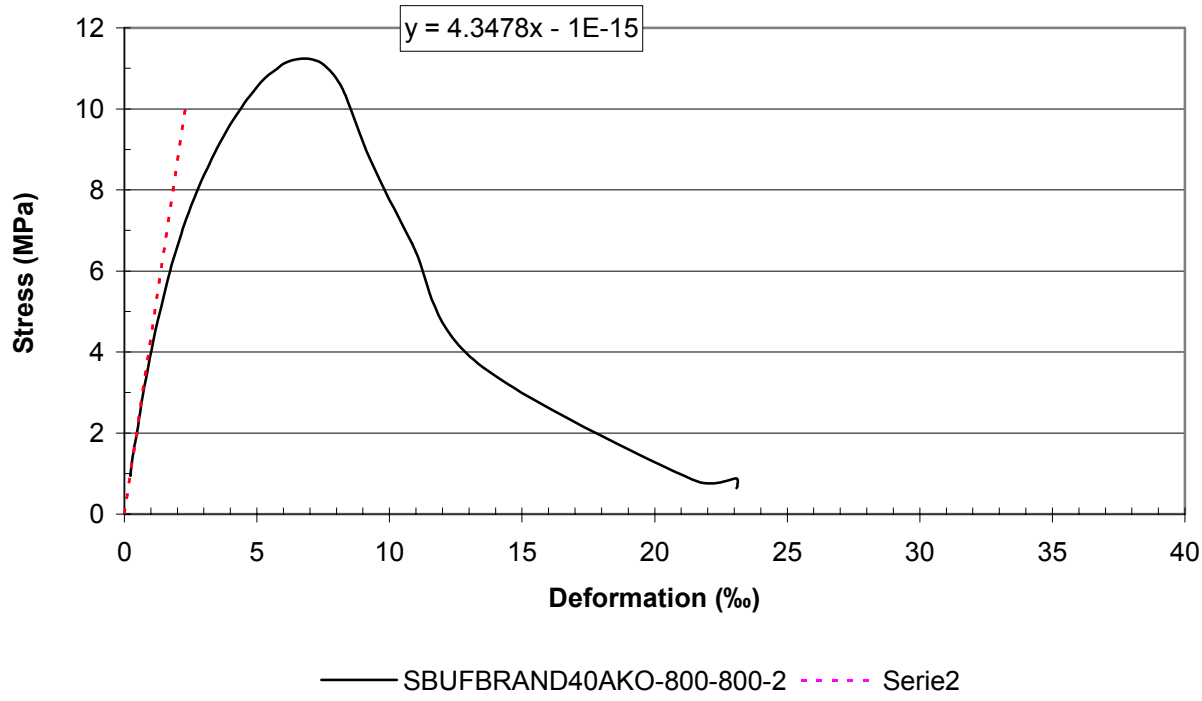

Appendix 4.22 – Stress/strain results of concrete 40AK2 at 20 °C.

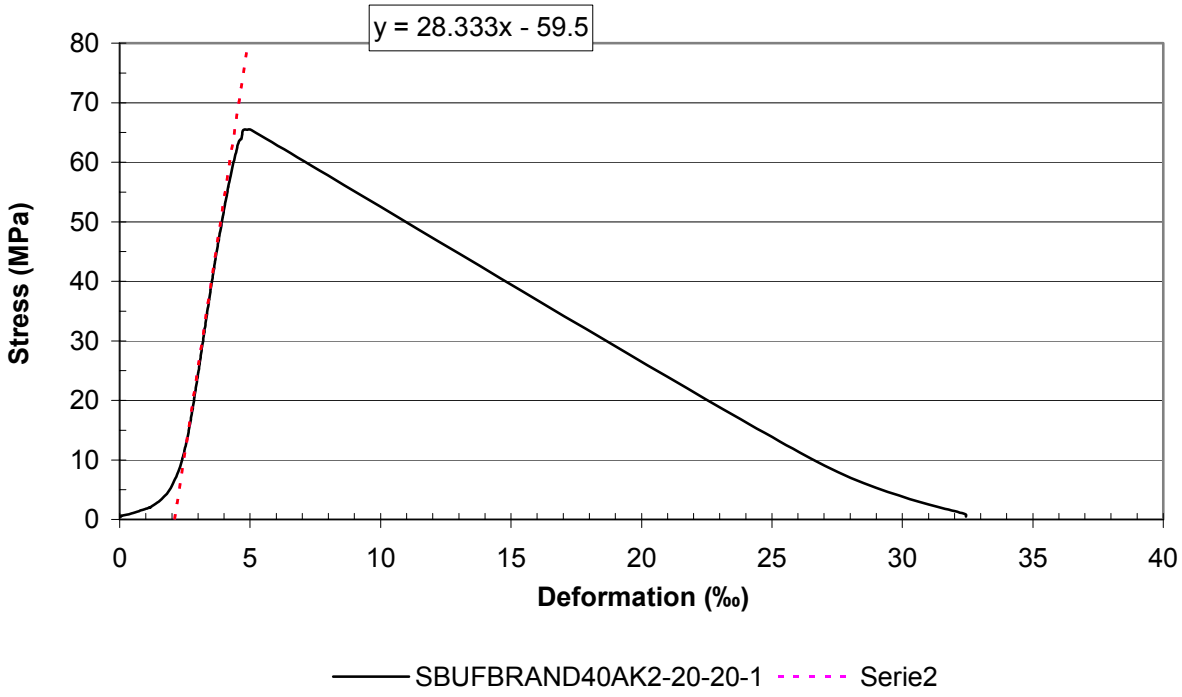

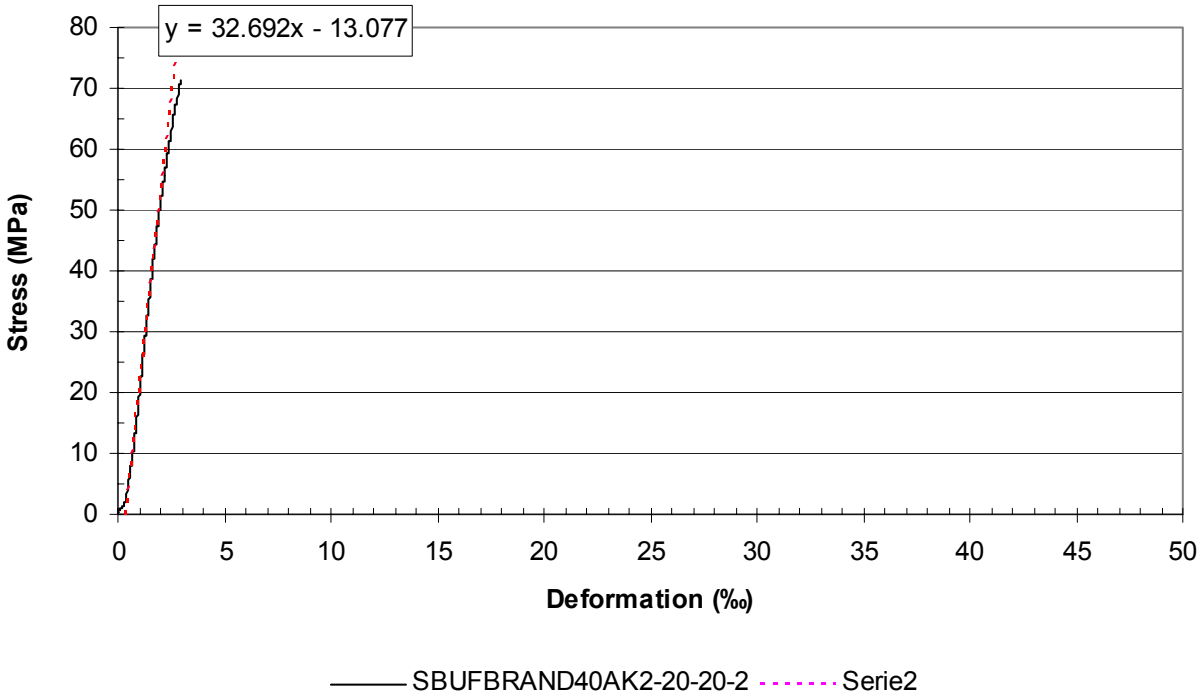

Appendix 4.23 – Stress/strain results of concrete 40AK2 at 200 °C – 20 °C.

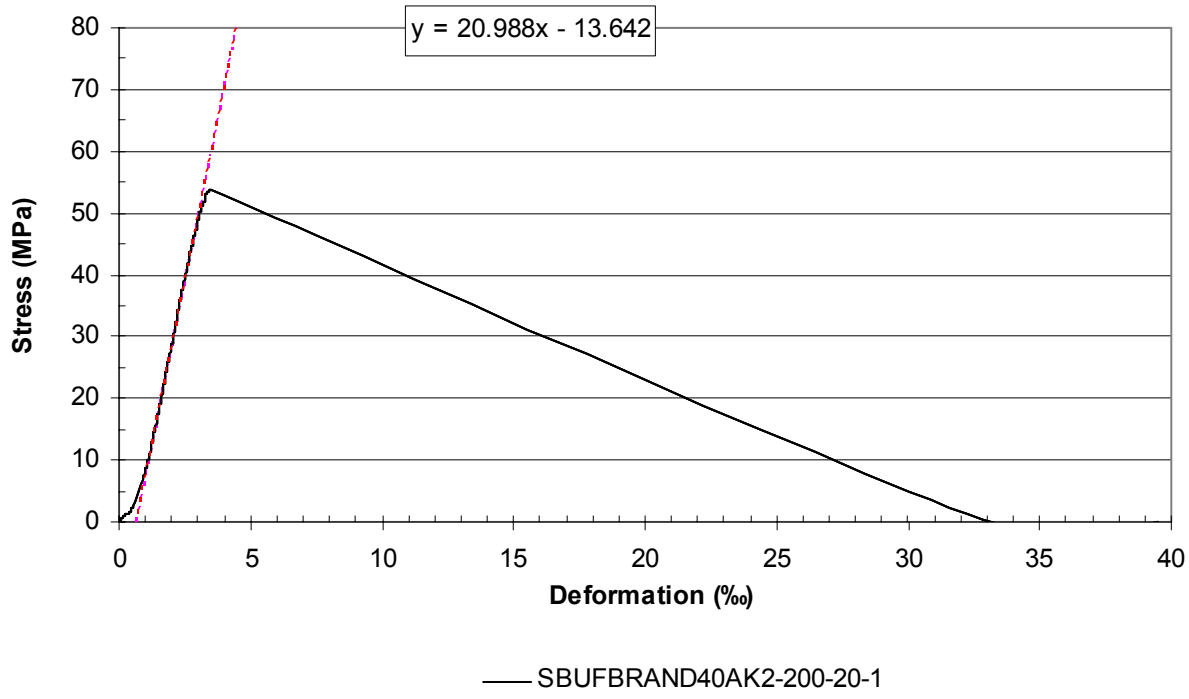

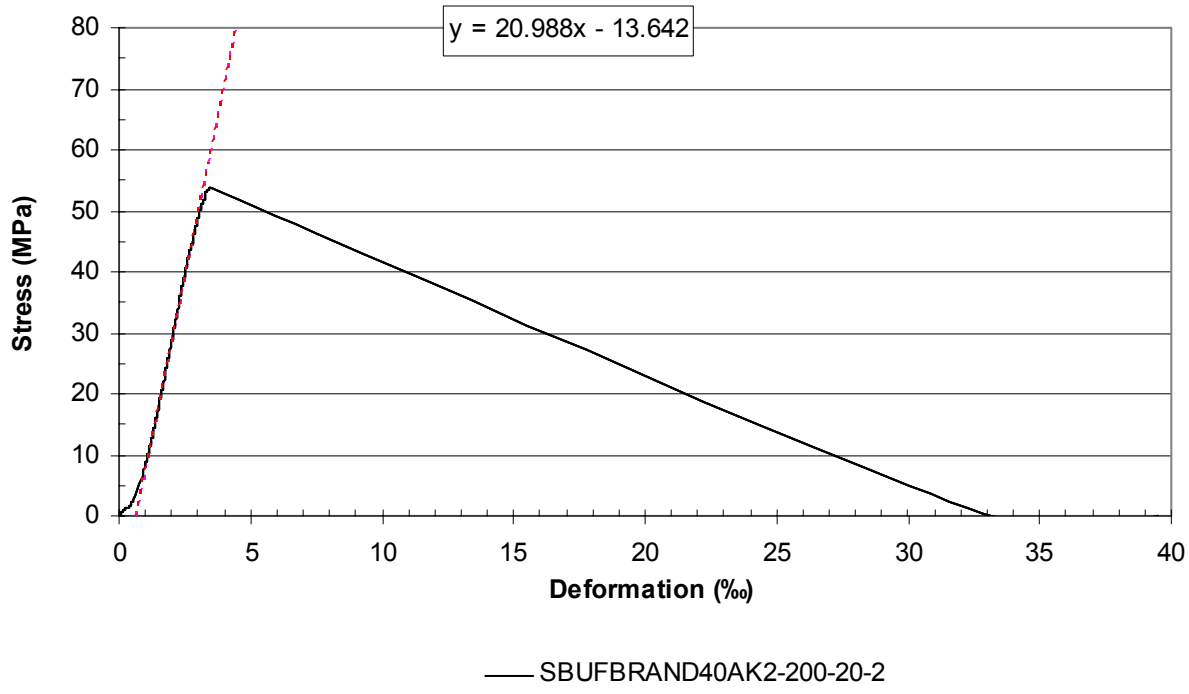

Appendix 4.24 – Stress/strain results of concrete 40AK2 at 200 °C – 200 °C.

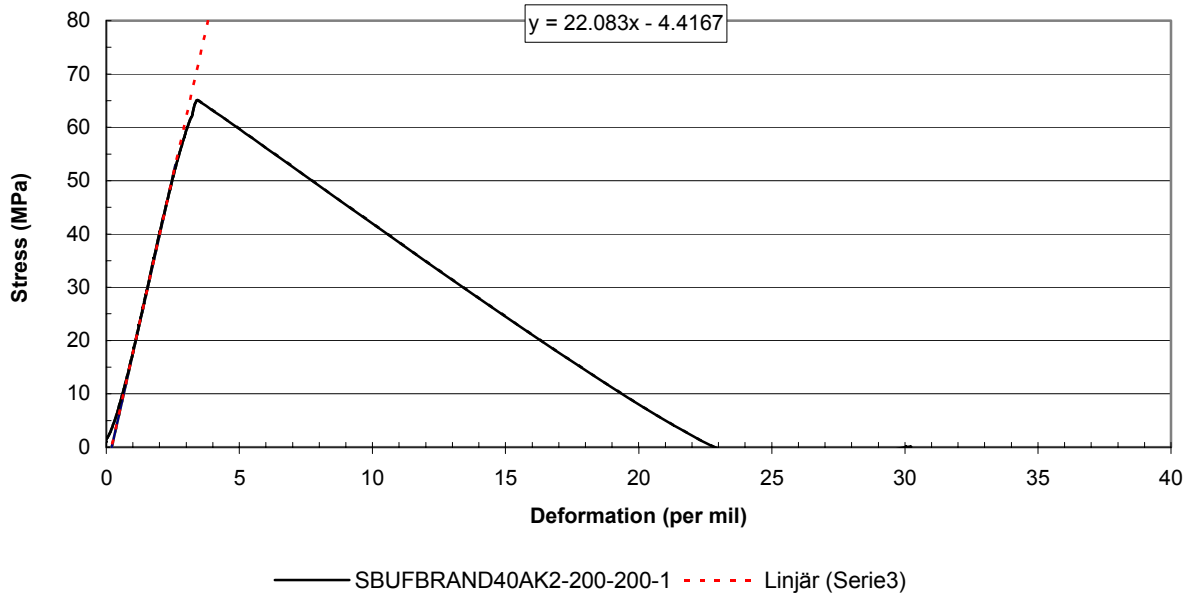

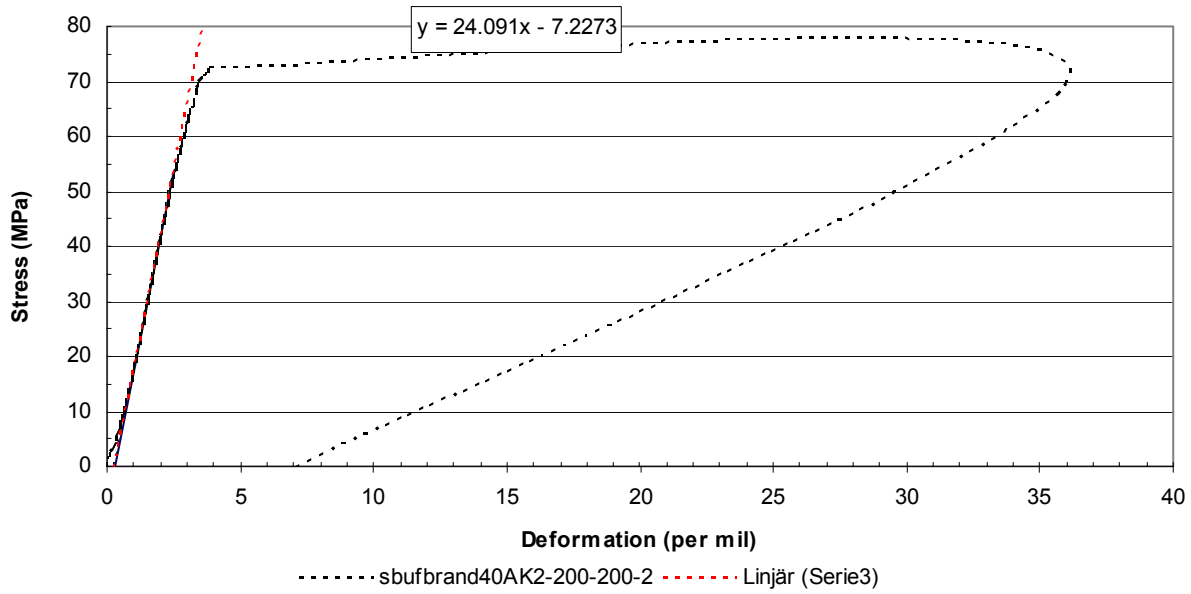

Appendix 4.25 – Stress/strain results of concrete 40AK2 at 400 °C – 20 °C.

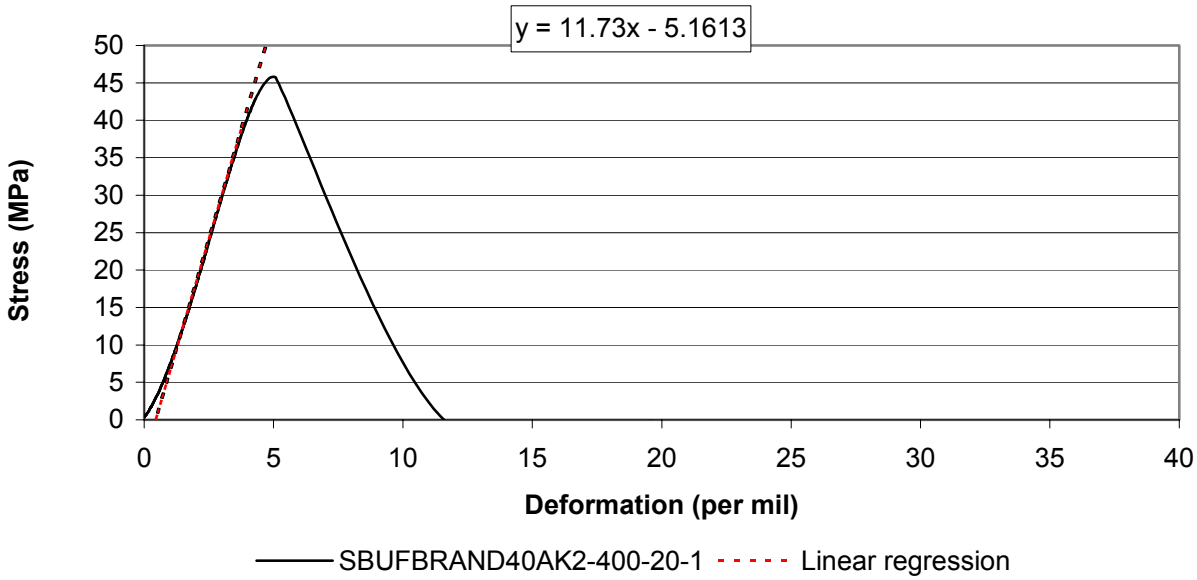

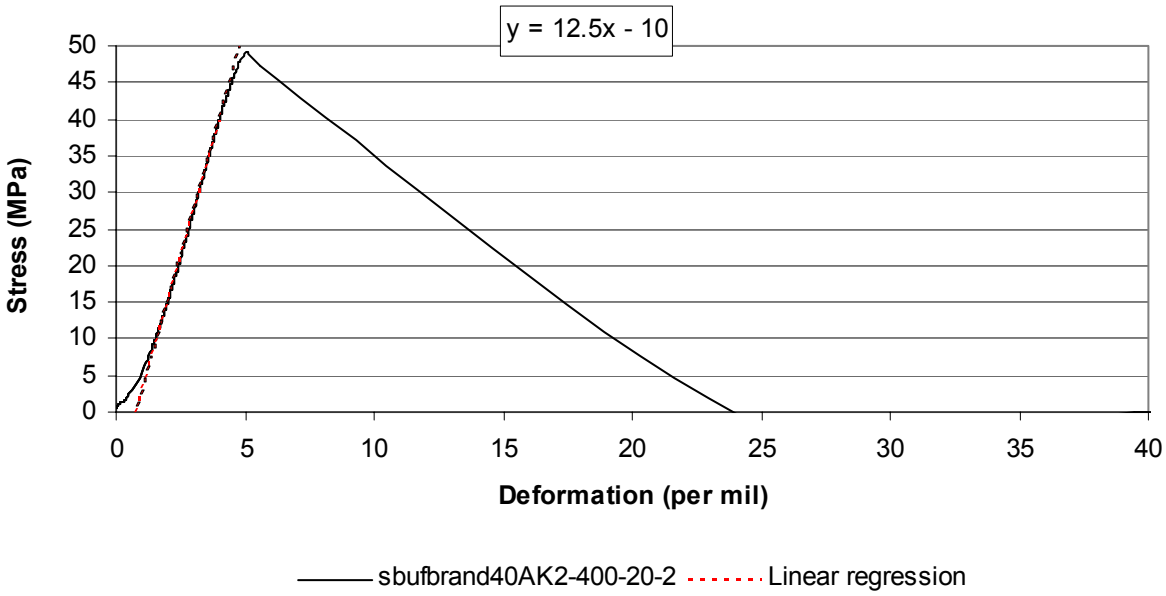

Appendix 4.26 – Stress/strain results of concrete 40AK2 at 400 °C – 400 °C.

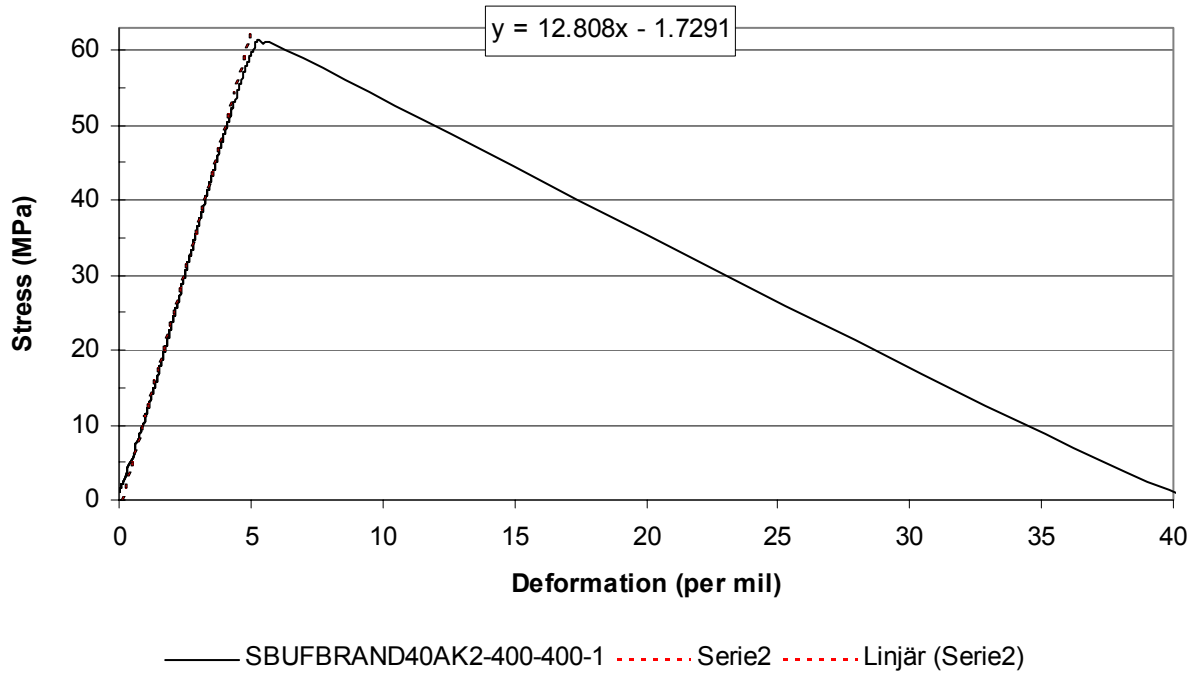

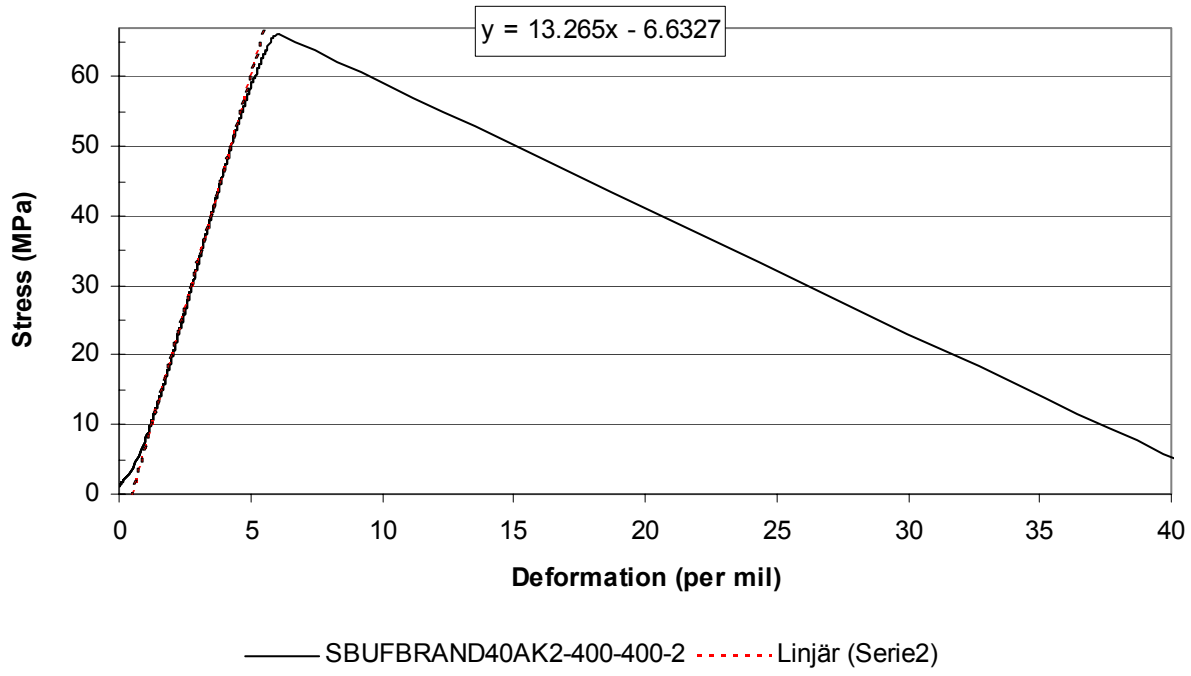

Appendix 4.27 – Stress/strain results of concrete 40AK2 at 800 °C – 800 °C.

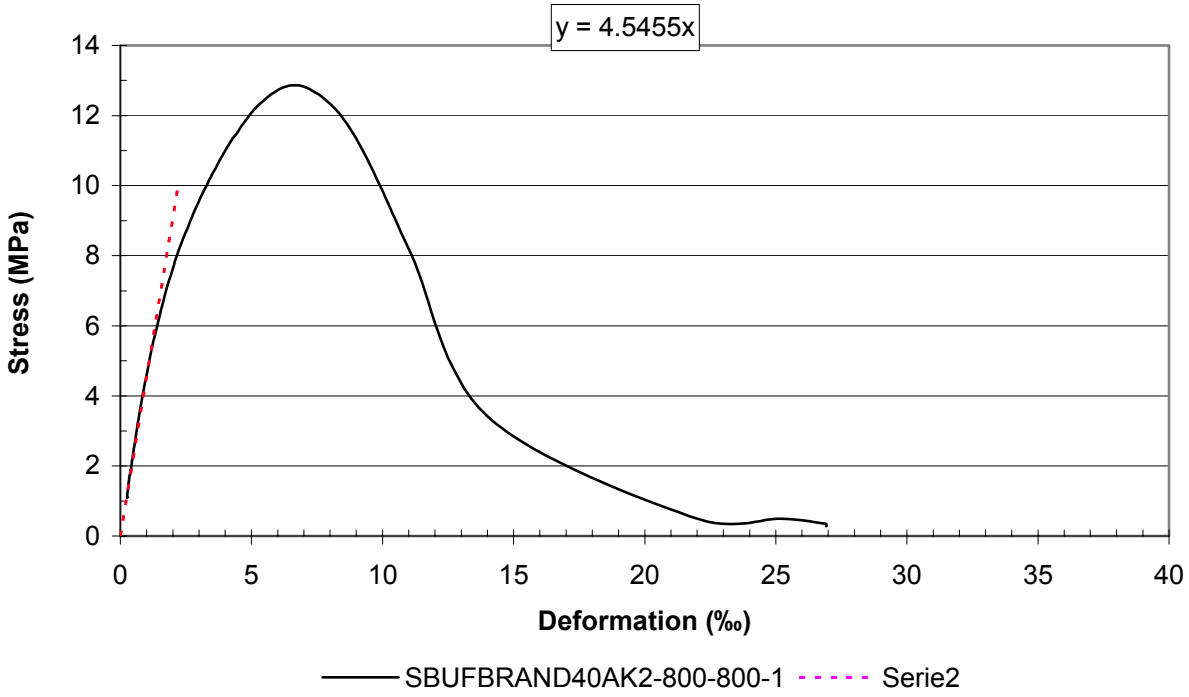

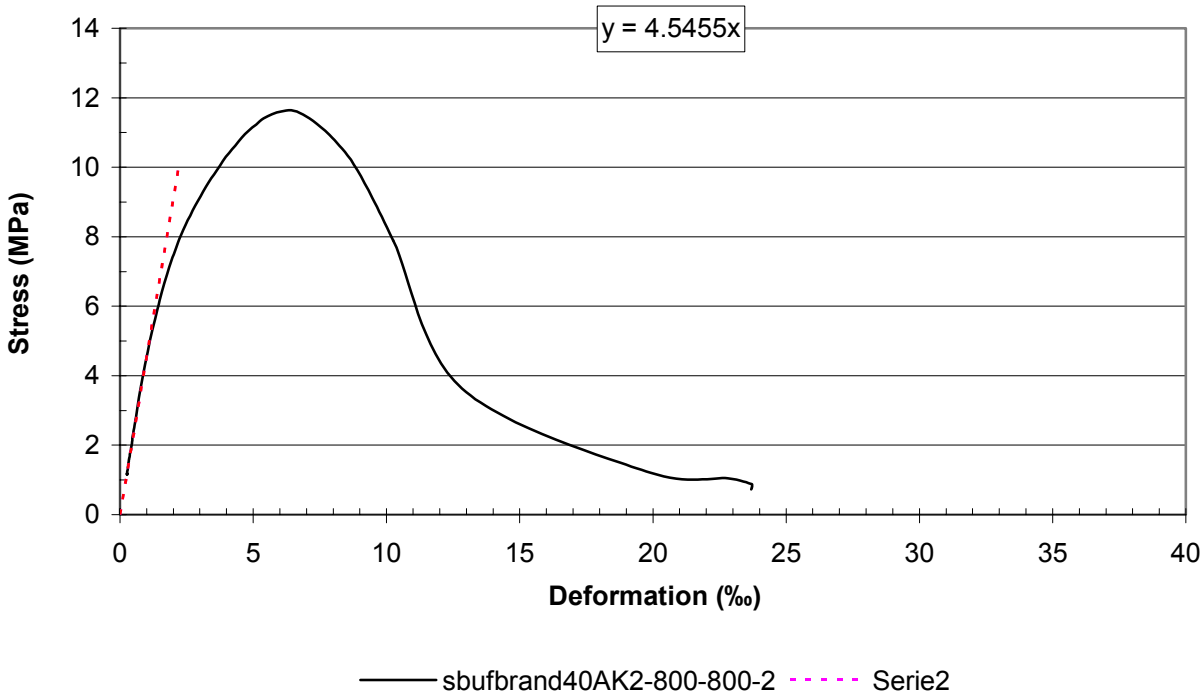

Appendix 4.28 – Stress/strain results of concrete 40AK4 at 20 °C.

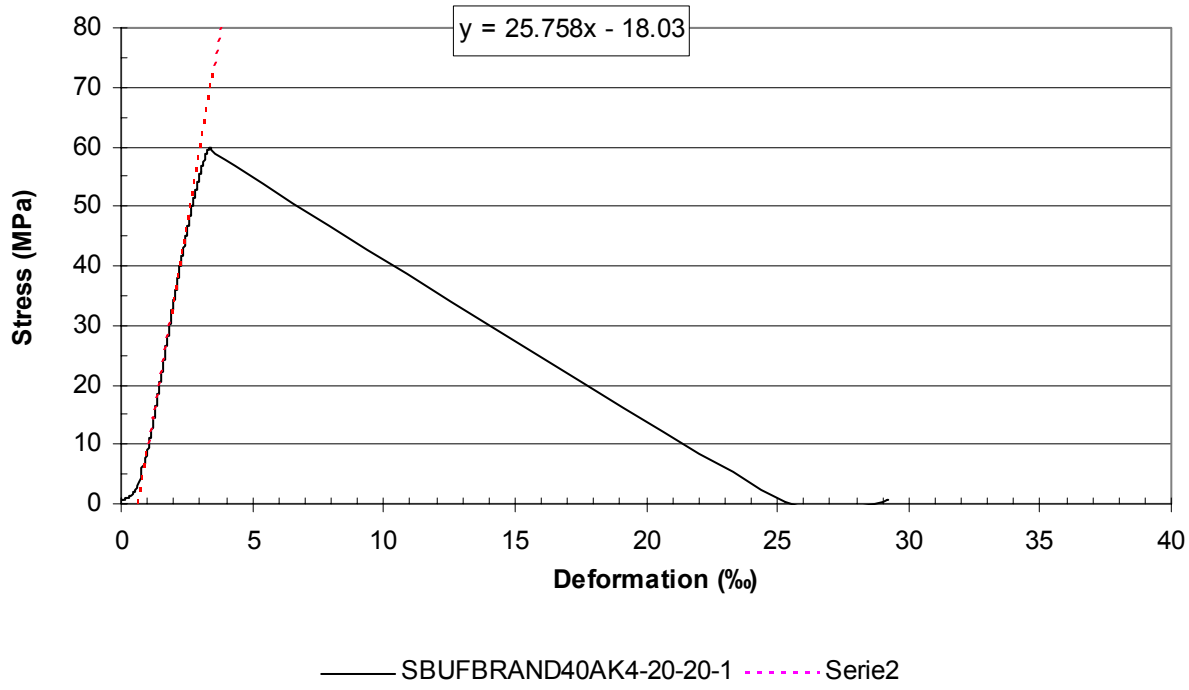

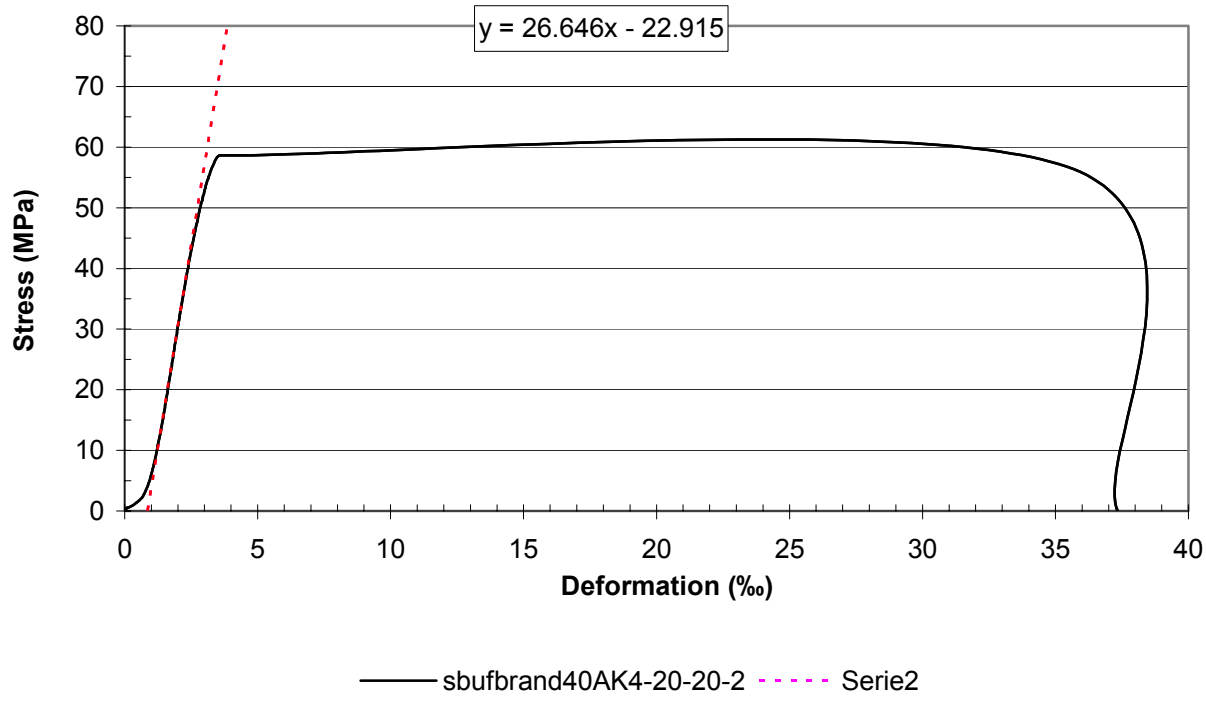

Appendix 4.29 – Stress/strain results of concrete 40AK4 at 200 °C – 20 °C.

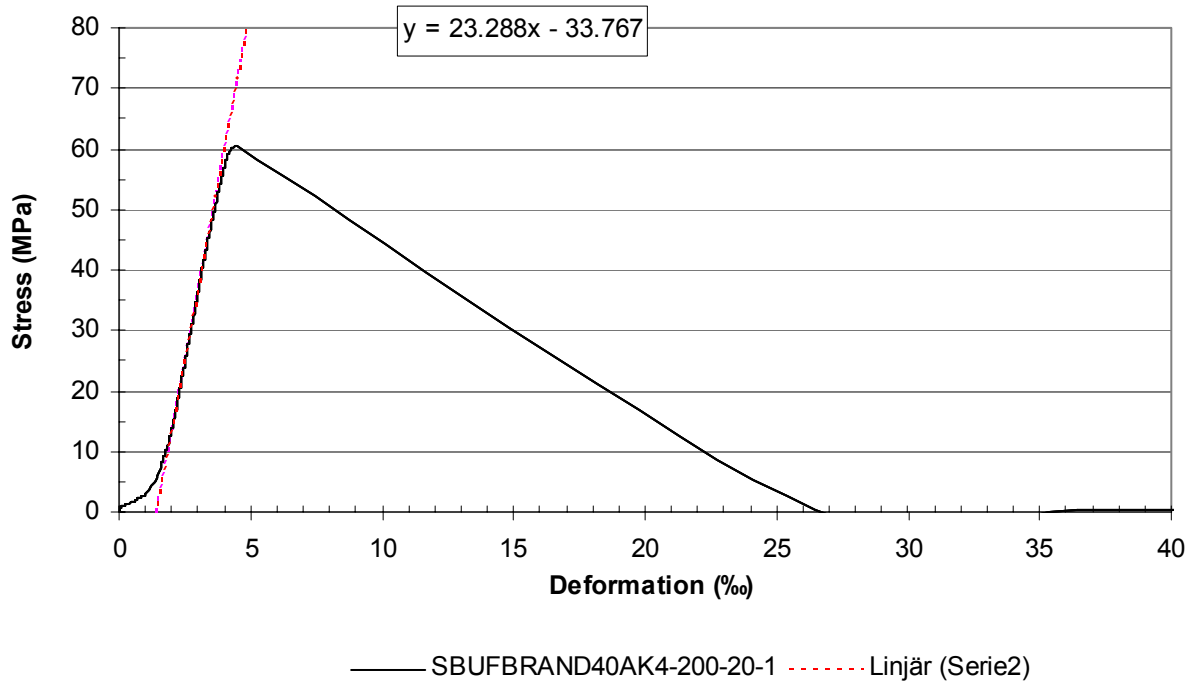

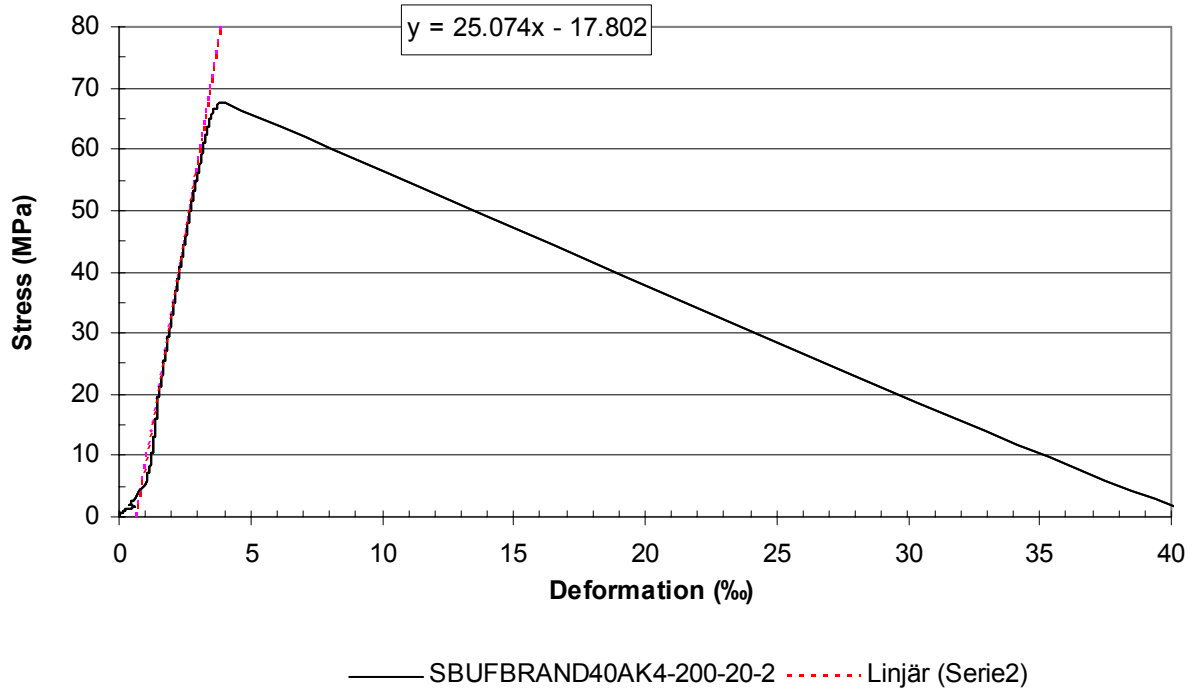

Appendix 4.30 – Stress/strain results of concrete 40AK4 at 200 °C – 200 °C.

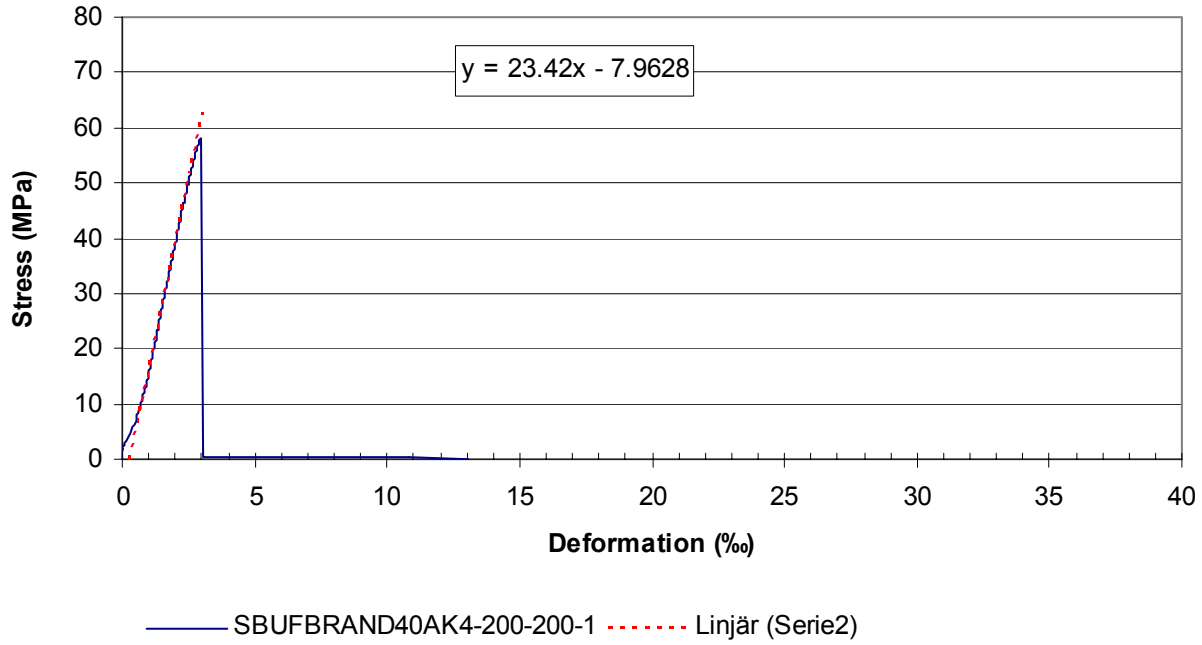

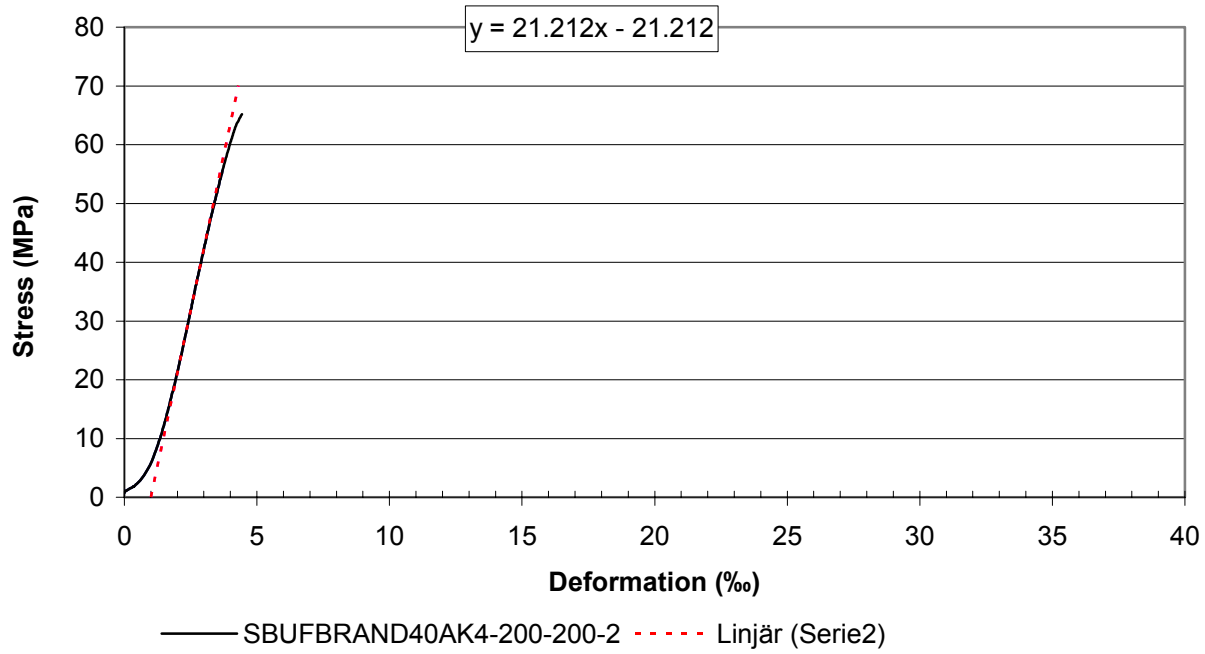

Appendix 4.31 – Stress/strain results of concrete 40AK4 at 400 °C – 20 °C.

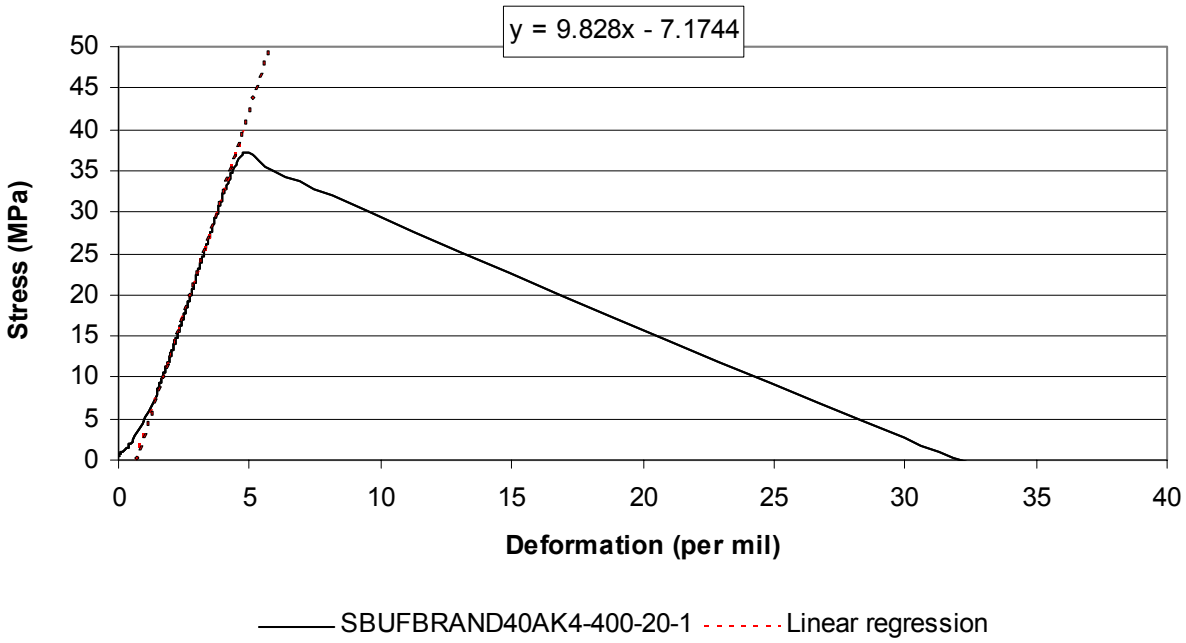

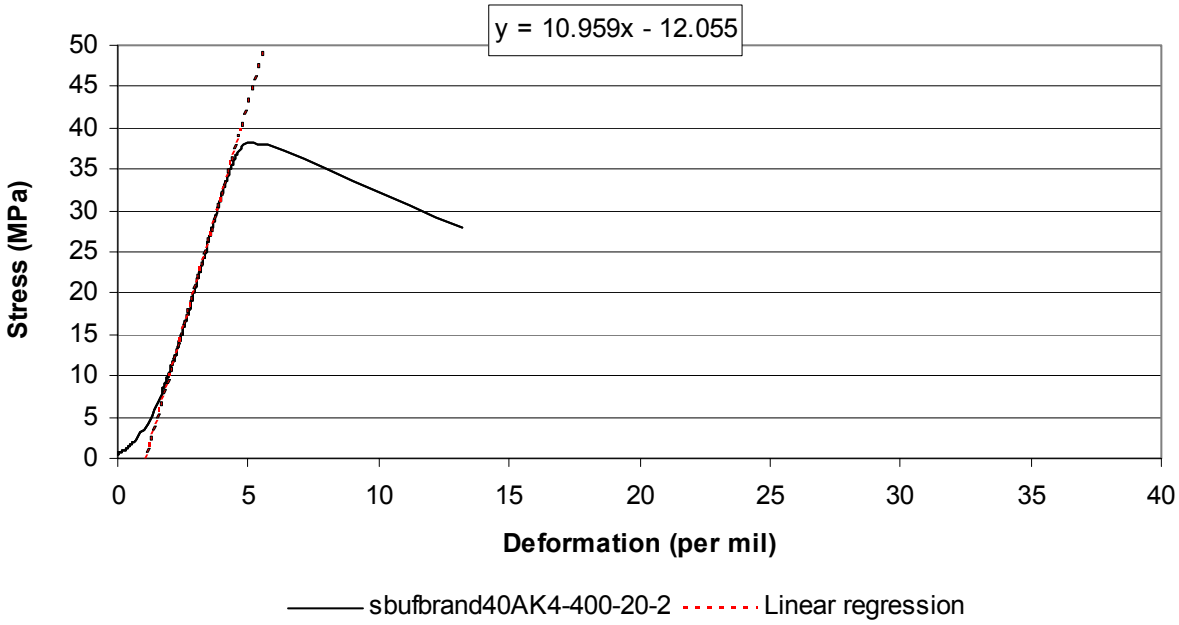

Appendix 4.32 – Stress/strain results of concrete 40AK4 at 400 °C – 400 °C.

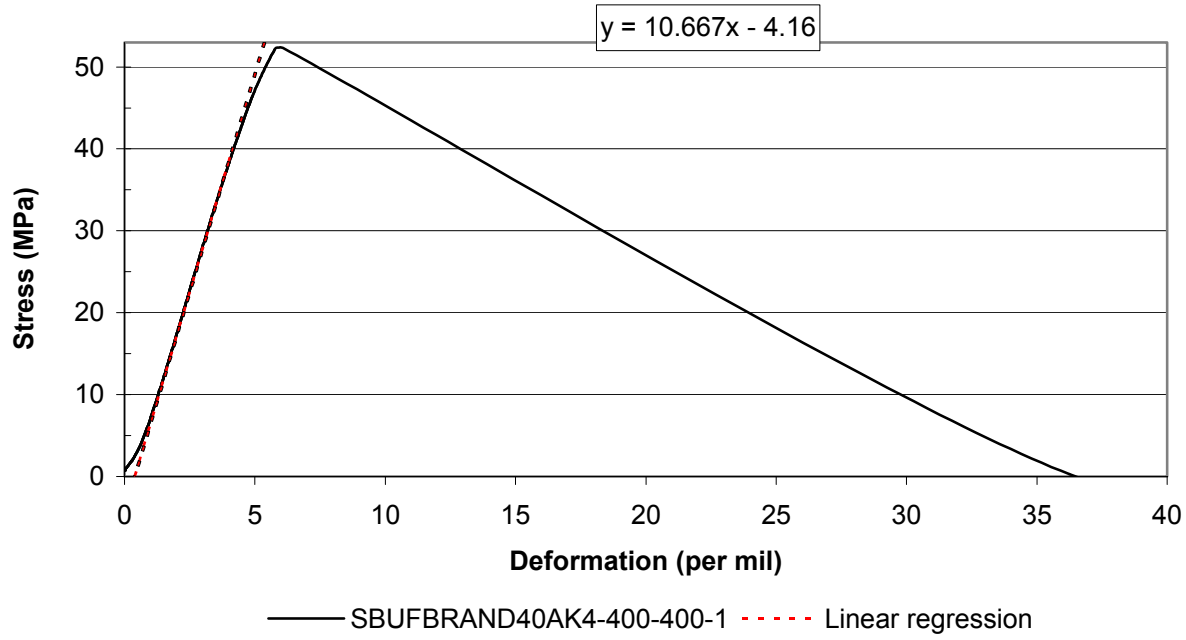

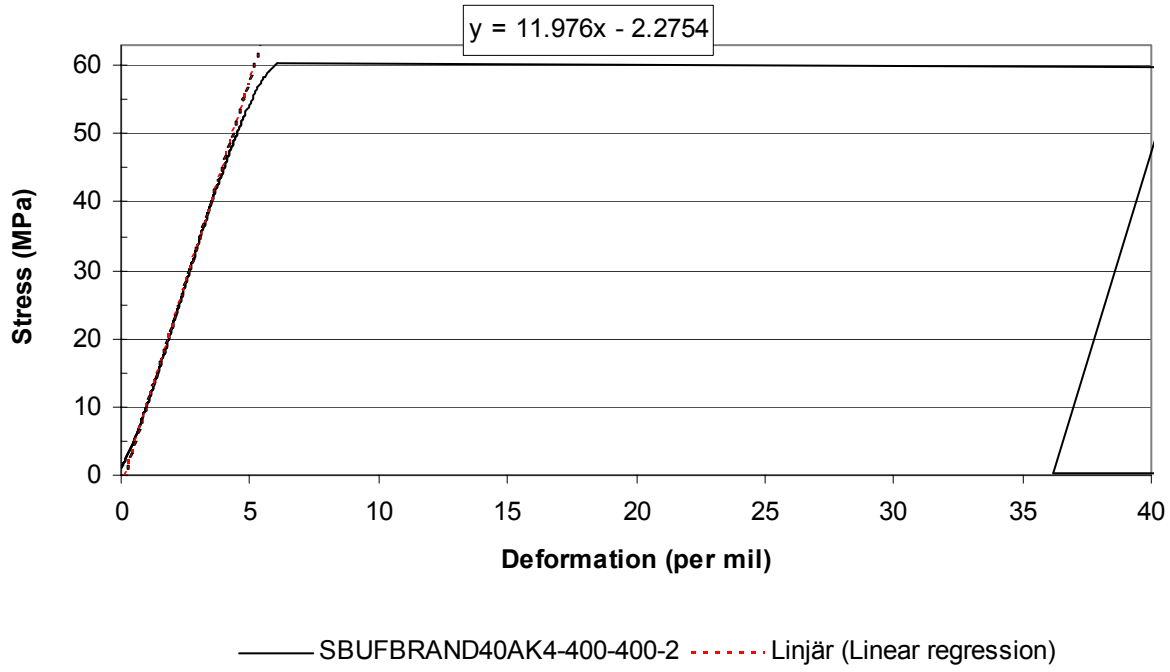

Appendix 4.33 – Stress/strain results of concrete 40AK4 at 800 °C – 800 °C.

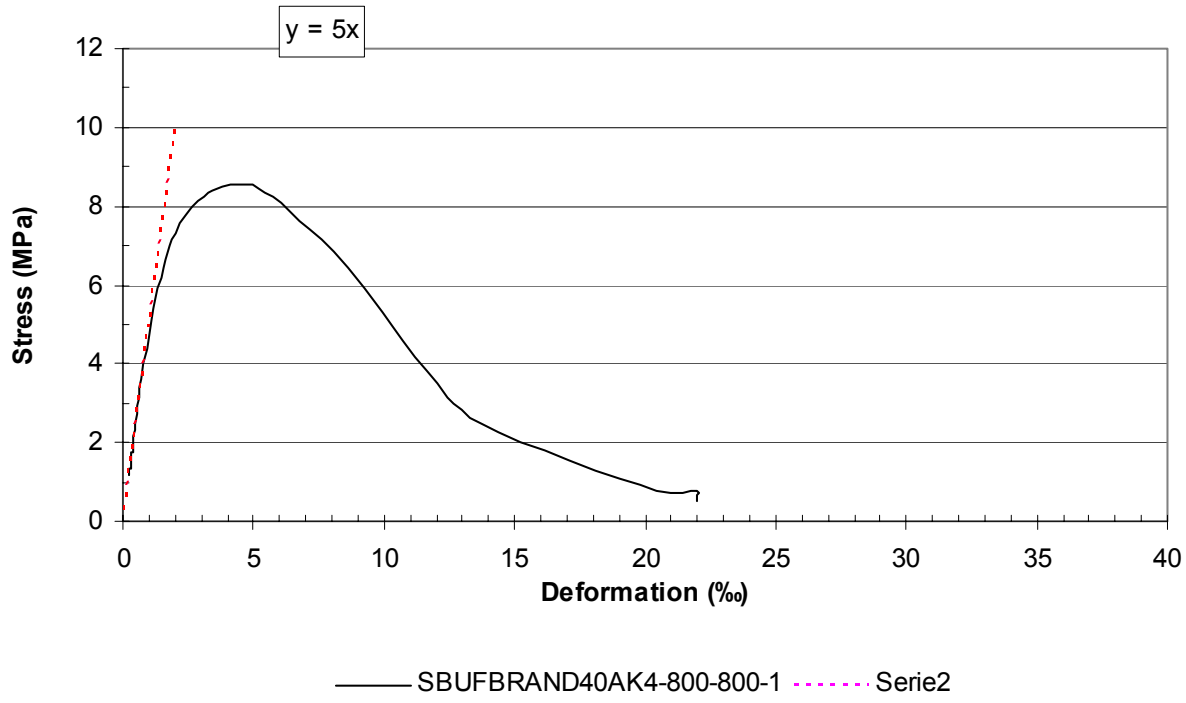

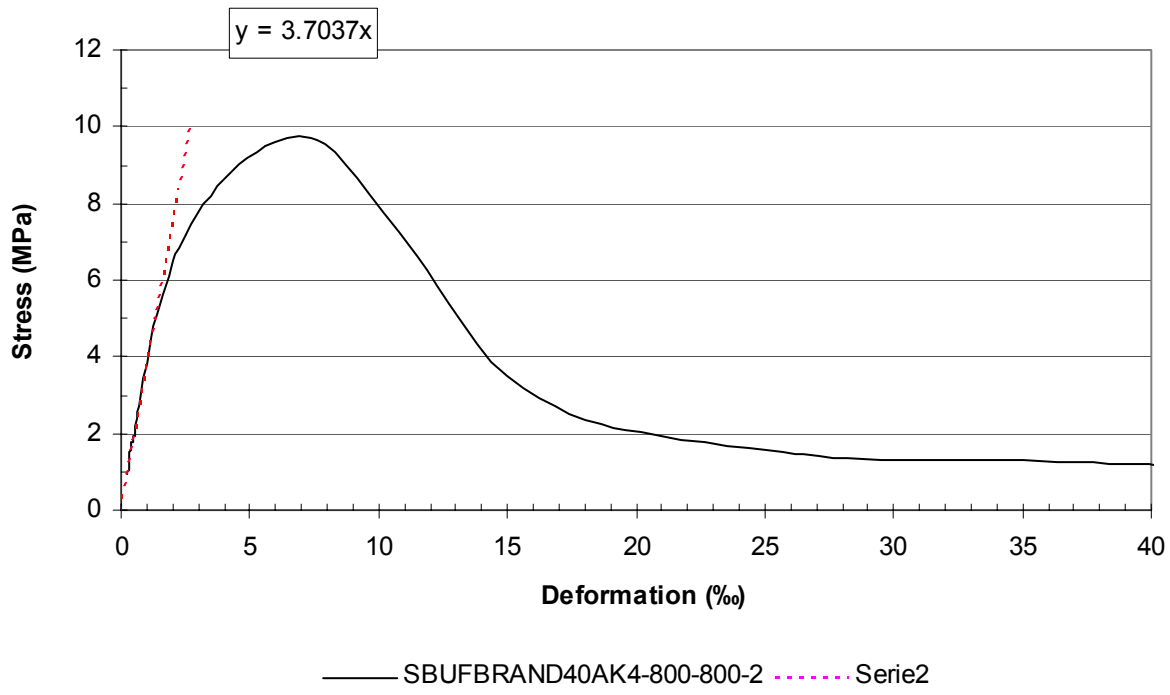

Appendix 4.34 – Stress/strain results of concrete 40BR0 at 20 °C.

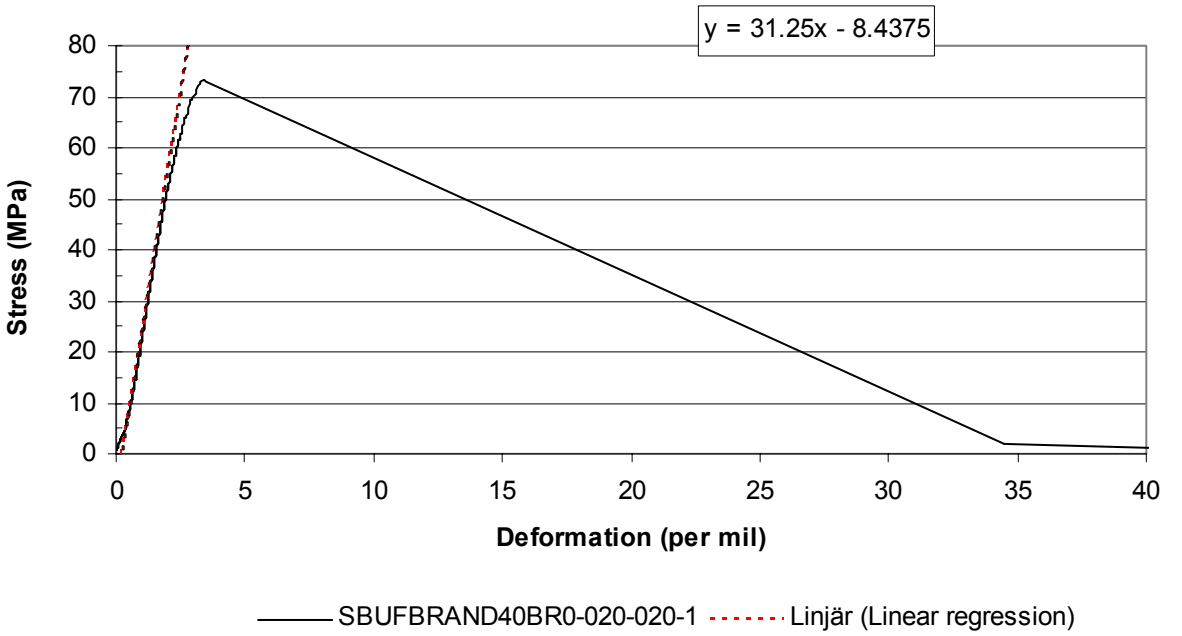

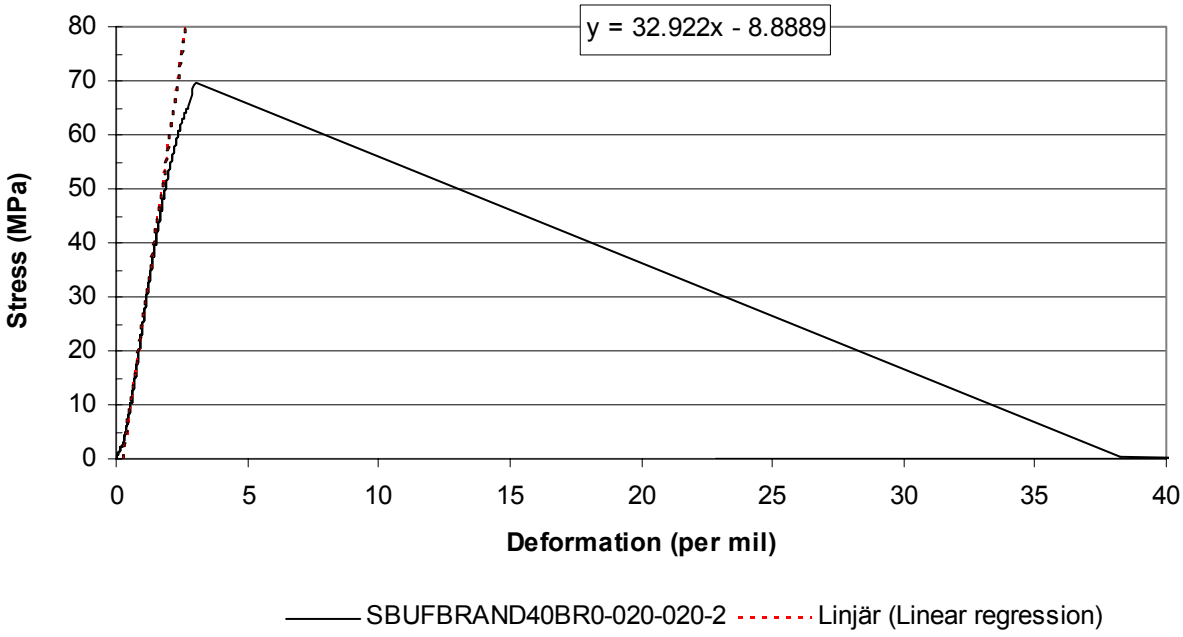

Appendix 4.35 – Stress/strain results of concrete 40BR0 at 200 °C – 20 °C.

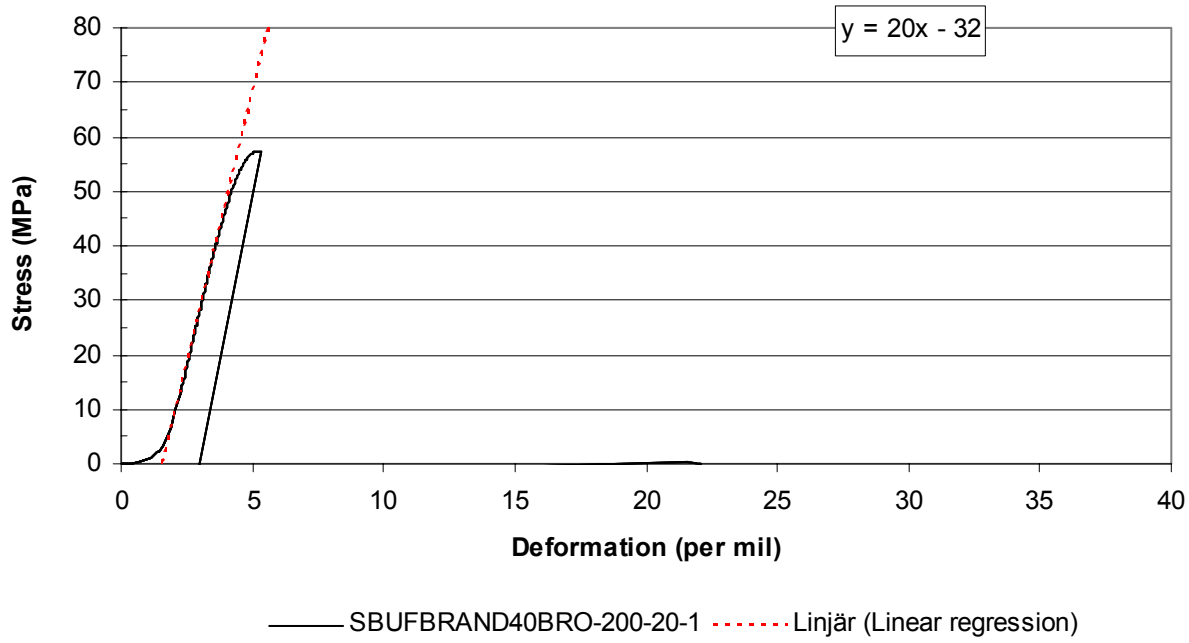

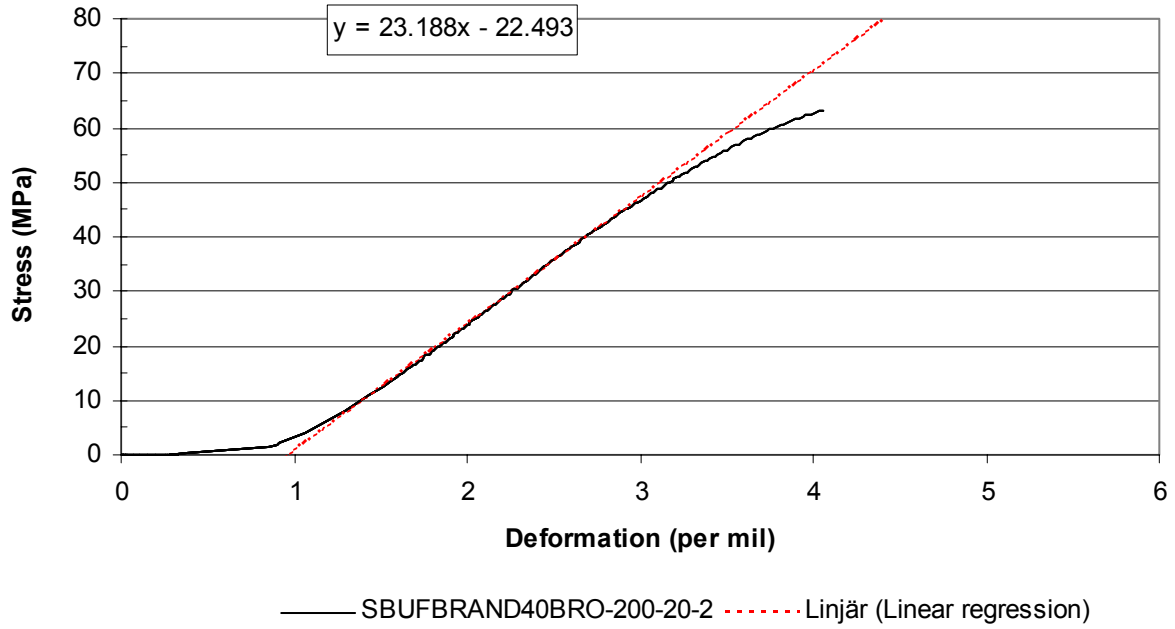

Appendix 4.36 – Stress/strain results of concrete 40BR0 at 200 °C – 200 °C.

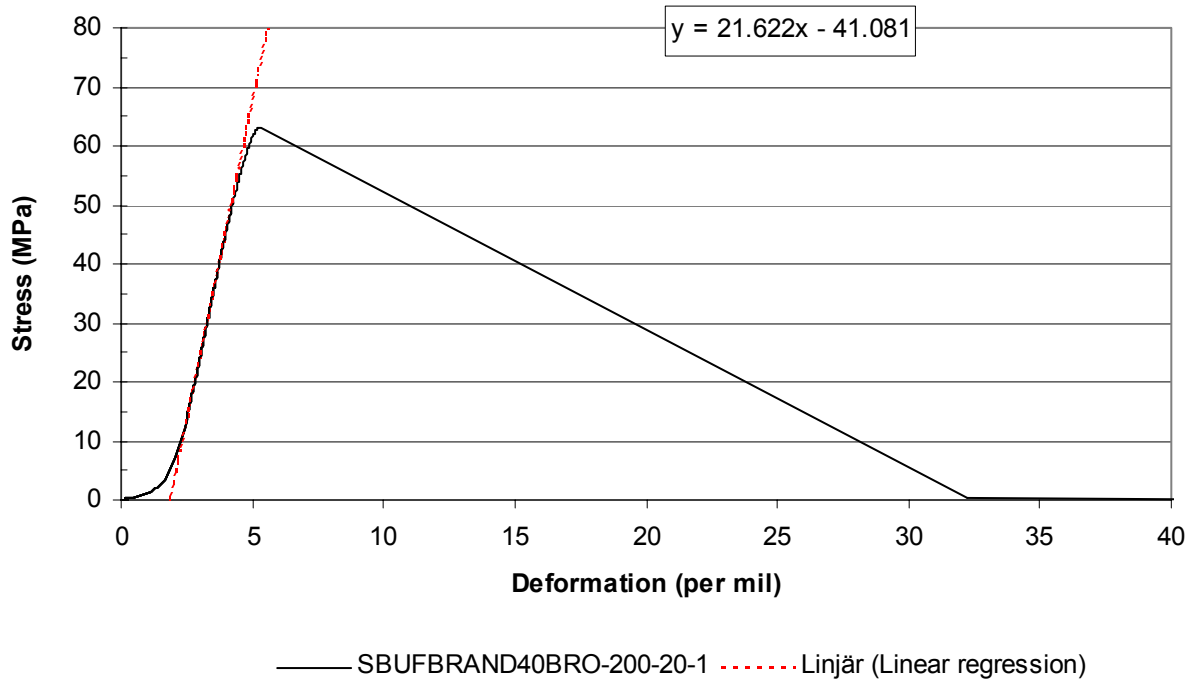

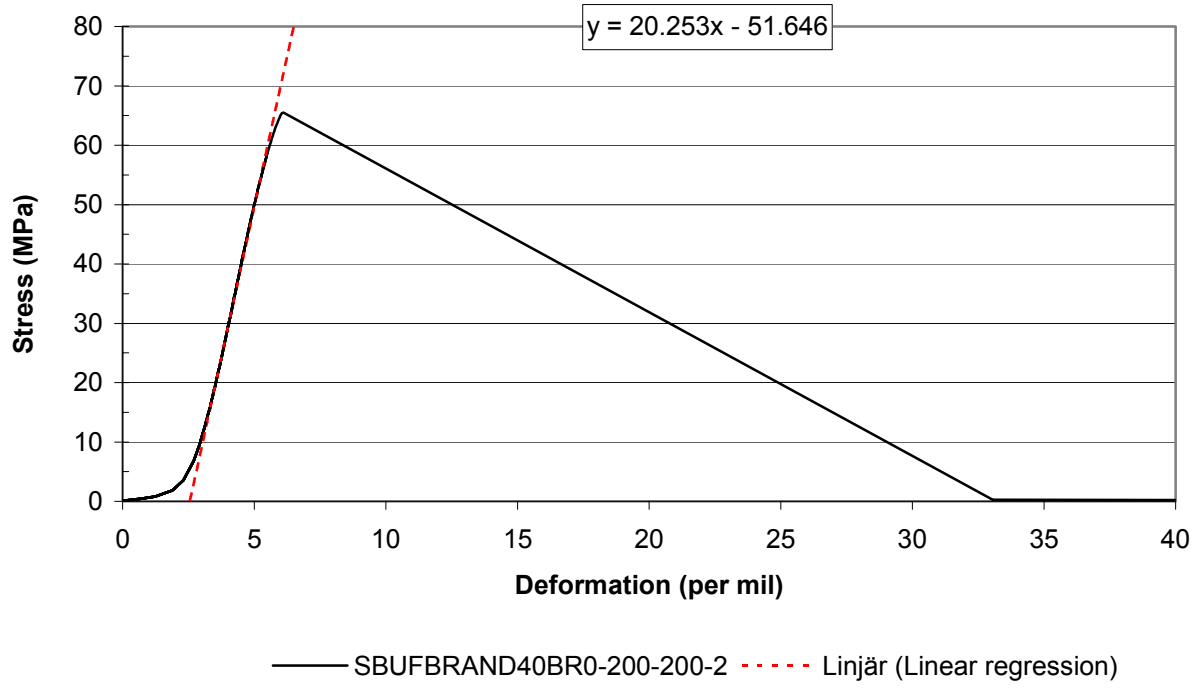

Appendix 4.37 – Stress/strain results of concrete 40BR0 at 400 °C – 20 °C.

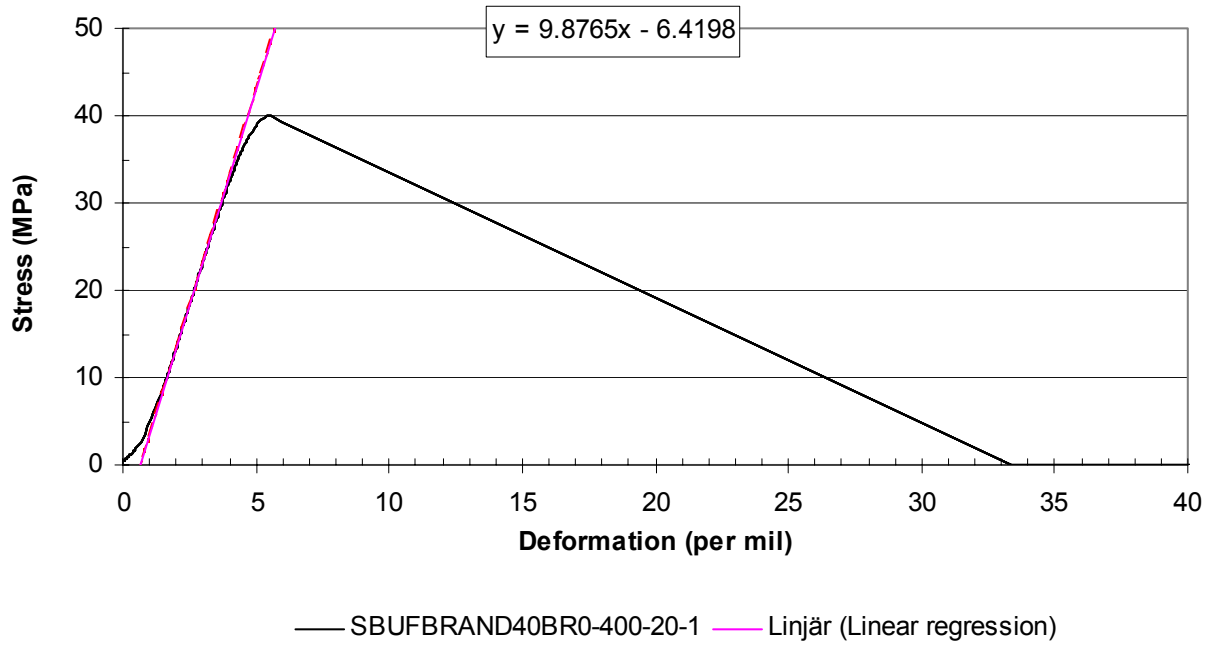

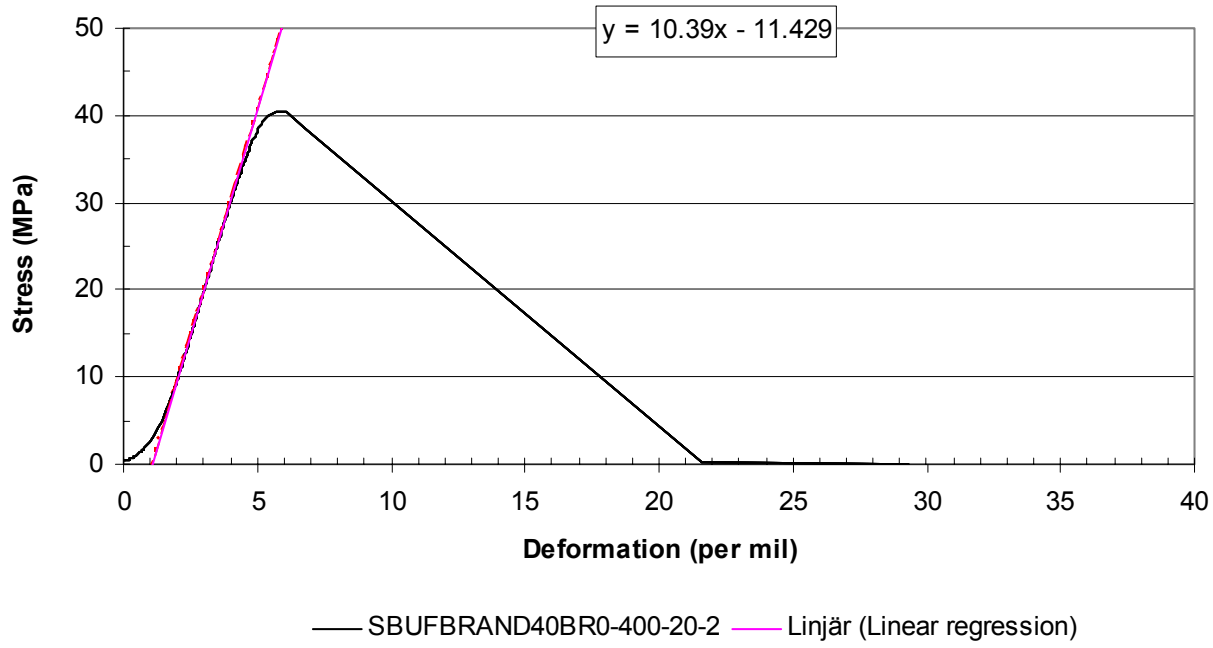

Appendix 4.38 – Stress/strain results of concrete 40BR0 at 400 °C – 400 °C.

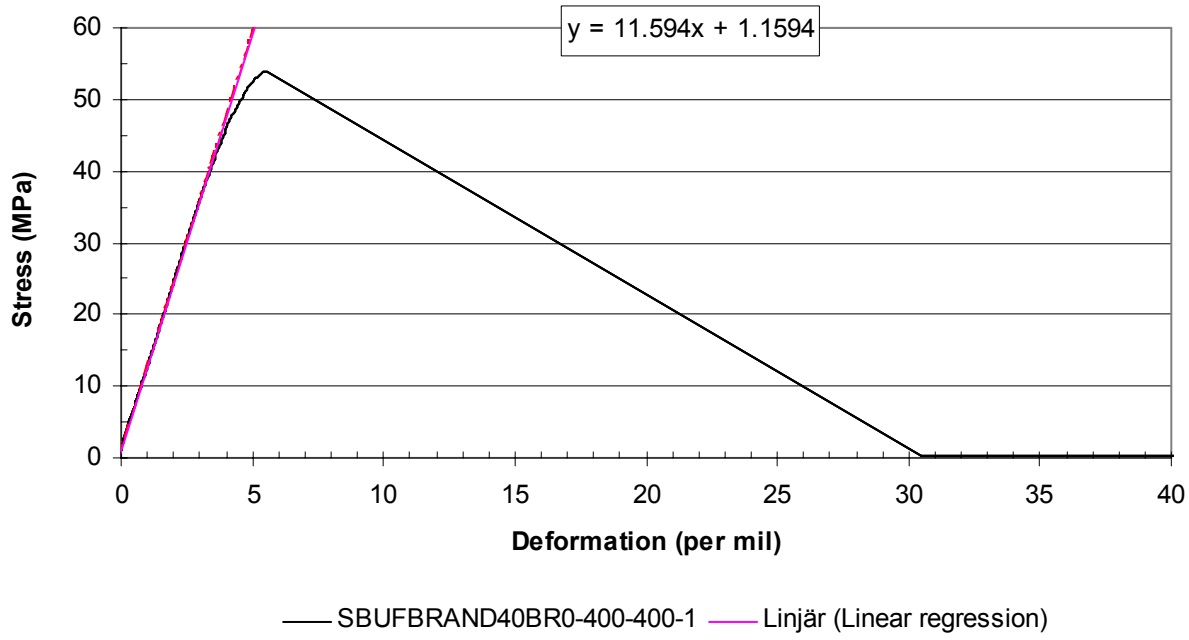

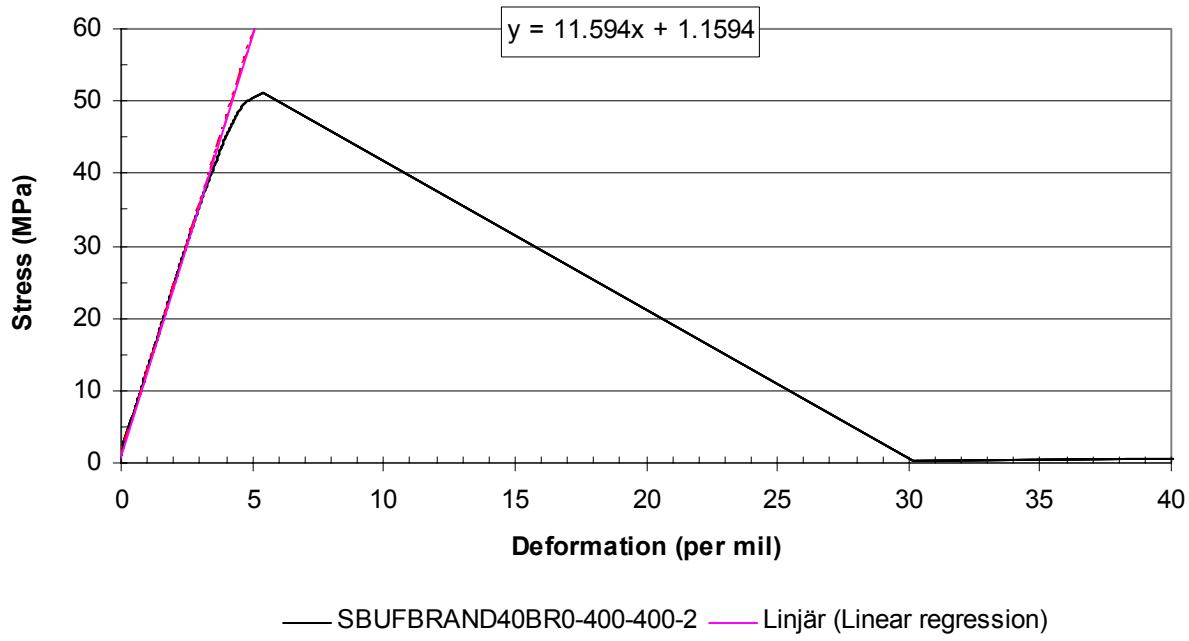

Appendix 4.39 – Stress/strain results of concrete 40BR0 at 800 °C – 20 °C.

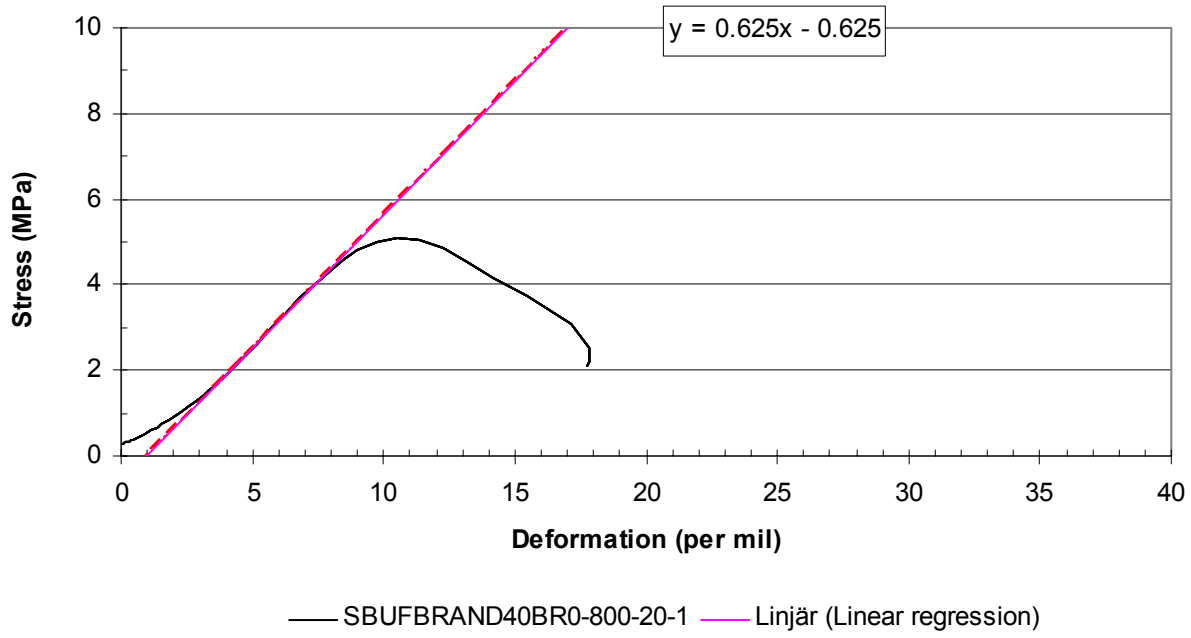

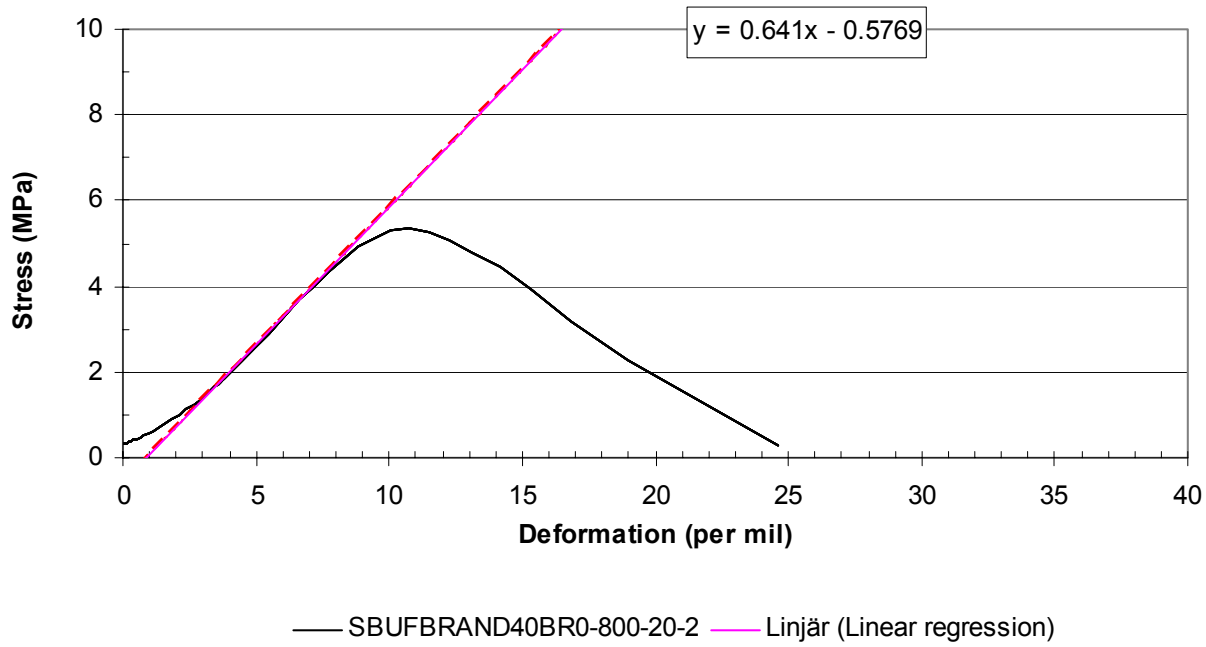

Appendix 4.40 – Stress/strain results of concrete 40BR0 at 800 °C – 800 °C.

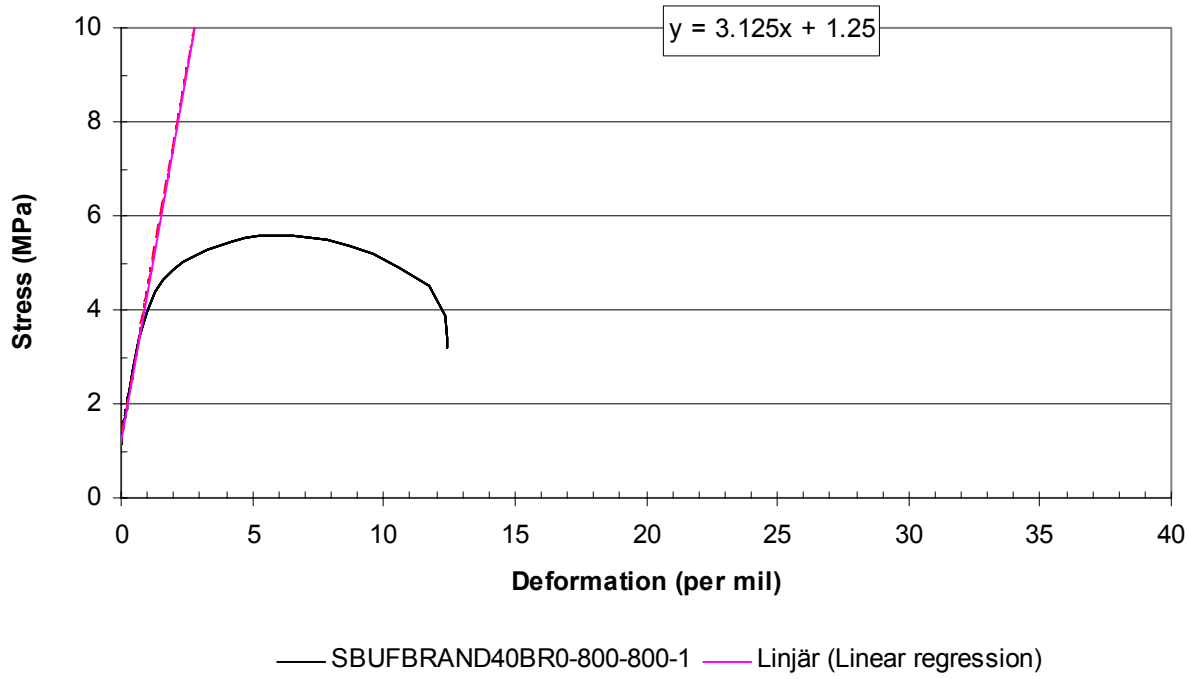

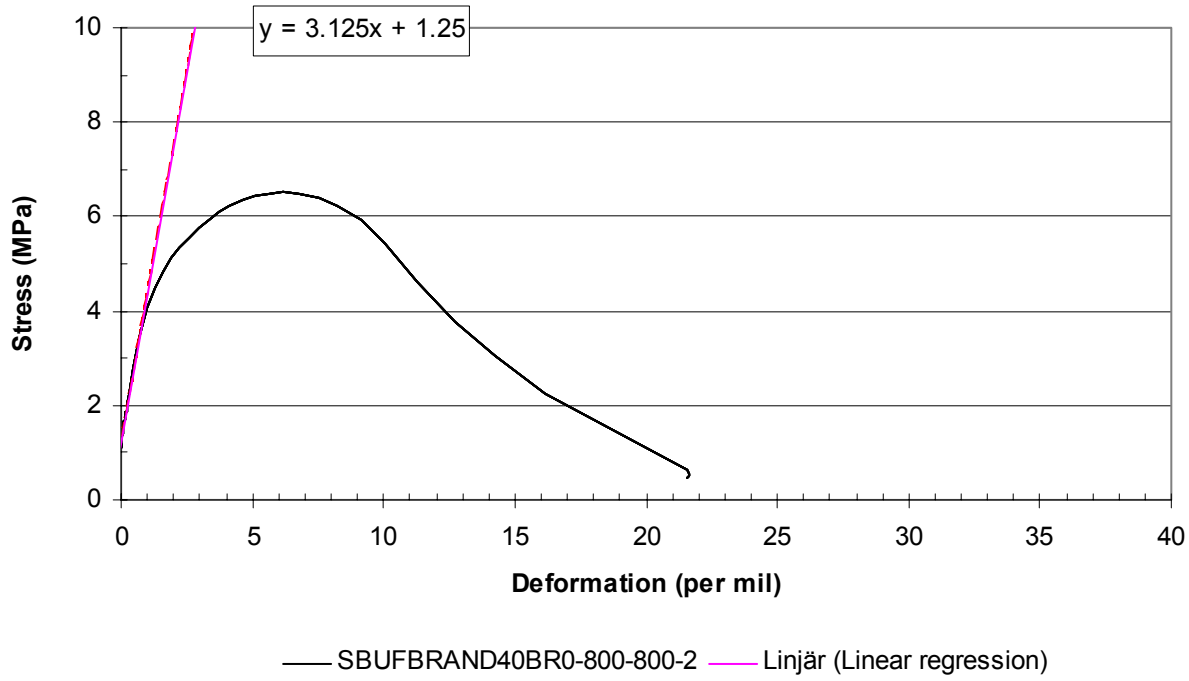

Appendix 4.41 – Stress/strain results of concrete 55BK0 at 20 °C.

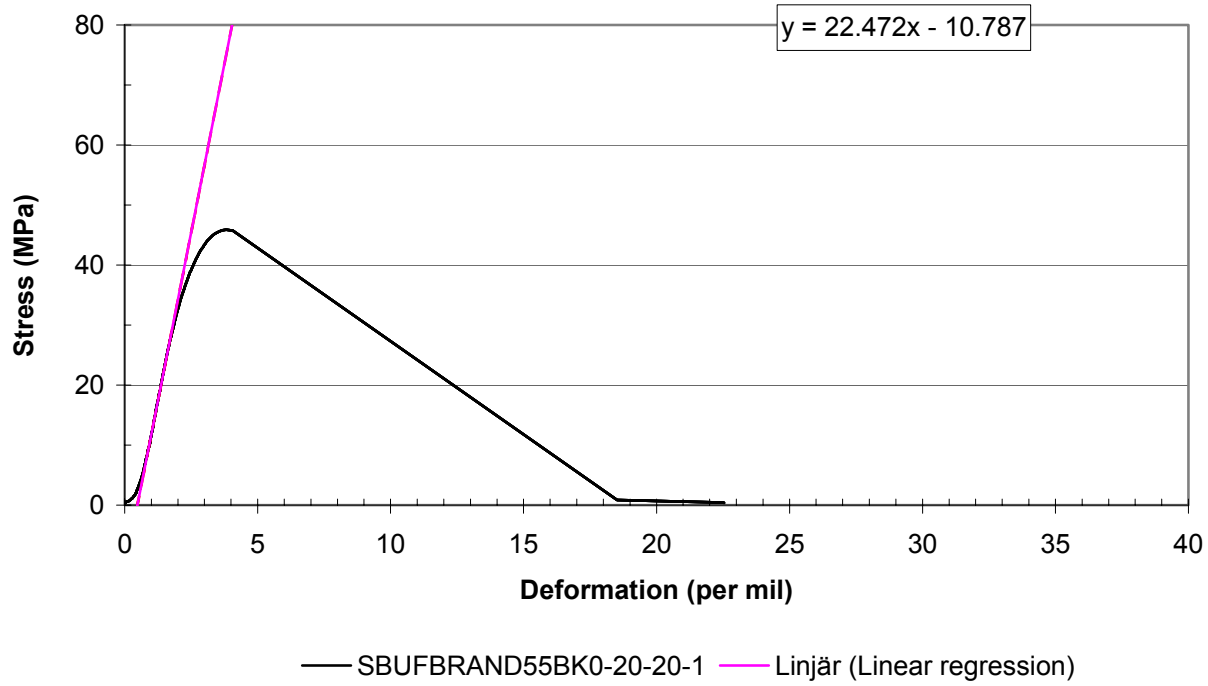

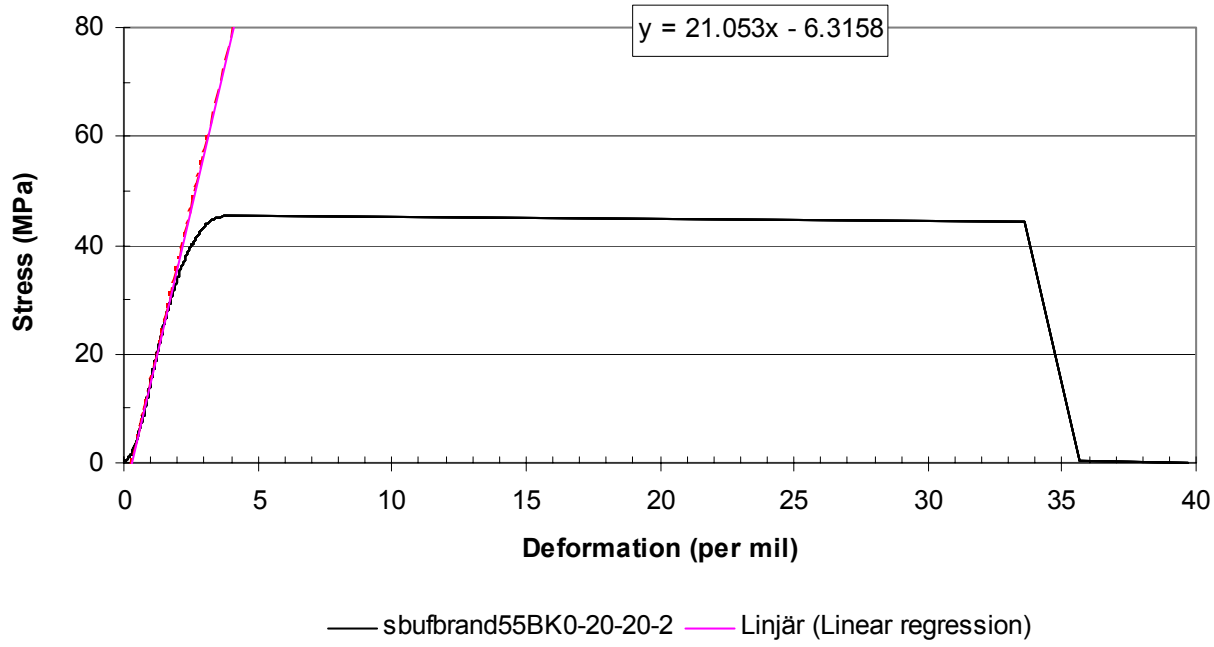

Appendix 4.42 – Stress/strain results of concrete 55BK0 at 200 °C – 20 °C.

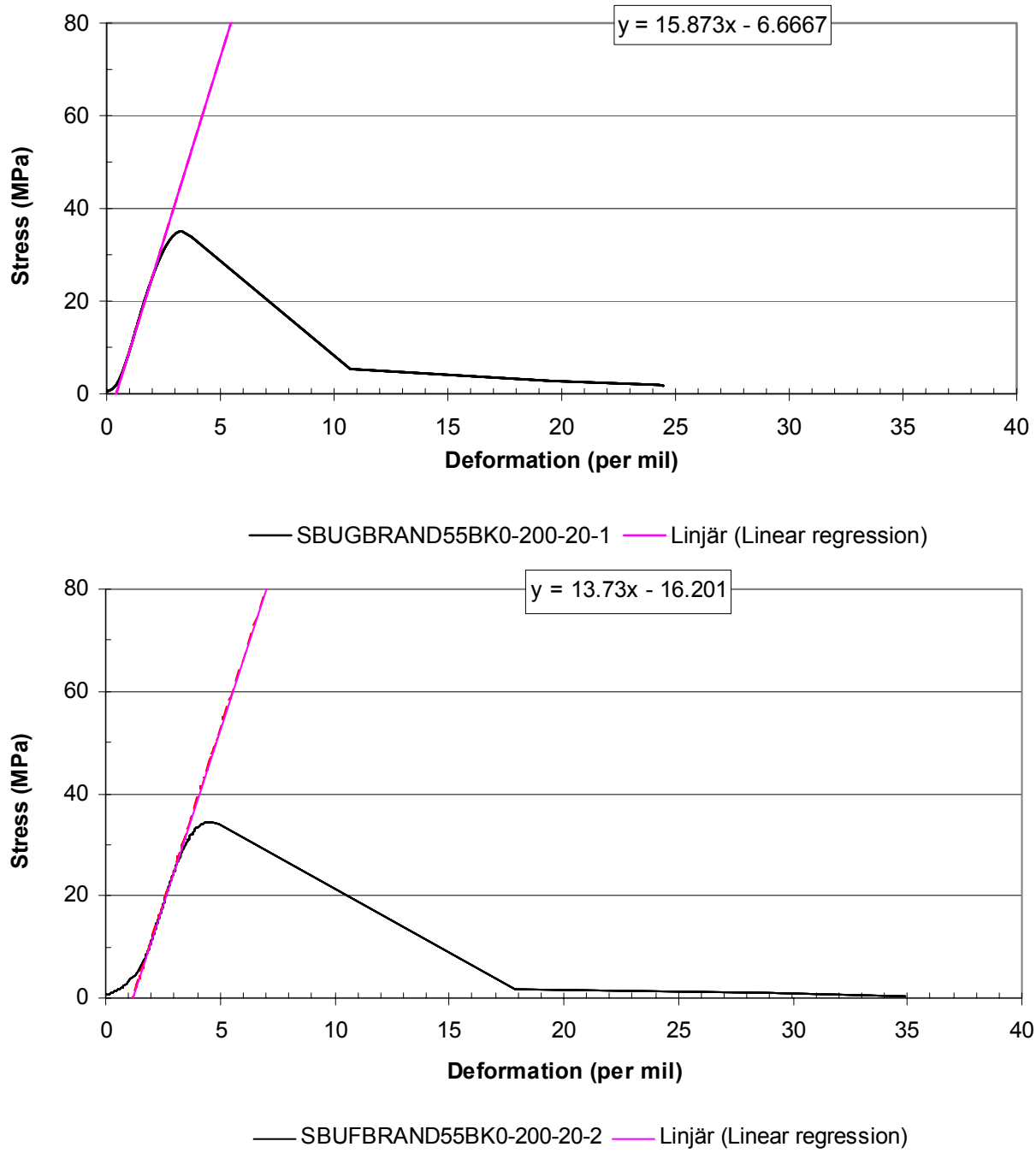

Appendix 4.43 – Stress/strain results of concrete 55BK0 at 200 °C – 200 °C.

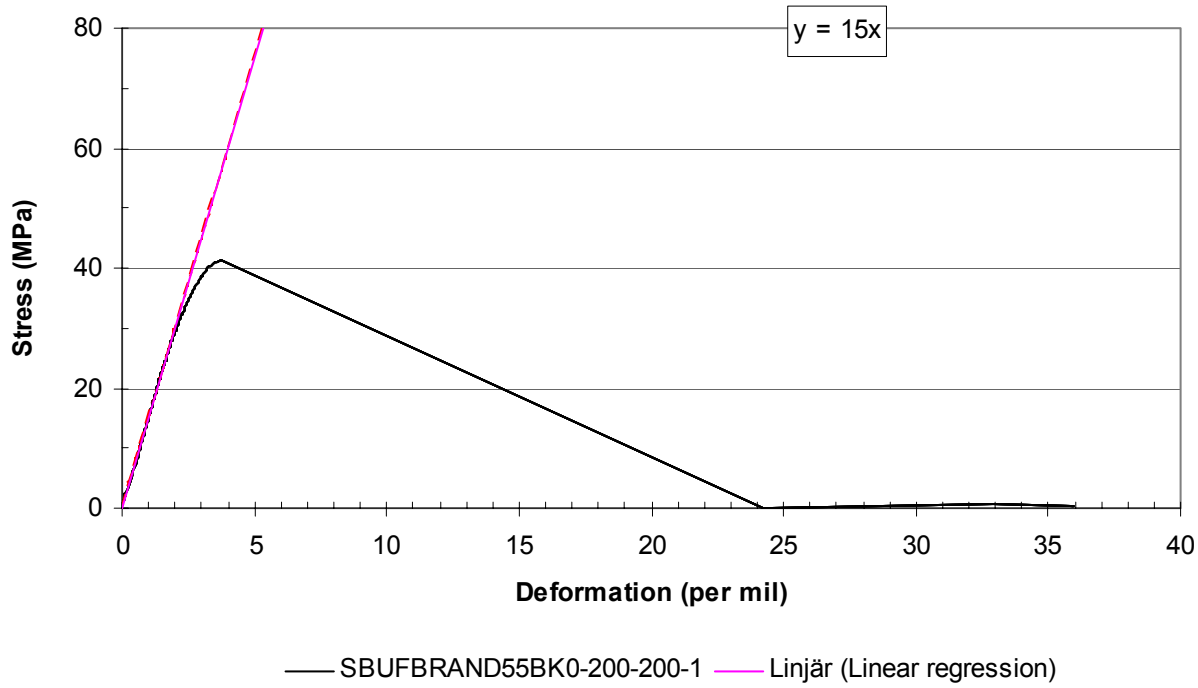

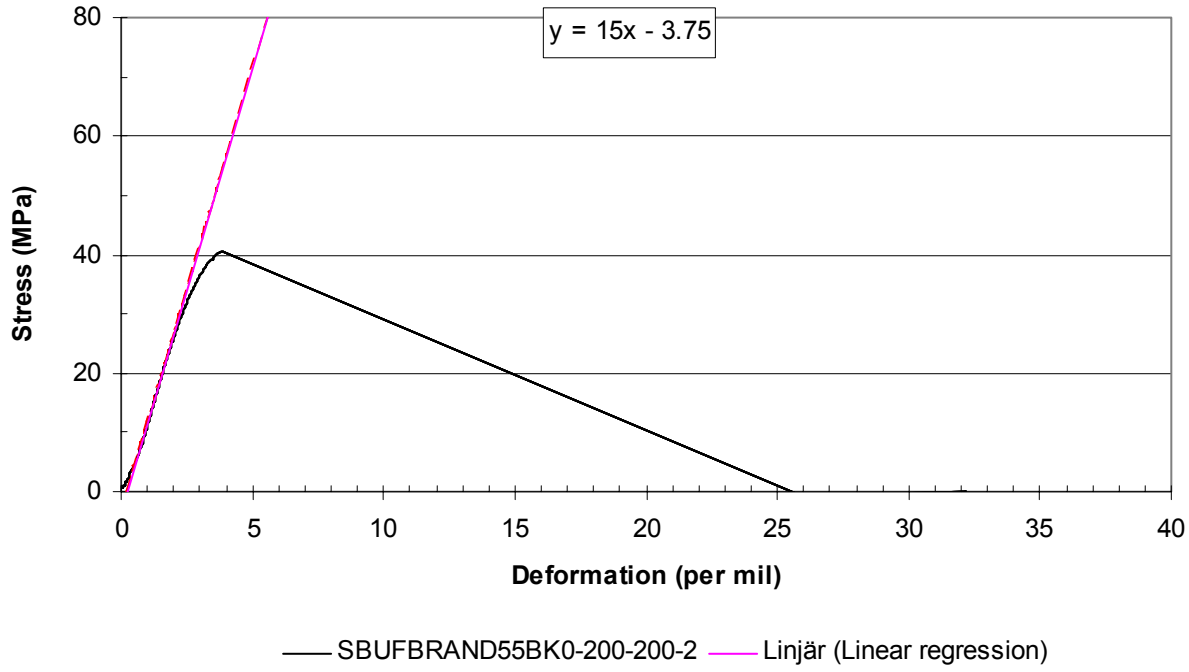

Appendix 4.44 – Stress/strain results of concrete 55BK0 at 400 °C – 20 °C.

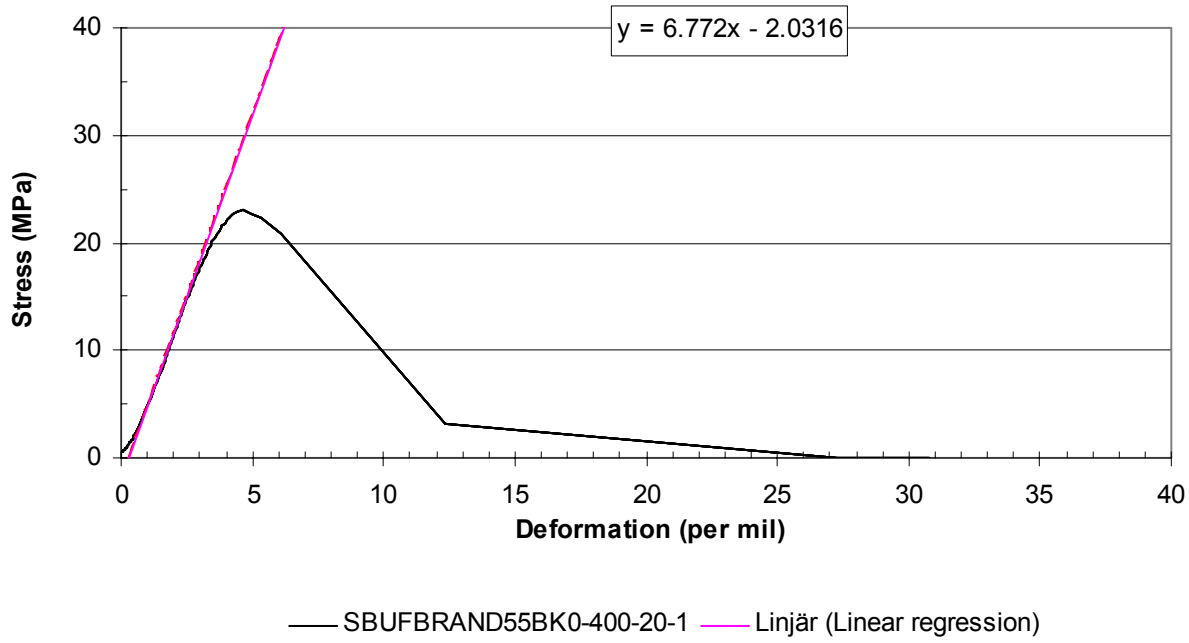

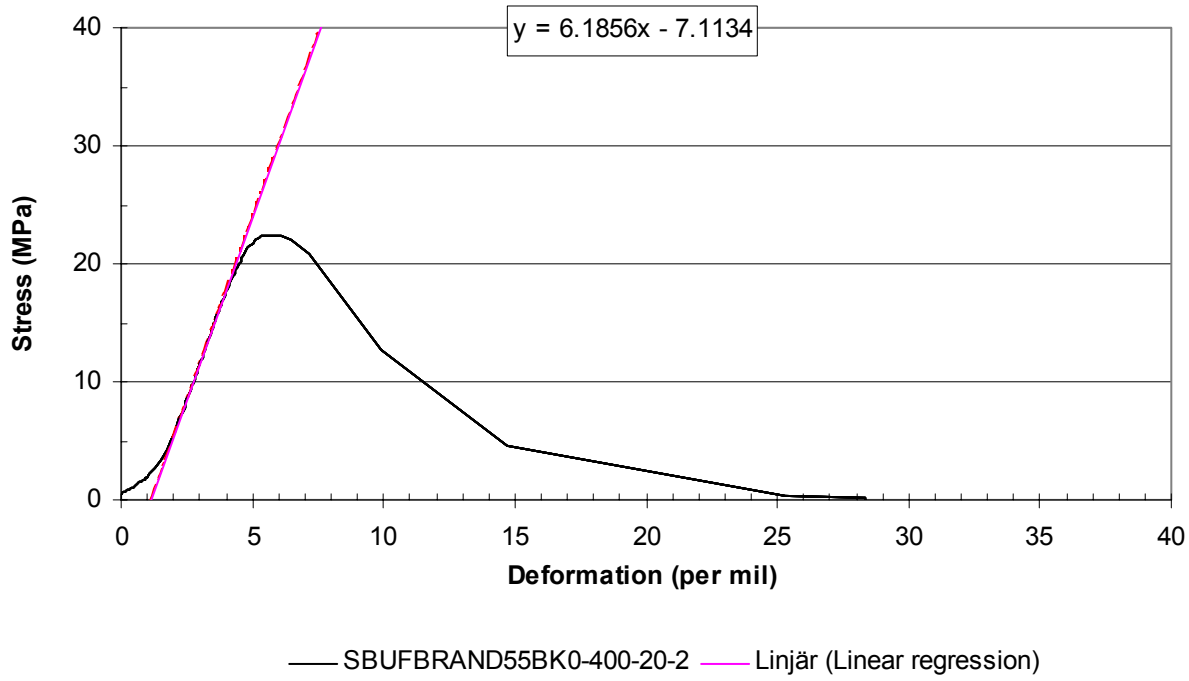

Appendix 4.45 – Stress/strain results of concrete 55BK0 at 400 °C – 400 °C.

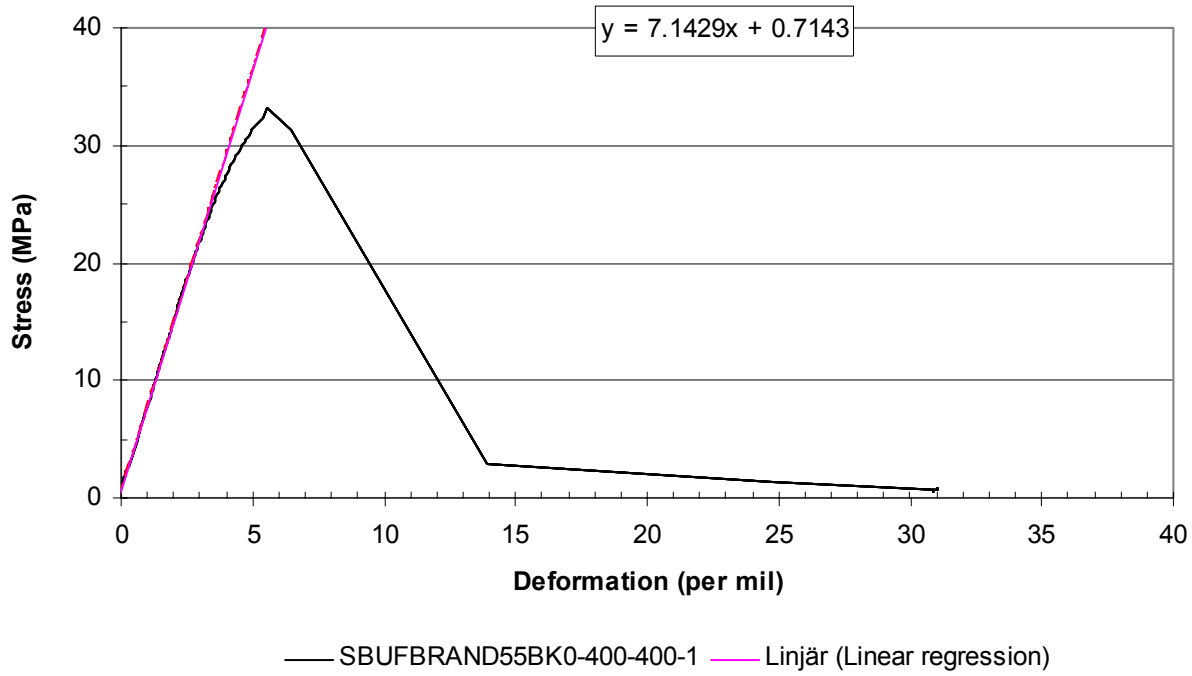

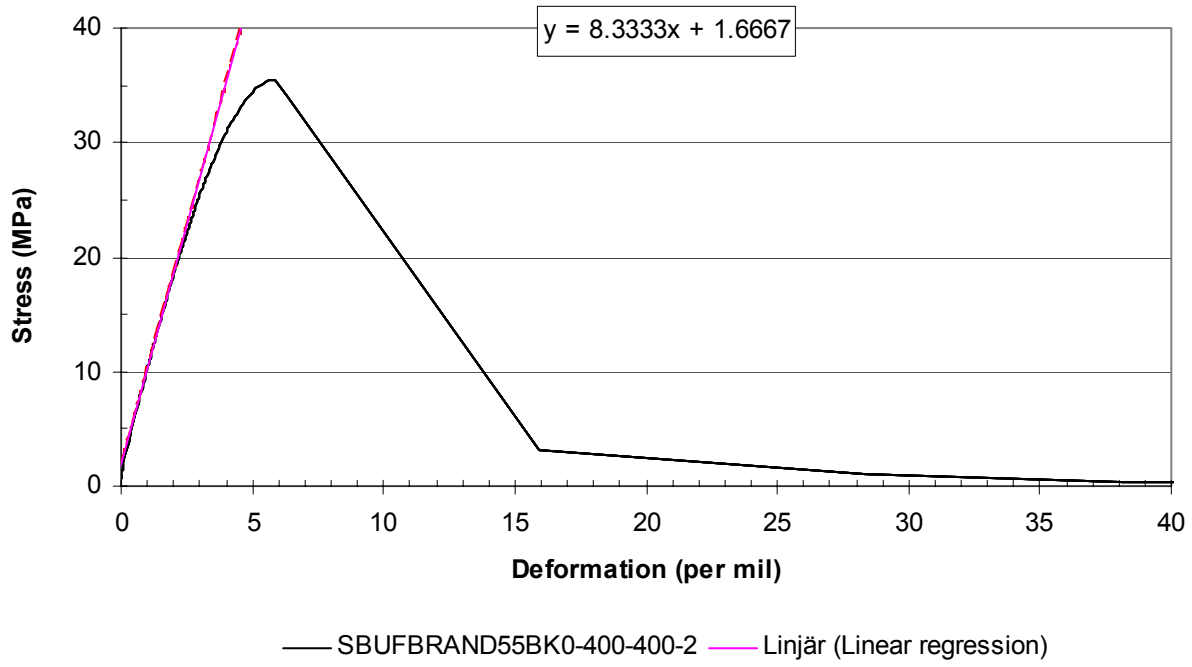

Appendix 4.46 – Stress/strain results of concrete 55BK0 at 800 °C – 800 °C.

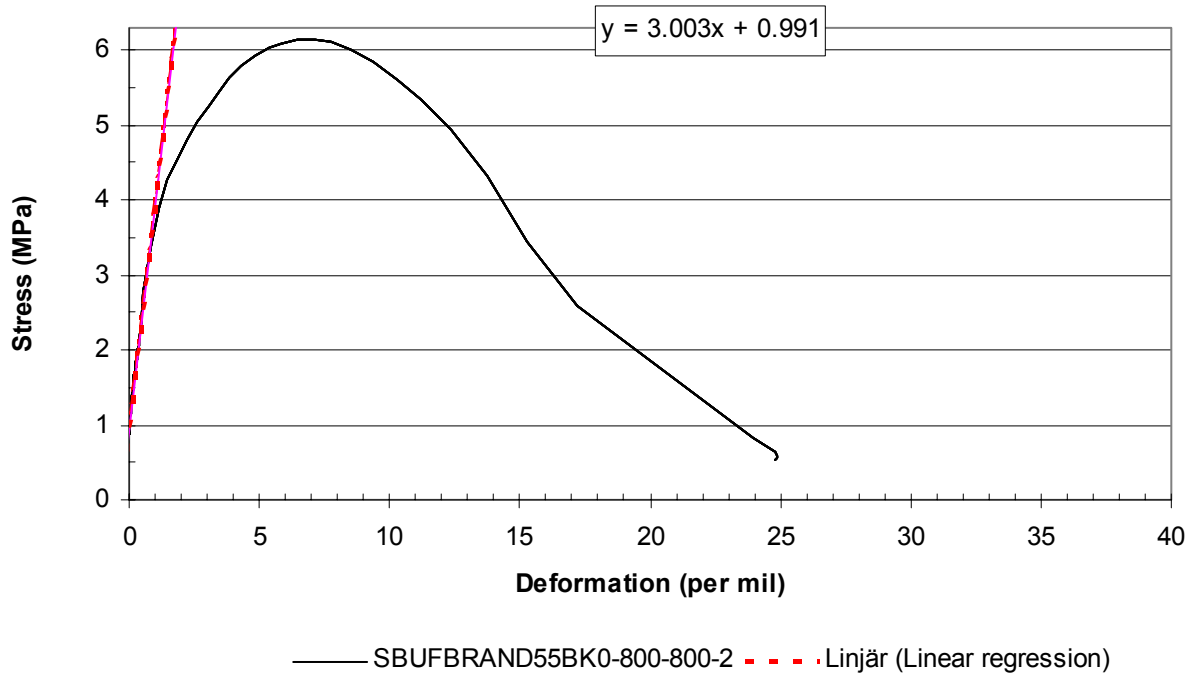

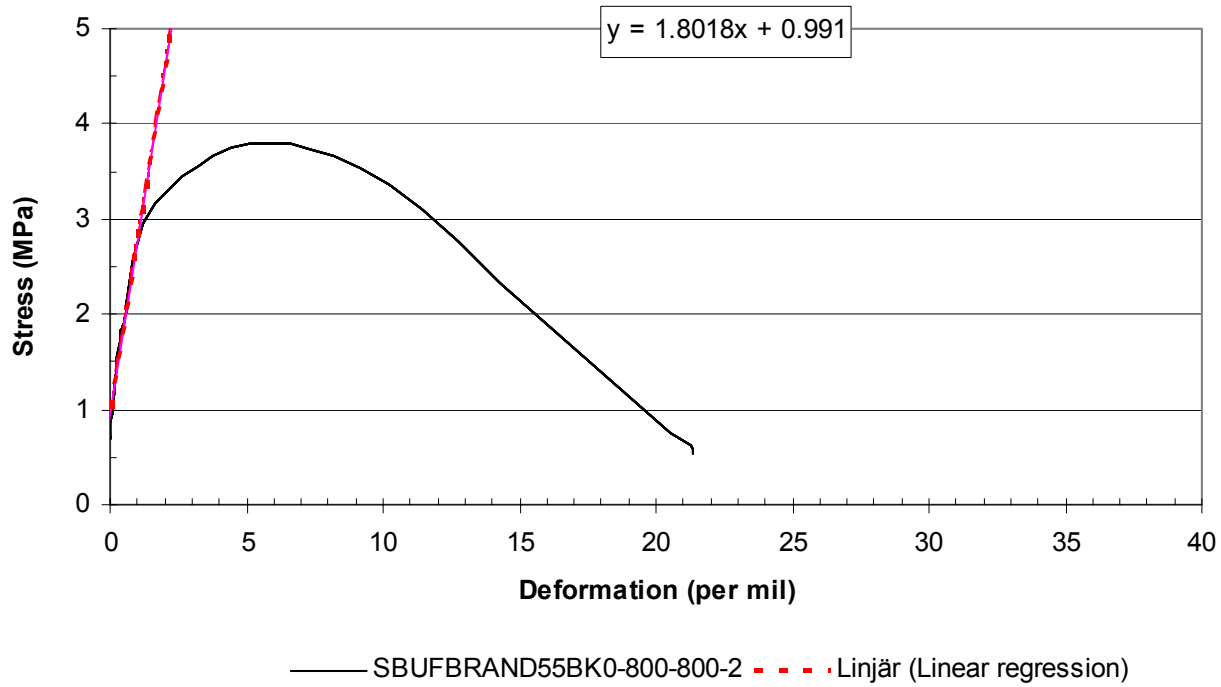

Appendix 4.47 – Stress/strain results of concrete 70BG0 at 20 °C.

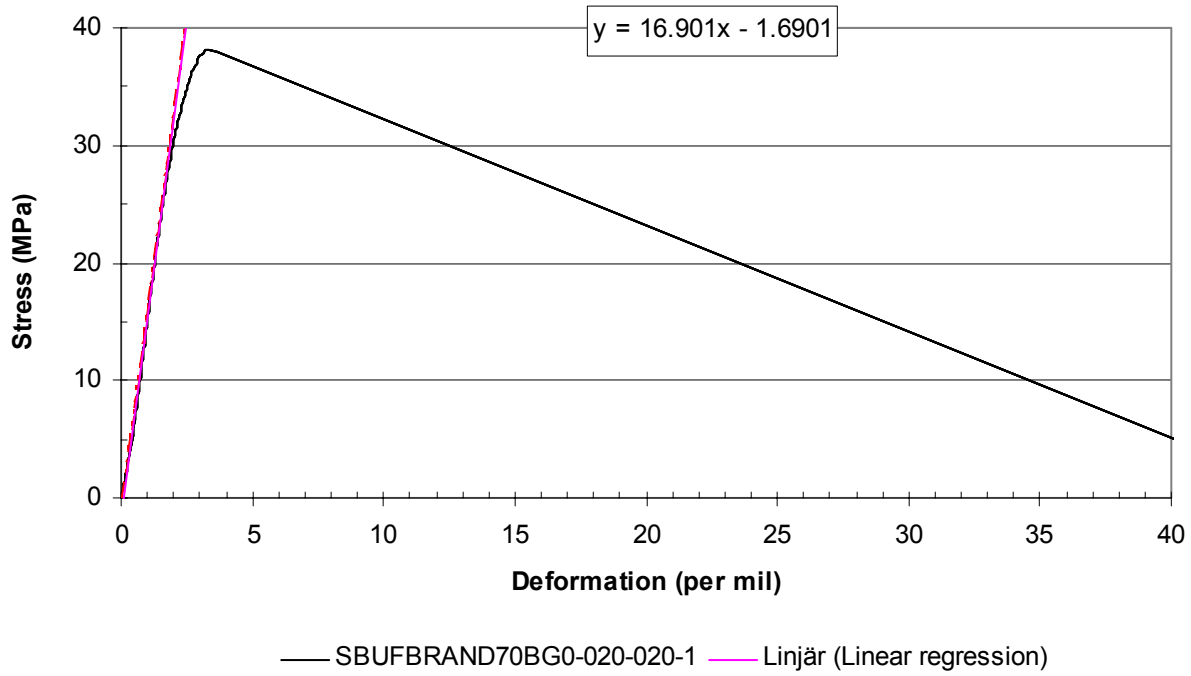

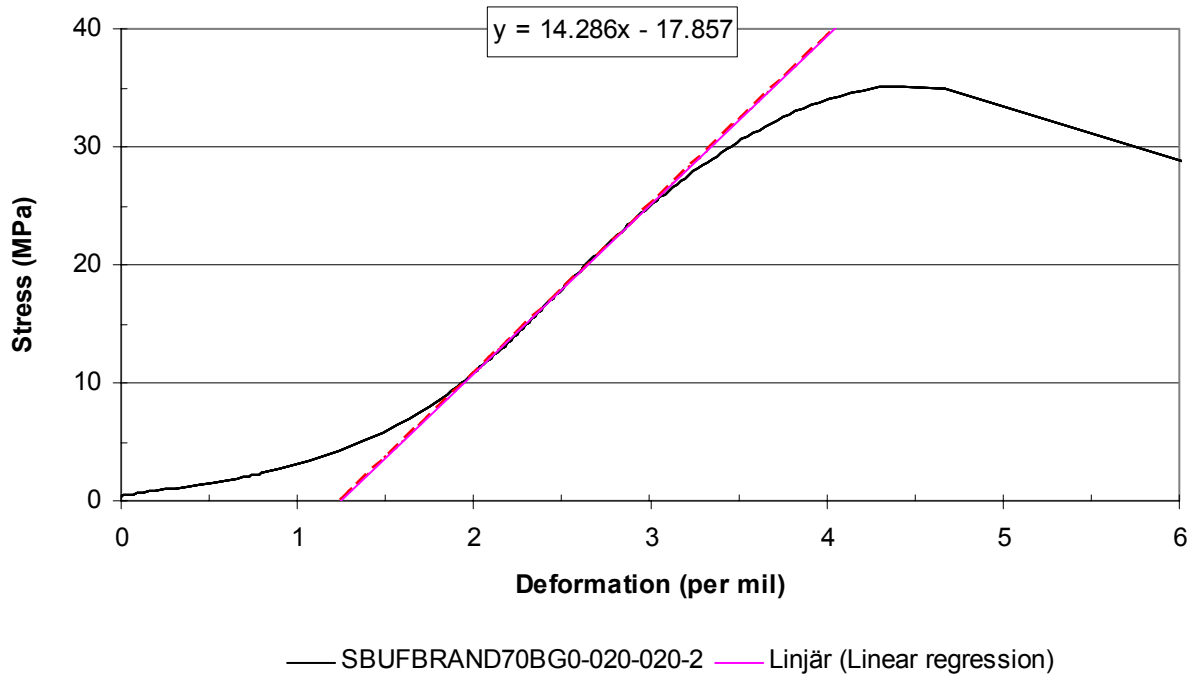

Appendix 4.48 – Stress/strain results of concrete 70BG0 at 200 °C – 20 °C.

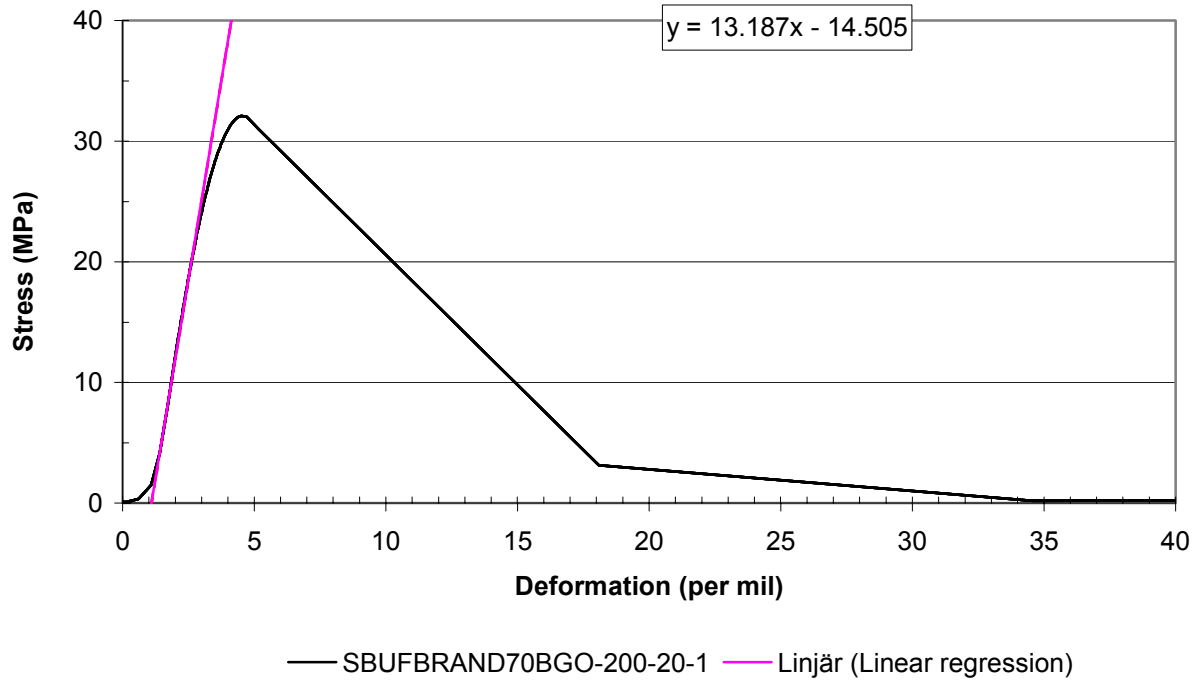

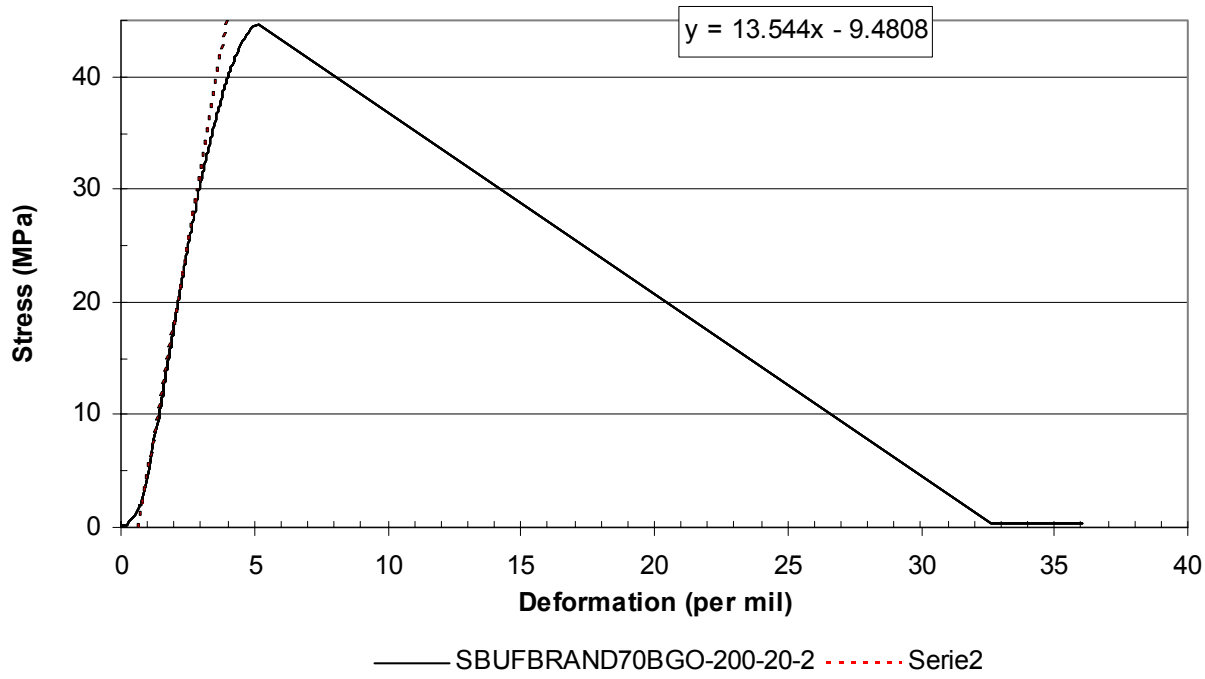

Appendix 4.49 – Stress/strain results of concrete 70BG0 at 200 °C – 200 °C.

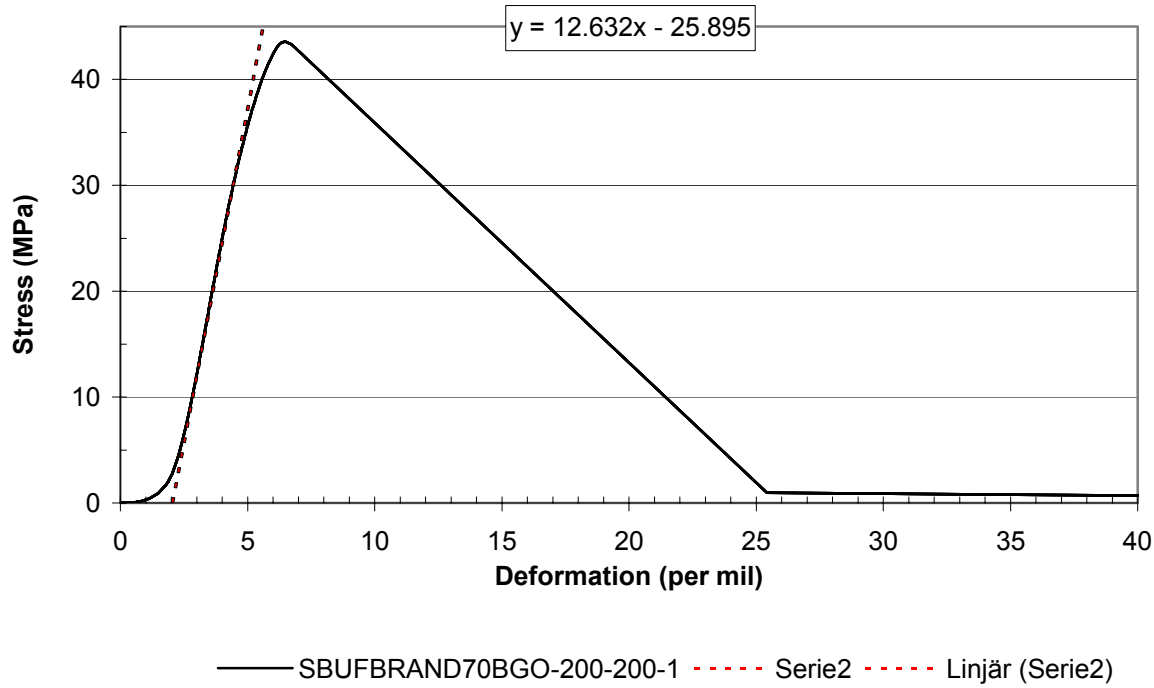

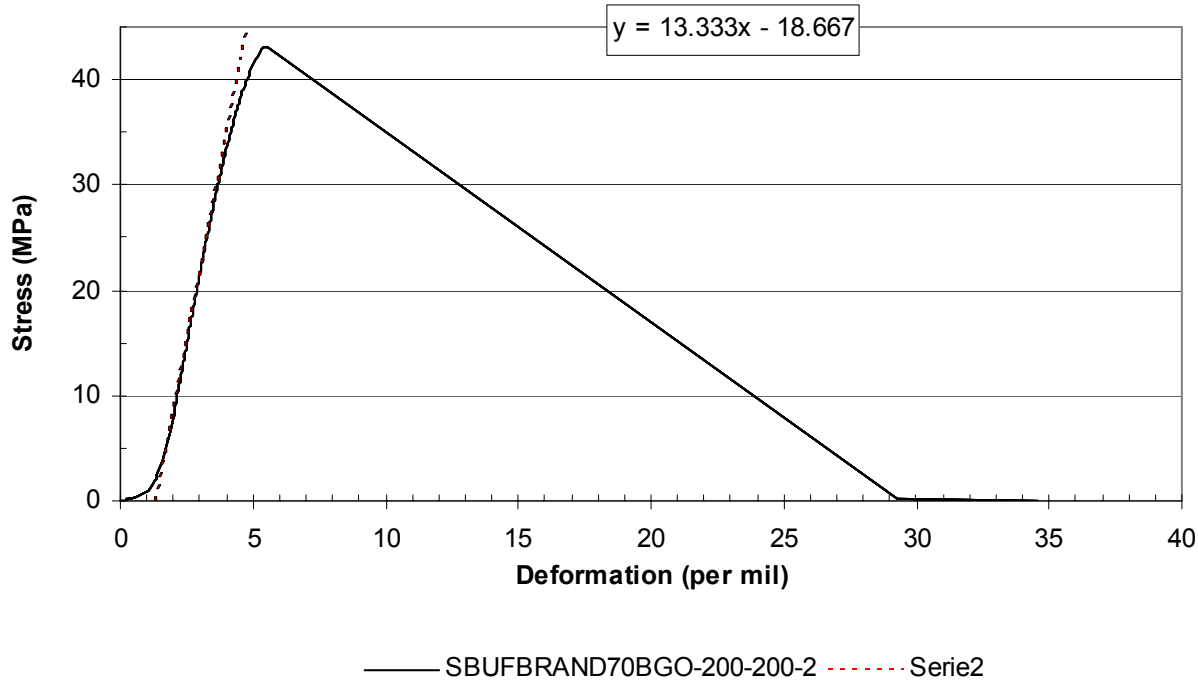

Appendix 4.50 – Stress/strain results of concrete 70BG0 at 400 °C – 20 °C.

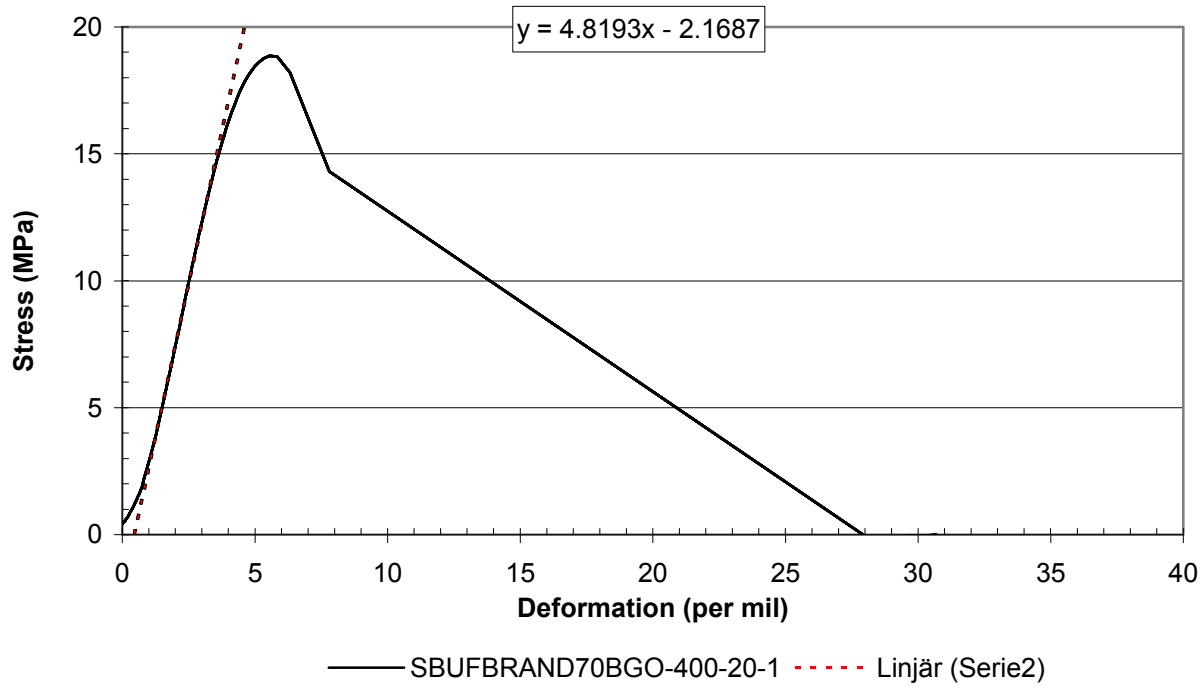

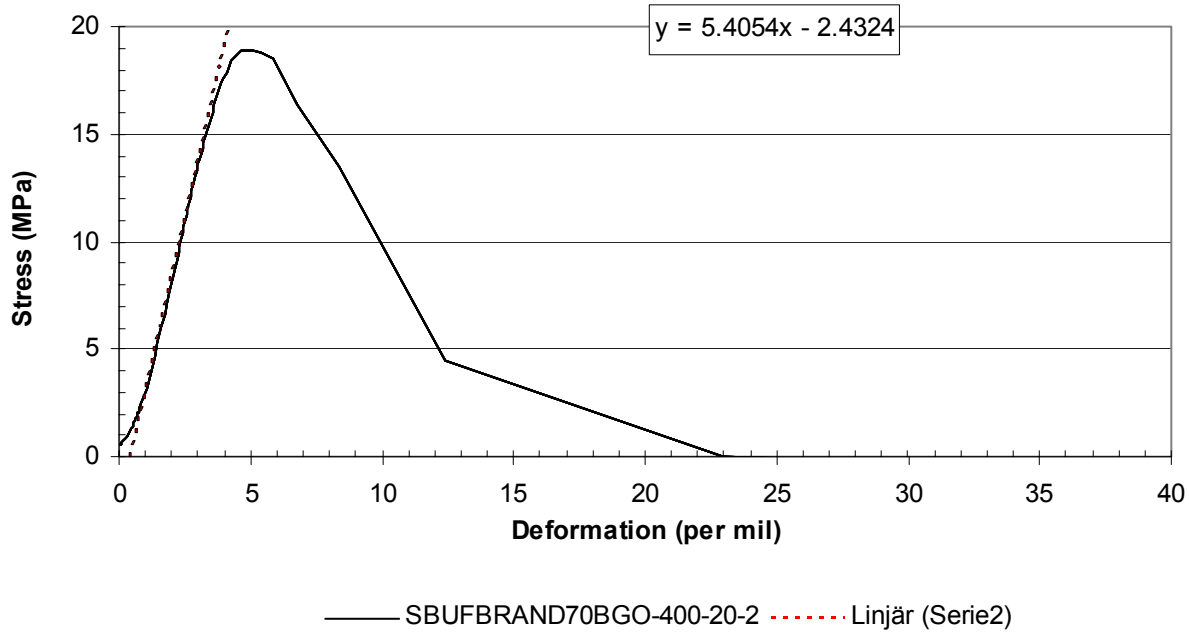

Appendix 4.51 – Stress/strain results of concrete 70BG0 at 400 °C – 400 °C.

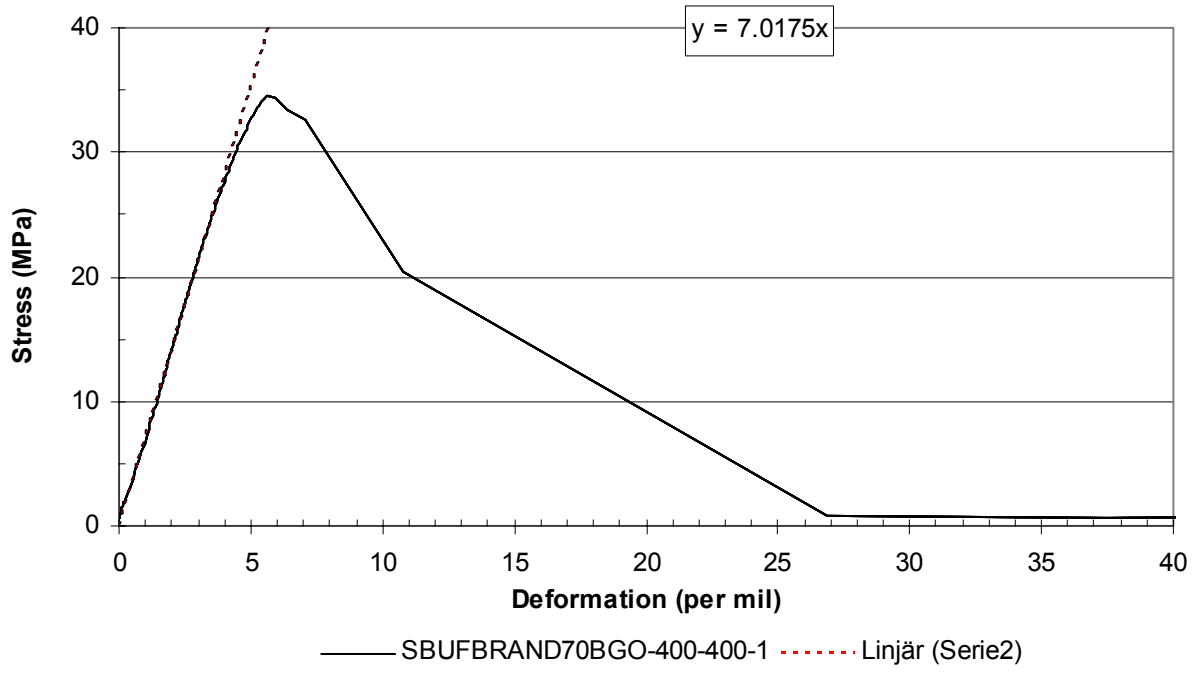

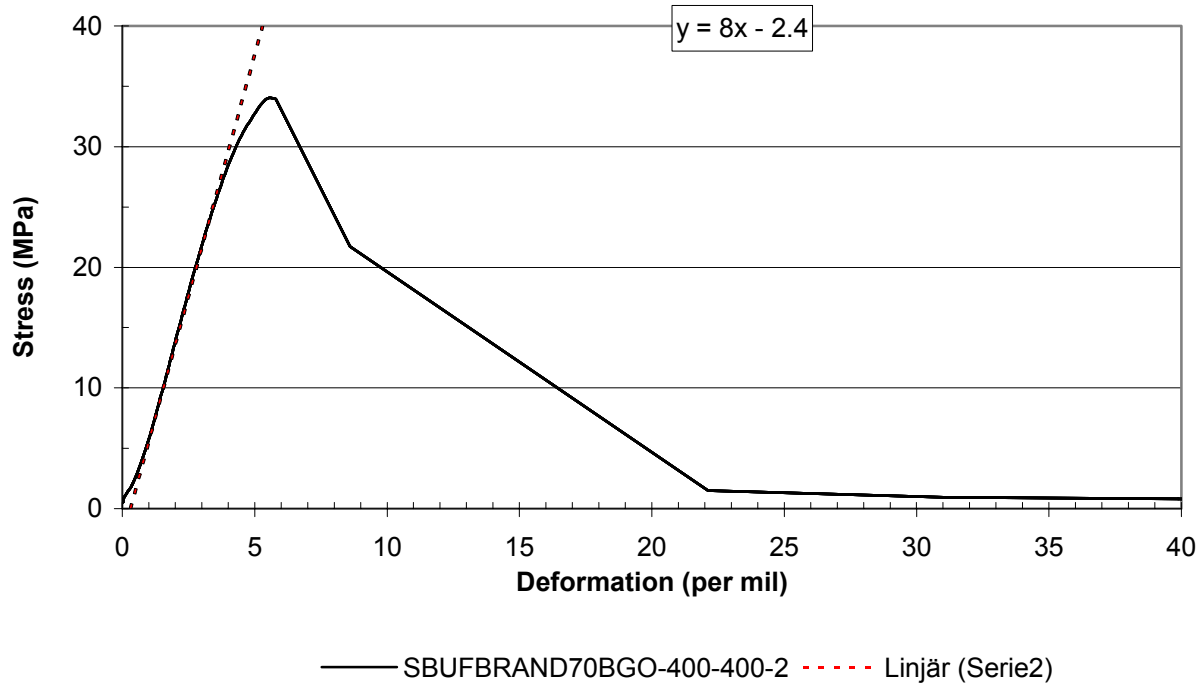

Appendix 4.52 – Stress/strain results of concrete 70BG0 at 800 °C – 20 °C.

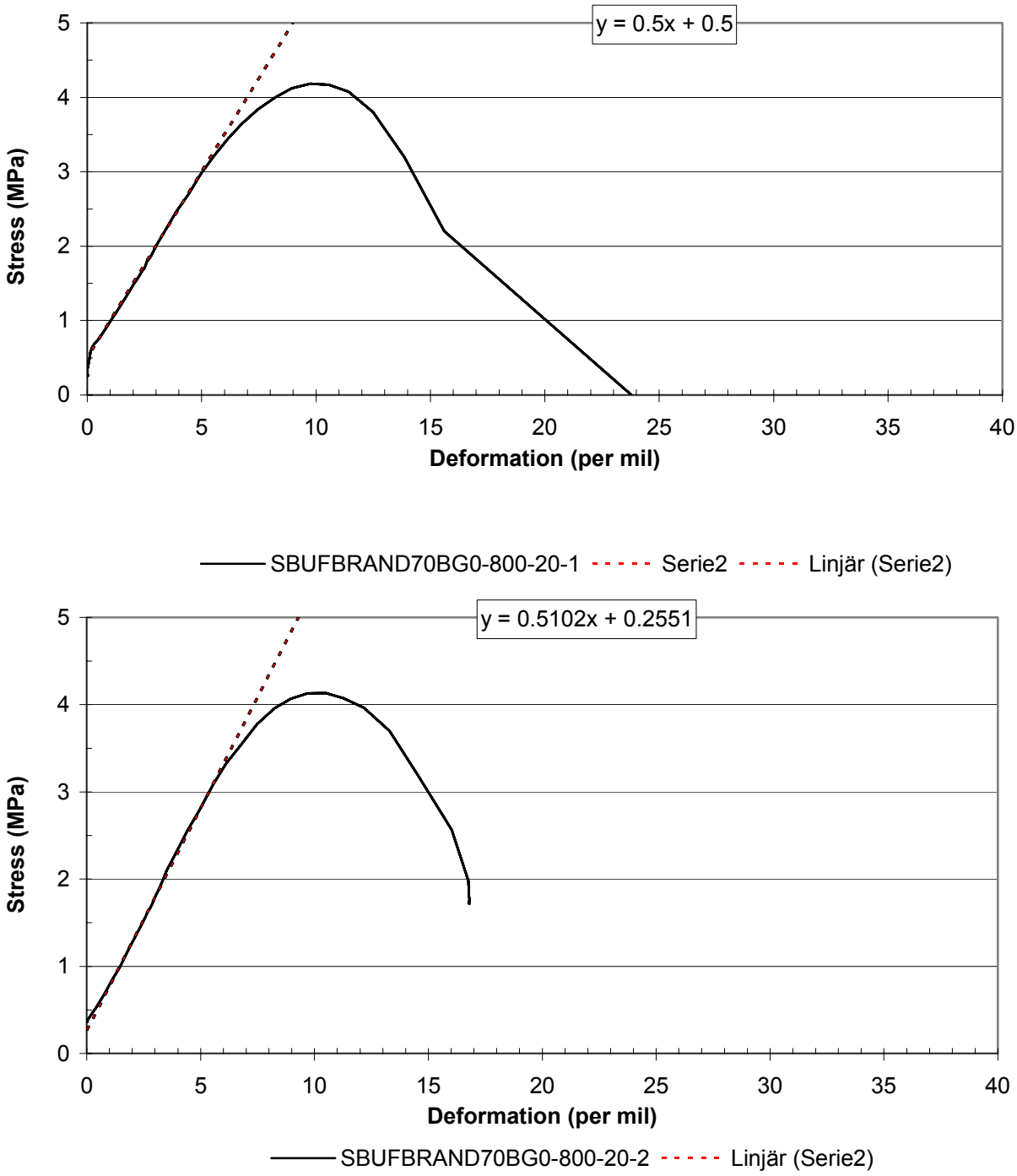

Appendix 4.53 – Stress/strain results of concrete 70BG0 at 800 °C – 800 °C.

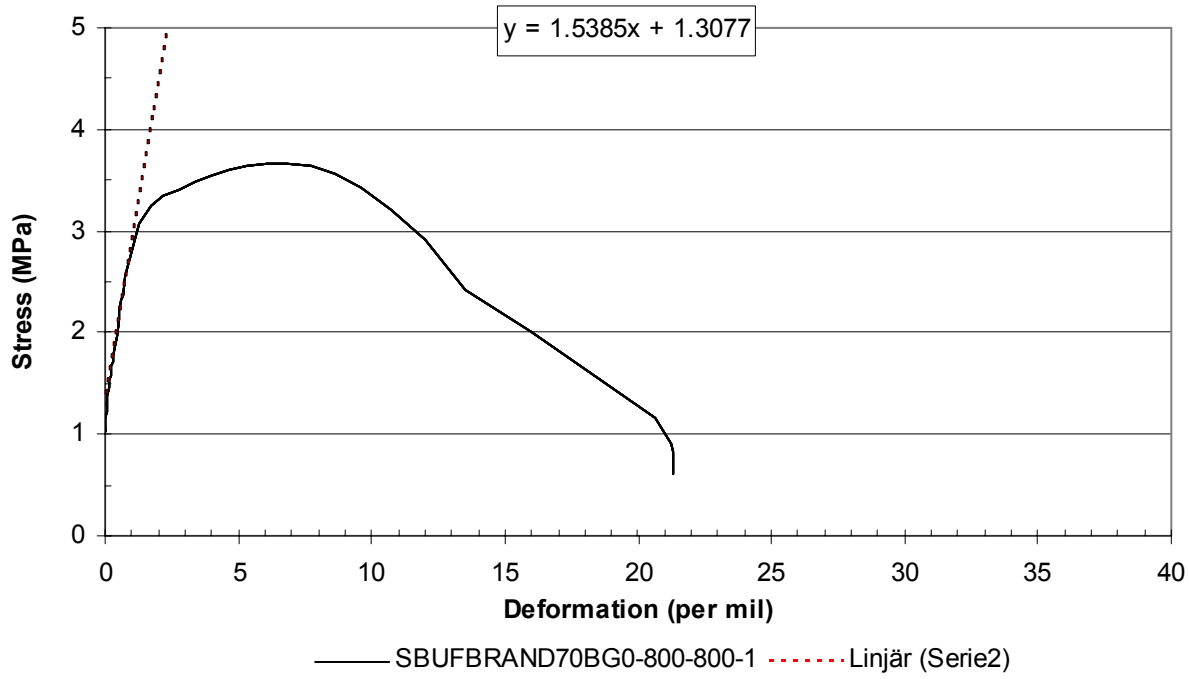

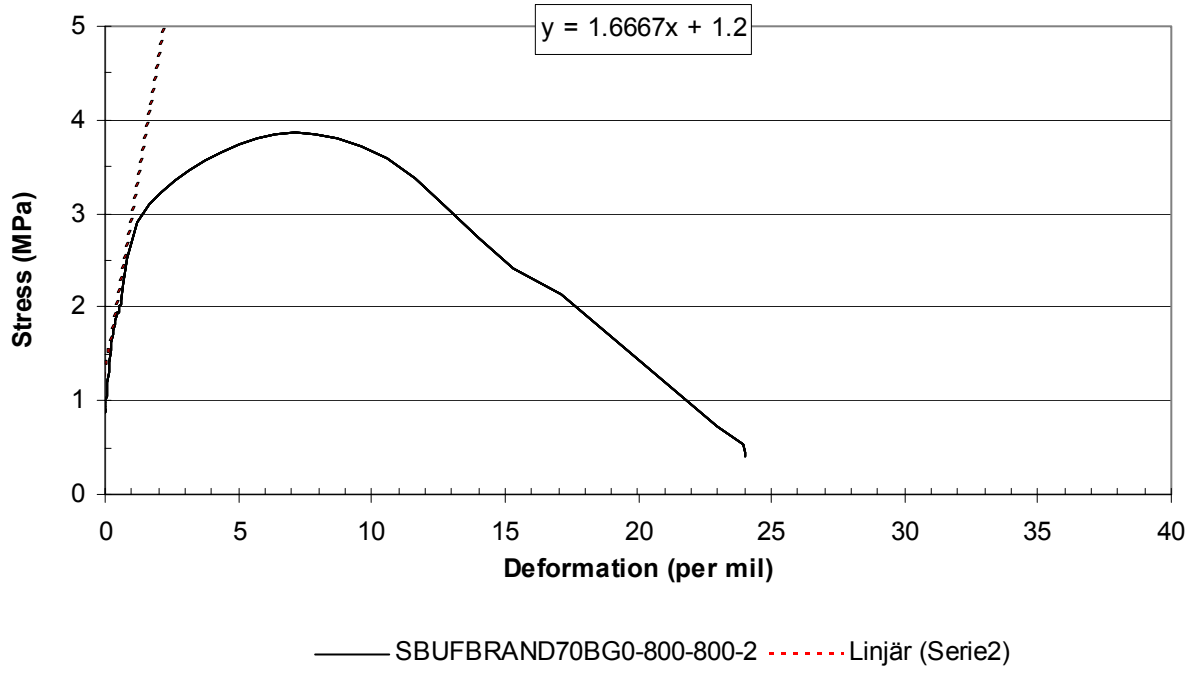

Appendix 4.54 – Stress/strain results of concrete 70BK0 at 20 °C.

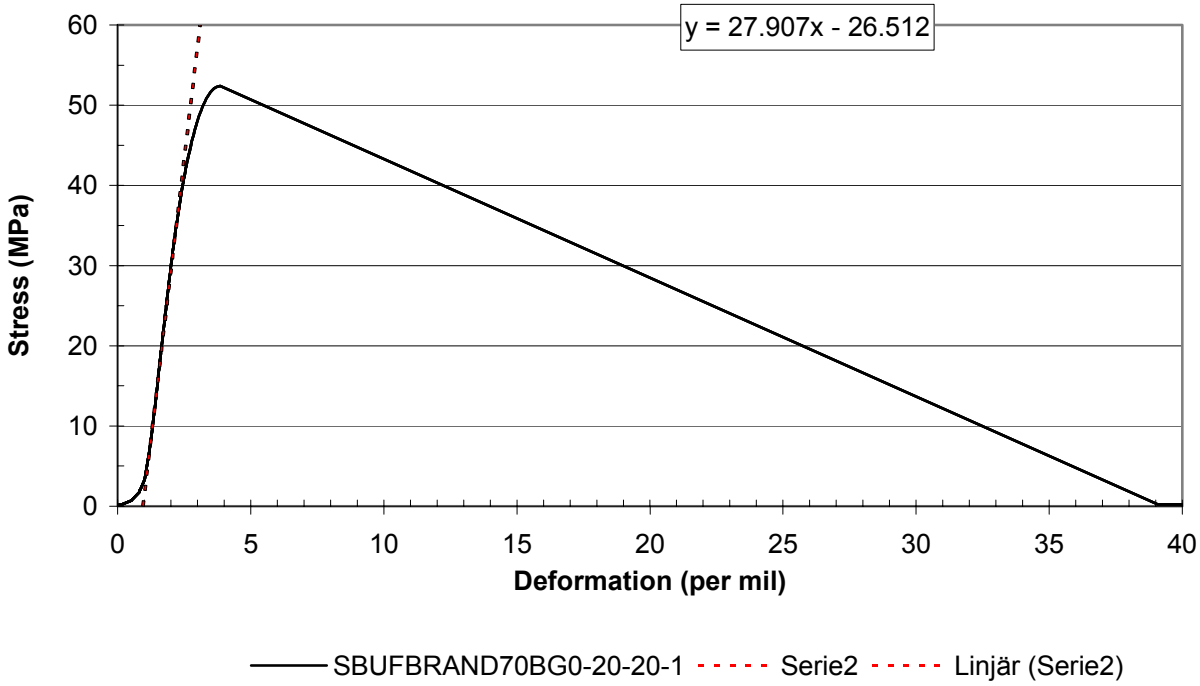

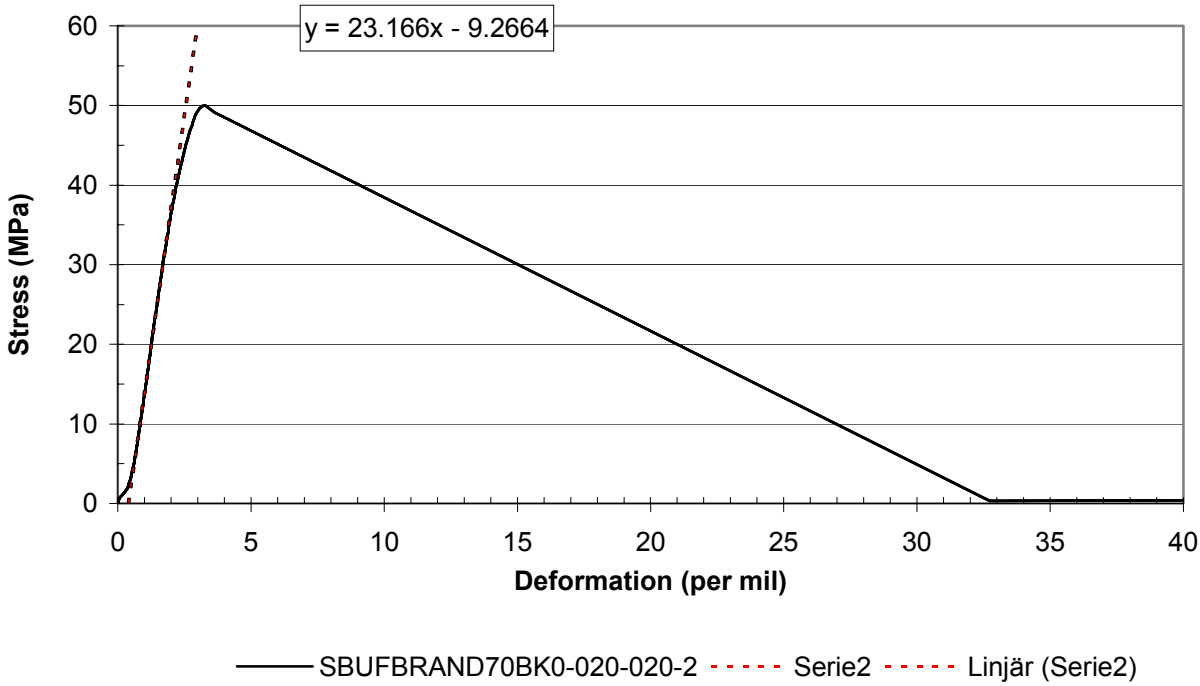

Appendix 4.55 – Stress/strain results of concrete 70BK0 at 200 °C – 20 °C.

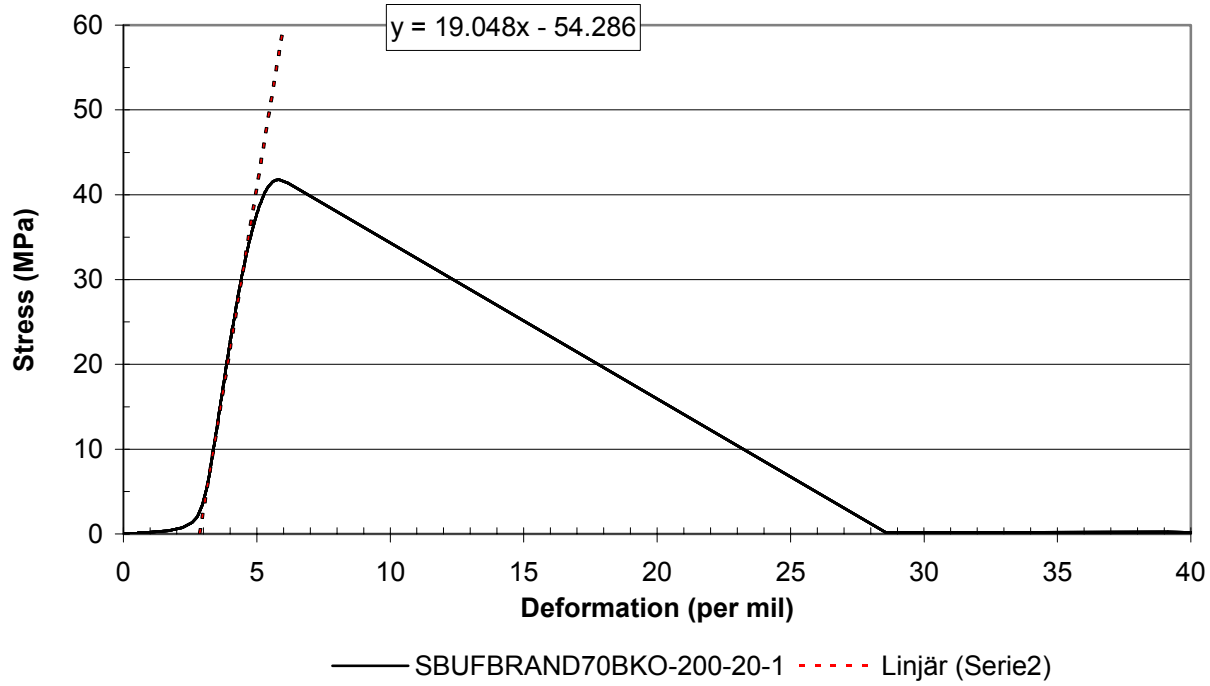

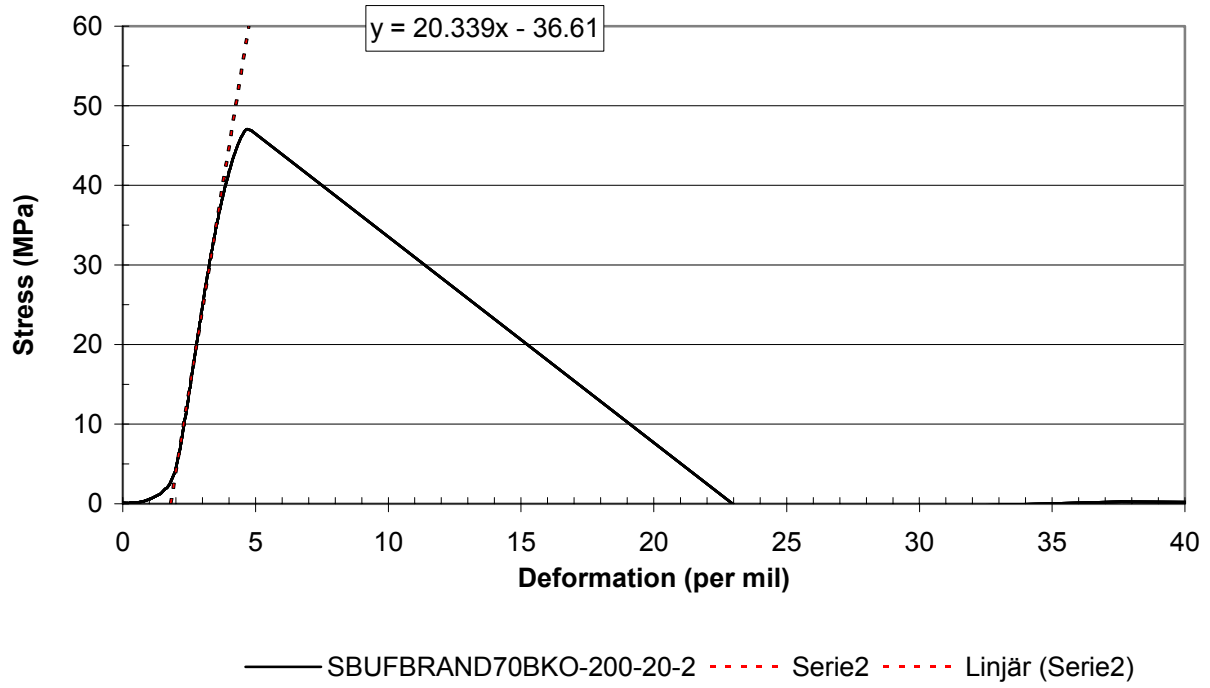

Appendix 4.56 – Stress/strain results of concrete 70BK0 at 200 °C – 200 °C.

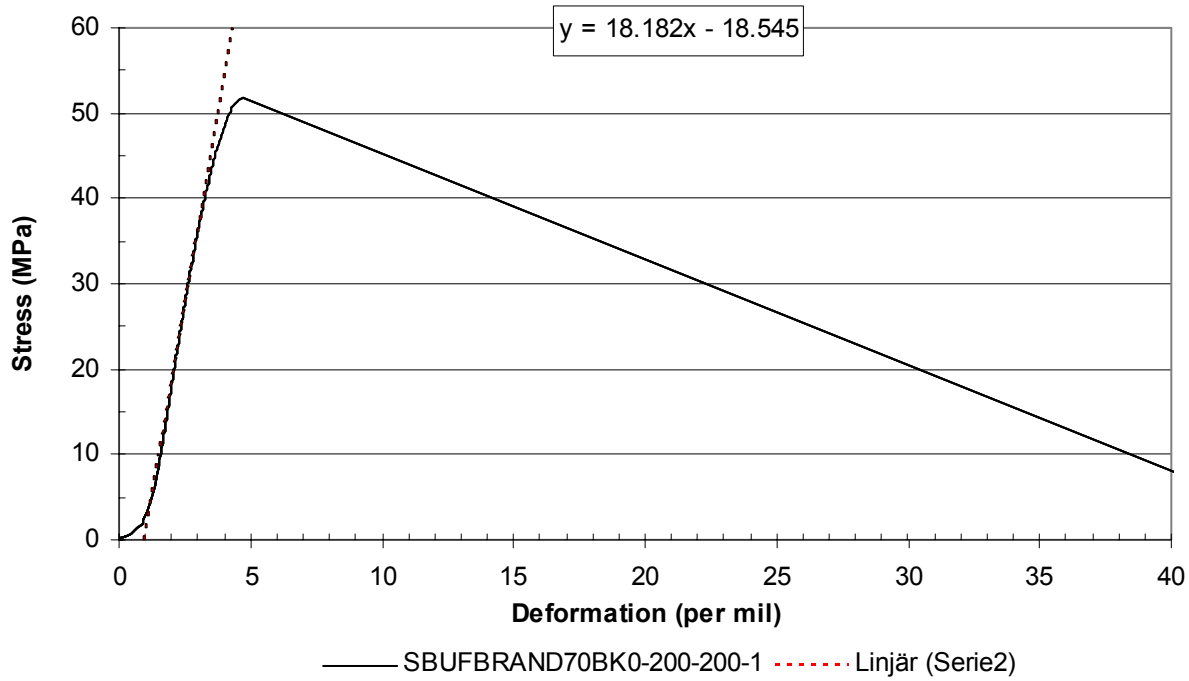

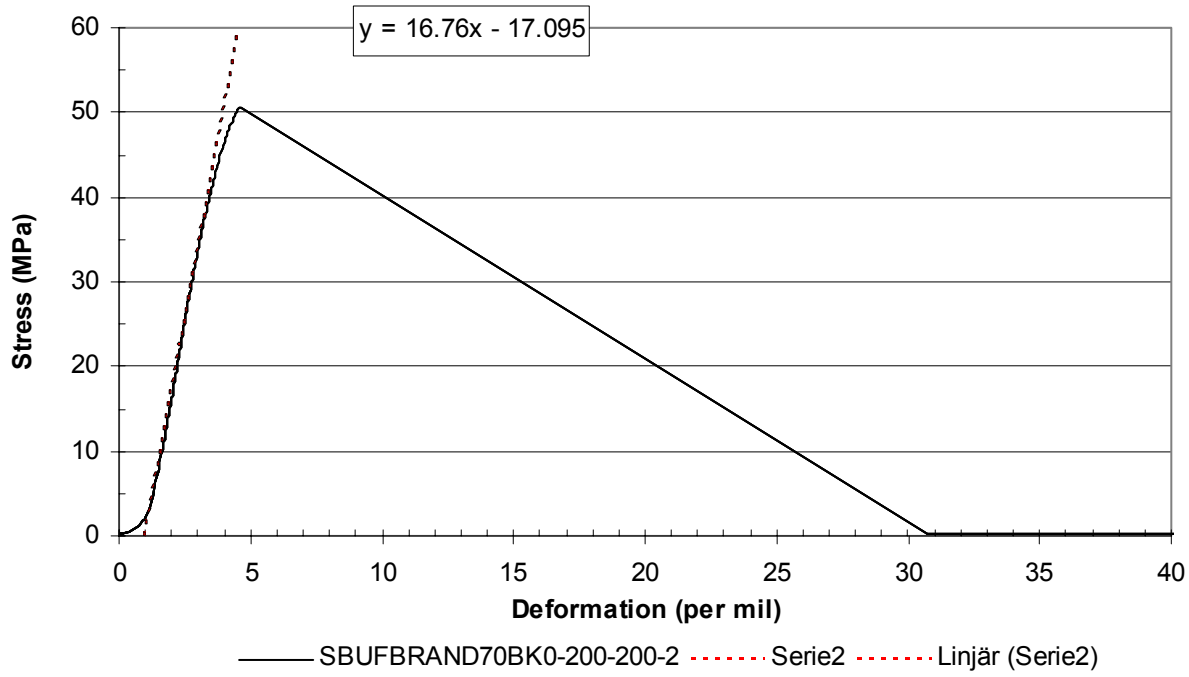

Appendix 4.57 – Stress/strain results of concrete 70BK0 at 400 °C – 20 °C.

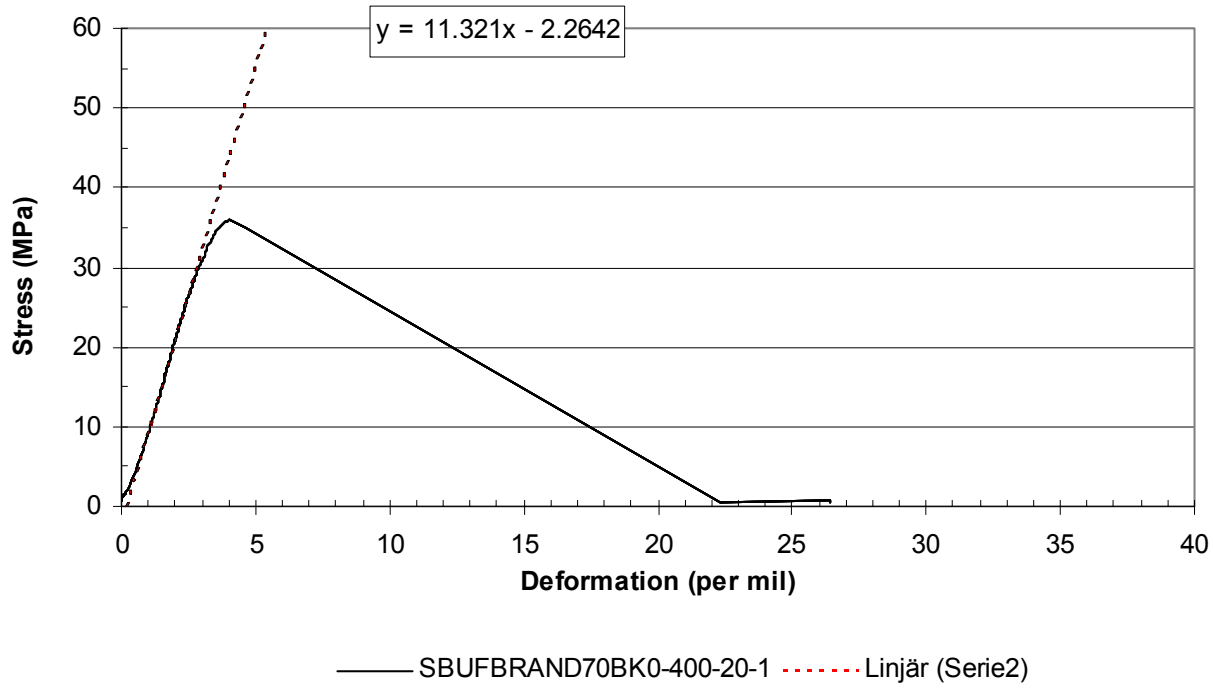

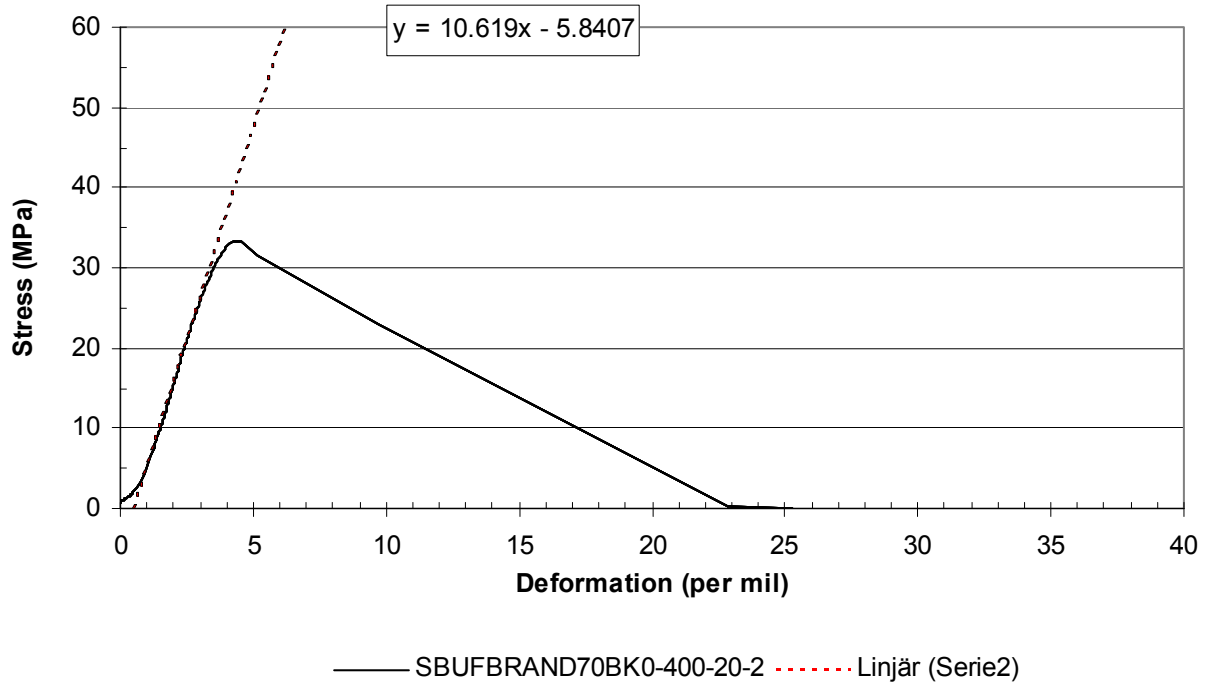

Appendix 4.58 – Stress/strain results of concrete 70BK0 at 400 °C – 400 °C.

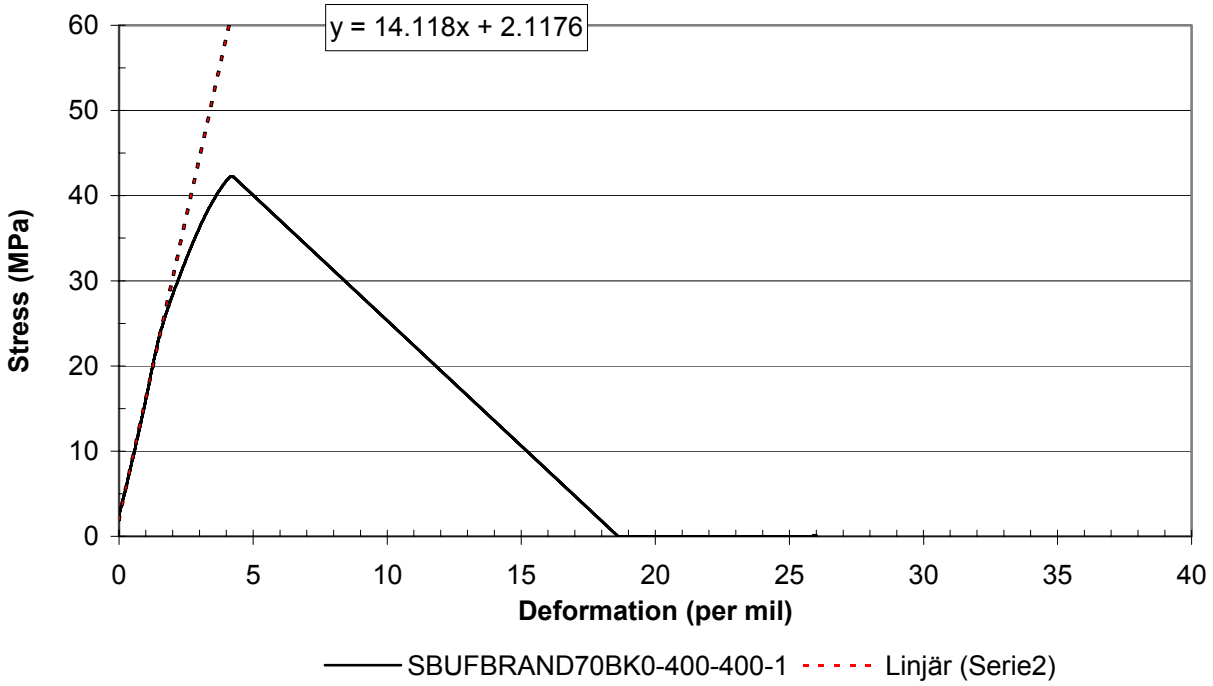

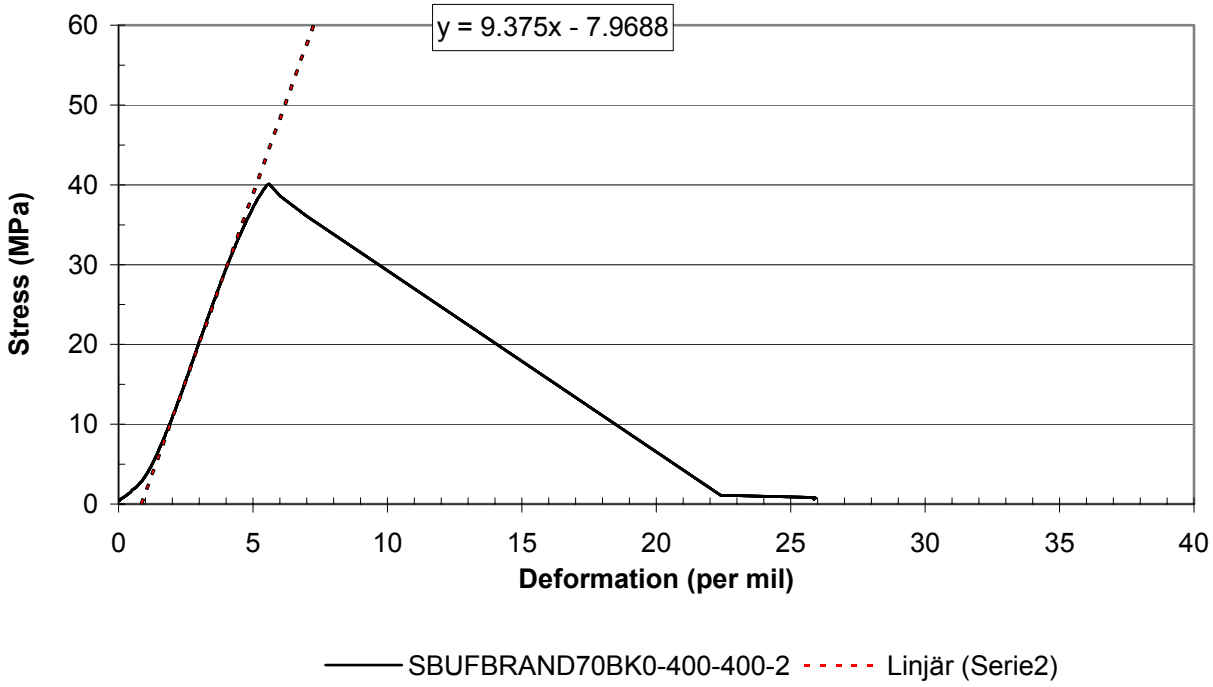

Appendix 4.59 – Stress/strain results of concrete 70BK0 at 800 °C – 800 °C.

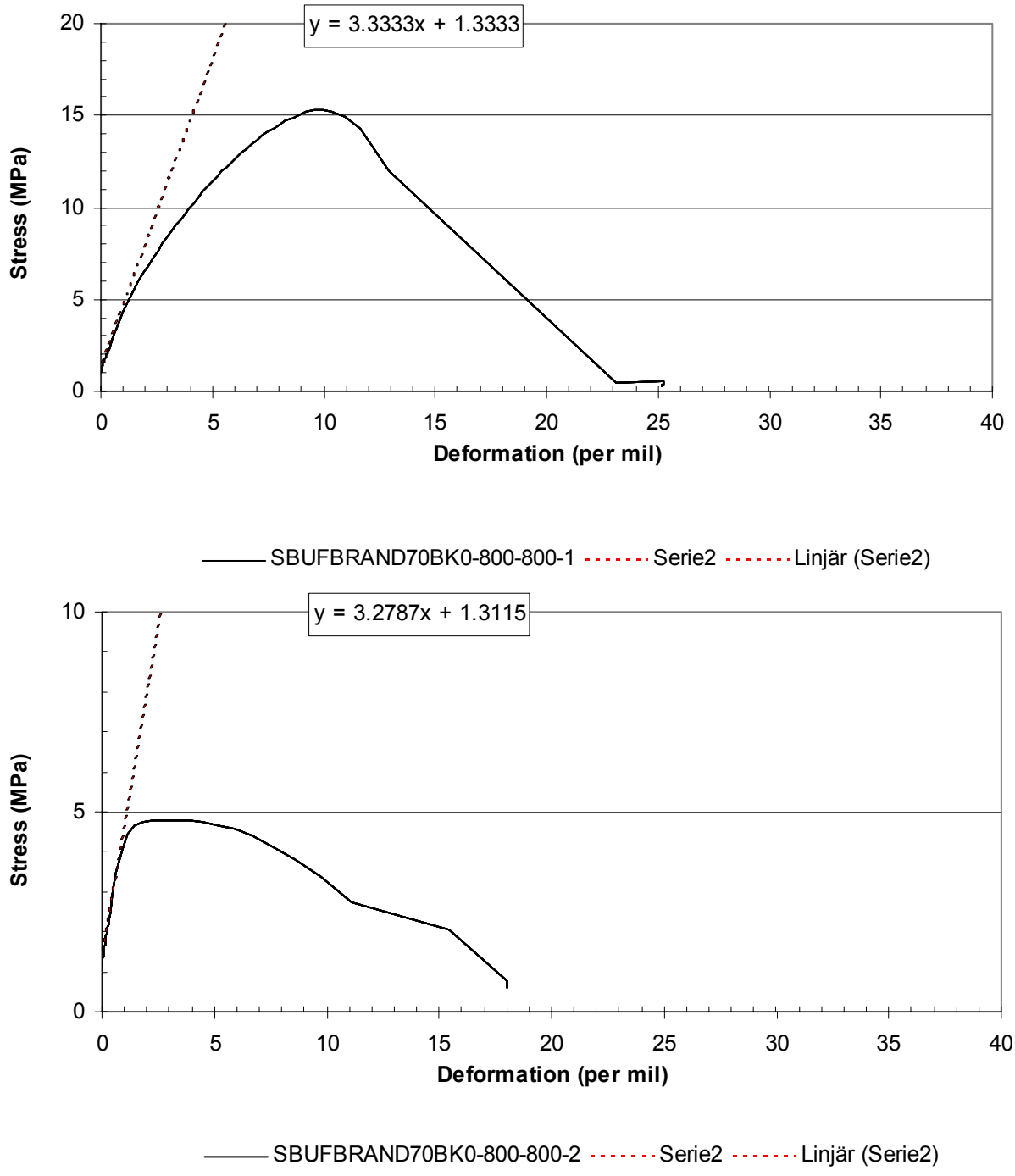

Appendices 5 - Analysis

Appendix 5.1 – Ideal distribution of particles in NC

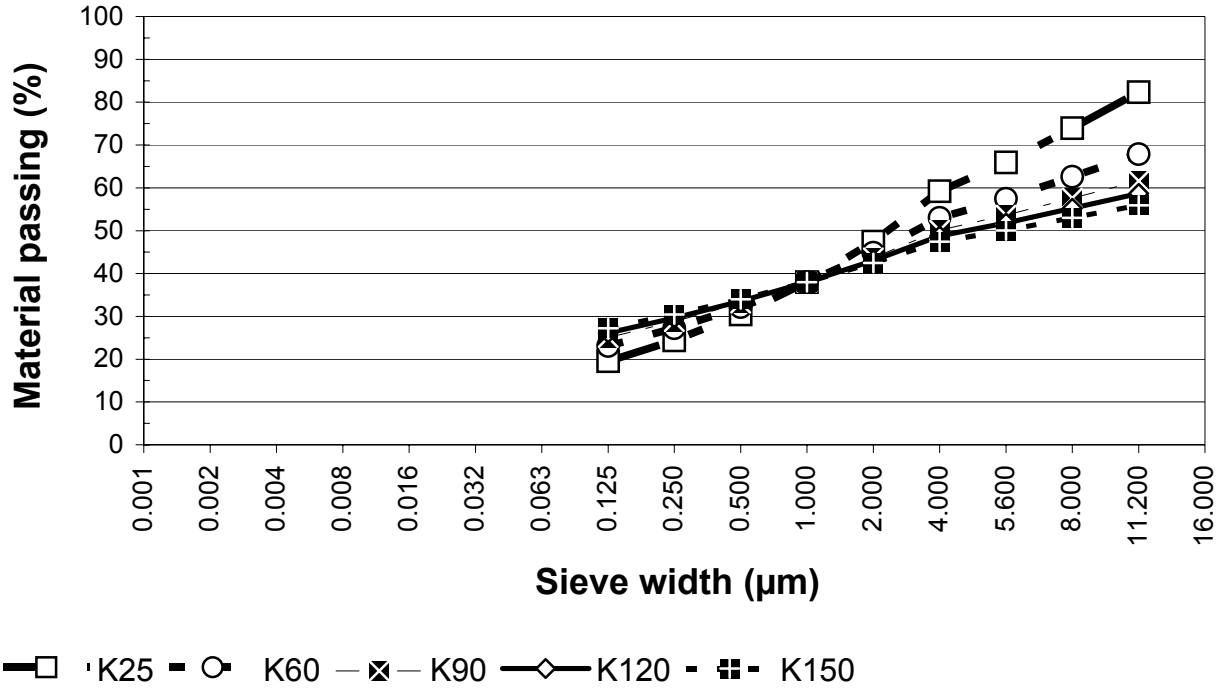

Appendix 5.2 – Particle grading of fresh concrete optimised by LTH.

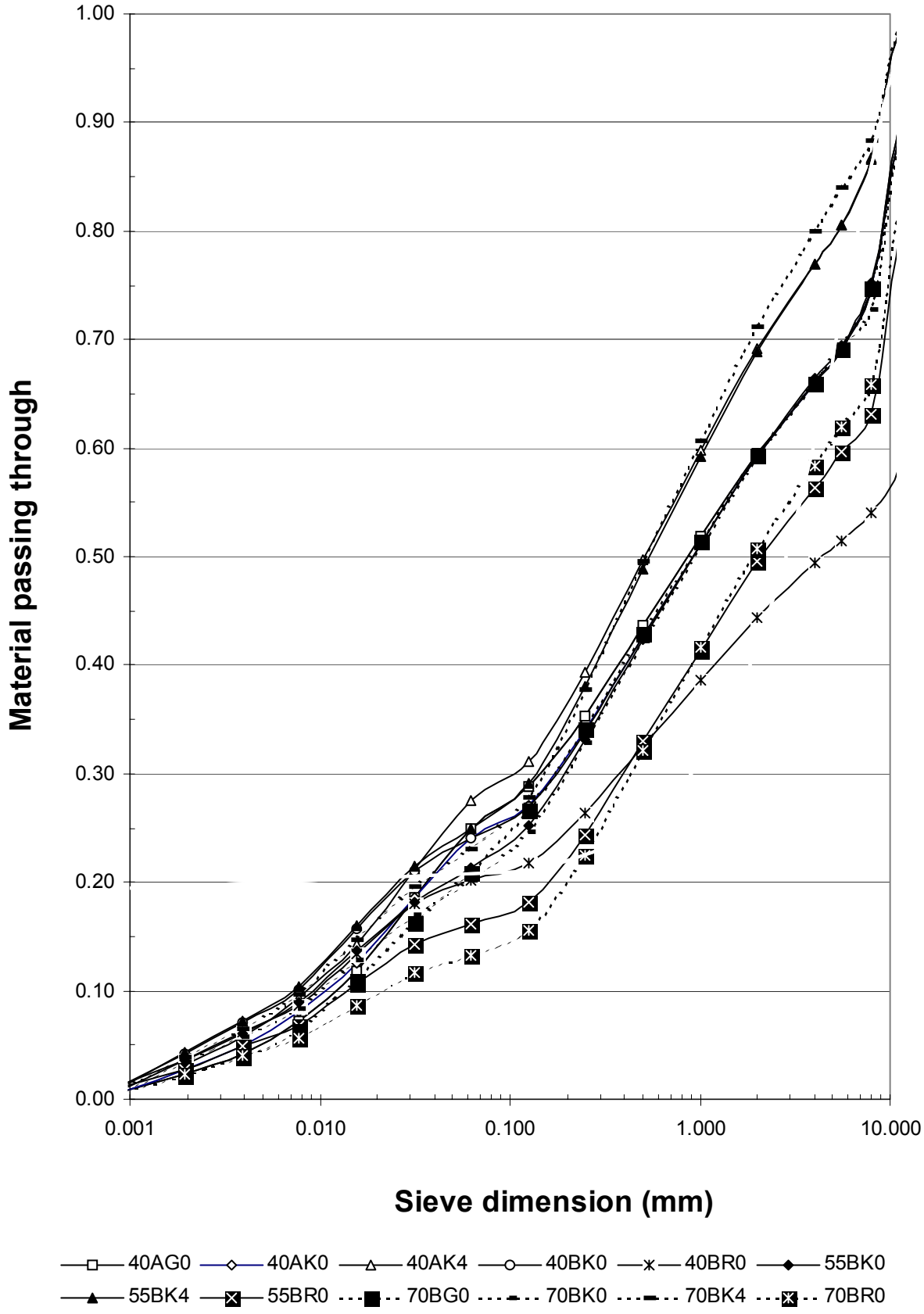

Appendix 5.3 Grading of fresh concrete optimised by Nordkalk and SGÅ

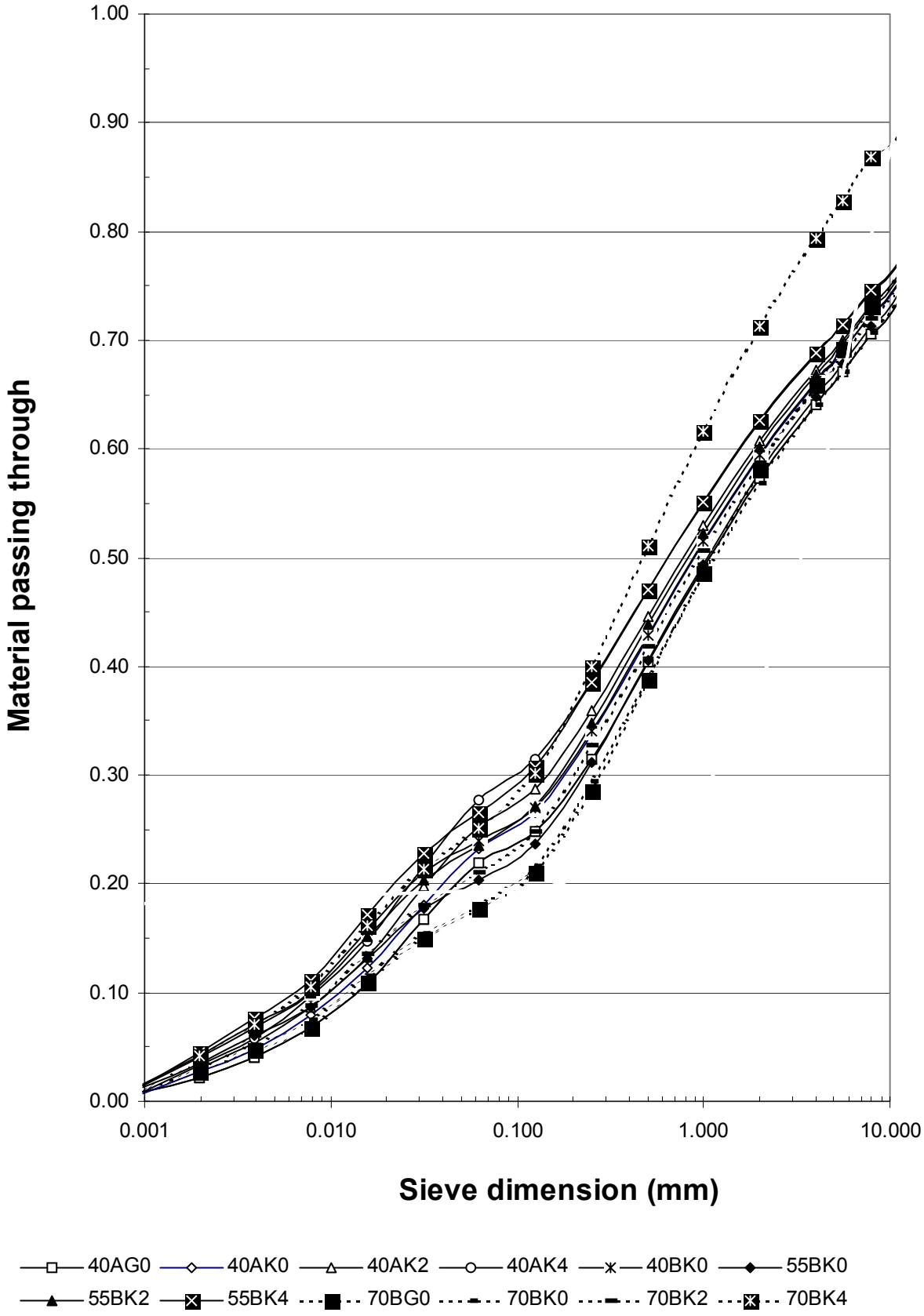

Appendix 5.4 – Results of residual properties after cooling at 20 °C and RH = about 40%.

Residual E-modulus (GPa)	40AG0	40AK0	40AK2	40AK4	40BR0	55BK0	70BG0	70BK0
20.00	31.00	25.60	28.33	25.76	31.25	21.05	16.90	27.91
20.00	27.00	23.00	32.70	26.65	32.92	22.47	14.29	23.17
200.00	22.40	20.60	25.80	23.29	20.00	13.73	13.18	19.05
200.00	24.60	21.00	19.30	25.07	23.19	15.87	13.54	20.34
400.00	9.30	9.83	11.70	9.83	9.88	6.19	4.82	11.32
400.00	8.70	9.76	12.50	11.00	10.39	6.77	5.41	10.62
800.00	1.32	0.00	0.00	0.00	0.63	0.00	0.50	0.00
800.00	1.32	0.00	0.00	0.00	0.64	0.00	0.51	0.00
On average residual E-modulus (GPa)	40AG0	40AK0	40AK2	40AK4	40BR0	55BK0	70BG0	70BK0
20 °C	29.00	24.30	30.52	26.21	32.09	21.76	15.60	25.54
200 °C	23.50	20.80	22.55	24.18	21.60	14.80	13.36	19.70
400 °C	9.00	9.80	12.10	10.42	10.14	6.48	5.12	10.97
800 °C	1.32	0.00	0.00	0.00	0.64	0.00	0.51	0.00
Residual strain (‰)	40AG0	40AK0	40AK2	40AK4	40BR0	55BK0	70BG0	70BK0
20.00	2.74	3.57	4.88	3.40	3.38	3.73	3.37	3.86
20.00	3.24	6.50	3.49	3.63	3.07	3.81	4.43	3.29
200.00	4.43	4.34	3.91	4.56	5.31	4.44	4.51	5.83
200.00	4.35	3.47	7.85	4.03	4.45	3.32	5.15	4.68
400.00	5.41	5.59	4.90	4.84	5.60	5.76	5.55	4.05
400.00	5.30	5.21	5.60	4.95	5.84	4.61	5.10	4.34
800.00	10.00	0.00	0.00	0.00	10.50	0.00	9.76	0.00
800.00	9.51	0.00	0.00	0.00	10.80	0.00	10.50	0.00
On average residual strain (‰)	40AG0	40AK0	40AK2	40AK4	40BR0	55BK0	70BG0	70BK0
20 °C	2.99	5.04	4.19	3.52	3.23	3.77	3.90	3.58
200 °C	4.39	3.91	5.88	4.30	4.88	3.88	4.83	5.26
400 °C	5.36	5.40	5.25	4.90	5.72	5.19	5.33	4.20
800 °C	9.76	0.00	0.00	0.00	10.65	0.00	10.13	0.00
Residual strength (MPa)	40AG0	40AK0	40AK2	40AK4	40BR0	55BK0	70BG0	70BK0
20.00	60.40	57.90	65.50	59.70	73.24	45.30	38.20	52.37
20.00	60.30	56.60	74.60	58.67	69.65	45.90	35.10	50.00
200.00	57.75	56.10	77.30	60.40	57.39	34.51	32.10	41.80
200.00	71.66	53.90	76.50	67.70	65.37	35.02	44.56	47.10
400.00	40.30	39.77	45.70	37.20	39.92	22.42	18.85	36.00
400.00	33.80	40.35	47.20	38.20	40.47	23.00	18.92	33.36
800.00	11.46	0.00	0.00	0.00	5.10	0.00	4.81	0.00
800.00	11.53	0.00	0.00	0.00	5.34	0.00	4.13	0.00
On average residual strength (MPa)	40AG0	40AK0	40AK2	40AK4	40BR0	55BK0	70BG0	70BK0
20 °C	60.35	57.25	70.05	59.19	71.45	45.60	36.65	51.19
200 °C	64.71	55.00	76.90	64.05	61.38	34.77	38.33	44.45
400 °C	37.05	40.06	46.45	37.70	40.20	22.71	18.89	34.68
800 °C	11.50	0.00	0.00	0.00	5.22	0.00	4.47	0.00
Relative residual E-modulus	40AG0	40AK0	40AK2	40AK4	40BR0	55BK0	70BG0	70BK0
20 °C	1.00	1.00	1.00	1.00	1.00	1.00	1.00	1.00
200 °C	0.81	0.86	0.74	0.92	0.67	0.68	0.86	0.77
400 °C	0.31	0.40	0.40	0.40	0.32	0.30	0.33	0.43
800 °C	0.05				0.02		0.03	
Relative residual strain	40AG0	40AK0	40AK2	40AK4	40BR0	55BK0	70BG0	70BK0
20 °C	1.00	1.00	1.00	1.00	1.00	1.00	1.00	1.00
200 °C	1.47	0.78	1.41	1.22	1.51	1.03	1.24	1.47
400 °C	1.79	1.07	1.25	1.39	1.77	1.38	1.37	1.17
800 °C	3.26	0.00	0.00	0.00	3.30	0.00	2.60	0.00
Relative residual strength	40AG0	40AK0	40AK2	40AK4	40BR0	55BK0	70BG0	70BK0
20 °C	1.00	1.00	1.00	1.00	1.00	1.00	1.00	1.00
200 °C	1.07	0.96	1.10	1.08	0.86	0.76	1.05	0.87
400 °C	0.61	0.70	0.66	0.64	0.56	0.50	0.52	0.68
800 °C	0.19	0.00	0.00	0.00	0.07	0.00	0.12	0.00

Appendix 5.5 – Results of hot properties at elevated temperatures.

Hot E-modulus (MPa)	40AG0	40AK0	40AK2	40AK4	40BR0	55BK0	70BG0	70BK0
20.00	31	25.6	28.33	25.76	31.25	21.05	16.90	27.91
20.00	27	23	32.7	26.65	32.92	22.47	14.29	23.17
200.00	16.6	22.27	22.1	23.42	20	15.00	12.63	18.18
200.00	21.25	18	24.1	21.21	23.19	15.00	13.33	16.76
400.00	8	10	12.81	10.67	9.88	8.33	7.02	14.11
400.00	9.41	11.11	13.27	11.98	10.39	7.14	8.00	9.38
800.00	4.55	4.54	4.55	5	0.63	1.80	1.67	1.91
800.00	4.26	4.35	4.55	5	0.64	3.13	1.54	3.28
On average hot E-modulus (MPa)	40AG0	40AK0	40AK2	40AK4	40BR0	55BK0	70BG0	70BK0
20 °C	29.00	24.30	30.52	26.21	32.09	21.76	15.60	25.54
200 °C	18.93	20.14	23.10	22.32	21.60	15.00	12.98	17.47
400 °C	8.71	10.56	13.04	11.33	10.14	7.74	7.51	11.75
800 °C	4.41	4.45	4.55	5.00	0.64	2.47	1.61	2.60
Hot strain (‰)	40AG0	40AK0	40AK2	40AK4	40BR0	55BK0	70BG0	70BK0
20.00	2.74	3.57	4.88	3.4	3.38	3.73	3.37	3.86
20.00	3.24	6.5	3.49	3.63	3.07	3.81	4.43	3.29
200.00	5.33	4	3.43	2.95	5.31	3.91	6.48	4.71
200.00	5.51	3.66	6.55	4.44	4.45	3.74	5.55	4.67
400.00	6.91	6.34	5.28	5.92	5.6	5.67	5.61	4.14
400.00	6.41	6.49	6.06	6.03	5.84	5.55	5.56	5.59
800.00	5.59	6.91	6.52	4.55	10.5	5.81	6.84	9.58
800.00	4.87	6.7	6.43	4.55	10.8	6.48	7.11	2.77
On average hot strain (‰)	40AG0	40AK0	40AK2	40AK4	40BR0	55BK0	70BG0	70BK0
20 °C	2.99	5.04	4.19	3.52	3.23	3.77	3.90	3.58
200 °C	5.42	3.83	4.99	3.70	4.88	3.83	6.02	4.69
400 °C	6.66	6.42	5.67	5.98	5.72	5.61	5.59	4.87
800 °C	5.23	6.81	6.48	4.55	10.65	6.15	6.98	6.18
Hot strength (MPa)	40AG0	40AK0	40AK2	40AK4	40BR0	55BK0	70BG0	70BK0
20.00	60.4	57.9	65.5	59.7	73.24	45.30	38.20	52.37
20.00	60.3	56.6	74.6	58.67	69.65	45.90	35.10	50.00
200.00	52.9	55.9	65.1	57.95	57.39	40.50	43.60	51.70
200.00	63.49	49.9	65.4	65.2	65.37	41.26	43.10	50.60
400.00	41.73	48.15	61.53	52.38	39.92	35.42	34.60	42.25
400.00	47.1	52.18	66	60.3	40.47	33.20	34.10	40.11
800.00	9.11	11.36	12.9	8.55	5.1	3.80	3.66	15.27
800.00	6.59	11.23	11.64	8.55	5.34	6.15	3.86	4.78
On average hot strength (MPa)	40AG0	40AK0	40AK2	40AK4	40BR0	55BK0	70BG0	70BK0
20 °C	60.35	57.25	70.05	59.19	71.45	45.60	36.65	51.19
200 °C	58.20	52.90	65.25	61.58	61.38	40.88	43.35	51.15
400 °C	44.42	50.17	63.77	56.34	40.20	34.31	34.35	41.18
800 °C	7.85	11.30	12.27	8.55	5.22	4.98	3.76	10.03
Relative hot E-modulus	40AG0	40AK0	40AK2	40AK4	40BR0	55BK0	70BG0	70BK0
20 °C	1.00	1.00	1.00	1.00	1.00	1.00	1.00	1.00
200 °C	0.65	0.83	0.76	0.85	0.72	0.52	0.45	0.60
400 °C	0.30	0.43	0.43	0.43	0.40	0.27	0.26	0.41
800 °C	0.15	0.18	0.15	0.19	0.11	0.09	0.06	0.09
Relative hot strain	40AG0	40AK0	40AK2	40AK4	40BR0	55BK0	70BG0	70BK0
20 °C	1.00	1.00	1.00	1.00	1.00	1.00	1.00	1.00
200 °C	1.81	0.76	1.19	1.05	1.90	1.28	2.01	1.57
400 °C	2.23	1.27	1.35	1.70	1.73	1.88	1.87	1.63
800 °C	1.75	1.35	1.55	1.29	2.01	2.06	2.33	2.07
Relative hot strength	40AG0	40AK0	40AK2	40AK4	40BR0	55BK0	70BG0	70BK0
20 °C	1.00	1.00	1.00	1.00	1.00	1.00	1.00	1.00
200 °C	0.96	0.92	0.93	1.04	1.06	0.68	0.72	0.85
400 °C	0.74	0.88	0.91	0.95	0.86	0.57	0.57	0.68
800 °C	0.13	0.20	0.18	0.14	0.10	0.08	0.06	0.17

Appendix 5.6 – Properties at 20 °C

Concrete		40AG0	40AK0	40AK2	40AK4	40BR0	55BKO	70BG0	70BK0
20 °C									
Specimen 1 (20 °C)	Date	28/08/2002	28/08/2002	28/08/2002	28/08/2002	13/06/2002	28/08/2002	13/06/2002	13/06/2002
	Weight (g)	3633	3604	3824	3765	3819	3641	3485	3742
	FRF (kHz)	6.54	6.44	7.02	6.87	6.55	6.2	5.53	6.26
	fc (MPa)	60.44	57.88	65.46	59.69	73.24	45.90	38.20	52.37
	Ult. load. (kN)	474.70	454.59	514.12	468.81	575.23	360.50	300.02	411.31
	RH -cal. (%)	97	97	94		68		68	71
Specimen 2 (20 °C)	Date	28/08/2002	28/08/2002	28/08/2002	28/08/2002	13/06/2002	28/08/2002	13/06/2002	13/06/2002
	Weight (g)	3637	3578	3804	3711	3790	3613	3504	3705
	FRF (kHz)	6.48	6.41	6.95	6.84	6.6	6.21	5.57	6.25
	fc (MPa)	60.29	56.58	74.62	58.67	69.65	45.30	35.07	50.02
	Ult. load. (kN)	473.52	444.38	586.07	460.79	547.03	355.79	275.44	392.86
	RH -cal. (%)	97	93	97		68		66	65
On average 20 °C	Weight (g)	3635	3591	3814	3738	3804.5	3627	3494.5	3723.5
	FRF (kHz)	6.51	6.425	6.985	6.855	6.575	6.205	5.55	6.255
	fc (MPa)	£60.37	£57.23	£70.04	£59.18	£71.45	£45.60	£36.64	£51.20
	RH -cal. (%)	97	95.0	95.5		67.5		67.0	67.8
Concrete		**40AG0**	**40AK0**	**40AK2**	**40AK4**	**40BR0**	**55BKO**	**70BG0**	**70BK0**
fc1 (MPa)		60.44	57.88	65.46	59.69	73.24	45.90	38.20	52.37
	Edyn1 (GPa)	33.25	31.99	40.33	38.03	35.06	29.95	22.81	31.38
	Estat1 (GPa)	31	25.7	28.33	25.76	31.25	22.47	16.9	27.91
Concrete		**40AG0**	**40AK0**	**40AK2**	**40AK4**	**40BR0**	**55BKO**	**70BG0**	**70BK0**
fc2 (MPa)		60.29	56.58	74.62	58.67	69.65	45.30	35.07	50.02
	Edyn2 (GPa)	32.68	31.46	39.32	37.15	35.33	29.82	23.26	30.97
	Estat2 (GPa)	27	23	32.7	26.65	32.92	21.05	14.29	23.17

Appendix 5.7 – Properties at 20 °C after heating to 200 °C.

Concrete		**40AG0**	**40AK0**	**40AK2**	**40AK4**	**40BR0**	**55BKO**	**70BG0**	**70BK0**
200 °C									
Specimen 1 (20 °C)	Date	30/08/2002	30/08/2002	30/08/2002	30/08/2002	04/07/2002	30/08/2002	04/07/2002	04/07/2002
	Weight (g)	3685	3570	3812	3715	3730	3628	3463	3591
	FRF (kHz)	6.56	6.4	6.97	6.67	4.79	6.17	4.47	5.37
	T (°C)	20	20	20	20	20	20	20	20
	Ult. load. (kN)	453.49	440.30	607.04	474.38	450.82	275.05	252.11	328.22
	fc (MPa)	57.74	56.06	77.29	60.40	57.40	35.02	32.10	41.79
Specimen 2 (20 °C)	Date	30/08/2002	30/08/2002	30/08/2002	30/08/2002	04/07/2002	30/08/2002	04/07/2002	04/07/2002
	Weight (g)	3749	3562	3798	3784	3696	3640	3387	3624
	FRF (kHz)	6.84	6.39	6.75	6.6	5.1	6.2	4.52	5.25
	T (°C)	20	20	20	20	20	20	20	20
	Ult. load. (kN)	562.82	423.09	600.99	531.48	513.42	271.04	350.05	369.61
	fc (MPa)	71.66	53.87	76.52	67.67	65.37	34.51	44.57	47.06
On average 20 °C	Weight (g)	3717	3566	3805	3749.5	3713	3634	3425	3607.5
	FRF (kHz)	6.7	6.395	6.86	6.635	4.945	6.185	4.495	5.31
	T (°C)	20	20	20	20	20	20	20	20
	fc (MPa)	64.70	54.97	76.91	64.04	61.39	34.77	38.34	44.43
Concrete		**40AG0**	**40AK0**	**40AK2**	**40AK4**	**40BR0**	**55BKO**	**70BG0**	**70BK0**
fc1 (MPa)		57.74	56.06	77.29	60.40	57.40	35.02	32.10	41.79
	Edyn1 (GPa)	33.94	31.29	39.63	35.37	18.31	29.56	14.81	22.16
	Estat1 (GPa)	22.4	20.63	25.8	23.29	20	15.87	13.18	19.05
Concrete		**40AG0**	**40AK0**	**40AK2**	**40AK4**	**40BR0**	**55BKO**	**70BG0**	**70BK0**
fc2 (MPa)		71.66	53.87	76.52	67.67	65.37	34.51	44.57	47.06
	Edyn2 (GPa)	37.54	31.13	37.03	35.27	20.57	29.94	14.81	21.38
	Estat2 (GPa)	24.6	21	19.3	25.08	23.19	13.73	13.54	20.34

Appendix 5.8 - E_{dyn}, E_{stat} and compressive strength after heating to 200 °C.

Concrete		**40AG0**	**40AK0**	**40AK2**	**40AK4**	**40BR0**	**55BKO**	**70BG0**	**70BK0**
200 °C									
Specimen 1 (200 °C)	Date	05/09/2002	05/09/2002	05/09/2002	05/09/2002	02/07/2002	05/09/2002	11/07/2002	09/07/2002
	Weight (g)	3750	3737	3751	3733	3695	3636	3428	3612
	FRF (kHz)	6.92	6.74	6.87	6.73	5.11	6.19	4.54	5.27
	T (°C)					200		200	200
	Ult. load. (kN)	415.16	439.27	511.22	455.14	495.67	324.06	342.36	406.29
	fc (MPa)	52.86	55.93	65.09	57.95	63.11	41.26	43.59	51.73
Specimen 2 (200 °C)	Date	05/09/2002	05/09/2002	05/09/2002	05/09/2002	03/07/2002	05/09/2002	11/07/2002	09/07/2002
	Weight (g)	3657	3510	3773	3755	3731	3689	3491	3589
	FRF (kHz)	6.57	6.27	6.9	6.78	5.05	6.27	4.53	5.25
	T (°C)					200		200	200
	Ult. load. (kN)	498.65	391.91	513.34	512.08	514.59	318.09	338.59	397.49
	fc (MPa)	63.49	49.90	65.36	65.20	65.52	40.50	43.11	50.61
On average 200 °C	Weight (g)	3703.50	3623.50	3762.00	3744.00	3713.00	3662.50	3459.50	3600.50
	FRF (kHz)	6.75	6.51	6.89	6.76	5.08	6.23	4.54	5.26
	T (°C)					200.00		200.00	200.00
	fc (MPa)	58.18	52.92	65.23	61.58	64.32	40.88	43.35	51.17
Concrete		**40AG0**	**40AK0**	**40AK2**	**40AK4**	**40BR0**	**55BKO**	**70BG0**	**70BK0**
fc1 (MPa)		52.86	55.93	65.09	57.95	63.11	41.26	43.59	51.73
	Estat1 (GPa)	16.6	22.27	22.1	23.47	21.62	15	12.63	18.18
Concrete		**40AG0**	**40AK0**	**40AK2**	**40AK4**	**40BR0**	**55BKO**	**70BG0**	**70BK0**
fc2 (MPa)		63.49	49.90	65.36	65.20	65.52	40.50	43.11	50.61
	Estat2 (GPa)	21.25	18	24.1	21.21	20.25	15	13.33	16.76

Appendix 5.9 – Properties at 20 °C after heating to 400 °C.

Concrete		40AG0	40AK0	40AK2	40AK4	40BR0	55BKO	70BG0	70BK0
Specimen 1 (20 °C)	Date	13/09/2002	13/09/2002	16/09/2002	16/09/2002	16/09/2002	16/09/2002	17/09/2002	17/09/2002
	Weight (g)	3610	3563	3753	3786	3820	3646	3548	3683
	FRF (kHz)	6.53	6.34	6.83	6.75	6.47	6.22	5.6	6.26
	T (°C)	25	25	22	22	22	22	22	22
	Ult. load. (kN)	316.59	312.35	359.08	292.09	313.53	180.64	148.13	282.74
	fc (MPa)	40.31	39.77	45.72	37.19	39.92	23.00	18.86	36.00
Specimen 2 (20 °C)	Date	13/09/2002	13/09/2002	16/09/2002	16/09/2002	16/09/2002	16/09/2002	17/09/2002	17/09/2002
	Weight (g)	3626	3582	3848	3774	3830	3632	3532	3675
	FRF (kHz)	6.52	6.33	6.96	6.8	6.54	6.28	5.61	6.23
	T (°C)	25	25	22	22	22	22	22	22
	Ult. load. (kN)	265.15	316.91	370.71	299.63	316.99	176.09	148.68	262.01
	fc (MPa)	33.76	40.35	47.20	38.15	40.36	22.42	18.93	33.36
On average 20 °C	Weight (g)	3618	3572.5	3800.5	3780	3825	3639	3540	3679
	FRF (kHz)	6.525	6.335	6.895	6.775	6.505	6.25	5.605	6.245
	T (°C)	25	25	22	22	22	22	22	22
	fc (MPa)	37.04	40.06	46.46	37.67	40.47	22.71	18.90	34.68
After cooling:	FRF (kHz) 1	3.72	3.88	4.03	3.7	3.29	3.65	3.32	4.27
	FRF (kHz) 2	3.69	3.79	4.05	3.84	3.49	3.72	3.45	4.15
	Weight (g) 1	3338	3294	3507	3538	3658	3458	3405	3582
	Weight (g) 2	3341	3319	3599	3528	3668	3452	3392	3573
fc1 (MPa)		40.31	39.77	45.72	37.19	39.92	23.00	18.86	36.00
	Edyn1 (GPa)	9.89	10.61	12.19	10.37	8.47	9.86	8.03	13.98
	Estat1 (GPa)	9.3	9.83	11.7	9.83	9.87	6.77	4.82	11.32
fc2 (MPa)		33.76	40.35	47.20	38.15	40.36	22.42	18.93	33.36
	Edyn2 (GPa)	9.74	10.20	12.63	11.13	9.56	10.22	8.64	13.17
	Estat2 (GPa)	8.7	9.76	12.5	11	10.39	6.19	5.41	10.62
	Moisture loss:	0.92	0.93	0.93	0.93	0.96	0.95	0.96	0.97

Appendix 5.10 – Properties after heating to 400 °C.

Concrete		**40AG0**	**40AK0**	**40AK2**	**40AK4**	**40BR0**	**55BKO**	**70BG0**	**70BK0**
400 °C									
Specimen 1 (400 °C)	Date	11/11/2002	06/11/2002	07/11/2002	08/11/2002	31/10/2002	29/10/2002	30/10/2002	28/10/2002
	Weight (g)	3627	3658	3806	3727	3813	3628	3603	3682
	FRF (kHz)	6.55	6.54	6.91	6.78	6.62	6.21	5.81	6.23
	T (°C)								
	Ult. load. (kN)	327.75	378.17	483.26	411.39	423.49	260.75	271.59	331.91
	fc (MPa)	41.73	48.15	61.53	52.38	53.92	33.20	34.58	42.26
Specimen 2 (400 °C)	Date	11/11/2002	05/11/2002	07/11/2002	08/11/2002	01/11/2002	30/10/2002	31/10/2002	29/10/2002
	Weight (g)	3631	3640	3878	3780	3822	3642	3600	3674
	FRF (kHz)	6.56	6.54	7.13	6.93	6.59	6.28	5.79	6.15
	T (°C)								
	Ult. load. (kN)	369.77	409.82	518.68	473.36	392.39	278.19	267.51	315.02
	fc (MPa)	47.08	52.18	66.04	60.27	49.96	35.42	34.06	40.11
On average 400 °C	Weight (g)	3629	3649	3842	3753.5	3817.5	3635	3601.5	3678
	FRF (kHz)	6.555	6.54	7.02	6.855	6.605	6.245	5.8	6.19
	T (°C)								
	fc (MPa)	44.41	50.17	63.79	56.33	51.94	34.31	34.32	41.19
Concrete		**40AG0**	**40AK0**	**40AK2**	**40AK4**	**40BR0**	**55BKO**	**70BG0**	**70BK0**
fc1 (MPa)		41.73	48.15	61.53	52.38	53.92	33.20	34.58	42.26
	Estat1 (GPa)	8	10	12.81	10.67	11.6	7.14	7.02	11.14
Concrete		**40AG0**	**40AK0**	**40AK2**	**40AK4**	**40BR0**	**55BKO**	**70BG0**	**70BK0**
fc2 (MPa)		47.08	52.18	66.04	60.27	49.96	35.42	34.06	40.11
	Estat2 (GPa)	9.4	11.11	13.27	11.98	11.59	8.33	8	9.38

Appendix 5.11 – Properties at 20 °C after heating to 800 °C.

Concrete		40AG0	40AK0	40AK2	40AK4	40BR0	55BKO	70BG0	70BK0
Specimen 1 (20 °C)	Date	07/10/2002				07/10/2002		07/10/2002	
	Weight (g)	3612	3633	3731	3774	3828	3596	3582	3693
	FRF (kHz)	6.56	6.53	6.86	6.8	6.6	6.23	5.73	6.22
	T (°C)								
	Ult. load. (kN)	90.09				40.06		32.83	
	fc (MPa)	11.47				5.10		4.18	
Specimen 2 (20 °C)	Date								
	Weight (g)	3587	3579	3740	3728	3838	3697	3548	3666
	FRF (kHz)	6.48	6.47	6.91	6.75	6.54	6.24	5.78	6.13
	T (°C)								
	Ult. load. (kN)	90.56				41.94		32.44	
	fc (MPa)	11.53				5.34		4.13	
On average 20 °C	Weight (g)	3599.5	3606	3735.5	3751	3833	3646.5	3565	3679.5
	FRF (kHz)	6.52	6.5	6.885	6.775	6.57	6.235	5.755	6.175
	T (°C)								
	fc (MPa)	11.50				5.22		4.16	
After cooling:	FRF (kHz) 1	1.83	Destroyed	Destroyed	Destroyed	0.99	Destroyed	1.27	Destroyed
	FRF (kHz) 2	1.97	Destroyed	Destroyed	Destroyed	1.06	Destroyed	1.29	Destroyed
	Weight (g) 1	3281	Destroyed	Destroyed	Destroyed	3581	Destroyed	3346	Destroyed
	Weight (g) 2	3243	Destroyed	Destroyed	Destroyed	3588	Destroyed	3312	Destroyed
fc1 (MPa)		11.47				5.10		4.18	
	Edyn1 (GPa)	2.35				0.75		1.15	
	Estat1 (GPa)	1.32				0.63		0.5	
fc2 (MPa)		11.53				5.34		4.13	
	Edyn2 (GPa)	2.69				0.86		1.18	
	Estat2 (GPa)	1.31				0.64		0.51	
	Moisture losses	0.91				0.94		0.93	

Appendix 5.12 – Properties after heating to 800 °C.

Concrete		**40AG0**	**40AK0**	**40AK2**	**40AK4**	**40BR0**	**55BKO**	**70BG0**	**70BK0**
800 °C									
Specimen 1 (800 °C)	Date	12/11/2002	29/11/2002	04/12/2002	06/12/2002	14/11/2002	21/11/2002	19/11/2002	25/02/2002
	Weight (g)	3760	3648	3782	3722	3824	3620	3567	3677
	FRF (kHz)	6.88	6.6	6.88	6.82	6.48	6.2	5.72	6.32
	T (°C)	800				800	793	800	791
	Ult. load. (kN)	71.79	89.22	101.08	67.23	43.90	48.30	28.75	119.93
	fc (MPa)	9.14	11.36	12.87	8.56	5.59	6.15	3.66	15.27
Specimen 2 (800 °C)	Date	13/11/2002	03/12/2002	05/12/2002		15/11/2002	22/11/2002	20/11/2002	26/11/2002
	Weight (g)	3810	3622	3876	3750	3811	3649	3620	3717
	FRF (kHz)	6.93	6.58	7.17	6.95	6.55	6.15	5.8	6.26
	T (°C)	800				800	800	800	817
	Ult. load. (kN)	51.68	88.28	91.42	76.50	51.29	29.85	30.24	37.62
	fc (MPa)	6.58	11.24	11.64	9.74	6.53	3.80	3.85	4.79
On average 800 °C	Weight (g)	3785	3635	3829	3736	3817.5	3634.5	3593.5	3697
	FRF (kHz)	6.905	6.59	7.025	6.885	6.515	6.175	5.76	6.29
	T (°C)	800				800	796.5	800	804
	fc (MPa)	7.86	11.30	12.26	9.15	6.06	4.98	3.76	10.03
Concrete		**40AG0**	**40AK0**	**40AK2**	**40AK4**	**40BR0**	**55BKO**	**70BG0**	**70BK0**
fc1 (MPa)		9.14	11.36	12.87	8.56	5.59	6.15	3.66	15.27
	Estat1 (GPa)	4.55	4.54	4.55	5	3.13	3.13	1.67	3.33
Concrete		**40AG0**	**40AK0**	**40AK2**	**40AK4**	**40BR0**	**55BKO**	**70BG0**	**70BK0**
fc2 (MPa)		6.58	11.24	11.64	9.74	6.53	3.80	3.85	4.79
	Estat2 (GPa)	4.26	4.35	4.55	3.7	3.13	1.8	1.54	3.28

Appendix 5.13 - E_{dyn} and E_{stat} versus compressive strength at 20 °C.

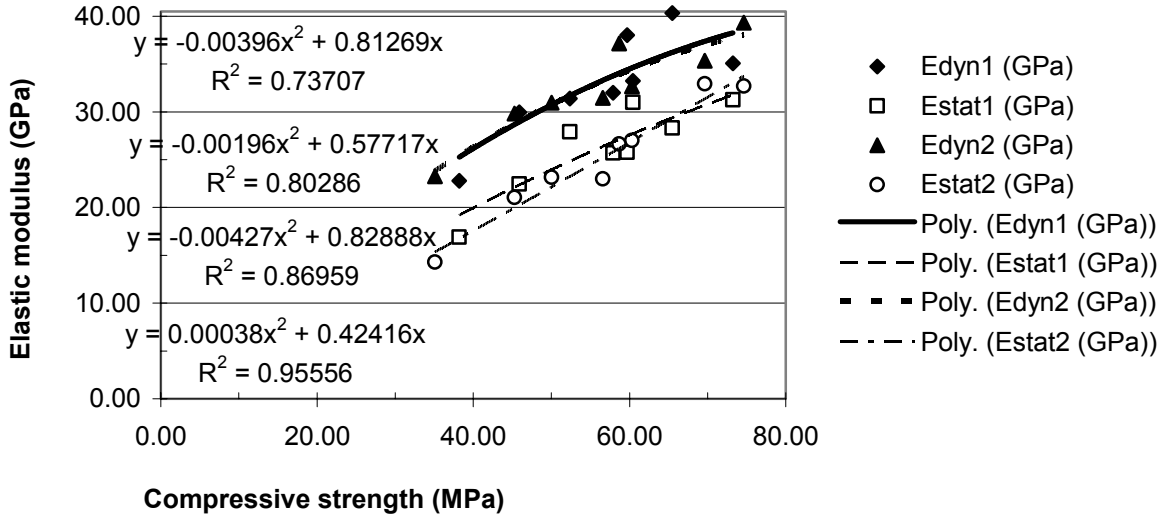

Appendix 5.14 - E_{dyn} and E_{stat} versus compressive strength at 20 °C after heating to 200 °C.

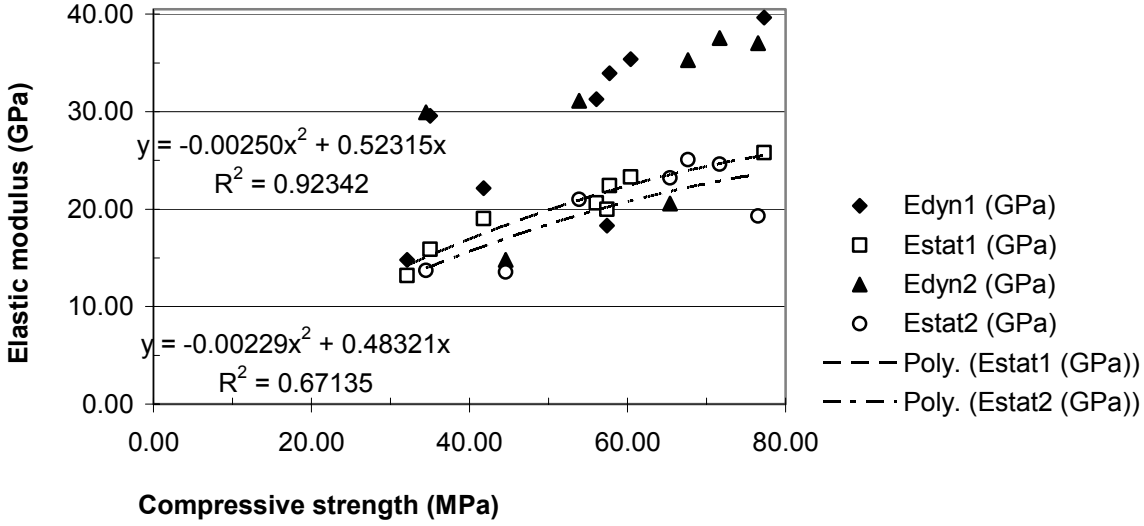

Appendix 5.15 - E_{dyn} and E_{stat} versus compressive strength after heating to 200 °C.

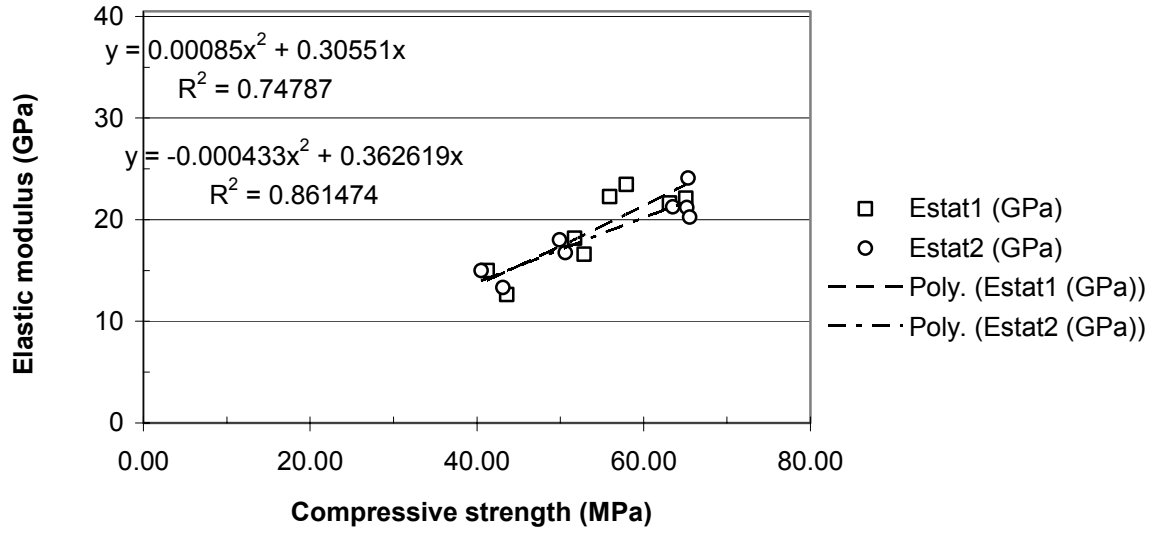

Appendix 5.16 - E_{dyn} and E_{stat} at 20 °C versus compressive strength after heating to 400 °C.

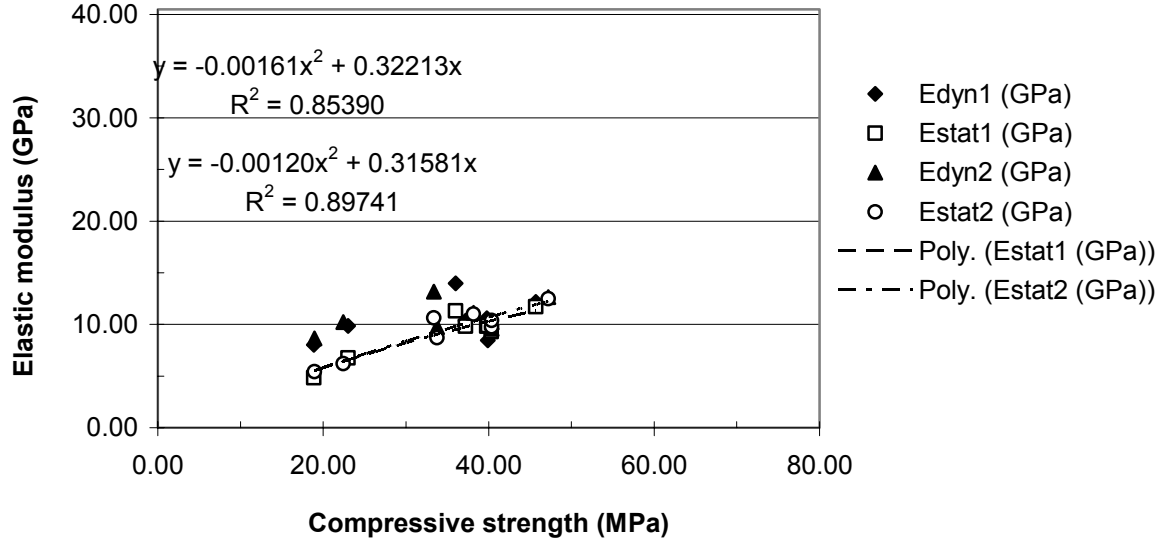

Appendix 5.17 - E_{dyn} and E_{stat} versus compressive strength after heating to 400 °C.

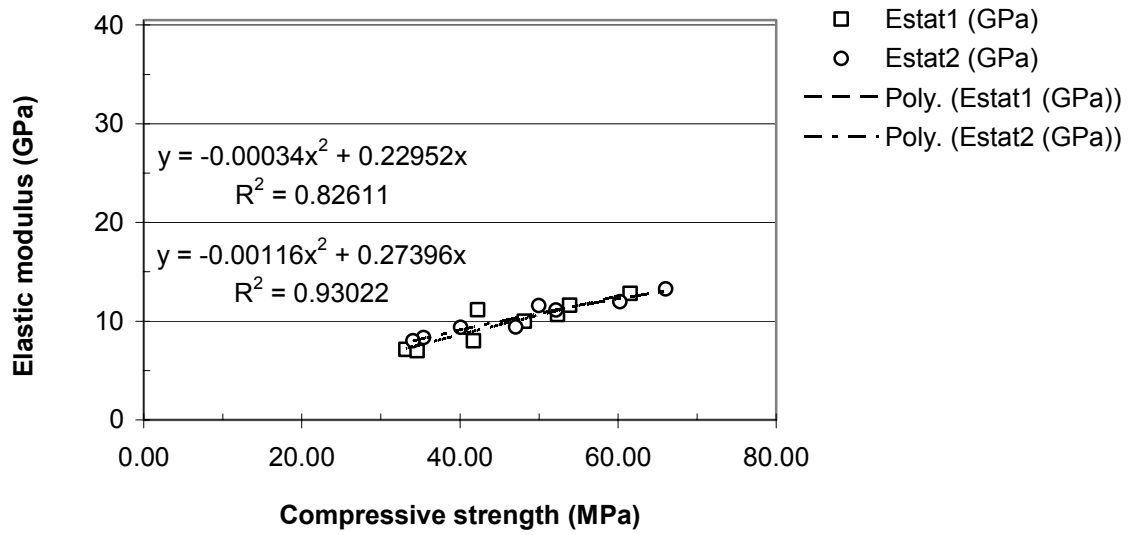

Appendix 5.18 - E_{dyn} and E_{stat} at 20 °C versus compressive strength after heating to 800 °C.

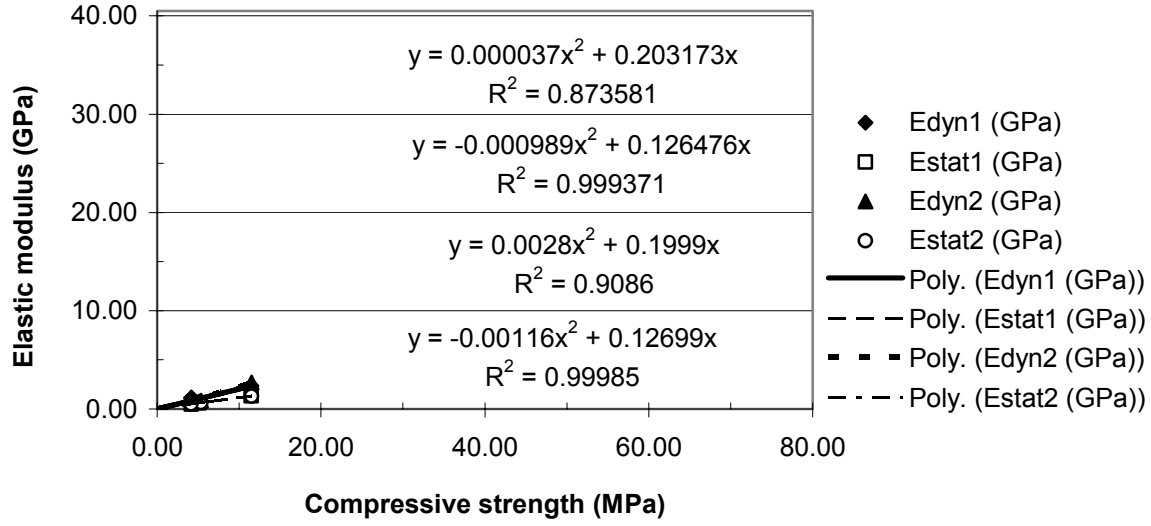

Appendix 5.19 - E_{dyn} and E_{stat} after heating to 800 °C.

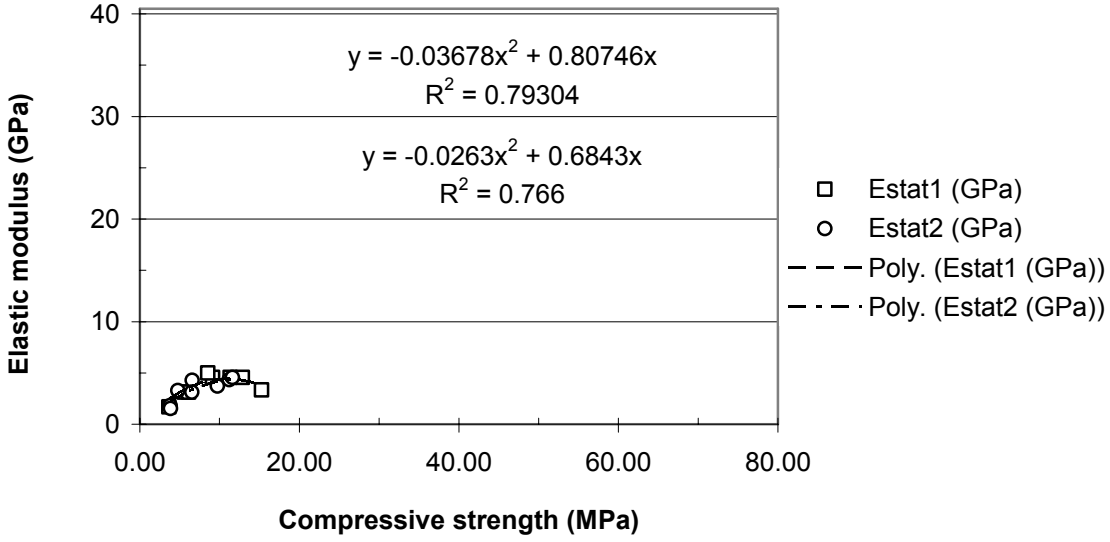

Appendix 5.20 – Moisture losses at 20 °C after heating to high temperatures.

Concrete	HPC [40]	NC [40]	40AG0	40AK0	40AK2	40AK4	40BR0	55BK0	70BG0	70BK0
20	1.000	1.000	1.000	1.000	1.000	1.000	1.000	1.000	1.000	1.000
100	0.984	0.972	0.926	0.947	0.948	0.943	0.966	0.959	0.961	0.971
130										
300	0.951	0.934								
400			0.923	0.926	0.935	0.935	0.958	0.949	0.960	0.972
450	0.923	0.913								
800			0.906	0.000	0.000	0.000	0.935	0.000	0.934	0.000

Appendix 5.21 – RH before heating in cylinders of present study and of columns 200x200 mm [94].

Concrete	40AG0	40AK0	40AK2	40AK4	40AR0	40BK0	40BR0	55BK0	55BR0	70BG0	70BK0	70BR0
Column	89.0	89.0			93.0	73.0		77.0	73.0	77.0	76.0	77.0
Cylinder 1	97.0	97.0	94.0				68.0			68.0	71.0	
Cylinder 2	97.0	93.0	97.0				68.0			66.0	65.0	
Cylinders, av.	97.0	95.0	95.5				67.5			67.0	67.8	

Appendices 6 – Statistical analysis and sources of error

Appendix 6.1 – Stress/strain results of concrete 40BR0 at 200 °C – 200 °C.

Appendix 6.2 – Stress/strain results of concrete 70BG0 at 200 °C – 200 °C

Appendix 6.3 – Stress/strain results of concrete 70BK0 at 200 °C – 200 °C.

Appendix 6.4 – Statistical analysis of stress/strain tests

Appendix 6.1 – Stress/strain results of concrete 40BR0 at 200 °C – 200 °C.

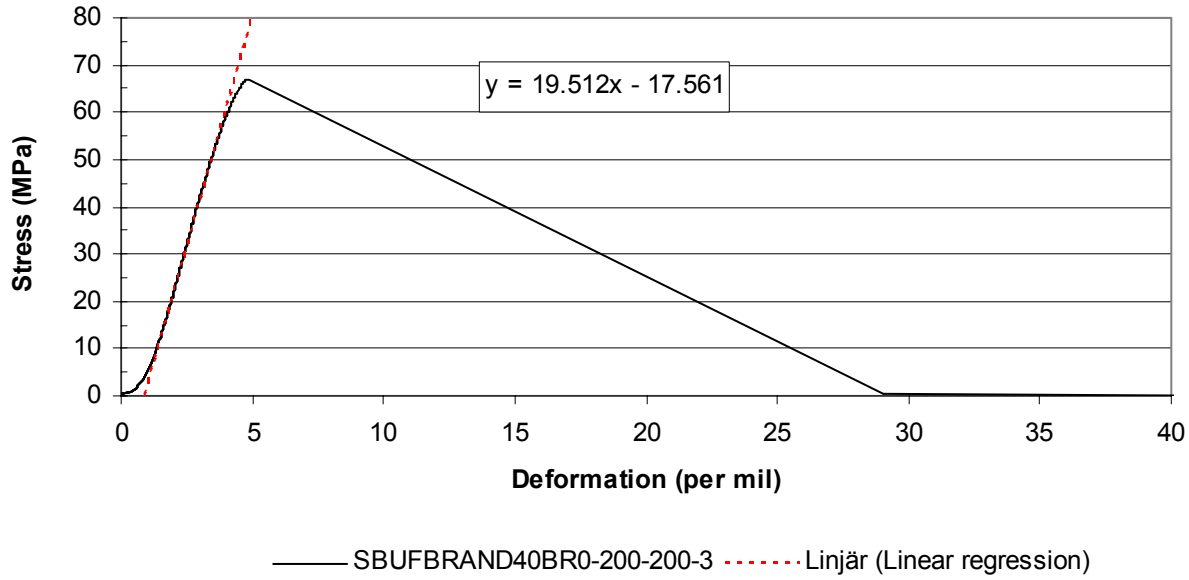

Appendix 6.2 – Stress/strain results of concrete 70BG0 at 200 °C – 200 °C

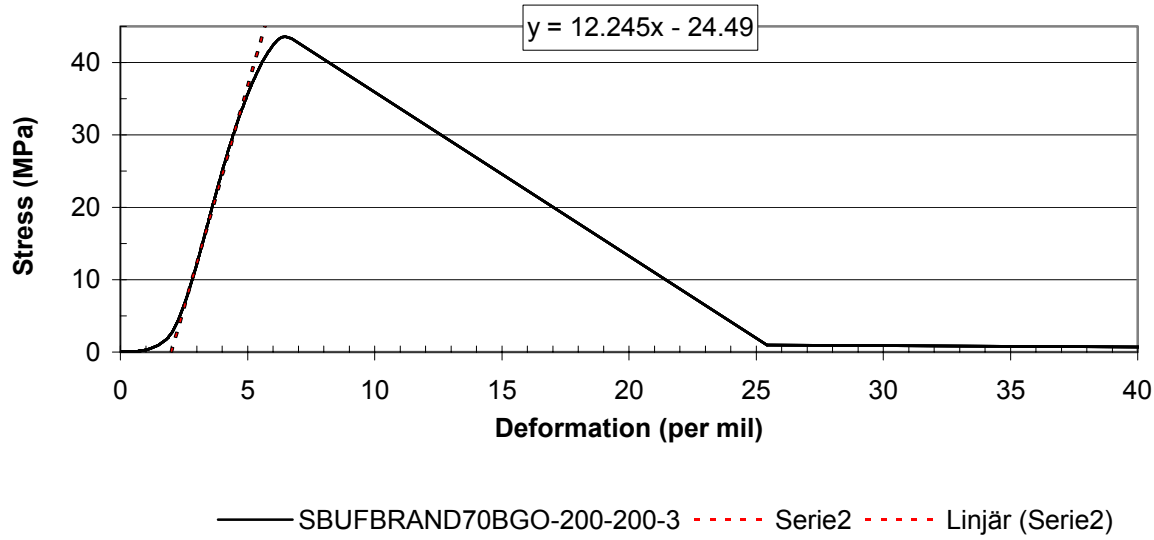

Appendix 6.3 – Stress/strain results of concrete 70BK0 at 200 °C – 200 °C.

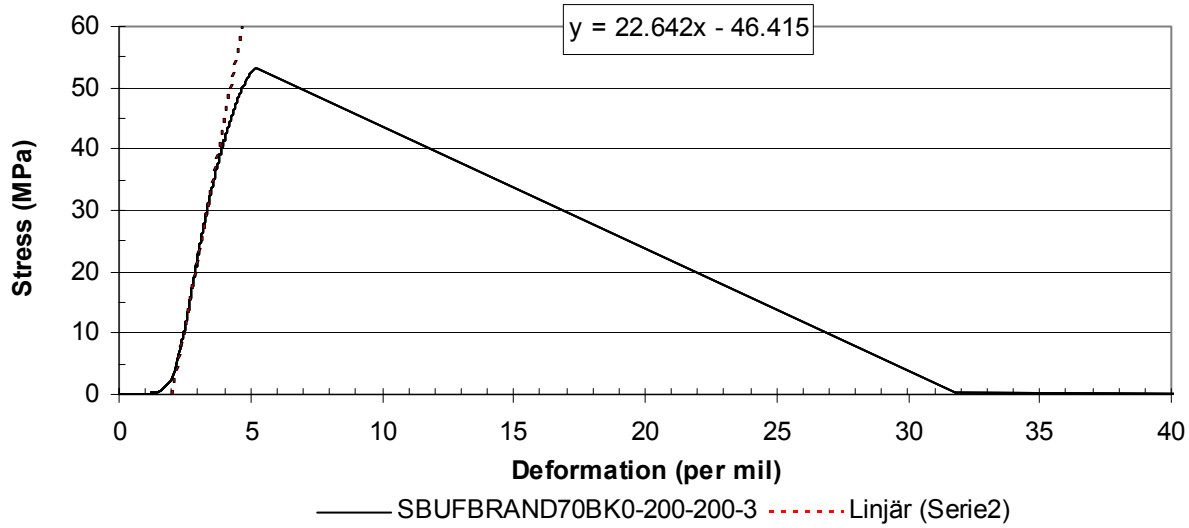

Appendix 6.4 – Accuracy of stress/strain tests

Elastic modulus (GPa)	1	2	3	Std	Average	Variance (%)
40BR0-200-200	21.62	20.25	19.51	0.87	20.46	4.27
70BG0-200-200	12.63	13.33	12.25	0.45	12.74	3.51
70BK0-200-200	18.18	16.76	22.64	2.51	19.19	13.05
Strain at max strain (‰)	1	2	3	Std	Average	Variance (%)
40BR0-200-200	5.25	6.11	4.87	0.52	5.41	9.59
70BG0-200-200	6.48	5.55	6.73	0.51	6.25	8.12
70BK0-200-200	4.71	4.67	5.21	0.25	4.86	5.05
Strength (MPa)	1	2	3	Std	Average	Variance (%)
40BR0-200-200	63.10	65.52	67.02	1.61	65.21	2.48
70BG0-200-200	43.59	43.11	43.30	0.20	43.33	0.46
70BK0-200-200	51.73	50.61	53.31	1.11	51.88	2.13

Appendices 7 – Supplementary tests

Appendix 7.1 - Stress/strain results of concrete 40AG0 at 600 °C – 20 °C.

Appendix 7.2 - Stress/strain results of concrete 40AK0 at 600 °C – 20 °C.

Appendix 7.3 - Stress/strain results of concrete 40AK2 at 600 °C – 20 °C.

Appendix 7.4 - Stress/strain results of concrete 40AK4 at 600 °C – 20 °C.

Appendix 7.5 - Stress/strain results of concrete 40BR0 at 600 °C – 20 °C.

Appendix 7.6 - Stress/strain results of concrete 55BK0 at 600 °C – 20 °C.

Appendix 7.7 - Stress/strain results of concrete 70BG0 at 600 °C – 20 °C.

Appendix 7.8 - Stress/strain results of concrete 70BK0 at 600 °C – 20 °C.

Appendix 7.1 - Stress/strain results of concrete 40AG0 at 600 °C – 20 °C.

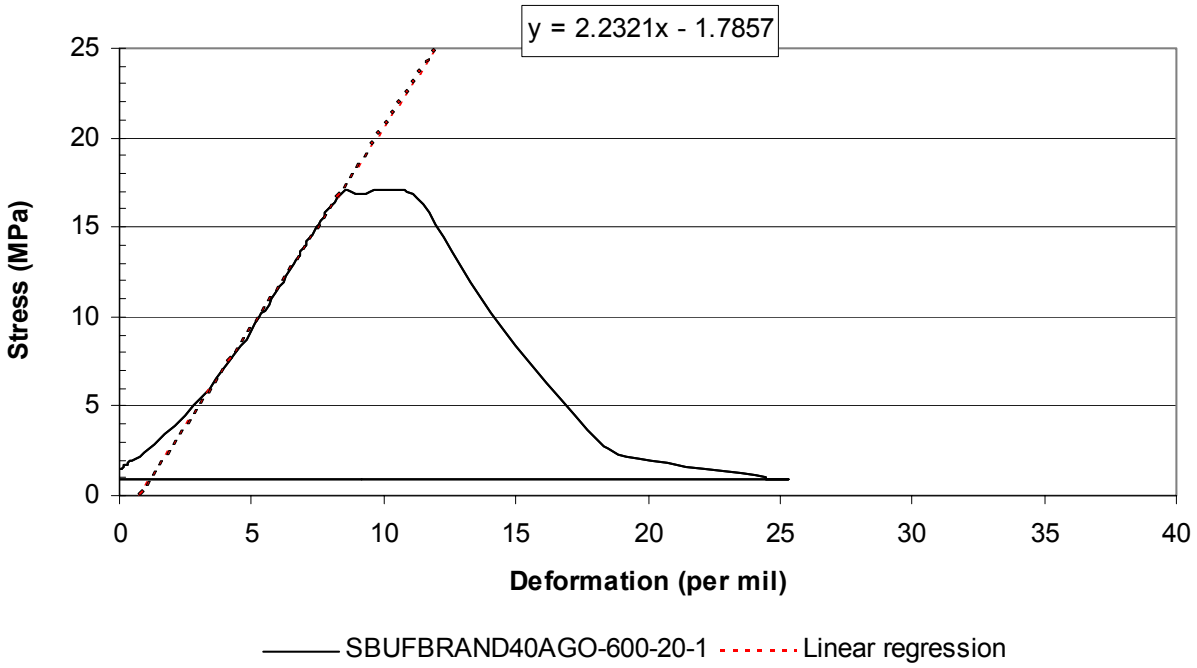

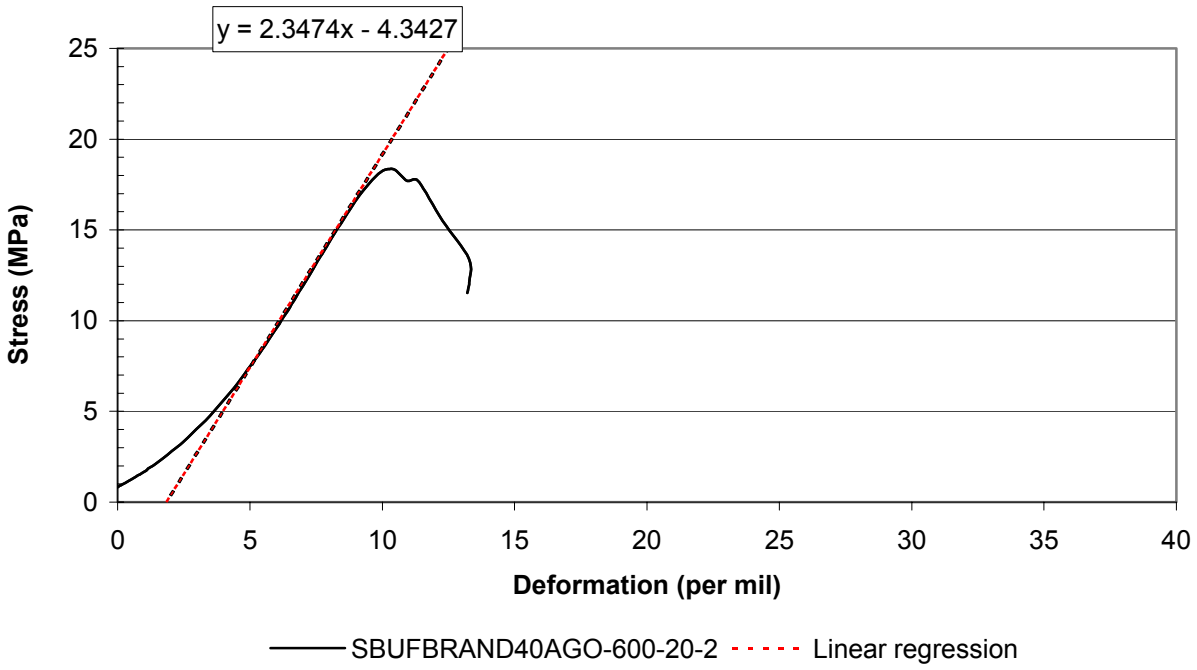

Appendix 7.2 - Stress/strain results of concrete 40AK0 at 600 °C – 20 °C.

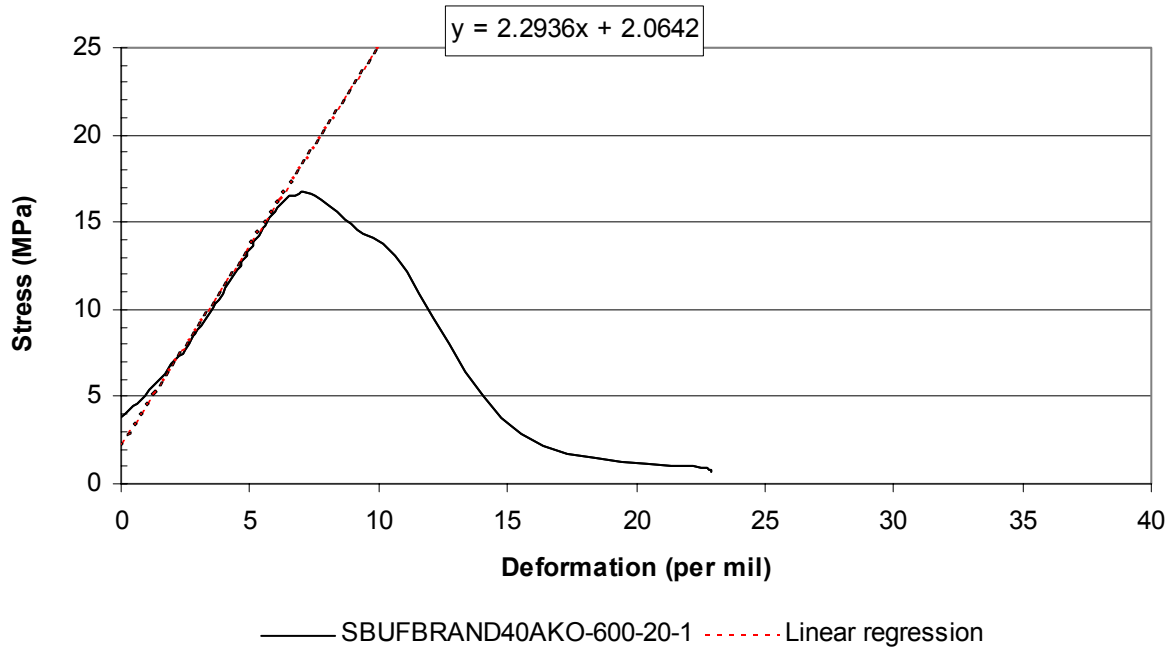

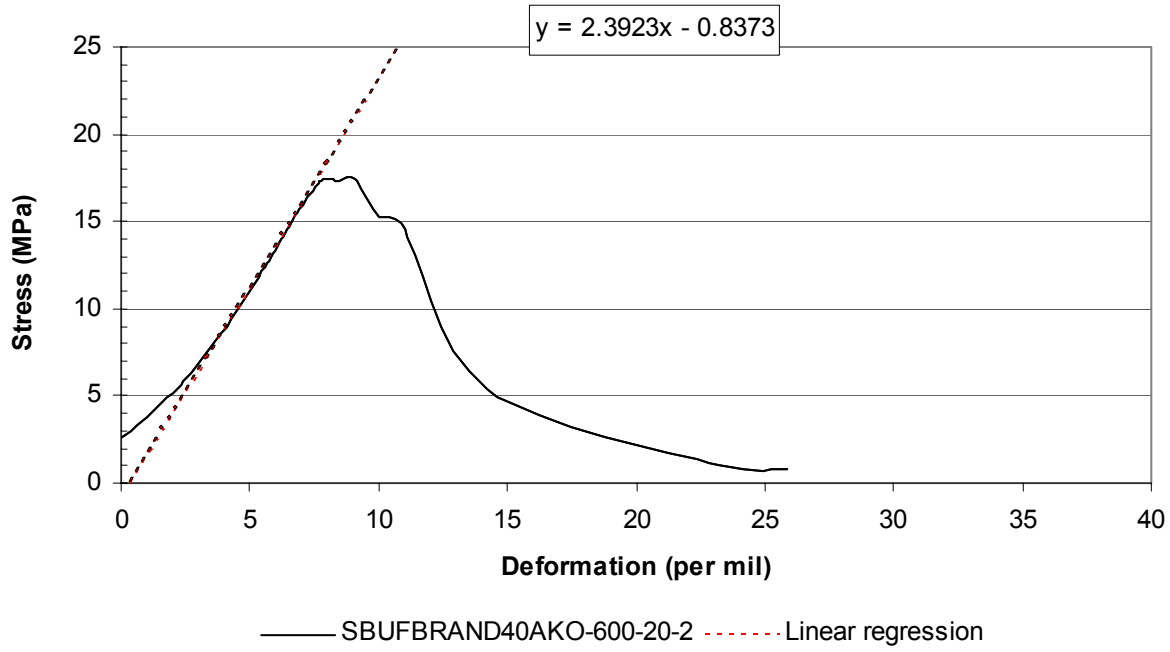

Appendix 7.3 - Stress/strain results of concrete 40AK2 at 600 °C – 20 °C.

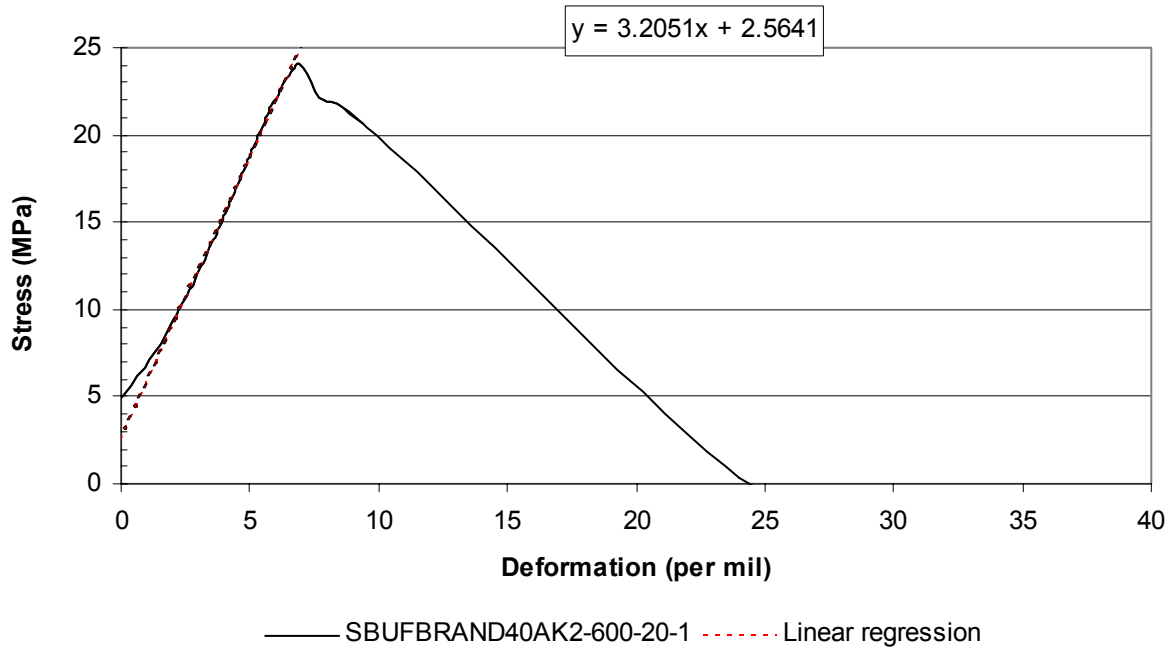

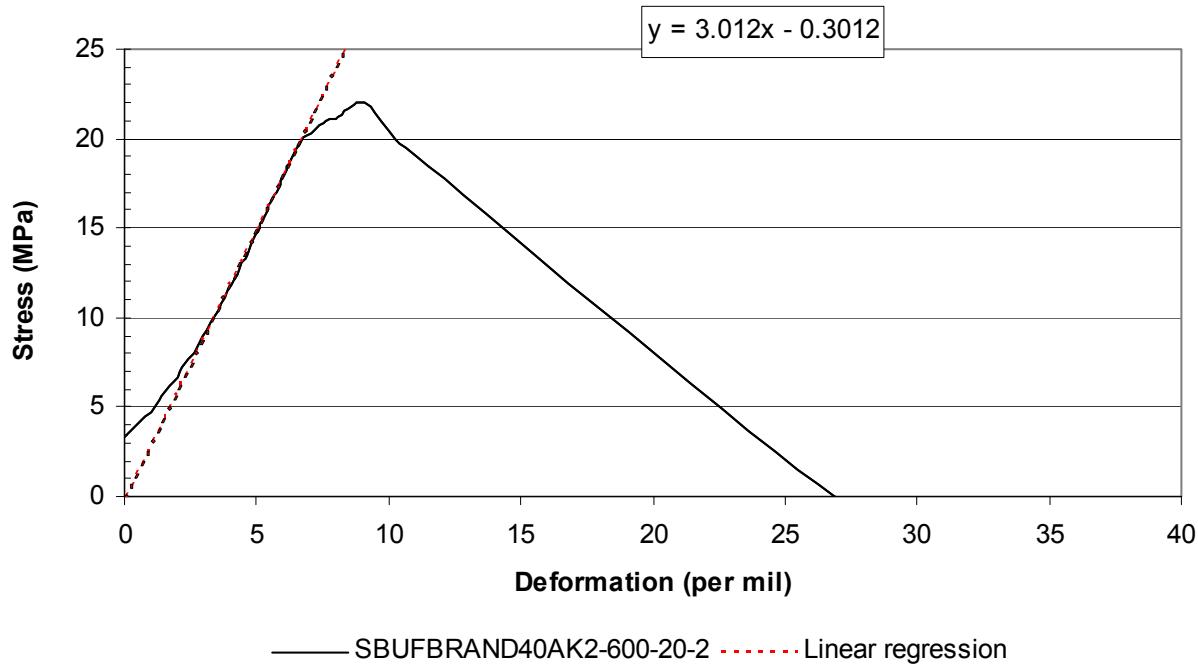

Appendix 7.4 - Stress/strain results of concrete 40AK4 at 600 °C – 20 °C.

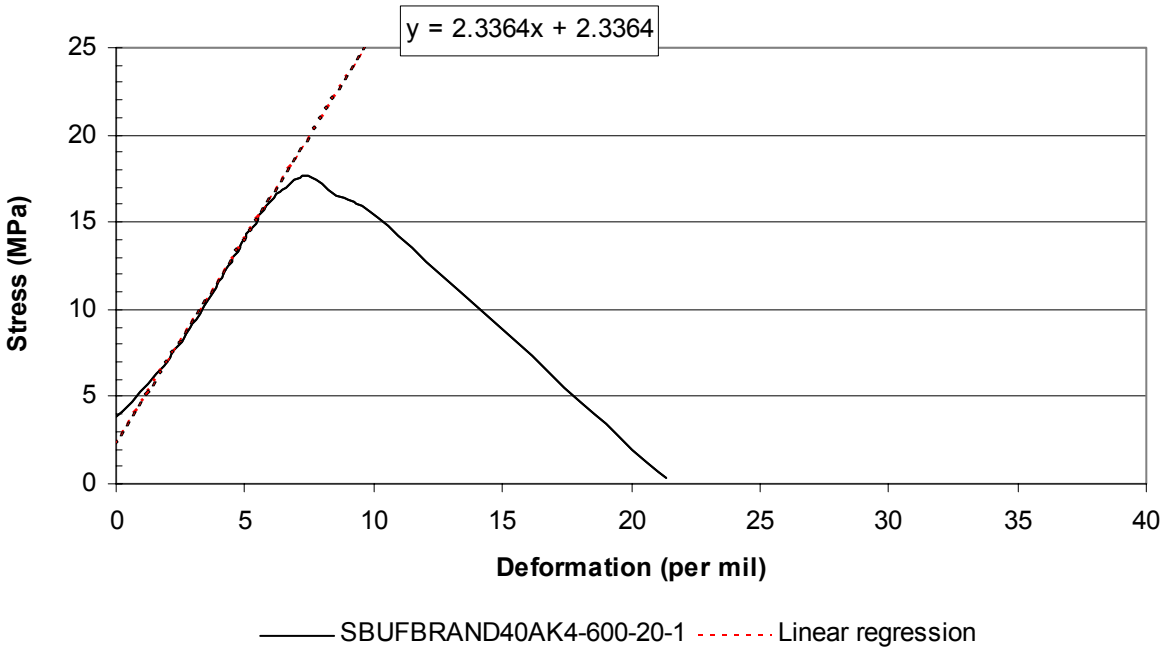

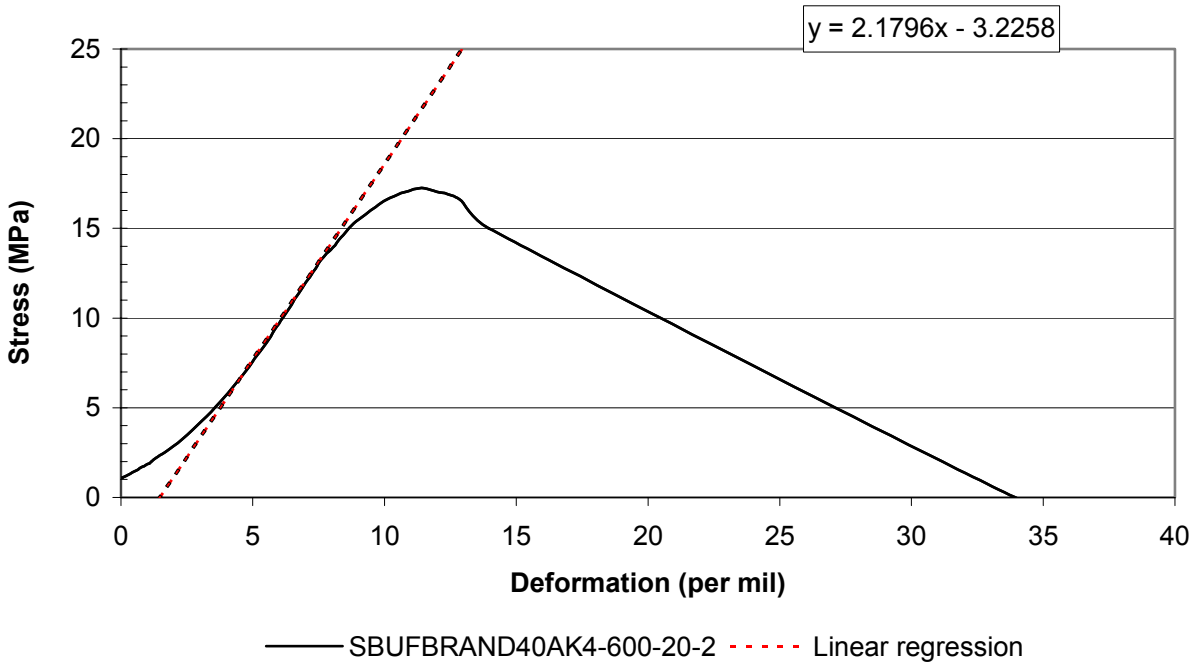

Appendix 7.5 - Stress/strain results of concrete 40BR0 at 600 °C – 20 °C.

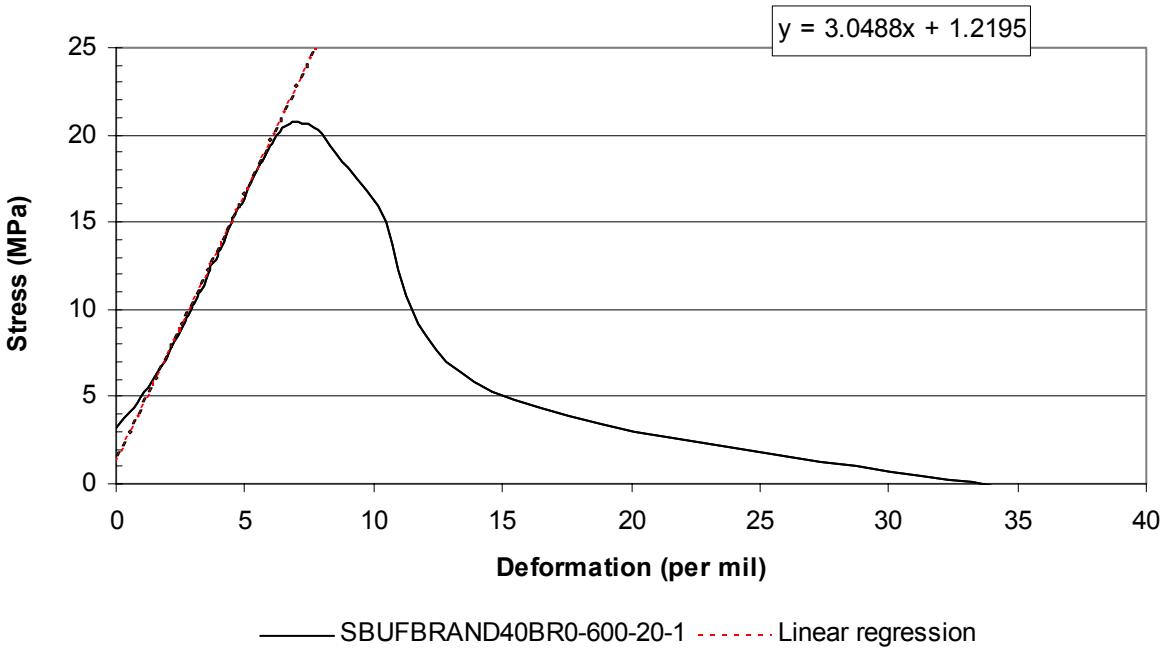

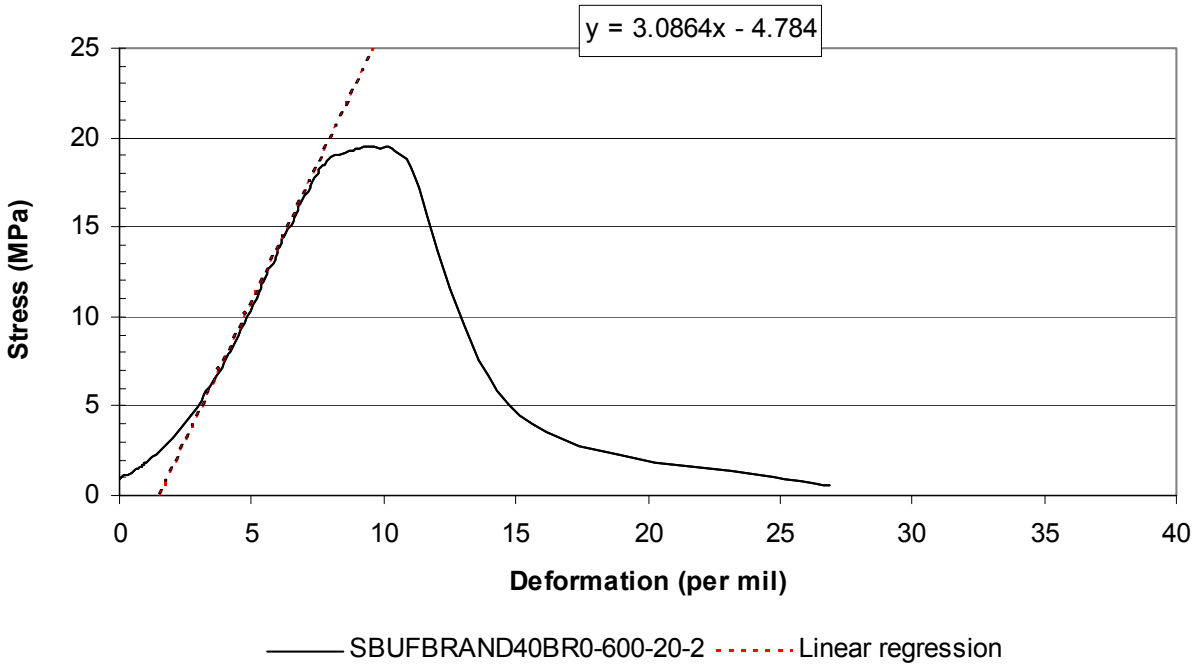

Appendix 7.6 - Stress/strain results of concrete 55BK0 at 600 °C – 20 °C.

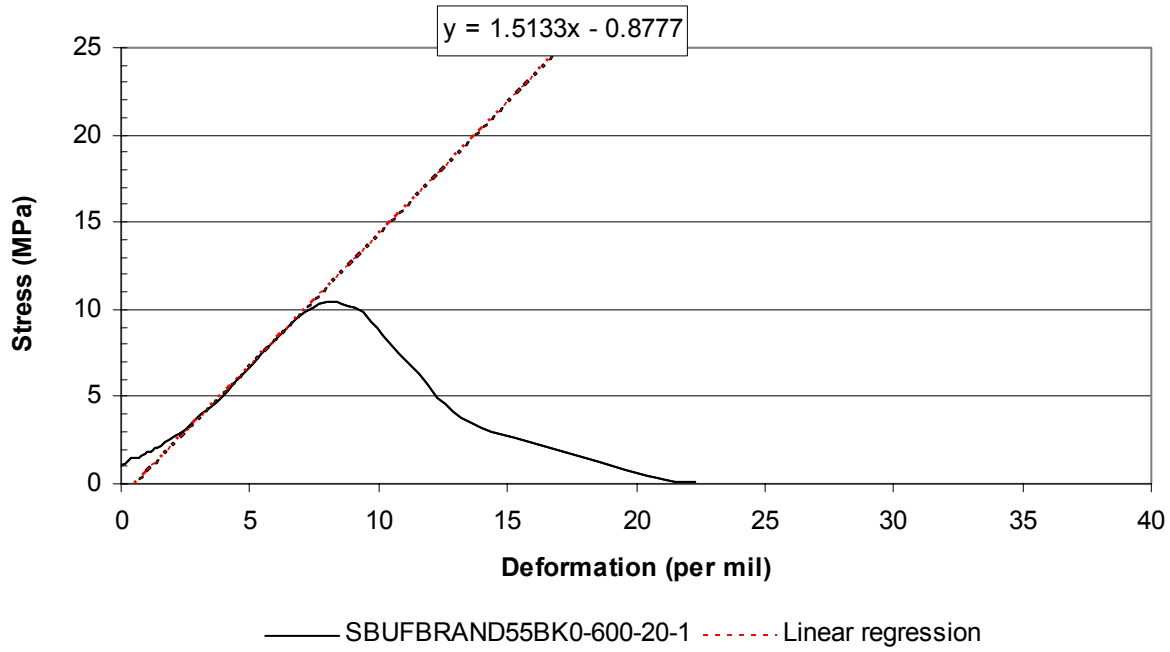

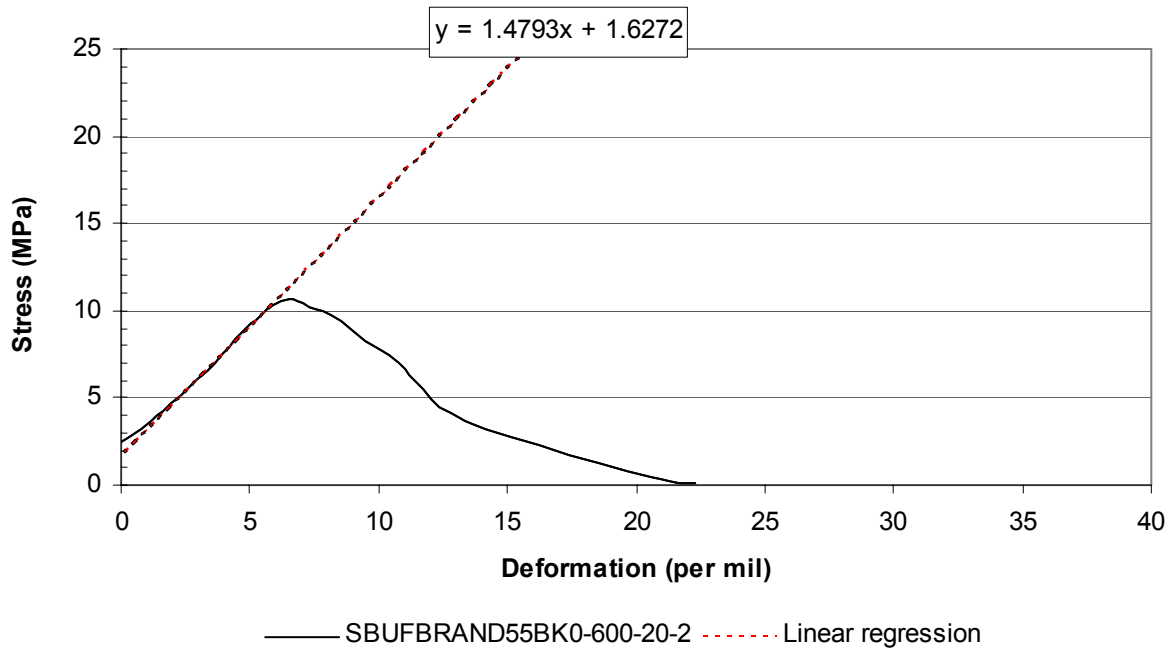

Appendix 7.7 - Stress/strain results of concrete 70BG0 at 600 °C – 20 °C.

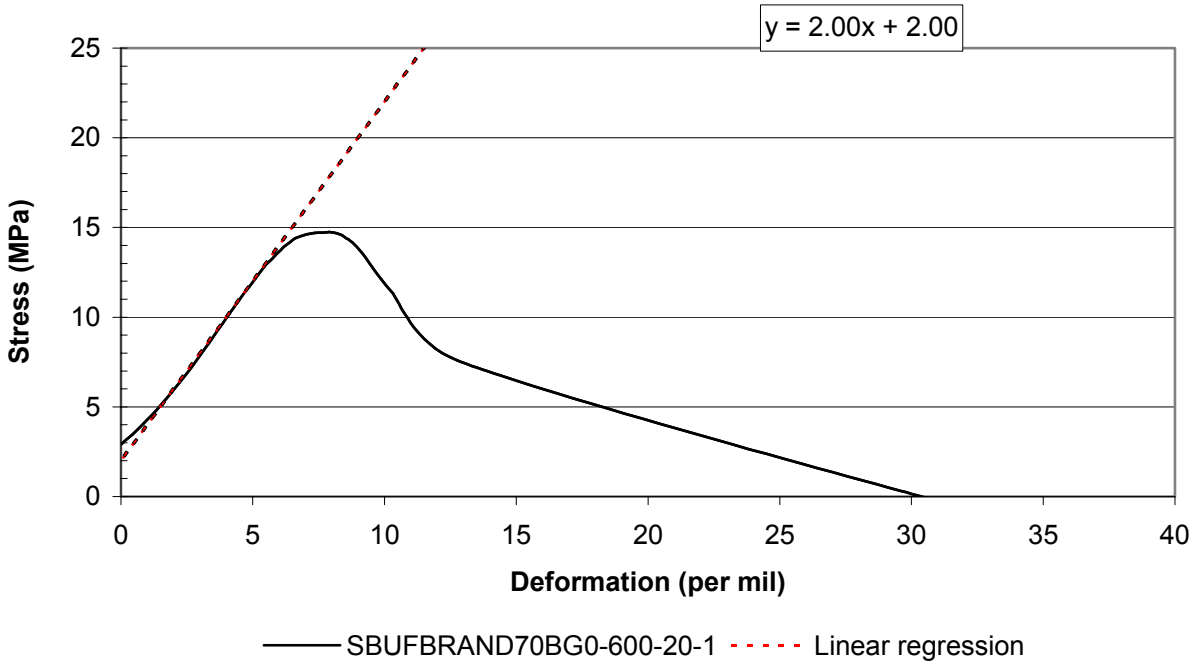

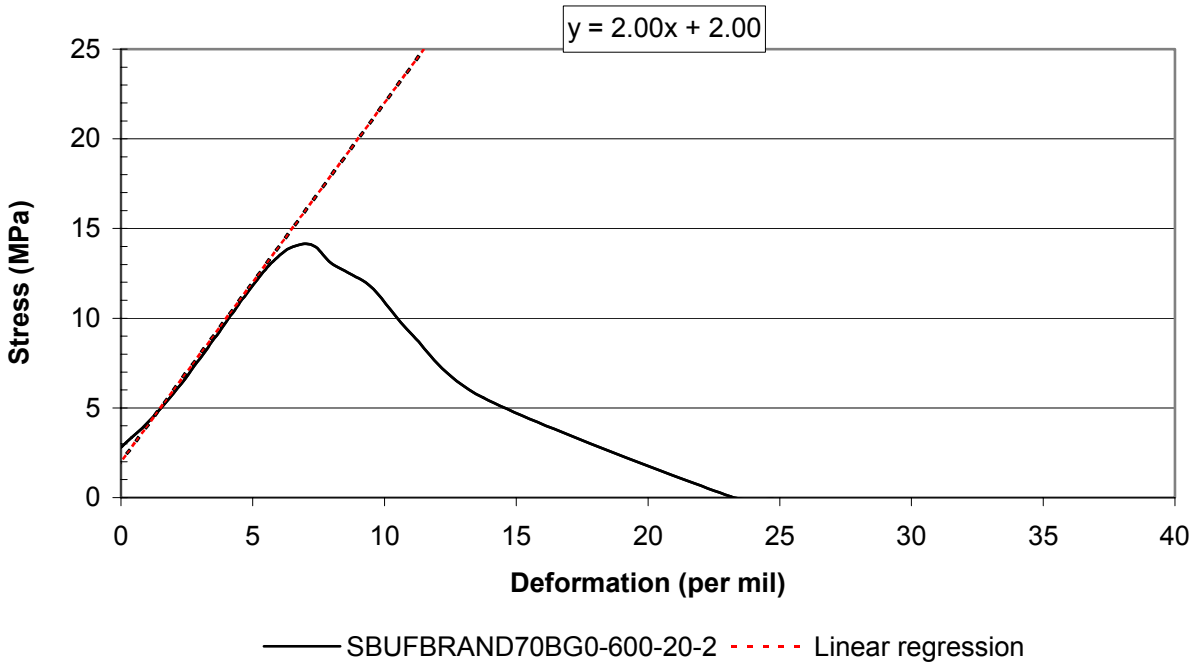

Appendix 7.8 - Stress/strain results of concrete 70BK0 at 600 °C – 20 °C.

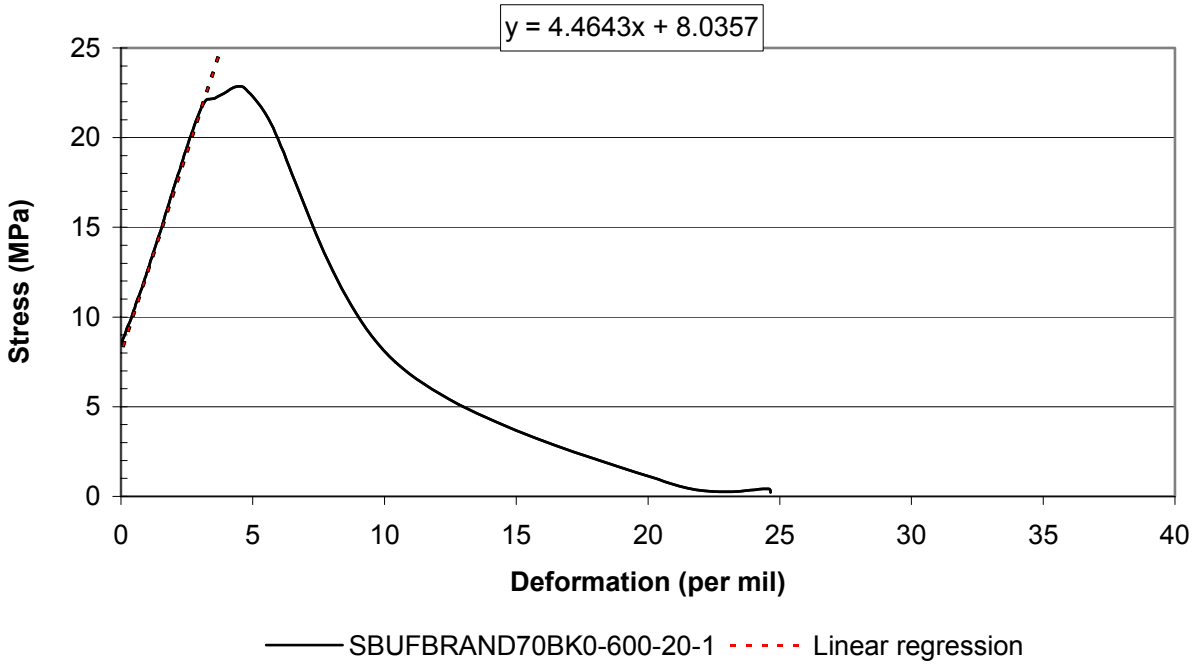

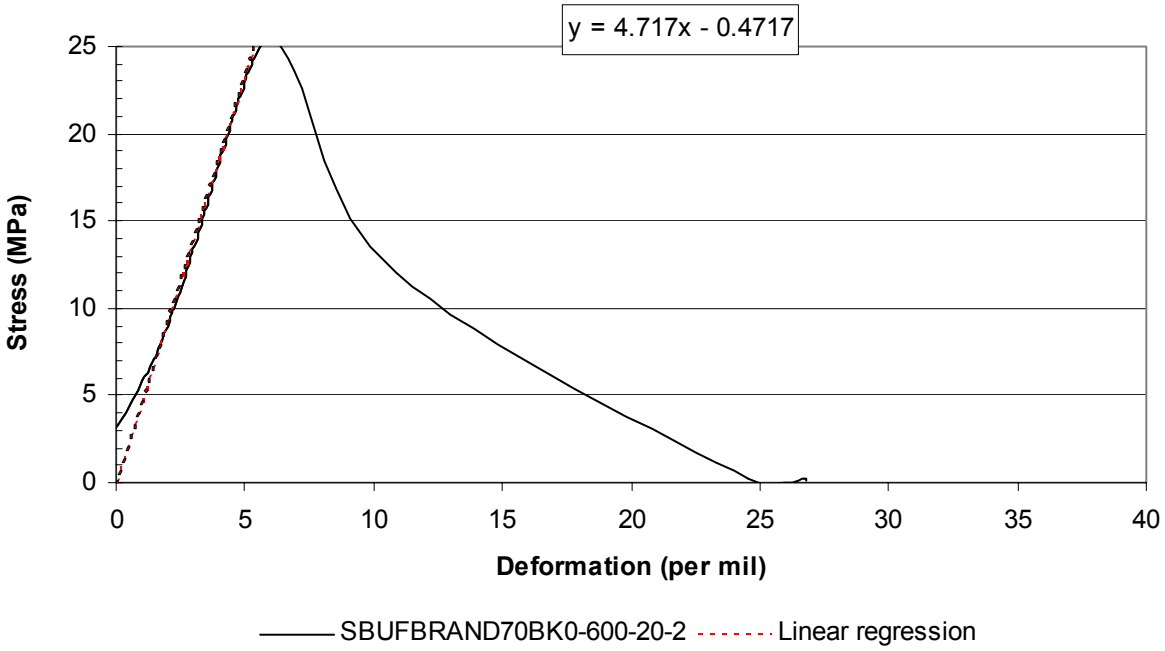

Appendix 7.9 - Resistance to water penetration after heating to 105 °C (s/m²·10^6).

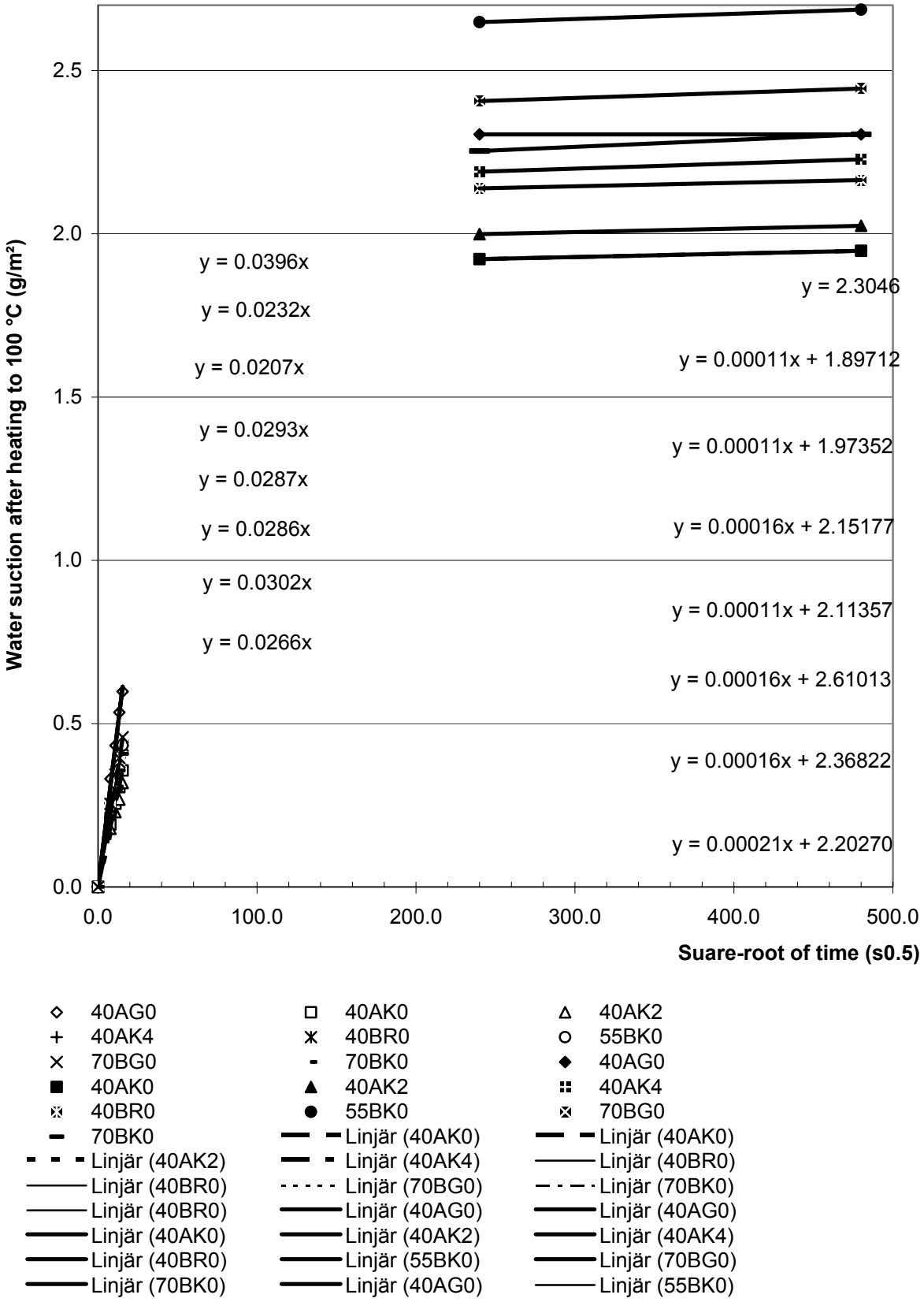

Appendix 7.10 - Resistance to water penetration after heating to 200 °C (s/m²·10^6).

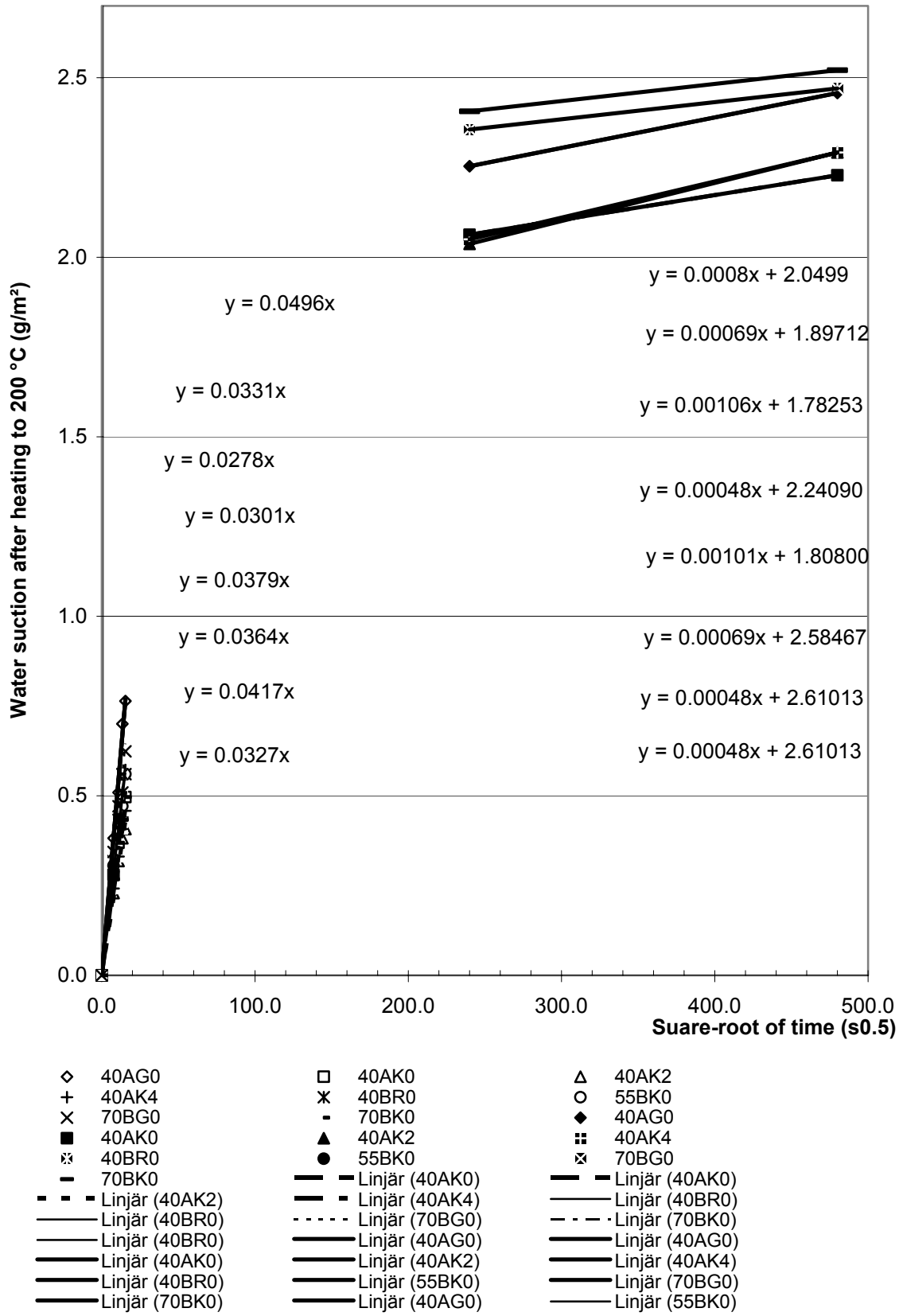

Appendix 7.11 - Resistance to water penetration after heating to 400 °C (s/m²·10^6).

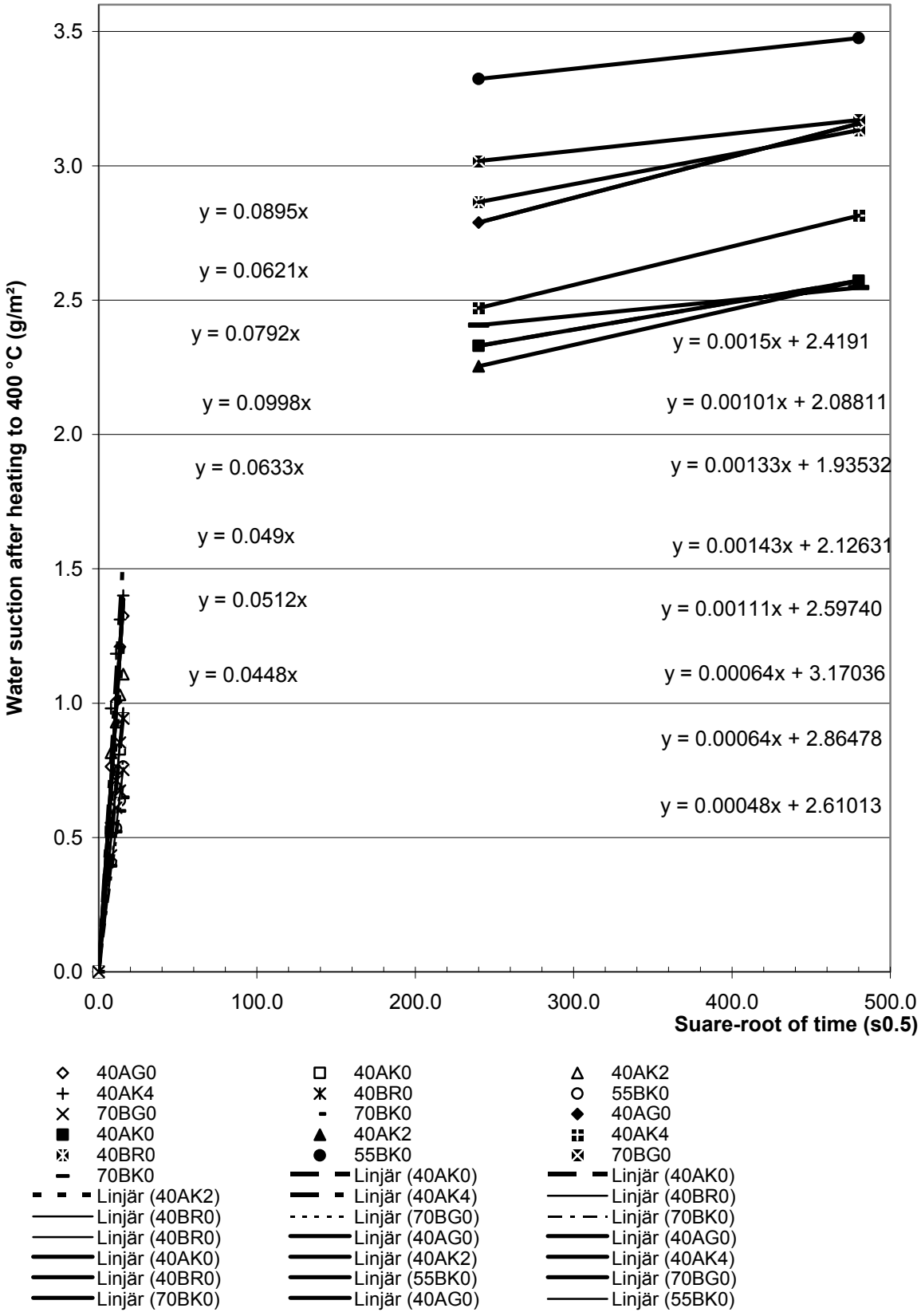

Appendix 7.12 - Resistance to water penetration after heating to 600 °C (s/m²·10^6).

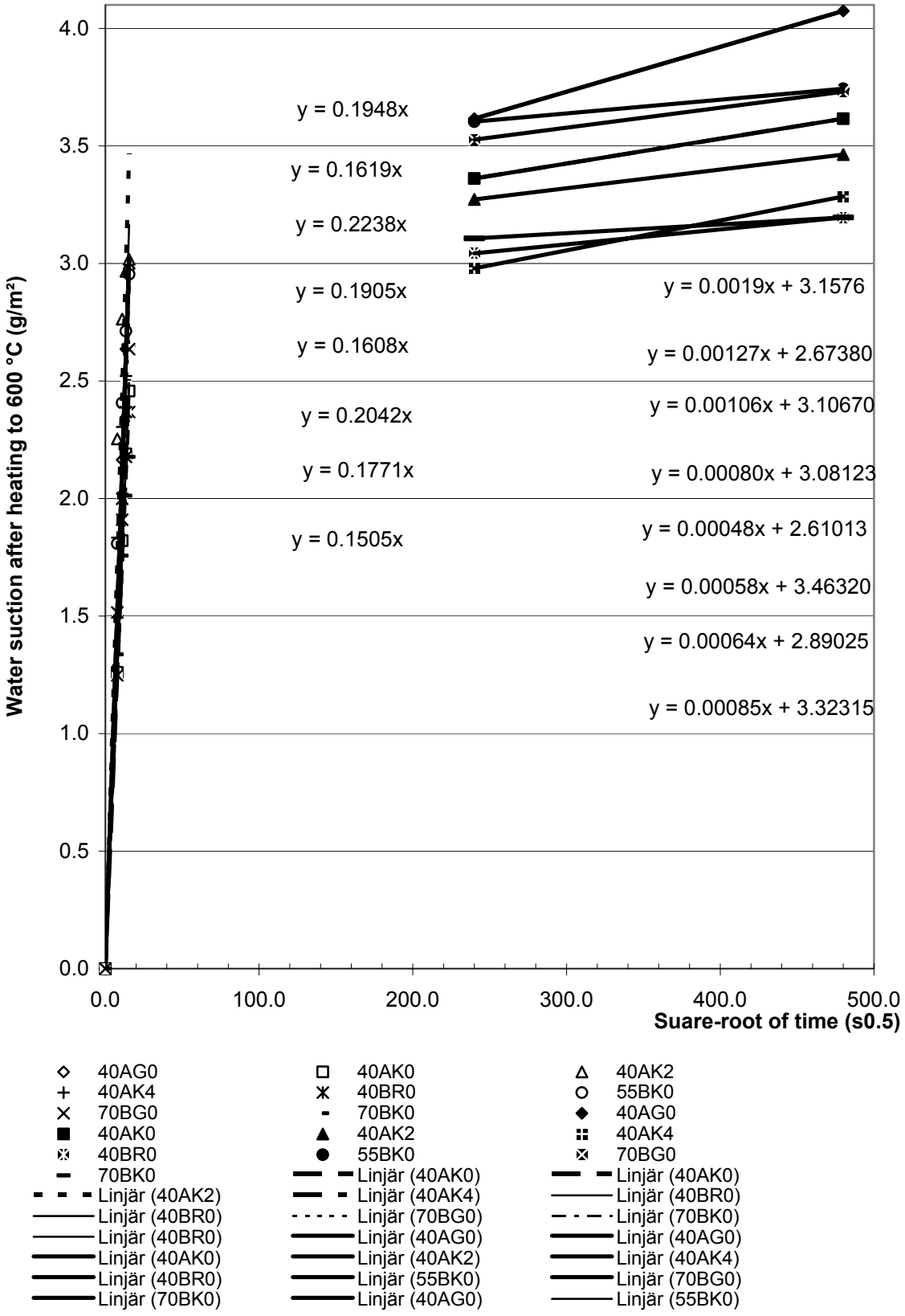

Appendix 8 – Discussion of data from fire spalling tests [94,107].

Con-crete	We-ight	w	c	f	w/p	RH	Mois-ture	Den-sity	12-16 mm	8-11 mm	0-8 mm	16 mm/p	11 mm/p	8 mm/p	c/p	f/p	a/p	16 mm/p	11 mm/p	8 mm/p	Age (days)
40AG0	0.82	172	430	62	0.35	0.89	0.037	2330	624		1042	1.27	0.00	2.12	0.87	0.13	3.39	1.27	0.00	2.12	170
40AK0	0.68	164	411	149	0.29	0.89	0.037	2360	595		1041	1.06	0.00	1.86	0.73	0.27	2.92	1.06	0.00	1.86	170
40AK2	0.88	173	433	181	0.28		0.037	2360	572		1001	0.93	0.00	1.63	0.71	0.29	2.56	0.93	0.00	1.63	170
40AK4	0.94	195	487	171	0.30		0.037	2370		326	1191	0.00	0.50	1.81	0.74	0.26	2.31	0.00	0.50	1.81	170
40AR0	0.93	206	518	0	0.40	0.93	0.037	2350	857		769	1.65	0.00	1.48	1.00	0.00	3.14	1.65	0.00	1.48	170
40BR0	0.95	175	436	0	0.40		0.031	2420	602		1207	1.38	0.00	2.77	1.00	0.00	4.15	1.38	0.00	2.77	170
40BK0	0.76	179	447	130	0.31	0.73	0.031	2360	1004		600	1.74	0.00	1.04	0.77	0.23	2.78	1.74	0.00	1.04	170
55BK0 -1 year	0.73	170	308	242	0.31	0.77	0.031	2380	234	362	1064	0.43	0.66	1.93	0.56	0.44	3.02	0.43	0.66	1.93	320
55BK2 -1 year	0.85	189	344	241	0.32		0.031	2390	119	244	1253	0.20	0.42	2.14	0.59	0.41	2.76	0.20	0.42	2.14	320
55BK4	0.86	210	382	233	0.34		0.031	2350		316	1209	0.00	0.51	1.97	0.62	0.38	2.48	0.00	0.51	1.97	160
55BR0 -1 year	0.86	192	348	0	0.55	0.73	0.031	2380	452	360	1028	1.30	1.03	2.95	1.00	0.00	5.29	1.30	1.03	2.95	320
70BG0	0.87	225	321	80	0.56	0.77	0.031	2340	551		1163	1.37	0.00	2.90	0.80	0.20	4.27	1.37	0.00	2.90	170
70BK0	0.82	188	268	189	0.41	0.76	0.031	2394	631		1118	1.38	0.00	2.45	0.59	0.41	3.83	1.38	0.00	2.45	170
70BK2	0.97	209	298	229	0.40		0.031	2330	583		1011	1.11	0.00	1.92	0.57	0.43	3.02	1.11	0.00	1.92	160
70BK4	0.86	214	306	331	0.34		0.031	2320		220	1249	0.00	0.35	1.96	0.48	0.52	2.31	0.00	0.35	1.96	160
70BR0	0.92	195	278	0	0.70	0.77	0.031	2250	351	356	1070	1.26	1.28	3.85	1.00	0.00	6.39	1.26	1.28	3.85	170